UNCUYO UNIVERSIDAD NACIONAL DE CUYO | FACULTAD DE INGENIERÍA | DIRECCIÓN DE POSGRADO

UNCUYO
UNIVERSIDAD
NACIONAL DE CUYO

THESIS OF MASTER

ANALYSIS OF THE INFLUENCE OF URBAN TUNNEL EXCAVATION ON PRE-EXISTING STRUCTURES

Student´s Name: Ing. David Enrique Agüero

Advisor´s Name: Dr. Ing. Juan Pablo Ibañez

Ingenieros J. 1400, Mendoza, Argentina. 2025

UNCUYO UNIVERSIDAD NACIONAL DE CUYO | FACULTAD DE INGENIERÍA | DIRECCIÓN DE POSGRADO

UNCUYO
UNIVERSIDAD
NACIONAL DE CUYO

ACADEMIC UNIT: FACULTY OF ENGINNERING

THESIS OF MASTER

ANALISYS OF THE INFLUENCE OF URBAN TUNNEL EXCAVATION ON PRE-EXISTING STRUCTURES

DOUBLE DEGREE

MASTER IN GEOTECHNICAL ENGINEERING

MASTER OF SCIENCES IN CIVIL ENGINEERING

Student´s Name: Ing. David Enrique Agüero

Advisor´s Name: Dr. Ing. Juan Pablo Ibañez

Ingenieros J. 1400, Mendoza, Argentina. 2025

DEDICATORIA

Dedico esta tesis en honor a mi padre: Cesar Alberto Agüero, cuya memoria vive en mi cada día.

Adicionalmente, a mi madre Olga y mi hermano Cesar, quienes son el tesoro más grande que Dios me ha regalado.

ACKNOWLEDGMENTS

I would like to express my most sincere gratitude first of all to God for being my support and fortitude at all times throughout my life and for giving me the opportunity to continue growing as a person and in this case as a professional.

To my professor Juan Pablo Ibañez, for taking on this job with such dedication and responsibility, making his knowledge and experience available to offer valuable contributions to its development.

To the teaching staff of the Geotechnics Department of UNCUYO and TUM for the knowledge provided throughout this professional training process. Very especially to Professor Roberto Cudmani, for all his support, help and willingness during my stay and that of my colleagues in Munich.

To the coordinator of the Master's Degree in Argentina Arnaldo Barchiesi and in Germany Nick Sommer, for their constant help and willingness to solve any problem or evacuate any concern that arose during this study process.

To my colleagues and friends, Franz Brücklmayr, Nicholas Shankie, Julio Lara, Cecilia Howe, Gabriel de Mula, Augusto Abdala and Emanuel Villegas, for their solidarity, affection and camaraderie. A special thanks to Dr. Sandra Ibañez, for teaching us with passion.

To my colleagues and Friends, Mauricio Toledo, Leonardo Bustamante, Victor Carcamo, Miguel Navarrete, Carlos Caro, Nicolas Zegpi, Juan Pablo Merello, Ignacio Arancibia, Sergio Gutierrez Pablo Tapia and Carlos Saldes.

To my family in Germany, Marti and Herb Muller Rossbach, Kenny Tam and Zenith Chan for their constant support, help and affection throughout the semester in Munich.

Last but not least, I would like to give a very special thanks to my family and friends in Chile, Edith Garrido, Luis Gonzales, Luis Perez, Felipe Perez, Eloy Peña, Vanessa Siqueira, Andres Vazques, who have accompanied me from a distance and have given me their unconditional support throughout this time.

GENERAL INDEX

Pág.

DEDICATORIA i

ACKNOWLEDGMENTS ii

GENERAL INDEX iii

LIST OF TABLES x

LIST OF FIGURES xiii

LIST OF GRAPHS xviii

ABSTRACT xix

RESUMEN xxi

I. INTRODUCTION 1
- 1.1. Objectives 2
  - 1.1.1. General Objective 2
  - 1.1.2. Specific Objectives 2
- 1.2. Methodology 3

II. HISTORICAL EVOLUTION AND CONSTRUCTION METHODS OF TUNNELS IN SOILS 7
- 2.1. Traditional Methods 9
  - 2.1.1 English Method (Tamesis Tunnel, 1843) 9
  - 2.1.2 Belgian Method (Charleroi Tunnel, 1828) 11
  - 2.1.3 German Method (Black Forest Tunnel, 1830) 13
  - 2.1.4 Swiss Method (Lötschberg Tunnel, 1996) 15
  - 2.1.5 Austrian Classic Method (Gumpoldskirchen, 1839) 17
- 2.2. Modern Methods 19
  - 2.2.1 New Austrian Tunnel Method (NATM) 19

2.2.2 Tunnel Boring Machine (TBM) 21
2.3. Support and Lining of Tunnels 23
2.3.1 Support 23
2.3.2 Lining 24

III. CASE STUDY: URBAN TUNNELS IN THE METROPOLITAN REGION OF SANTIAGO DE CHILE 26
3.1. The Study Area 26
3.1.1 Location 26
3.1.2 Distribution of Population 27
3.1.3 Urban Transport 28
3.1.4 Projected Situation 29
3.2. Geology of Santiago de Chile 30
3.2.1 Gravel of Santiago 32
3.2.2 Fine of Santiago 33
3.2.3 Mixed of Santiago 34
3.3. Characteristics of the New Road Tunnels Projected 35
3.3.1 Geometry Road Tunnels 35
3.3.2 Structural Elements of the New Road Tunnels 36
3.3.3 Construction Sequence with the NATM (New Austrian Tunnel Method) 36
3.4. Pre-existing Situation with Metro Tunnel 38
3.4.1 Line of the Metro of Santiago 38
3.4.2 Geometric Section of the Metro Tunnel 39
3.4.3 Structural Elements of the Metro Tunnel 39
3.4.4 Location of Metro Tunnel on the Soil Profiles 41
3.5. Pre-existing Situation with Important Building 42
3.5.1 Structural Characteristics of Building 43
3.5.2 Location of Building on the Soil Profiles 44
3.6. Final Profiles with the Projected and Existing Situation 45
3.6.1 Final Profiles considering the Pre-existing Metro Tunnel 45
3.6.2 Final Profiles considering the Pre-existing Building 46
3.7. Limitations and Acceptance Criteria 47
3.7.1 On the Pre-existing Metro Tunnel 47
3.7.2 On the Pre-existing Building 48

3.7.3 On the New Road Tunnels 52
3.7.4 Verification of the Bearing Capacity of Soil 54

IV. NUMERICAL MODELLING 55
4.1. General Modeling Consideration 55
4.1.1 Model Dimensions 55
4.1.2 Boundary Conditions 56
4.1.3 Water Pressures 56
4.1.4 Surface Loads: Traffic Overload 57
4.1.5 Service Loads for tunnels 57
4.1.6 Finite Element Mesh 58
4.2. Soil Modeling Considerations 59
4.2.1 Constitutive Models 59
4.2.2 Soil Input Parameters for the models 59
4.2.3 Initial Conditions of Soil 62
4.3. Pre-existing Metro Tunnel Modeling Consideration 63
4.3.1 Geometry of the Pre-existing Metro Tunnel 63
4.3.2 Support Parameters of the Pre-existing Metro Tunnel 64
4.3.3 Lining Parameters of the Pre-existing Metro Tunnel 66
4.3.4 Backfill Parameters of the Pre-existing Metro Tunnel 67
4.3.5 Plate Slab of Road Parameters of the Pre-existing Metro Tunnel . 67
4.3.6 Relaxation Parameters of the Pre-existing Metro Tunnel 68
4.3.7 Sequence Construction of the Pre-existing Metro Tunnel 69
4.4. Pre-existing Building Modeling Consideration 73
4.4.1 Geometry of the Pre-existing Building 73
4.4.2 Load to be Applied 75
4.4.3 Structure and Foundation Input Parameters for the models 75
4.5. New Tunnels Modeling Consideration 77
4.5.1 Geometry of the New Tunnels 77
4.5.2 Support Parameters of the New Tunnels 78
4.5.3 Lining Parameters of the New Road Tunnels 81
4.5.4 Temporal Walls of New Tunnels 82
4.5.5 Backfill Parameters of the New Road Tunnels 82
4.5.6 Plate Slab of Road Parameters of the New Road Tunnels 82
4.5.7 Relaxation Parameters of the New Road Tunnels 83

4.5.8 Sequence Construction of the New Road Tunnels 87
4.6. Interfaces 94

V. ANALYSIS OF THE INFLUENCE OF THE NEW ROAD TUNNELS EXCAVATION ON THE PRE-EXISTING METRO TUNNEL 96
5.1. Variation of the Constitutive Soil Model with Plane Sole section in the new Tunnels 96
5.1.1 Summary of Structural Verifications 97
5.1.2 Comments on the Results 98
5.2. Variation of the Constitutive Soil Model with Counter-vault section in the new Tunnels for Mixed and Fine Soils 99
5.2.1 Summary of Structural Verifications 100
5.2.2 Comments on the Results 101
5.3. Variation of the Constitutive Soil Model with four Phases of Excavation of the New Road Tunnels for Fine Soil 102
5.3.1 Summary of Structural Verifications 104
5.3.2 Comments on the Results 105

VI. ANALYSIS OF THE INFLUENCE OF EXCAVATION OF THE NEW ROAD TUNNELS ON THE PRE-EXISTING BUILDING 106
6.1. Variation of the Constitutive Soil Model with Plane Sole section in the new Tunnels 106
6.1.1 Summary of Structural Verifications 108
6.1.2 Comments on the Results 108
6.2. Variation of the Constitutive Soil Model with Counter-vault in the new Tunnels for Mixed and Fine Soils 110
6.2.1 Summary of Structural Verifications 111
6.2.2 Comments on the Results 112
6.3. Variation of the Constitutive Soil Model with four Phases of Excavation of the New Road Tunnels for Fine Soil 113
6.3.1 Summary of Structural Verifications 114
6.3.2 Comments on the Results 114
6.4. Mitigation Measure in fine soil applying a Micropile Wall 115
6.4.1 Description of the Micropile Wall 115
6.4.2 Summary of Structural Verifications 116

6.4.3 Comments on the Results 117

VII. CONCLUSIONS 118
7.1. Future Lines of Investigation 120
7.2. Bibliography 121

I. ANNEX: REASONS FOR SOME NATM FAILURES (MULLER, 1978) 124
1.1. Failure to control the length of the advance ("step") 124
1.2. Waiting too long to close the section 124
1.3. Absence of section closure (counter-vault) 125
1.4. Degradation of the ground due to big deformations 125

II. ANNEX: CONSTITUTIVE MODELS OF SOILS AND STRUCTURAL ELEMENTS 127
2.1. Constitutive Models of Soils 127
2.1.1 Mohr Coulomb Model 127
2.1.2 Hardening Soil Model 130
2.1.3 Hardening Soil with Small Deformations Model 133
2.1.4 Comparison between Constitutive Models 137
2.2. Constitutive Models of Structural Elements 140
2.2.1 Volumetric Element: Concrete Model 140
2.2.2 Shell Element: Plate Element 144

III. ANNEX: STRUCTURAL VERIFICATION WITH PRE-EXISTING METRO TUNNEL 146
3.1. Variation of the Constitutive Soil Model with Plane Sole Section in New Tunnels 146
3.1.1 Verification of the Deformation in the Metro Tunnel 147
3.1.2 Verification of the Resistance in the Pre-existing Metro Tunnel considering Sole Plane section in the new tunnels. 171
3.1.3 Verification of the Deformation in the New Road Tunnels 181
3.1.4 Verification of the Resistance in the New Road Tunnels 187
3.1.5 Verification of the Capacity of the Soil 190
3.2. Variation of the Constitutive Soil Model with Counter-vault Section in two excavation phases in Mixed and Fine Soil 192
3.2.1 Verification of the Deformation in the Metro Tunnel (MT) 192

3.2.2 Verification of the Resistance in the Pre-existing Metro Tunnel considering Counter-vault section in the new tunnels. 209
3.2.3 Verification of the Deformation in the New Road Tunnels..... 216
3.2.4 Verification of the Resistance in the New Road Tunnels 218
3.2.5 Verification of the Capacity of the Soil 223
3.3. Variation of the Constitutive Soil Model with Counter-vault Section in four excavation phases in Fine Soil 226
3.3.1 Verification of the Deformation in the Metro Tunnel (MT)..... 226
3.3.2 Verification of the Resistance in the Pre-existing Metro Tunnel considering Counter-vault section in the new tunnels and four phases of excavation. 235
3.3.3 Verification of the Deformation in the New Road Tunnels..... 240
3.3.4 Verification of the Resistance in the New Road Tunnels 241
3.3.5 Verification of the Capacity of the Soil 244

IV. ANNEX: STRUCTURAL VERIFICATION WITH PRE-EXISTING BUILDING 246
4.1. Variation of the Constitutive Soil Model with Plane Sole Section in New Tunnels 246
4.1.1 Verification of the Deformation in the Pre-existing Building (B)246
4.1.2 Verification of the Deformation in the New Road Tunnels..... 267
4.1.3 Verification of the Resistance in the New Road Tunnels 269
4.1.4 Verification of the Capacity of the Soil 272
4.2. Variation of the Constitutive Soil Model with Counter-vault Section in two excavation phases in Mixed and Fine Soil 274
4.2.1 Verification of the Deformation in the Pre-existing Building (B)274
4.2.2 Verification of the Deformation in the New Road Tunnels..... 288
4.2.3 Verification of the Resistance in the New Road Tunnels 289
4.2.4 Verification of the Capacity of the Soil 292
4.3. Variation of the Constitutive Soil Model with Counter-vault Section in four excavation phases in Fine Soil 294
4.3.1 Verification of the Deformation in the Pre-existing Building (B)294
4.4. Variation of the Constitutive Soil Model with Counter-vault Section in four excavation phases in Fine Soil applying Mitigation measure. 301
4.4.1 Verification of the Deformation in the Pre-existing Building (B)301

4.4.2 Verification of the Deformation in the New Road Tunnels..... 308
4.4.3 Verification of the Resistance in the New Road Tunnels..... 309
4.4.4 Verification of the Capacity of the Soil..... 312

V. PLANS..... 314
5.1. Plan N°1: Pre-existing Metro Tunnel- Soil Profiles with Tunnels Excavated in Two phases with Plane Sole Section..... 314
5.2. Plan N°2: Pre-existing Metro Tunnel- Soil Profiles with Tunnels Excavated in Two phases with Counter-vault Section. 314
5.3. Plan N°3: Pre-existing Metro Tunnel- Soil Profiles with Tunnels Excavated in Four phases with Counter-vault Section. 314
5.4. Plan N°4: Pre-existing Building- Soil Profiles with Tunnels Excavated in Two phases with Plane Sole Section..... 314
5.5. Plan N°5: Pre-existing Building- Soil Profiles with Tunnels Excavated in Two phases with Counter-vault Section..... 314
5.6. Plan N°6: Pre-existing Building- Soil Profiles with Tunnels Excavated in Four phases with Counter-vault Section. 314
5.7. Plan N°7: Pre-existing Building- Soil Profiles with Tunnels Excavated in Four phases with Counter-vault Section applying Mitigation measure. 314

LIST OF TABLES

Table III-1: Classification of damage to buildings according to Burland et al (1977). [6] 49
Table IV-1: Geotechnical Properties of Gravel Profile- Model MC- Musante e Ingenieros (2019) [11].....59
Table IV-2: Geotechnical Properties of Mixed Profile - Model MC- Musante e Ingenieros (2019) [11].....60
Table IV-3: Geotechnical Properties of Fine Profile- Model MC- Musante e Ingenieros (2019) [11].....60
Table IV-4: Geotechnical Properties of Gravel Profile- Model HS- Pinto and Ledezma (2019) [12].....60
Table IV-5: Geotechnical Properties of Mixed Profile - Model HS- Pinto and Ledezma (2019) [12].....61
Table IV-6: Geotechnical Properties of Fine Profile- Model HS- Rafael Iglesias (2014) [4] 61
Table IV-7: Geotechnical Properties of Gravel Profile- Model HSs- Pinto and Ledezma (2019) [12].....62
Table IV-8: Geotechnical Properties of Mixed Profile - Model HSs- Pinto and Ledezma (2019) [12].....62
Table IV-9: Geotechnical Properties of Fine Profile- Model HSs- Rafael Iglesias (2014) [4].....62
Table IV-10: Geometry of Metro Tunnel to represent the section in the “tunnel designer module”.....63
Table IV-11: Parameters of the Concrete Model for Support of Metro Tunnel 65
Table IV-12: Parameters of the Plate Element for Vault Lining of Metro Tunnel 66
Table IV-13: Parameters of the Plate Element for Counter-vault Lining of Metro Tunnel.....67
Table IV-14: Parameters of the Elastic Model for Backfill of Metro Tunnel.....67

Table IV-15: Parameters of the Plate Element for Slab of Metro Tunnel.....68
Table IV-16: Parameters of the Plate Element for Structures of Walls and Slabs.....75
Table IV-17: Parameters of the Plate Element for Structures of Underground walls.76
Table IV-18: Parameters of the Volumetric Element for Superficial Foundation of Building in Gravel.....76
Table IV-19: Parameters of the Embedded bean row for Deep Foundation of Building in Mixed and Fine 76
Table IV-20: Geometry of New East Tunnel to represent the section in the "tunnel designer module".....77
Table IV-21: Geometry of New West Tunnel to represent the section in the "tunnel designer module".....77
Table IV-22: Parameters of the Concrete Model for Support of New Road Tunnels.78
Table IV-23: Parameters of the Plate Element for Lining of New Road Tunnels 81
Table IV-24:Parameters of the Plate Element for Slab of New Road Tunnels.....82
Table IV-25:Summary Relaxation adopted for New Road Tunnels 87
Table IV-26: Definition of Interfaces in the models 95
Table V-1: Summary of Checks on Metro Tunnel – Pre-existing Metro Tunnel – First Analysis 97
Table V-2:Summary of Checks on New Tunnels – Pre-existing Metro Tunnel - First Analysis 97
Table V-3: Summary of Checks on Soil – Pre-existing Metro Tunnel – First Analysis 98
Table V-4: Summary of Checks on Metro Tunnel – Pre-existing Metro Tunnel – Second Analysis 100
Table V-5: Summary of Checks on New Tunnels – Pre-existing Metro Tunnel – Second Analysis 100
Table V-6: Summary of Checks on Soil – Pre-existing Metro Tunnel – Second Analysis 100
Table V-7: Summary of Checks on Metro Tunnel – Pr-eexisting Metro Tunnel – Third Analysis 104

Table V-8: Summary of Checks on New Tunnels– Pre-existing Metro Tunnel – Third Analysis 104
Table V-9: Summary of Checks on Soil – Pre-existing Metro Tunnel – Third Analysis 104
Table VI-1: Summary of Checks on Building – Pre-existing Building- First Analysis 108
Table VI-2:Summary of Checks on New Tunnels – Pre-existing Building- First Analysis 108
Table VI-3: Summary of Checks on Soil – Pre-existing Building – First Analysis .108
Table VI-4: Summary of Checks on Building – Pre-existing Building- Second Analysis 111
Table VI-5: Summary of Checks on New Tunnels – Pre-existing Building – Second Analysis 111
Table VI-6: Summary of Checks on Soil – Pre-existing Building – Second Analysis 111
Table VI-7: Summary of Checks on Building – Pre-existing Building – Third Analysis 114
Table VI-8: Parameters of the Embedded bean row for Micropile Wall in Fine Soil 115
Table VI-9: Summary of Checks on Building – Pre-existing Building – Fourth Analysis 116
Table VI-10: Summary of Checks on New Tunnels – Pre-existing Building – Fourth Analysis 116
Table VI-11: Summary of Checks on Soil – Pre-existing Building – Fourth Analysis 117

LIST OF FIGURES

Figure I-1: Work Organization (Chart II-III-IV).....5
Figure I-2: Work Organization (Chart V-VI)- Part 1.....5
Figure I-3: Work Organization (Chart V-VI)- Part 2.....6
Figure I-4: Work Organization (Chart V-VI)- Part 3.....6
Figure II-1: Historical Evolution of Tunnels (CTES [2]).....8
Figure II-2: Historical Evolution of Tunneling Methods (CTES [2]).....8
Figure II-3: Excavation with English Method (Soto Saavedra, P.S., 2004 [3]).....9
Figure II-4: Tamesis Tunnel with English Excavation Method, 1843.....10
Figure II-5: Excavation with Belgian Method (Soto Saavedra, P.S., 2004 [3]).....11
Figure II-6: Model Belgian Method (TUM Laboratory).....12
Figure II-7: Excavation with German Method (Soto Saavedra, P.S., 2004 [3]).....13
Figure II-8: Buenos Aires Subway Line E Tunnel, 1943 (AATES [1]).....14
Figure II-9: Excavation with Swiss Method (Soto Saavedra, P.S., 2004 [3]).....15
Figure II-10: Bernold Plates of Swiss Method.....16
Figure II-11: Excavation with Austrian Method (Soto Saavedra, P.S., 2004 [3]).....17
Figure II-12: Model Classic Austrian Method (TUM Laboratory).....18
Figure II-13: Characteristic curve of the ground and support. NATM Concept.....20
Figure II-14: Carmel Tunnel (left) and Sao Paulo Metro (right) Subsidence.....20
Figure II-15: Gripper TBM.....21
Figure II-16: Shield TBM in the La Fabrique du metro- Paris, France.....22
Figure II-17: Support with Shotcrete, construction of the Kramer Tunnel.....23
Figure II-18: Reticulate Steel Frame, construction of the Kramer Tunnel.....24
Figure II-19: Lining with Molded Concrete, construction of the Kramer Tunnel.....25
Figure II-20: Lining with Prefabricated Segments, construction of.....25
Figure III-1: Population of Santiago from 1820 to 2020. (from Wikipedia).....27
Figure III-2: Map of Santiago depicting main streets. (from Wikipedia).....28

Figure III-3: Proposed Road Tunnels underneath the Metro Tunnel (José Miguel Galera, 2020 [5]) 29
Figure III-4: Proposed Road Tunnels underneath the Building (José Miguel Galera, 2020 [5]) 29
Figure III-5: Geology of the city of Santiago [16] 30
Figure III-6: Satellite Image of Santiago de Chile city. (Web) 31
Figure III-7: Gravel Profile 32
Figure III-8: Fine Profile 33
Figure III-9: Mixed Profile 34
Figure III-10: Section Geometry of three way with Plane Sole (superior) and Counter-vault section (inferior) 35
Figure III-11: Construction Sequence- Two Phases of Excavation- Section with plane sole 37
Figure III-12: Excavation Section with plane sole- Corte A-A and Corte B- B 37
Figure III-13: Map of Metro of Santiago de Chile 38
Figure III-14: Typical Section of Metro Tunnel (Rafael Iglesias, 2014 [4]) 39
Figure III-15: Reinforcement in Lining with ACMA mesh of Typical Section of Metro Tunnel (Rafael Iglesias, 2014 [4]) 40
Figure III-16: Location of Metro Tunnel on the Gravel (superior), Mixed (center) ...41
Figure III-17: Typical Building in the city of Santiago de Chile (Illustrative Image of Google Earth) 42
Figure III-18: Building Structure in Gravel Profile 43
Figure III-19: Building Structure in Mixed and Fine Profile 43
Figure III-20: Location of Building 44
Figure III-21: Final Situation of Gravel (superior), Mixed (center) and Fine (inferior) Profiles 45
Figure III-22: Final Situation of Gravel (superior), Mixed (center) and Fine (inferior) Profiles 46
Figure III-23: AASHTO standard axial-moment interaction diagram [7] 47
Figure III-24: Representation of the Boscardin and Cording damage criterion. [6] ...50

Figure III-25: Definition of damage verification parameters in Building (β, ε) [6]....50
Figure III-26: Equivalent Beam Model [6] 51
Figure III-27: Relationship between category of damage and limiting tensile strain (after Boscardin and Cording, 1989 [6]) 51
Figure III-28: Plastification Criteria....54
Figure IV-1: Numerical Model Dimensions [m]....55
Figure IV-2: Boundary Conditions of the Models 56
Figure IV-3: Water Table in the Models....56
Figure IV-4: Type Vehicle for design 57
Figure IV-5: Traffic overload in the models 57
Figure IV-6: Service Loads for Metro Tunnel 57
Figure IV-7: Service Loads applied in Metro Tunnel and New Road Tunnels in the models 57
Figure IV-8: Coarseness factor for the definition of the mesh....58
Figure IV-9: Finite Element Mesh 58
Figure IV-10: Magnitude and orientation of initial stresses 63
Figure IV-11: Draw of the Metro Tunnel in “Tunnel Designer Module”....64
Figure IV-12: Schematic representation of the β-method for the analysis of NATM tunnels (Plaxis V24 Manual [19]) 69
Figure IV-13: Phase 1- Definition the Initial Stress State (left) and Phase 2- Activation of Traffic Overload (right) 70
Figure IV-14: Phase 3- Excavation of Metro Tunnel in Full Section 70
Figure IV-15: Phase 4- Interface and Support activated 71
Figure IV-16: Phase 5- Interface and Lining activated and 71
Figure IV-17: Definition of degraded soil area of the Metro Tunnel....72
Figure IV-18: Phase 7- Degradation of Support of the Metro Tunnel 72
Figure IV-19: Phase 8- Degradation of Soil around of the Metro Tunnel 73
Figure IV-20: Building Modeling for Gravel (Left), Mixed (Center) and Fine (Right). 73

Figure IV-21: Modeling of the Superficial Foundation of the Building, for Gravel only 74
Figure IV-22: Modeling of the deep Foundation of the Building, for Mixed and Fine 74
Figure IV-23: Modeling of the Building Loads 75
Figure IV-24: Draw of the New East and West Tunnels in “Tunnel Designer Module” 77
Figure IV-25: Graph of Vlanchopuolus & Diederichs.....84
Figure IV-26: Phase 9 and Phase 10- Excavation and Installation of support of Phase I of the West Road Tunnel 87
Figure IV-27: Phase 11 and Phase 12- Excavation and Installation of support of Phase II of the West Road Tunnel.....88
Figure IV-28: Phase 13-Demolition Temporal Wall of the West RoadTunnel 88
Figure IV-29: Phase 14- Excavation and Installation Support of Phase I of the East Road Tunnel.....89
Figure IV-30: Phase 15- Excavation and Installation Support of Phase II of the East Road Tunnel.....89
Figure IV-31: Phase 16 - Demolition Temporal Wall of the East Road Tunnel.....90
Figure IV-32: Phase 17- Installation of the Lining in the both New Road Tunnels ...90
Figure IV-33: Definition Degradation Area for New Road Tunnels 91
Figure IV-34: Phase 18- Application of the Service Loads 92
Figure IV-35: Phase 19- Degradation of the Support of the new road Tunnels.....93
Figure IV-36: Phase 20- Degradation of the Soil of the new road Tunnels.....93
Figure V-1: Gravel (superior), Mixed (center), Fine (inferior) Profiles with Sole Plane Section.....97
Figure V-2: Final Profile for Gravel Excavation with preexisting Metro Tunnel 98
Figure V-3: Mixed (superior) and Fine (inferior) Profiles Model with Counter-vault Section in.....99
Figure V-4: Final Profile for Mixed Excavation with pre-existing Metro Tunnel....101
Figure V-5: Excavation Section in Multiple Phases (4 Phases).....102

Figure V-6. Multi-phase Excavation Methodology 103
Figure V-7: Fine Profile Model with Counter-vault Section Excavated in four Phases in New Tunnels and Pre-existing Metro Tunnel 103
Figure V-8: Final Profile for Fine Excavation with pre-existing Metro Tunnel.....105
Figure VI-1: Gravel (superior), Mixed (center) and Fine (inferior) Profiles with Sole Plane Section in the New Tunnels and Building.....107
Figure VI-2: Final Profile for Gravel Excavation with pre-existing Building.....109
Figure VI-3: Mixed (superior) and Fine (inferior) Profile Model with Counter-vault Section.....110
Figure VI-4: Final Profile for Mixed Excavation with pre-existing Building 112
Figure VI-5: Excavation Section in Multiple Phases (4 Phases) 113
Figure VI-6: Fine Profile Model with Counter-vault Section Excavated in four Phases in New Tunnels and Pre-existing Building 113
Figure VI-7: Fine Profile Model with Counter-vault Section Excavated in four Phases in New Tunnels and Pre-existing Building, applying mitigation measure. 116
Figure VI-8: Final Profile for Fine Excavation with pre-existing Building.....117

LIST OF GRAPHS

Graph IV-1: Law of variation of compressive strength (f´c) with time (t) 80
Graph IV-2: Law of variation of Young´s module (Ec) with time (t).....81
Graph IV-3: Convergence – Confinement Curve of Gravel Profile 85
Graph IV-4: Convergence – Confinement Curve of Mixed Profile.....86
Graph IV-5: Convergence – Confinement Curve of Fine Profile 86

ABSTRACT

Large engineering projects increasingly require advanced field investigations, materials, designs and calculations, with a growing degree of sophistication and detail. This demand is being met by the development of methods, techniques, technologies and software that complement traditional engineering tools for such works.

In the field of geotechnical engineering in particular, the use of modern calculation tools has allowed substantial progress to be made in describing the behaviour of soils and rocks in their interaction with structures and stresses. The use of numerical methods such as the finite element method, and the development of specific constitutive models for soils and rocks, allow increasingly accurate estimates of stresses, deformations and settlements to be obtained.

One of the most complex challenges of these projects is the impact on pre-existing works, which generally occurs in urban areas. Tunnel construction projects of any kind in populated areas in particular generate great challenges for civil engineering. In addition to the complexity of the construction processes, the lack of space and logistical difficulties, the impact on pre-existing structures (old and modern buildings, other tunnels, service installations, etc.) must be controlled and limited according to their degree of sensitivity to ground movements. This last demand requires an adequate knowledge and modelling of the characteristics of the geotechnical profiles.

In the present thesis work, the influence on pre-existing structures of the excavation of two road tunnels in the Metropolitan Region of Santiago de Chile is analysed. This is a densely populated area of the Chilean capital, characterised by the presence of an important underground metro network, a large number of high-rise buildings and very diverse ground conditions, with gravelly, mixed and fine soils in the northern, central and southern sectors of the region respectively. Advanced finite element software was used to model the geometric domain of the problem for typical 2D sections in three different soil profiles. Three constitutive models were used to represent the mechanical behaviour of the soils with an increasing degree of detail: Mohr-Coulomb, Hardening Soil and Hardening Soil Small. The geotechnical parameters of the models were obtained from available reports of a comprehensive geotechnical survey campaign. The models included the pre-existing structures, as well as the construction and long-term stages of the newly constructed tunnels and all soil-structure interactions between them.

The model also took into account the stages of the conventional excavation method known as the New Austrian Tunnelling Method (NATM). The simulations made it possible to evaluate the cumulative effects of the excavation of these two tunnels on the ground and nearby structures. The case of a tunnel in the Metro network was analysed separately from the case of a typical reinforced concrete building in the city. Different project designs were studied: tunnel sections with and without counter-vault, and construction procedures with two or four excavation stages. Structural and serviceability acceptance criteria were applied to evaluate different designs. Finally, mitigation measures were evaluated in order to meet the acceptance criteria. The results obtained allowed conclusions to be drawn on the influence of the different design and material characterisation topics on the impact of the new project on the terrain and pre-existing structures.

RESUMEN

Los grandes proyectos de ingeniería requieren cada vez más investigaciones de campo, materiales, diseños y cálculos avanzados, con un grado de sofisticación y detalle crecientes. Esta demanda viene siendo atendida mediante el desarrollo de métodos, técnicas, tecnologías y software que complementan a las herramientas tradicionales de la ingeniería para encarar ese tipo de obras.

En el campo de la geotecnia en particular, el uso de herramientas modernas de cálculo ha permitido avanzar sustancialmente en la descripción del comportamiento de suelos y rocas en su interacción con las estructuras y las solicitaciones. El empleo de métodos numéricos como el método de los elementos finitos, y el desarrollo de modelos constitutivos específicos para suelos y rocas, permite obtener estimaciones cada vez mas ajustadas de las tensiones, deformaciones y asientos desarrollados.

Uno de los desafíos mas complejos de estos proyectos lo constituye la afectación de obras preexistentes, lo que se da generalmente en ámbitos urbanos. En especial los proyectos de ejecución de túneles de cualquier tipo en zonas pobladas generan grandes desafíos para la ingeniería civil. Sumado a la complejidad de los procesos constructivos, la falta de espacio y dificultades de logística, se debe controlar y acotar la afectación de las estructuras preexistentes según su grado de sensibilidad a los movimientos del terreno (edificios antiguos y modernos, otros túneles, instalaciones de servicios, etc.). Esta última demanda requiere de un conocimiento y modelado adecuado de las características de los perfiles geotécnicos.

En el presente trabajo de tesis se analiza la influencia sobre estructuras preexistentes de la excavación de dos túneles viales en la Región metropolitana de Santiago de Chile. Se trata de un área densamente poblada de la capital chilena, caracterizada por la presencia de una importante red de Metro subterráneo, un gran número de edificaciones de gran altura y condiciones del terreno muy diversas, con presencia de suelos gravosos, mixtos y finos en los sectores norte, centro y sur de la región respectivamente. Para ello se utilizó software de elementos finitos avanzado, para modelar el dominio geométrico del problema para secciones típicas 2D en tres diferentes perfiles de suelo. Se emplearon tres modelos constitutivos para representar el comportamiento mecánico de los suelos con un grado de detalle creciente: Mohr-Coulomb, Hardening Soil y Hardening Soil Small. Los parámetros geotécnicos de los mismos fueron obtenidos de los informes disponibles de una campaña completa de estudios geotécnicos. Los modelos incluyeron las estructuras preexistentes, así como las etapas constructivas y de largo plazo de los nuevos túneles ejecutados y todas las interacciones suelo-estructura entre ellos.

El modelo contempló a su vez las etapas del método de excavación convencional denominado Nuevo Método Austriaco (NATM). Las simulaciones permitieron evaluar los efectos acumulados de la excavación de estos dos túneles en el terreno y en las estructuras cercanas. Se analizó separadamente el caso de un túnel de la red de Metro, y el caso de un edificio de hormigón armado típico de la ciudad. Se estudiaron distintos diseños de proyecto: secciones de túnel con y sin contra bóveda, y procedimientos constructivos con dos o cuatro etapas de excavación. Se aplicaron criterios de aceptación estructurales y de servicio para evaluar diferentes diseños. Finalmente se evaluaron medidas de mitigación a fin de atender los criterios de aceptación. Los resultados obtenidos permitieron obtener conclusiones sobre la influencia de los distintos tópicos de diseño y de caracterización de los materiales en la afectación del nuevo proyecto al terreno y a las estructuras preexistentes

I. INTRODUCTION

In a world of ever larger cities, urban space is becoming increasingly valuable, making the construction of urban subway projects economically viable. Among these engineering project, urban tunnels allow us to materialize infrastructure and transportation lines, optimizing the operation of large cities. Additionally, transportation times are reduced for both people and goods, as well as environmental impacts such as noise and climate change gas emissions, contributing to greater sustainability and quality of life.

The design and execution of tunnels involves a complexity of phenomena that includes the structural behavior of the tunnel and especially its interaction with the ground. Tunnel construction modify the tensional equilibrium of the ground around them, and can affect the stability of other structures. This requires extensive ground investigation for the elaboration of representative geotechnical profiles and the estimation of parameters of the materials, soils or rocks, with the highest degree of reliability.

With these structure and ground data, it is possible to perform computational modeling to obtain estimates of stresses and strain fields. With these tools, it is also possible to evaluate the impact on nearby structures already existing in the urban environment, both above and below ground, which should be avoided or minimized in all cases.

The present thesis proposes to study by numerical modeling the impact of urban tunnels executed in soils on pre-existing structures. Specifically, it is proposed to evaluate the incidence, in terms of stresses, deformations or settlements, of some geotechnical, geometric, and constructive parameters. For this purpose, the execution of tunnels for communication roads in the Metropolitan Region of Santiago de Chile is adopted as a case study.

1.1. Objectives

1.1.1. General Objective

To investigate the influence of tunnel construction in soils on nearby pre-existing structures, considering different geotechnical and construction hypotheses.

1.1.2. Specific Objectives

- To describe the different excavation methods, traditional (Belgian, Swiss, German, English, etc.) and modern (NATM and TBM).

- To evaluate the performance of the New Austrian Method (NATM) by revision of some historic examples.

- To make a numerical modeling of tunnels excavation with the New Austrian Method (NATM) using 2d finite element analysis.

- To Apply and compare different constitutive soil models for three different typologies (gravel, mixed, fine).

- To evaluate the effect of some design hypotheses, such as the geometry of tunnels, as well as the construction methodology used (construction sequences and phases) on pre-existing Metro Tunnel and important Building separately.

- To Analyze the efficiency the mitigation measures (micropile walls, soil improvement, compensation injections, soil freezing, etc.) to minimize impact on pre-existing structures. The most appropriate option is chosen according to the situation obtained from each analysis.

1.2. Methodology

In compliance with the objectives of this work, the following methodology is proposed:

Initially, a general review of the historical evolution in the construction of tunnels in soils and the most widespread traditional and modern excavation methods is given to contextualize the present use of NATM (Chapter II).

Next, the case study corresponding to the Metropolitan Region of Santiago de Chile and the geological and geotechnical framework is presented. In this region, the excavation of two 3-lane roads tunnels has been projected under an existing Metro line and with a very marked development of urbanization and building in the area and acceptance criteria is also established, where the limits of deformations and stresses considered acceptable for a good design of the excavations are fixed. (Chapter III).

Based on the proposal of three geotechnical profiles representative of the study region: a) with gravel soils, b) with fine soils and c) with gravel and fine soils (mixed), three numerical models are presented, one for each geotechnical profile, using the commercial software Plaxis, in its 2D version. (Chapter IV).

Subsequently, stress-strain analyses including the construction stages of the tunnels (short term) and in service (long term) are performed using the new Austrian method of excavation in two advance stages and their impact on a pre-existing Metro Tunnel on the one hand and on an important building on the other hand are studied (Chapters V and VI).

For each of these pre-existing structures studied separately (tunnel and building), variations of the basic design and construction hypotheses are analyzed:

- Constitutive soil model for soils: The Mohr- Coulomb, Hardening Soil and Hardening Soil with small deformations Models are employed.

- Variation of the Geometry of the New Road Tunnels to be excavated: an ovoid section with several radius of circle with plane slab sole is used, and another section where a counter vault is introduced.

- Variation the sequence and number of excavation phases of the New Austrian Method. Initially it is excavated in two phases, but the increase and sequence of excavation in 4 phases is studied.

- Mitigation measure: according to the results obtained in the previous analysis, some mitigation measures are proposed in order to reduce the deformations of the ground.

Results sought: a) impact on the soils around the excavated tunnels (stresses and strains), b) impact on the pre-existing tunnel (stresses and strains), c) impact on the pre-existing building (settlements) and d) bearing capacity of the soil. For all the analyses, an admissibility criterion is established.

After completing all the analyses described above, the results are studied and comparisons are made to arrive at the final conclusions of this thesis (Chapters VII).

The flow charts in Figure I-1, Figure I-2, Figure I-3 and Figure I-4 shows the details of the process described above.

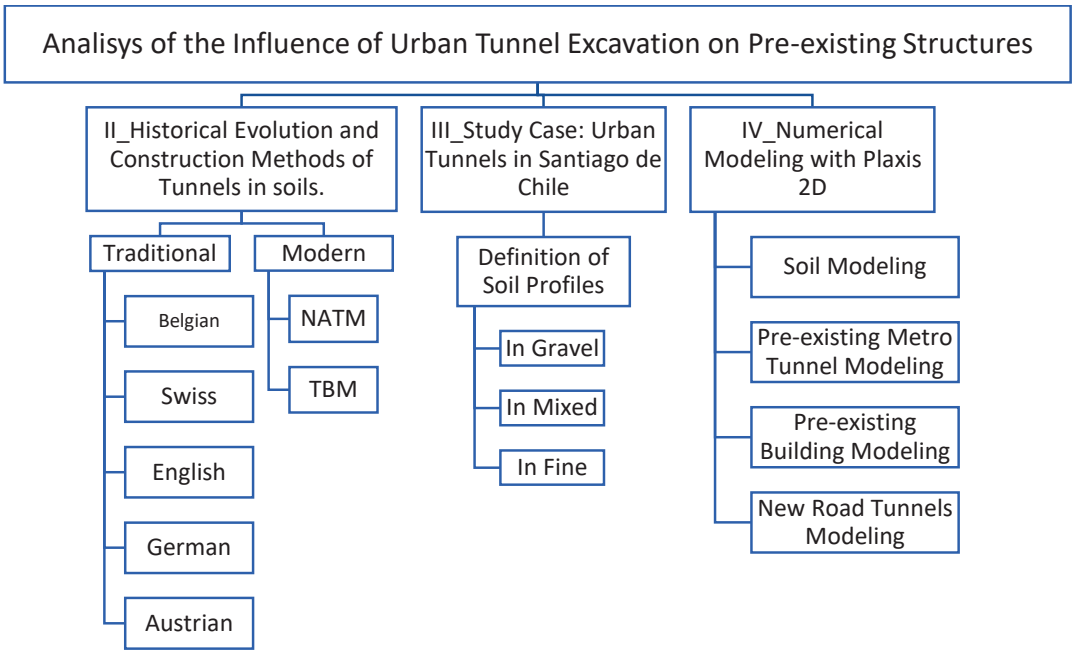


Figure I-1: Work Organization (Chart II-III-IV)

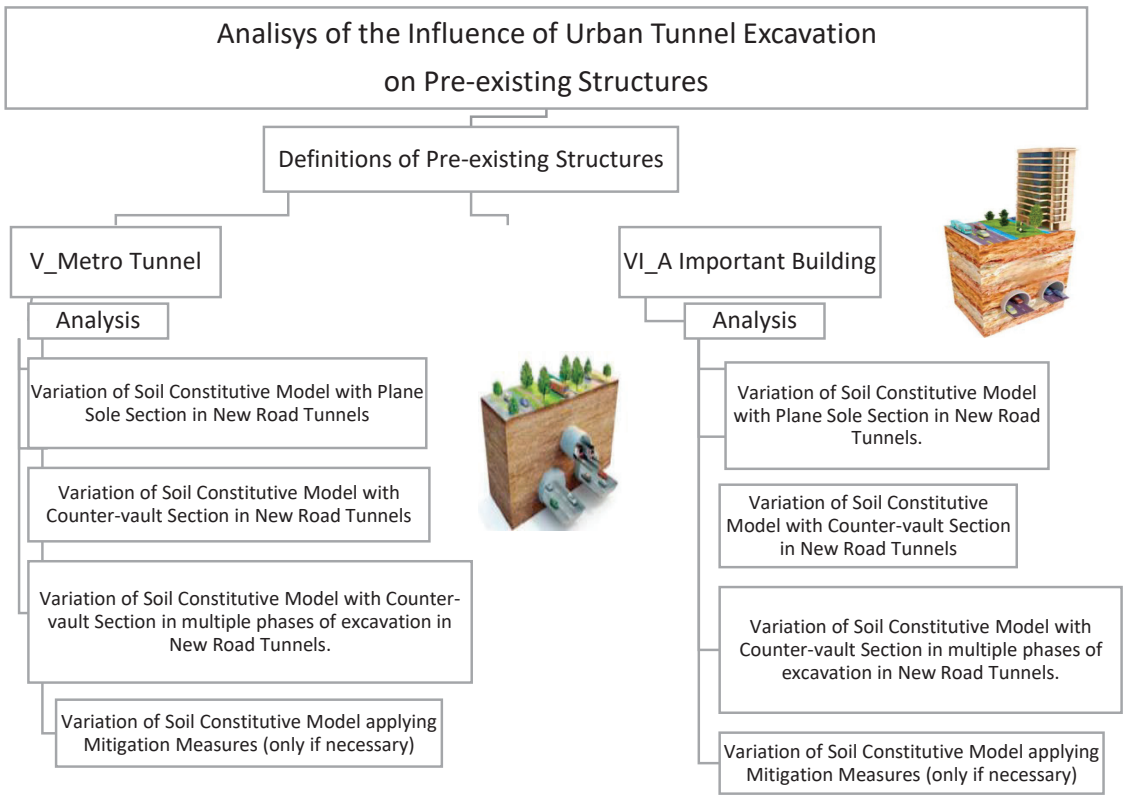


Figure I-2: Work Organization (Chart V-VI)- Part 1

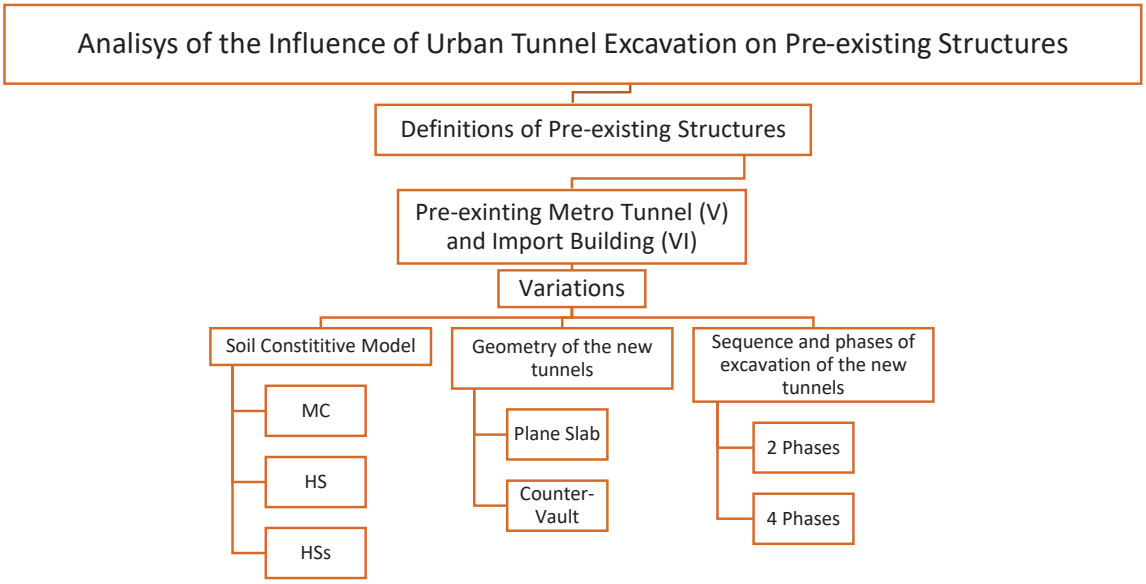


Figure I-3: Work Organization (Chart V-VI)- Part 2

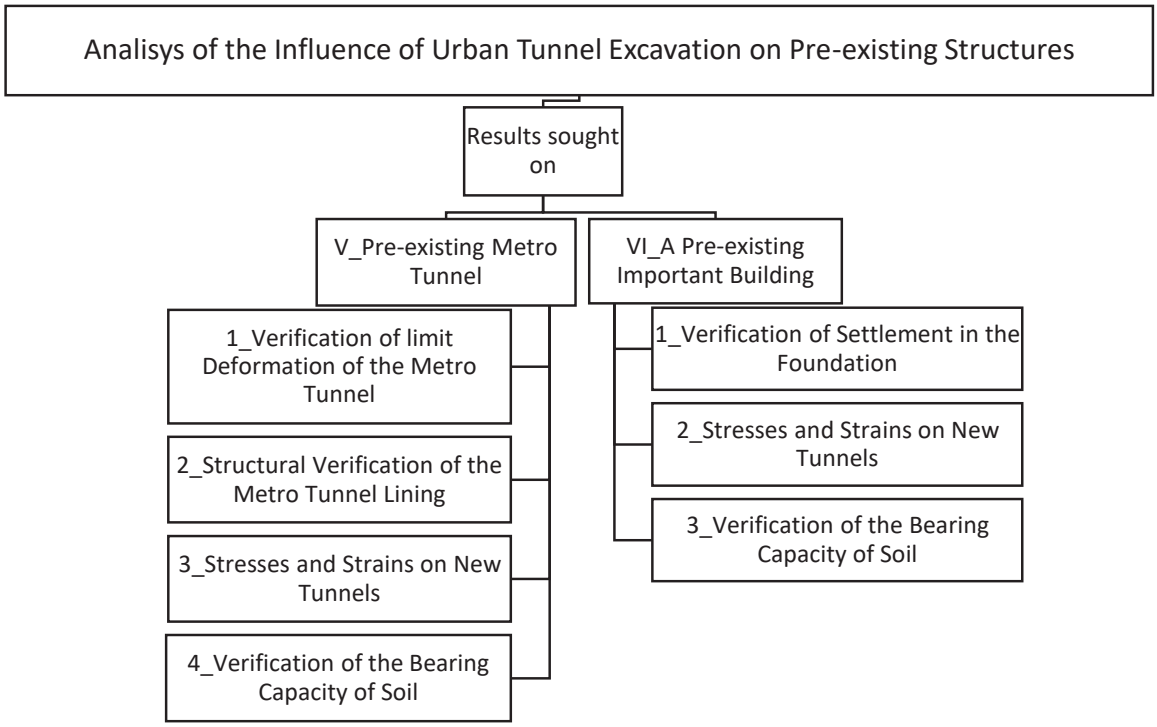


Figure I-4: Work Organization (Chart V-VI)- Part 3

II. HISTORICAL EVOLUTION AND CONSTRUCTION METHODS OF TUNNELS IN SOILS

In olden times, the first known tunnels were built by the ancient Egyptians and Mesopotamians for irrigation and drainage systems. In addition, the Romans perfected the construction of tunnels for aqueducts and subway roads, using advanced techniques such as the use of arches and vaults. During the Middle Ages, tunnel construction was mainly used for mining and military fortifications. Medieval miners developed manual excavation techniques and the use of rudimentary explosives.

In the Renaissance and 18th century, tunneling techniques were improved, especially in Italy and France, where tunnels were built for canals and roads. The Canal du Midi tunnel in France is a notable example. In the Industrial Revolution, the invention of gunpowder and the development of heavy machinery allowed the construction of longer and deeper tunnels. The Standedge Tunnel in England, completed in 1811, is a prime example.

In the 19th century, the expansion of railroads spurred the construction of tunnels all over the world. The Mont Cenis tunnel in the Alps, completed in 1871, was one of the first important railway tunnels. Subsequently, underwater tunnels began to be built, such as the Thames Tunnel in London, completed in 1843, which was the first tunnel under a navigable river.

In the 20th century, the construction of road tunnels became common, with notable examples such as the Mont Blanc tunnel between France and Italy, inaugurated in 1965. Cities also began to build underground subway systems, such as the New York subway (1904), the London subway (1863) and Buenos Aires sudway (1913).

In the 21st century, modern technology has enabled the construction of longer and more complex tunnels, such as the Channel Tunnel (1994) and the Gotthard Base Tunnel in Switzerland (2016), the longest railway tunnel in the world.

The summary evolution of tunnel engineering throughout history is presented below.

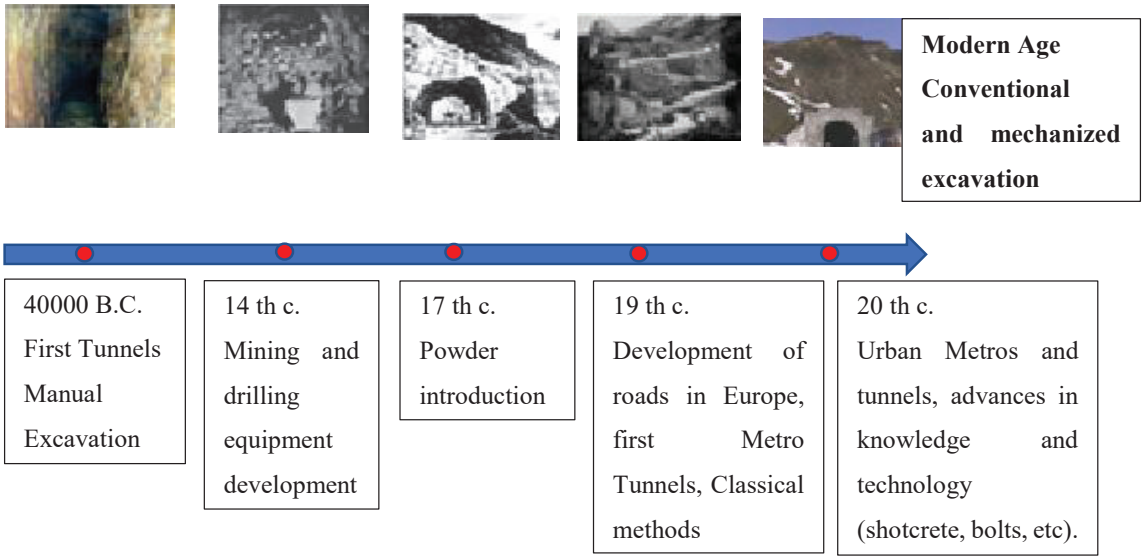


Figure II-1: Historical Evolution of Tunnels (CTES [2])

The historical evolution of tunnel excavation methods is presented below

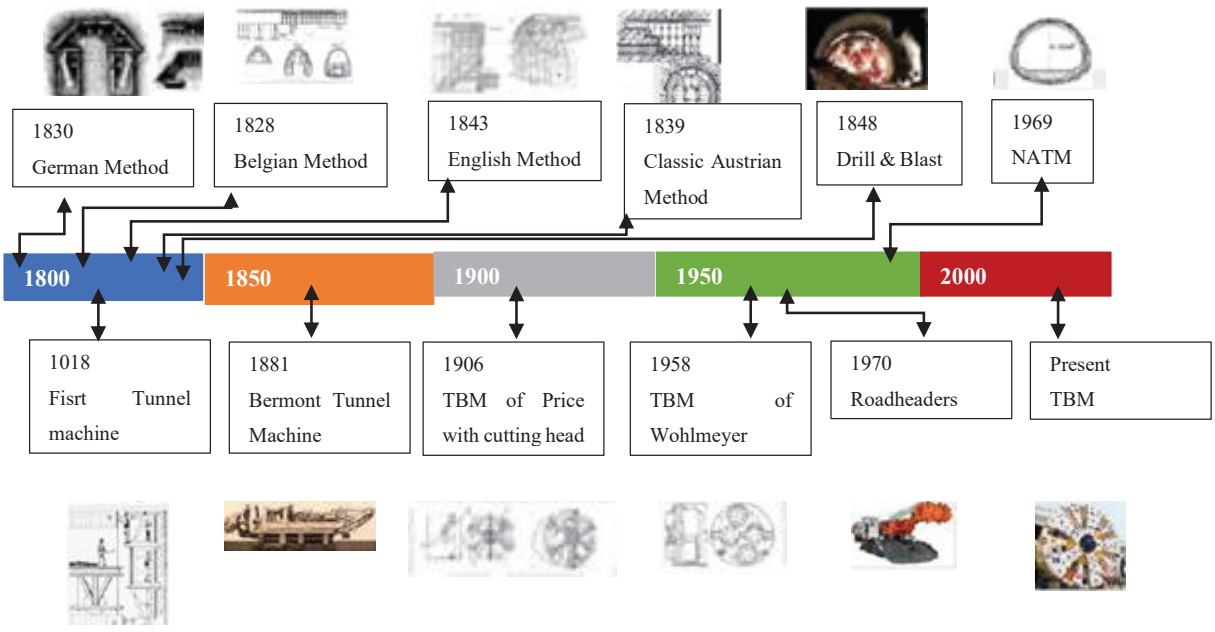


Figure II-2: Historical Evolution of Tunneling Methods (CTES [2])

2.1. Traditional Methods

The traditional methods most used in history for tunnel construction in soils will be described below.

2.1.1 English Method (Tamesis Tunnel, 1843)

The English Method, also known as the Full Section Attack Method, is a technique used in tunnel construction. This method is usually used for small section tunnels (less than 15 m^2), or in very good soil in larger sections, and of course in rock.

A solution for lower quality soils is to use the attack at full section but with several attack steps. The excavation is carried out in horizontal strips starting with the vault, with the disadvantage that the evacuation of the material requires several actions until reaching the level where the transport system to the outside is installed.

The excavation process by this system can be seen in Figure II-3.

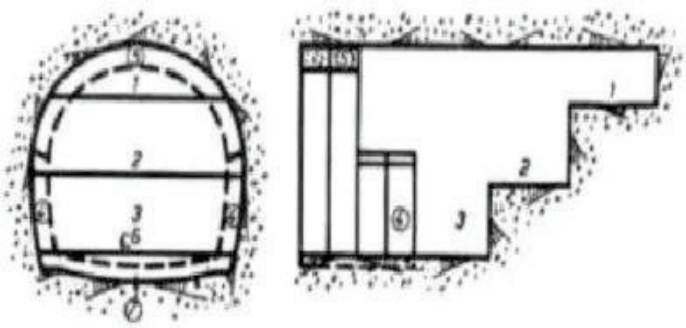


Figure II-3: Excavation with English Method (Soto Saavedra, P.S., 2004 [3])

https://www.youtube.com/watch?v=zV6iXvAjaeM

(a) Construction Phases

1. Excavation of the keystone area of tunnel.
2. Excavation of central destroy.
3. Excavation of inferior destroy.
4. Support of the gables.
5. Support of the keystone.
6. Excavation of the sole or counter-vault (only is necessary).
7. Concreting of the sole or counter-vault.

(b) Characteristics of the English Method

- In this method the area of advancement is very small and it is possible to correct any unforeseen event that may arise.
- It also has the advantage that the concrete is made in one go, avoiding joints and possible settlements.
- This method is more dangerous because the section is not concreted until the end of the excavation, so a failure can occur at any time.
- Therefore, this method requires small thrusts, since otherwise the shoring would be excessive.
- It is also necessary that the material has a minimum of cohesion, since otherwise it would be impossible to excavate the vault and the counter-vault.

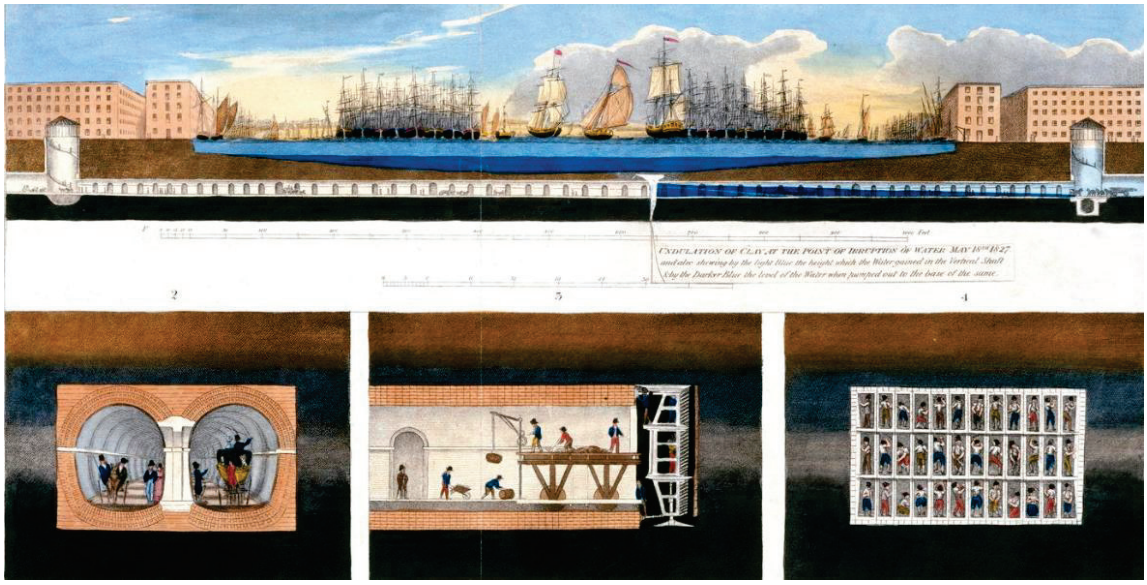


Figure II-4: Tamesis Tunnel with English Excavation Method, 1843

(www.worldhistory.org)

2.1.2 Belgian Method (Charleroi Tunnel, 1828)

The Belgian Method, also known as the Classical Madrid Method or the Keystone Gallery Method, is a technique used in tunnel construction.
Method of excavation of tunnels in soils that consists of excavating a gallery in the keystone and widening it little by little, protecting and support the front, until the entire vault can be concreted. The excavation process by this system can be seen in Figure II-5.

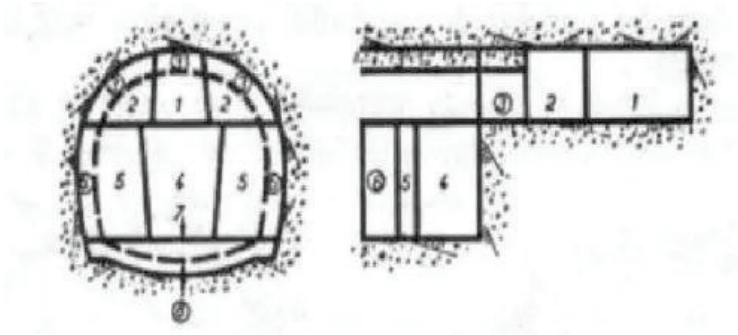


Figure II-5: Excavation with Belgian Method (Soto Saavedra, P.S., 2004 [3])

https://www.youtube.com/watch?v=uRZbKqM4TUs

https://www.youtube.com/watch?v=olE1S9qhtrQ

(a) Construction Phases

1. Excavation and support of the advance central keystone gallery.
2. Excavation of the vault.
3. Support of the vault.
4. Excavation in destroy of the central corridor.
5. Excavation of the lateral berms and construction of the gables.
6. Support of the gables.
7. Excavation of the sole or counter-vault (only if necessary).
8. Concreting of the sole or counter-vault.

(b) Characteristics of the Belgian Method

- The Belgian Method can be used whenever the ground is good enough to support the removal of part of the vault to carry out the staged construction of gables (not suitable for sandy ground with abundant water).
- Manual method that does not require advanced machinery or large investments.
- Progress of between 30 and 50 m/month depending on the quality of the ground (24 hours of work). Small performance.
- When removing the vault from the ground to build the gables, cracks or breakage of the vault may occur (large tunnel diameters or stations). This would lead to greater settlements. As an alternative, the German method is applied.
- Maximum safety for workers inside the tunnel, and for buildings and other elements on the ground surface.
- Minimized open face area of the tunnel at all times, being able to solve any instability problems that may occur.



Figure II-6: Model Belgian Method (TUM Laboratory)

2.1.3 German Method (Black Forest Tunnel, 1830)

The German Method, also known as the three galleries, it is used in sections larger than 50 m^2. It is characterized by the preservation of the structure until the support of the vault and the gables is completed.

The excavation process by this system can be seen in Figure II-7.

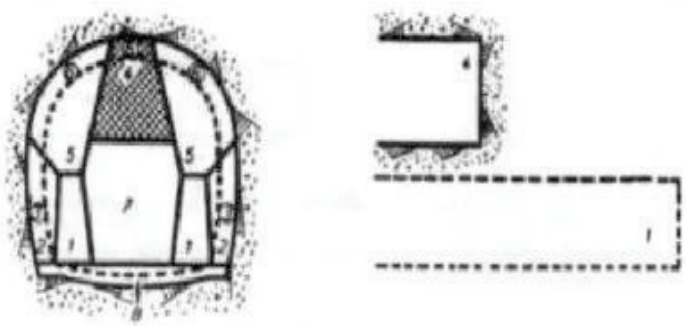


Figure II-7: Excavation with German Method (Soto Saavedra, P.S., 2004 [3])

https://www.youtube.com/watch?v=S0HA7avKQXw
https://www.youtube.com/watch?v=rRjaUpK8qnE

(a) Construction Phases

1. Excavation of two lateral galleries, to the right and left of the tunnel axis.
2. Expansion of the galleries.
3. Support of the gables.
4. Excavation of central keystone gallery.
5. Expansion of central gallery.
6. Support of the vault.
7. Excavation in destroy.
8. Excavation and concreting of the sole or counter-vault (only if necessary).

(b) Characteristics of the German Method

- Typically used for poor geotechnical conditions.
- A large tunnel section is preferable for applying this method, spans greater than 8 m.
- With this method, it is possible to react faster than with the Belgian method if water appears in loose soils or sandy layers.
- Reduces possible differential settlements that would produce cracks in the vault and settlements on the surface.



Figure II-8: Buenos Aires Subway Line E Tunnel, 1943 (AATES [1])

2.1.4 Swiss Method (Lötschberg Tunnel, 1996)

The Swiss Method, also known as the Bernold Method, is a technique used in tunnel construction. This method is one of the most widely used methods of advancing tunnels at full section. The excavation process by this system can be seen in Figure II-9.



Figure II-9: Excavation with Swiss Method (Soto Saavedra, P.S., 2004 [3]).

(a) Construction Phases

1. Full section excavation of the tunnel.
2. Installation of the steel frames.
3. Installation of the Bernold Plate.
4. The concreting behind the plate serves as a lost shuttering and reinforcement.

(b) Characteristics of the Swiss Method

- The Bernold system approximates the ideal case of excavation, which is to install the support just after the tunnel has been excavated, with the ground suffering small deformations.
- The Bernold system is a convenient way to install shotcrete in the presence of abundant water.
- This method is a valid option for ground of poor or very poor quality.

- The characteristic element of the Swiss Method are specially shaped and perforated plates (See Figure II-10), which can be installed to form a shuttering and reinforcement, leaving a distance equal to the thickness of the excavation to the surface.
- These plates, thanks to their special form, are on the one part rigid enough to absorb the pressure of the shuttering and, on the other part, sufficiently closed to prevent a plastic concrete consistency from escaping during the hardening process.
- The Bernold sheet system or Swiss Method provides two functions at the same time, that of metallic support and that of definitive covering of the soil.
- The vibrated concrete is introduced through the grooves of the sheet and together with the soil and the Bernold sheet, forming a homogeneous structure that allows a good load distribution.



Figure II-10: Bernold Plates of Swiss Method

(https://victoryepes.blogs.upv.es/2016/05/18/metodo-bernold-de-ejecucion-de-tuneles/)

2.1.5 Austrian Classic Method (Gumpoldskirchen, 1839)

The Austrian Method, also known as the two-gallery method, is characterized by the use of an advance gallery in the axis and base of the tunnel. An escape way is installed in it, which is used during the entire construction work.
The excavation process by this system can be seen in Figure II-11.

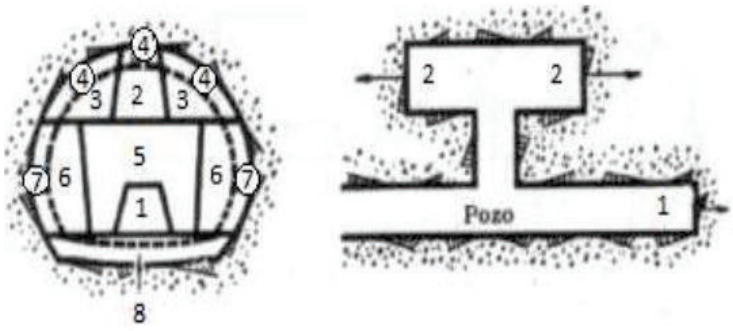


Figure II-11: Excavation with Austrian Method (Soto Saavedra, P.S., 2004 [3]).

(a) Construction Phases

1. Excavation of the central inferior gallery.
2. Excavation of the central superior gallery and connection shaft.
3. Excavation of the vault.
4. Support of the vault.
5. Excavation in destroy of the central corridor.
6. Excavation of the lateral berms and construction of the gables.
7. Support of the gables.
8. Excavation and concreting of the sole or counter-vault (only if necessary).

(b) Characteristics of the Austrian Classic Method

- When the inferior gallery has advanced a certain length, a shaft is drilled upwards and a second gallery is dug in both directions. Once the upper gallery has been drilled, it is followed as in the Belgian method.
- The lower gallery method can be used for the evacuation and elimination of debris and infiltration water, respectively.
- It is possible to have more than one excavation attack front, which speeds up tunnel construction.



Figure II-12: Model Classic Austrian Method (TUM Laboratory)

2.2. Modern Methods

The most commonly used modern methods today for tunnel construction in soils will be described below.

2.2.1 New Austrian Tunnel Method (NATM)

The New Austrian Method, known by the acronym NATM, is one of the most widely used and successful methods for designing and executing tunnels in rock and soil in the world within the field of civil engineering.

This method, also called "Advance and Destroy", was developed and patented by Rabcewickz, Müller and Pacher between 1948 and 1964, and was presented in Salzburg (Austria). The first urban application in soil was in the Frankfurt subway (1969), becoming generalized in the late 1980s and early 1990s.

In essence, NATM is based on five fundamental principles:

- It uses the ground itself as a resistant element against the local stress increases that occur during excavation.
- It uses the excavation methods that minimize damage to the ground, with protective umbrella before excavation.
- Continuous monitoring of deformations inside the excavation as a function of time, and comparison with the expected deformations according to soil classifications and geomechanical parameters determined by laboratory tests.
- Install flexible initial supports, protecting the ground from meteorizations, decompression and decohesion, etc., with the adequate speed, to prevent the start of damage.
- To install the definitive lining, if necessary, also flexible, minimizing bending moments, adding additional strength with trusses or bolts, but do not with rigid sections.

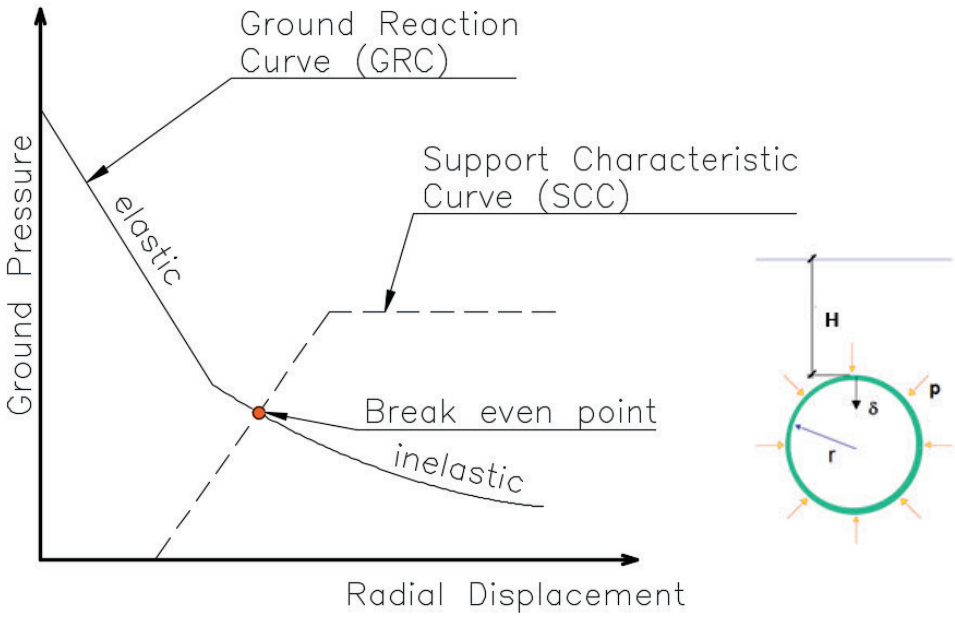


Figure II-13: Characteristic curve of the ground and support. NATM Concept

This rapid implementation of NATM sometimes led to poor design, poor execution and poor supervision, causing some collapses, for example the Carmel Tunnel in Barcelona, Madrid Metro, London Metro, Metro Munich, Sao Paulo, among other more. Some possible reasons for these collapses are discussed in greater detail in Appendix I.



Figure II-14: Carmel Tunnel (left) and Sao Paulo Metro (right) Subsidence

https://www.youtube.com/watch?v=y4pUgchcGcs

https://es.euronews.com/next/2022/02/01/brasil-metro-hundimiento

2.2.2 Tunnel Boring Machine (TBM)

In urban area, the tendency today is to carry out the construction of tunnels by means of tunnel boring machines, using traditional methods only occasionally, such as in the construction of connecting galleries between tunnels, access tunnels to stations and caverns. The use of tunnel boring machines is preferred to traditional methods mainly because the machines can ensure greater stability (especially of the face) and control of the excavation, especially in soft ground, on which cities are usually built.

The tunnel boring machines (TBM) existing today can be classified, in a general form, in two big groups:

- Machines for hard rock.
- Shields (machines for soft rocks and soils).

Hard rock TBMs are, in general, machines without total protection that excavate the face by means of their mechanical cutting elements, applying the rotation (torque) of the head and the longitudinal thrust obtained by reaction against the rock, against which they are supported by means of extensible arms called “grippers”. These machines are also known by the name of “topo” in Spanish or “mole” in English.

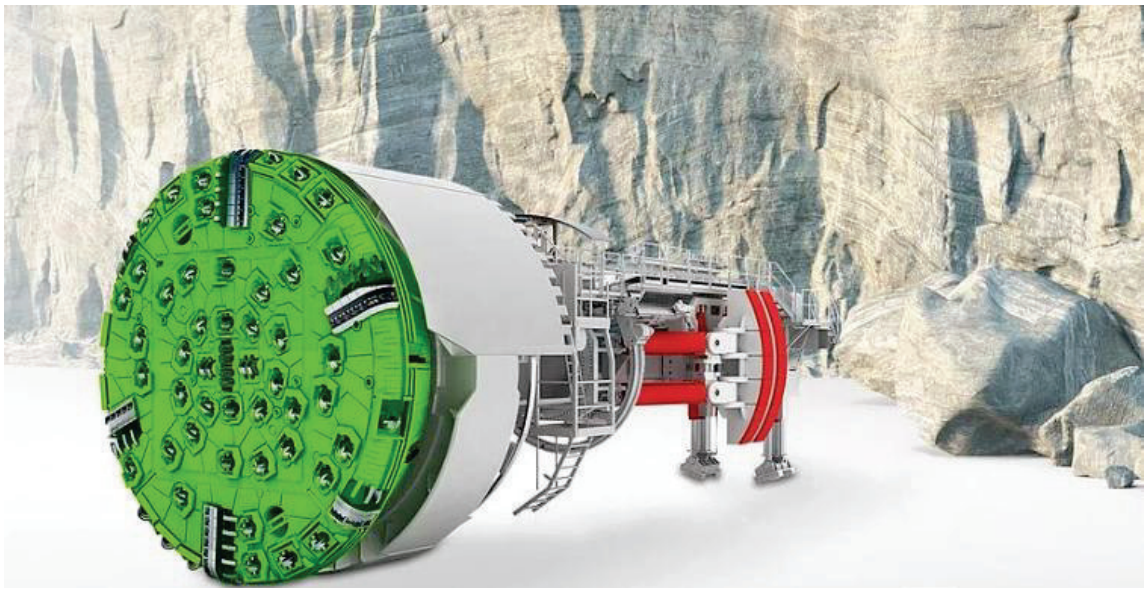


Figure II-15: Gripper TBM

https://www.herrenknecht.com/es/productos/productdetail/tuneladora-gripper/

In the case of the shield, the advance of the machine is achieved by pushing jacks against a rigid casing installed by the machine itself (generally precast concrete segments), since the grounds in which this type of machine is used are not sufficiently competent for the use of grippers. The shield is a machine that, unlike the hard rock TBM, incorporates an integral protection system. The main characteristic elements of shields are:

- The TBM itself is housed in a laminated steel structure or shell called shield. The mission of this shield is to guarantee the support and stability of the excavation in the excavated area still occupied by the machine.
- The machine is equipped with a robot in charge of the construction and installation of the lining rings, formed by concrete or metal segments. This lining completes the advance of the cycle by replacing the shield in its mission of supporting the walls of the excavation.
- The procedure described above allows these machines to work in highly unstable terrain, as the machine head guarantees the stability of the face, and the shield and the lining guarantee the stability of the excavation as the machine advances. They are therefore the ideal machines for working in an urban environment, as they guarantee the necessary safety conditions.



Figure II-16: Shield TBM in the La Fabrique du metro- Paris, France.

(Visit of UNCUYO students with the TUM in the great civil engineering excursion, 2023)

https://www.grandparisexpress.fr/fabrique-du-metro/visiter

2.3. Support and Lining of Tunnels

2.3.1 Support

The primary lining or support consists of a thin layer of sprayed concrete (See Figure II-17), combined with any or all of the following support elements:

- Bolts (do not provide significant resistance in soils, they are little used).
- Welded steel mesh.
- Steel or synthetic fibers.
- Steel frames (See Figure II-18).
- Marchiavantis.

The support or primary lining of the tunnel has the mission of stabilizing the excavations during its construction, in which there is no other action than the one derived from the thrust of the ground. If there is a water table in the ground, it must be depressed to allow excavation. Therefore, it should only be designed according to the characteristics of the ground.



Figure II-17: Support with Shotcrete, construction of the Kramer Tunnel

Between Garmisch- Partenkirchen, Germany

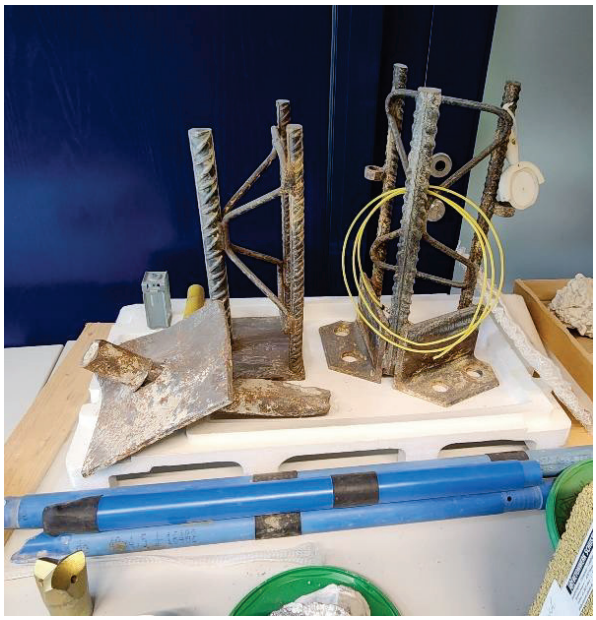


Figure II-18: Reticulate Steel Frame, construction of the Kramer Tunnel

Between Garmish- Partenkirchen, Germany

2.3.2 Lining

The secondary lining or simply lining consists of a thin layer of sprayed concrete or molded concrete (See Figure II-19) or prefabricated segments (See Figure II-20), if used TBM as excavation method. Any of these types of lining can be combined with any or all of the following lining elements:

- Welded steel mesh or Steel Bars (used when a concrete or prefabricated segment lining is defined)
- Steel or synthetic fibers (used when a Shotcrete lining is defined)
- Waterproofing of PVC Sheet (used when there is a water table in the ground)

The tunnel lining or secondary lining is designed to ensure, on the one part, the water tightness of the tunnel and to resist the loads associated with the water pressure, if the water table is affected. In addition, taking into account, if necessary, seismic or other time-dependent action (expansivity, creep, flow, etc.).

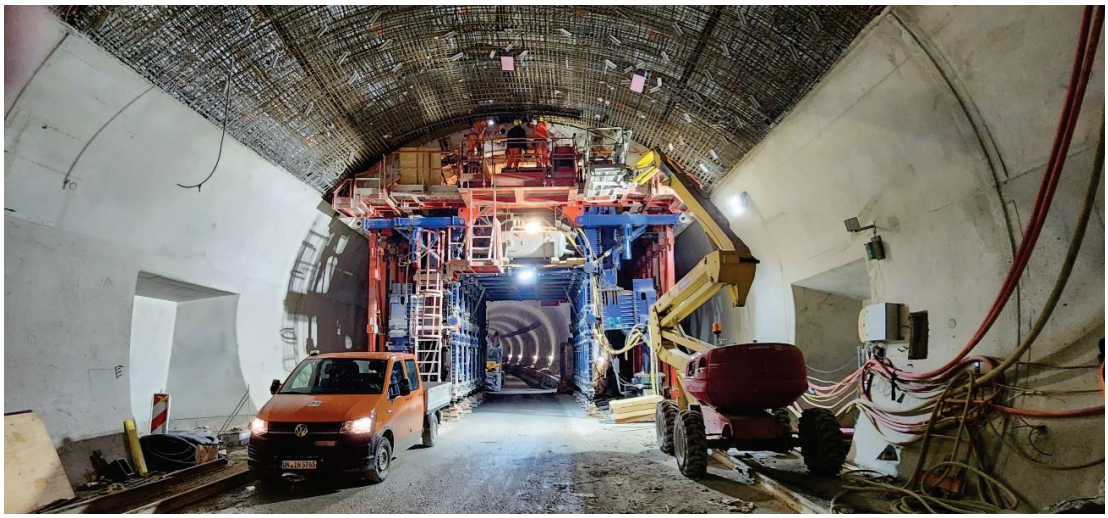


Figure II-19: Lining with Molded Concrete, construction of the Kramer Tunnel

Between Garmisch- Partenkirchen, Germany



Figure II-20: Lining with Prefabricated Segments, construction of

Metro Line 17, Paris, France (Visit of UNCUYO students with the TUM

in the great civil engineering excursion, 2023)

III. CASE STUDY: URBAN TUNNELS IN THE METROPOLITAN REGION OF SANTIAGO DE CHILE

3.1. The Study Area

3.1.1 Location

The urban road situation in the Metropolitan Region of Santiago de Chile confront several challenges. The city has experienced significant growth in its population and vehicle fleet, which has generated problems of congestion and accessibility. Main road problems:

- Congestion: Streets and avenues have become insufficient to handle the current volume of traffic.

- Infrastructure: There is a deficit in road infrastructure, especially in peripheral areas, which affects connectivity and accessibility.

- Public transport: Although the Santiago Metro is one of the most used transport systems, it does not always manage to meet demand, especially during rush hour.

The Santiago 2030 Metropolitan Mobility Plan seeks to address these challenges by improving road infrastructure, promoting more sustainable modes of transport and integrating new technologies to optimize urban mobility, such as the inclusion of avenues in tunnels.

3.1.2 Distribution of Population

Due to the great expansion that Santiago has had throughout its history, its population has expanded the initial limits of the city from Santa Lucía Hill to sectors of the foothills and the banks of the Maipo River in the east to the Maipú plains in the west. This caused a constant displacement of the main centers of population concentration from the center, which adopted the style of a financial district, to the periphery.

This trend, however, has slowed in the last decade. The most central communes have experienced significant processes of densification and verticalization. According to the 2017 census, the commune of Santiago became the third most populated in the country, with a total of 404,495 inhabitants, doubling its population in 15 years. As can be seen in the Figure III-1.

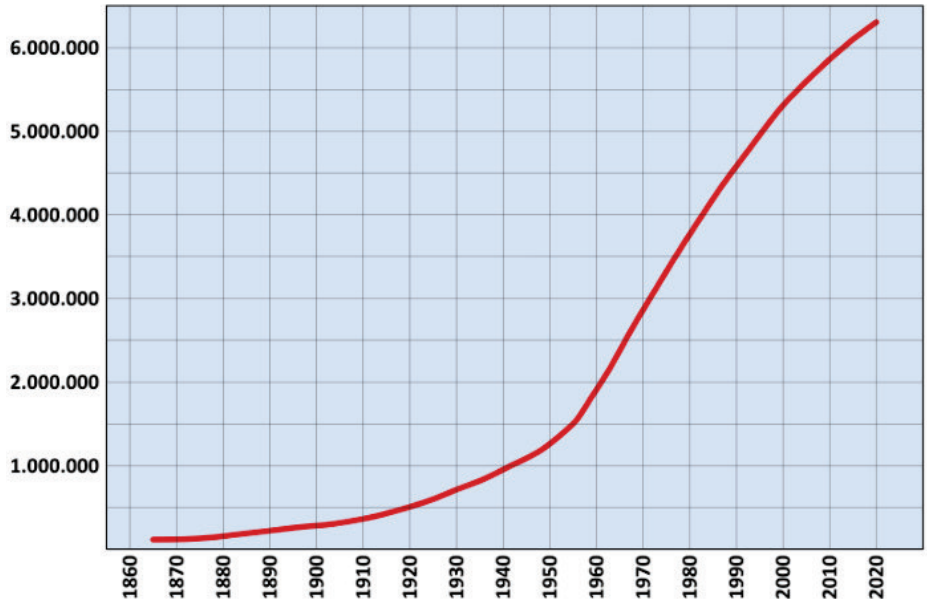


Figure III-1: Population of Santiago from 1820 to 2020. (from Wikipedia)

3.1.3 Urban Transport

Santiago accounts for 38.96% of the Chilean vehicle fleet in 2019, with a total of 2,228,385 vehicles, of which 2,197,683 are motorized and the city has 1,553,704 cars travelling, which is equivalent to 41.76% of the national total. To support this enormous fleet, an extensive network of avenues and streets extends throughout Santiago in order to provide connectivity to the different communes that make up the metropolitan area.

The Américo Vespucio ring road Avenue surrounds the inner sector of the city, facilitating the connection of the various axes.

During the 2000s, and in order to improve vehicular transport in Santiago, various urban highways were built throughout the capital. General Velásquez and the sections of the Panamericana highway that cross the city were converted into the Autopista Central, while Américo Vespucio gave way to the Vespucio Norte Express, Vespucio Sur and the future Vespucio Oriente highways. Following the edge of the Mapocho River, the Costanera North highway was built, connecting the northeastern part of the capital with the airport and the downtown area more quickly. All of these concessioned highways, which total 210 km in length, have a free flow toll system. As can be seen in the Figure III-2.



Figure III-2: Map of Santiago depicting main streets. (from Wikipedia)

3.1.4 Projected Situation

(a) Considering the Pre-existing Metro Tunnel

Two road tunnels are planned to be built under the pre-existing Metro tunnel with several lanes in both directions of advance, west and east. As can be seen in the Figure III-3.

The new east and west tunnels are defined in details in section 3.3, and the Metro tunnel is defined in section 3.4.

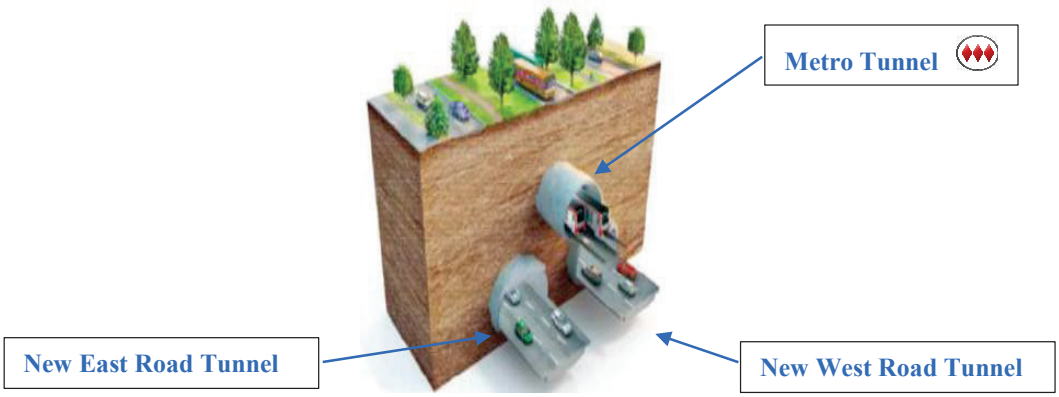


Figure III-3: Proposed Road Tunnels underneath the Metro Tunnel (José Miguel Galera, 2020 [5])

(b) Considering the Important Pre-existing Building

Two road tunnels are planned to be built under the pre-existing building with several lanes in both directions of advance, west and east. As can be seen in the Figure III-4.

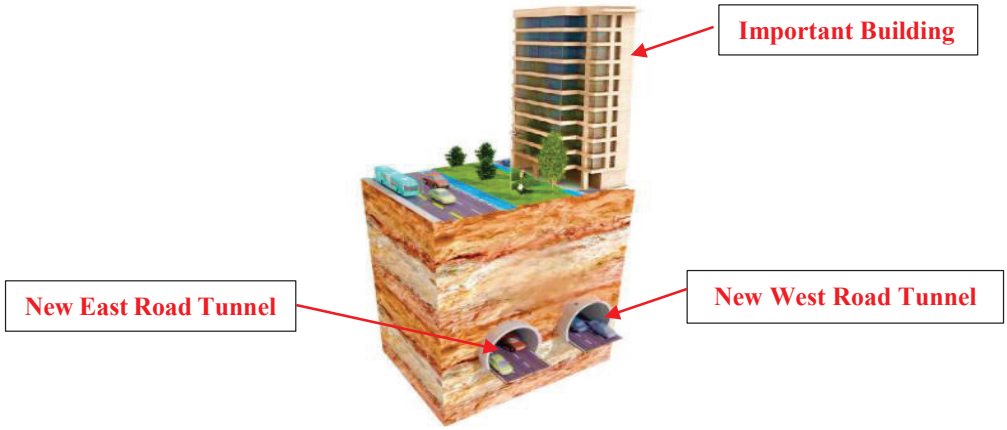


Figure III-4: Proposed Road Tunnels underneath the Building (José Miguel Galera, 2020 [5])

The new east and west tunnels are defined in details in section 3.3, and the important building is defined in section 3.5.

3.2. Geology of Santiago de Chile

The metropolitan region is made up mainly of alluvial and colluvial deposits, and to a lesser degree, by material from mass removals, both with an origin associated with the Pleistocene - Holocene age.

This can be seen in the following Figure III-5 in which it can be seen that the city of Santiago is located in unit Q1.

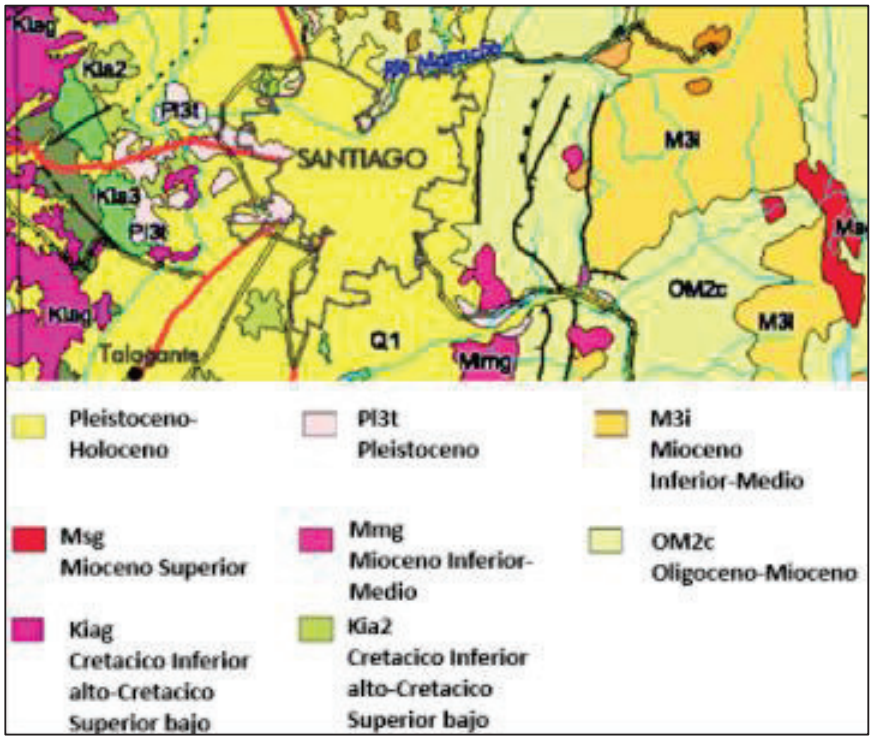


Figure III-5: Geology of the city of Santiago [16]

As mentioned, three zones will be studied, all associated with future road tunnel projects, some of which are currently under construction. These zones correspond to the northeast zone where gravel predominate, better known as “Gravel of Santiago”, the south-central zone where fines deposits predominate and the central-east zone with a predominance of a mixture of soils, including gravels with sandy and clayey matrix, as well as silt and clay layers.

These three study zones are presented below in a satellite image of Figure III-6, where three profiles of soils can be defined.

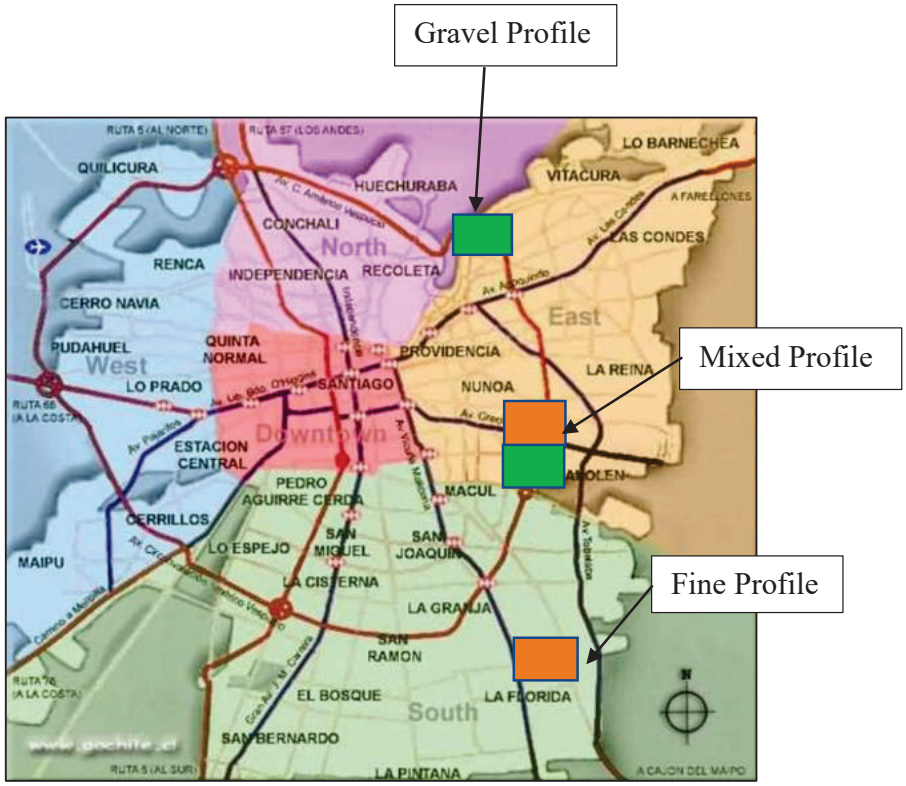


Figure III-6: Satellite Image of Santiago de Chile city. (Web)

3.2.1 Gravel of Santiago

The first profile corresponds to Santiago Gravel, which is a coarse granular soil transported by the Mapocho River. It is made up of sub-rounded to subangular particles with a very sporadic presence of lenses of fine gravel without fines and thin lenses of sand. It is a very compact soil with high mechanical interlock and high shear strength and rigidity. It can be classified according to USCS (Unified Soil Classification System) in Well Graded Gravel (GW).

The first few meters of the profile are an anthropic fill, composed mainly of clays with gravel. The thickness varies between 1.6 and 5.4 m, generally presenting about 5.0 m.
The 2st deposition (upper level) is made up of clean sandy gravel or with very little presence of silty fines. It has high homogeneity and an increase in the quantity and plasticity of the fines is observed as it approaches its contact with the first deposition.

The most competent soil is gravel of the 1st deposition, formed by sandy gravel and sandy-clay gravel. In the following Figure III-7 shows the described profile.

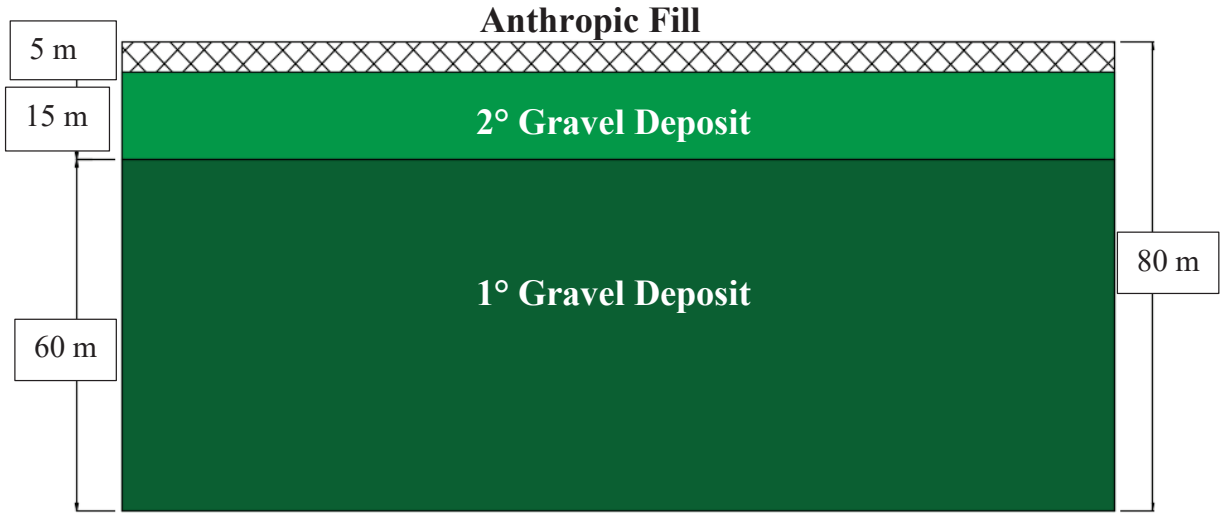


Figure III-7: Gravel Profile

3.2.2 Fine of Santiago

The second profile corresponds to deposits of Alluvial Fans (alluvial sandy clay). An important formation in the south-eastern sector of Santiago, they have a clay subsoil resulting from the successive accumulation of alluvial materials from the Andean foothills during heavy torrential rains and rapid snow melting that tend to occur recurrently every few winters. It can be classified according to USCS (Unified Soil Classification System) in low-plasticity clay and low-plasticity silt (CL, ML).

A top and bottom layers of dejection cones is distinguished, which are differentiated by the increase in cohesion with depth and the decrease in the coefficient of earth pressure at rest. In the followinokg Figure III-8 shows the described profile.

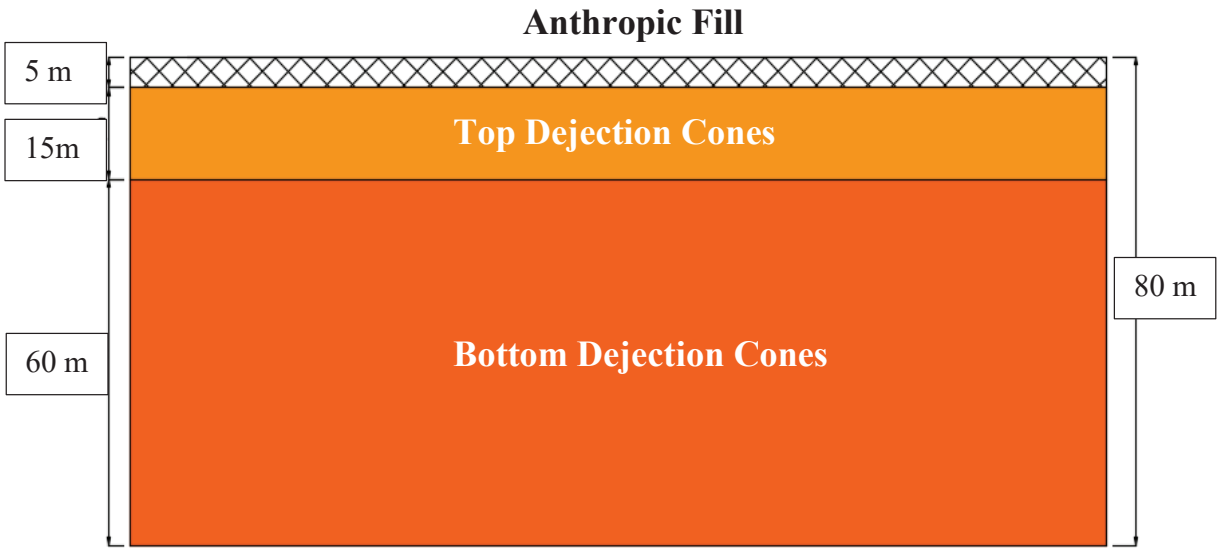


Figure III-8: Fine Profile

3.2.3 Mixed of Santiago

This profile is made up of medium-plastic, brown-colored silty and clayey materials with intercalations of sandy and gravelly lenses. The soil particles come from the decomposition of sedimentary and volcanic rocks from the nearby Andes mountain ranges. In the following Figure III-9 shows the described profile.

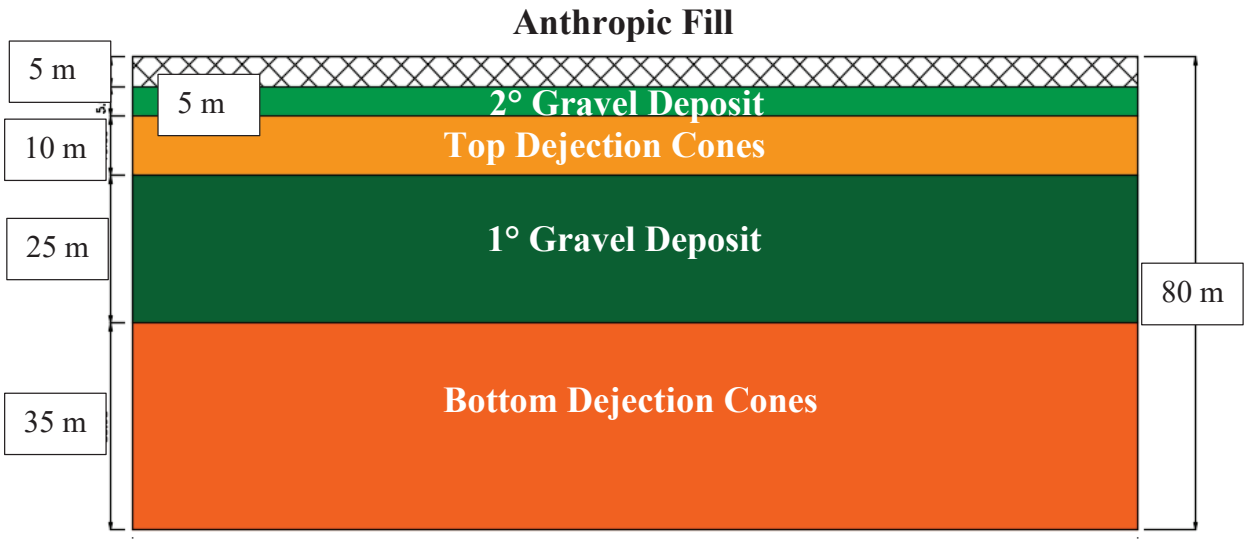


Figure III-9: Mixed Profile

3.3. Characteristics of the New Road Tunnels Projected

3.3.1 Geometry Road Tunnels

Two geometries are proposed for the analysis tunnel sections, a first section, with plan slab, a second section with counter-vault, both with various radios of circular in vault. (See Figure III-10). These sections correspond to those indicated in the Chilean road manual [9].

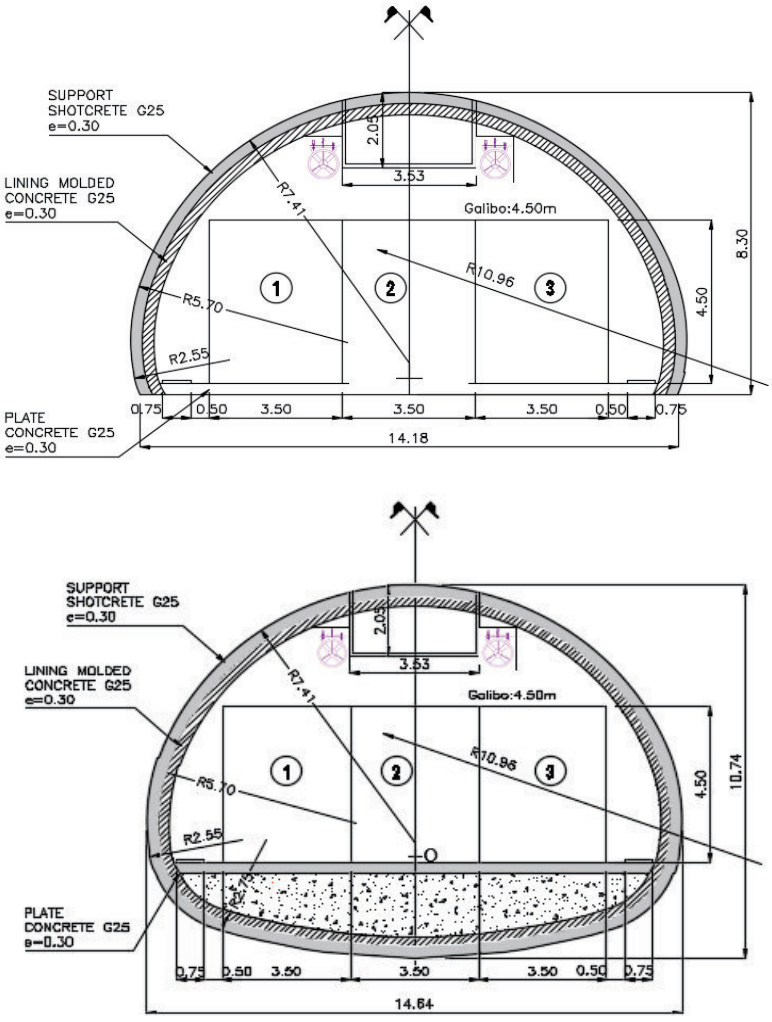


Figure III-10: Section Geometry of three way with Plane Sole (superior) and Counter-vault section (inferior)

3.3.2 Structural Elements of the New Road Tunnels

(a) Support of New East and West Road Tunnels

The support of the New East and West tunnels are formed by 0.30 m thick shotcrete reinforcement with steel fiber “3c”, and G25 quality with a characteristic resistance of 25 MPa at 28 days and reinforcement with steel frame LG 115/32/22 and Young´s module of 12500MPa.

(b) Lining of New East and West Road Tunnels

The lining of the news East and West tunnels are formed by 0.30 m thick molded concrete of G25 quality with a characteristic resistance of 25 MPa at 28 days and Young´s module of 23500 MPa. In addition, it has a reinforcement composed of ACMA electro-welded mesh 335 in the both faces.

(c) Backfill of Simple Concrete of New East and West Road Tunnels

A simple G10 quality concrete filler is used in the counter-vault with a characteristic resistance of 10 MPa after 28 days and Young´s Modulus of 15000 MPa.

(d) Plate of Reinforcement Concrete of New East and West Road Tunnels

The reinforced concrete slab that forms the tunnel floor is formed by 0.30 m thick molded concrete of G25 quality reinforced with steel bars with a characteristic resistance of 25 MPa after 28 days and Young´s Modulus of 23500 MPa.

3.3.3 Construction Sequence with the NATM (New Austrian Tunnel Method)

The proposed construction sequence is presented below and can observed in Figure III-11 y Figure III-12:

- **Phase I:** Excavation and installation of the support of the first phase, with an excavation section of 51.32m2. It will be excavated in advances of 1.00m.

- **Phase II:** The excavation of the section is completed with the excavation of phase II, with an excavation section of 44.48m2. A minimum offset of 20m must be maintained with the advance front. It will also be excavated in 1.00m advances.

- **Phase III:** Maintaining a minimum offset of 20m, with respect to the advance front of Phase II, the demolition of the intermediate wall that forms the temporary support of the tunnel will be executed, in 1.00m steps.

- **Phase IV:** Execution of lining.

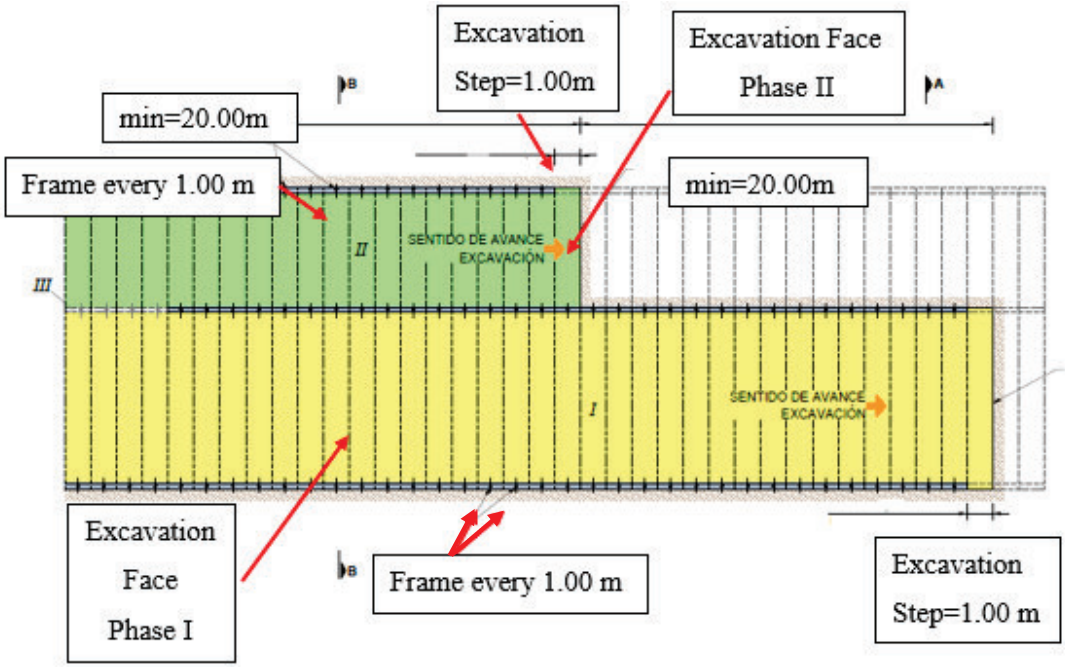


Figure III-11: Construction Sequence- Two Phases of Excavation- Section with plane sole

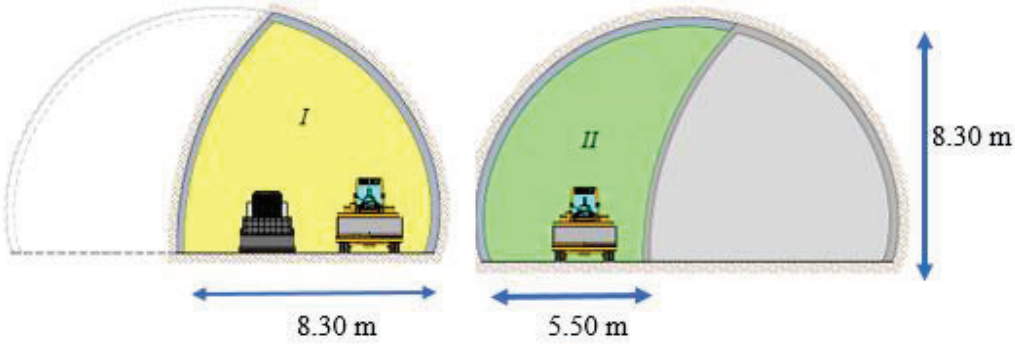


Figure III-12: Excavation Section with plane sole- Corte A-A and Corte B- B

3.4. Pre-existing Situation with Metro Tunnel

3.4.1 Line of the Metro of Santiago

Santiago Metro has seven operating lines (1, 2, 3, 4, 4A, 5 and 6), extending over 149 km and connecting 143 stations. The system carries around 2.400.000 passengers per day.
In addition, 3 more lines were planned (7, 8, 9), which will connect the outskirts and reduce travel times to the city center.
The following is the Metro line of Santiago de Chile, in the Figure III-13.

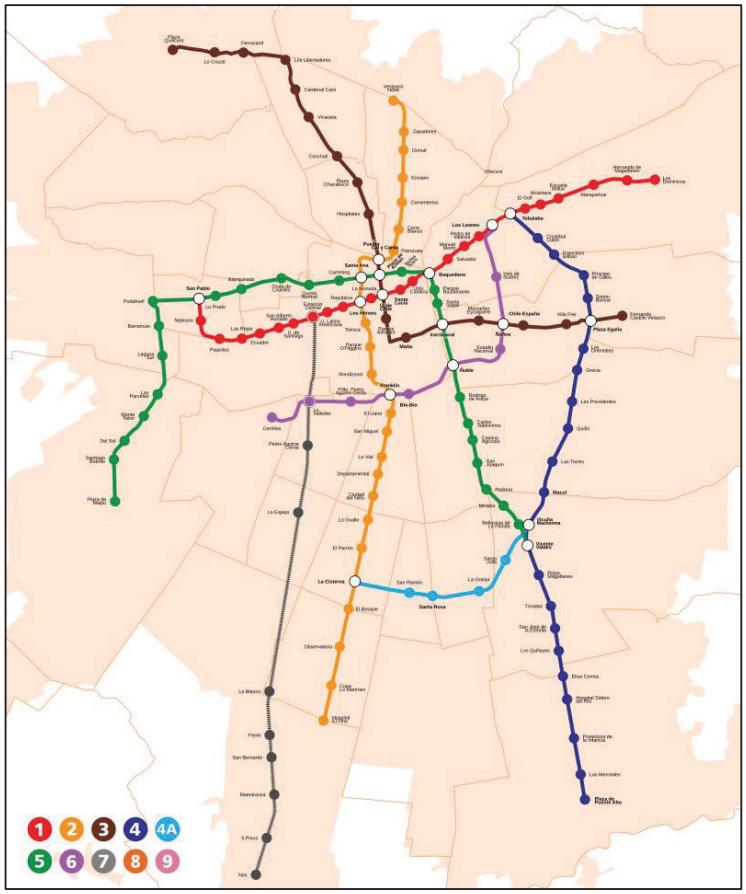


Figure III-13: Map of Metro of Santiago de Chile

3.4.2 Geometric Section of the Metro Tunnel

A typical section of metro tunnels is presented below, in the Figure III-14, where an excavated area of 68.90 m2 is observed, with a support and lining of shotcrete, which defines two railways.

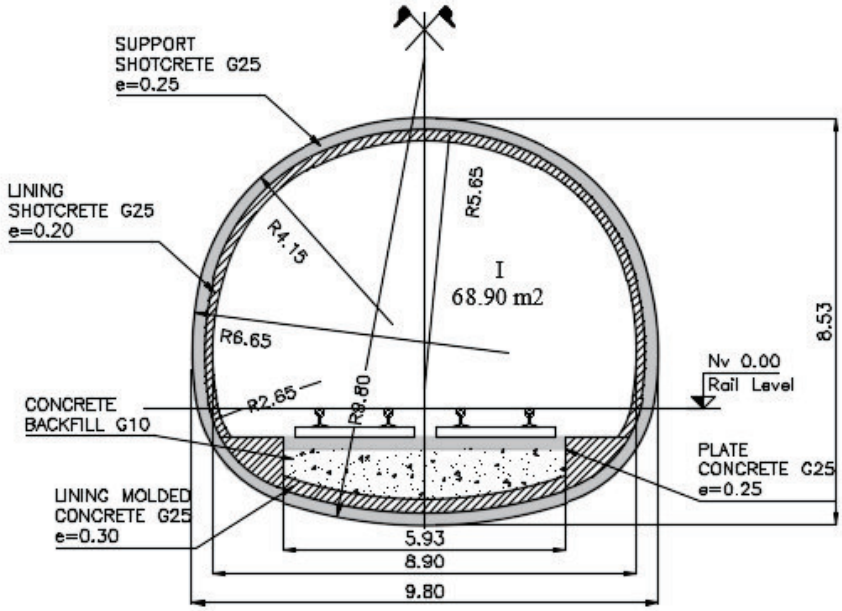


Figure III-14: Typical Section of Metro Tunnel (Rafael Iglesias, 2014 [4])

3.4.3 Structural Elements of the Metro Tunnel

(a) Support of Metro Tunnel

The support of the Metro tunnel is formed by 0.25 m thick shotcrete of G25 quality with a characteristic resistance of 25 MPa at 28 days and Young´s module of 12500 MPa.

(b) Lining of Metro Tunnel

The lining of the Vault of Metro tunnel is formed by 0.20 m thick shotcrete of G25 quality with a characteristic resistance of 25 MPa at 28 days and Young´s module of 12500 MPa. The lining of the Counter-vault of Metro tunnel is formed by 0.30 m thick molded concrete of G25 quality with a characteristic resistance of 25 MPa at 28 days and Young´s module of 23500 MPa.

In addition, it has a reinforcement composed of ACMA electro-welded mesh, according to the arrangement shown in Figure III-15.

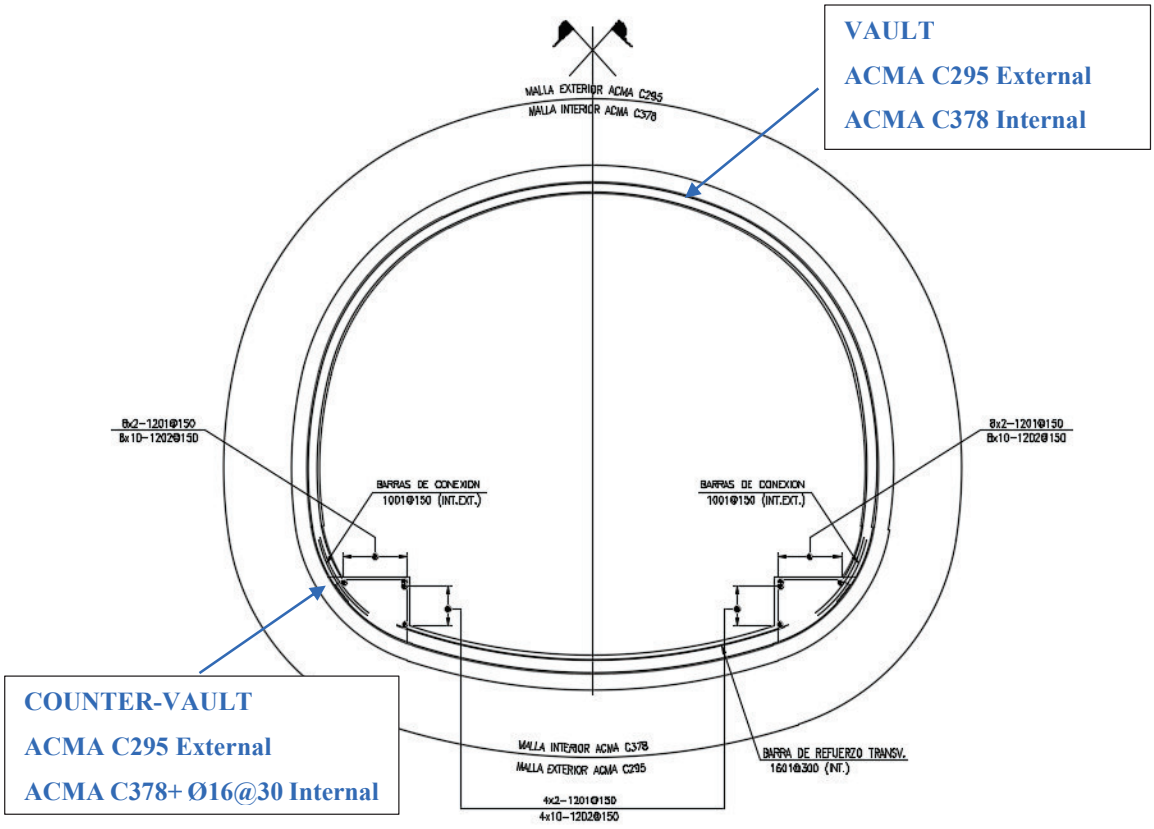


Figure III-15: Reinforcement in Lining with ACMA mesh of Typical Section of Metro Tunnel (Rafael Iglesias, 2014 [4]).

(c) Backfill of Simple Concrete of Metro Tunnel

A simple G10 quality concrete filler is used in the counter-vault with a characteristic resistance of 10 MPa after 28 days and Young´s Modulus of 15000 MPa.

(d) Plate of Concrete with Reinforcement Steel of Metro Tunnel

The reinforced concrete slab of 0.25 m thickness that forms the tunnel floor is composed of G25 quality molded concrete reinforced with steel bars with a characteristic resistance of 25 MPa after 28 days and Young´s Modulus of 23500 MPa.

3.4.4 Location of Metro Tunnel on the Soil Profiles

The Metro line 4, which runs parallel to the Americo Vespucio ring road has a keystone located at a depth of 10 m from the ground surface in all soil profiles. See Figure III-16.

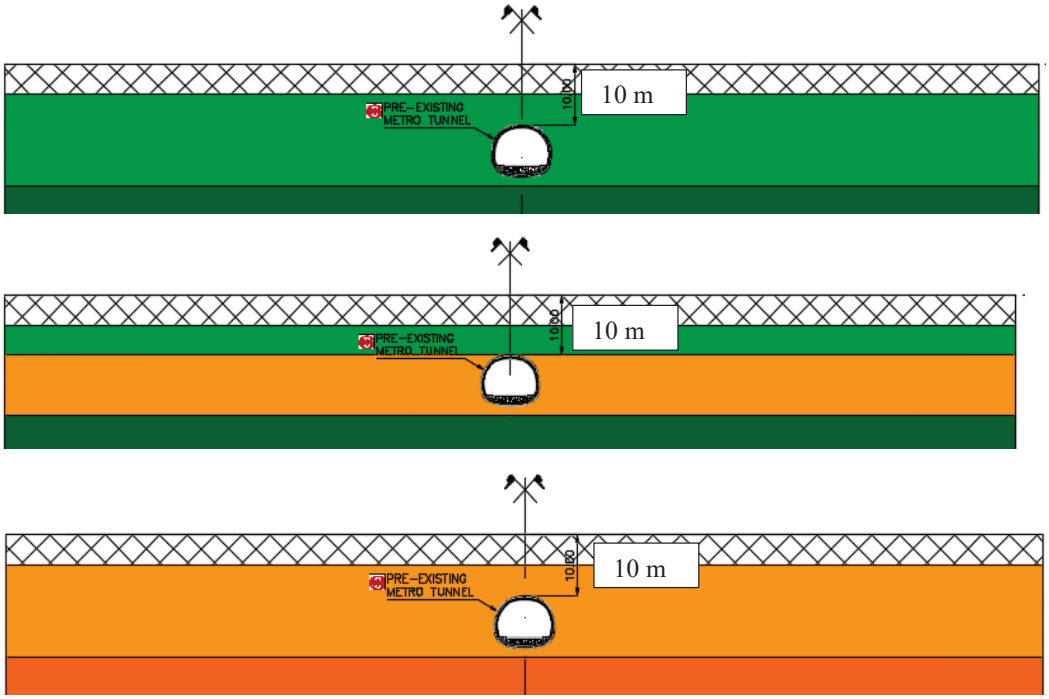


Figure III-16: Location of Metro Tunnel on the Gravel (superior), Mixed (center) and Fine (inferior) Profiles

The same support and lining are used in all soil profiles as described in sections 3.4.3(a) and 3.4.3(b).

3.5. Pre-existing Situation with Important Building

For the analysis made in this thesis, a 22-story reinforced concrete building is adopted, as shows in the Figure III-17. This building is located on the same trace of the L4 Metro line and the Americo Vespucio Oriente ring road, and is representative of any building that can be found in any profile.



Figure III-17: Typical Building in the city of Santiago de Chile (Illustrative Image of Google Earth)

3.5.1 Structural Characteristics of Building

The structure of the building is composed of 0.50 m thick underground walls, 0.25 m thick elevation walls and 0.25 m thick slabs. For all soil profiles the structure of the building is the same.

But the foundation of the building is studied in two typologies, superficial (for gravel soil) and deep foundations (for mixed and fine soils).

The superficial foundation consisting of four continuous bases, with 3 m width and 1.50 m high, founded at 6.50 m depth, (See Figure III-18)

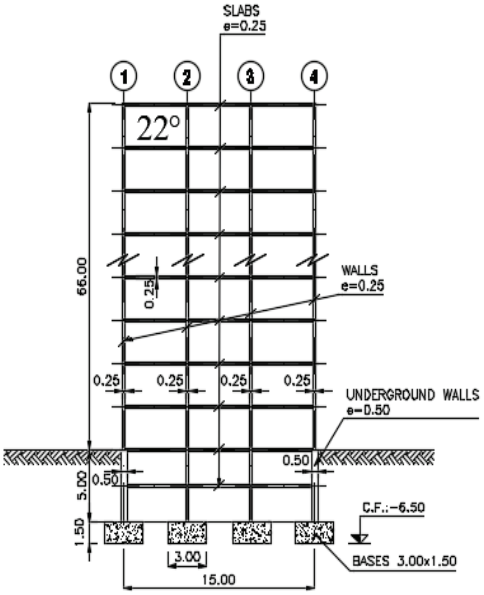


Figure III-18: Building Structure in Gravel Profile

The deep foundation consisting of two micropiles of reinforcement concrete of 0.30 m diameter in each bases and founded at 26.50 m depth, (See Figure III-19).

The structural analysis is considered for a building length of 1 m.

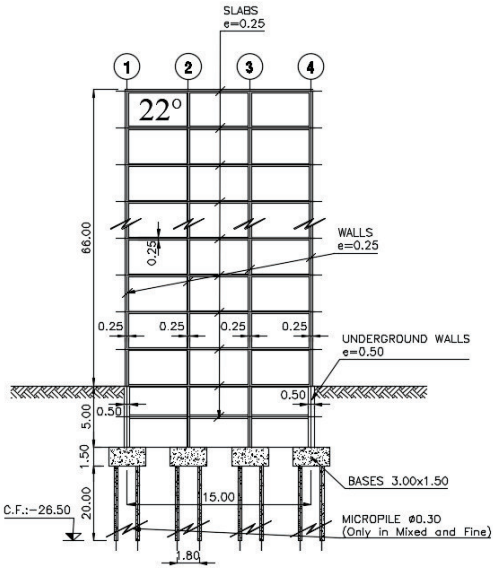


Figure III-19: Building Structure in Mixed and Fine Profile

3.5.2 Location of Building on the Soil Profiles

From the right edge to the west tunnel to the left edge of the building there are 1.10 m horizontally, obtaining a total distance of 23 m from the axis of symmetry of the profile and from the keystone of the tunnels to the last basement of the building there are 32.00 m depth. As can be seen in the Figure III-20.

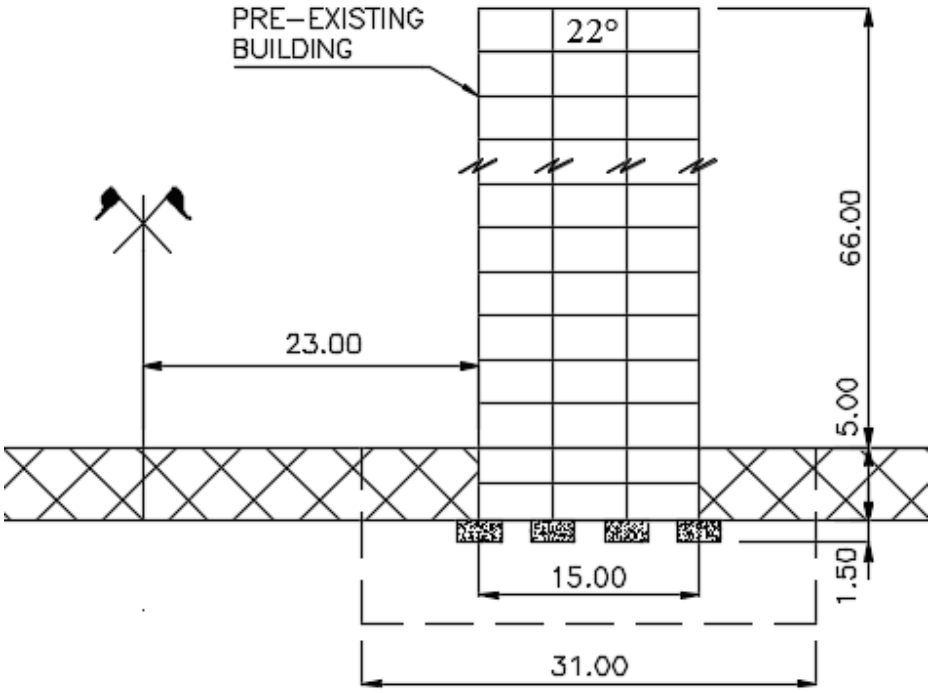


Figure III-20: Location of Building

3.6. Final Profiles with the Projected and Existing Situation

Below are the 6 scenarios studied, as can be seen Figure III-21 and Figure III-22.

3.6.1 Final Profiles considering the Pre-existing Metro Tunnel

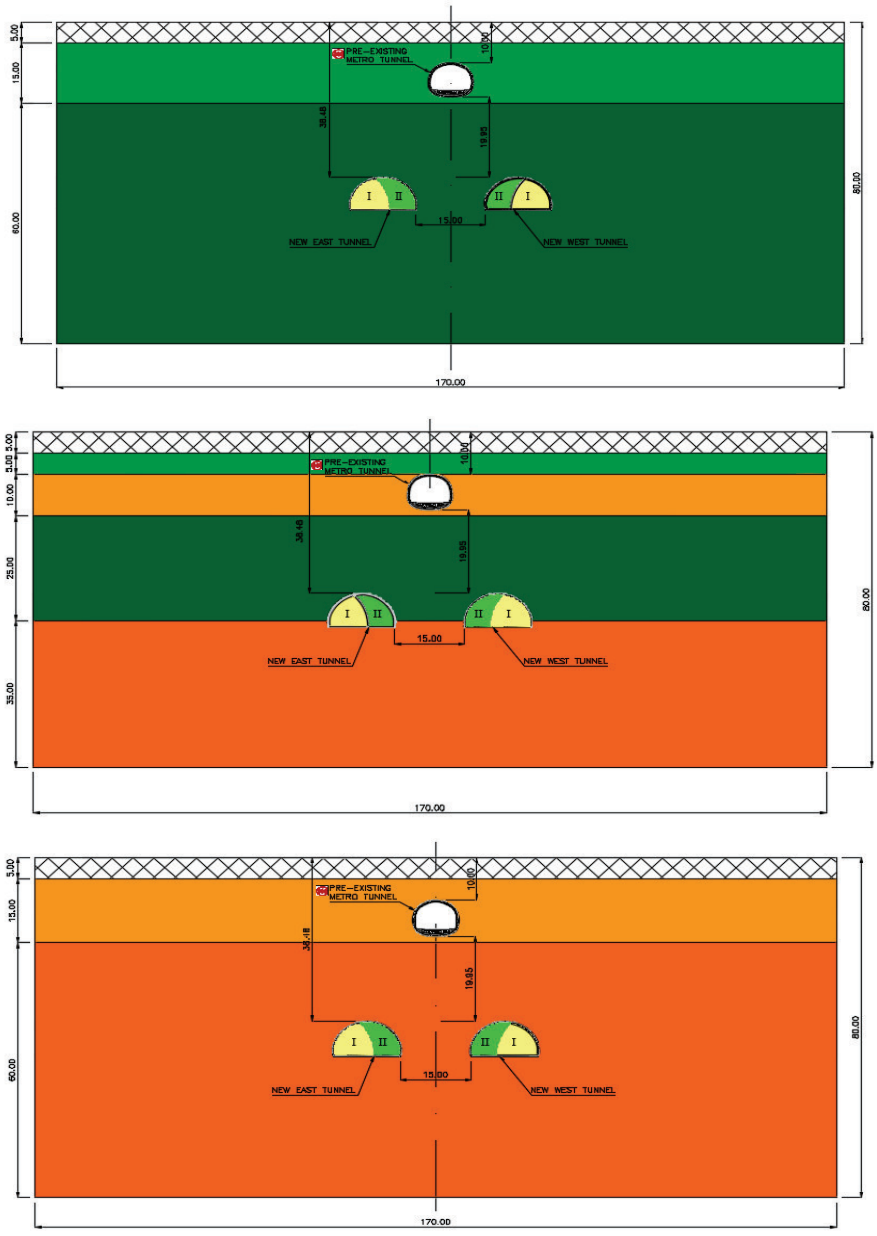


Figure III-21: Final Situation of Gravel (superior), Mixed (center) and Fine (inferior) Profiles with Pre-existing Metro Tunnel

3.6.2 Final Profiles considering the Pre-existing Building

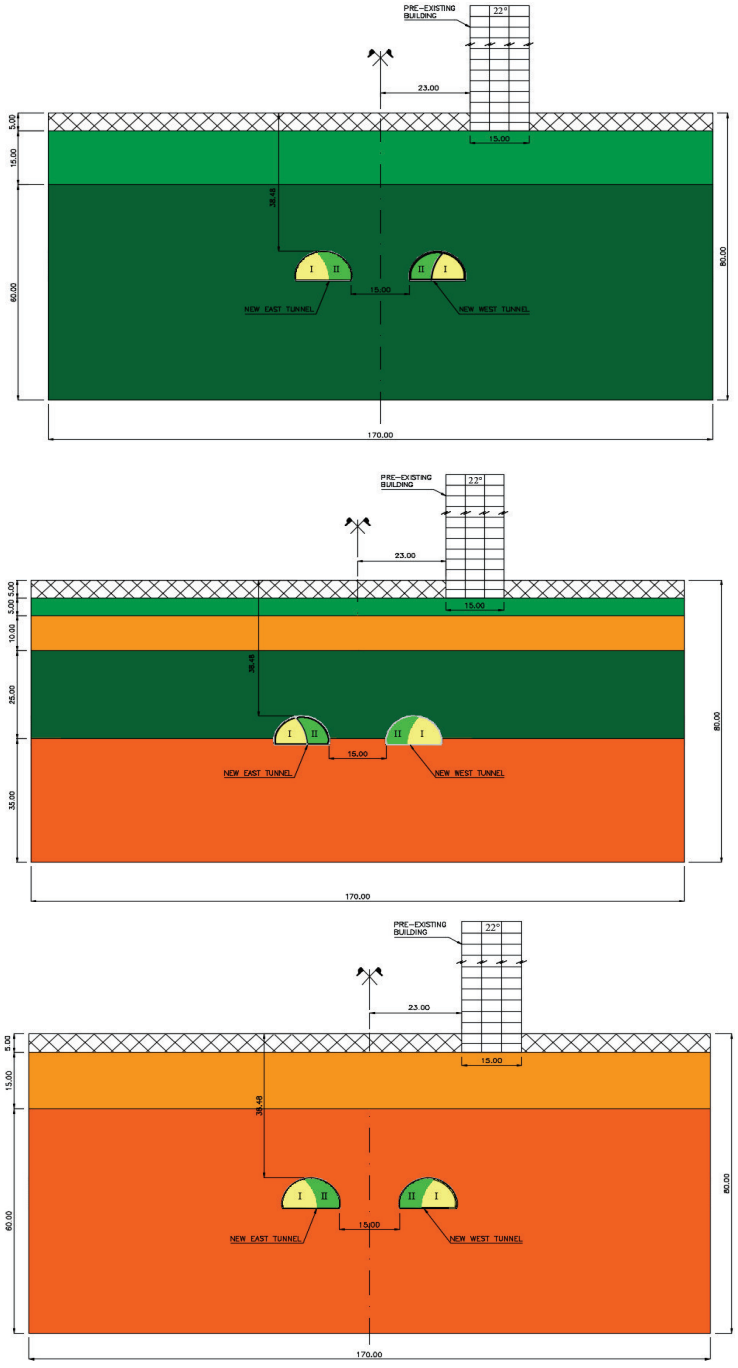


Figure III-22: Final Situation of Gravel (superior), Mixed (center) and Fine (inferior) Profiles with Pre-existing Building.

3.7. Limitations and Acceptance Criteria

3.7.1 On the Pre-existing Metro Tunnel

In order to determine the effect on the Metro Tunnel in terms of induced deformations and stress resulting from the excavation of the new road east and west tunnels, the following limits established by METRO S.A. must be met:

(a) Verification of Deformation in the Metro Tunnel

In a transversal sense, for straight sections, the height of one rail in relation to the other, on the same track, cannot exceed **+2 mm.**

(b) Verification of Resistance in the Metro Tunnel

Structural verification of the Metro lining of shotcrete reinforced with mesh and steel bars in the Construction Phase (Short Time) of the new tunnels and in the Service Phase (Long Time) through the interaction diagrams of flexural-compressed (M-N) and shear verification elements according to AASHTO standards [7].

It is noted that for the verification of the lining it is considered that the support and the around soil have degraded by a factor of α=0.5 (they provide half of the resistance).

The diagrams used can be seen in Figure III-23.

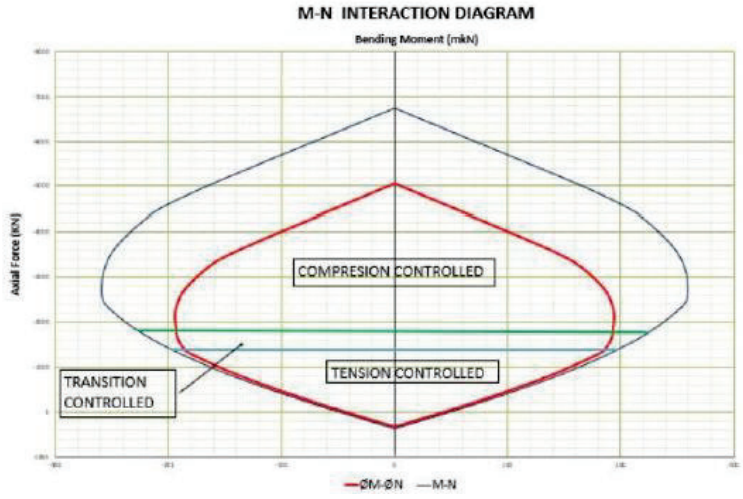


Figure III-23: AASHTO standard axial-moment interaction diagram [7]

3.7.2 On the Pre-existing Building

(a) Verification of Settlements in the Building Foundation

The effect of tunnels on surface structures will be evaluated on the base of the recommendations of the ITA [6].
This document establishes a three-stage assessment procedure:

1) **First Stage**: If the tunneling induces a settlement in the buildings of less than 10 mm and also the slope of the settlement curve is less than 1/500, the risk of damage is assumed to be insignificant and the evaluation process is finished.

2) **Second Stage:** If the settlement in the buildings exceeds that established in the first stage, each building should be evaluated by calculating the horizontal deformation under the building and assigning a damage category. The Boscardin Cording or Burland methodology can be used for this purpose.

3) Third Stage: This stage will only be performed if the evaluated building(s) have shown a damage level of "Light" or higher in stage two. In this case, specific building details and/or building protection measures should be considered in the three-dimensional numerical model in order to reduce the level of damage estimated in stage two. This last stage of analysis is out of scope of the present thesis.

(a.1) Boscardin Cording or Burland Criteria

Initially, the classification of damages in BURLAND (1977), reference [6], buildings is defined

Table III-1: Classification of damage to buildings according to Burland et al (1977). [6]

TYPES OF DAMAGE	DESCRIPTION OF DAMAGE	APPROXIMATE WIDTH OF CRACKS [mm]
Negligible	Almost imperceptible cracks.	< 0.1
Very Slight	Fine cracks that are easily repairable and occasional larger cracks. Cracks in facades that are visible on careful inspection.	< 1
Slight	Cracks that can be filled without problems. Slight fractures inside the buildings and visible on the outside. Doors and windows close with difficulty.	< 5
Moderate	Repairing the cracks requires major work, both inside and outside. Doors and windows do not close. Use of the building must be interrupted until repair is complete.	5 to 15
Severe	Intensive repairs to the partitions. Doors and windows do not close and floors have noticeable slopes. The building must be evacuated.	15 to 25
Very Severe	Repair may involve partial reconstruction of the building. Cracks affect the structure and there is a risk of collapse.	> 25

BOSCARDIN and CORDING (1989), reference [6], published a criterion for damage to buildings caused by tunnel excavation based on the combination of the parameters: Horizontal deformation in traction and inclination of the surface (see Figure III-24).

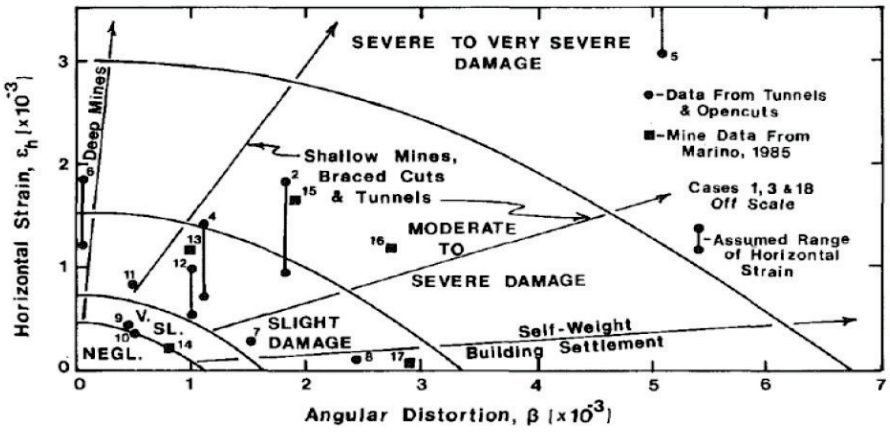


Figure III-24: Representation of the Boscardin and Cording damage criterion. [6]

For the study of the effect of ground settlement on existing buildings and structures, the following parameters are defined (see Figure III-25):

- Settlement (uz): Vertical displacement of a point.
- Relative settlement (Δuz): Value of the difference between two settlements.
- Angular distortion (β): Rotation between two points separated by a straight line.
- Horizontal deformation (εh): Defined as the average relative horizontal movement between two reference points.

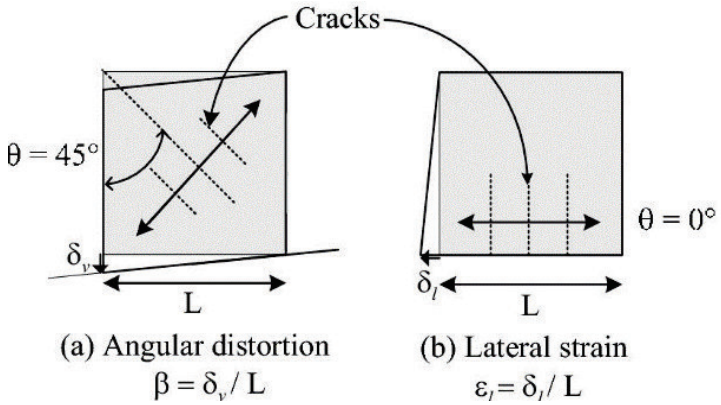


Figure III-25: Definition of damage verification parameters in Building (β, ε) [6]

Both the Burland and Boscardin and Cording criteria are based on the equivalent beam model in which the building is modeled as if it were a beam subjected to the displacements induced by a point load. Likewise, both criteria establish that tensile deformation is the criterion that controls the structural damage, which can be produced by flexural bending, by shear deformation or by a combination of both (See Figure III-26).

The difference between both methods is that Burland evaluates the maximum deflection ratio (Δ/L) while Boscardin and Cording introduce the concept of angular distortion that represents the deflection angle with respect to the horizontal.

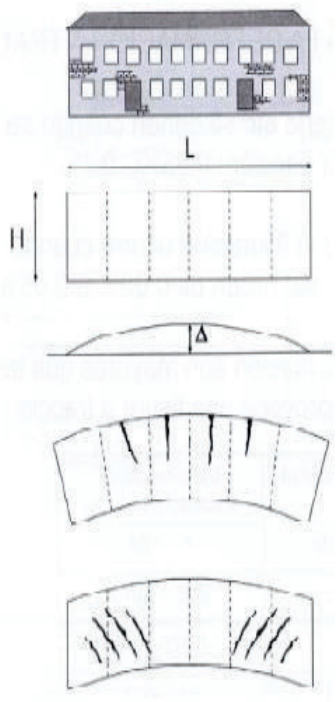


Figure III-26: Equivalent Beam Model [6]

The acceptance criterion followed for the analysis carried out is buildings with a damage category lower than or equal to "**Very Slight**".

Category of damage	Normal degree of severity	Limiting tensile strain (ε_{lim}) (%)
0	Negligible	0–0.05
1	Very slight	0.05–0.075
2	Slight	0.075–0.15
3	Moderate*	0.15–0.3
4 to 5	Severe to very severe	> 0.3

*Note: Boscardin and Cording (1989) describe the damage corresponding to ε_{lim} in the range 0.15–0.3 per cent as "moderate to severe". However, none of the cases quoted by them exhibits severe damage for this range of strains. There is therefore no evidence to suggest that tensile strains up to 0.3 per cent will result in severe damage.

Figure III-27: Relationship between category of damage and limiting tensile strain (after Boscardin and Cording, 1989 [6])

3.7.3 On the New Road Tunnels

(a) Verification of Deformation in the New Road Tunnels

Normally, the absolute magnitude of movements (the convergence) should not exceed a percentage of the tunnel width (B= 14 m). Therefore, the following values are established:

- For Gravel: 0.0005 - 0.002 B δ_{max} **< 30 mm**
- For Mixed: 0.002 - 0.0035 B δ_{max} **< 50 mm**
- For Fine: 0.0035 - 0.005 B δ_{max} **< 70 mm**

This criterion is established as good engineering practice in the area of tunnel geotechnics.

(b) Verification of Resistance in the New Road Tunnels

The support of shotcrete reinforced with steel frame and fiber steel will be designed according to CEB-FIP (Reference [8]), which establishes the format of partial safety factors, which consists of increasing the loads by a partial safety factor in order to obtain the design value (F_d) according to the following generic equation:

$$F_d = \gamma_F \times F_{rep} = 1.05 \times F_{rep}$$

Where:

F_{rep} is the representative value of a solicitation

γ_F is a partial safety factor (1.05 for Permanent Load).

To verify the support, a simplified method is initially used in terms of the maximum admissible stresses in the concrete.

$$\sigma_{c,max} \leq f_{cd} = \frac{f_{ck}}{\gamma_c}$$

$$\sigma_{t,max} \leq f_{ctd} = \frac{f_{ctk}}{\gamma_t}$$

Where:

$\sigma_{c,max}$: maximum compressive strength obtained in the model.

$\sigma_{t,max}$: maximum tensile strength obtained in the model.

f_{ck}: characteristic compressive strength of shotcrete G25 (25 MPa)

$f_{ct,k}$: characteristic tensile strength of shotcrete. ($0.6 \times \sqrt{f_{ck}} = 3MPa$)

γ_c: safety factor for the characteristic compressive strength of shotcrete (1.5)

γ_t: safety factor for the characteristic tensile strength of shotcrete (1.5)

f_{cd}: design compressive strength of shotcrete G25 (16.67 MPa)

$f_{ct,d}$: design tensile strength of shotcrete. (2 MPa)

Finally, we have:

$$\sigma_{c,max} \leq f_{cd} = -16.67\ MPa$$

$$\sigma_{t,max} \leq f_{ctd} = 2\ MPa$$

In case this last condition is not satisfied, a detailed verification of the fiber-reinforced shotcrete must be carried out through the flexural-normal (M-N) and shear-normal (V-N) interaction diagrams according to the guidelines of the 2010 Model Code.

The lining of molded concrete reinforced with steel mesh will be designed according to AASHTO [7], which consists of increasing the loads by a major factor in order to obtain the design value (F_d) according to the following generic equation:

$$F_d = \gamma_p \times F_{rep} = 1.50 \times F_{rep}$$

Where:

F_{rep} is the representative value of a solicitation

γp is a major factor (1.50 for Permanent Load).

To verify the lining of concrete molded, the interaction diagram (M-N) and shear-verification is used according to the guidelines of the AASHTO standards [7].

It is noted that for the verification of the lining it is considered a support with steel fiber degradation (the fiber does not provide resistance) and the around soil degraded by a factor α=0.66.

3.7.4 Verification of the Bearing Capacity of Soil

The state of plastification of the ground around the excavations (both the Metro tunnel, the new road tunnels and foundation of building) will be presented, taking into consideration that in all underground excavations a radius of plastification is generated, which depends on the dimensions of the tunnel, the state of stress in situ and the geomechanical parameters of the soil. Those crowns of plastification less than one (1) tunnel diameter or the largest dimension of the tunnel (14 m) are considered admissible in the analysis, in other words when the plastic crown has a radius less than twice the radius of the tunnel or its with (14 m). (See Figure III-28)

The deformation and resistance verifications of the new road tunnels and Bearing Capacity of soil are only carried out in case the verifications carried out on the pre-existing structures are positive.

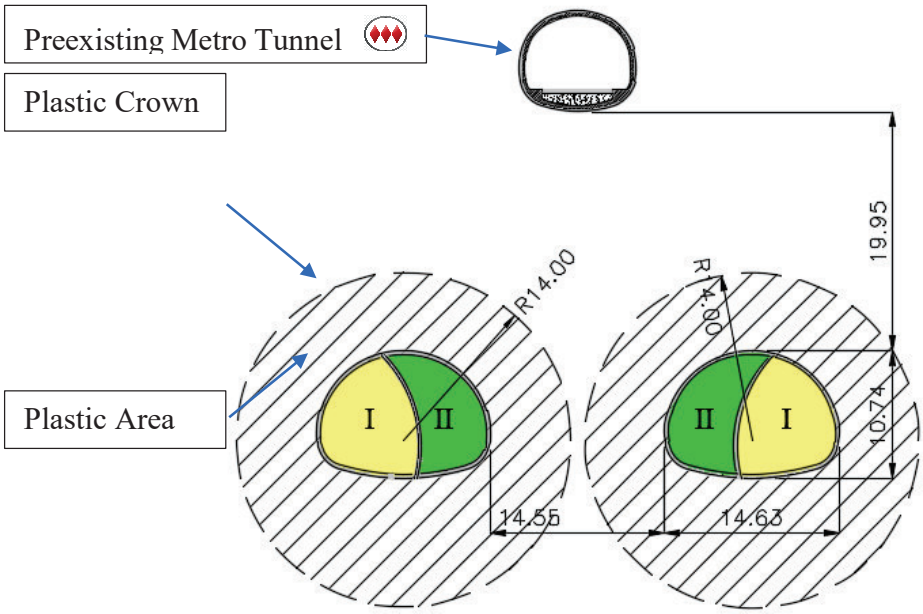


Figure III-28: Plastification Criteria

IV. NUMERICAL MODELLING

The software Plaxis, in its 2D version, is used. This program performs numerical calculations by means of Finite Elements Method (FEM), especially designed for the analysis of geotechnical problems. It is possibly the most widespread numerical calculation program worldwide in the field of tunnel engineering and geotechnical engineering.

4.1. General Modeling Consideration

4.1.1 Model Dimensions

The size of the model is defined as follows:

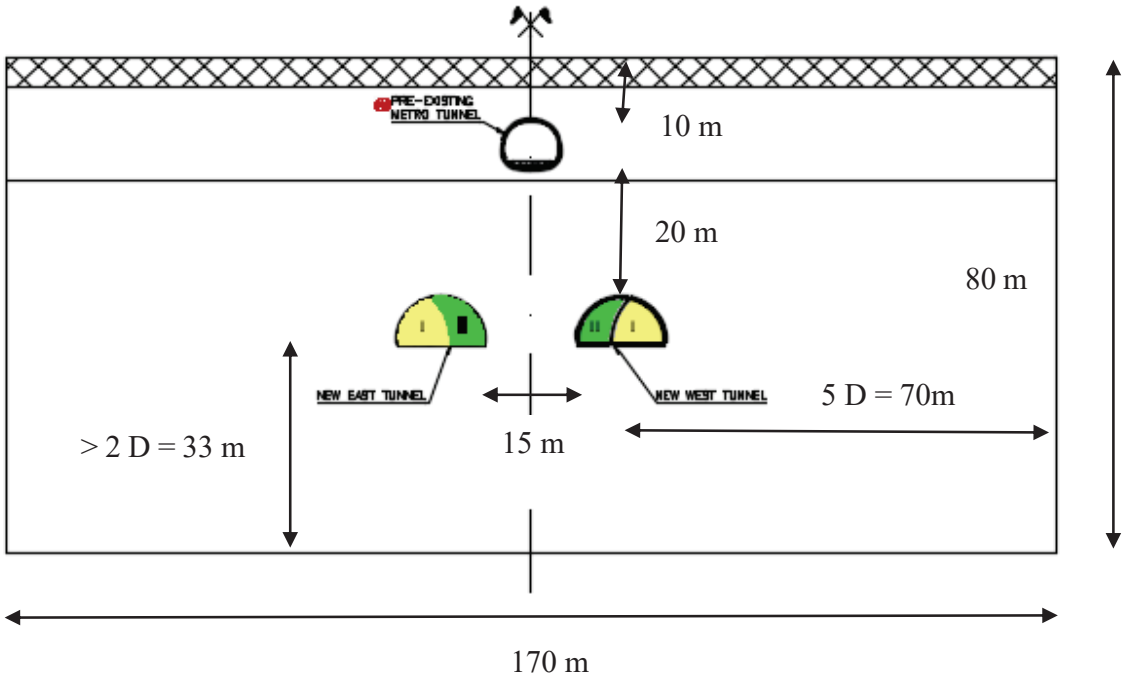


Figure IV-1: Numerical Model Dimensions [m]

Where, $D \approx 14\ m$

Model width = 170 m

Model Depth = 80 m

4.1.2 Boundary Conditions

The boundary conditions of the model are defined as follows:

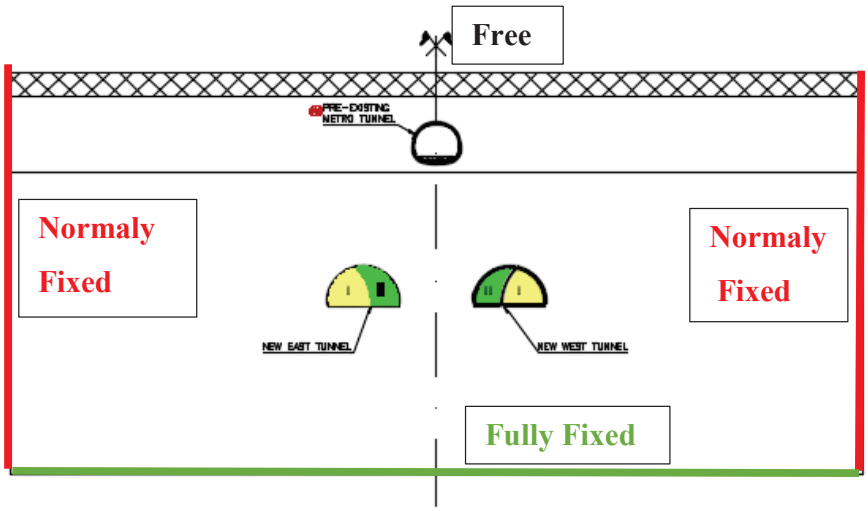


Figure IV-2: Boundary Conditions of the Models

4.1.3 Water Pressures

In the Metropolitan region of Santiago de Chile, the water table is located at a depth of more than 80 m, so water is not considered in the present models. However, the program requires the definition of a water table, which is placed at the bottom of the model where it will have no repercussions for the calculation.

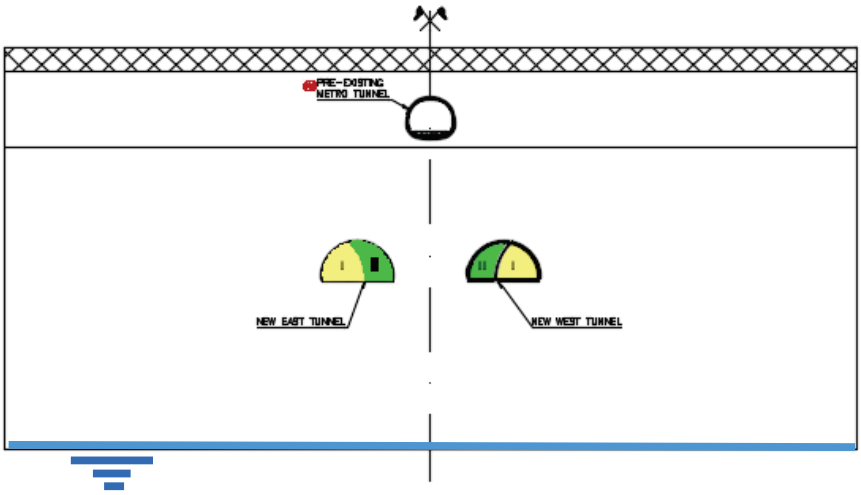


Figure IV-3: Water Table in the Models

4.1.4 Surface Loads: Traffic Overload

For the development of the modeling, a traffic overload has been considered for which a value of 10kPa has been adopted for the entire surface of the model, which corresponds to the value suggested in the Road Manual standard [9] for a double axle and single track type vehicle (see Figure IV-4).

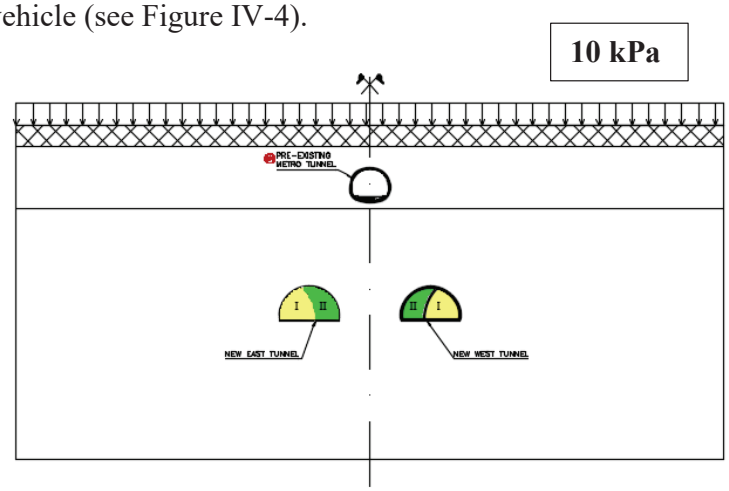


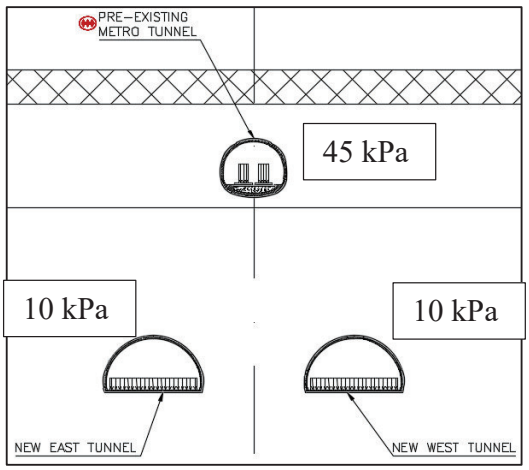


Figure IV-4: Type Vehicle for design

Figure IV-5: Traffic overload in the models

4.1.5 Service Loads for tunnels

A service load of 45 kN/m is considered for the Metro Tunnel roadway with 1.435 m of width, corresponding to a design train stipulated in Road Manual [9]. (See Figure IV-6).
A traffic load of 10 kN/m is considered on the new road tunnels, corresponding to that stipulated in the Road Manual standard. Both loads are shown below.



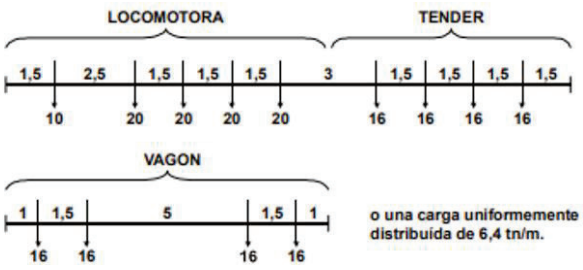


Figure IV-6: Service Loads for Metro Tunnel

Figure IV-7: Service Loads applied in Metro Tunnel and New Road Tunnels in the models

4.1.6 Finite Element Mesh

A 60 m x 60 m region is defined where the finite element mesh is densified. This densification is defined through the coarseness factor (CF), as shown in the following Figure IV-8.

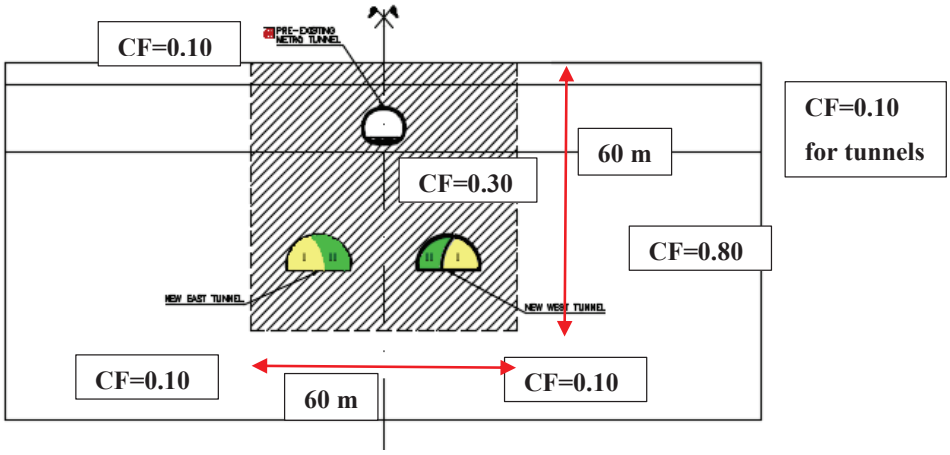


Figure IV-8: Coarseness factor for the definition of the mesh

A mesh with distribution elements of the type “Very Fine” is defined.

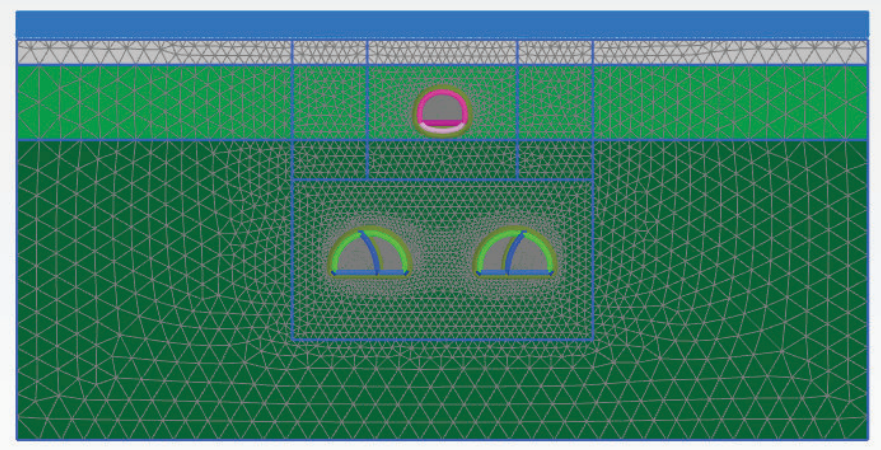


Figure IV-9: Finite Element Mesh

We obtain 10201 elements, 84209 nodes. This mesh is used in all models.

4.2. Soil Modeling Considerations

4.2.1 Constitutive Models

The constitutive model defines the response and behavior of the material to the action (loading, unloading, thermal action, etc.) to which it is subjected. All constitutive models are an approximation, idealization and theoretical and mathematical conceptualization of the real behavior of materials. The most advanced constitutive models can recreate and reproduce some of the more complex aspects of material behavior, but none can reproduce absolutely all aspects of a material's behavior. Therefore, knowing which aspects of a material's behavior a given constitutive model can simulate is as important as knowing which aspects of behavior it cannot simulate.

In the present thesis, three constitutive models of soil behavior are used: Mohr-Coulomb, Hardening Soil and Hardening Soil Small. For a brief presentation of these models, see Annex II.

4.2.2 Soil Input Parameters for the models

All geomechanical parameters were obtained from soil mechanics studies done in the region metropolitan of Santiago de Chile [11].

(a) Geotechnical Properties of the Soil for Mohr-Coulomb Model

The Mohr-Coulomb elasto-plastic model involves only five parameters, Young's modulus E and Poisson's coefficient ν for soil elasticity, internal friction angle φ and cohesion c for strength and plasticity, and ψ as the dilatancy angle.

Table IV-1: Geotechnical Properties of Gravel Profile- Model MC- Musante e Ingenieros (2019) [11]

Lithological Unit	Geotechnical Parameters						
	γ (kN/m3)	Cmax (kPa)	ϕm(°)	E (kPa)	ν	ψ(°)	Ko
Anthropic Fill	19	10	33	20000	0.3	0	0.65
2°Deposit Gravel	22.5	20	45	46000*z^0.50	0.25	12	0.80
1°Deposit Gravel	22.5	35	45	65000*z^0.50	0.25	12	0.53

Table IV-2: Geotechnical Properties of Mixed Profile - Model MC- Musante e Ingenieros (2019) [11]

Lithological Unit	Geotechnical Parameters						
	γ (kN/m3)	Cmax (kPa)	ϕm(°)	E (kPa)	ν	ψ(°)	Ko
Anthropic Fill	19	10	33	20000	0.30	0	0.65
2°Deposit Gravel	22.5	20	45	46000*z^0.50	0.25	12	0.80
Top Dejection Cones	18.5	50	31	20000 + 2750*z	0.30	0	0.65
1°Deposit Gravel	22.5	35	45	65000*z^0.50	0.25	12	0.53
Bottom Dejection Cones	18.5	50	31	20000 + 2750*z	0.30	0	0.45

Table IV-3: Geotechnical Properties of Fine Profile- Model MC- Musante e Ingenieros (2019) [11]

Lithological Unit	Geotechnical Parameters						
	γ (kN/m3)	Cmax (kPa)	ϕm(°)	E (kPa)	ν	ψ(°)	Ko
Anthropic Fill	19	10	33	20000	0.3	0	0.65
Top Dejection Cones	18.5	30 (z<=10) 50 (z>10m)	31	20000 + 2750*z	0.3	0	0.65
Bottom Dejection Cones	18.5	50	31	20000 + 2750*z	0.3	0	0.45

(b) Geotechnical Properties of the Soil for Hardening Soil Model

This model includes all the parameters defined in the previous section for the Mohr Coulomb model plus the following parameters:

Table IV-4: Geotechnical Properties of Gravel Profile- Model HS- Pinto and Ledezma (2019) [12]

Lithological Unit	Geotechnical Parameters							
	ν_{ur}	p_{ref} [kPa]	K_o^{nc}	E_{50}^{ref}(MPa)	E_{oed}^{ref}(MPa)	E_{ur}^{ref}(MPa)	m	R_f
2°Deposit Gravel	0.3	100	0.65	80	130	350	0.55	0.9
1°Deposit Gravel	0.2	100	0.43	275	190	900	0.51	0.9

Table IV-5: Geotechnical Properties of Mixed Profile - Model HS- Pinto and Ledezma (2019) [12]

Lithological Unit	Geotechnical Parameters							
	v_{ur}	p_{ref} [kPa]	K_o^{nc}	E_{50}^{ref}(MPa)	E_{oed}^{ref}(MPa)	E_{ur}^{ref}(MPa)	m	R_f
2°Deposit Gravel	0.3	100	0.65	80	130	350	0.55	0.9
Top Dejection Cones	0.3	100	0.65	21	21	150	0.7	0.9
1°Deposit Gravel	0.2	100	0.43	275	190	900	0.51	0.9
Bottom Dejection Cones	0.3	100	0.55	55	53.8	220	1	0.9

Table IV-6: Geotechnical Properties of Fine Profile- Model HS- Rafael Iglesias (2014) [4]

Lithological Unit	Geotechnical Parameters							
	v_{ur}	p_{ref} [kPa]	K_o^{nc}	E_{50}^{ref}(MPa)	E_{oed}^{ref}(MPa)	E_{ur}^{ref}(MPa)	m	R_f
Top Dejection Cones	0.3	100	0.65	21	21	150	0.7	0.9
Bottom Dejection Cones	0.3	100	0.55	55	53.8	220	1	0.9

(c) Geotechnical Properties of the Soil for Hardening Soil Small Model

The Hardening Soil model with small-strain stiffness is based on the Hardening Soil model and uses almost entirely the same parameters.

In fact, only two additional parameters are needed to describe the variation of stiffness with strain:

- the initial or very small-strain shear modulus G_o.
- the shear strain level $\gamma 0.7$ at which the secant shear modulus G_s is reduced to about 70% of G_o.

Table IV-7: Geotechnical Properties of Gravel Profile- Model HSs- Pinto and Ledezma (2019) [12]

Lithological Unit	Geotechnical Parameters	
	G_o^{ref} [MPa]	$\gamma_{0.7}$
2°Deposit Gravel	400	0.0008
1°Deposit Gravel	750	0.0011

Table IV-8: Geotechnical Properties of Mixed Profile - Model HSs- Pinto and Ledezma (2019) [12]

Lithological Unit	Geotechnical Parameters	
	G_o^{ref} [MPa]	$\gamma_{0.7}$
2°Deposit Gravel	400	0.0008
Top Dejection Cones	140	0.0001
1°Deposit Gravel	750	0.0011
Bottom Dejection Cones	240	0.0001

Table IV-9: Geotechnical Properties of Fine Profile- Model HSs- Rafael Iglesias (2014) [4]

Lithological Unit	Geotechnical Parameters	
	G_o^{ref} [MPa]	$\gamma_{0.7}$
Top Dejection Cones	140	0.0001
Bottom Dejection Cones	240	0.0001

4.2.3 Initial Conditions of Soil

When excavating a tunnel, the magnitude of the initial stress to be used as the starting point must be considered. In this thesis the "k_o procedure" type of calculation is used:
Ko procedure: Direct generation of initial effective stresses, pore pressures and states parameters.

The thrust coefficient at rest (k_o) is the ratio of the effective horizontal stress and the effective vertical stress.

$$\sigma'_v = \Sigma_i \gamma_i \cdot \Delta_{hi} - u_i$$

$$\sigma'_h = k_o \cdot \sigma'_v$$

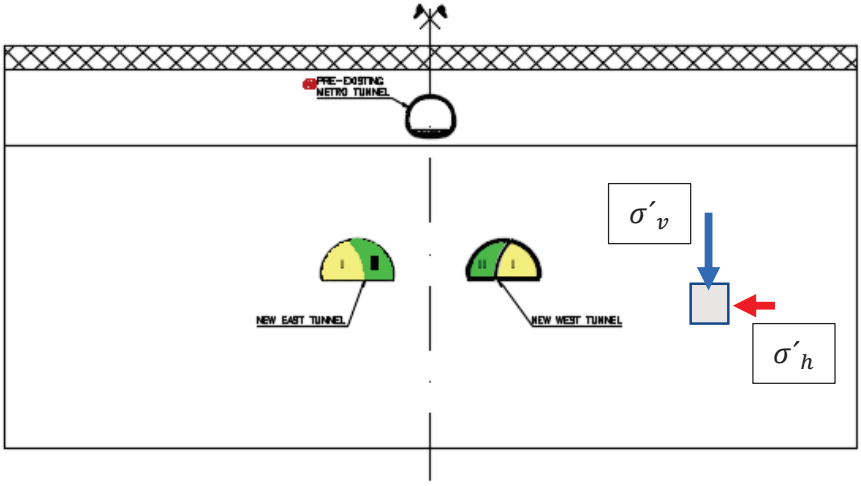


Figure IV-10: Magnitude and orientation of initial stresses

The k_o values used correspond to those shown in the Table IV-1, Table IV-2 and Table IV-3 for every soil type.

4.3. Pre-existing Metro Tunnel Modeling Consideration

4.3.1 Geometry of the Pre-existing Metro Tunnel

The geometry of the Metro Tunnel shown in Figure IV-11 is drawn in Plaxis through the "Tunnel Designer" module, where this objective is achieved through the radius of the circle, segment angles and start angles.

Table IV-10: Geometry of Metro Tunnel to represent the section in the “tunnel designer module”

Radius [m]	Segment angle [°]	Start angle [°]
9.80	17.95	0
2.65	63.32	19.88
6.65	22.92	83.21
4.15	49.11	107.69
5.65	23.19	156.81

The section drawn in the section design is as follows:

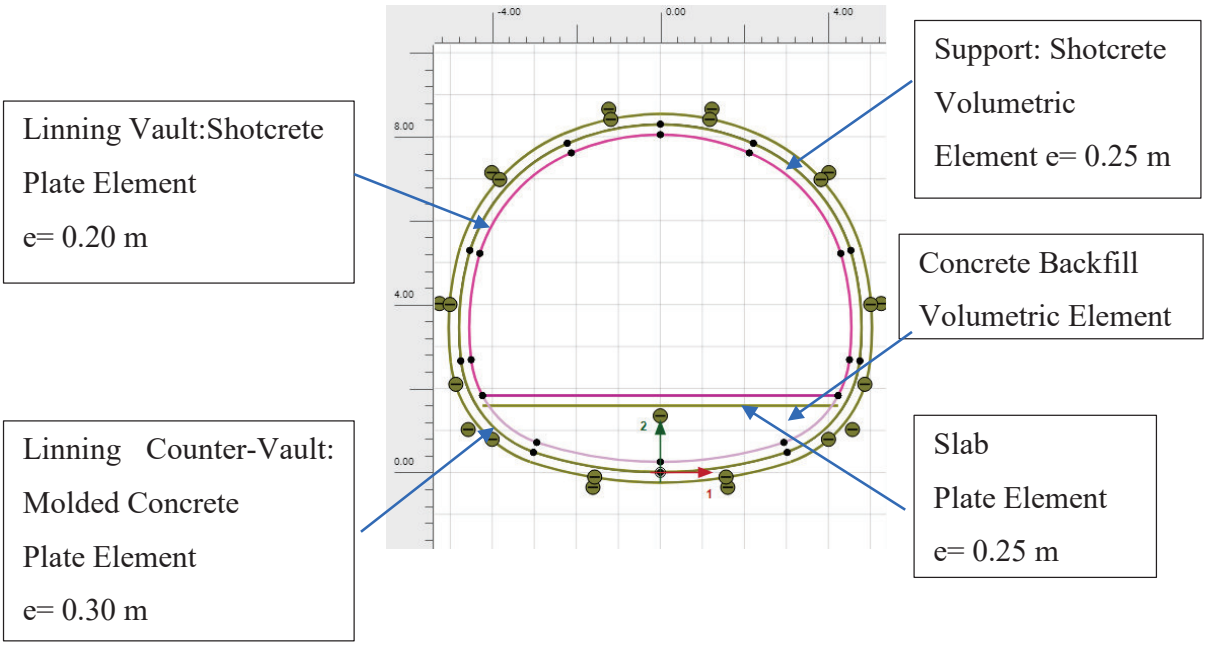


Figure IV-11: Draw of the Metro Tunnel in "Tunnel Designer Module"

4.3.2 Support Parameters of the Pre-existing Metro Tunnel

For modelling the shotcrete support (see Figure III-14), volumetric elements defined through the "Concrete Model" is used. To know in detail consists of it is recommended to review Annex II in section 2.2.1.

(a) Support Input Parameter for the Concrete Model

The parameters used in the concrete model for modelling the metro tunnel support are presented below.

Table IV-11: Parameters of the Concrete Model for Support of Metro Tunnel

SUPPORT: VOLUMETRIC ELEMENTS - CONCRETE MODEL			
Shotcrete G25 without Fiber, without Reinforcement of Steel			
Thickness	e	0.25	m
Unit weight of concrete	δ	25	kN/m^3
1_Stiffness Parameters (non-time dependent)			
Young's modulus	E28	12500	MPa
Poisson´s ratio	ν	0.2	-
2a_ Strength Parameters in Compression			
Uniaxial compressive strength 28 days	fc28	25	MPa
Normalised initially mobilised strength	fc0n	0.1	-
Normalised failure strength	fcfn	0.1	-
Normalised residual strength	fcun	0.1	-
Compressive fracture energy	Gc28	30	kN/m
Maximun Friction angle	ϕ	35	°
Dilatancy angle	ψ	0	°
Safety factor for compressive strength	γfc	1	-
2b_ Strength Parameters in Tension			
Uniaxial tensile strength 28 days	ft28	2.5	MPa
Ratio of residual vs peak tensile strength	ftun	0	-
Tensile fracture energy	Gt,28	0.05	kN/m
Safety factor for tensile strength	γft	1	-
2c_ Ductility			
Uniaxial plastic failure strain	εcp	-0.001	-
Increase εcp with increase of p	a	18	-
3_ Time dependent Parameters			
not employed			

The use of safety factors equal to 1 is because it is desired to bring the support of the Metro tunnel up to its capacity. Additionally, the time dependence of the strength and stiffness parameters is not considered because it is desired to know a final state of tensions.

4.3.3 Lining Parameters of the Pre-existing Metro Tunnel

For modelling the shotcrete reinforced with mesh and bars of steel lining (See Figure III-15), shell elements defined through the "Plate Element" from the PLAXIS is used. To know in detail consists of it is recommended to review in section 2.2.2 of Annex II.

(a) Lining Input Parameter for the Plate Element

The parameters used in the plate elements for modelling the lining are presented below.

Table IV-12: Parameters of the Plate Element for Vault Lining of Metro Tunnel

VAULT LINING: ELEMENT PLATE PLASTIC			
Shotcrete G25 without Fiber, with Reinforcement of Steel Mesh (C295 Ext, C378 Int)			
Thickness	e	0.2	m
Uniaxial compressive strength 28 days	f´c	25	MPa
Young's modulus	Ec	12500	MPa
Axial Stiffness	EA	2500000	kN m/m
Bending Stiffness	EI	8333.33	kN m^2/m
Poisson´s Ratio	v	0.2	
Unit weight of concrete Lining	δ	25	kN/m^3
Unit weight of concrete Support	γh	25	kN/m^3
Section Unit Weight	w	2.5	kN/m^2
Maximum bending moment	Mp	95	kN m/m
Maximum axial force	Np	4565	kN/m

Table IV-13: Parameters of the Plate Element for Counter-vault Lining of Metro Tunnel

CONTRAVAULT LINING: ELEMENT PLATE PLASTIC			
Molded concrete G25 without Fiber, with Reinforcement of steel mesh and bars (C295 Ext, C378 + Ø16 @30 Int)			
Thickness	e	0.3	m
Uniaxial compressive strength 28 days	f´c	25	MPa
Young's modulus	Ec	23500	MPa
Axial Stiffness	EA	7050000	kN m/m
Bending Stiffness	EI	52875.00	kN m^2/m
Poisson´s Ratio	v	0.2	
Unit weight of concrete Lining	δ	25	kN/m^3
Unit weight of concrete Support	γh	25	kN/m^3
Section Unit Weight	w	3.75	kN/m^2
Maximum bending moment	Mp	199	kN m/m
Maximum axial force	Np	7004	kN/m

4.3.4 Backfill Parameters of the Pre-existing Metro Tunnel

For modelling the backfill, volumetric elements defined through the "Elastic Model" from the PLAXIS constitutive models gallery are used.

Table IV-14: Parameters of the Elastic Model for Backfill of Metro Tunnel

CONCRETE BACKFILL: VOLUMETRIC ELEMENT – ELASTIC MODEL			
Molded Concrete G10			
Uniaxial compressive strength 28 days	f´c	10	MPa
Young's modulus	Ec	14863	MPa
Poisson´s ratio	v	0.2	
Unit weight of concrete	δ	25	kN/m^3

4.3.5 Plate Slab of Road Parameters of the Pre-existing Metro Tunnel

The parameters used in the plate elements for modelling the metro tunnel slab of floor are presented below.

Table IV-15: Parameters of the Plate Element for Slab of Metro Tunnel

ROAD SLAB: ELEMENT PLATE ELASTIC			
Molded Concrete G25			
Thickness	e	0.25	m
Uniaxial compressive strength 28 days	f´c	25	MPa
Young's modulus	Ec	23500	MPa
Axial Stiffness	EA	5875000	kN m/m
Bending Stiffness	EI	30598.96	kN m^2/m
Poisson´s Ratio	v	0.2	
Unit weight of concrete plate	δ	25	kN/m^3
Unit weight of concrete backfill	γh	25	kN/m^3
Section Unit Weight	w	3.125	kN/m^2

4.3.6 Relaxation Parameters of the Pre-existing Metro Tunnel

(a) Deconfinement (β-Method)

In PLAXIS 2D it is possible to simulate the construction process of tunnels with a sprayed concrete lining (NATM). The major point in such an analysis is to account for the three-dimensional arching effect that occurs within the soil and the deformations that occur around the unsupported tunnel face. A method that takes these effects into account is described below. There are various methods described in the literature for the analysis of tunnels constructed according to the New Austrian Tunnelling Method. One of these is the so-called convergence confinement method or β-method (Schikora & Fink, 1982 [13]).

The idea is that the initial stresses P_k acting around the location where the tunnel is to be constructed are divided into a part $(1 - \beta)\ P_k$ that is applied to the unsupported tunnel and a part $\beta\ P_k$ that is applied to the supported tunnel (Figure IV-12). The β-value is an 'experience value', which, among other things, depends on the ratio of the unsupported tunnel length and the equivalent tunnel diameter.

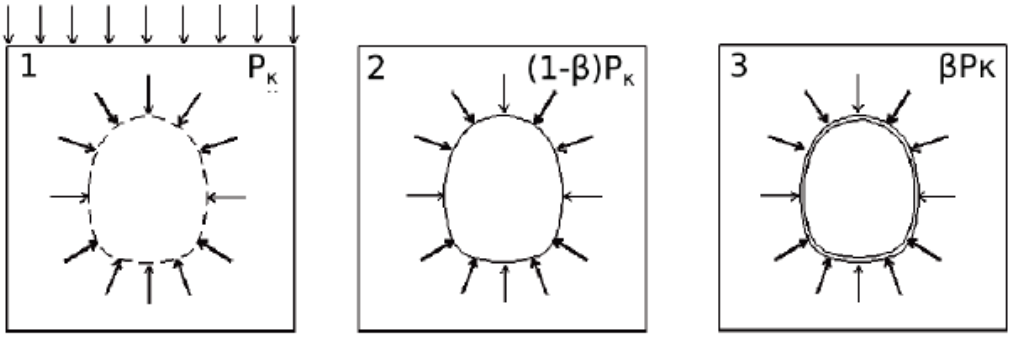


Figure IV-12: Schematic representation of the β-method for the analysis of NATM tunnels (Plaxis V24 Manual [19])

The process is summarized below:

1. Generate the initial stress field and apply eventual external loads that are present before the tunnel is constructed.
2. De-activate the tunnel clusters without activation of the tunnel lining and apply a deconfinement value of 1- β. The value entered is in percentage.
3. Activate the tunnel lining to the soil clusters inside the tunnel and check that deconfinement of the soil clusters inside the tunnel is set to 100%.

(b) Relaxation Parameters used for Modelling Metro Tunnel

In studies carried out for the design of tunnels in Santiago (Bard et al, 2008 [14]), with characteristics and dimensions similar to those considered in the models analyzed, a stress relaxation prior to the placement of the support of the order of 60% has been estimated, and of 80% after the placement of the support. Thus, the relaxation values adopted for the respective construction sequences are the following:

Excavation: (1-β) = 60%

Application and Hardening of the Support: 100%

4.3.7 Sequence Construction of the Pre-existing Metro Tunnel

The construction of the Metro tunnel is considered to have been carried out in full section, that is, the 68.90 m2 were excavated in a single phase. The modeled construction process is described below.

(a) Construction Stage of the Pre-existing Metro Tunnel

- **Phase 1:** Initial Stress and Phase 2: Activation Traffic Overload

In the first phase, the initial stress state is defined using the "ko procedure" method, as explained in the section 4.2.3. In the next phase the 10 kPa traffic overload defined in section 4.1.4 is activated.

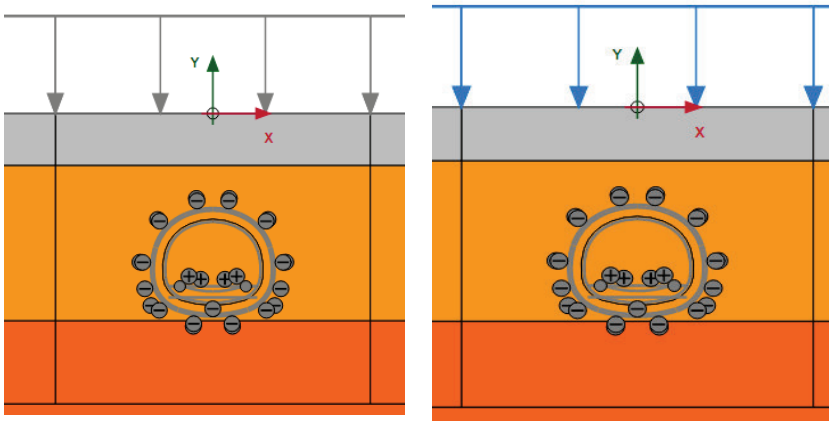


Figure IV-13: Phase 1- Definition the Initial Stress State (left) and Phase 2- Activation of Traffic Overload (right)

- **Phase 3:** Full Section Excavation

  In the third phase, the tunnel is excavated in full section with the relaxation defined in section 4.3.6(a).

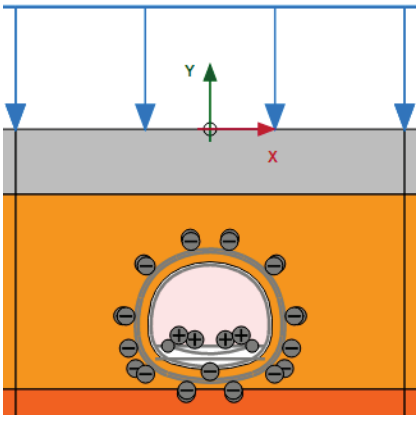


Figure IV-14: Phase 3- Excavation of Metro Tunnel in Full Section

- **Phase 4:** Installation of Support

The interface is activated according to the guidelines defined in section 4.6 and the support defined in section 4.3.2 is installed.

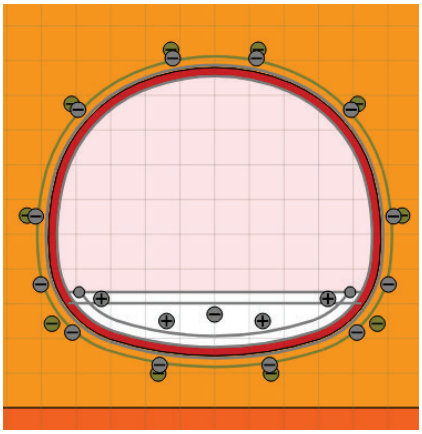


Figure IV-15: Phase 4- Interface and Support activated

- **Phase 5:** Installation of Lining and Phase 6: Backfill Concrete and Road Slab construction

The interface is activated according to the guidelines defined in section 4.6 and the lining defined in section 4.3.3 is installed.

The backfill concrete is installed as defined in section 3.4.3(c) and the road slab is constructed as defined in section 3.4.3(d).

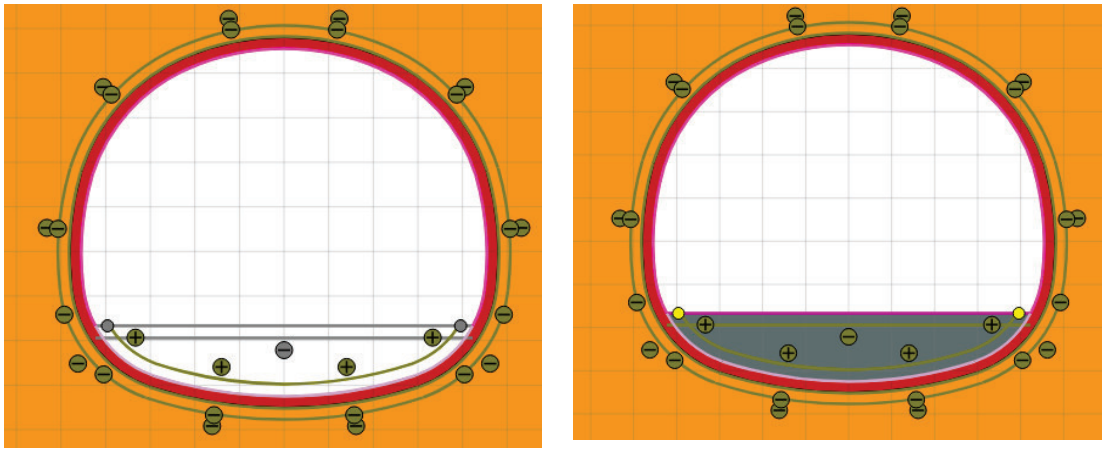


Figure IV-16: Phase 5- Interface and Lining activated and

Phase 6- Backfill concrete and Road Slab are installed

(b) Final Stage of the Pre-existing Metro Tunnel

A long-term situation is studied where the support and the soil are degraded. This hypothesis is a conservative criterion considering that many lines of the Santiago de Chile Metro are around 20 years old since their construction until now. For this purpose, a degradation parameter α is used and the soil area involved is defined as follows.

Where:

$H = 3R = 15\ m$ Degradation Distance,

R= Equivalent Radio of the Tunnel.

$\alpha = 0.5$ Degradation Factor

Area with properties degraded

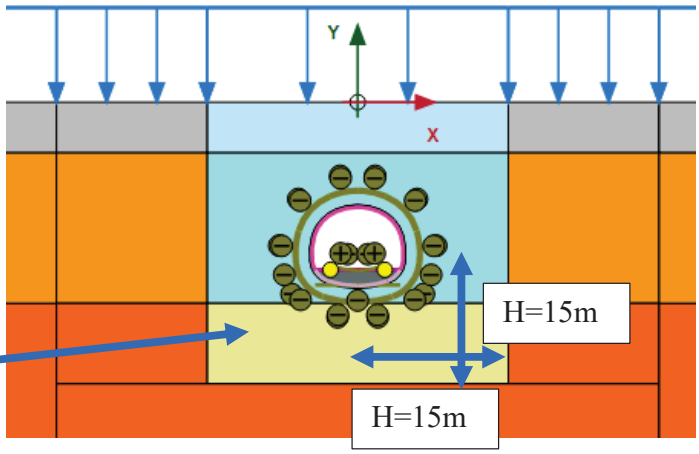


Figure IV-17: Definition of degraded soil area of the Metro Tunnel

- **Phase 7:** Degradation of Support

Support is degraded using the same factor α=0.5 defined above.

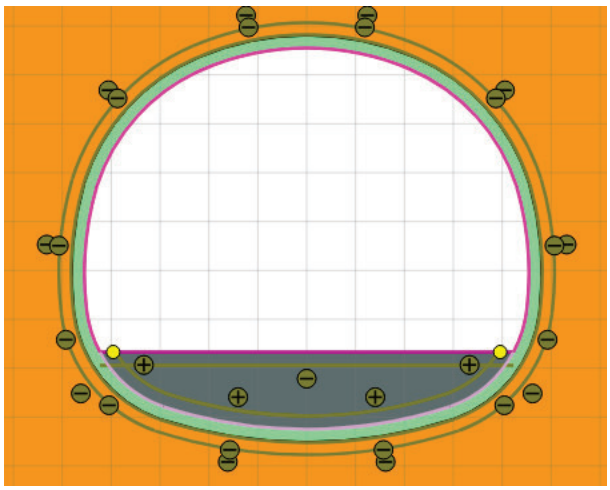


Figure IV-18: Phase 7- Degradation of Support of the Metro Tunnel

- **Phase 8:** Degradation of Soil

The soil around the tunnel is degraded using the factor a=0.5 defined above.

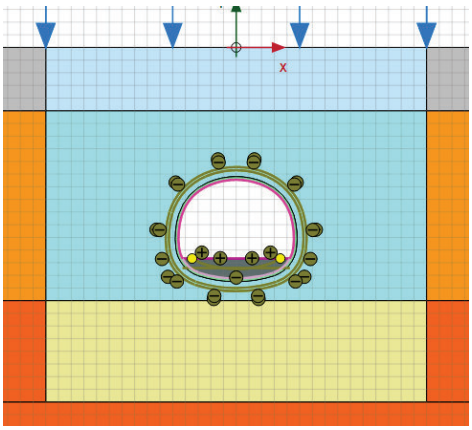


Figure IV-19: Phase 8- Degradation of Soil around of the Metro Tunnel

4.4. Pre-existing Building Modeling Consideration

4.4.1 Geometry of the Pre-existing Building

The walls and slabs of the building structure are modeled as *plate elements*, with elastic behavior (Figure IV-20). While the superficial foundation bases are modeled as *volumetric elements*, with elastic behavior (See Figure IV-21), and deep foundation with *embedded bean row*. (See Figure IV-22).

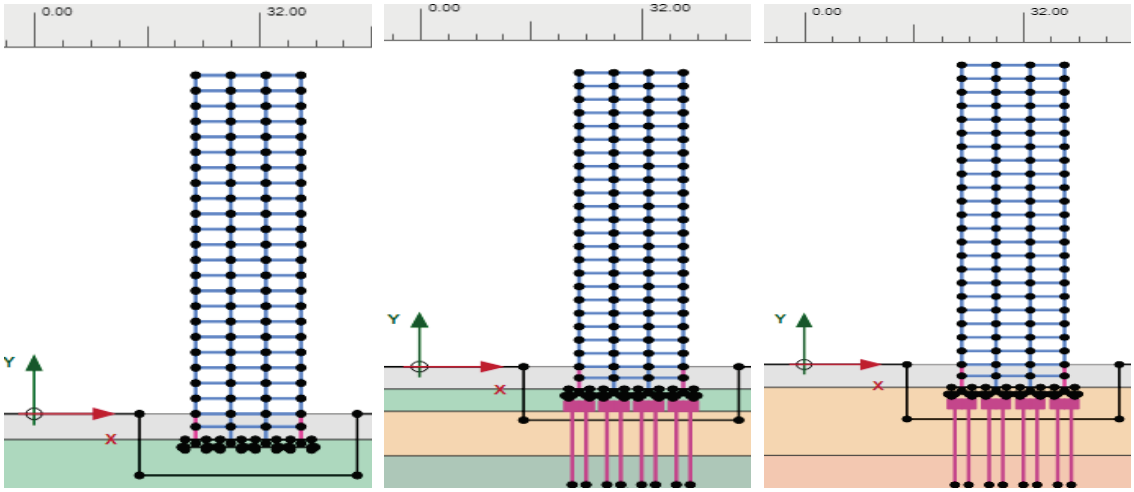


Figure IV-20: Building Modeling for Gravel (Left), Mixed (Center) and Fine (Right).

In addition, the superficial foundation of the study building with its respective interfaces is shown.

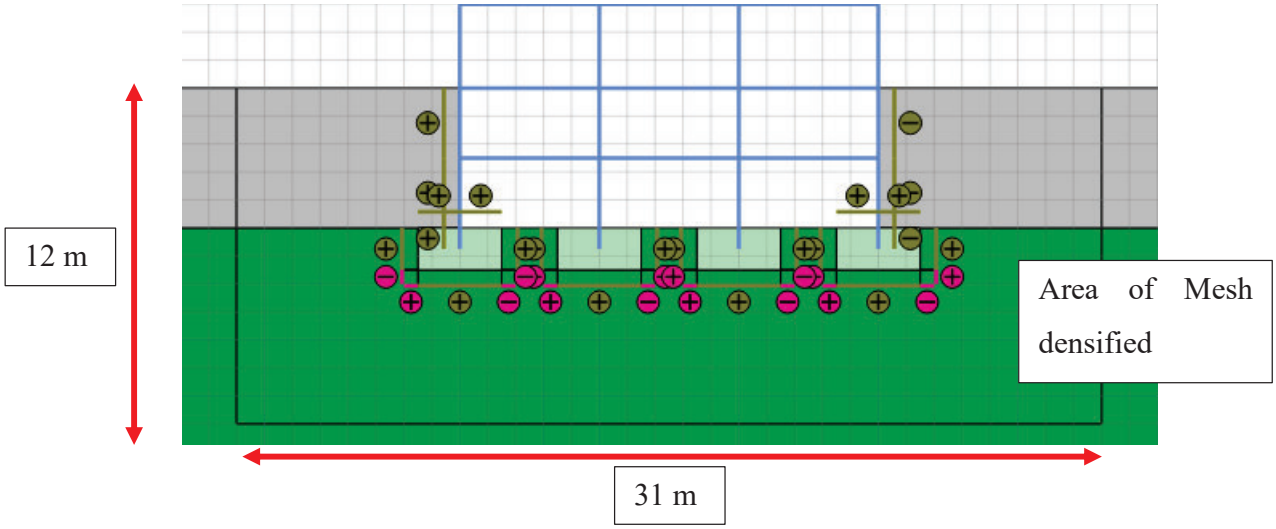


Figure IV-21: Modeling of the Superficial Foundation of the Building, for Gravel only

Also in the previous image you can see the delimited area where the finite element mesh is densified.

Finally, the deep foundation of the study building with its respective interfaces is shown.

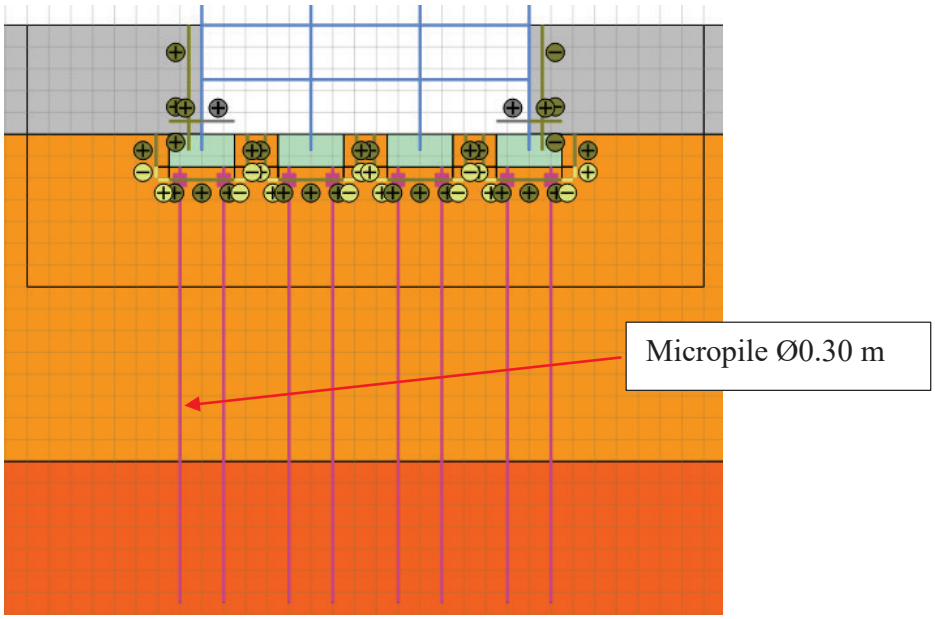
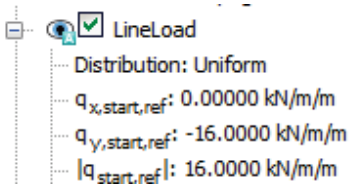


Figure IV-22: Modeling of the deep Foundation of the Building, for Mixed and Fine

4.4.2 Load to be Applied

The linearly distributed load of 16 kPa over each slab of the building is shown below.



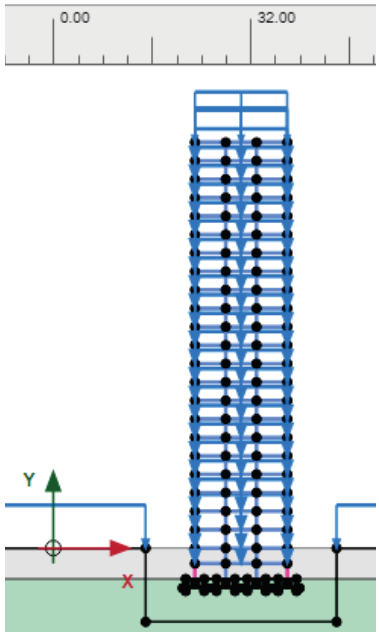


Figure IV-23: Modeling of the Building Loads

4.4.3 Structure and Foundation Input Parameters for the models

The parameters used in modelling the building structure (Table IV-16 y Table IV-17), modelling the isolated foundations in gravel soil (Table IV-18), and modelling the micropiles in mixed and fine soils (Table IV-19) are presented below.

Table IV-16: Parameters of the Plate Element for Structures of Walls and Slabs

STRUCTURES OF WALLS - SLABS: ELEMENT PLATE - ELASTIC			
Molded concrete G25 Reinforcement with Steel Bars			
Thickness	e	0.25	m
Uniaxial compressive strength 28 days	f´c	25	MPa
Young's modulus	Ec	23500	MPa
Axial Stiffness	EA	5875000	kN m/m
Bending Stiffness	EI	30598.96	kN m^2/m
Poisson´s Ratio	v	0.2	
Unit weight of concrete Lining	δ	25	kN/m^3
Section Unit Weight	w	6.25	kN/m^2

Table IV-17: Parameters of the Plate Element for Structures of Underground walls

STRUCTURES OF UNDERGROUND WALLS: ELEMENT PLATE - ELASTIC			
Molded concrete G25 Reinforcement with Steel Bars			
Thickness	e	0.5	m
Uniaxial compressive strength 28 days	f´c	25	MPa
Young's modulus	Ec	23500	MPa
Axial Stiffness	EA	11750000	kN m/m
Bending Stiffness	EI	244791.67	Kn m^2/m
Poisson´s Ratio	ν	0.2	
Unit weight of concrete Lining	δ	25	kN/m^3
Section Unit Weight	w	12.5	kN/m^2

Table IV-18: Parameters of the Volumetric Element for Superficial Foundation of Building in Gravel

FOUNDATION BASES: VOLUMETRIC ELEMENT - ELASTIC			
Molded Concrete G25			
Uniaxial compressive strength 28 days	f´c	25	MPa
Young's modulus	Ec	23500	MPa
Poisson´s ratio	ν	0.2	
Unit weight of concrete	δ	25	kN/m^3

Table IV-19: Parameters of the Embedded bean row for Deep Foundation of Building in Mixed and Fine

MICROPILE: ELEMENT EMBEDDED BEAM ROWS - ELASTIC			
Molded concrete G25: massive circular beam			
Young's modulus of concrete	Ec	23500	MPa
Unit weight of Micropile	γ	25	kN/m^3
Diameter of the Micropile	Ø	0.3	m
Longitudinal Separation	Lspacing	1.00	m
For Mixed Soil			
Axial skin resistance	Tmax	107	kN/m
Base Resistance	Fmax	0	kN
For Fine Soil			
Axial skin resistance	Tmax	93	kN/m
Base Resistance	Fmax	0	kN

4.5. New Tunnels Modeling Consideration

4.5.1 Geometry of the New Tunnels

The geometry of the new road Tunnels shown in Figure IV-24 is drawn in Plaxis through the "Tunnel Designer" module, where this objective is achieved through the radius of the circle, segment angles and start angles.

Table IV-20: Geometry of New East Tunnel to represent the section in the "tunnel designer module"

Radius [m]	Segment angle [°]	Start angle [°]
2.55	14.71	67.59
5.70	27.15	83.15
7.40	55.21	110.30
7.40	14.48	165.52
10.96	44.20	90.00

Table IV-21: Geometry of New West Tunnel to represent the section in the "tunnel designer module"

Radius [m]	Segment angle [°]	Start angle [°]
2.55	14.71	67.59
5.70	27.15	83.15
7.40	55.21	110.30
7.40	14.48	165.52
-10.96	44.20	90.00

The section drawn in the section design is as follows:

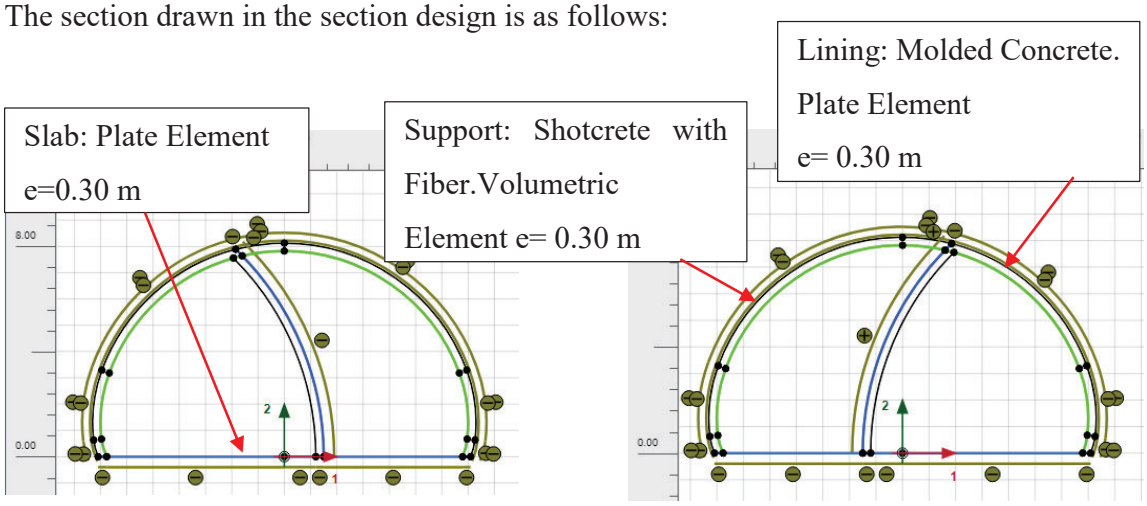


Figure IV-24: Draw of the New East and West Tunnels in "Tunnel Designer Module"

The last row of Table IV-20 and Table IV-21 correspond to the geometric properties of the temporary wall of each of the new tunnels.

4.5.2 Support Parameters of the New Tunnels

For modelling the shotcrete reinforced with fiber and frame steel as support, volumetric elements defined through the "Concrete Model" from the PLAXIS constitutive models gallery are used. This model is explained in detail in the section 2.2.1, Annex II, and the parameters used for the modeling are presented below.

Table IV-22: Parameters of the Concrete Model for Support of New Road Tunnels

SUPPORT: VOLUMETRIC ELEMENTS - CONCRETE MODEL			
Shotcrete G25 with Fiber Steel "3c", with Frame Steel LG 115/32/22			
Thickness	e	0.3	m
Unit weight of concrete	δ	25	kN/m^3
1_Stiffness Parameters (non-time dependent)			
Young's modulus	E28	12500	MPa
Poisson´s ratio	v	0.2	-
2a_ Strength Parameters in Compression			
Uniaxial compressive strength 28 days	fc28	25	MPa
Normalized initially mobilized strength	fc0n	0.1	-
Normalized failure strength	fcfn	0.1	-
Normalized residual strength	fcun	0.1	-
Compressive fracture energy	Gc,28	30	kN/m
Maximum Friction angle	ϕ	35	°
Dilatancy angle	ψ	0	-
Safety factor for compressive strength	γfc	1.5	-
2b_ Strength Parameters in Tension			
Uniaxial tensile strength 28 days	ft28	2.5	MPa
Ratio of residual vs peak tensile strength	ftun	0	-
Tensile fracture energy	Gt,28	0.71	kN/m
Safety factor for tensile strength	γft	1.5	-
3_Time- dependent parameters			
Time for full hydration	thydr	28	days
Continuation			

3a_Stiffness			
Time- dependency ratio of elastic stiffness	E1/E28	0.4	-
3b_Strength			
Time- dependency of compressive strength	f'c1/f'c28	0.4	-
3c_Ductility			
Uniaxial plastic failure strain at 1 hour	εcp.1h	-0.01	-
Uniaxial plastic failure strain at 8 hour	εcp.8h	-0.001	-
Uniaxial plastic failure strain at 24 hour	εcp.24h	-0.0007	-
Increase εcp with increase of p	a	18	-
3d_Shrinkage			
Not employed			
3e_Creep			
Not employed			

The following parameters are highlighted as being used in the concrete model of the new road tunnels.

(a) Safety Factors

Safety factors of 1.5 for compression and tension are used because the support for the new tunnels is being designed. Unlike the support for the metro tunnel, where a value of 1 was used because it was desired to know the stress state with the maximum capacity of the support.

(b) Consideration of Steel Fibers

The concrete model allows to consider the contribution of the fiber through the parameter G_{t28}. Which can be estimated through the correlation proposed by Barros & Figueiras (1999) [15].

$$G_{t28} = \left(1 + 13.159 \cdot w_f^{1.827}\right) \cdot G_{t0}$$

Where:

G_{t28}: The fracture energy of plain shotcrete in the 28 days

$G_{t0} = 0.05 \frac{kN}{m}$: The fracture energy of plain shotcrete

$W_f = 25 \frac{kg}{m^3}$: fiber content [kg/m3]

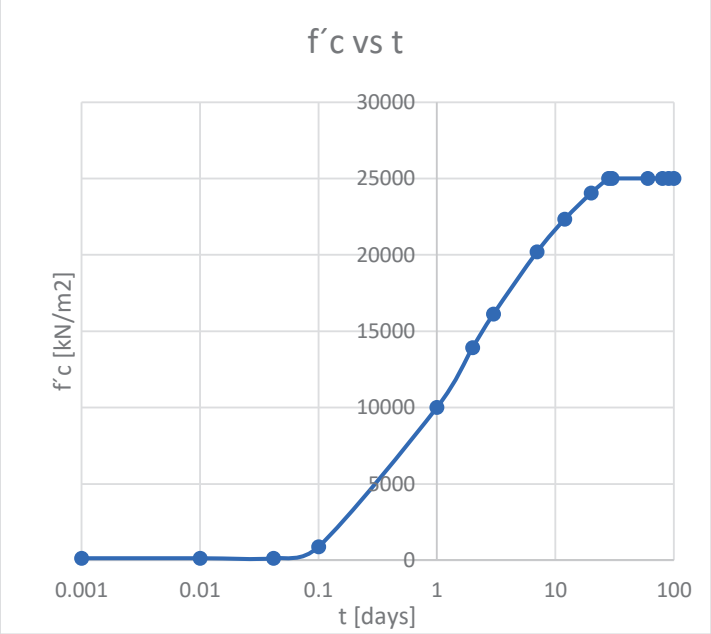
$w_f = 1\%$: fiber percentage in weigh

Finally:

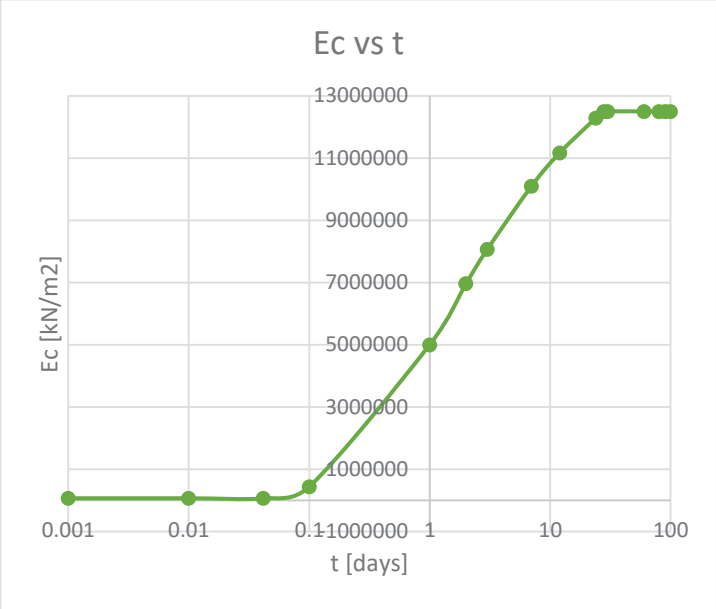
$$G_{t28} = (1 + 13.159 \cdot 1^{1.827}) \cdot 0.05 \frac{kN}{m} = 0.71 \frac{kN}{m}$$

(c) Time- dependent parameters

The hardening process of concrete is considered over time, through the following laws of variation of the Young modulus and the characteristic compressive strength, according to the guidelines explained in Annex II, section 2.2.1.



Graph IV-1: Law of variation of compressive strength (f´c) with time (t)



Graph IV-2: Law of variation of Young´s module (Ec) with time (t)

4.5.3 Lining Parameters of the New Road Tunnels

For modelling the molded concrete reinforced with mesh of steel lining, shell elements defined through the "Plate Element" from the PLAXIS is used.

Table IV-23: Parameters of the Plate Element for Lining of New Road Tunnels

LINING: ELEMENT PLATE ELASTIC			
Molded concrete G25 Reinforcement with Steel Mesh ACMA 335 (Ext, Int)			
Thickness	e	0.3	m
Uniaxial compressive strength 28 days	f´c	25	MPa
Young's modulus	Ec	23500	MPa
Axial Stiffness	EA	7050000	kN m/m
Bending Stiffness	EI	52875.00	kN m^2/m
Poisson´s Ratio	v	0.2	
Unit weight of concrete Lining	δ	25	kN/m^3
Unit weight of concrete support	γh	25	kN/m^3
Section Unit Weight	w	3.75	kN/m^2

Elastic behaviour is adopted to design the lining because the final stress state in service involves soil degradation. For this to be possible, it is necessary for the lining to have elastic behaviour, obtaining a very rigid structure (conservative design criterion).

4.5.4 Temporal Walls of New Tunnels

The temporary walls have a 0.30 m thick support with the same characteristics defined in section 4.5.2.

4.5.5 Backfill Parameters of the New Road Tunnels

In cases where a section of the new tunnels with a counter-vault section is being studied, it will be necessary to backfill concrete; for this, the same material defined in section 4.3.4 and the Table IV-14 is used.

4.5.6 Plate Slab of Road Parameters of the New Road Tunnels

The parameters used in the plate elements for modelling the new road tunnels slab of floor are presented below.

Table IV-24:Parameters of the Plate Element for Slab of New Road Tunnels

ROAD SLAB: ELEMENT PLATE - ELASTIC			
Molded concrete G25 Reinforcement with Steel Bars			
Thickness	e	0.3	m
Uniaxial compressive strength 28 days	f´c	25	MPa
Young's modulus	Ec	23500	MPa
Axial Stiffness	EA	7050000	kN m/m
Bending Stiffness	EI	52875.00	kN m^2/m
Poisson´s Ratio	ν	0.2	
Unit weight of concrete plate	δ	25	kN/m^3
Unit weight of concrete Backfill	γh	25	kN/m^3
Section Unit Weight	w	3.75	kN/m^2

4.5.7 Relaxation Parameters of the New Road Tunnels

For the simulation of the construction process of new road tunnels, the Convergence confinement method or β-method described in section 4.3.6(a) is used.

To determine the relaxation values used, the convergence curve of the soil and the moment where the shotcrete support is applied must be determined.

To do this, a simplified auxiliary model is created in the Plaxis program with the equivalent radius of the section of the phase to be excavated, without modeling the support, with the objective of obtaining the characteristic convergence curve of each soil.

Subsequently, the Vlanchopuolus & Diederichs [10] criterion is used to determine the deformation at which the support is installed. For this, the equivalent radius, the advance pass and the plastic radius (determined in the numerical modeling) are required as input data. For example, for the gravel profile, we have:

At	51.320	m2	Tunnel Area		
Plaxis Model with equivalent Radius (Re) for circular Tunnel					
De	8.09	m	Equivalent Diámeter		
r0	4.045	m	Tunnel Radius (equivalent)		
rpm	7	m	Circular Tunnel Plastic Radius (equivalent) Plaxis model		
x	1	m	Distance from tunnel face		

Input parameters of the diagram V&D

Diagram Vlanchopuolus & Diederichs		
x/r0	0.25	
rpm/r0	1.73	
Output parameters of the diagram V&D		
ui/uim	**0.42**	Deformations Ratio from Diagram Vlanchopuolus & Diederichs

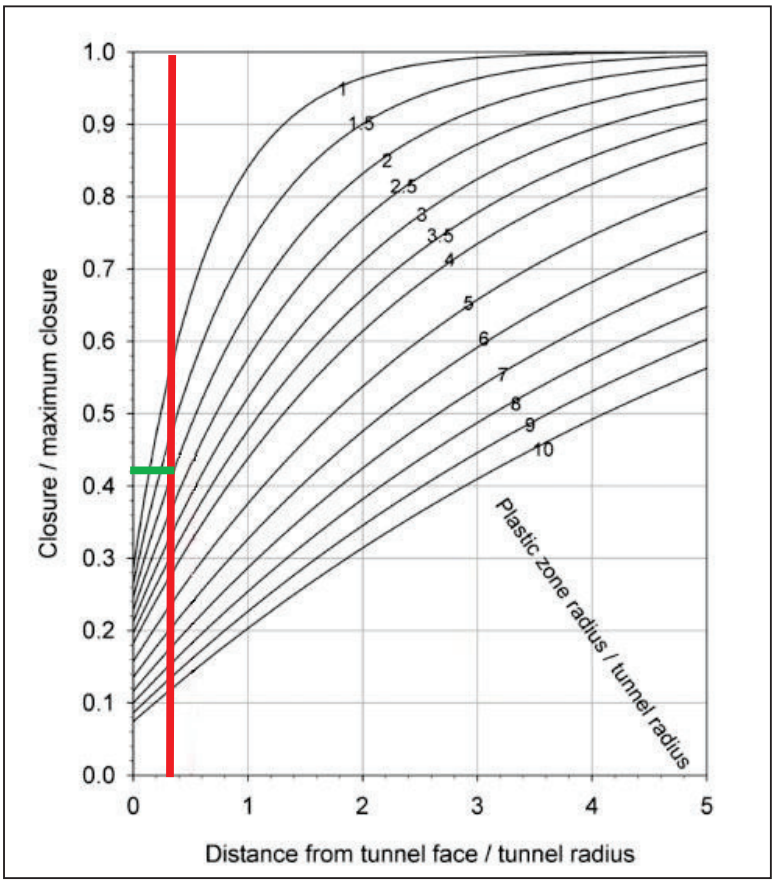
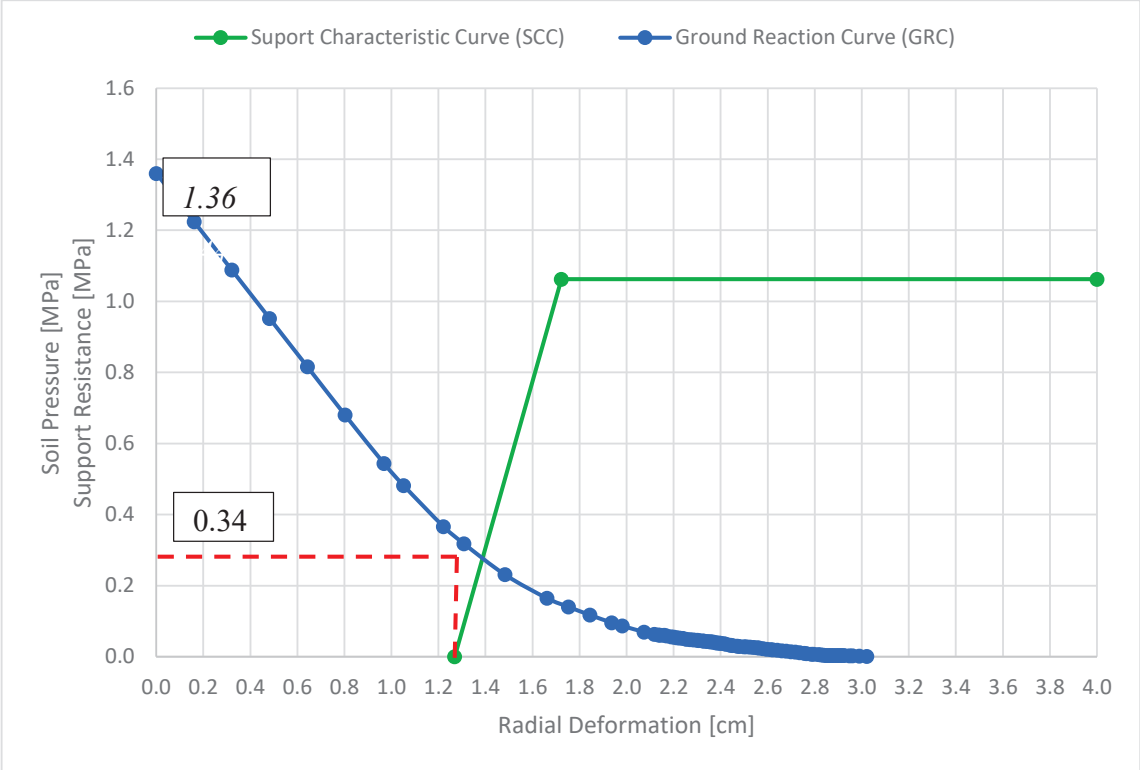


Figure IV-25: Graph of Vlanchopuolus & Diederichs

From Plaxis model with Equivalent Section

uim	0.0302	m	Maximum Deformation Plaxis model
ui	0.0127	m	Deformation where the support is installed

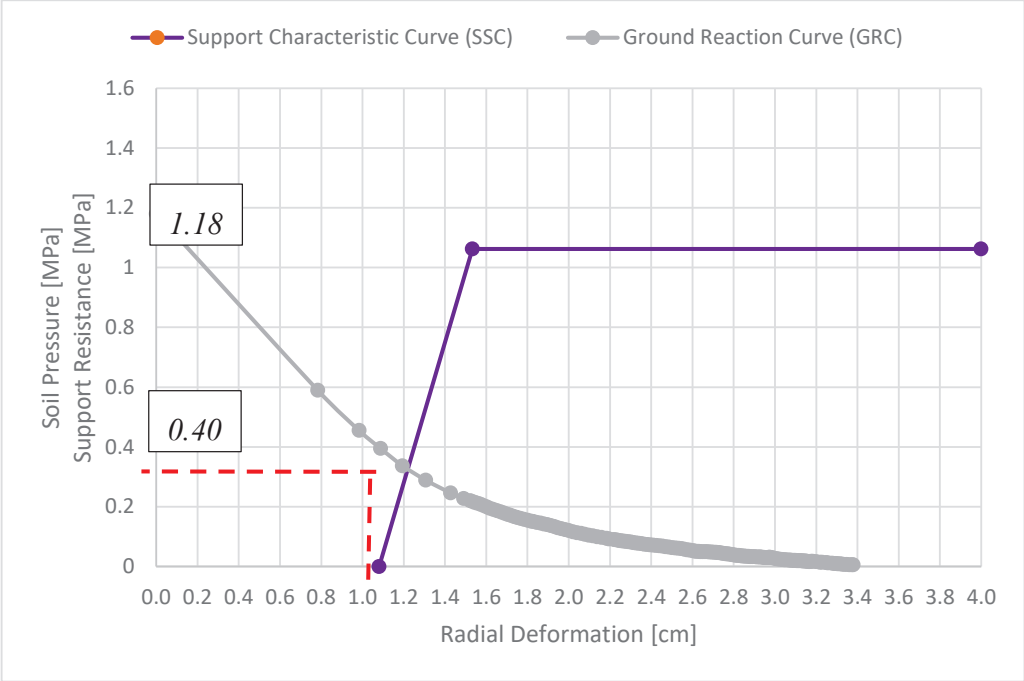
Finally, we have:



Graph IV-3: Convergence – Confinement Curve of Gravel Profile

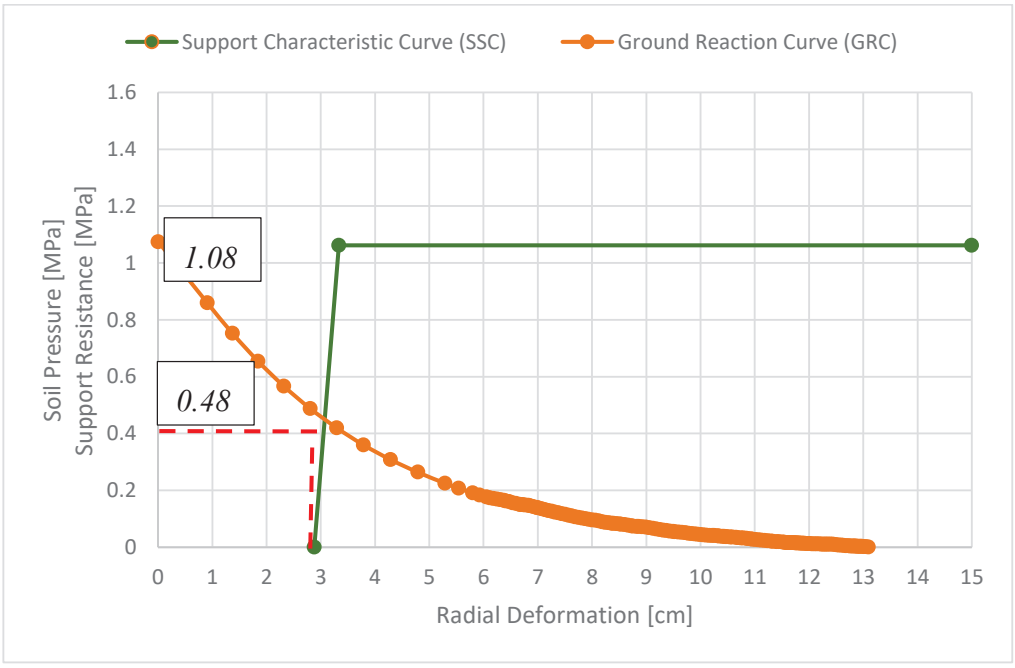
$$Deconfinement = (1-\beta) = \left(\frac{P_o - P_{support}}{P_0}\right) = \left(\frac{1.36 - 0.34}{1.36MPa}\right) MPa \times 100 = 75\%$$

Applying the same procedure for the mixed and fine profiles, the following characteristic curves are obtained.



Graph IV-4: Convergence – Confinement Curve of Mixed Profile

$$Deconfinement = (1-\beta) = \left(\frac{P_o - P_{support}}{P_0}\right) = \left(\frac{1.18 - 0.40}{1.18MPa}\right) MPa \times 100 = 66\%$$



Graph IV-5: Convergence – Confinement Curve of Fine Profile

$$Deconfinement = (1-\beta) = \left(\frac{P_o - P_{support}}{P_0}\right) = \left(\frac{1.08 - 0.48}{1.08MPa}\right) MPa \times 100 = 55\%$$

The relaxation or deconfinement values adopted in the modeling are summarized below.

Table IV-25:Summary Relaxation adopted for New Road Tunnels

Section	N° Phases	Phase	Req	Gravel	Mixed	Fine
With Slab of Floor Plane	2	I/II	4.00	75%	65%	55%

4.5.8 Sequence Construction of the New Road Tunnels

The construction of the new road tunnels is considered to be carried out in two areas, according to the methodology described in section 3.3.3. The modeled construction process is described below.

(a) Construction Stage of the New Road Tunnels

- **Phase 9:** Excavation Phase I of the West Road Tunnel

Previous to the beginning of the first phase of excavation of the west tunnel, the displacements are reset to zero, so that all the observed deformations correspond to those produced by the excavation of the new road tunnels. Phase I of the west tunnel is excavated.

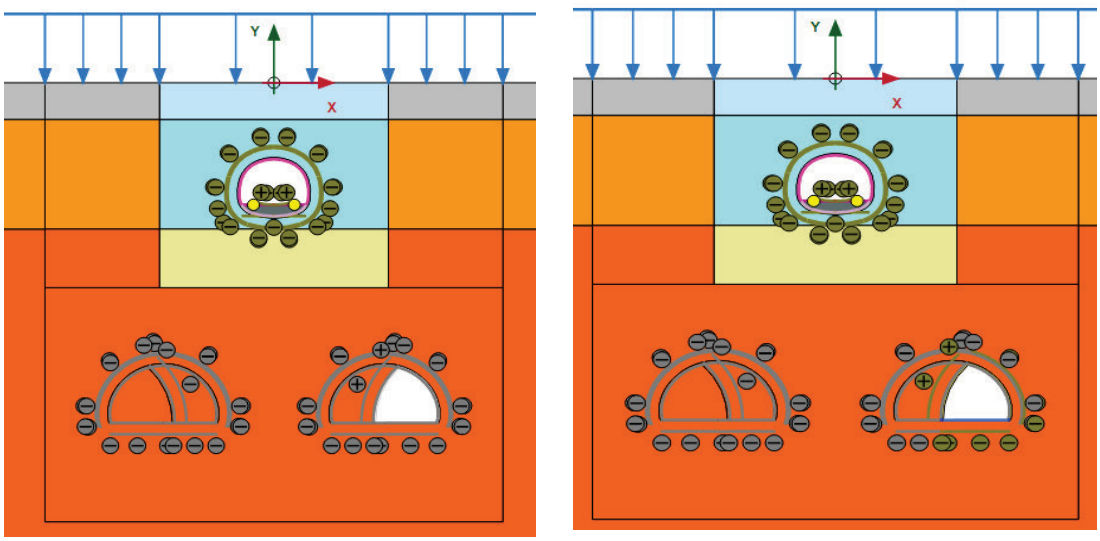


Figure IV-26: Phase 9 and Phase 10- Excavation and Installation of support of Phase I of the West Road

- **Phase 10:** Installation of Support

The interface is activated according to the guidelines defined in section 4.6 and the support defined in section 4.5.2 is installed.

- **Phase 11 y 12:** Excavation and Installation Support of Phase II of the West Road Tunnel

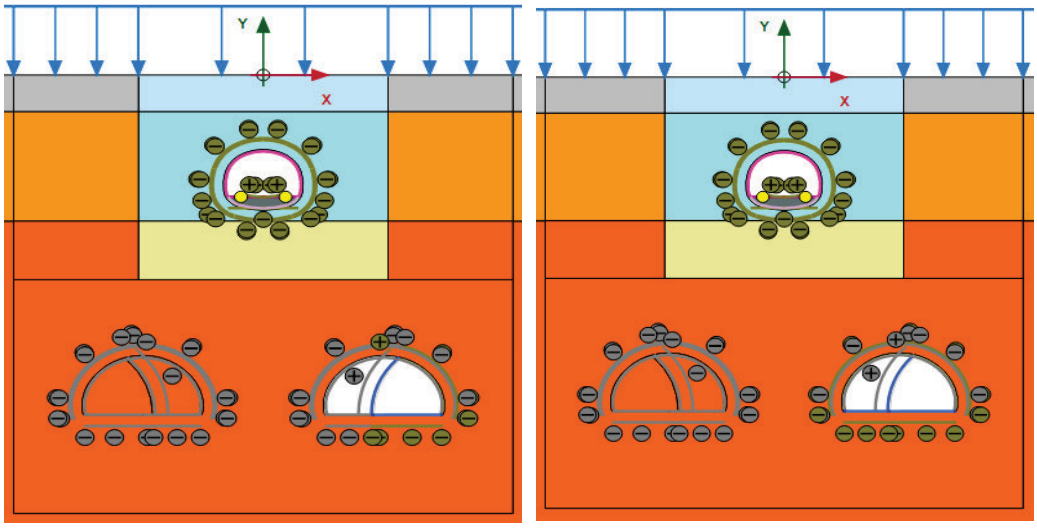


Figure IV-27: Phase 11 and Phase 12- Excavation and Installation of support of Phase II of the West Road Tunnel

- **Phase 13:** Demolition Temporal Wall of the West Road Tunnel

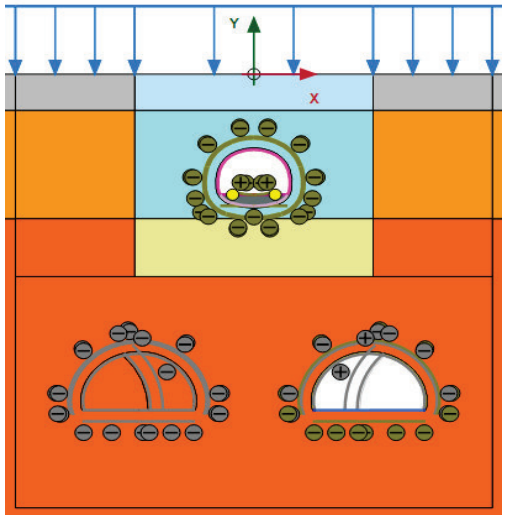


Figure IV-28: Phase 13-Demolition Temporal Wall of the West RoadTunnel

- **Phase 14:** Excavation and Installation Support of Phase I of the East Road Tunnel

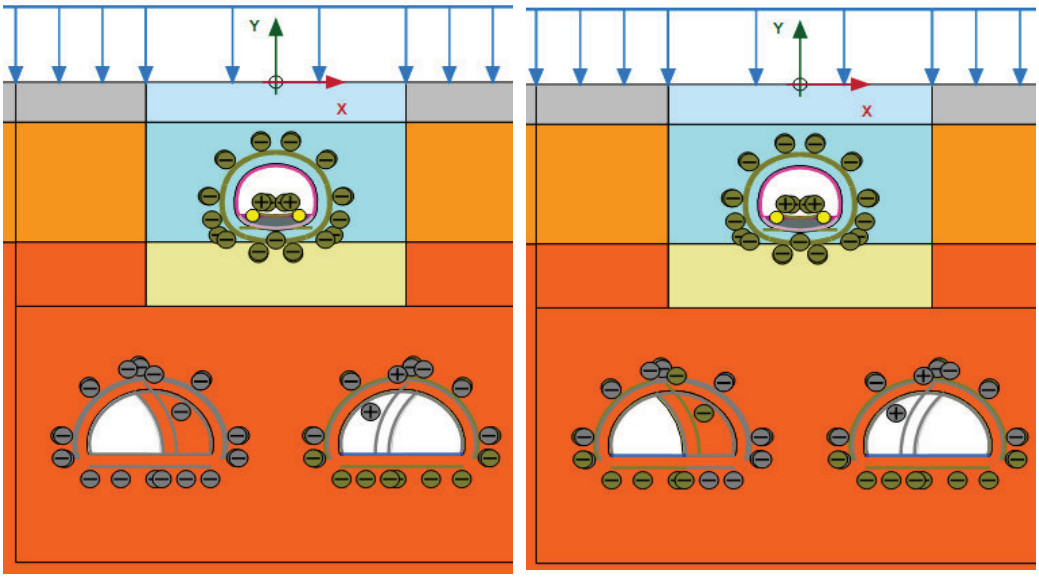


Figure IV-29: Phase 14- Excavation and Installation Support of Phase I of the East Road Tunnel

- **Phase 15:** Excavation and Installation Support of Phase II of the East Road Tunnel

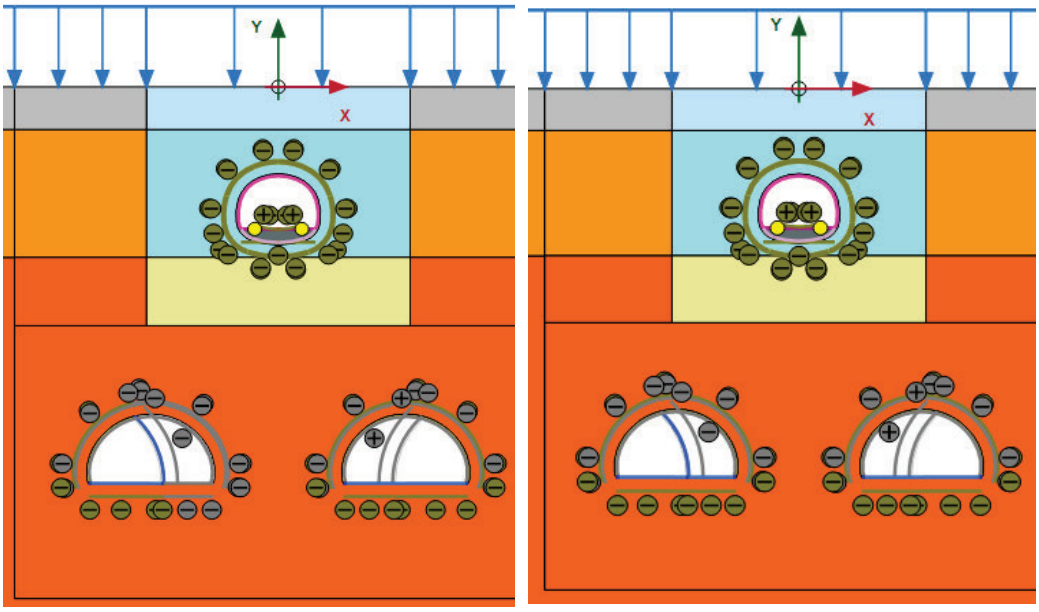


Figure IV-30: Phase 15- Excavation and Installation Support of Phase II of the East Road Tunnel

- **Phase 16:** Demolition Temporal Wall of the East Road Tunnel

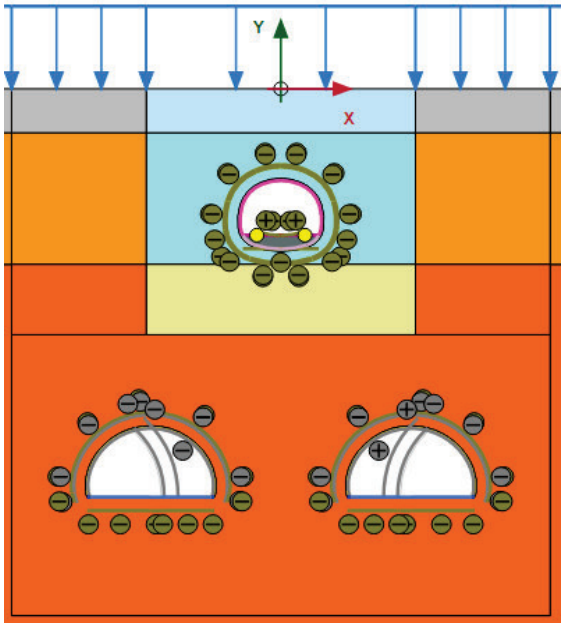


Figure IV-31: Phase 16 - Demolition Temporal Wall of the East Road Tunnel

- **Phase 17:** Installation of the lining in the both New Road Tunnels

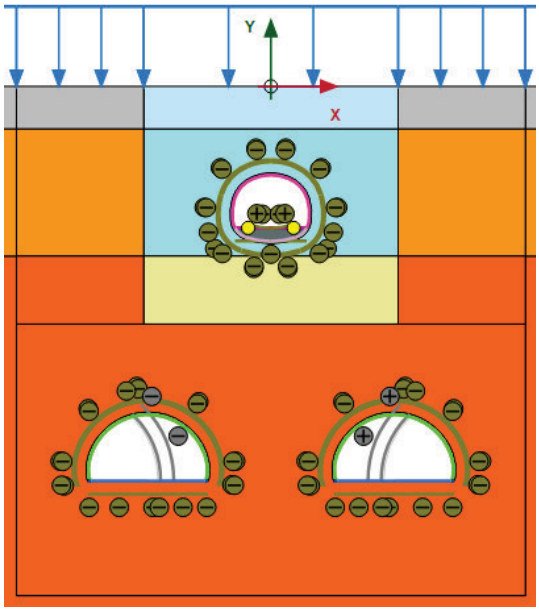


Figure IV-32: Phase 17- Installation of the Lining in the both New Road Tunnels

(b) Final Stage of the New Road Tunnels

The stresses and deformations produced by the degradation of the support and the soil are studied as a long-term service scenario. The following hypotheses are considered:

- **Service Loads:** a traffic load of 10 kN/m2 is applied to the road surfaces of the new road tunnels and a load of 45 kN/m is applied to the road surfaces of the Metro tunnel, according section 4.1.5
- **Support degradation:** the support is considered to have degraded over the long term, losing the resistance provided by the steel fibers.
- **Soil degradation:** the support is considered to have degraded over the long term, losing the resistance provided by the steel fibers.

  Soil degradation: a degradation length of 15 m is considered on each side of the new road tunnels, a concept identical to that used in Figure IV-17 for Metro Tunnel, obtaining an area of 60m x 32m of soil, degrading its resistant properties by a factor α=0.667.

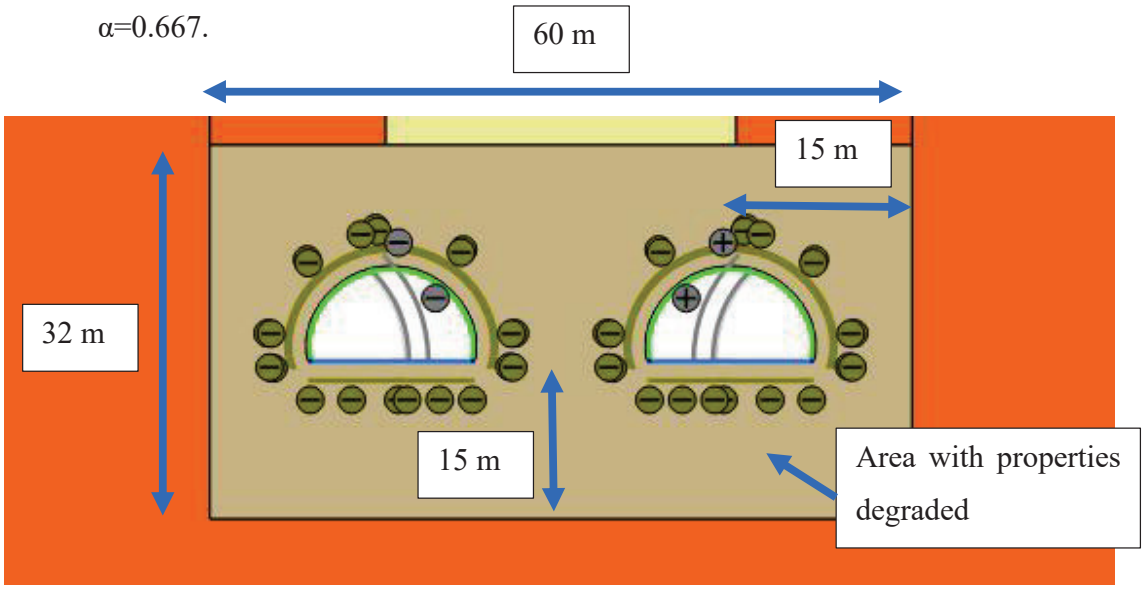


Figure IV-33: Definition Degradation Area for New Road Tunnels

Where:

H=2R = 15 m Degradation Distance

R= Equivalent Radio of the Tunnel

α=0.667 Degradation Factor

Important Note: the degradation factor of α= 0.667 is higher than that used for the metro tunnel of α= 0.5 because the new tunnels are located at a greater depth, which means that the plastification or softening could be less.

Finally, the final phases of excavation will be:

- **Phase 18:** Application of the Service Loads

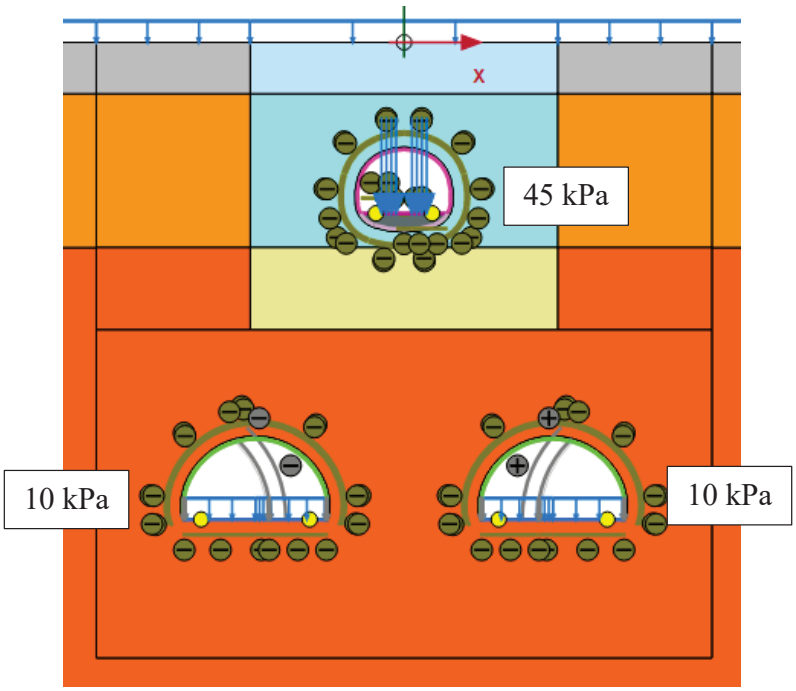


Figure IV-34: Phase 18- Application of the Service Loads

- **Phase 19:** Degradation of the Support of the New Road Tunnels

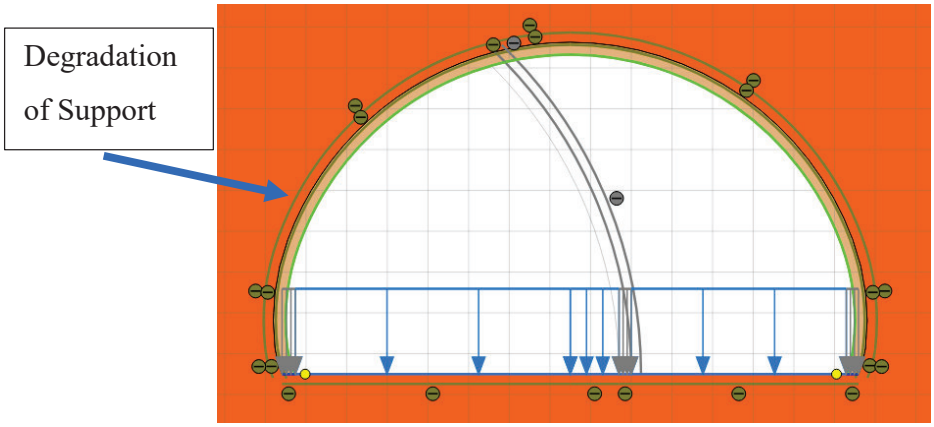


Figure IV-35: Phase 19- Degradation of the Support of the new road Tunnels

- **Phase 20:** Degradation of the Soil around of the New Road Tunnels

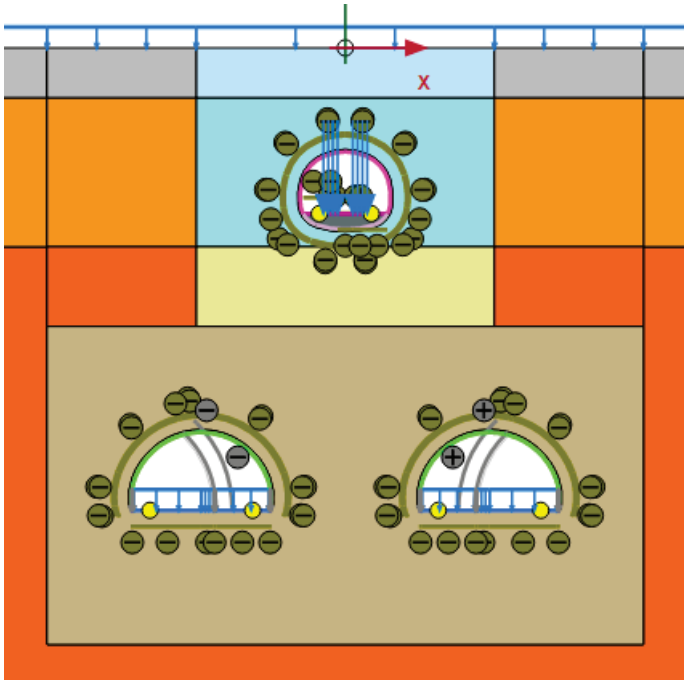


Figure IV-36: Phase 20- Degradation of the Soil of the new road Tunnels

4.6. Interfaces

Interfaces are joint elements to be added to plates to allow for a proper modelling of soil-structure interaction. Interfaces may be used to simulate, the thin zone of intensely shearing material at the contact between a plate and the surrounding soil. Interfaces can be created next to plate elements or between two soil polygons, according to the Reference Manual [19]. The interface's stiffness and strength must be defined. Stiffness is defined as follows:

- Standard: With this option, is calculated the interface stiffness directly from the following expressions

$$E_{oed,i} = 2 \cdot G_i \cdot \frac{(1-\nu_i)}{1-2\cdot\nu_i} \qquad G_i = R_{int}^2 \cdot G_{soil} \leq G_{soil} \qquad \nu_i = 0.45$$

In the above expressions, G_i is the transverse stiffness modulus of the interface, $E_{oed,i}$ is the oedometric Young's modulus of the interface, ν_i is the Poisson's ratio of the interface, G_{soil} is the transverse stiffness modulus of the soil, and R_{int} is the strength reduction factor.

The interface strength is defined in the Strength section. In general, for most constitutive models, and especially the most widely used ones, the fundamental parameter determining the interface strength is the strength reduction factor Rinter. In relation to this strength reduction factor, the interface strength for modelling the soil-structure interaction is taken into account by means of a Mohr-Coulomb type elastoplastic behavior model. The Mohr-Coulomb elastoplastic model allows to distinguish between the elastic behavior of the interface, for which small displacements occur, and the plastic behavior of the interface in which sliding can occur between the interface and the soil, and therefore between the structure and the soil. The shear stress at the interface is calculated as:

$$\tau_i = c_i + \sigma'_n \cdot tan\,\varphi_i$$

Where φ_i and c_i are the angle of friction and cohesion respectively of the interface and σ'_n is the effective normal stress acting perpendicularly on the interface that Plaxis automatically calculates as:

$$\sigma'_n = \frac{(\sigma'_2+\sigma'_3)}{2}$$

For the elastic behavior of the interface, it is true that:

$$\tau_i < c_i + \sigma'_n \cdot tan\,\varphi_i$$

For the plastic behavior of the interface, it is true that:

$$\tau_i = c_i + \sigma'_n \cdot tan\,\varphi_i$$

The resistant properties of the interface (φi and ci) are linked to the resistant properties of the ground by means of the factor $Rinter$ from the following expressions.

$$c_i = R_{int} \cdot c_{soil}$$

$$tan\,\varphi_i = R_{int} \cdot tan\,\varphi_{soil}$$

$$\psi_i = 0\ for\ R_{int} = 0\ otherwise\ \psi_i = \psi_{soil}$$

$$\sigma_t < \sigma_{t,i} = R_{int} \cdot \sigma_{t,soil}$$

In the above expressions φ_i and c_i are the angle of friction and the cohesion respectively of the interface and φ_{soil} and c_{soil} are the angle of friction and the cohesion respectively of the soil ψ_i and ψ_{soil} are the dilatancy angles of the interface and the soil respectively and R_{int} is the strength reduction factor. $\sigma_{t,i}$ is the tensile strength of the interface, σ_t is the tensile stress applied to the interface, and $\sigma_{t,soil}$ is the tensile strength of the soil.

Within the Strength section, the Strength section presents a drop-down menu offering the user the following options:

- Rigid: This is the option that the user should use when the interface does not have a lower strength than the surrounding soil, but has the same strength. Therefore, in this case, the value of Rinter = 1.
- Manual: This option allows the user to manually enter the value of Rinter. Typically, to account for the actual soil-structure interaction, the interface is weaker and more flexible than the surrounding soil, meaning that Rinter < 1. Typically, values of Rinter = 2/3 are considered acceptable. A value of Rinter > 1 is not common and should not be used.

The values for R_{int} employed in the present thesis are:

Table IV-26: Definition of Interfaces in the models

Interfaces	Rint
Interaction Support-Lining	1
Interaction Plate Slab-Backfill Concrete	1
Interaction Soil - Support	0.667

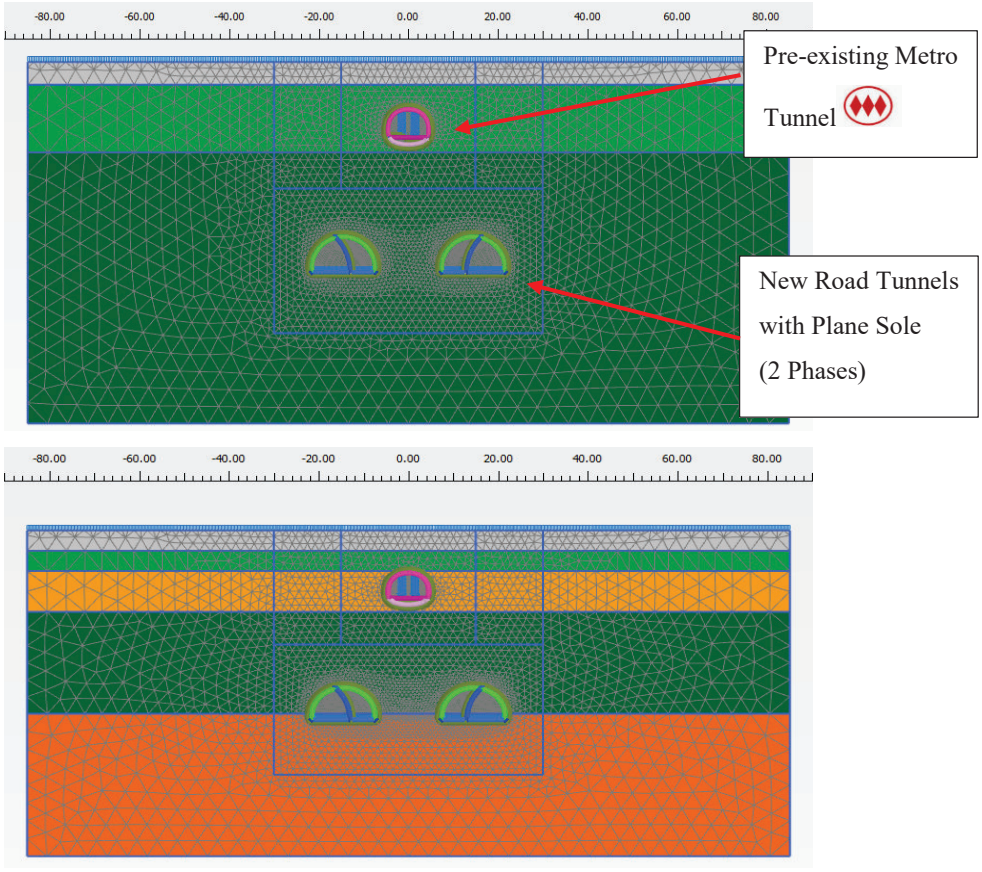
V. ANALYSIS OF THE INFLUENCE OF THE NEW ROAD TUNNELS EXCAVATION ON THE PRE-EXISTING METRO TUNNEL

5.1. Variation of the Constitutive Soil Model with Plane Sole section in the new Tunnels

Initially, in the first simple analysis, more simple (See Plan N°1 in section 5.1, Annex V), three soil constitutive models were studied:

- Mohr Coulomb Model
- Hardening Soil Model
- Hardening Soil Small Model

In the nine models at this stage, a section with a plane sole is used for the new road tunnels and these are excavated in two phases. As shown below:



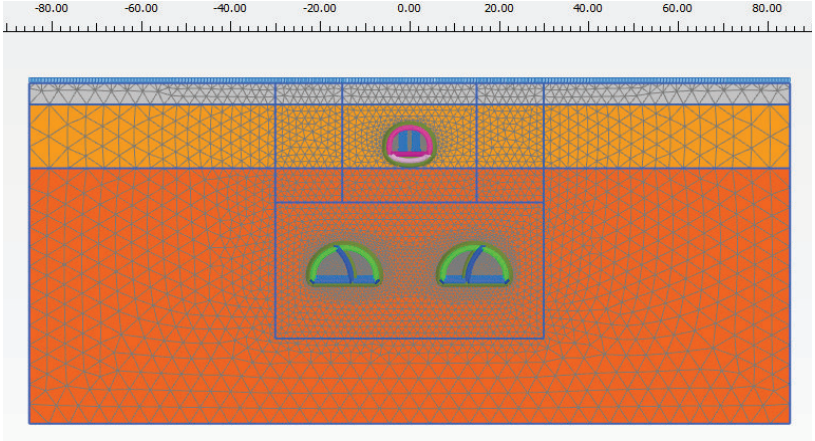


Figure V-1: Gravel (superior), Mixed (center), Fine (inferior) Profiles with Sole Plane Section in New Tunnels and Metro Tunnel

5.1.1 Summary of Structural Verifications

From the deformation and strength verifications presented in Annex III and described in detail in chapter 3.1, the following summary of checks is obtained

Table V-1: Summary of Checks on Metro Tunnel – Pre-existing Metro Tunnel – First Analysis

1_Variation of the Constitutive Soil Model with Sole Plane Section in the New Tunnels												
Soil	On Metro Tunnel											
	Construction Stage						Service Stage					
	Deformation			Resistance			Deformation			Resistance		
	MC	HS	HSs	MC	HS	HSs	MC	HS	HSs	MC	HS	HSs
Gravel	✓	✓	✓	✓	✓	✓	✓	✓	✓	✓	✓	✓
Mixed	✓	×	✓	×	✓	✓	✓	✓	✓	×	✓	✓
Fine	×	×	×	-	-	-	✓	×	×	×	-	-

Table V-2:Summary of Checks on New Tunnels – Pre-existing Metro Tunnel - First Analysis

1_Variation of the Constitutive Soil Model with Sole Plane Section in the New Tunnels												
Soil	On New Tunnels (Section with Plane Sole)											
	Construction Stage						Service Stage					
	Deformation			Resistance			Deformation			Resistance		
	MC	HS	HSs	MC	HS	HSs	MC	HS	HSs	MC	HS	HSs
Gravel	×	×	✓	-	-	✓	×	×	✓	-	-	✓
Mixed	-	×	×	-	-	-	-	×	×	-	-	-

Table V-3: Summary of Checks on Soil – Pre-existing Metro Tunnel – First Analysis

1_Variation of the Constitutive Soil Model						
Soil	On Soil (Section with Plane Sole)					
	Construction Stage			Service Stage		
	Plastification			Plastification		
	MC	HS	HSs	MC	HS	HSs
Gravel	-	-	✓	-	-	✓

5.1.2 Comments on the Results

Comments from the first analysis done:

- Excavation of gravel profile using section with plane sole section in two phases requires a constitutive model of Hardening Soil Small to satisfy all the acceptance criteria.
- Excavation of mixed and fine profile using plane sole section in two phases is not possible because the acceptance criteria are not verified.
- Excavation of fine profile using plane sole section in two phases requires shotcrete application on the plane sole during the construction process due to strong elastic bounces.

With this first, more simple analysis, to verify for the excavation of the new road tunnels under a pre-existing Metro tunnel in the gravel profile the admissibility criterion using a section without counter-vault (smaller excavation area) and excavating in two phases (faster execution), i.e. with the geometry presented below.

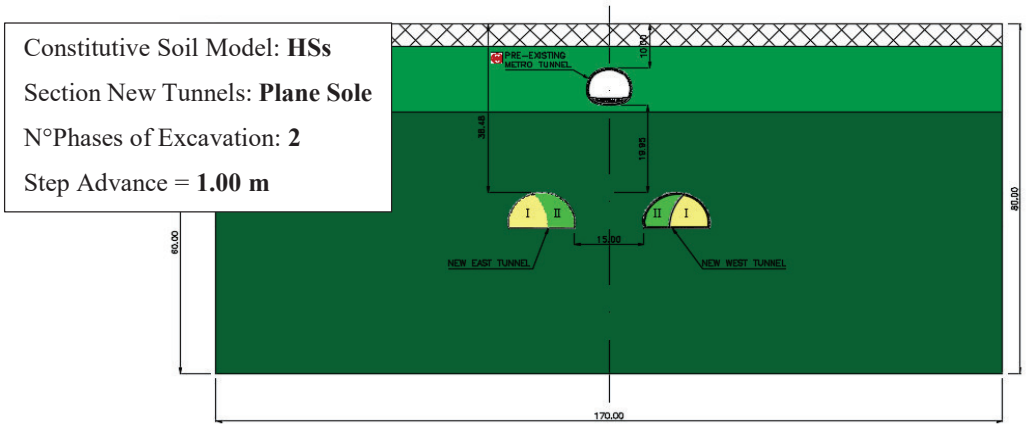


Figure V-2: Final Profile for Gravel Excavation with preexisting Metro Tunnel

5.2. Variation of the Constitutive Soil Model with Counter-vault section in the new Tunnels for Mixed and Fine Soils

In a second analysis, more refined (See Plan N°2 in section 5.2, Annex V), it is proposed to use a section of excavation with a counter-vault in the new road tunnels for the mixed and fine profiles.

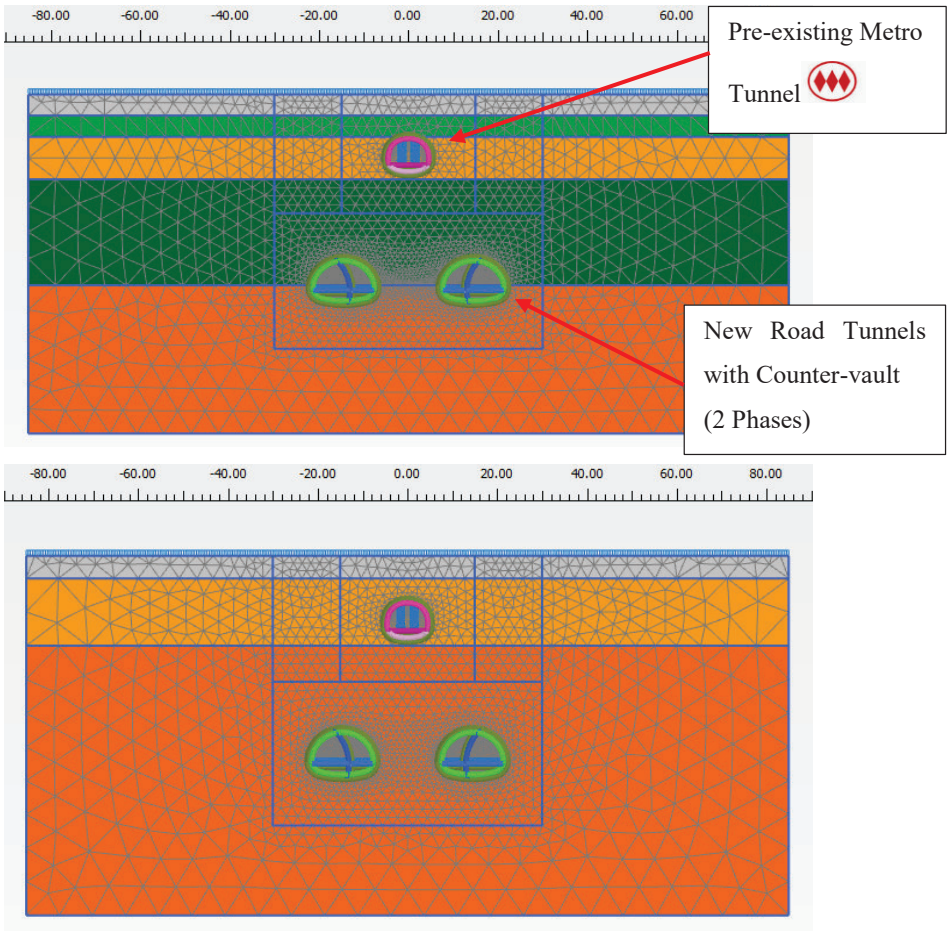


Figure V-3: Mixed (superior) and Fine (inferior) Profiles Model with Counter-vault Section in New Tunnels and Metro Tunnel

5.2.1 Summary of Structural Verifications

From the deformation and strength verifications presented in Annex III and described in detail in chapter 3.2, the following summary of checks is obtained.

Table V-4: Summary of Checks on Metro Tunnel – Pre-existing Metro Tunnel – Second Analysis

2_Variation of the Constitutive Soil Model with Counter-Vault Section in the New Tunnels												
Soil	On Metro Tunnel											
	Construction Stage						Service Stage					
	Deformation			Resistance			Deformation			Resistance		
	MC	HS	HSs	MC	HS	HSs	MC	HS	HSs	MC	HS	HSs
Mixed	✓	✓	✓	×	✓	✓	✓	✓	✓	×	✓	✓
Fine	×	×	×	-	-	-	✓	✓	✓	✓	✓	✓

Table V-5: Summary of Checks on New Tunnels – Pre-existing Metro Tunnel – Second Analysis

2_Variation of the Constitutive Soil Model with Counter-Vault Section in the New Tunnels												
Soil	On New Tunnels (Section with Counter-Vault)											
	Construction Stage						Service Stage					
	Deformation			Resistance			Deformation			Resistance		
	MC	HS	HSs	MC	HS	HSs	MC	HS	HSs	MC	HS	HSs
Mixed	-	✓	✓	-	✓	✓	-	✓	✓	-	✓	✓

Table V-6: Summary of Checks on Soil – Pre-existing Metro Tunnel – Second Analysis

2_Variation of the Constitutive Soil Model						
Soil	On Soil (Section with Counter-Vault)					
	Construction Stage			Service Stage		
	Plastification			Plastification		
	MC	HS	HSs	MC	HS	HSs
Mixed	-	✓	✓	-	✓	✓

5.2.2 Comments on the Results

Comments from the second analysis done:

- We can see the importance to verifying the intermediate stages of excavation, for example in fines, because it is verified in the service stage, but not in the construction stages.

- Excavation in mixed soil is possible to use the Hardening Soil and Hardening Soil Small models when introducing counter-vault.

- Excavation in fine soils is not possible even with the introducing of counter-vault in the section because it does not verify the criterion of transverse deformations in the pre-existing structures.

With this second, more refined analysis, to verify for the excavation of the new road tunnels under a pre-existing Metro tunnel in the mixed profile the admissibility criterion using a section with counter-vault (larger excavation area) and excavating in two phases (faster execution), i.e. with the geometry presented below.

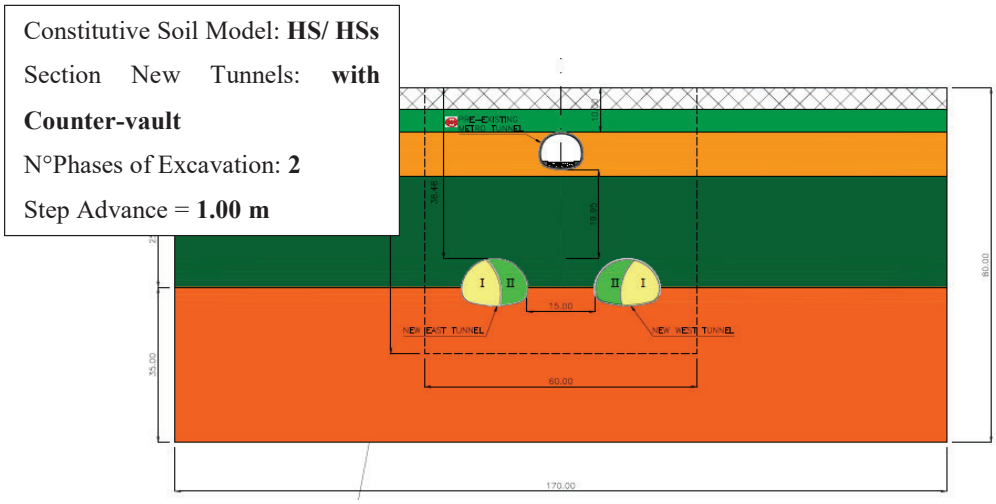


Figure V-4: Final Profile for Mixed Excavation with pre-existing Metro Tunnel

5.3. Variation of the Constitutive Soil Model with four Phases of Excavation of the New Road Tunnels for Fine Soil

In a third analysis, more sophisticated, (See Plan N°3 in section 5.3, Annex V), it is proposed to use a four-phase (Side Drifts) excavation section in the new road tunnels, with a step advance of 0.75 m, for the fine profile. See Figure V-5 and Figure V-6.

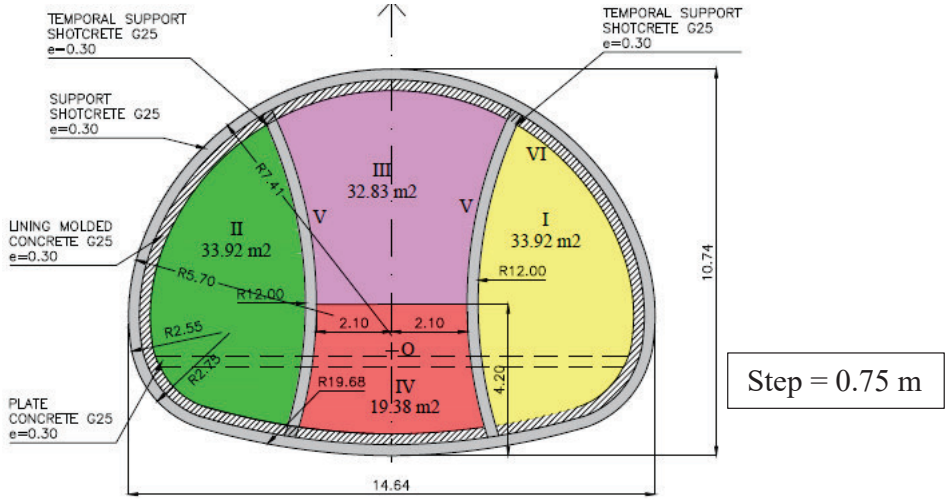


Figure V-5: Excavation Section in Multiple Phases (4 Phases)

The following is a description of the construction methodology in multiple phases, which can be observed in the Figure V-6:

- Phase I: Excavation and installation of the support of the first phase, with an excavation section of 33.92m2. It will be excavated in advances of 0.75 m.

- Phase II: Identical to phase I, but a minimum offset of 20 m must be respected with respect to the excavation front of phase I. It will also be excavated in 0.75 m advances.

- Phase III: Maintaining a minimum offset of 20m, with respect to the advance front of Phase II, Excavation and installation of the support of the third phase, with an excavation section of 32.83m2, in 0.75 m advances.

- Phase IV: Maintaining a minimum offset of 20m, with respect to the advance front of Phase III, Excavation and installation of the support of the fourth phase, with an excavation section of 19.38m2, in 0.75 m advances.

- Phase V: Maintaining a minimum offset of 20m, with respect to the advance front of Phase IV, the demolition of the intermediate wall that forms the temporary support of the tunnel will be executed, in 0.75 m steps.

- Phase VI: Execution of lining.

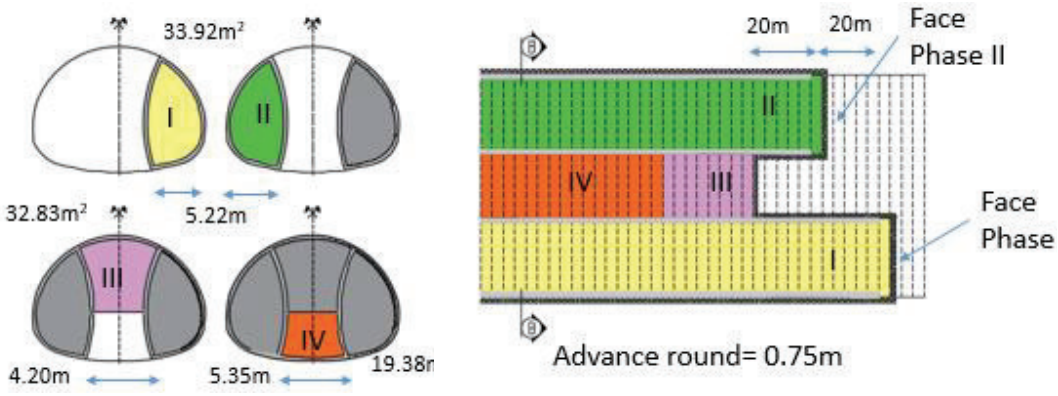


Figure V-6. Multi-phase Excavation Methodology

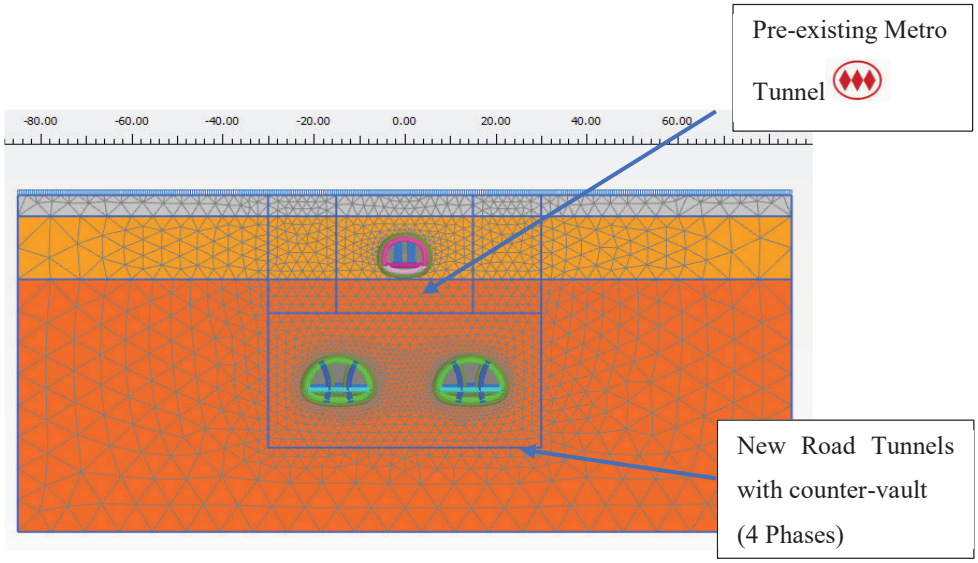


Figure V-7: Fine Profile Model with Counter-vault Section Excavated in four Phases in New Tunnels and Pre-existing Metro Tunnel

5.3.1 Summary of Structural Verifications

From the deformation and strength verifications presented in Annex III and described in detail in chapter 3.3, the following summary of checks is obtained

Table V-7: Summary of Checks on Metro Tunnel – Pr-eexisting Metro Tunnel – Third Analysis

3_Variation of the Constitutive Soil Model with 4 Phases of Excavation in the New Tunnels												
Soil	On Metro Tunnel											
	Construction Stage						Service Stage					
	Deformation			Resistance			Deformation			Resistance		
	MC	HS	HSs	MC	HS	HSs	MC	HS	HSs	MC	HS	HSs
Fine	✗	✗	✓	✗	✓	✓	✓	✓	✓	✗	✓	✓

Table V-8: Summary of Checks on New Tunnels– Pre-existing Metro Tunnel – Third Analysis

3_Variation of the Constitutive Soil Model with 4 Phases of Excavation in the New Tunnels												
Soil	On New Tunnels (Section with Counter-Vault and 4 Phases of Excavation)											
	Construction Stage						Service Stage					
	Deformation			Resistance			Deformation			Resistance		
	MC	HS	HSs	MC	HS	HSs	MC	HS	HSs	MC	HS	HSs
Fine	-	-	✓	-	-	✓	-	-	✓	-	-	✓

Table V-9: Summary of Checks on Soil – Pre-existing Metro Tunnel – Third Analysis

3_Variation of the Constitutive Soil Model						
Soil	On Soil (Section with Counter-Vault					
	Construction Stage			Service Stage		
	Plastification			Plastification		
	MC	HS	HSs	MC	HS	HSs
Fine	-	-	✓	-	-	✓

5.3.2 Comments on the Results

Comments from the third analysis done:

- Excavation in fine soils is possible only in multiple phases (4 phases) and is possible only when using the Hardening Soil Small model.
- There are occasions where the strength of the structural elements can be verified, but not the deformation criterion, for example with the Hardening Soil model.
- Verifications of transverse deformations in the pre-existing Metro tunnel reveal that the critical stage of deformation corresponds to the construction stage of the new western road tunnel.
- In the shear verification of Metro's pre-existing tunnel lining, in situations that do not verify the Q-N interaction diagram coinciding with the junction between the vault and the counter-vault, the concrete overthickness and the additional steel bars placed in that junction must be considered.

With this third, more sophisticated analysis, to verify for the excavation of the new road tunnels under a pre-existing Metro tunnel in the fine profile the admissibility criterion using a section with counter-vault (larger excavation area) and excavating in four phases and lower advance step (slower execution), i.e. with the geometry presented below.

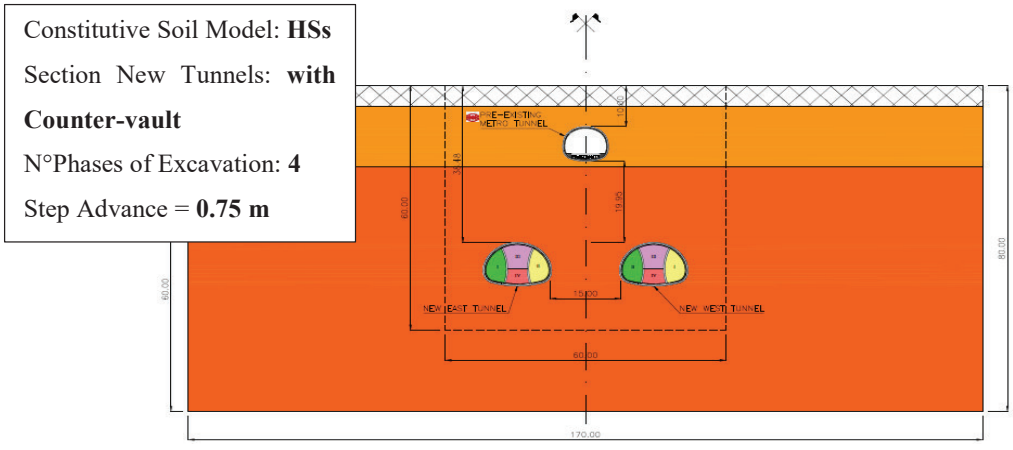


Figure V-8: Final Profile for Fine Excavation with pre-existing Metro Tunnel

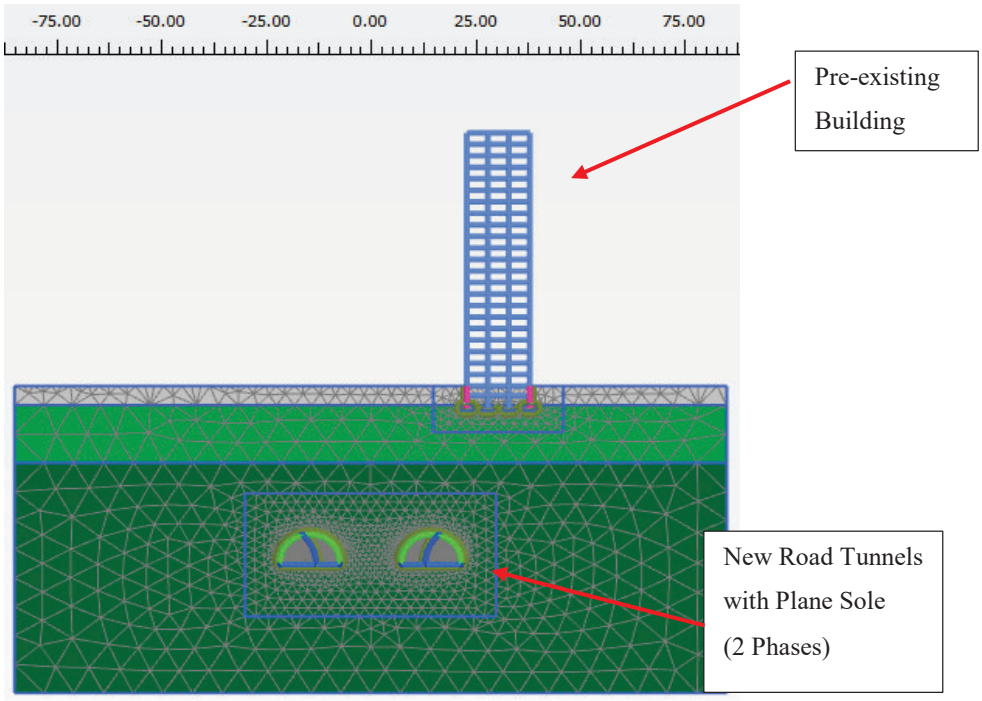
VI. ANALYSIS OF THE INFLUENCE OF EXCAVATION OF THE NEW ROAD TUNNELS ON THE PRE-EXISTING BUILDING

6.1. Variation of the Constitutive Soil Model with Plane Sole section in the new Tunnels

Initially, in the first, more simple analysis, (See Plan N°4 in section 5.4, Annex V), three soil constitutive models were studied:

- Mohr Coulomb Model
- Hardening Soil Model
- Hardening Soil Small Model

In the nine models at this stage, a section with a plane sole is used for the new road tunnels and these are excavated in two phases. As shown below:



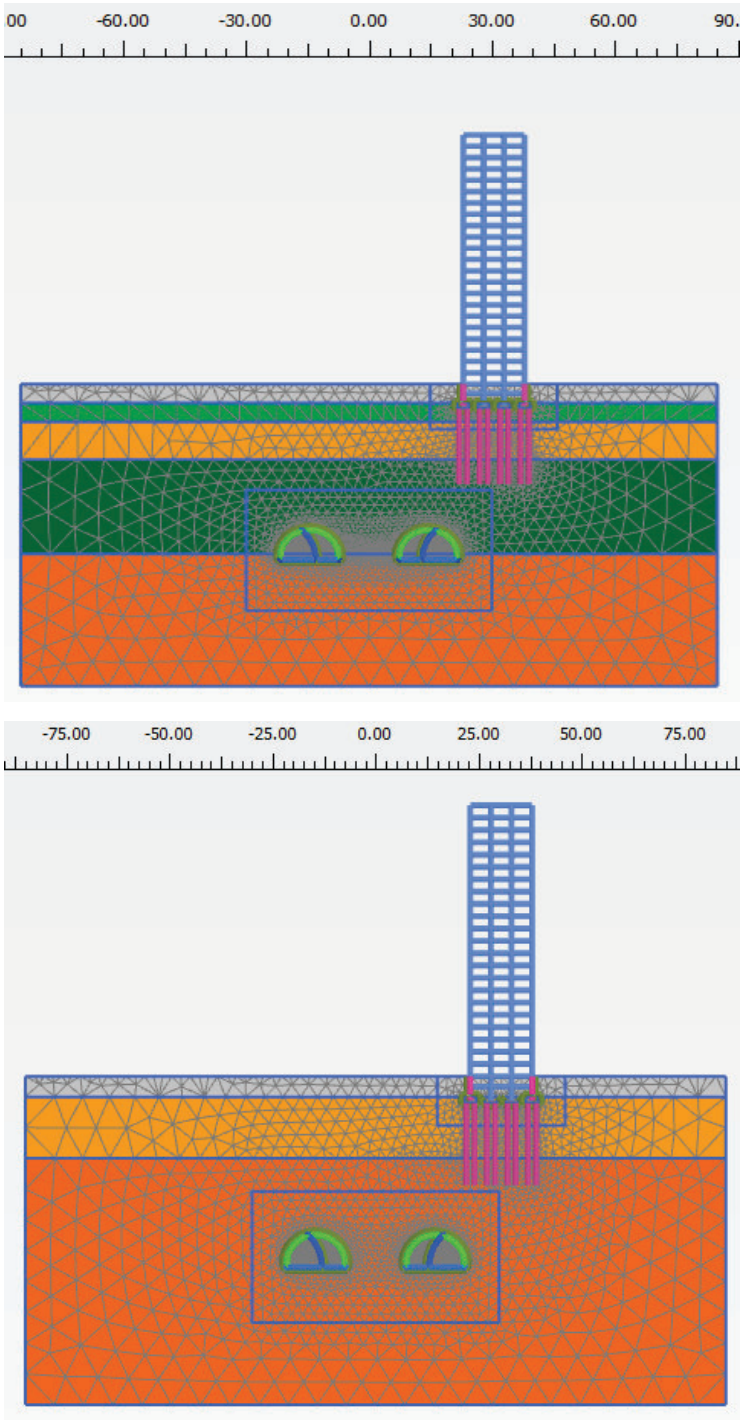


Figure VI-1: Gravel (superior), Mixed (center) and Fine (inferior) Profiles with Sole Plane Section in the New Tunnels and Building

6.1.1 Summary of Structural Verifications

From the deformation and strength verifications presented in Annex IV and described in detail in chapter 4.1, the following summary of checks is obtained

Table VI-1: Summary of Checks on Building – Pre-existing Building- First Analysis

1_Variation of the Constitutive Soil Model			
Soil	On Building		
	Deformation		
	MC	HS	HSs
Gravel	×	✓	✓
Mixed	×	×	×
Fine	×	×	×

Table VI-2:Summary of Checks on New Tunnels – Pre-existing Building- First Analysis

1_Variation of the Constitutive Soil Model												
Soil	On New Tunnels (Section with Plane Sole)											
	Construction Stage						Service Stage					
	Deformation			Resistance			Deformation			Resistance		
	MC	HS	HSs	MC	HS	HSs	MC	HS	HSs	MC	HS	HSs
Gravel	-	×	✓	-	-	✓	-	×	✓	-	-	✓

Table VI-3: Summary of Checks on Soil – Pre-existing Building – First Analysis

1_Variation of the Constitutive Soil Model						
Soil	On Soil					
	Construction Stage			Service Stage		
	Plastification			Plastification		
	MC	HS	HSs	MC	HS	HSs
Gravel	-	-	✓	-	-	✓

6.1.2 Comments on the Results

- Excavation of gravel profile using section with plane sole in two phases requires a constitutive model of Hardening Soil Small to satisfy all the acceptance criteria.
- Excavation of mixed and fine profile using plane sole section in two phases is not possible because the acceptance criteria are not verified.

- Excavation of fine profile using plane sole section in two phases requires shotcrete application on the plane sole during the construction process due to strong elastic bounces.
- Excavation of mixed profile using plane sole section shows “slight” to “moderate” damage to the building, but the design criteria establishes “very slight” or “negligible”.
- Excavation of fine profile using plane sole section shows “moderate” to “several” damage to the building, but the design criteria establishes “very slight” or “negligible”.

With this first, more simple analysis, to verify for the excavation of the new road tunnels under a pre-existing building in the gravel profile the admissibility criterion using a section without counter-vault (smaller excavation area) and excavating in two phases (faster execution), i.e. with the geometry presented below.

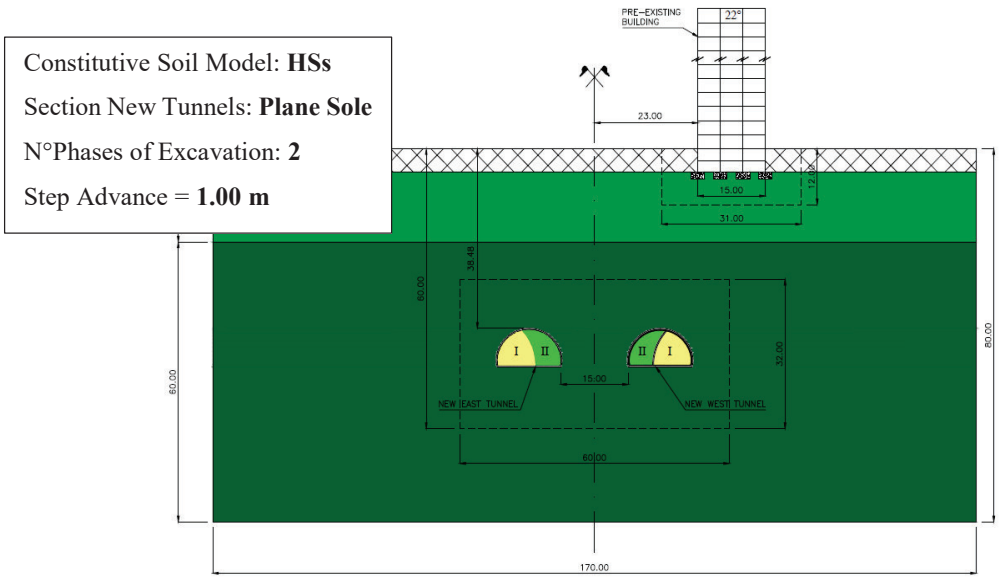


Figure VI-2: Final Profile for Gravel Excavation with pre-existing Building

6.2. Variation of the Constitutive Soil Model with Counter-vault in the new Tunnels for Mixed and Fine Soils

In a second analysis, more refined (See Plan N°5 in section 5.5, Annex V), it is proposed to use a section with a counter-vault.

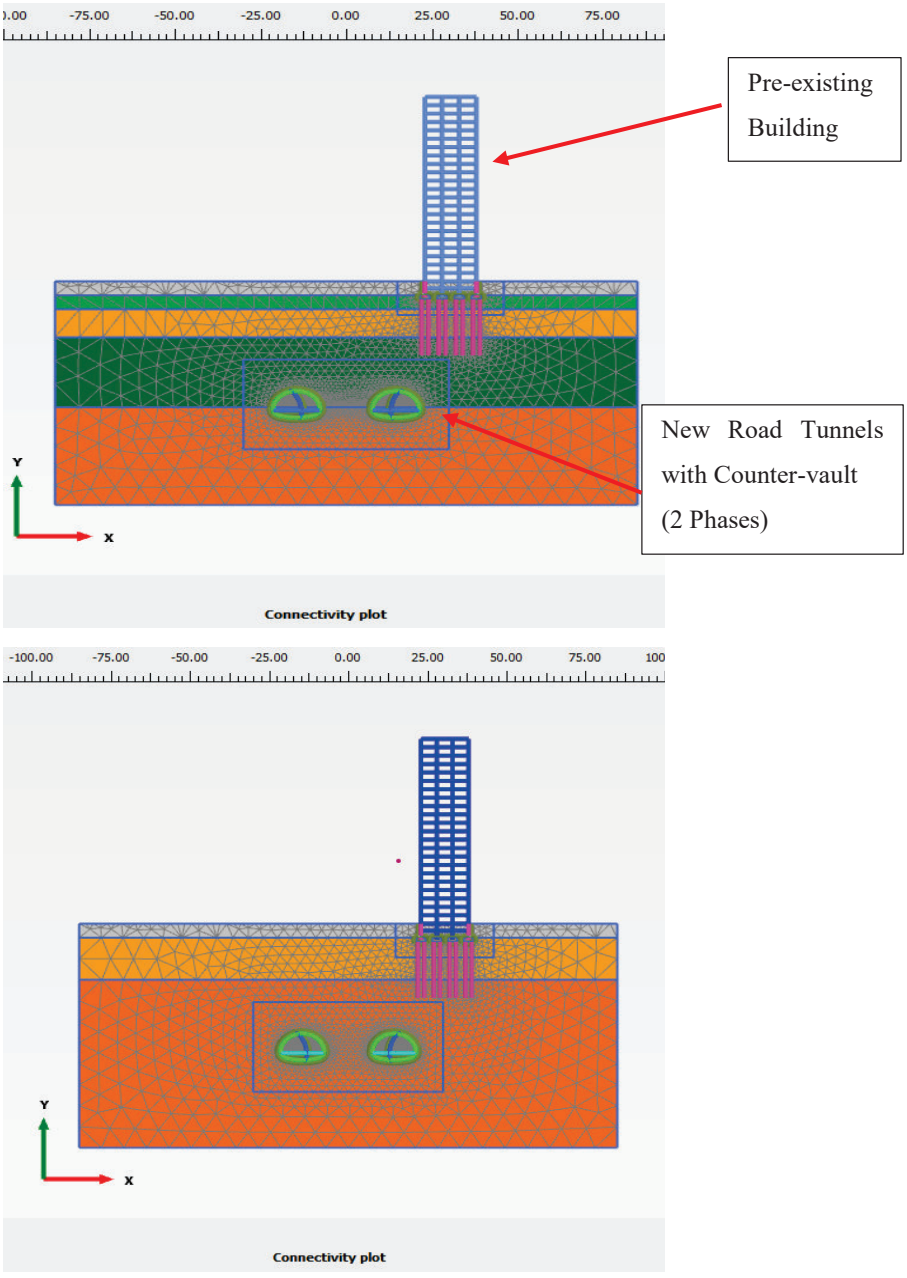


Figure VI-3: Mixed (superior) and Fine (inferior) Profile Model with Counter-vault Section in New Tunnels and Building

6.2.1 Summary of Structural Verifications

From the deformation and strength verifications presented in Annex IV and described in detail in chapter 4.2, the following summary of checks is obtained.

Table VI-4: Summary of Checks on Building – Pre-existing Building- Second Analysis

2_Variation of the Constitutive Soil Model			
Soil	On Building		
	Deformation		
	MC	HS	HSs
Mixed	×	×	✓
Fine	×	×	×

Table VI-5: Summary of Checks on New Tunnels – Pre-existing Building – Second Analysis

Soil	On New Tunnels (Section with Counter- Vault)											
	Construction Stage						Service Stage					
	Deformation			Resistance			Deformation			Resistance		
	MC	HS	HSs	MC	HS	HSs	MC	HS	HSs	MC	HS	HSs
Mixed	-	-	✓	-	-	✓	-	-	✓	-	-	✓

Table VI-6: Summary of Checks on Soil – Pre-existing Building – Second Analysis

Soil	On Soil					
	Construction Stage			Service Stage		
	Plastification			Plastification		
	MC	HS	HSs	MC	HS	HSs
Mixed	-	-	✓	-	-	✓

6.2.2 Comments on the Results

Comments from the second analysis done:

- Excavation in gravel and mixed soil is possible to use only Hardening Soil Small models when introducing counter-vault.

- Excavation in fine soils is not possible even with the introducing of counter-vault in the section because it does not verify the criterion of deformations in the pre-existing structures. Because damages were obtained “Slight” to “Moderate”.

With this second, more refined analysis, to verify for the excavation of the new road tunnels under a pre-existing building in the mixed profile the admissibility criterion using a section with counter-vault (larger excavation area) and excavating in two phases (faster execution), i.e. with the geometry presented below.

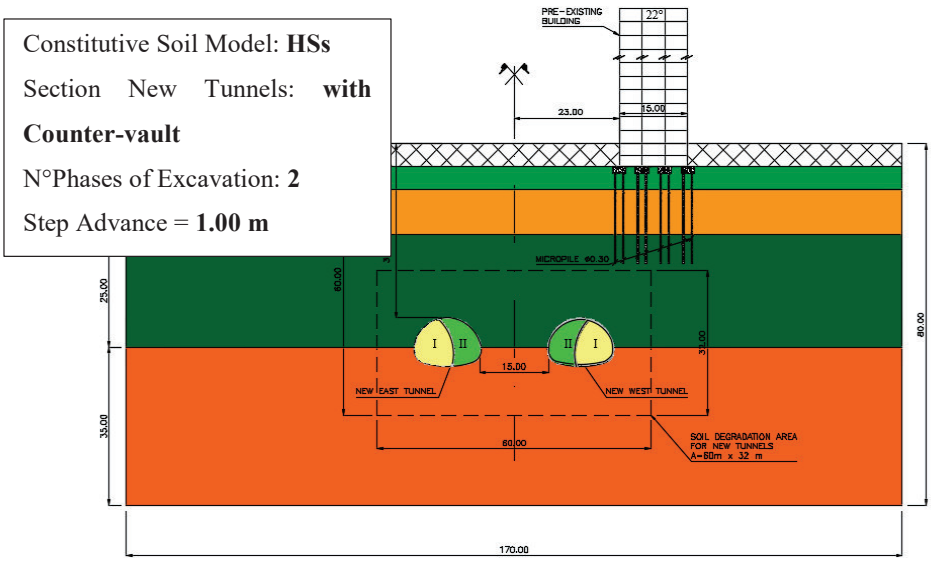


Figure VI-4: Final Profile for Mixed Excavation with pre-existing Building

6.3. Variation of the Constitutive Soil Model with four Phases of Excavation of the New Road Tunnels for Fine Soil

In a third analysis, more sophisticated (See Plan N°6 in section 5.6, Annex V), it is proposed to use a four-phase (Side Drifts) excavation section in the new road tunnels, with a step advance of 0.75 m, for the fine profile.

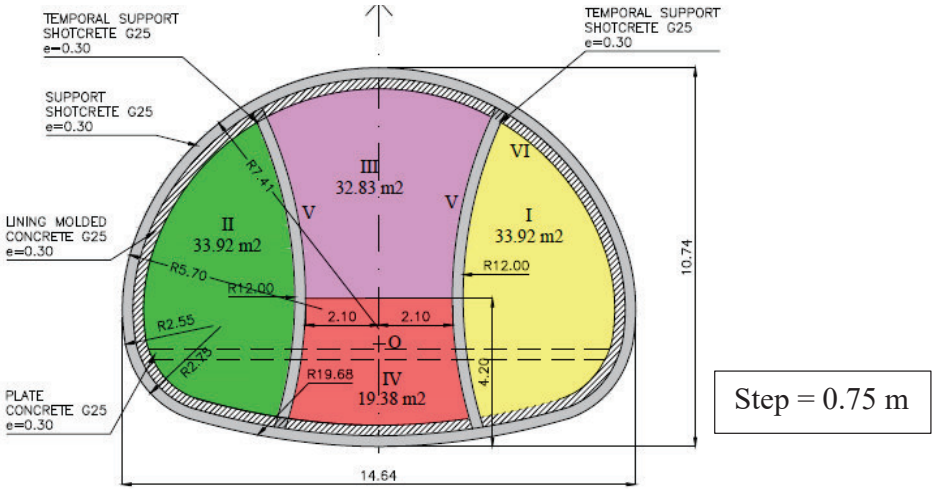


Figure VI-5: Excavation Section in Multiple Phases (4 Phases)

The construction process is the same as shown in section 5.3.

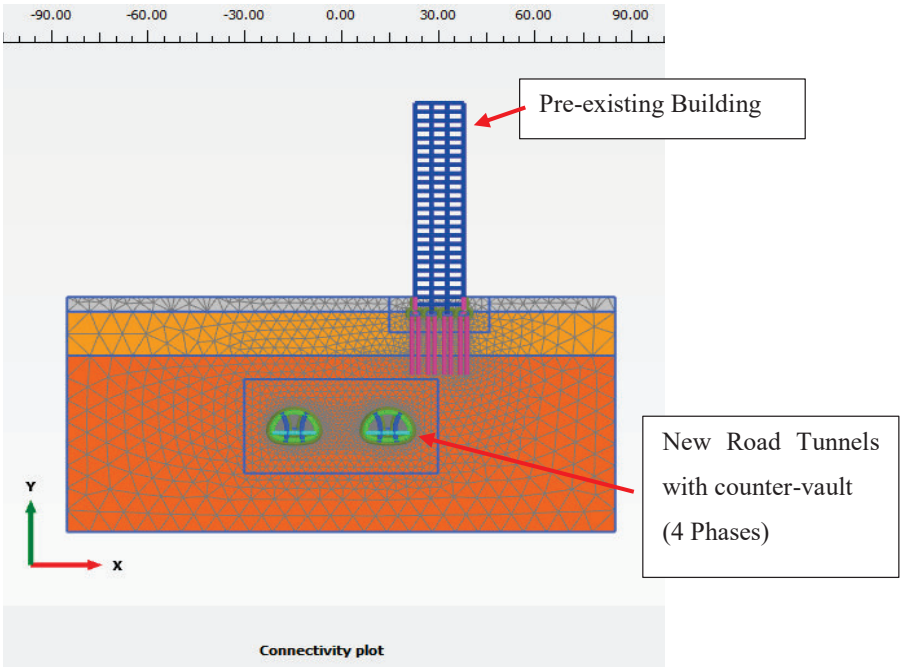


Figure VI-6: Fine Profile Model with Counter-vault Section Excavated in four Phases in New Tunnels and Pre-existing Building

6.3.1 Summary of Structural Verifications

From the deformation and strength verifications presented in Annex IV and described in detail in chapter 4.3, the following summary of checks is obtained

Table VI-7: Summary of Checks on Building – Pre-existing Building – Third Analysis

3_Variation of the Constitutive Soil Model with 4 Phases			
Soil	On Building		
	Deformation		
	MC	HS	HSs
Fine	×	×	×

6.3.2 Comments on the Results

Comments from the third analysis done:

- Excavation in fine soils is not possible in multiple phases (4 phases) because it does not verify the criterion of deformations in the pre-existing structures. Because damages were obtained “Slight” to “Moderate”.

- It is necessary to implement some mitigation measures, which are proposed in the following analysis.

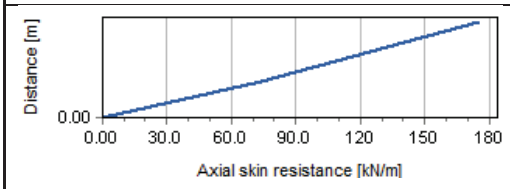
A fourth, more sophisticated analysis is proposed, implementing a mitigation measure consisting of two micropile walls, as presented in the following section:

6.4. Mitigation Measure in fine soil applying a Micropile Wall

6.4.1 Description of the Micropile Wall

A micropile wall of 0.25 m diameter and 55 m in length of G25 concrete reinforced with an S-275 steel tube, 0.20 m diameter and 20 mm thick, separated every 0.50 m longitudinally, is designed. See Plan N°7 in section 5.7, Annex V.

Table VI-8: Parameters of the Embedded bean row for Micropile Wall in Fine Soil

MICROPILE: ELEMENT EMBEDDED BEAM ROWS - ELASTIC			
Inyection concrete G25 Reinforcement with Steel Tube S-275			
External Diameter of the Micropile	Øe	0.25	m
External Diameter of Steel Tube	Øes	0.20	m
Thickness of Steel Tube	e	0.02	m
Internal Diameter of Steel Tube	Øi	0.16	m
Total Area	At	0.049087	m^2
Total Inertia	It	0.000238	m^4
Uniaxial compressive strength of Inyection	f´c	25	MPa
Young's modulus of concrete	Ec	23500	MPa
Young's modulus of steel	Es	210000	MPa
Young's modulus of Micropile	Et	66470	MPa
Unit weight of Micropile	γ	37.33	kN/m^3
Separation bewten micropile	Lspacing	0.5	m
Unit weight of Micropile	γ	9555.68	kN/m^3
Separation bewten micropile	Lspacing	0.5	m
Axial Skin resistance			
z = 20 m	Tz	74	kN/m
z = 54 m	Tz	175	kN/m
			
Base resistance	Fmax	0	kN

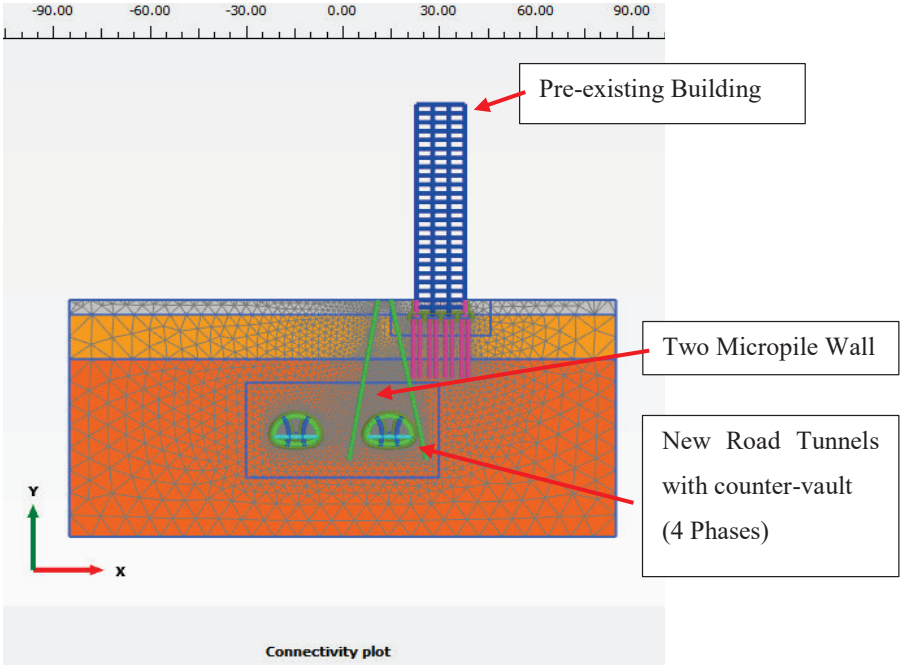


Figure VI-7: Fine Profile Model with Counter-vault Section Excavated in four Phases in New Tunnels and Pre-existing Building, applying mitigation measure.

6.4.2 Summary of Structural Verifications

From the deformation and strength verifications presented in Annex IV and described in detail in chapter 4.4, the following summary of checks is obtained.

Table VI-9: Summary of Checks on Building – Pre-existing Building – Fourth Analysis

3_Variation of the Constitutive Soil Model with 4 Phases			
Soil	On Building		
	Deformation		
	MC	HS	HSs
Fine	×	×	✓

Table VI-10: Summary of Checks on New Tunnels – Pre-existing Building – Fourth Analysis

Soil	On New Tunnels (Section with Counter- Vault)											
	Construction Stage						Service Stage					
	Deformation			Resistance			Deformation			Resistance		
	MC	HS	HSs	MC	HS	HSs	MC	HS	HSs	MC	HS	HSs
Fine	-	-	✓	-	-	✓	-	-	✓	-	-	✓

Table VI-11: Summary of Checks on Soil – Pre-existing Building – Fourth Analysis

Soil	On Soil					
	Construction Stage			Service Stage		
	Plastification			Plastification		
	MC	HS	HSs	MC	HS	HSs
Fine	-	-	✓	-	-	✓

6.4.3 Comments on the Results

Comments from the fourth analysis done:

- Excavation in fine soils is possible in multiple phases (4 phases), with a step advance of 0.75 m and applying a micropile wall as mitigation measure.
- The first micropile wall reduces the displacements produced by the excavation of the western tunnel in relation to the building and the second wall reduces the displacements produced by the excavation of the eastern tunnel

With this fourth, more sophisticated analysis, which includes a mitigation measure, the admissibility criterion for the excavation of new road tunnels under a pre-existing building is verified in the fine profile, i.e., with the geometry presented below.

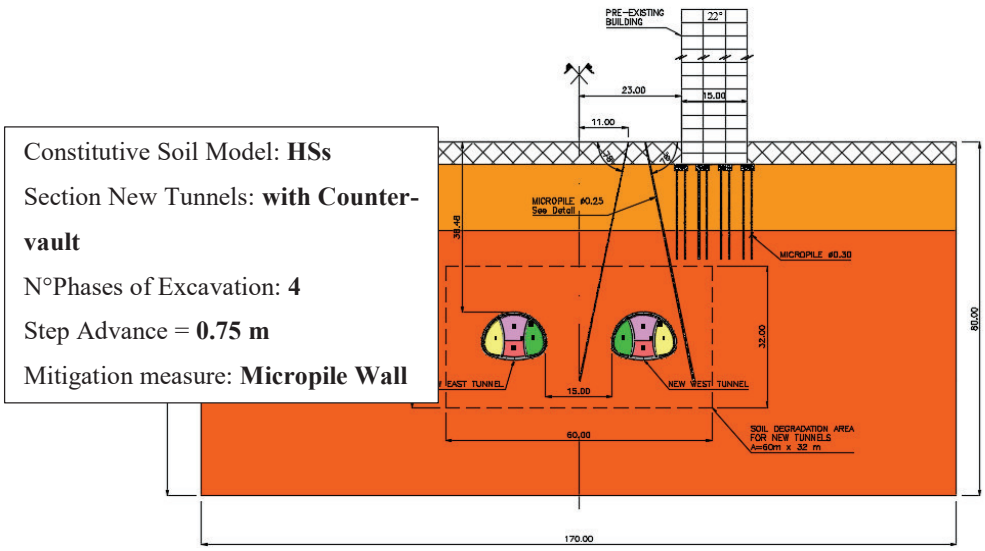


Figure VI-8: Final Profile for Fine Excavation with pre-existing Building

VII. CONCLUSIONS

Tunnel projects represent one of the most demanding areas of civil engineering, as they involve a complex interaction of geotechnical, structural, and environmental factors. The effective execution of such undertakings, particularly within densely built urban environments, has been made possible through the development and application of advanced numerical analysis tools, such as the Finite Element Method (FEM) and sophisticated constitutive models. These techniques allow for accurate representation of soil behavior and for assessing the impacts of excavation processes on surrounding structures. The tunnels analyzed in this research—located in the Metropolitan Region of Santiago, Chile—exemplify this complexity, as they must coexist with sensitive buildings, other underground infrastructures, and soils with generally unfavorable geomechanical properties, all of which demand high standards in planning, modeling, and execution.

The study of traditional excavation methods (German, Belgian, Swiss, English, among others) demonstrates the evolution of the discipline over time, in which the excavation of different types of soils and geological conditions has been achieved. These have laid the foundations for the emergence of the New Austrian method, the application of which has revolutionized the tunneling industry. This method exposes its versatility in the present thesis, allowing the excavation of tunnels in gravelly, fine and mixed soils.

This thesis reveals the importance of numerical modelling of tunnels, which is an essential tool in modern geotechnical engineering. It allows engineers to predict and analyses the behavior of the ground, and the effect on new or pre-existing structures during the excavation process, which is crucial to ensure the stability and safety of underground structures. One of the main benefits of numerical modelling is its ability to simulate different scenarios and ground conditions. In the present thesis, a total of 39 scenarios with three different soil profiles (gravel, mixed and fine) were studied, evaluating stresses, strains and settlements in the soil, in the new and around pre-existing structures. Therefore, the investigation enables the design of the tunnels to be optimized, reducing costs and minimizing risks.

The choice of the constitutive model has a direct impact on the prediction of ground deformations and their effect on pre-existing structures, therefore three of the most used soil constitutive models in geotechnical engineering (Mohr Coulomb, Hardening Soil and Hardening Soil Small) were studied and different stress distributions, settlements and plasticity zones were observed. It is shown that using the Hardening Soil Small model gives the lowest settlements and stresses on the pre-existing structures, while the Mohr Coulomb model gives the highest deformations and stresses, and the Hardening Soil model gives results intermediate to the other models. This exposes the importance of evaluating and choosing the constitutive soil model. At the same time, the modelling assumptions would be always be verified by monitoring the displacements around the excavations and on the surface.

The study of the geometry of the new tunnels reveals that the inclusion of a section with a counter-vault, or in general terms designing a section as similar as possible to a circle, results in a better distribution of stresses (greater arch effect) in the excavation, generating less level of deformations and stresses around the tunnels. The disadvantage is a larger excavation volume, around 27%, which generates higher construction costs, not only because of the additional volume to be excavated, as well as the additional volume of backfill to obtain a plane base for the construction of the roadway or roadbed of the tunnels.

By dividing the excavation process into phases, the behavior of the ground and adjacent structures can be better controlled, resulting in safer construction. At the same time, the variation of the advance pass is a critical factor influencing the stability and design of new tunnels and the impact on pre-existing structures. In soils with adverse geotechnical conditions (e.g. fines) small advance passes are required to reduce the risk of collapse and excessive deformation, while in more competent soils (e.g. gravels) larger advances can be adopted.

The application of mitigation measures to reduce the induced settlement is essential in fine soils in urban areas. In the present thesis, soil reinforcement with micropile walls was applied, demonstrating its effectiveness in this objective for the analysis of the pre-existing building, where admissible settlements were obtained only with its inclusion.

As a result of the present work, we can state that the construction of tunnels in urban areas requires careful planning and execution to avoid damage to pre-existing structures. Proper design, construction method and mitigation measures are recommended to ensure the safety and stability of the news tunnels and nearby structures preexisting.

7.1. Future Lines of Investigation

The following lines of future research related to the present thesis are recommended:

- Front stability in urban tunnels, analysis 3D.
- Application of the NATM in Rocks. Study and application of soil constitutive models for rocks (Mohr Coulomb, Hoek Brown, Jointed rock).
- Other solicitation in tunnels: dynamic analysis (vibrations and seismic analysis) and thermic effect for fire of tunnels.
- Tunnel excavation with tunnel boring machines (TBM)

7.2. Bibliography

[1] ARGENTINE ASSOCIATION OF TUNNELS AND UNDERGROUND SPACES (AATES)

[2] CHILEAN ASSOCIATION OF TUNNELS AND UNDERGROUND SPACES- (CTES)

[3] SOTO SAAVEDRA, P.S., 2004. "Tunnels Construction". Thesis to opt for the Degree of Civil Constructor, Austral University of Chile.

[4] RAFAEL IGLESIAS ALVAREZ, 2014. "Seismic Analysis of Shallow Depth Tunnels in the Soils of Santiago". Thesis to opt for the Degree of Civil Engineer, University of Chile.

[5] JOSE MIGUEL GALERA, 2020. "Considerations for the design and construction of excavated tunnels in urban context". XXXV national congress of engineering, Cartagena, Colombia.

[6] ITA/AITES REPORT 2006. "Settlements induced by tunneling in Soft Ground". Tunnelling and Underground Space Technology.

[7] AASHTO LRFD, 2024. American Association of State Highway and Transportation Officials, 10ta edition.

[8] CEB-FIP MODEL CODE 2010. Federation International of Concrete.

[9] ROAD MANUAL, 2016. Volume N°3: Instructions and Design Criteria. Directorate of Roads. Ministry of Public Works

[10] VLANCHOPOULOS & DIEDERICHS, 2009. "Improved Longitudinal Displacement Profiles for Convergence Confinement Analysis of Deep Tunnels".

[11] MUSANTE E INGENIEROS, 2019. "Soil Mechanics Report of the Metropolitan Region of Santiago de Chile".

[12] PINTO & LEDEZMA, 2021. "Dynamic Response of tall Building with Basement considering Soil- Structure Interaction".

[13] SCHIKORA & FINK, 1982. “Berechnungsmethoden moderner bergmäannischer Bauweisen beim U-BahnBau. Bauingenieur 57, 193–198”.

[14] BARD, E., LEON, R. & ANABALON. 2004. “Dynamic analysis of tunnels in Santiago gravels”. Chilean Geotechnical Congress. Santiago, University of Chile.

[15] BARROS & FIGUEIRAS, 1999. “Flexural Behavior of SFRC: Testing and Modeling, Journal of Materials in Civil Engineering”.

[16] NATIONAL GEOLOGY AND MINING SERVICE, 2003. “Geological Map of Chile: Digital Version’. Santiago of Chile. Scale 1:1.000.000”

[17] THOMAS BENZ, 2007. “Small Strain Stiffness of Soils and its Numerical Consequences”

[18] R. OBRZUD, A. TRUTY. "The Hardening Soil Model a Practical Guidebook”.

[19] REFERENCE MANUAL 2D, 2024. Plaxis 2D- Bentley Advancing Infrastructure.

[20] MATERIAL MODELS MANUAL 2D, 2024. Plaxis 2D- Bentley Advancing Infrastructure

[21] MÜLLER & SPAUN, 1978. “Reasons for some NATM failures”

ANNEXES

I. ANNEX: REASONS FOR SOME NATM FAILURES (MULLER, 1978)

1.1. Failure to control the length of the advance ("step")

Tunnel in Austria. Alterable rock. The graph shows the influence of the length of the advance on the measured horizontal deformations (Spaun 1976 [21]).

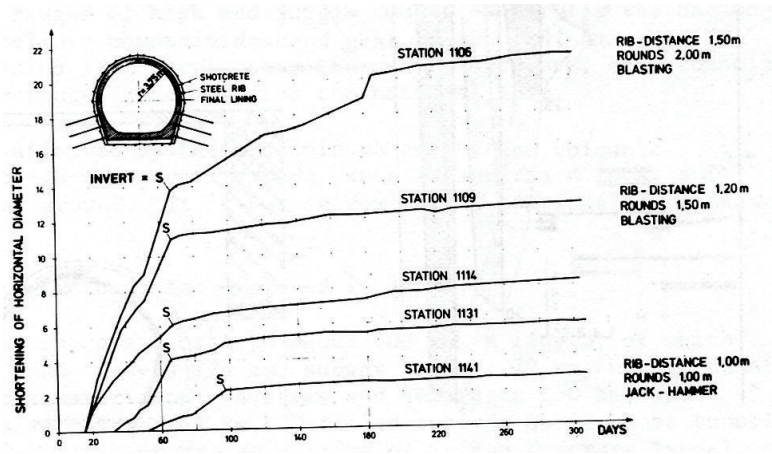


Figure I-1: Curve of horizontal deformations over time (Spaun, 1976 [21])

1.2. Waiting too long to close the section

Three examples of tunnels in soft rocks showing the influence of the time to section closure has on the vertical movements of the keystone.

A few hours or a few days can lead to an increase in seating by 200% or more (Muller ad Spaun, 1977 [21]).

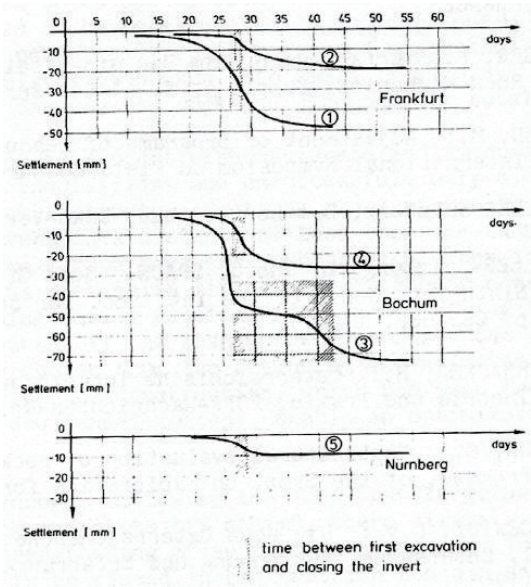


Figure I-2: Settlement vs Days (Muller ad Spaun, 1977 [21])

1.3. Absence of section closure (counter-vault)

Subway tunnel in Germany, excavated in marl. In the lower part of the geological profile there was a "solid" sandstone bank. It was judged that a concrete counter-vault was not necessary. But in one area the sandstone joints were parallel to the tunnel and dipped as shown. The excavation of the calotte was done in small steps. The same process must have been followed when the counter-vault was excavated. However, a length of 15 m was excavated all at once. A break occurred along the stratification planes along the layering planes and the shotcrete, steel frames and anchors collapsed into the tunnel (Muller, 1978 [21]) .

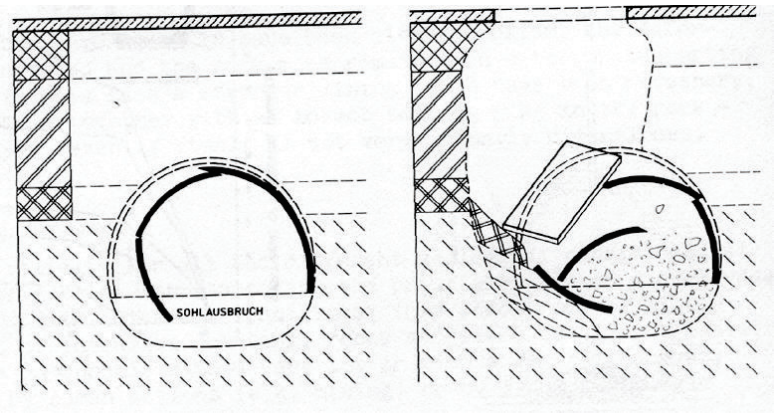


Figure I-3: Description of the failure occurred (Muller, 1978 [21])

1.4. Degradation of the ground due to big deformations

On the right the traditional form of mining galleries in the Ruhr basin with overburden up to 1000 m. Deformation of the sill is frequent (up to 30 cm of excavation every year to maintain the shape). Attempts were made to correct this by means of shotcrete and bolts but without success. Only one only a circular section supported with 25 cm of shotcrete, heavy trusses and few bolts, and an immediate closure of the section at less than one diameter distance to the advancing face managed to solve the problem (Muller 1978 [21]),

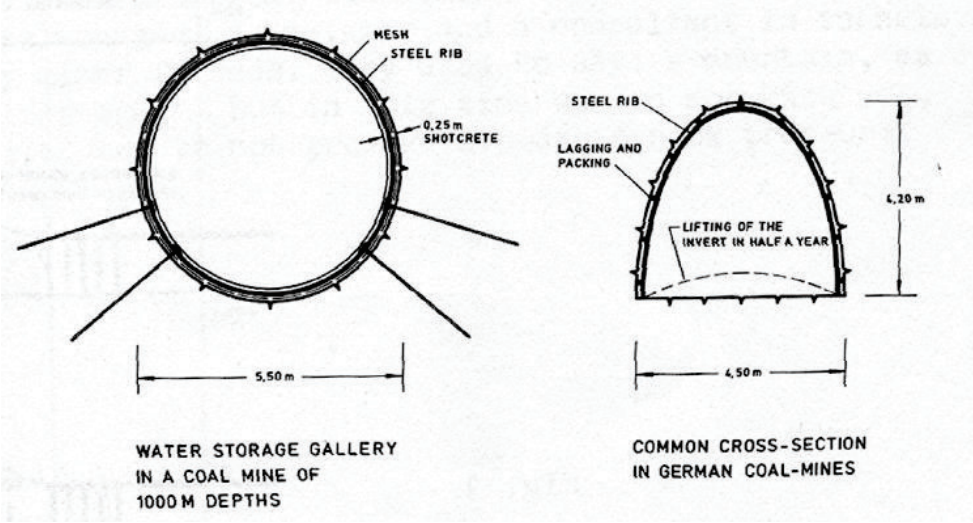


Figure I-4: Description of the problem and solution (Muller, 1978 [21])

The main lessons that can be learned from these collapses are:

- Collapses can happen in any of the excavation phases.
- All actors, designer, constructor and supervisor must have previous experience.
- Collapses are usually associated with geological-geotechnical conditions that were not foreseen and/or where appropriate measures have not been taken.
- In addition to a good design, it is essential to have effective real-time instrumentation of the deformations and stresses that are being produced.
- In relation to the application of NATM in soils, the shotcrete ring should be closed as soon as possible, especially in the case of soft soils with little cover. This may be necessary even in temporary excavation phases.

II. ANNEX: CONSTITUTIVE MODELS OF SOILS AND STRUCTURAL ELEMENTS

2.1. Constitutive Models of Soils

2.1.1 Mohr Coulomb Model

The Mohr-Coulomb model is a well-known linear elastic perfectly plastic model, which can be used as a first approximation of soil behaviour. The linear elastic part of the Mohr-Coulomb model is based on Hooke's law of isotropic elasticity. The perfectly plastic part is based on the Mohr-Coulomb failure criterion, formulated in a non-associated plasticity framework. Plasticity involves the development of irreversible strains.

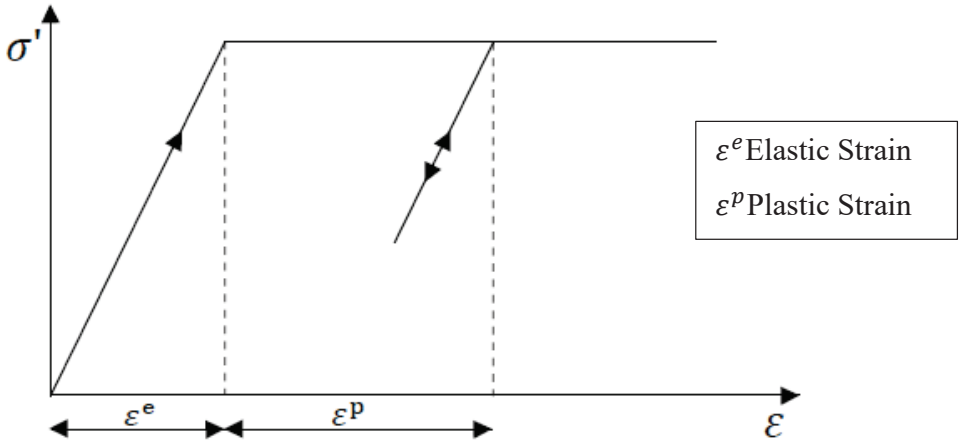


Figure II-1: Basic idea of an elastic perfectly plastic model- Mohr Coulomb (Plaxis V24 Manual [20])

The law of resistance of a material according to Coulomb depends on two fundamental parameters, its cohesion and its angle of internal friction, and can be stated as

$$\tau = c' + \sigma' \times tan\,\emptyset'$$

Where:

c': is the effective cohesion of the material.

$\emptyset'$: is the effective internal friction angle.

σ': is the effective stress acting normal (perpendicular) to the shear or failure plane.

τ: is the tangential or shear stress acting on the shear or failure plane. As can be observed, it is dependent on the value of σ. The higher the σ, the higher the shear stress. Therefore, in the case of the Mohr-Coulomb criterion, the strength of the material is dependent on the normal stress applied on the shear plane.

The Mohr plane is defined by two perpendicular axes. The vertical axis (ordinate) corresponds to the shear stress and the horizontal axis (abscissa) corresponds to the normal stress. If we draw on this plane the Coulomb line, defined by means of the previous equation, we would obtain the graphical representation shown in the following Figure II-2.

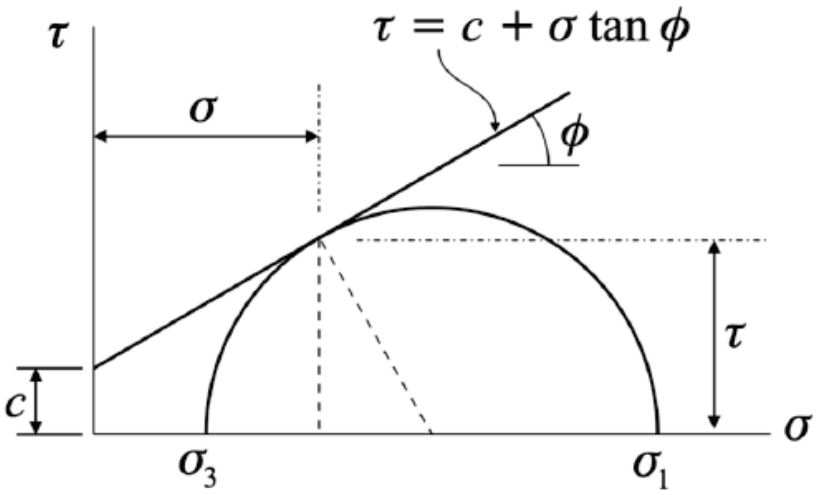


Figure II-2: Mohr-Coulomb criterion in the Mohr plane (Plaxis V24 Manual [20])

As can be seen in Figure II-2 above, the Mohr circle defined by the minimum principal stress and the maximum principal stress is tangent to the Coulomb line (the Coulomb line and Mohr circle intersect at a single point), then the stress state at the point in question corresponds to a stress state on the Mohr-Coulomb yield surface, i.e. it corresponds to a stress state for which the soil has reached, at that point in question, plastification (or the plastic state, in which plastic deformations start to occur). If, on the other hand, the Mohr circle is not tangent to the Coulomb line, but is entirely below it, then the stress state at the point in question corresponds to an elastic state.

The full Mohr-Coulomb yield condition consists of six yield functions when formulated in terms of principal stresses

$$f_{1a} = \frac{1}{2}(\sigma'_2 - \sigma'_3) + \frac{1}{2}(\sigma'_2 + \sigma'_3)\sin\emptyset - c \cdot \cos\emptyset \leq 0$$

$$f_{2a} = \frac{1}{2}(\sigma'_3 - \sigma'_2) + \frac{1}{2}(\sigma'_3 + \sigma'_2)\sin\emptyset - c \cdot \cos\emptyset \leq 0$$

$$f_{2a} = \frac{1}{2}(\sigma'_3 - \sigma'_1) + \frac{1}{2}(\sigma'_3 + \sigma'_1)\sin\emptyset - c \cdot \cos\emptyset \leq 0$$

$$f_{2b} = \frac{1}{2}(\sigma'_1 - \sigma'_3) + \frac{1}{2}(\sigma'_1 + \sigma'_3)\sin\emptyset - c \cdot \cos\emptyset \leq 0$$

$$f_{3a} = \frac{1}{2}(\sigma'_1 - \sigma'_2) + \frac{1}{2}(\sigma'_1 + \sigma'_2)\sin\emptyset - c \cdot \cos\emptyset \leq 0$$

$$f_{3b} = \frac{1}{2}(\sigma'_2 - \sigma'_1) + \frac{1}{2}(\sigma'_2 + \sigma'_1)\sin\emptyset - c \cdot \cos\emptyset \leq 0$$

The two plastic model parameters appearing in the yield functions are the well-known friction angle $\emptyset$ and the cohesion c. The condition $f_i = 0$ for all yield functions together (where f_i is used to denote each individual yield function) represents a fixed hexagonal cone in principal stress space as shown in Figure II-3.

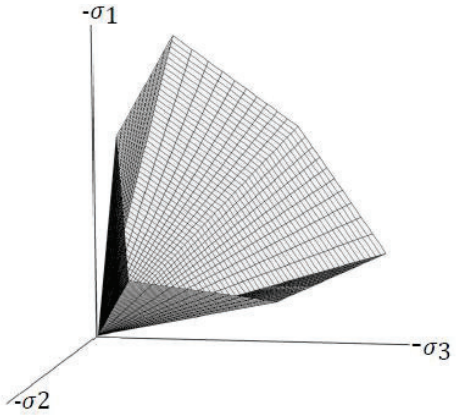


Figure II-3: The Mohr-Coulomb yield surface in principal stress space (c = 0)

The Mohr Coulomb model is widely used in geotechnics because it is a very intuitive behavioral model, defined by parameters (cohesion, friction angle, Young's modulus, etc.) that have a very obvious physical meaning and are easily measurable and quantifiable and its plasticization criterion is very accurate and reflects very appropriately the change or transition from the elastic to the plastic stress regime. Therefore, is used in the vast majority of advanced constitutive models (Hardeing Soil, etc.), which subsequently complement and extend it.

2.1.2 Hardening Soil Model

In contrast to an elastic perfectly-plastic model, the yield surface of a hardening plasticity model is not fixed in principal stress space, but it can expand due to plastic straining. Distinction can be made between two main types of hardening, namely shear hardening and compression hardening. Shear hardening is used to model irreversible strains due to primary deviatoric loading. Compression hardening is used to model irreversible plastic strains due to primary compression in oedometer loading and isotropic loading. Both types of hardening are contained in the present model.

A basic idea for the formulation of the Hardening Soil model is the hyperbolic relationship between the vertical strain, ε_1, and the deviatoric stress, q, in primary triaxial loading. Here standard drained triaxial tests tend to yield curves that can be described by:

$$-\varepsilon_1 = \frac{1}{E_i} \times \frac{q}{1 - \frac{q}{q_a}} \; for \; q < q_f$$

where

q_a = Asymptotic value of the shear strength.

E_i = Initial stiffness.

E_i is related to E_{50} by:

$$E_i = \frac{2E_{50}}{2 - R_f}$$

where

R_f is the failure ratio, which should obviously be smaller than or equal to 1

In PLAXIS, $R_f = 0.9$ is chosen as a suitable default setting.

The behavior defined by the above equation has the following graphical form, which is the basic idea for the hyperbolic formulation of the Hardening Soil model:

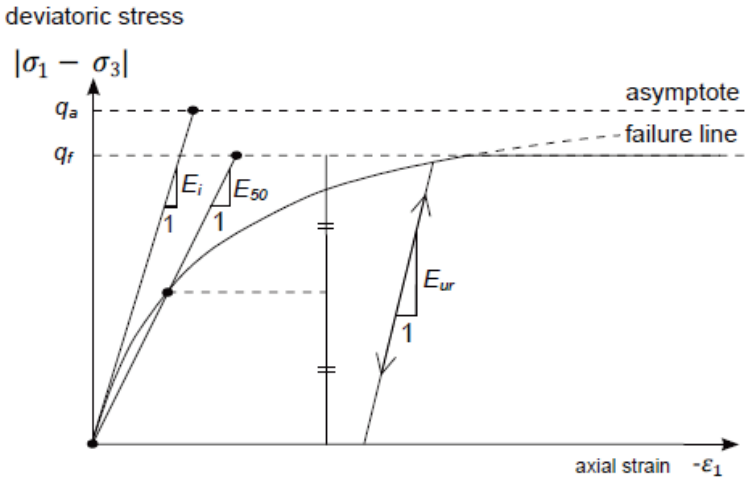


Figure II-4: Hardening Soil type behavior (Plaxis V24 Manual [20])

In the above expression, q_a is the asymptotic value defining the strength, and E_{50} is the deformation modulus at 50% of the deviatoric stress for rupture (q_f). The expression to determine qf comes from the failure criterion defined by Mohr Coulomb, which considers the shear strength parameters associated with cohesion and frictional angle, while q_a is a fraction of q_f, as shown in the following expressions:

$$q_f = (c' \cdot cot\, \emptyset' - \sigma'_3) \times \frac{2 \cdot sin\, \emptyset'}{3 - sin\, \emptyset'} \qquad and \qquad q_a = \frac{q_f}{R_f}$$

The Young's modulus for 50% deformation (E_{50}), for primary oedometer loading (E_{oed}) and for unloading/ reloading (E_{ur}) are defined by the following expressions:

$$E_{50} = E_{50}^{ref} \times \left(\frac{c' \cdot cos\, \emptyset' - \sigma_3' \cdot sin\, \emptyset'}{c' \cdot cos\, \emptyset' + p^{ref} \cdot sin\, \emptyset'} \right)^m$$

$$E_{oed} = E_{oed}^{ref} \times \left(\frac{c' \cdot cos\, \emptyset' - \frac{\sigma'_3}{K_O^{nc}} \cdot sin\, \emptyset'}{c' \cdot cos\, \emptyset' + p^{ref} \cdot sin\, \emptyset'} \right)^m$$

$$E_{ur} = E_{ur}^{ref} \times \left(\frac{c' \cdot cos\, \emptyset' - \sigma_3' \cdot sin\, \emptyset'}{c' \cdot cos\, \emptyset' + p^{ref} \cdot sin\, \emptyset'} \right)^m$$

Where:

m: is an exponential parameter, obtained experimentally, which determines the relationship (variation) of the E50 modulus with the stress level.

c': is the effective cohesion.

$\emptyset'$ is the effective internal friction angle

E_{50}^{ref}: is the value of the secant modulus corresponding to a value of the horizontal stress $\sigma'_3 = p_{ref}$.

p_{ref}: is the reference pressure for which the value of E_{50}^{ref} is obtained. In most numerical calculation software, a value of 100 kPa is used.

σ'_3 : is the value of the horizontal effective stress.

E_{ur}^{ref}: is the value of the load/unload modulus corresponding to a value of the horizontal stress $\sigma'_3 = p_{ref}$.

E_{oed}^{ref}: is the value of the vertical compressive modulus corresponding to a value of the vertical stress $\sigma'_3 = p_{ref}$.

Note: In many practical cases it is appropriate to set $E_{ur}^{ref} = 3 \cdot E_{50}^{ref}$; this is the default setting used in PLAXIS. Regardless the previous value of E50, a new value will be automatically assigned according to: $E_{50}^{ref} = 1.25 \cdot E_{oed}^{ref}$.

The main difference (and advantage) compared to the Mohr-Coulomb model is that it allows taking into account the variation of soil stiffness (i.e. Young's modulus) with the level of stresses and allows taking into account the different components of soil stiffness, namely stiffness against a deviatoric (or shear) stress, stiffness against a vertical compression (edometric type) and stiffness against an unloading and reloading situation.

2.1.3 Hardening Soil with Small Deformations Model

The original Hardening Soil model assumes elastic material behaviour during unloading and reloading. However, the strain range in which soils can be considered truly elastic, i.e. where they recover from applied straining almost completely, is very small. With increasing strain amplitude, soil stiffness decays nonlinearly. Plotting soil stiffness against log(strain) yields characteristic S-shaped stiffness reduction curves. Figure II-5 gives an example of such a stiffness reduction curve. It outlines also the characteristic shear strains that can be measured near geotechnical structures and the applicable strain ranges of laboratory tests.

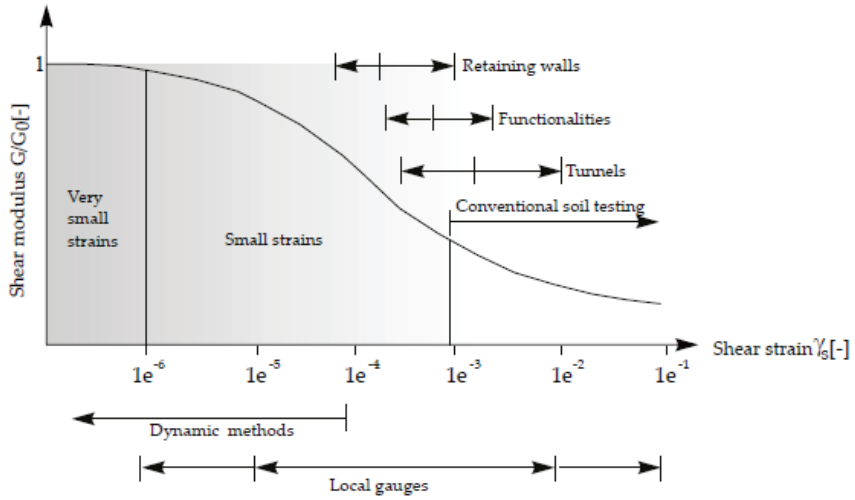


Figure II-5: Characteristic stiffness-strain behaviour of soil with typical strain ranges for laboratory tests and structures (after Atkinson & Sallfors,1991)- (Plaxis V24 Manual [20])

Therefore, from the above figure, it can be concluded that, in order to carry out a rigorous and accurate analysis of soil deformations, it is necessary to take into account its stiffness (modulus) at small initial deformations and its variation (non-linear) with the level of shear deformation, and not the stiffnesses (modulus) corresponding to the "large deformations" that occur during and at the end of the construction of the work in question. This aspect is precisely what allows the Hardening Soil Small model to be taken into account, as shown in the Figure II-6 below.

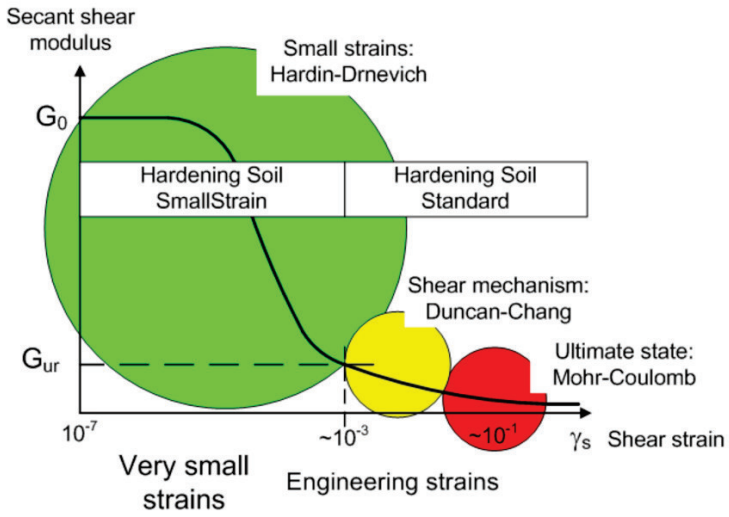


Figure II-6: Decreasing soil modulus with shear deformation and application on the different models (The Hardening Soil Model a Practical Guidebook –Zsoil [18])

Looking at the Figure II-6 above, we see that the Mohr-Coulomb model (red circle) provides acceptable results only for "large" deformations, when the modulus (stiffness) of the soil has decreased considerably with respect to its initial value. Likewise, although it allows stiffness (modulus) to be taken into account for smaller deformations, the Hardening Soil model only provides acceptable results for deformations greater than 1 x 10-3. It is the Hardening Soil Small model (green circle) that allows to take into account not only the value of stiffness (modulus) suitable for small deformations, but also its decrease, in a non-linear way, with increasing shear deformation. This is the main difference with the Hardening Soil model, as well as the main advantage of the Hardening Soil Small model.

The modulus (stiffness) of the soil at small deformations is a soil property that has been widely studied and used in the field of soil dynamics. Its transposition to the static cases is that it can be considered as equivalent to the dynamic modulus Ed and the modulus at small deformations E0, such that E0 = Ed. Both moduli are related to the transverse modulus of elasticity by means of the elasticity expression already discussed in previous sessions.

$$G_o = \frac{E_o}{2 \cdot (1 + \nu)} = \frac{E_o}{2 \cdot (1 + \nu_{ur})}$$

In the case of Poisson's coefficient, in the Hardening Soil Small model it is usually considered that υ=υ_{ur}, where υ_{ur}=0.2 is usually taken. If the soil is subjected to a drained triaxial test, a hyperbolic type curve can be observed between the stress deviator q=σ'1 - σ'3, and the axial deformation ε1, as shown in the following figure.

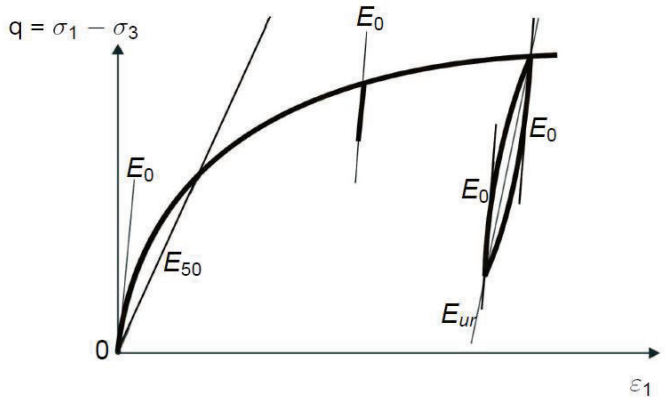


Figure II-7: Stiffness parameters E50, Eur, and Eo of the Hardening Soil model with small-strain stiffness in a triaxial test (Plaxis V24 Manual [20])

The E_O modulus, which is tangent to the curve at the origin and to the load-discharge branch at its upper and lower points, is the modulus at small deformations. In addition to the triaxial test, there are numerous correlations that allow determining the E_O value of the soil from certain in-situ tests and tests that allow directly determining its magnitude, such as the seismic wave propagation velocity test. One of the best known correlations in this sense is that of Alpan (1970) shown in the figure below, in which $E_d = E_O$ and $E_s = E_{ur}$. Generally, it is usually considered that, at most $E_o = 10 \cdot E_{ur}$.

For the Hardening Soil Small model, the modulus G_O is determined from the following expression:

$$G_O = G_O^{ref} \times \left(\frac{c' \cdot cos\,\emptyset' - \sigma_3' \cdot sin\,\emptyset'}{c' \cdot cos\,\emptyset' + p^{ref} \cdot sin\,\emptyset'} \right)^m$$

G_O^{ref}: Reference shear modulus at very small strains ($\varepsilon < 10^{-6}$)

The above equations have made it possible to establish the relationship of G_O with the stress state to which the soil is subjected. It would therefore remain to establish the nonlinear variation of G_O with the tangential or shear deformation. For this purpose, the most commonly used model is the Hardin-Drnevich and Santos y Correia (2001), which was

defined for application in soil dynamics. From experimental data and measurements, the authors determined that the relationship between the transverse deformation modulus and the tangential or shear deformation follows a hyperbolic law with the following form:

$$\frac{G_t}{G_o} = \frac{1}{\left(1 + a \cdot \frac{\gamma}{\gamma_{0.7}}\right)^2} \quad a = 0.385$$

In the case of modulus variation at small deformations with shear deformation, it is not allowed to decrease continuously with deformation until it practically cancels out, as this would lack physical sense. Therefore, when applying the Hardening Soil Small model, we limit the degradation of the modulus Gt with shear deformation until it reaches the value of Gur, which, as we know, is equal to:

$$G_{ur} = \frac{E_{ur}}{2 \cdot (1 + \nu_{ur})}$$

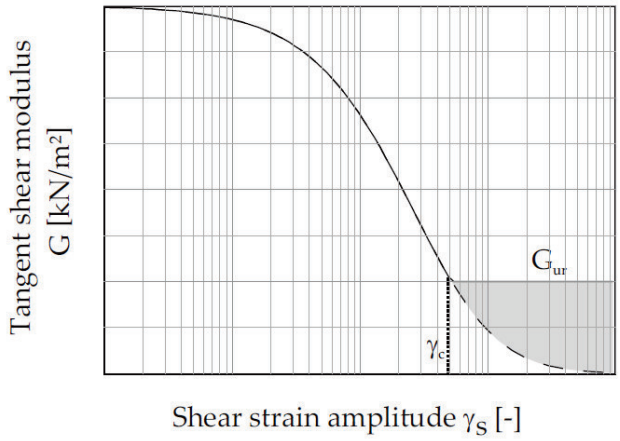


Figure II-8: Cut-off in the tangent stiffness degradation curve (Thomas Benz, 2007 [17])

2.1.4 Comparison between Constitutive Models

A comparison of the three constitutive models used was carried out by means of a triaxial test on the gravel and fine soil, with the geomechanical properties described in the Table IV-1 and Table IV-3, Table IV-4 and Table IV-6, Table IV-7 and Table IV-9.

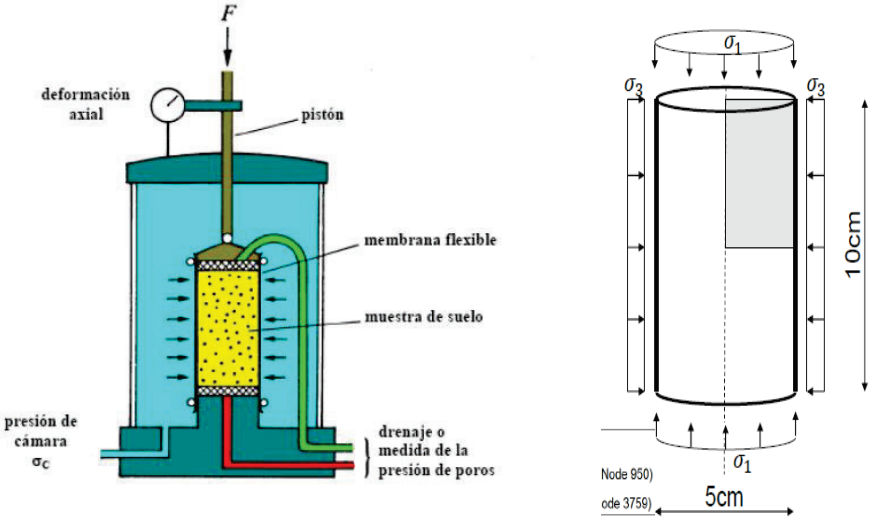
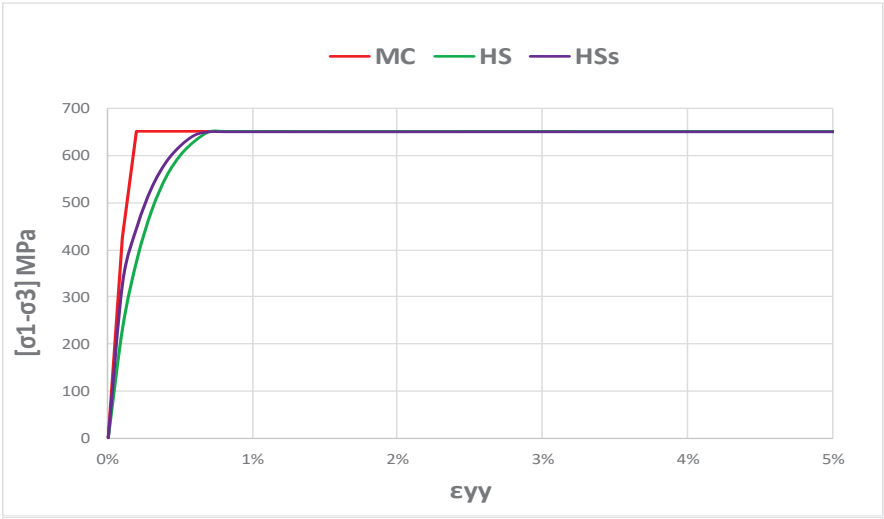


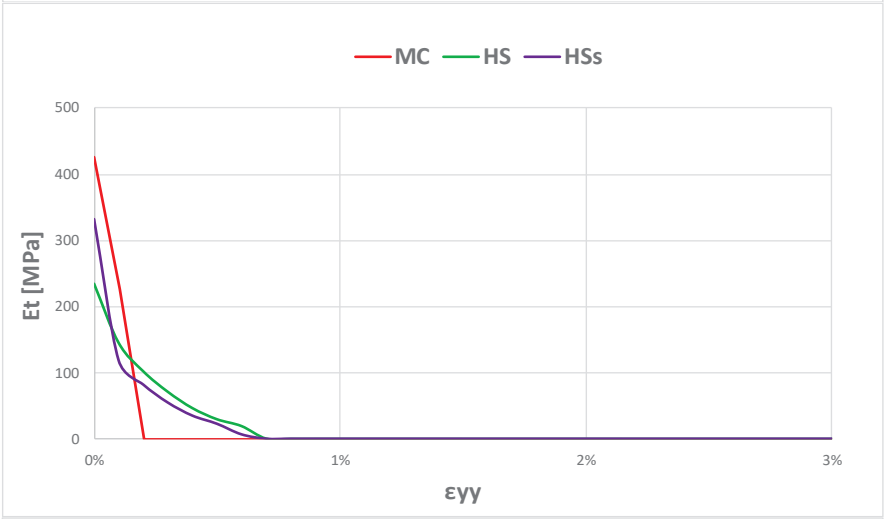
Figure II-9: Triaxial Test on the gravel and fine soils

The following are a different diagrams of the gravel and fine soil sample analyzed. (see Figure II-10 and Figure II-11).

a)



b)



c)

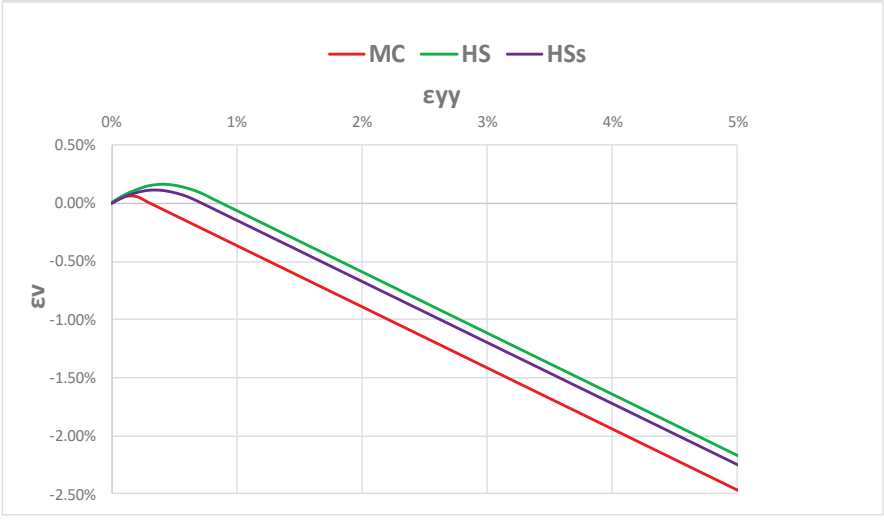
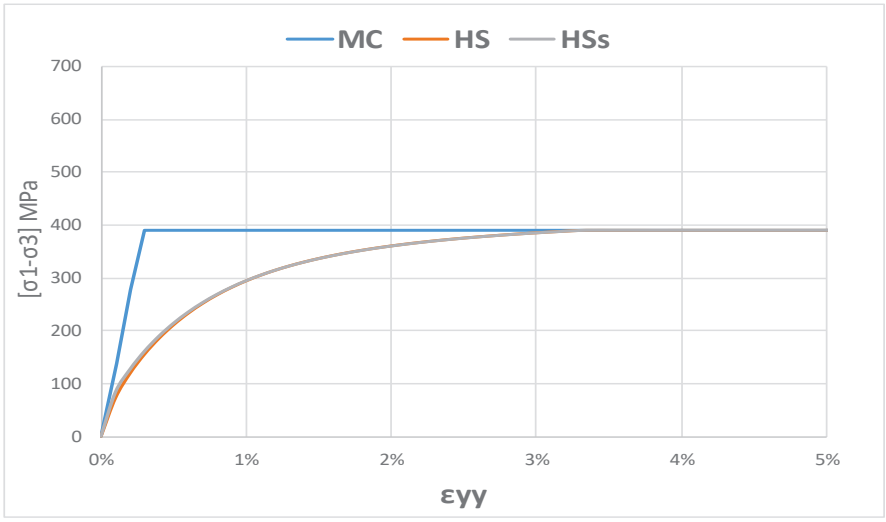


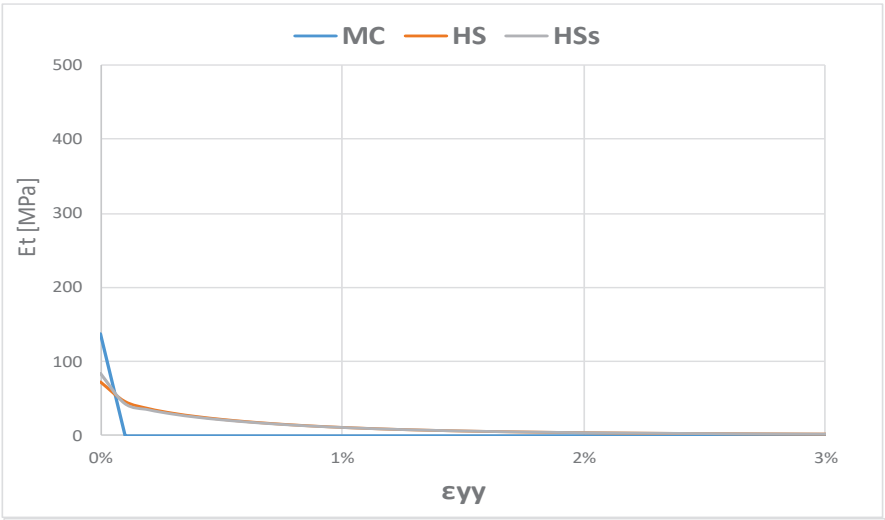
Figure II-10: a) Stress-Strain diagram b) Young´s modulus –Strain diagram

c) Axial Strain – Volumetric Strain diagram, all for Gravel Soil

a)



b)



c)

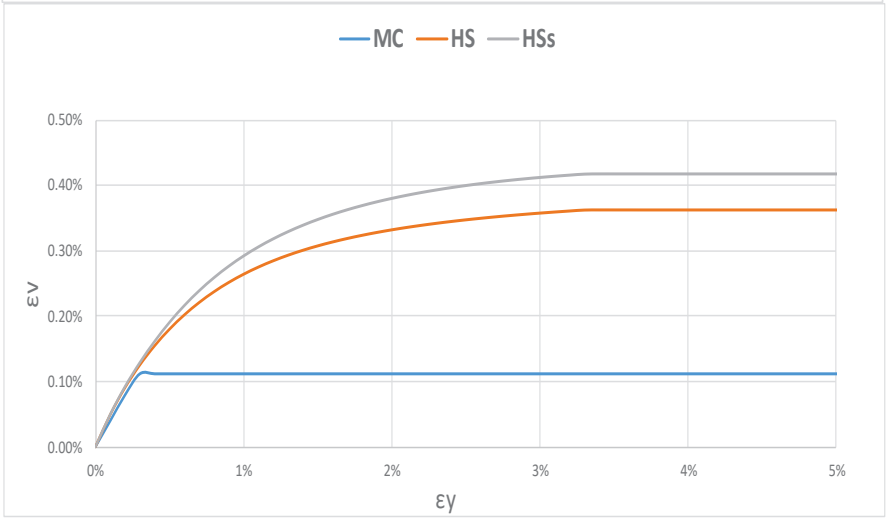


Figure II-11: a) Stress-Strain diagram b) Young´s modulus –Strain diagram

c) Axial Strain – Volumetric Strain diagram, all for Fine Soil

2.2. Constitutive Models of Structural Elements

2.2.1 Volumetric Element: Concrete Model

Generally, for concrete structure elements, a linear elastic material model is adopted due to their strength compared to the one of the soil. However, in some kind of geotechnical problems, the complex non-linear behavior of the concrete structures must be inspected for a reliable redistribution of stress-strain in the continuum and a correct design. Distinction can be made between the main features of the complex concrete behavior: limited strength in compression and tension, time-dependent strength and stiffness, strain hardening/softening, creep and shrinkage.

With the Concrete model more realistic stress distributions can be obtained, as the non-linearity of the material behavior is taken into account.

When subjected to deviatoric loading, concrete shows different behaviors: in compression, the strength increases non-linearly up to a peak value and then softens to a residual one; in tension, it's considered linear elastic until reaching the tensile strength and then softens to the residual value. The Concrete model employs a Mohr-Coulomb yield surface for deviatoric loading, combined with a Rankine yield surface in the tensile regime.

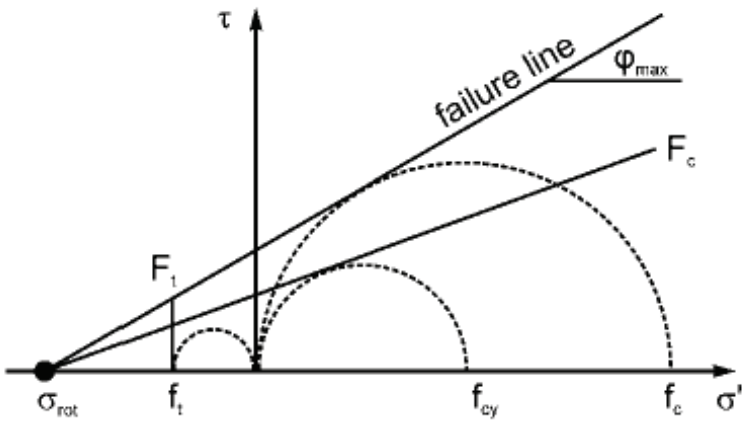


Figure II-12: Yield Surfaces and failure envelope for Concrete model (Plaxis V24 Manual [20])

(a) Strain hardening and softening

In compression, the Concrete model follows the approach proposed by Schütz, Potts & Zdravkovi´c (2011). The stress-strain curve is divided in four parts (Figure II-13):

- Part I - quadratic strain hardening
- Part II - linear strain softening
- Part III - linear strain softening
- Part IV - constant residual strength

Due to the time-dependency of the involved material parameters, a normalised hardening/softening parameter $H_c = \frac{\varepsilon_c^p}{\varepsilon_{cp}^p}$ is used, with ε_c^p = minor plastic strain and ε_{cp}^p = plastic peak strain in uniaxial compression.

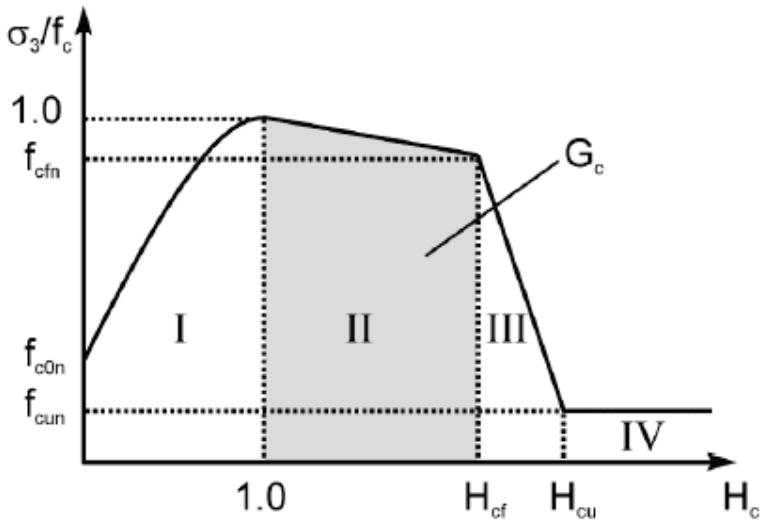


Figure II-13: Normalised stress-strain curve in compression (Plaxis V24 Manual [20])

The Concrete model behaviour in tension is linear elastic until the tensile strength f_t is reached, then softens with a linear strain softening (Figure II-14). The strain softening is governed by the normalized tension softening parameter $H_t = \frac{\varepsilon_1^p}{\varepsilon_{tu}^p}$ with ε_1^p = major principal plastic strain and ε_{tu}^p =Plastic ultimate strain in uniaxial tension.

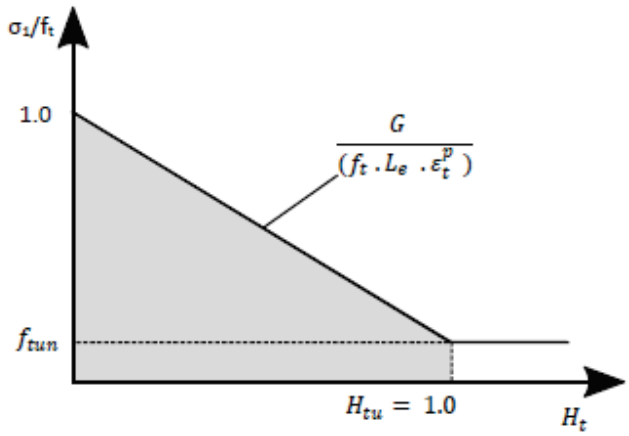


Figure II-14: Tension softening (Plaxis V24 Manual [20])

(b) Time-dependency of the Concrete model

The Concrete model takes into account the time-dependent behavior of material parameters. The stiffness and strength of concrete increase rapidly with time due to the hydration of the cement paste. The increase of Young's modulus E in the model follows an approach similar to the recommendation of CEB-FIP model code (1990) [8]

$$E_{(t)} = E_{28} \times e^{s_{stiff}\cdot\left(1-\sqrt{\frac{t_{hydr}}{t}}\right)}$$

Where:

E_{28}= Young´s modulus of cured concrete

t_{hydr}= Time until curing (e.g. usually taken as 28 days)

t= time (days)

s_{stiff}= Parameter governing stiffness evolution with time

$s_{stiff}$is related to the stiffness ratio at 1 day, E_1/E_{28}, and t_{hydr} as:

$$s_{stiff} = -\frac{ln\left(\frac{E_1}{E_{28}}\right)}{\sqrt{\frac{t_{hydr}}{t_{1d}}} - 1}$$

where t_{1d} is the duration of one day in the unit time. The Young's modulus is constant for $t < t_{1d}$and for $t > t_{hydr}$.

For the uniaxial compressive strength f_c, the Concrete model implements approaches is similar to the recommendation of CEB-FIP model code (1990) [8] for concrete. The relations are the same as before but exchanging s_{stiff} with $s_{strength}$, which depends now on the strength ratio at 1 day, $\frac{f_{c1}}{f_{c28}}$, and t_{hydr}. A lower limit of $f_c = 0.005 \cdot f_{c28}$ is used at very early age. The CEB-FIP [8] type approach yields very low concrete strength at ages < 2h.

$$f_{c(t)} = f_{c28} \times e^{s_{strength} \cdot \left(1 - \sqrt{\frac{t_{hydr}}{t}}\right)} \qquad s_{strength} = -\frac{ln\left(\frac{f_{c1}}{f_{c28}}\right)}{\sqrt{\frac{t_{hydr}}{t_{1d}}} - 1}$$

(c) Plastic Deformability

The ability of young concrete to withstand large deformations is not only a result of its low elastic modulus at this age, but also due to its high plastic ductility. With concrete aging this ductile behavior decreases.

In the Concrete model this behavior is represented by a time-dependent plastic peak strain ε_{cp}^{p}. Similar to the approach proposed by Meschke, Kropik & Mang (1996), a tri-linear function in time is adopted. Input values are the plastic peak strains at t = 1h, 8h and 24h. Beyond 24h, ε_{cp}^{p} is assumed to be constant.

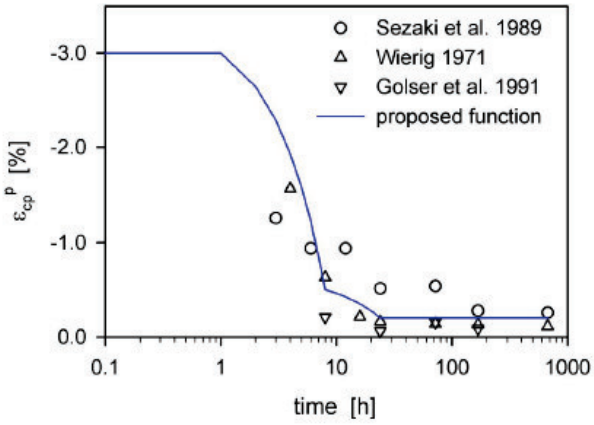


Figure II-15: Reduction of ε_{cp}^{p} with aging in the Concrete model compared to experimental data from uniaxial compression tests. The chosen ε_{cp}^{p} p values are -3%, -0.5% and -0.2%. (Plaxis V24 Manual [20])

In this thesis, creep and shrinkage phenomena are not considered, but the concrete model allows them to be considered.

2.2.2 Shell Element: Plate Element

The PLAXIS 2D program allows for orthotropic elasto-plastic material behaviour in plate elements. The elastic behaviour is defined by the parameters: Axial Stiffness (EA), Bending Stiffness (EI), Poisson´s ratio (ν) and plastic behavior is defined by the parameters: Maximum bending moment (M_p) and Maximum axial force (N_p).

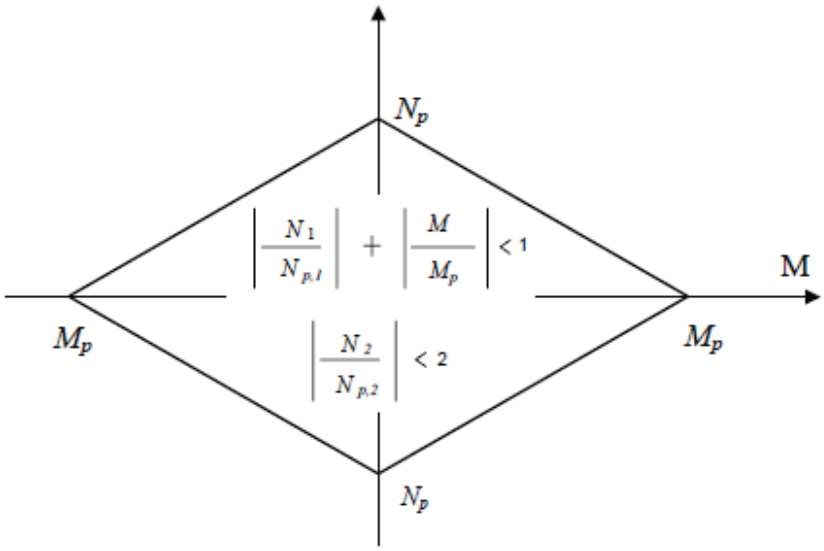


Figure II-16: Combinations of maximum bending moment and axial force (Plaxis V24 Manual [20])

The material behavior in plate elements is defined by the following relationship between strains and stresses.

$$\begin{bmatrix} \sigma_N \\ \Sigma_2 \\ \tau \end{bmatrix} = \begin{bmatrix} \frac{2 \cdot G}{1-\nu} & \frac{2 \cdot G}{1-\nu} & 0 \\ \frac{2 \cdot G}{1-\nu} & \frac{2 \cdot G}{1-\nu} & 0 \\ 0 & 0 & k \cdot G \end{bmatrix} \times \begin{bmatrix} \varepsilon_N \\ \varepsilon_2 \\ \gamma \end{bmatrix}$$

In which k is the shear correction factor, which is taken as 5/6. For isotropic material:

$$G = \frac{E}{2 \cdot (1 + \nu)}$$

The material behavior in plate elements is defined by the following relationship between structural forces and strains:

Axil Force	$N = E \cdot A \cdot \varepsilon$
Shear Force	$Q = \frac{k \cdot E \cdot A}{2 \cdot (1+\nu)}$
Bending Moment	$M = E \cdot I \cdot \kappa$

Where

k=5/6 is the shear correction factor

$\kappa = \frac{\ddot{u}}{x}$ is the curvature

III. ANNEX: STRUCTURAL VERIFICATION WITH PRE-EXISTING METRO TUNNEL

3.1. Variation of the Constitutive Soil Model with Plane Sole Section in New Tunnels

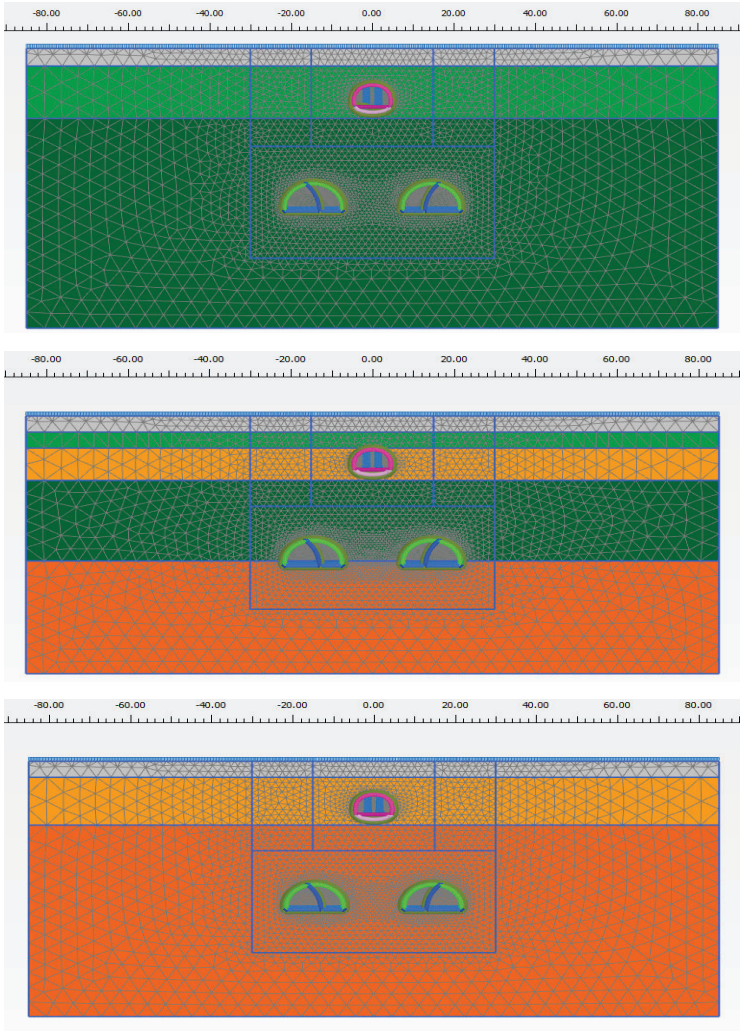


Figure III-1: Soils Models (Gravel-superior, Mixed-central and Fine-inferior) with Pre-existing Metro Tunnel and Plane Sole section in New Tunnels

3.1.1 Verification of the Deformation in the Metro Tunnel

Initially, the vertical deformations or settlements are shown for each soil profile, in the most important construction phases and for each soil constitutive model. Then, the settlement profiles located at the inferior level, 18.50 m, and the verification of the acceptance criterion of transverse deformation of the rails of the Metro Tunnel (See Chapter 3.7.1(a)), are presented.

(a) Analysis of the Gravel Profile

(a.1) Construction Stage

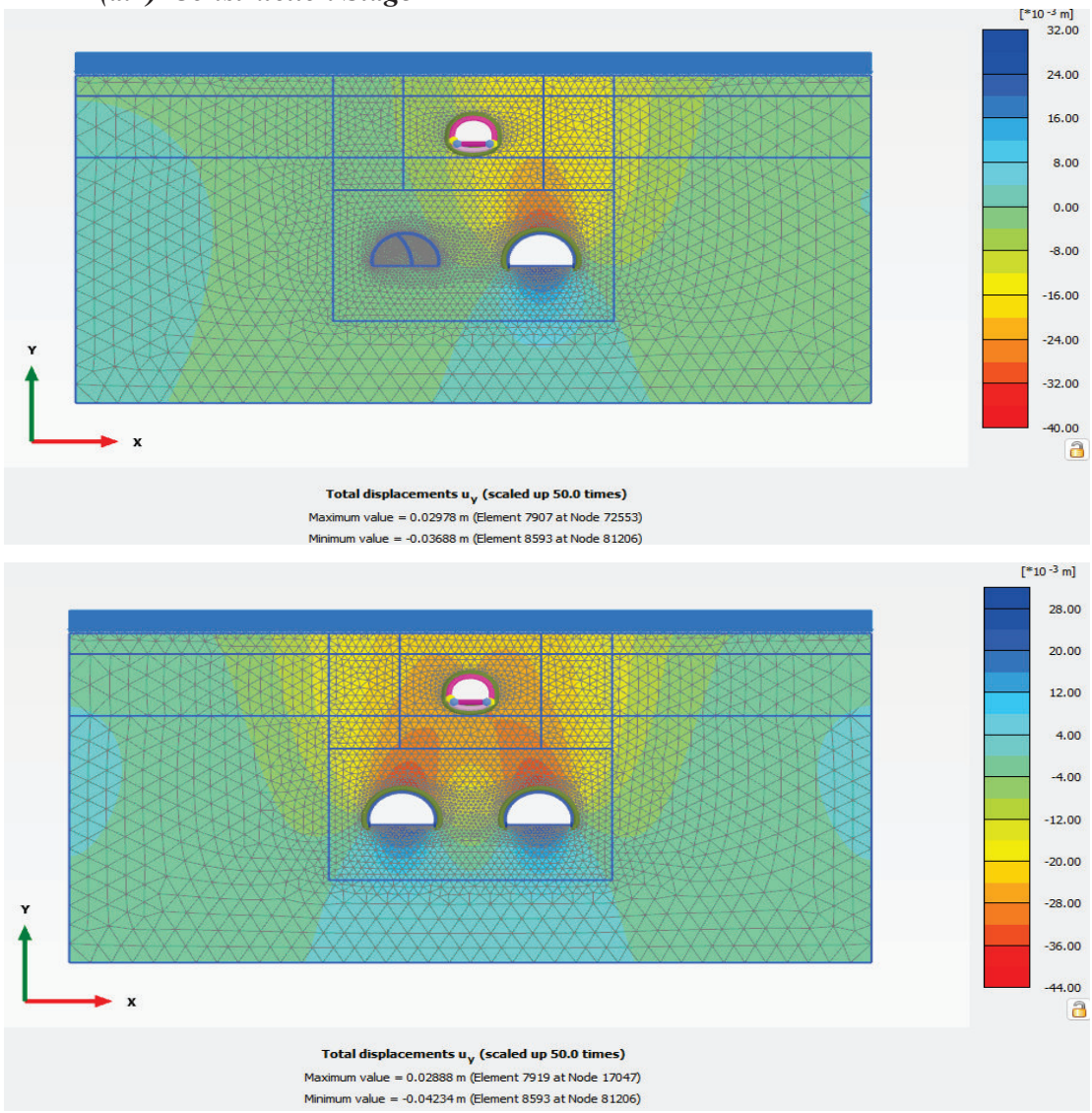
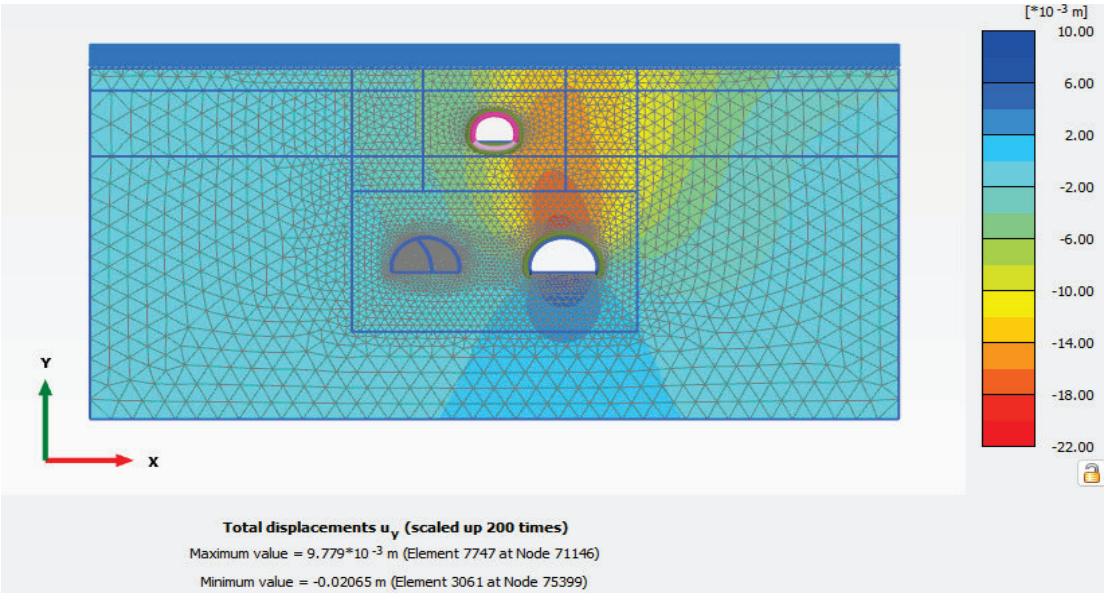


Figure III-2: Vertical Settlement in Construction- (WT and ET)- MC- Gravel Plane Sole Section in New Tunnels



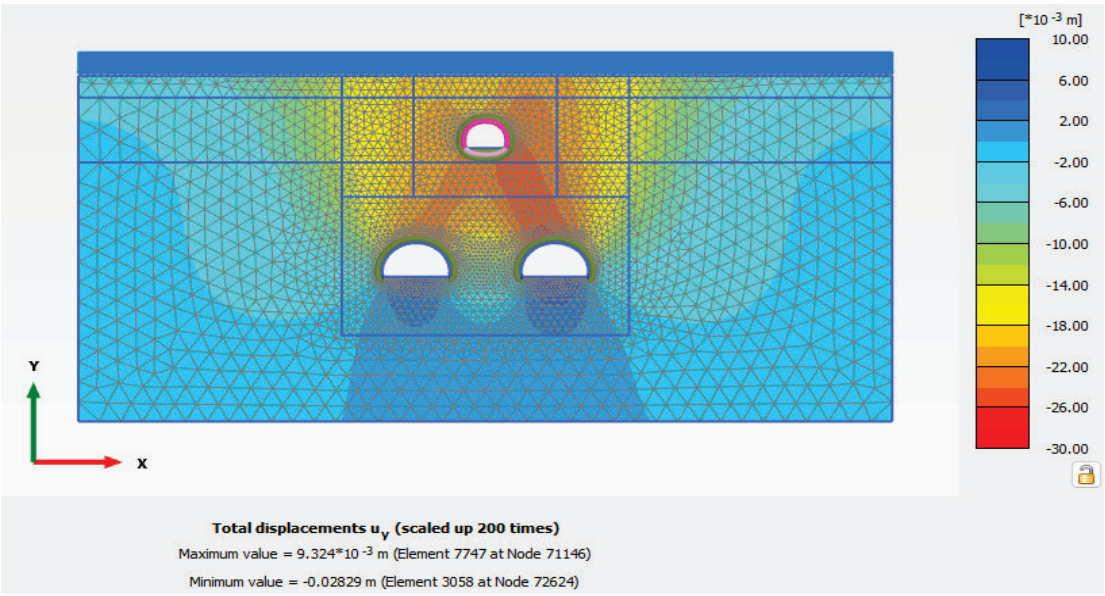
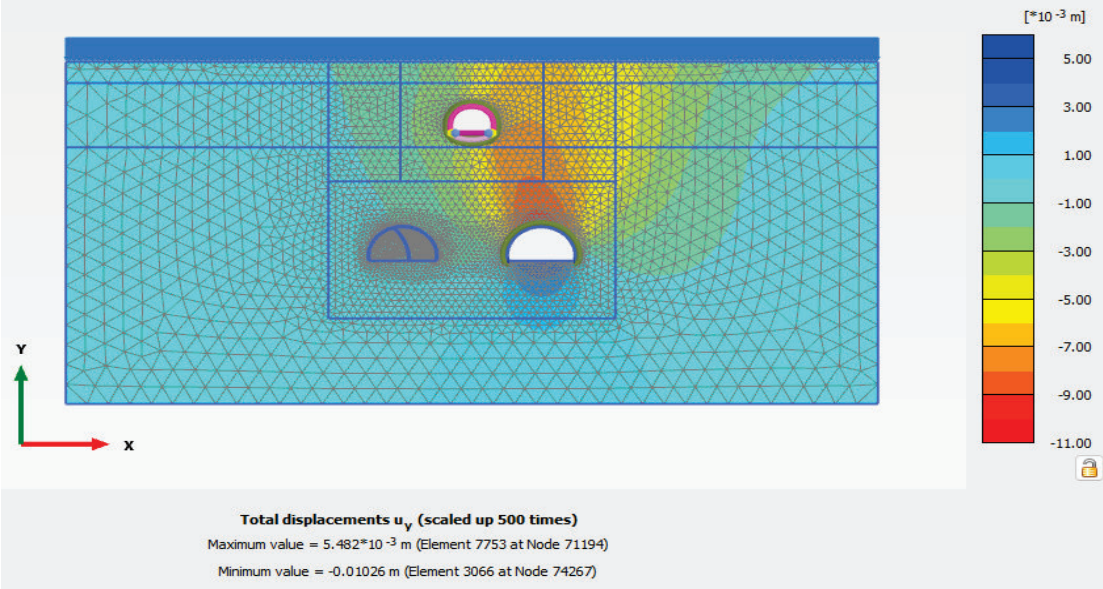


Figure III-3: Vertical Settlement in Construction (WT and ET)- HS- Gravel

Plane Sole Section in New Tunnels



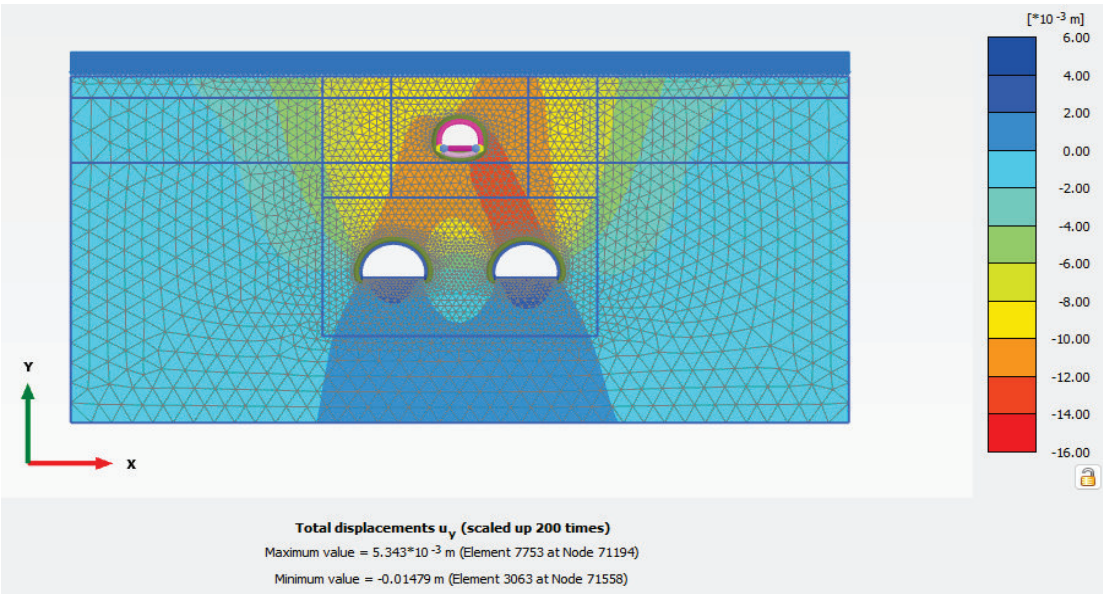
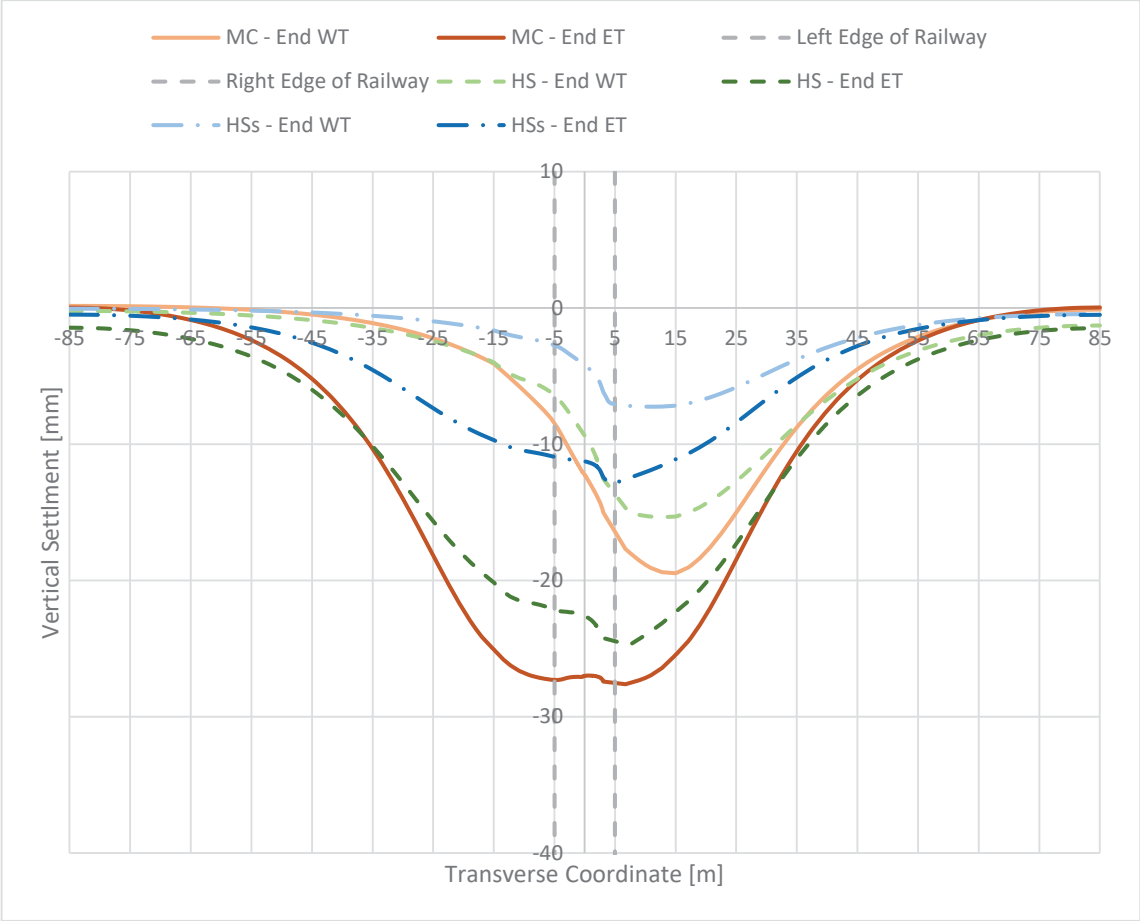


Figure III-4: Vertical Settlement in Construction (WT and ET)- HSs- Gravel Plane Sole Section in New Tunnels.



Graph III-1: Diagram of Transverse Settlement on Metro Tunnel - Construction Stage – Model with Plane Sole Section in New Tunnels- Gravel

Table III-1: Verification of the Transverse Settlement Limit- MC Model- Construction Stage- Gravel- Plane Sole Section in New Tunnels

Phase	Rial 1 Settl (mm)	Rial 2 Settl (mm)	Δ Settl (mm)	Δ Limit (mm)	Verification
Settlement of West Rial					
Excavation WT	-12.79	-13.97	1.18	2	**CHECK**
Excavation ET	-26.99	-27.07	0.09	2	**CHECK**
Settlement of East Rial					
Excavation WT	-11.77	-10.64	1.13	2	**CHECK**
Excavation ET	-27.09	-27.10	0.02	2	**CHECK**

Table III-2: Verification of the Transverse Settlement Limit - HS Model- Construction Stage- Gravel- Plane Sole Section in New Tunnels

Phase	Rial 1 Settl (mm)	Rial 2 Settl (mm)	Δ Settl (mm)	Δ Limit (mm)	Verification
Settlement of West Rial					
Excavation WT	-9.92	-11.40	1.48	2	**CHECK**
Excavation ET	-22.81	-23.56	0.75	2	**CHECK**
Settlement of East Rial					
Excavation WT	-8.90	-7.96	0.94	2	**CHECK**
Excavation ET	-22.50	-22.35	0.15	2	**CHECK**

Table III-3: Verification of the Transverse Settlement Limit- HSs Model- Construction Stage- Gravel- Plane Sole Section in New Tunnels

Phase	Rial 1 Settl (mm)	Rial 2 Settl (mm)	Δ Settl (mm)	Δ Limit (mm)	Verification
Settlement of West Rial					
Excavation WT	-4.48	-5.23	0.76	2	**CHECK**
Excavation ET	-11.34	-11.72	0.38	2	**CHECK**
Settlement of East Rial					
Excavation WT	-3.96	-3.50	0.46	2	**CHECK**
Excavation ET	-11.18	-11.11	0.07	2	**CHECK**

(a.2) Service Stage

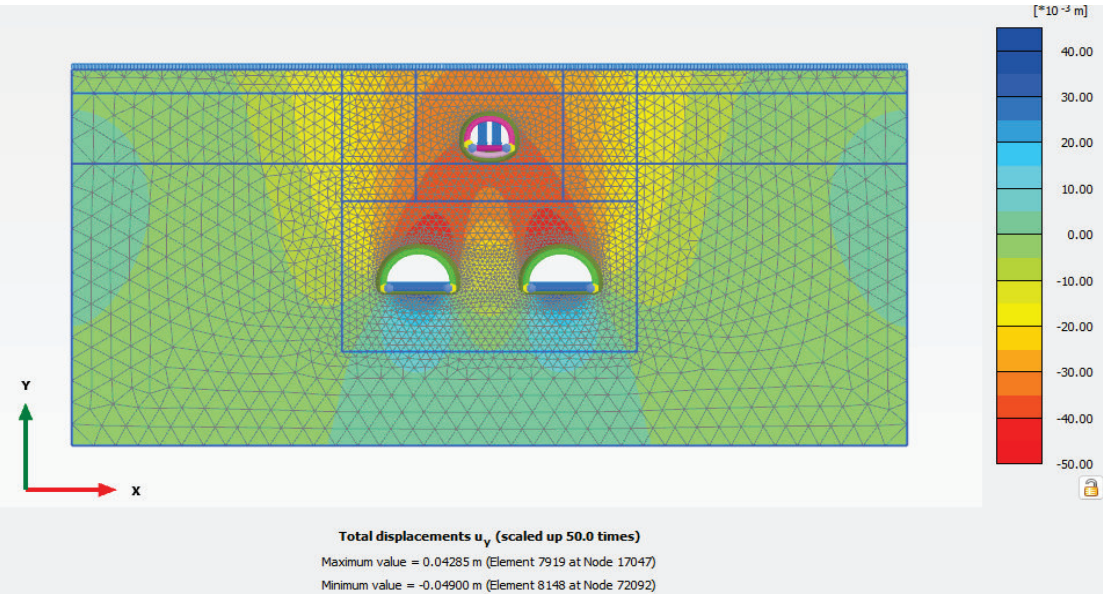


Figure III-5: Vertical Settlement in Service- MC- Gravel- Plane Sole Section in New Tunnels

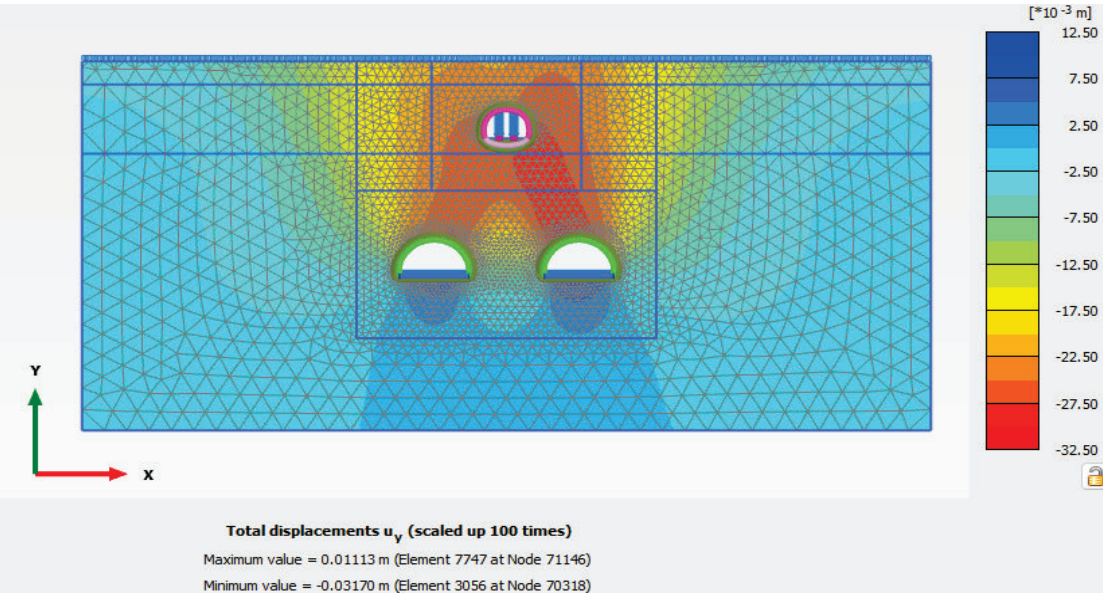


Figure III-6: Vertical Settlement in Service- HS- Gravel-

Plane Sole Section in New Tunnels

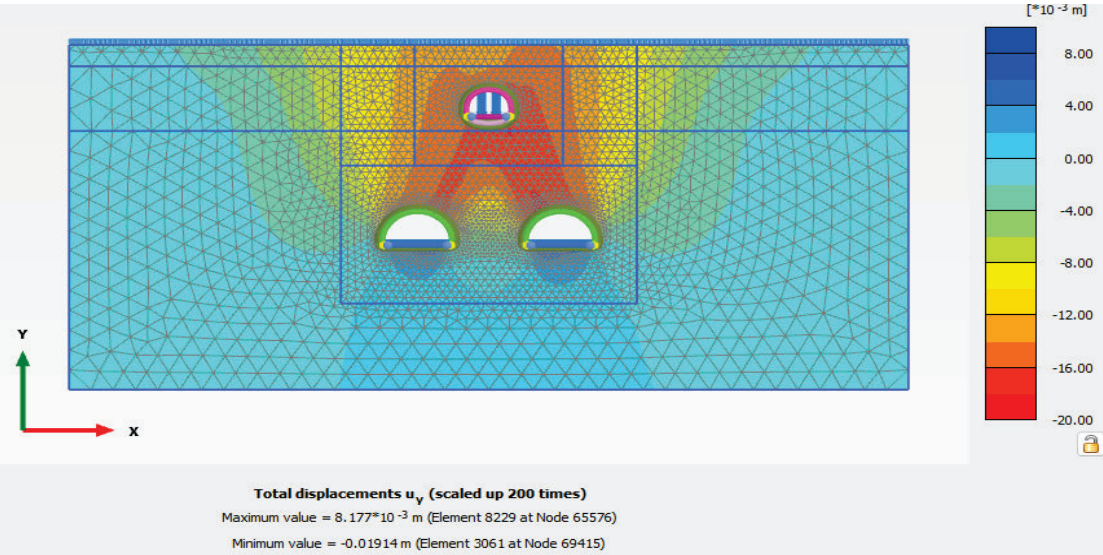
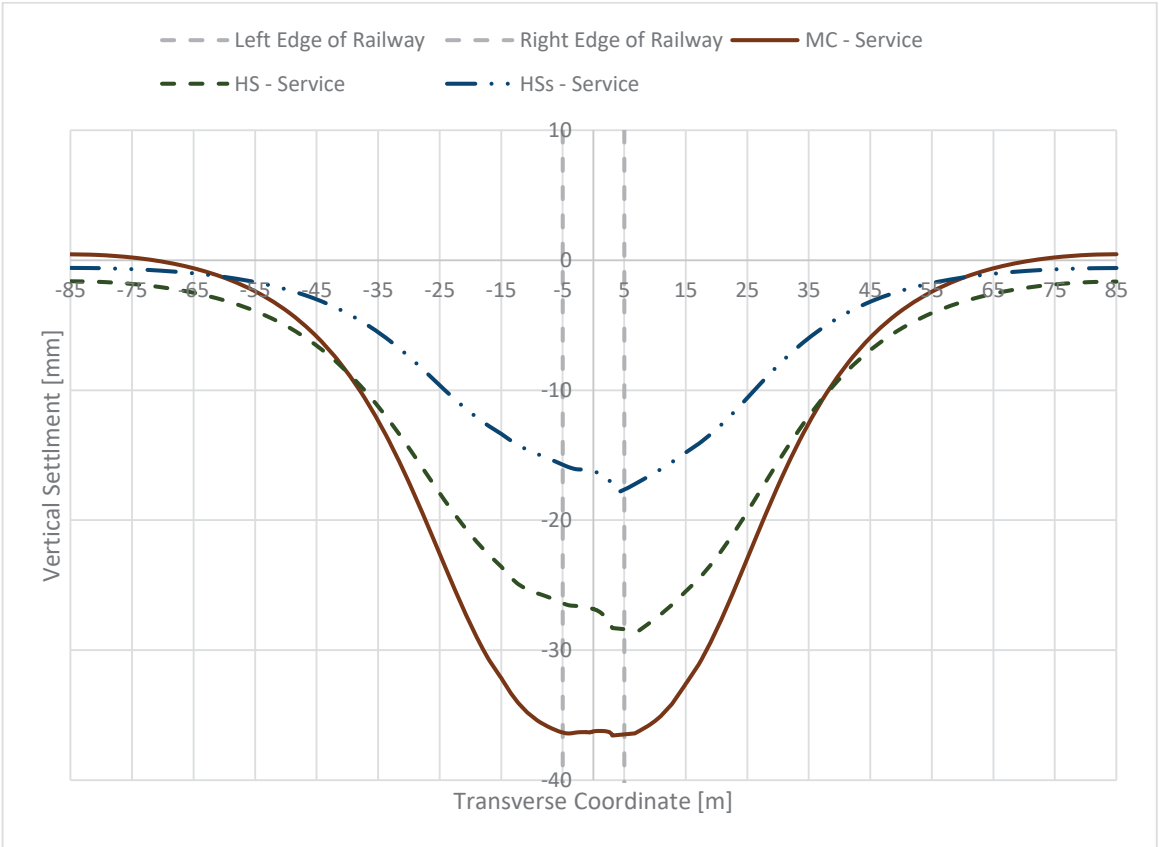


Figure III-7: Vertical Settlement in Service- HSs- Gravel-

Plane Sole Section in New Tunnels



Graph III-2: Diagram of Transverse Settlement on Metro Tunnel - Service Stage –

Model with Plane Sole Section in New Tunnels- Gravel

Table III-4: Verification of the Transverse Settlement Limit- MC Model- Service Stage- Gravel Plane Sole Section in New Tunnels

Phase	Rial 1 Settl (mm)	Rial 2 Settl (mm)	Δ Settl (mm)	Δ Limit (mm)	Verification
Settlement of West Rial					
Service	-36.15	-36.20	0.05	2	**CHECK**
Settlement of East Rial					
Service	-36.24	-36.22	0.02	2	**CHECK**

Table III-5: Verification of the Transverse Settlement Limit- HS Model- Service Stage- Gravel Plane Sole Section in New Tunnels

Phase	Rial 1 Settl (mm)	Rial 2 Settl (mm)	Δ Settl (mm)	Δ Limit (mm)	Verification
Settlement of West Rial					
Service	-26.99	-27.68	0.69	2	**CHECK**
Settlement of East Rial					
Service	-26.73	-26.62	0.11	2	**CHECK**

Table III-6: Verification of the Transverse Settlement Limit- HSs Model- Service Stage- Gravel Plane Sole Section in New Tunnels

Phase	Rial 1 Settl (mm)	Rial 2 Settl (mm)	Δ Settl (mm)	Δ Limit (mm)	Verification
Settlement of West Rial					
Service	-16.35	-16.71	0.36	2	**CHECK**
Settlement of East Rial					
Service	-16.18	-16.09	0.08	2	**CHECK**

(b) Analysis of the Mixed Profile

(b.1) Construction Stage

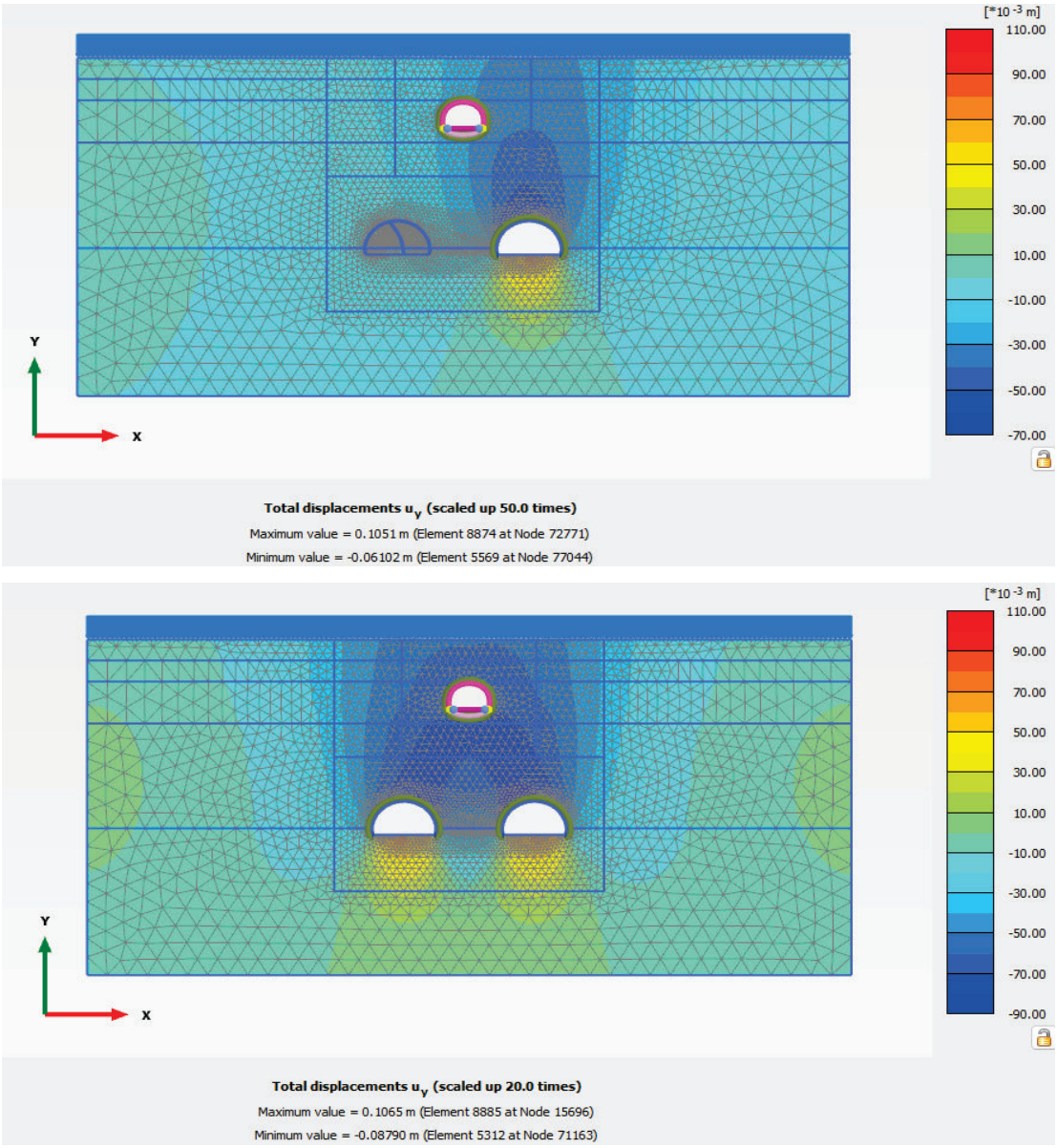


Figure III-8: Vertical Settlement in Construction (WT and ET)- MC- Mixed-Plane Sole Section in New Tunnels

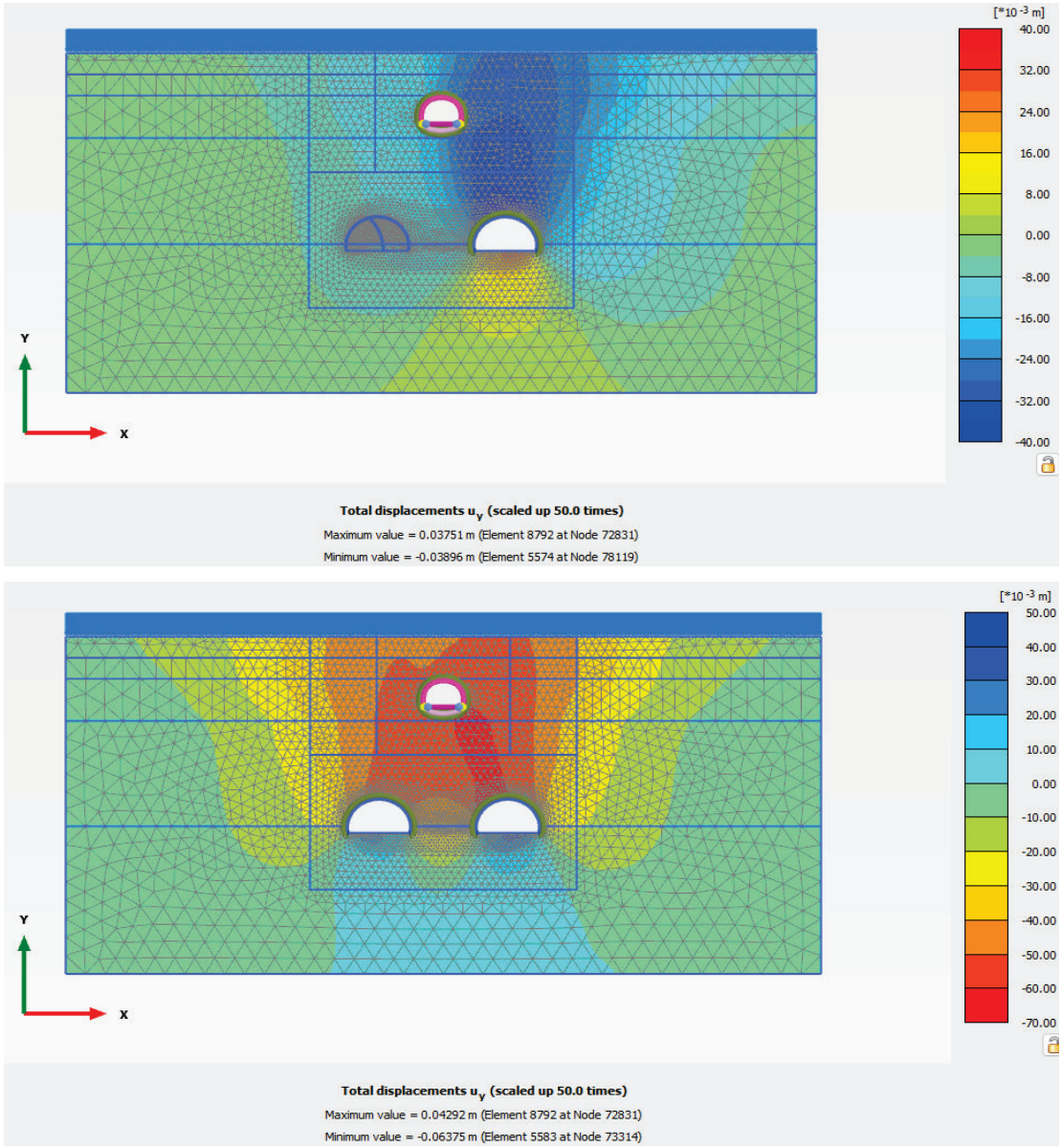
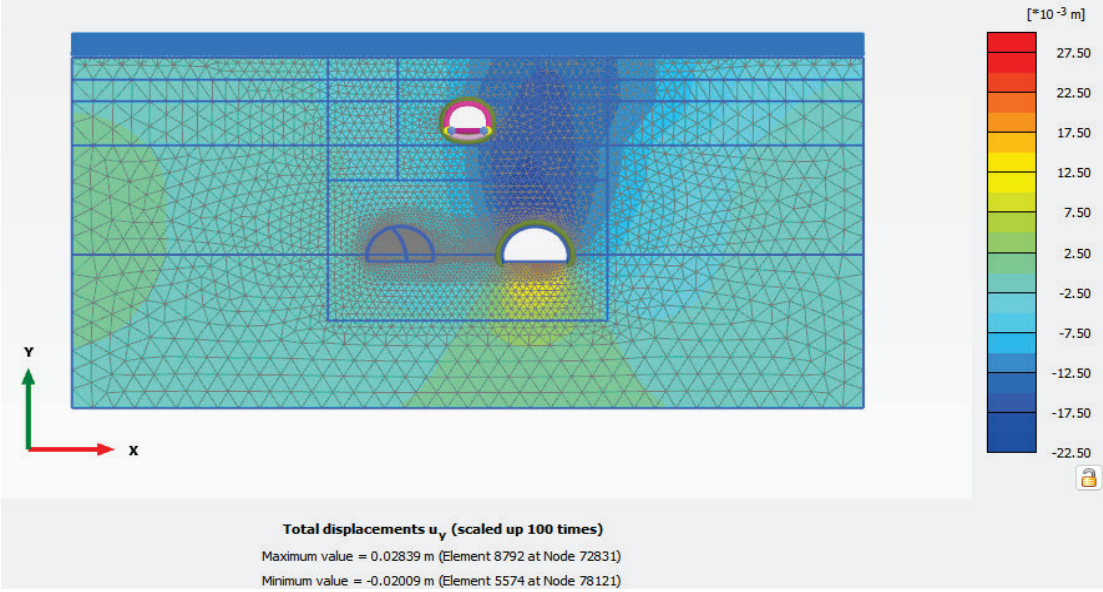


Figure III-9: Vertical Settlement in Construction (WT and ET)- HS- Mixed-Plane Sole Section in New Tunnels



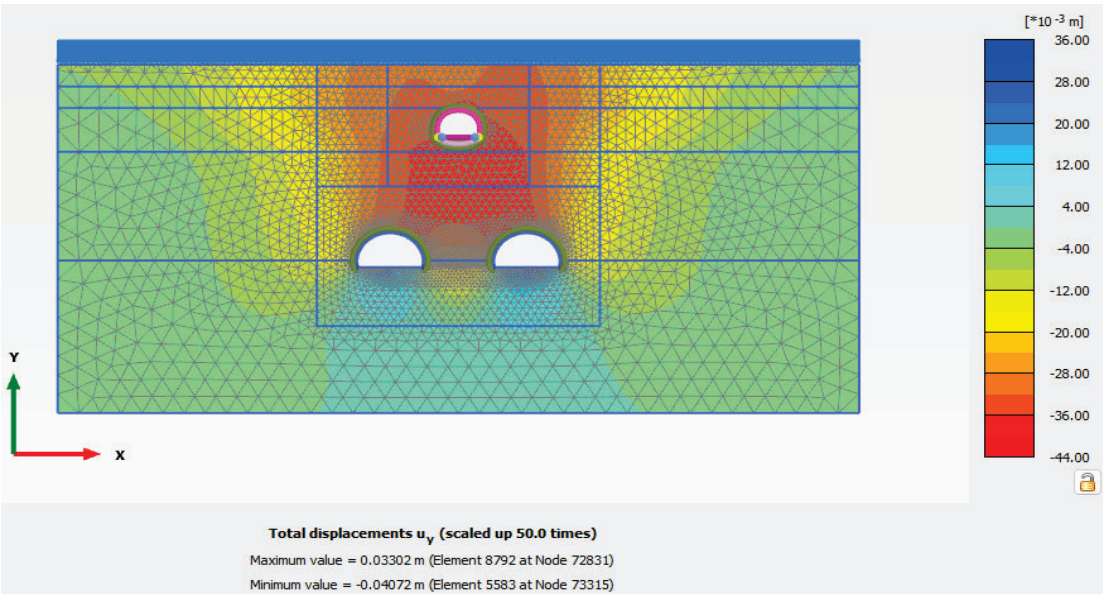
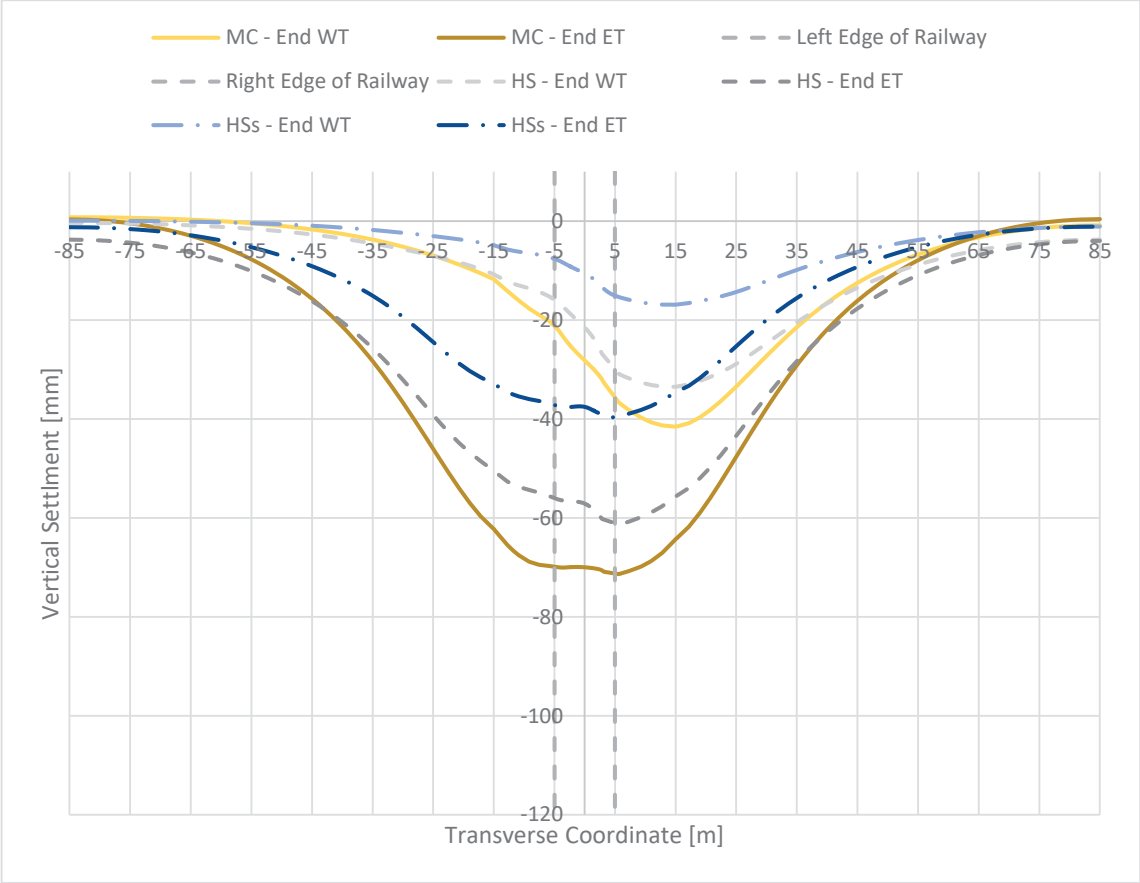


Figure III-10: Vertical Settlement in Construction (WT and ET)- HSs- Mixed-Plane Sole Section in New Tunnels



Graph III-3: Diagram of Transverse Settlement on Metro Tunnel - Construction Stage –

Model with Plane Sole Section in New Tunnels- Mixed

Table III-7: Verification of the Transverse Settlement Limit- MC Model- Construction Stage- Mixed Plane Sole Section in New Tunnels

Phase	Rial 1 Settl (mm)	Rial 2 Settl (mm)	Δ Settl (mm)	Δ Limit (mm)	Verification
Settlement of West Rial					
Excavation WT	-29.06	-30.92	1.87	2	**CHECK**
Excavation ET	-70.03	-70.30	0.27	2	**CHECK**
Settlement of East Rial					
Excavation WT	-27.28	-25.44	1.83	2	**CHECK**
Excavation ET	-69.89	-69.90	0.01	2	**CHECK**

Table III-8: Verification of the Transverse Settlement Limit- HS Model- Construction Stage- Mixed Plane Sole Section in New Tunnels

Phase	Rial 1 Settl (mm)	Rial 2 Settl (mm)	Δ Settl (mm)	Δ Limit (mm)	Verification
Settlement of West Rial					
Excavation WT	-22.53	-25.14	2.61	2	**NOT CHECK**
Excavation ET	-57.59	-59.10	1.51	2	**CHECK**
Settlement of East Rial					
Excavation WT	-20.61	-18.95	1.66	2	**CHECK**
Excavation ET	-56.78	-56.61	0.17	2	**CHECK**

Table III-9: Verification of the Transverse Settlement Limit- HSs Model- Construction Stage- Mixed Plane Sole Section in New Tunnels

Phase	Rial 1 Settl (mm)	Rial 2 Settl (mm)	Δ Settl (mm)	Δ Limit (mm)	Verification
Settlement of West Rial					
Excavation WT	-11.09	-12.41	1.32	2	**CHECK**
Excavation ET	-37.84	-38.71	0.88	2	**CHECK**
Settlement of East Rial					
Excavation WT	-10.11	-9.27	0.84	2	**CHECK**
Excavation ET	-37.42	-37.53	0.12	2	**CHECK**

(b.2) Service Stage

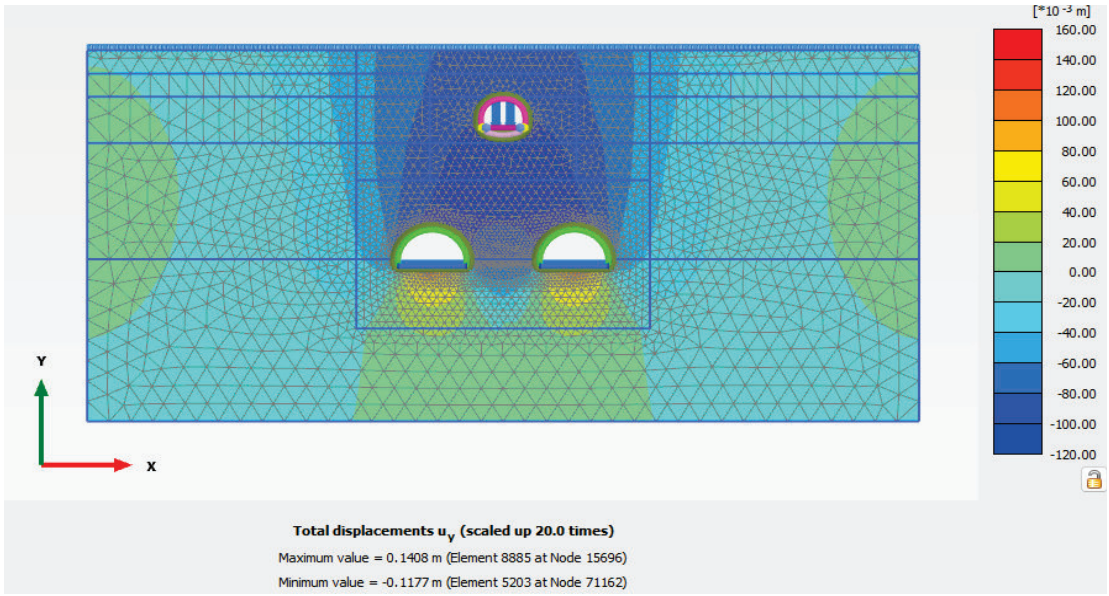


Figure III-11: Vertical Settlement in Service- MC- Mixed

Plane Sole Section in New Tunnels

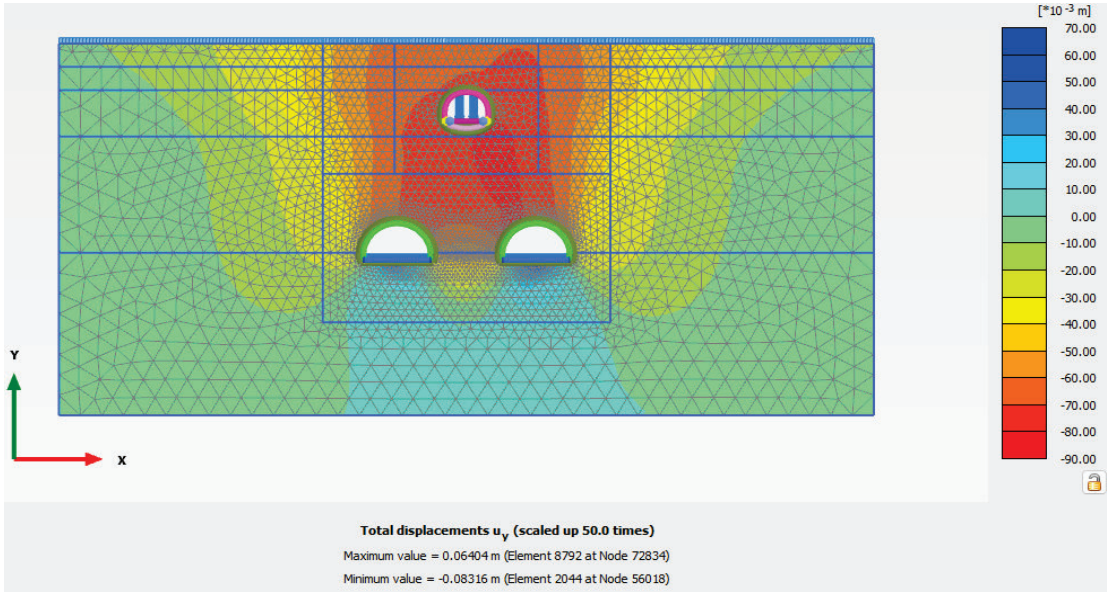


Figure III-12: Vertical Settlement in Service- HS- Mixed

Plane Sole Section in New Tunnels

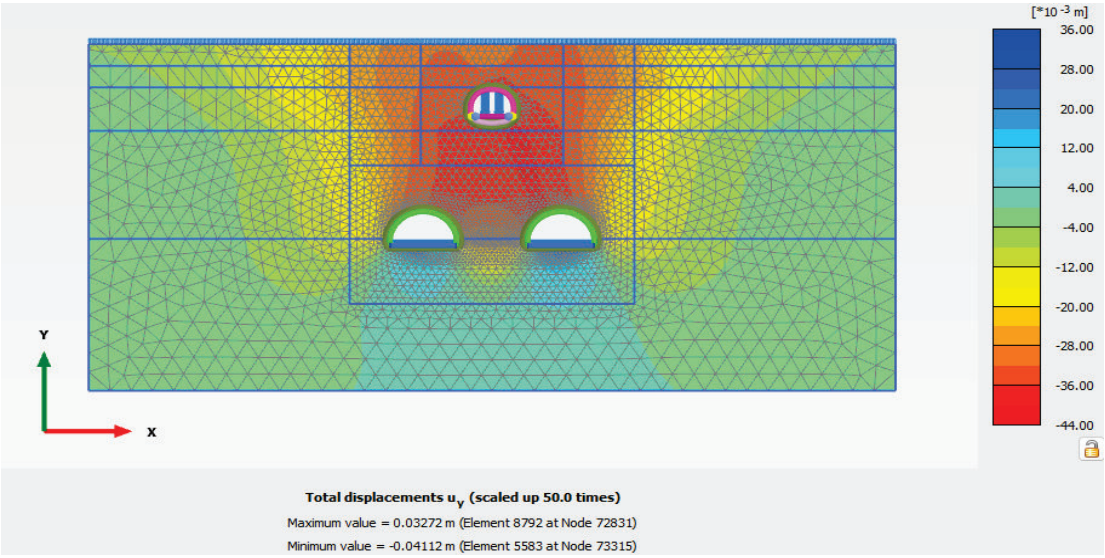
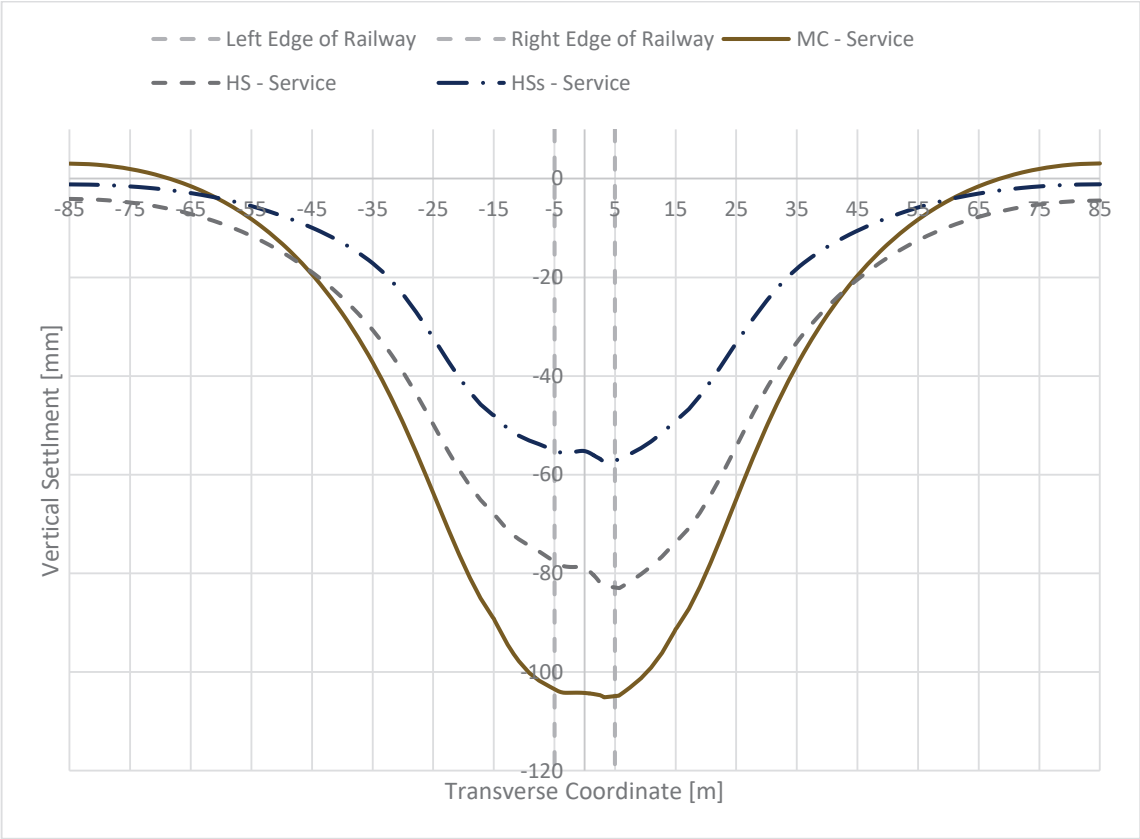


Figure III-13: Vertical Settlement in Service- HSs- Mixed

Plane Sole Section in New Tunnels



Graph III-4: Diagram of Transverse Settlement on Metro Tunnel - Service Stage –

Model with Plane Sole Section in New Tunnels- Mixed

Table III-10: Verification of the Transverse Settlement Limit- MC Model- Service Stage- Mixed Plane Sole Section in New Tunnels

Phase	Rial 1 Settl (mm)	Rial 2 Settl (mm)	Δ Settl (mm)	Δ Limit (mm)	Verification
Settlement of West Rial					
Service	-104.34	-104.62	0.28	2	**CHECK**
Settlement of East Rial					
Service	-104.20	-104.20	0.00	2	**CHECK**

Table III-11: Verification of the Transverse Settlement Limit- HS Model- Service Stage- Mixed Plane Sole Section in New Tunnels

Phase	Rial 1 Settl (mm)	Rial 2 Settl (mm)	Δ Settl (mm)	Δ Limit (mm)	Verification
Settlement of West Rial					
Service	-79.54	-81.37	1.83	2	**CHECK**
Settlement of East Rial					
Service	-78.72	-78.72	0.00	2	**CHECK**

Table III-12: Verification of the Transverse Settlement Limit- HSs Model- Service Stage- Mixed Plane Sole Section in New Tunnels

Phase	Rial 1 Settl (mm)	Rial 2 Settl (mm)	Δ Settl (mm)	Δ Limit (mm)	Verification
Settlement of West Rial					
Service	-55.58	-56.59	1.01	2	**CHECK**
Settlement of East Rial					
Service	-55.22	-55.54	0.31	2	**CHECK**

(c) Analysis of the Fine Profile

(c.1) Construction Stage

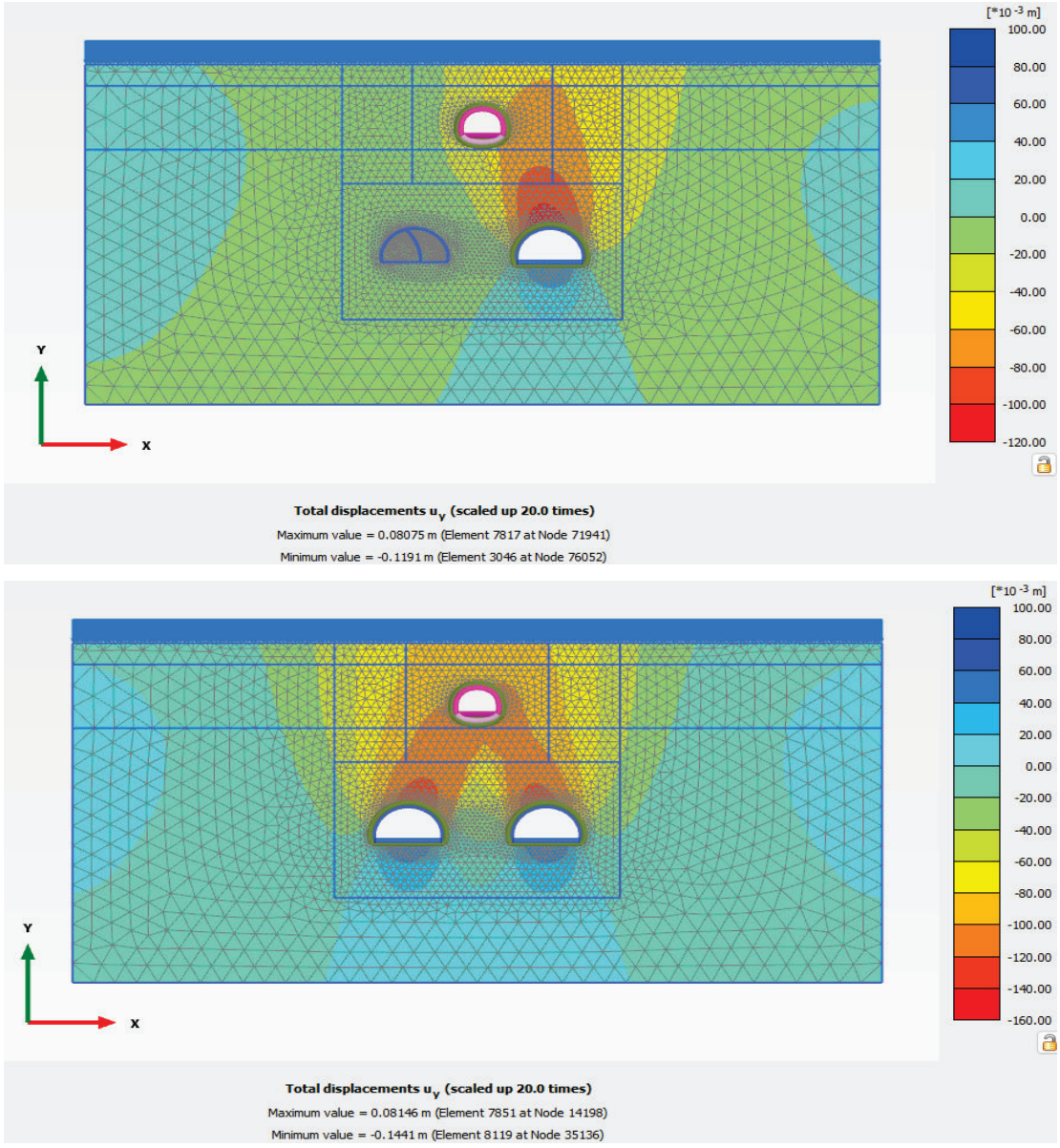
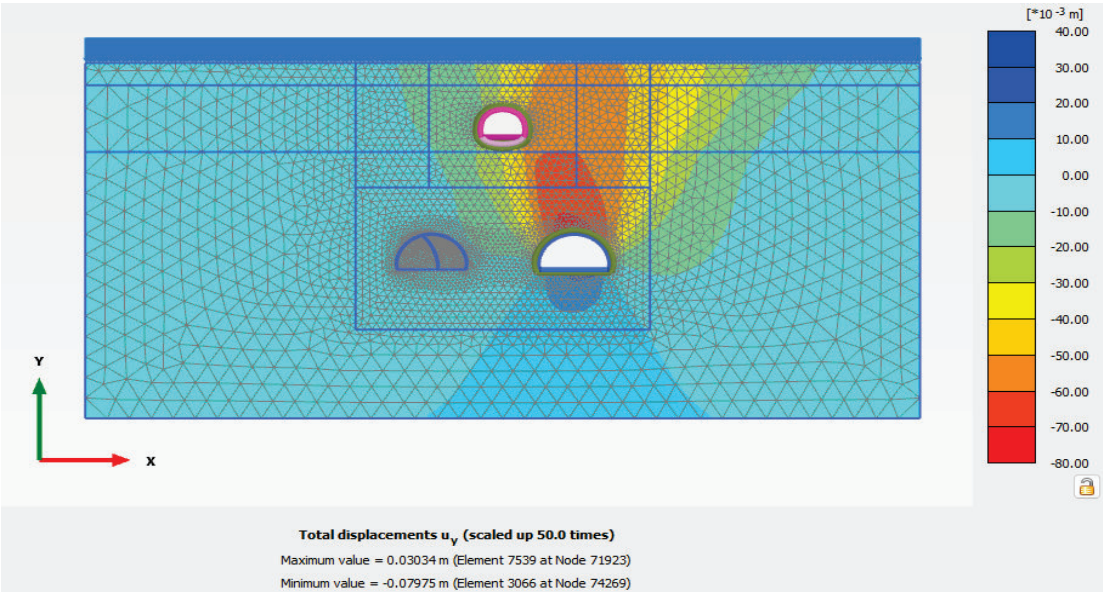


Figure III-14: Vertical Settlement in Construction (WT and ET)- MC- Fine Plane Sole Section in New Tunnels



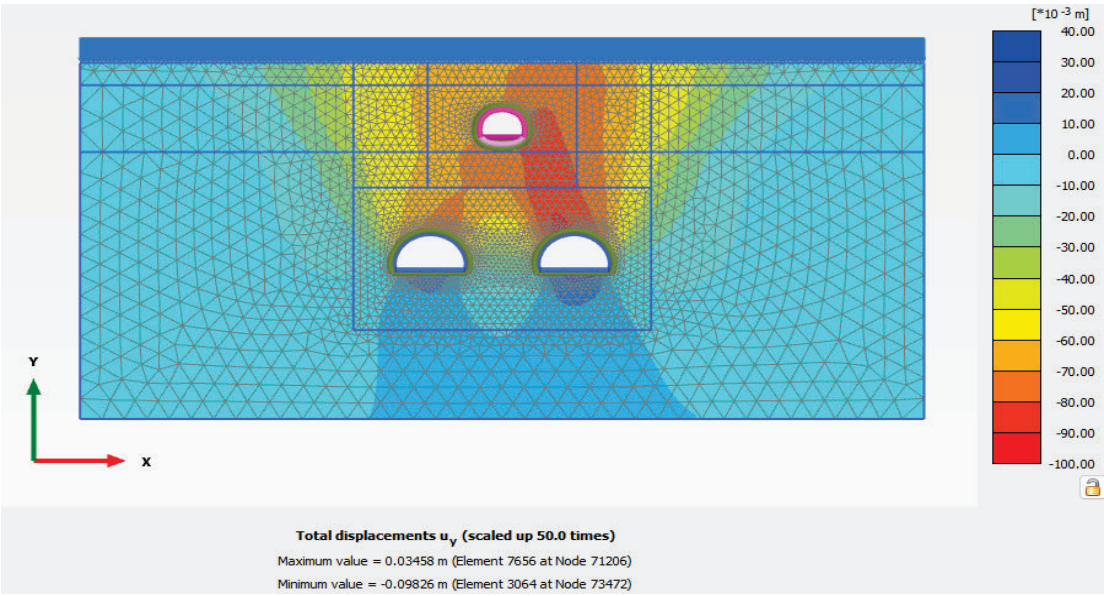


Figure III-15: Vertical Settlement in Construction (WT and ET)- HS- Fine Plane Sole Section in New Tunnels

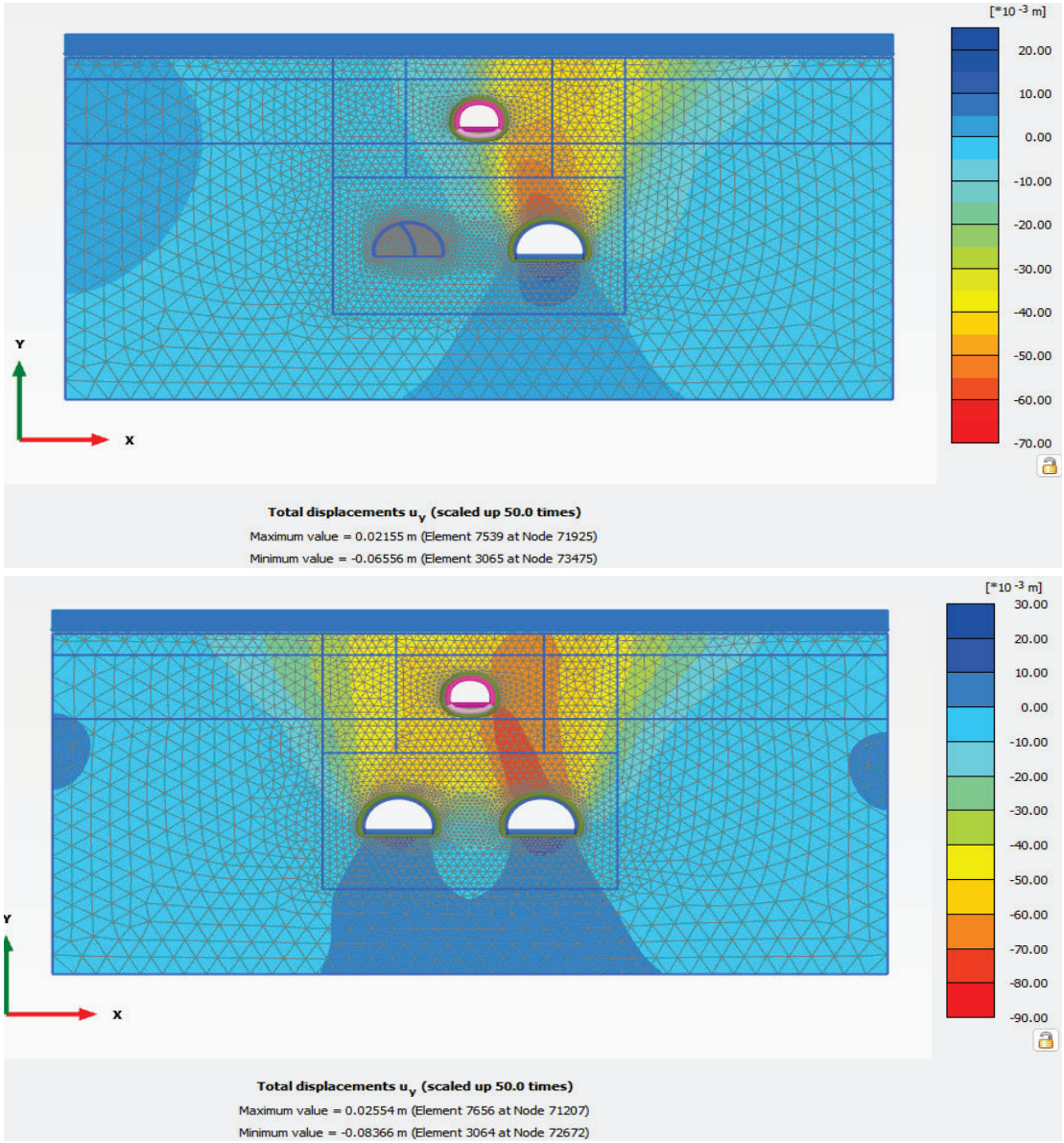
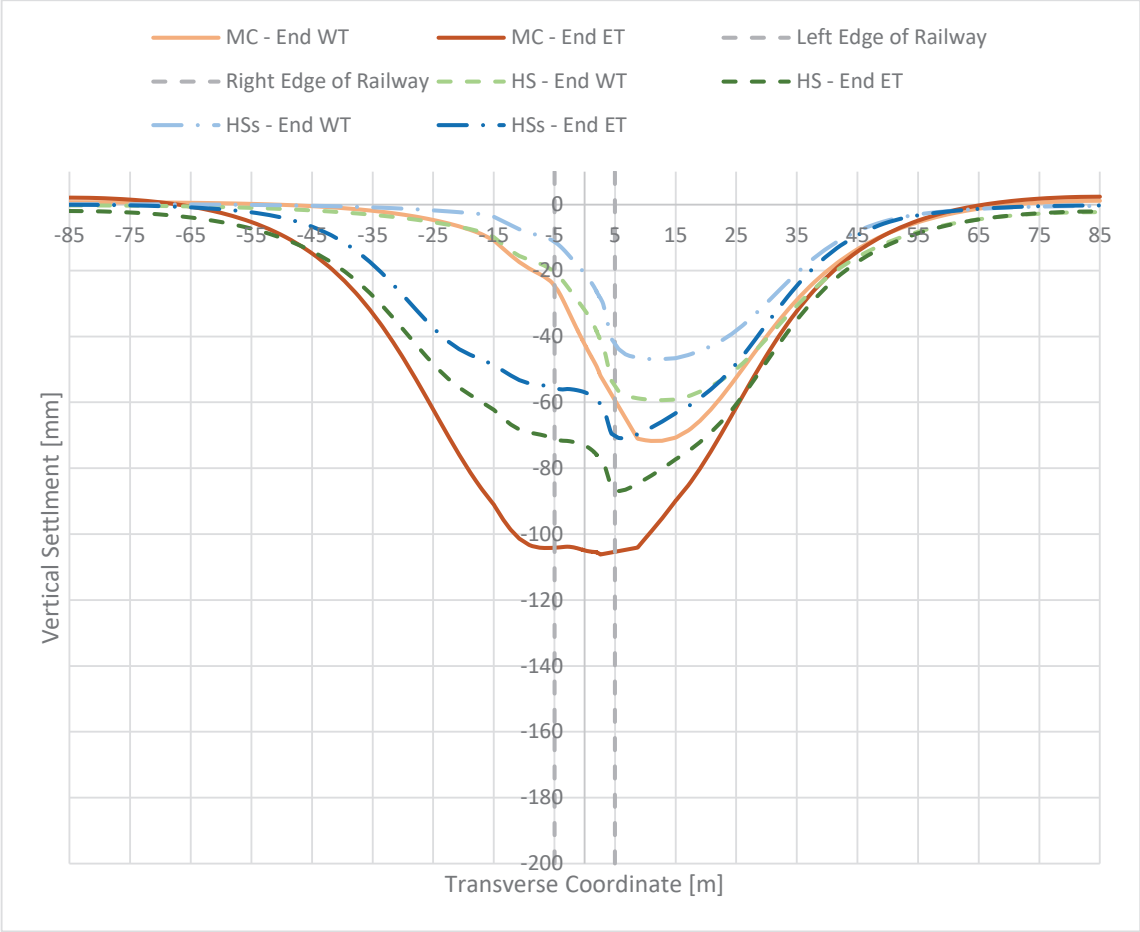


Figure III-16: Vertical Settlement in Construction (WT and ET)- HSs- Fine Plane Sole Section in New Tunnels



Graph III-5: Diagram of Transverse Settlement on Metro Tunnel - Construction Stage – Model with Plane Sole Section in New Tunnels- Fine

Table III-13: Verification of the Transverse Settlement Limit- MC Model- Construction Stage- Fine Plane Sole Section in New Tunnels

Phase	Rial 1 Settl (mm)	Rial 2 Settl (mm)	Δ Settl (mm)	Δ Limit (mm)	Verification
Settlement of West Rial					
Excavation WT	-45.02	-50.09	5.08	2	**NOT CHECK**
Excavation ET	-105.27	-105.74	0.48	2	**CHECK**
Settlement of East Rial					
Excavation WT	-39.73	-34.29	5.44	2	**NOT CHECK**
Excavation ET	-104.56	-103.94	0.63	2	**CHECK**

Table III-14: Verification of the Transverse Settlement Limit- HS Model- Construction Stage- Fine Plane Sole Section in New Tunnels

Phase	Rial 1 Settl (mm)	Rial 2 Settl (mm)	Δ Settl (mm)	Δ Limit (mm)	Verification
Settlement of West Rial					
Excavation WT	-34.13	-39.44	5.31	2	**NOT CHECK**
Excavation ET	-73.88	-76.46	2.58	2	**NOT CHECK**
Settlement of East Rial					
Excavation WT	-30.13	-26.57	3.56	2	**NOT CHECK**
Excavation ET	-72.56	-71.89	0.67	2	**CHECK**

Table III-15: Verification of the Transverse Settlement Limit- HSs Model- Construction Stage- Fine Plane Sole Section in New Tunnels

Phase	Rial 1 Settl (mm)	Rial 2 Settl (mm)	Δ Settl (mm)	Δ Limit (mm)	Verification
Settlement of West Rial					
Excavation WT	-22.67	-27.17	4.51	2	**NOT CHECK**
Excavation ET	-57.59	-59.80	2.21	2	**NOT CHECK**
Settlement of East Rial					
Excavation WT	-19.27	-16.27	3.00	2	**NOT CHECK**
Excavation ET	-56.50	-56.01	0.48	2	**CHECK**

(c.2) Service Stage

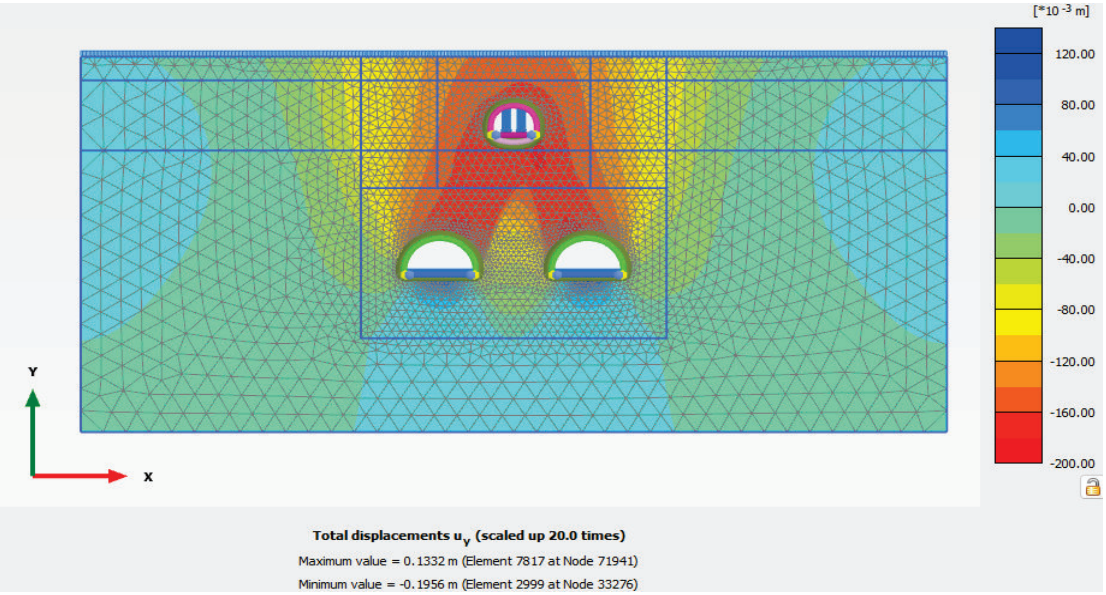


Figure III-17: Vertical Settlement in Service- MC- Fine- Plane Sole Section in New Tunnels

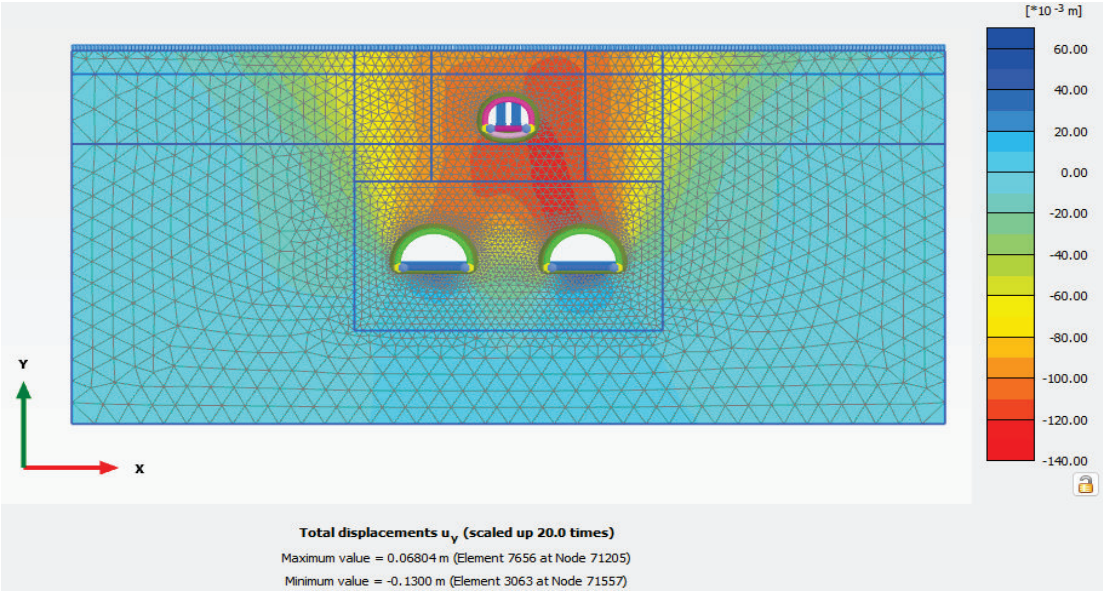


Figure III-18: Vertical Settlement in Service- HS- Fine- Plane Sole Section in New Tunnels

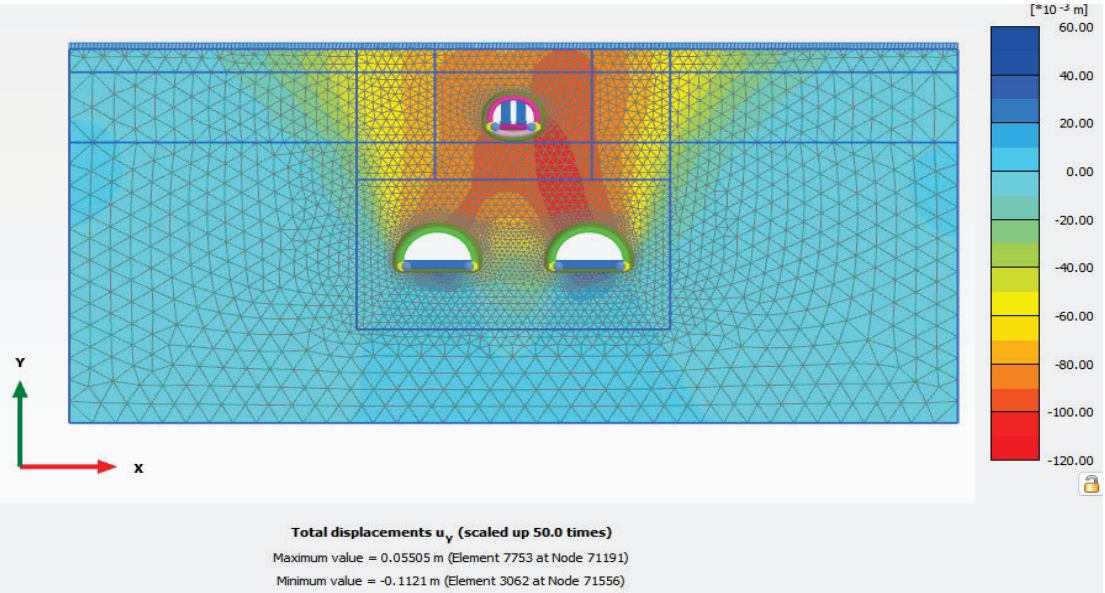
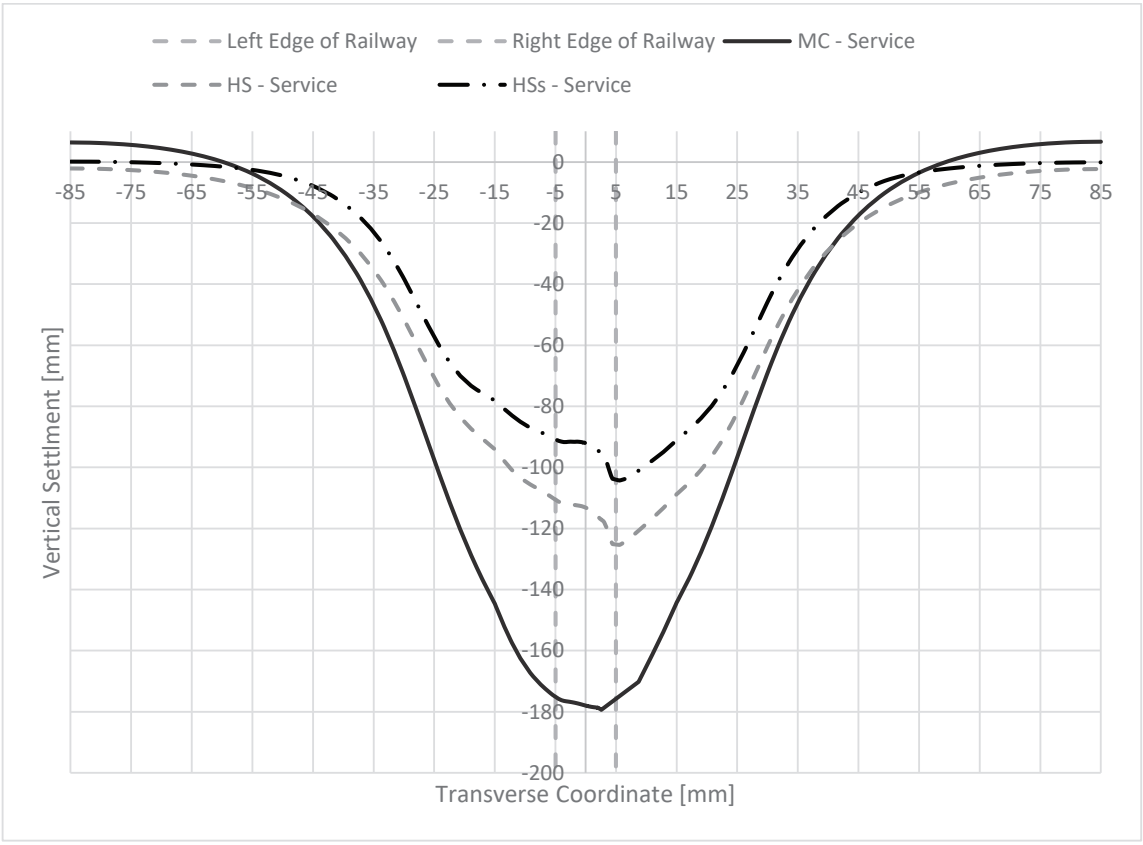


Figure III-19: Vertical Settlement in Service- HSs- Fine- Plane Sole Section in New Tunnels



Graph III-6: Diagram of Transverse Settlement on Metro Tunnel - Service Stage –

Model with Plane Sole Section in New Tunnels- Fine

Table III-16: Verification of the Transverse Settlement Limit- MC Model- Service Stage- Fine Plane Sole Section in New Tunnels

Phase	Rial 1 Settl (mm)	Rial 2 Settl (mm)	Δ Settl (mm)	Δ Limit (mm)	Verification
Settlement of West Rial					
Service	-178.38	-178.96	0.58	2	**CHECK**
Settlement of East Rial					
Service	-177.63	-176.96	0.67	2	**CHECK**

Table III-17: Verification of the Transverse Settlement Limit- HS Model- Service Stage- Fine Plane Sole Section in New Tunnels

Phase	Rial 1 Settl (mm)	Rial 2 Settl (mm)	Δ Settl (mm)	Δ Limit (mm)	Verification
Settlement of West Rial					
Service	-114.04	-116.49	2.45	2	**NOT CHECK**
Settlement of East Rial					
Service	-112.71	-112.22	0.49	2	**CHECK**

Table III-18: Verification of the Transverse Settlement Limit- HSs Model- Service Stage- Fine Plane Sole Section in New Tunnels

Phase	Rial 1 Settl (mm)	Rial 2 Settl (mm)	Δ Settl (mm)	Limit (mm)	Verification
Settlement of West Rial					
Service	-92.74	-94.75	2.01	2	**NOT CHECK**
Settlement of East Rial					
Service	-91.73	-91.62	0.11	2	**CHECK**

3.1.2 Verification of the Resistance in the Pre-existing Metro Tunnel considering Sole Plane section in the new tunnels.

At the beginning, the axial force, bending and shear diagrams on the metro-tunnel are presented and then the structural verification is realized through the M-N and N-Q interaction diagrams, as presented in chapter 3.7.1(b).
First the vault and then the counter-vault of the Metro tunnel are verified, with their corresponding concrete thicknesses and reinforcement, as defined in Figure III-14 and Figure III-15.

- Vault of the Metro Tunnel

$e = 0.325\ m$ Concrete thicknesses for the calculation
(Lining thicknesses = 0.20 m + ½ Support thicknesses = 0.125 m)

$A_{s.i} = 3.780\ cm^2/m$ ACMA378 Mesh in Internal face
$A_{s.e} = 2.95\ cm^2/m$ ACMA295 Mesh in External face

- Counter-Vault of the Metro Tunnel

$e = 0.425\ m$ Concrete thicknesses for the calculation
(Lining thicknesses = 0.30 m + ½ Support thicknesses = 0.125 m)

$A_{s.i} = 3.780\ cm^2/m$ ACMA378 Mesh in Internal face
$A_{s.ref} = 6.70\ cm^2/m$ Reinforcement with bars steel 16@30 in Internal face
$A_{s.e} = 2.95\ cm^2/m$ ACMA295 Mesh in External face

(a) Analysis of the Gravel Profile

(a.1) Construction Stage

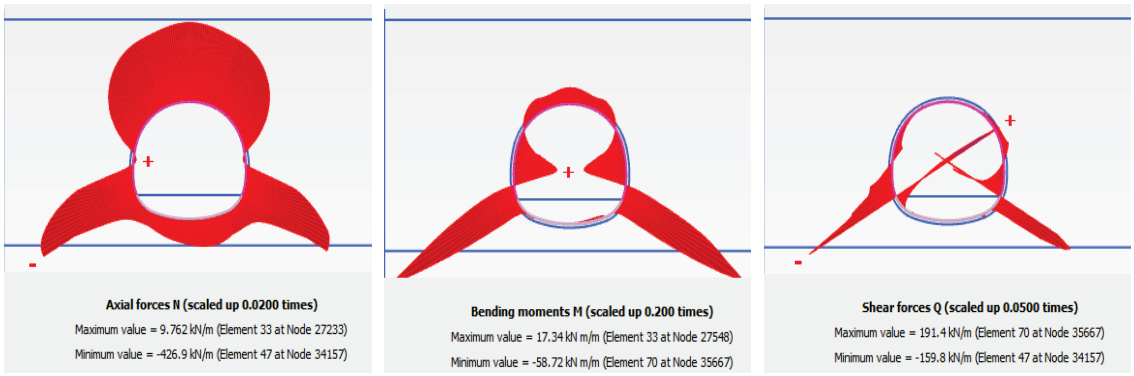


Figure III-20: Forces Diagram, Axial, Bending and Shear- Construction Stage- MC- Gravel Plane Sole Section in New Tunnels

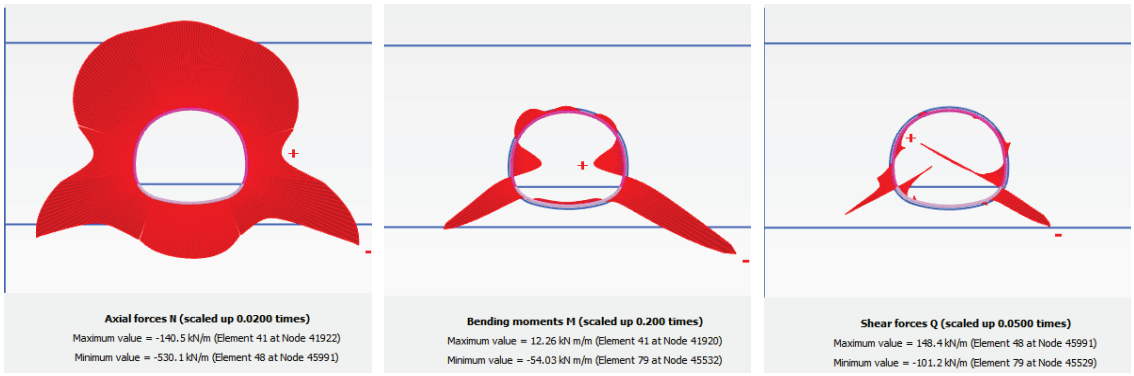


Figure III-21: Forces Diagram, Axial, Bending and Shear- Construction Stage- HS- Gravel Plane Sole Section in New Tunnels

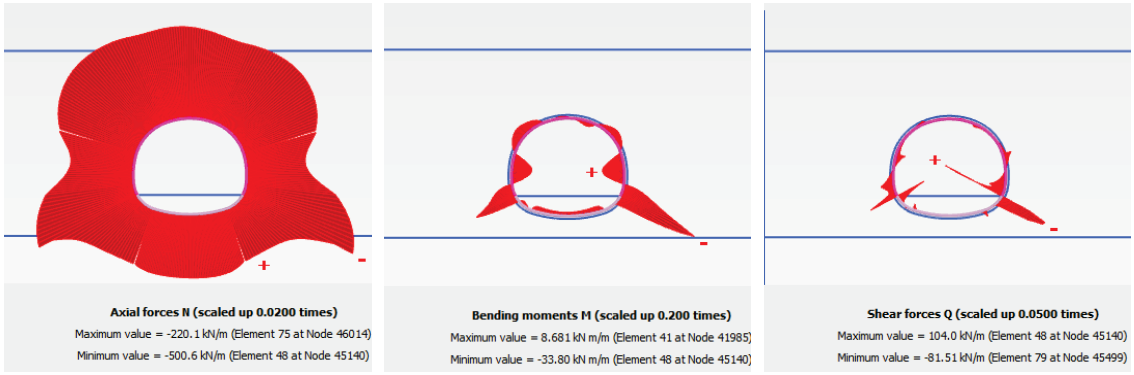
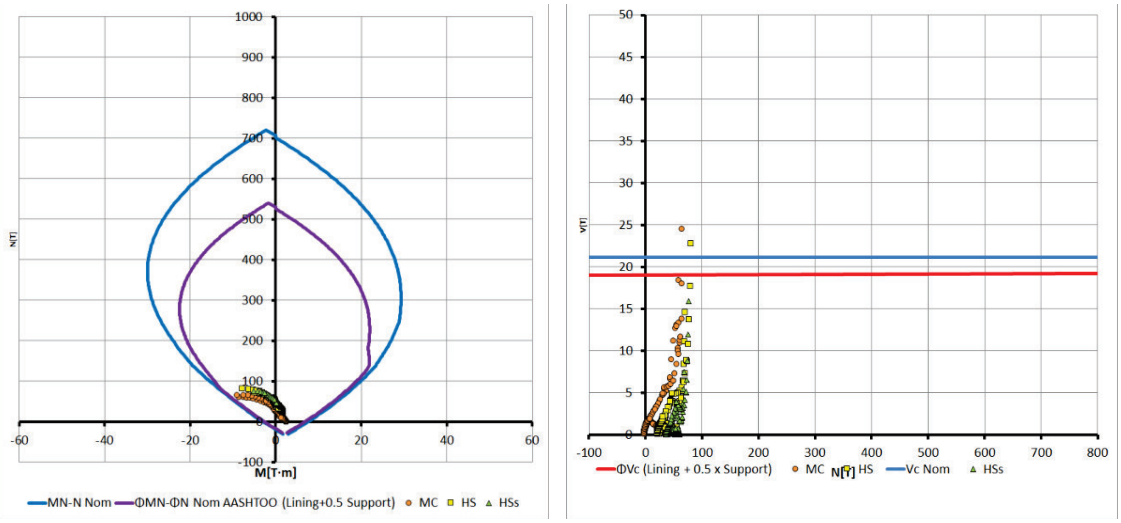
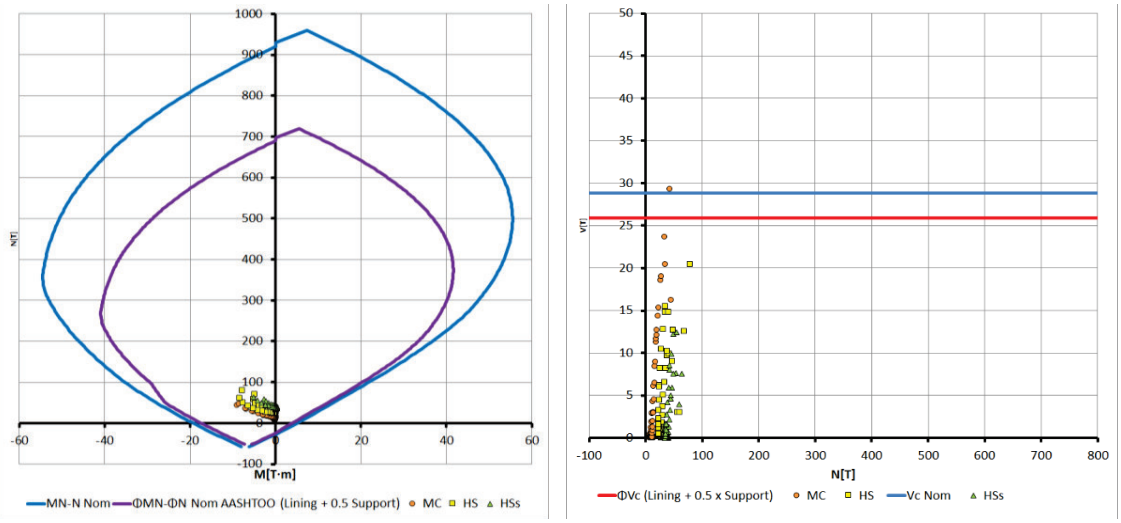


Figure III-22: Forces Diagram, Axial, Bending and Shear - Construction Stage- HSs- Gravel- Plane Sole Section in New Tunnels



Graph III-7: Interaction M-N and N-Q Diagram- Vault of Metro Tunnel- Construction Stage- Gravel- Plane Sole Section in New Tunnels



Graph III-8: Interaction M-N and N-Q Diagram- Counter vault of Metro Tunnel- Construction Stage- Gravel- Plane Sole Section in New Tunnels

(a.2) Service Stage

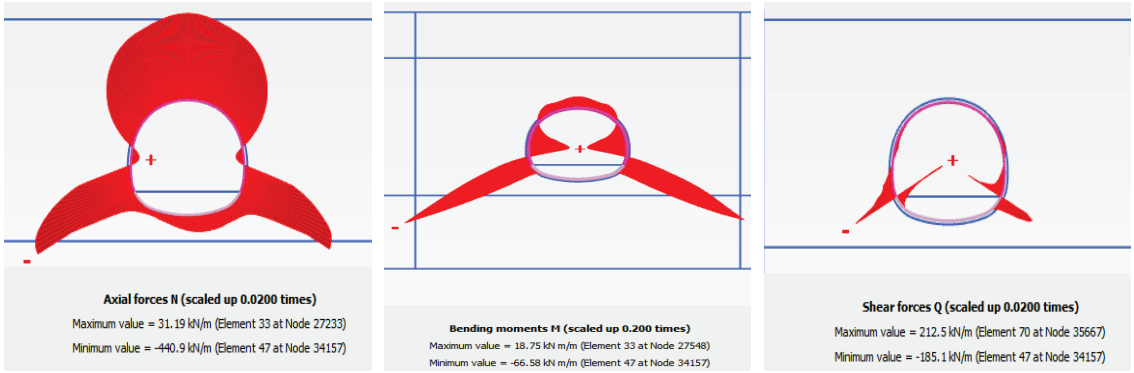


Figure III-23: Forces Diagram, Axial, Bending and Shear- Service Stage- MC- Gravel-

Plane Sole Section in New Tunnels

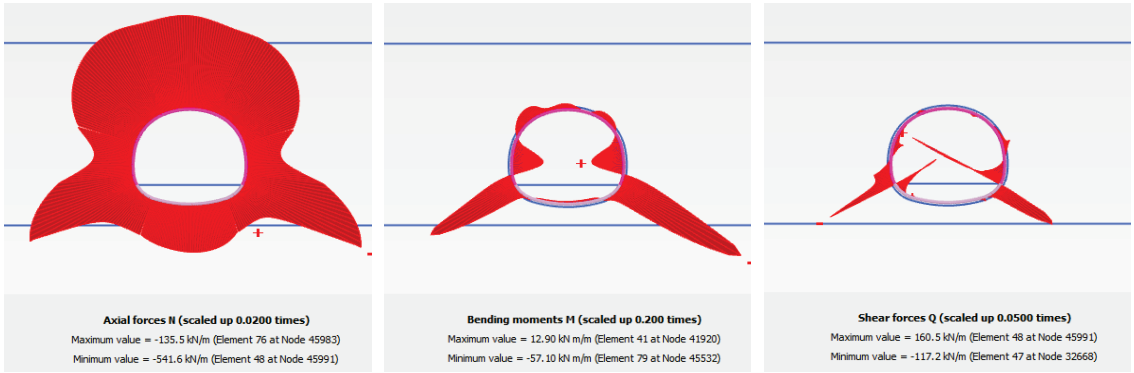


Figure III-24: Forces Diagram, Axial, Bending and Shear- Service Stage- HS- Gravel-

Plane Sole Section in New Tunnels

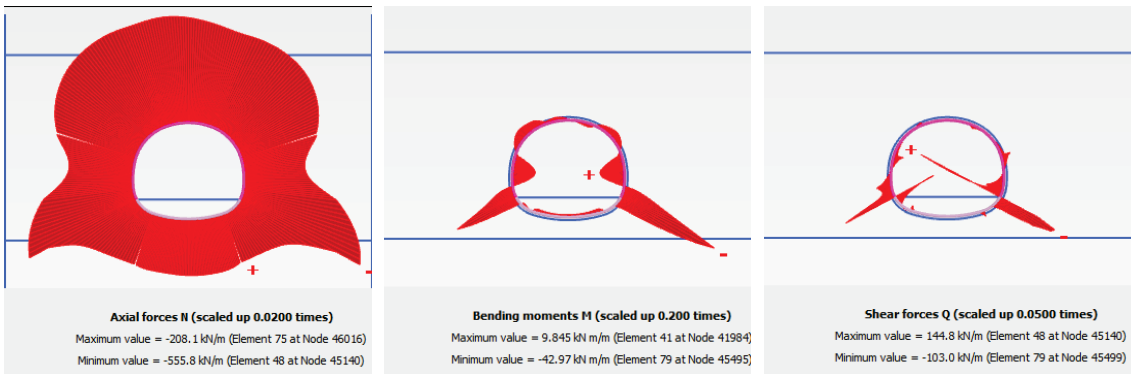
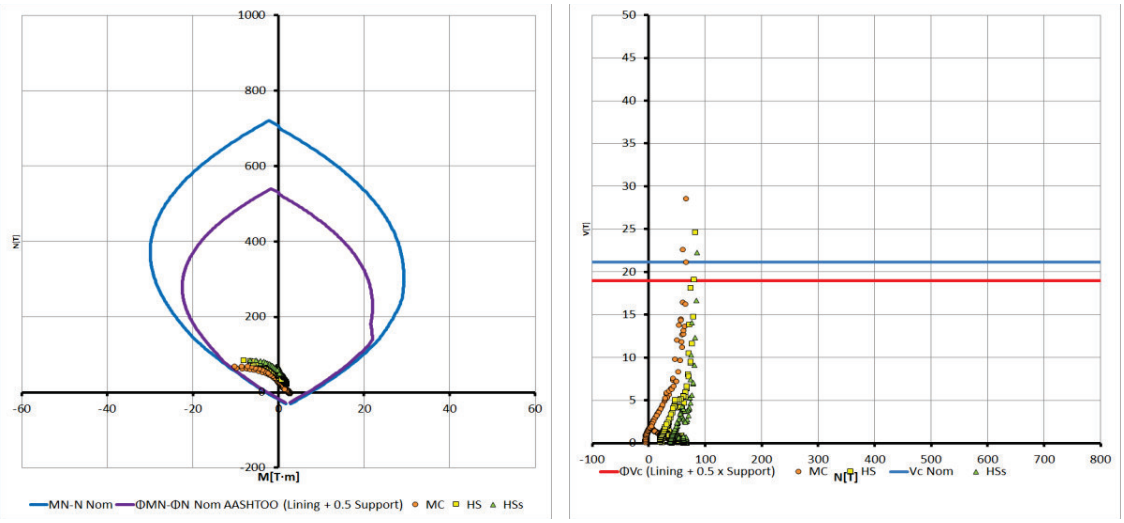
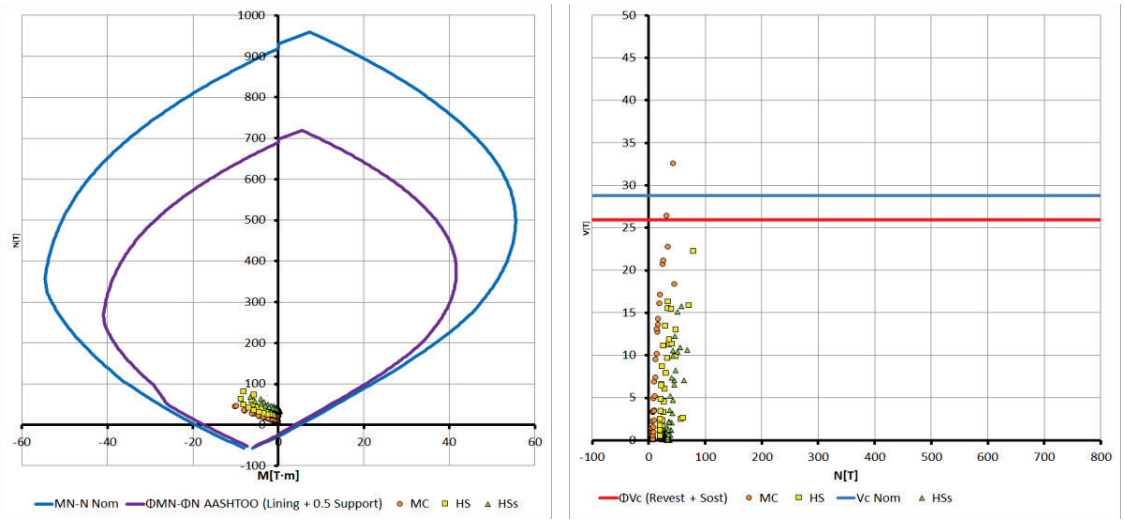


Figure III-25: Forces Diagram, Axial, Bending and Shear- Service Stage- HSs- Gravel-

Plane Sole Section in New Tunnels



Graph III-9: Interaction M-N and N-Q Diagram- Vault of Metro Tunnel- Service Stage- Gravel- Plane Sole Section in New Tunnels



Graph III-10: Interaction M-N and N-Q Diagram- Counter vault of Metro Tunnel- Service Stage- Gravel- Plane Sole Section in New Tunnels

(b) Analysis of the Mixed Profile

(b.1) Construction Stage

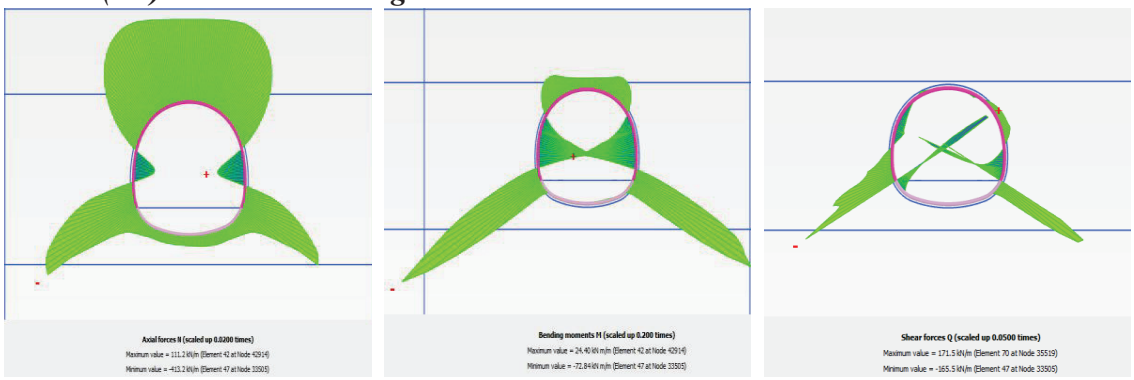


Figure III-26: : Forces Diagram, Axial, Bending and Shear- Construction Stage- MC- Mixed-Plane Sole Section in New Tunnels

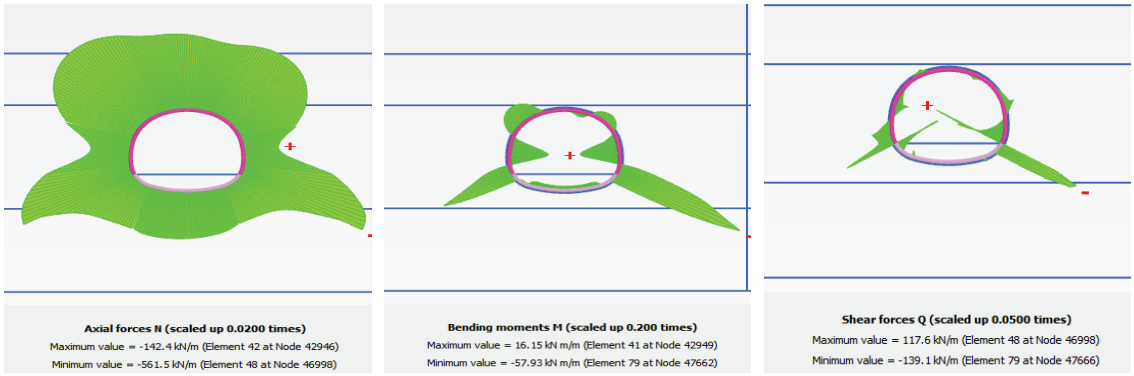


Figure III-27: Forces Diagram, Axial, Bending and Shear- Construction Stage- HS- Mixed- Plane Sole Section in New Tunnels

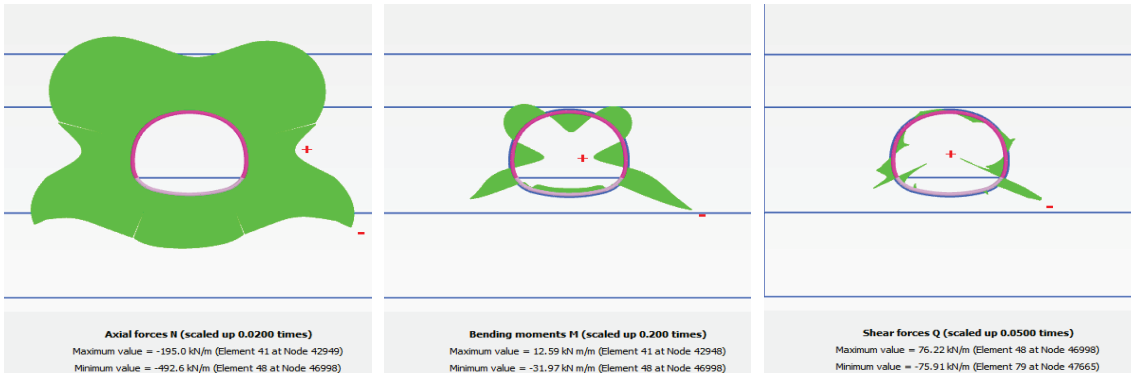
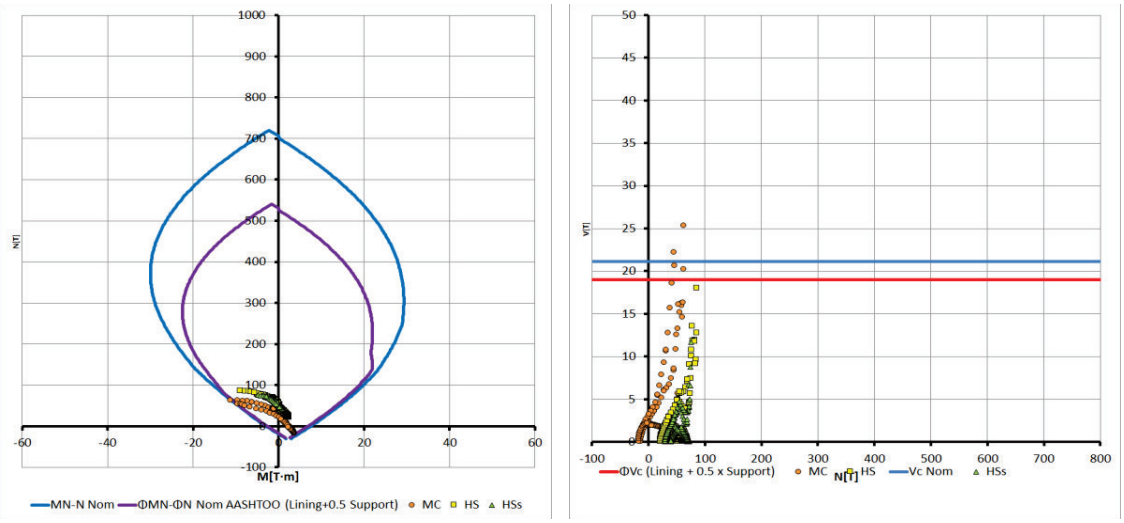
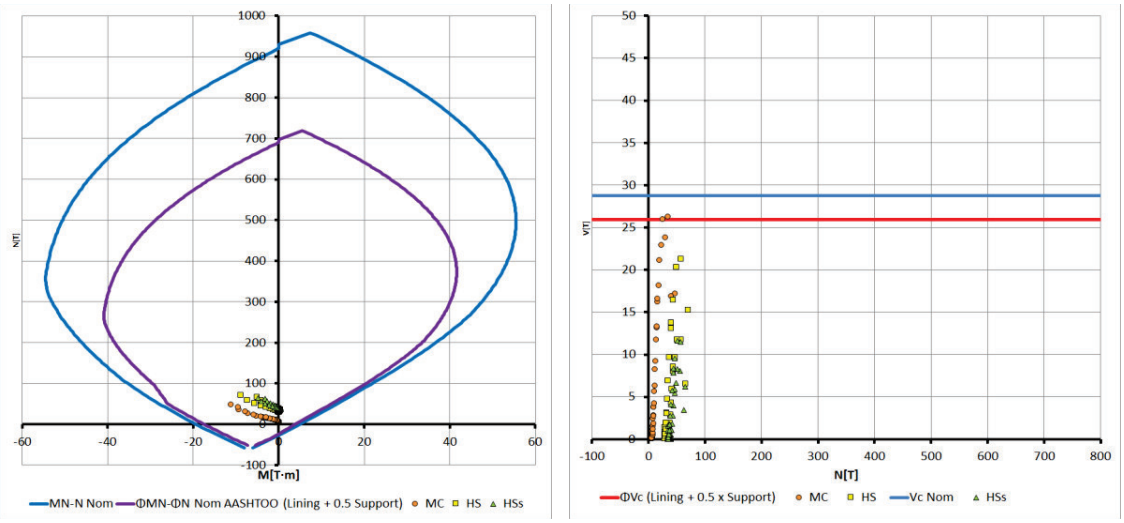


Figure III-28: Forces Diagram, Axial, Bending and Shear- Construction Stage- HSs- Mixed Plane Sole Section in New Tunnels



Graph III-11: Interaction M-N and N-Q Diagram- Vault of Metro Tunnel-

Construction Stage- Mixed- Plane Sole Section in New Tunnels



Graph III-12: Interaction M-N and N-Q Diagram- Counter vault of Metro Tunnel-

Construction Stage- Mixed- Plane Sole Section in New Tunnels

(b.2) Service Stage

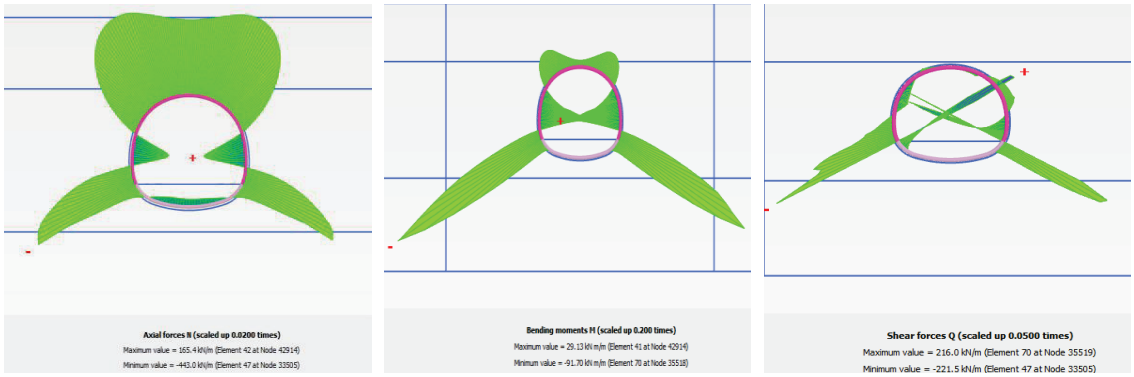


Figure III-29: Forces Diagram, Axial, Bending and Shear- Service Stage- MC- Mixed-Plane Sole Section in New Tunnels

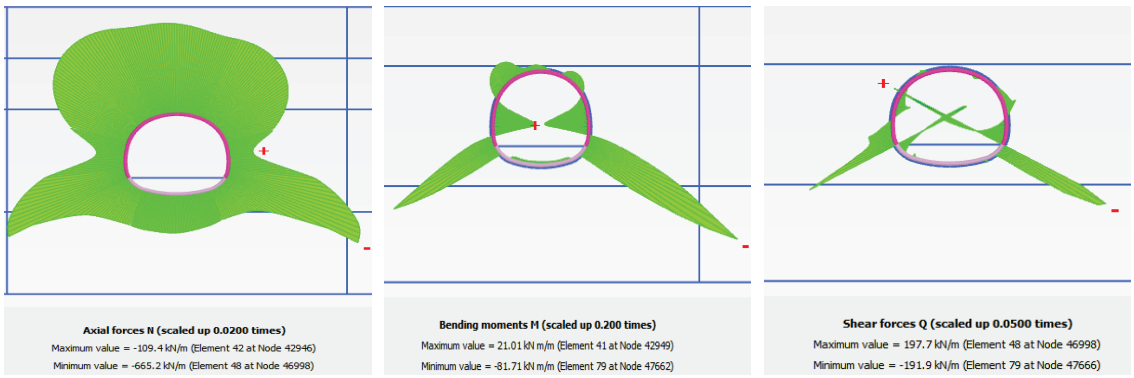


Figure III-30: Forces Diagram, Axial, Bending and Shear- Service Stage- HS- Mixed-Plane Sole Section in New Tunnels

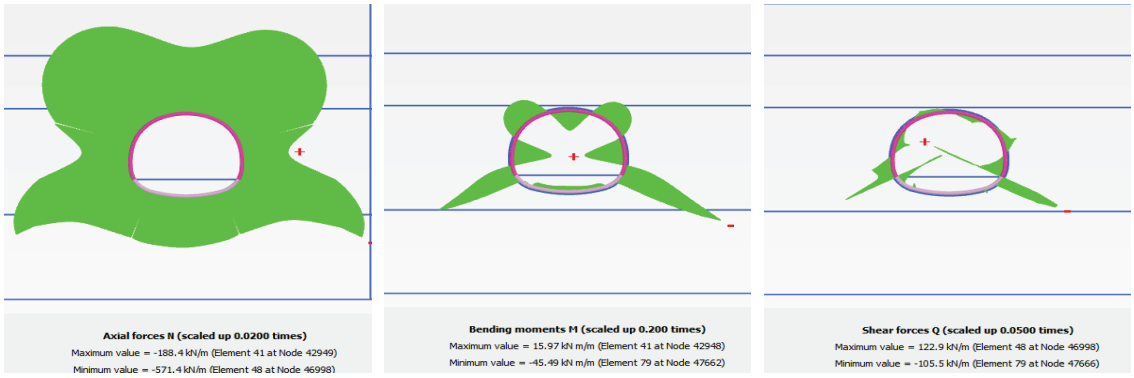
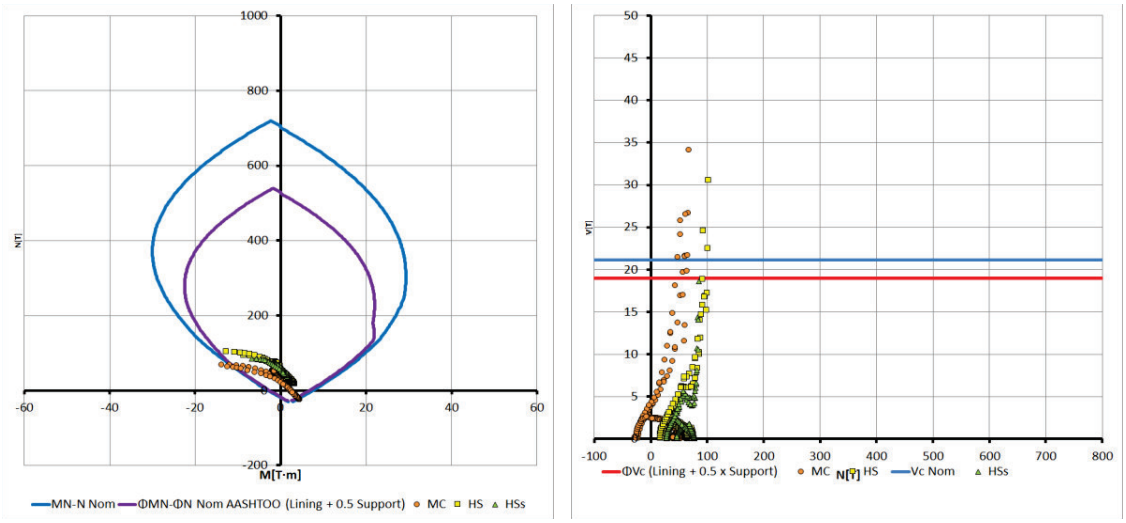
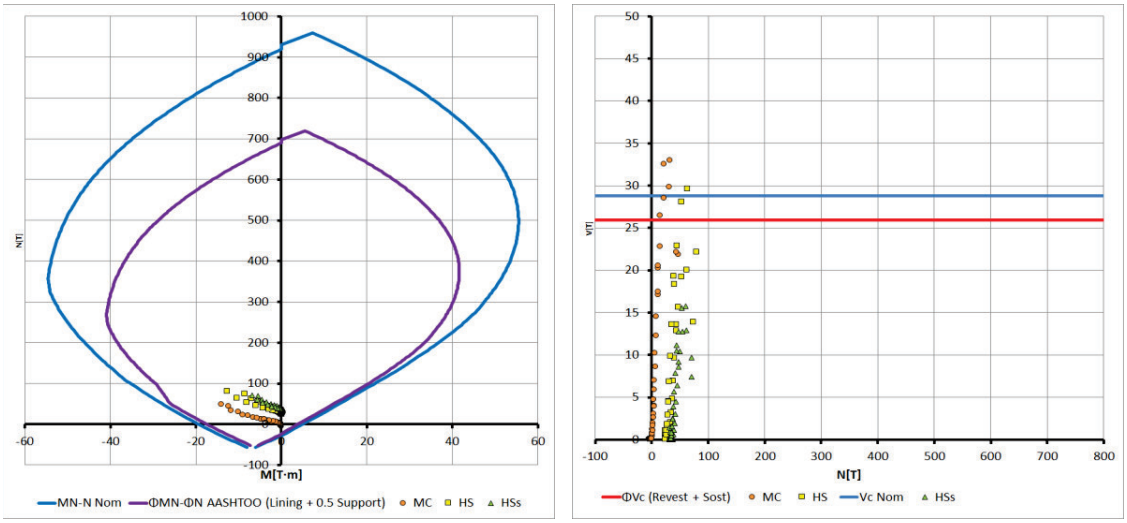


Figure III-31: Forces Diagram, Axial, Bending and Shear- Service Stage- HSs- Mixed-Plane Sole Section in New Tunnels



Graph III-13: Interaction M-N and N-Q Diagram- Vault of Metro Tunnel-

Service Stage- Mixed- Plane Sole Section in New Tunnels



Graph III-14: : Interaction M-N and N-Q Diagram- Counter vault of Metro Tunnel-

Service Stage- Mixed- Plane Sole Section in New Tunnels

(c) Analysis of the Fine Profile

(c.1) Service Stage

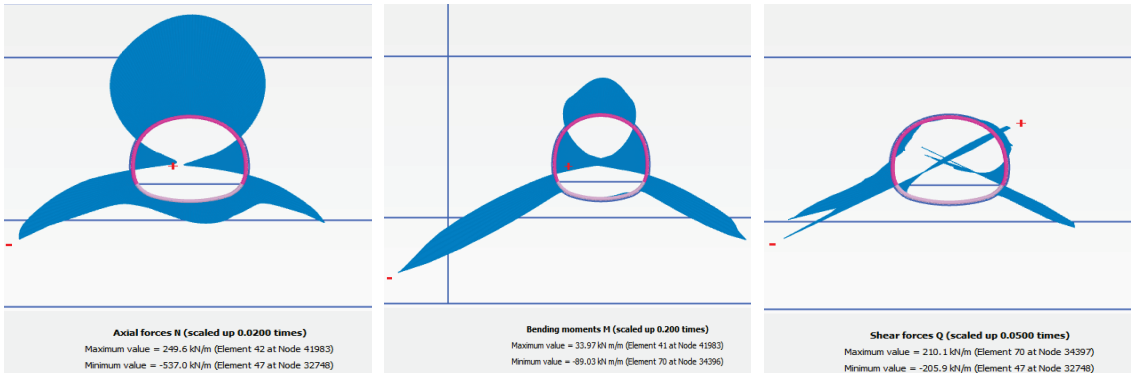
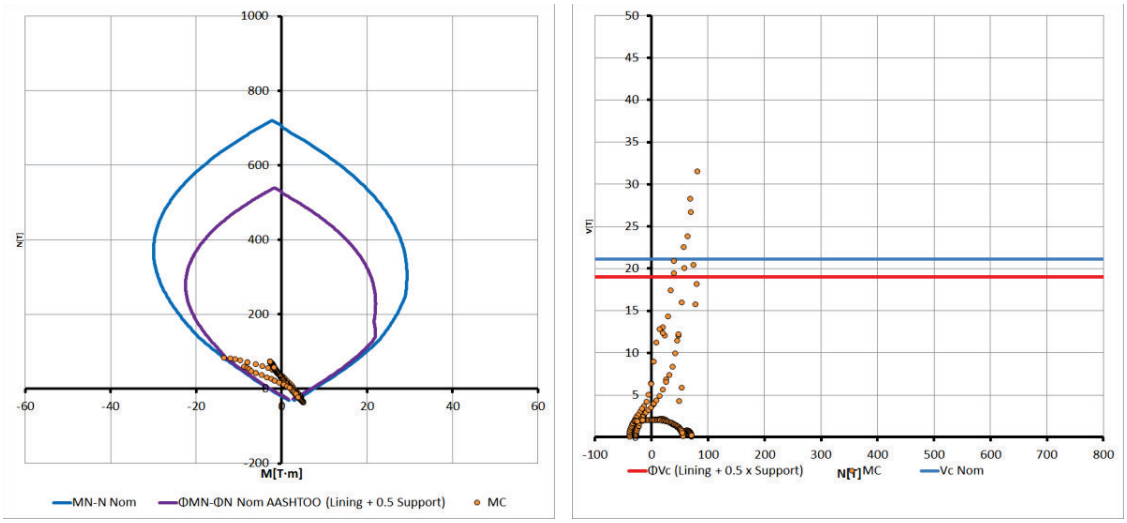
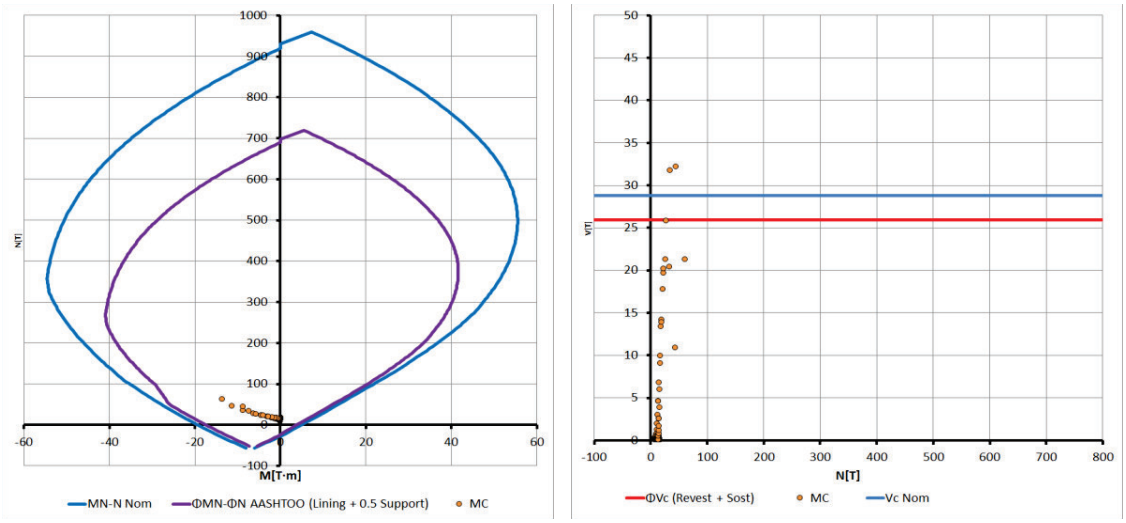


Figure III-32: Forces Diagram, Axial, Bending and Shear- Service Stage- MC- Fine-Plane Sole Section in New Tunnels



Graph III-15: Interaction M-N and N-Q Diagram- Vault of Metro Tunnel- Service Stage- Fine- Plane Sole Section in New Tunnels



Graph III-16: Interaction M-N and N-Q Diagram- Counter vault of Metro Tunnel-

Service Stage- Fine- Plane Sole Section in New Tunnels

3.1.3 Verification of the Deformation in the New Road Tunnels

The maximum convergence deformations must be verified with the criterion established in chapter 3.7.3(a).

(a) Analysis of the Gravel Profile

(a.1) Construction Stage

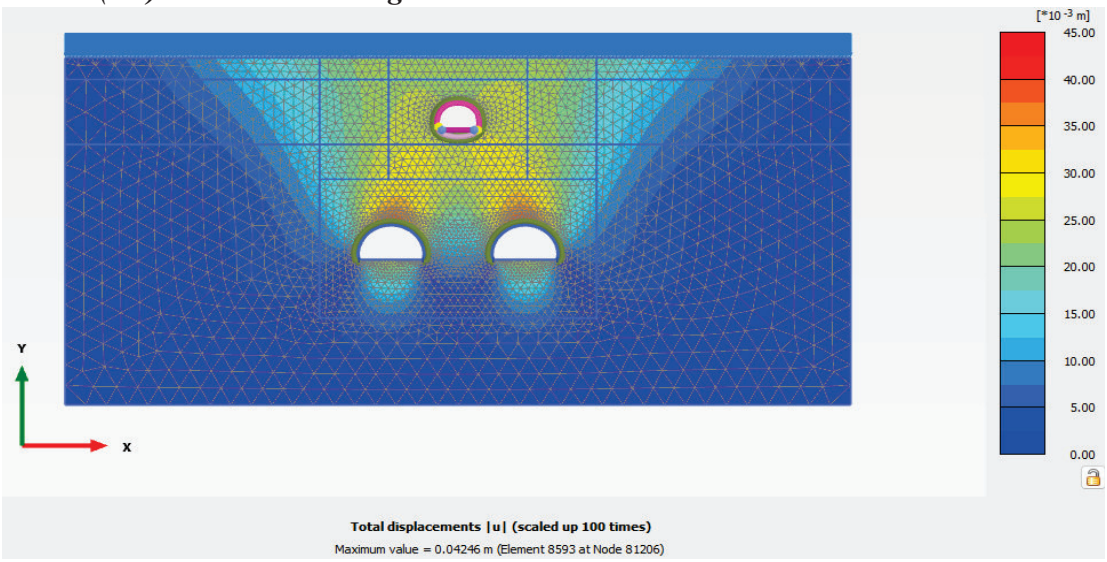


Figure III-33: Maximum Displacement in Construction- MC- Gravel

Plane Sole Section in New Tunnels

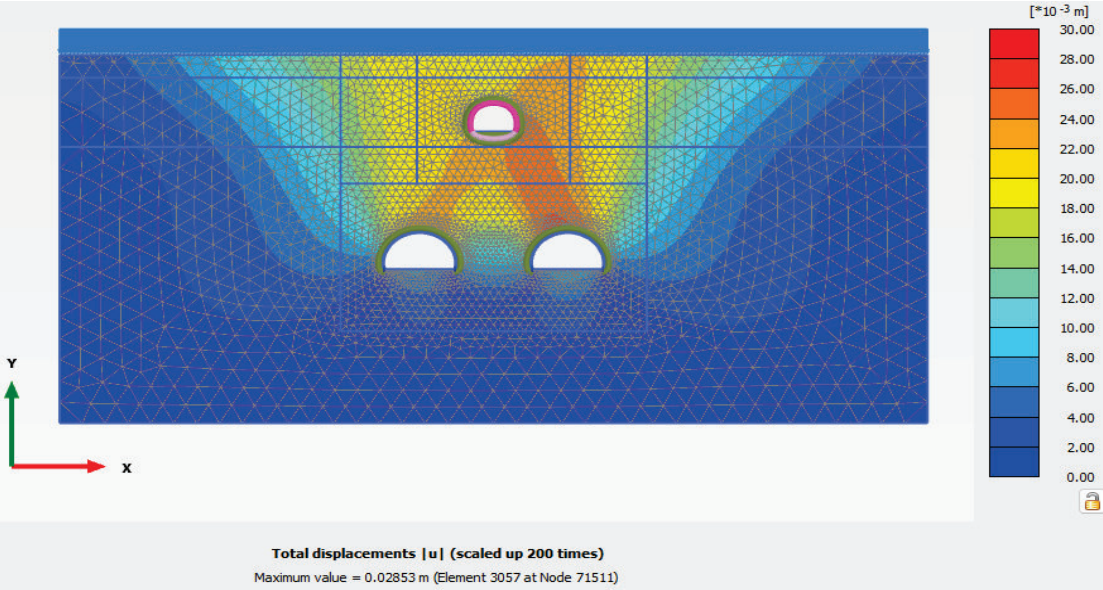


Figure III-34: Maximum Displacement in Construction- HS- Gravel-

Plane Sole Section in New Tunnels

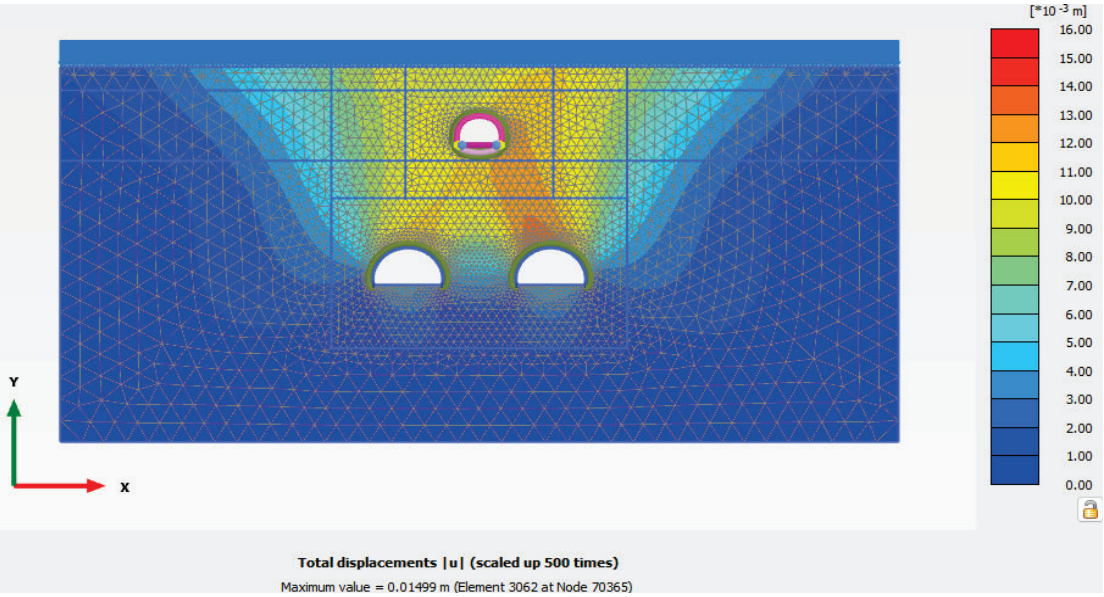


Figure III-35: Maximum Displacement in Construction- HSs- Gravel-

Plane Sole Section in New Tunnels

(a.2) Service Stage

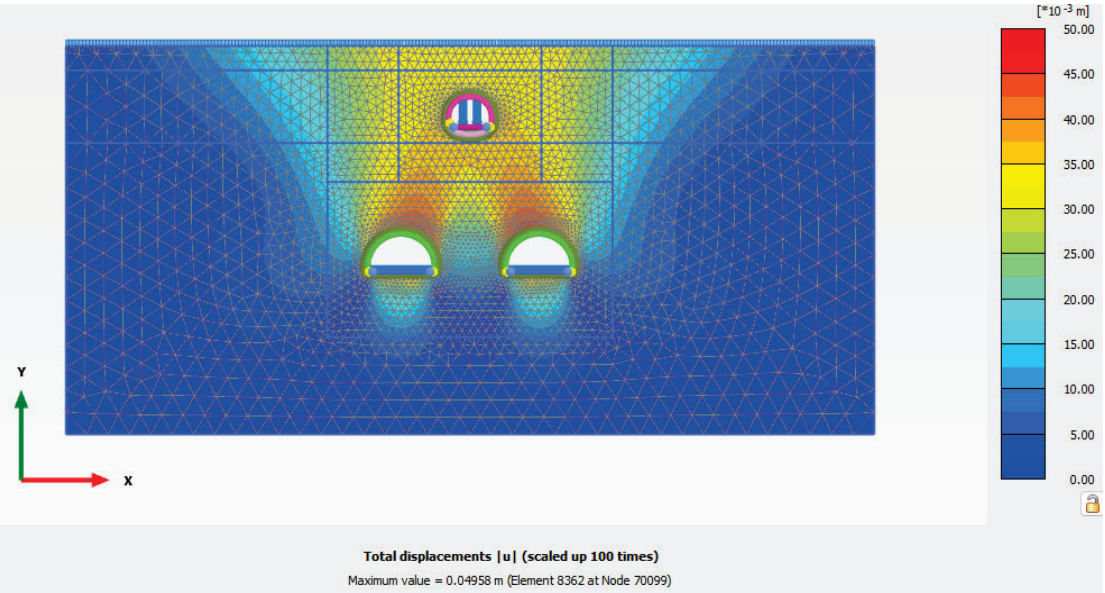


Figure III-36: Maximum Displacement in Service- MC- Gravel-Plane Sole Section in New Tunnels

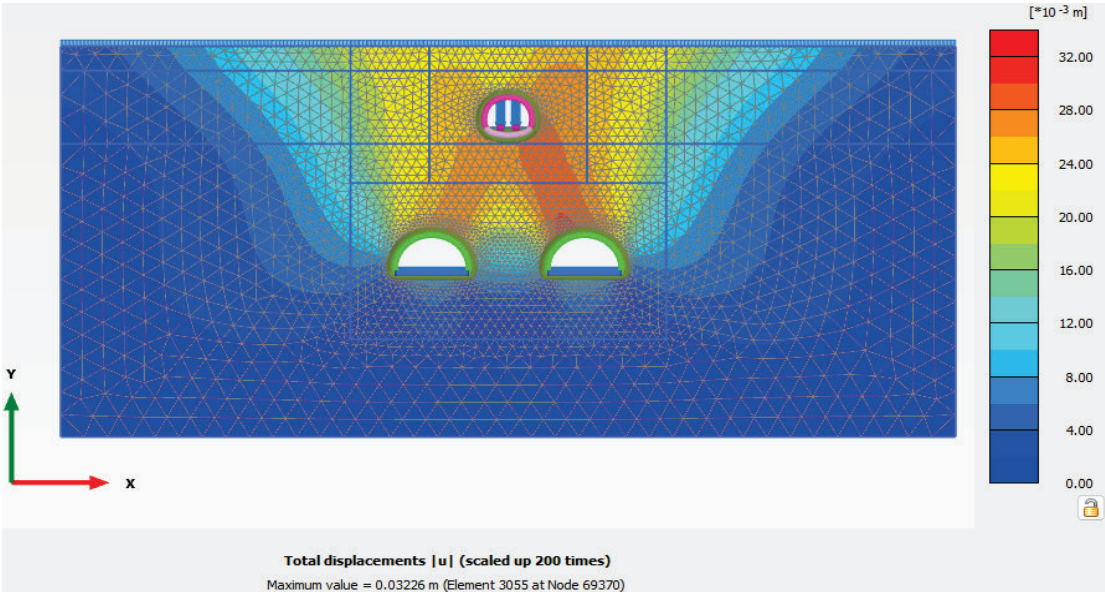


Figure III-37: Maximum Displacement in Service- HS- Gravel-Plane Sole Section in New Tunnels

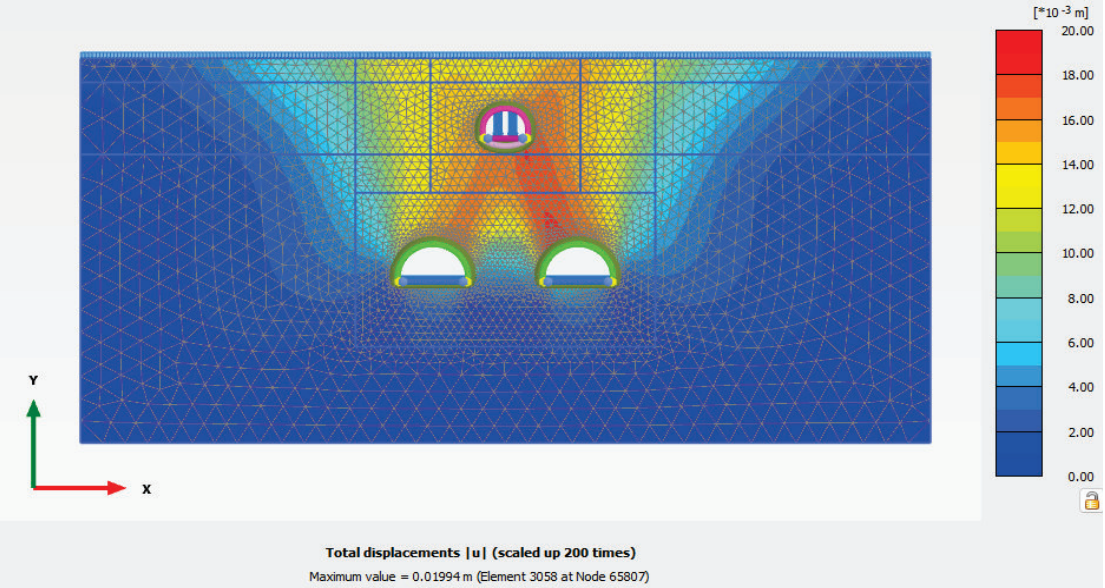


Figure III-38: Maximum Displacement in Service- HSs- Gravel- Plane Sole Section in New Tunnels

Table III-19: Summary of Maximum Displacement Checks on New Road Tunnels– Pre-existing Metro Tunnel – Gravel- Plane Sole Section in New Tunnels

Maximum Displacement [mm]							
Soil	Construction Stage			Service Stage			Admissible
	MC	HS	HSs	MC	HS	HSs	
Gravel	42.46	28.53	14.99	49.58	32.26	19.94	30

(b) Analysis of the Mixed Profile

(b.1) Construction Stage

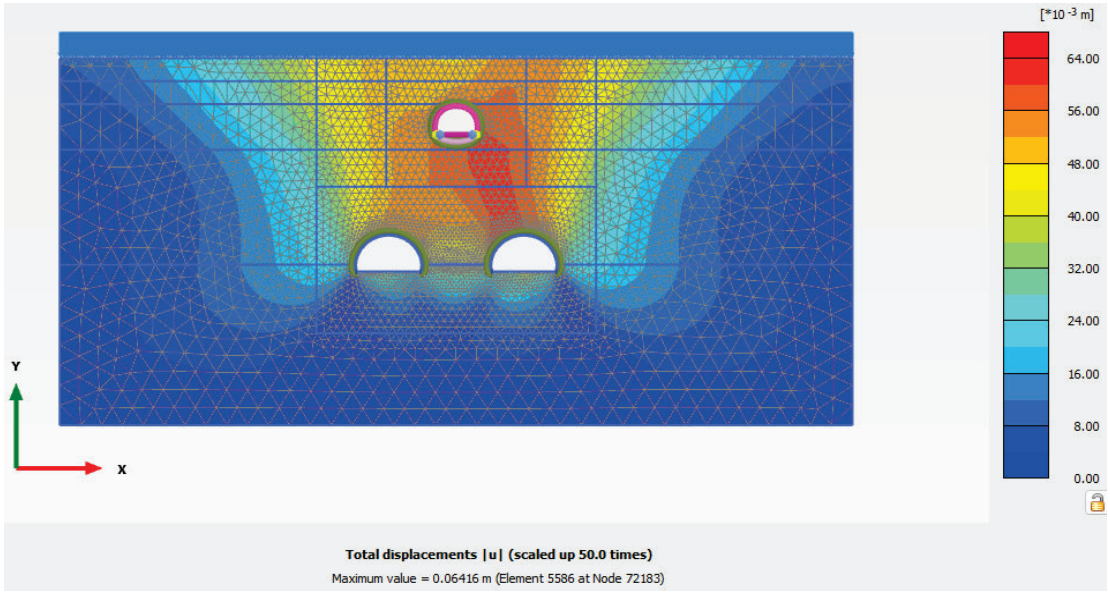


Figure III-39: Maximum Displacement in Construction- HS- Mixed-Plane Sole Section in New Tunnels

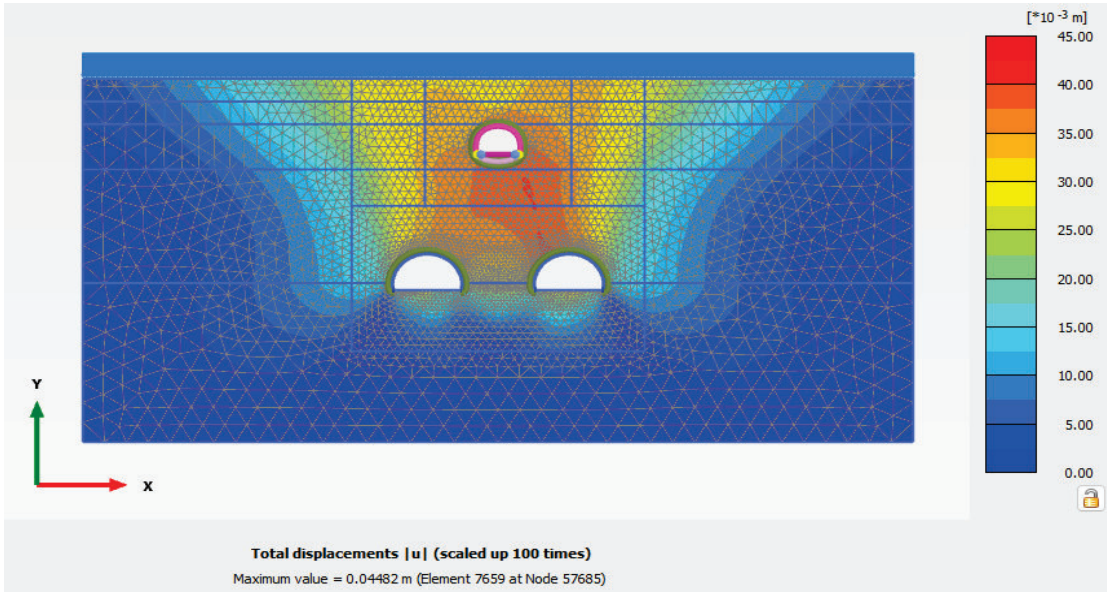


Figure III-40: Maximum Displacement in Construction- HSs- Mixed-Plane Sole Section in New Tunnels

(b.2) Service Stage

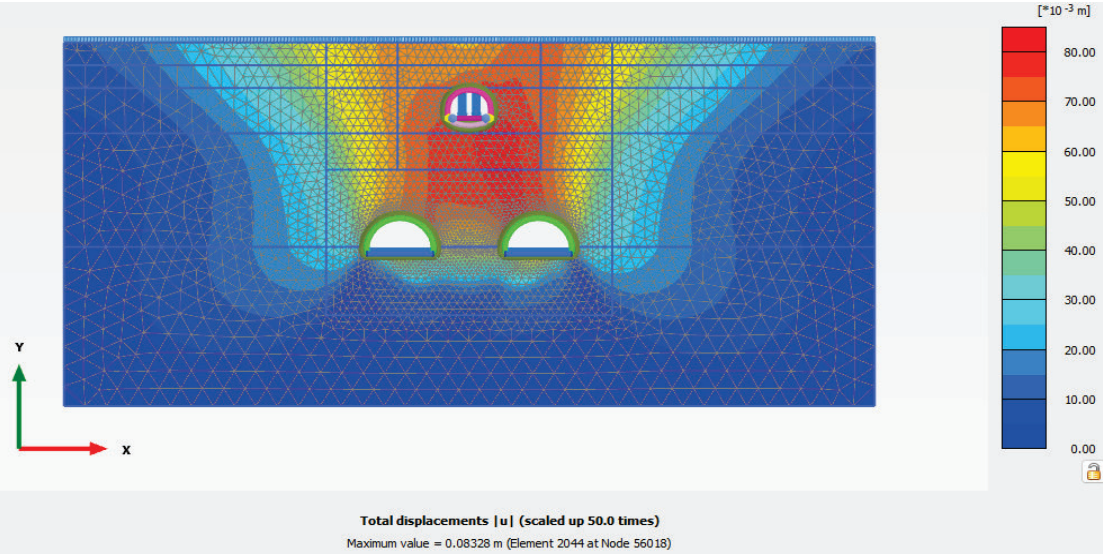


Figure III-41: Maximum Displacement in Service- HS- Mixed- Plane Sole Section in New Tunnels

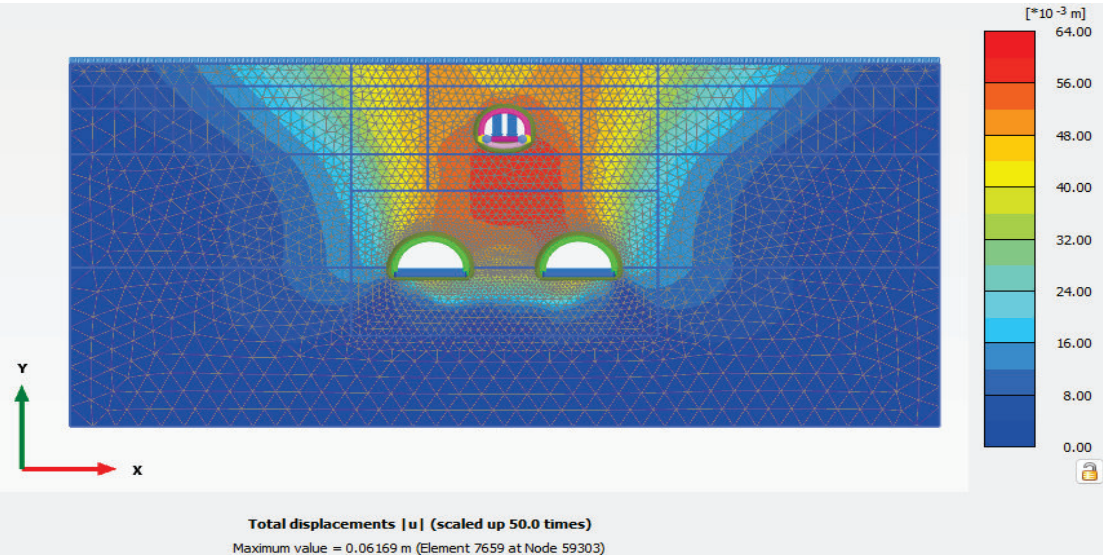


Figure III-42: Maximum Displacement in Service- HSs- Mixed- Plane Sole Section in New Tunnels

Table III-20: Summary of Maximum Displacement Checks on New Road Tunnels–

Pre-existing Metro Tunnel – Mixed- Plane Sole Section in New Tunnels

Maximum Displacement [mm]							
Soil	Construction Stage			Service Stage			Admissible
	MC	HS	HSs	MC	HS	HSs	
Mixed	-	64.16	44.82	-	83.28	61.69	50

3.1.4 Verification of the Resistance in the New Road Tunnels

In the construction stage, the support of the new road tunnels must be verified through the criterion of admissible stresses, as defined in section 3.7.3(b).

In the service stage, the lining of the new road tunnels must be verified through the interaction diagram M-N and N-Q, as defined in section 3.7.3(b)..

The lining of the new road tunnels are verified, with their corresponding concrete thicknesses and reinforcement, as defined in Figure III-10 and sections 3.3.2 and 3.3.2(b).

$e = 0.50\ m$ Concrete thicknesses for the calculation

(Lining thicknesses = 0.30 m + 2/3 Support thicknesses = 0.20 m)

$A_s = 3.35\ cm^2/m$ ACMA335 Mesh in Internal and External face

$A_{s1} = 7.60\ cm^2/m$ 2Ø22 Bar of the Reticulate Frame in Internal face

$A_{s1} = 8.04\ cm^2/m$ 1Ø32 Bar of the Reticulate Frame in External face

(a) Analysis of the Gravel Profile

(a.1) Construction Stage

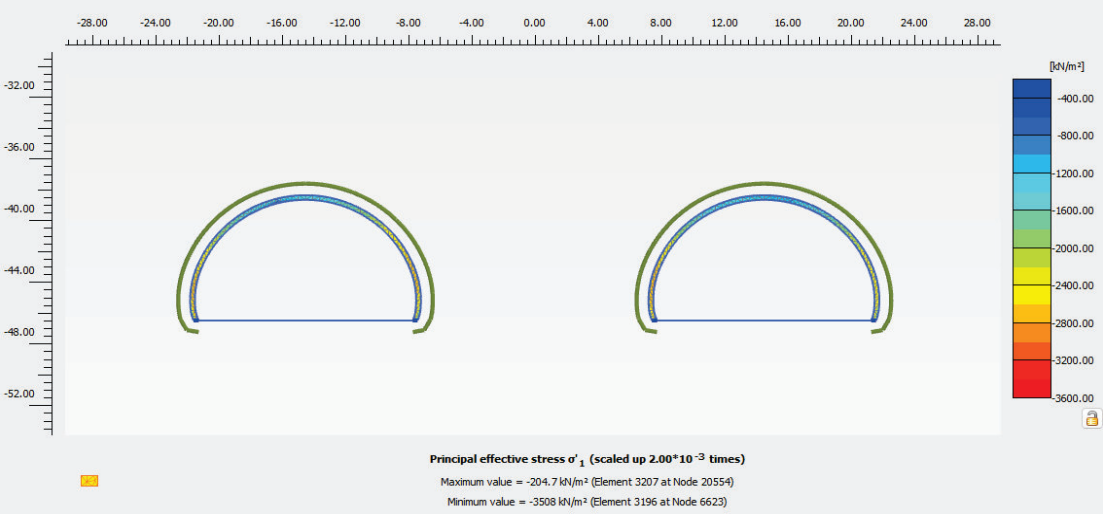


Figure III-43: Major Principal effective Stress on Support- HSs – Gravel-Plane Sole Section in New Tunnels

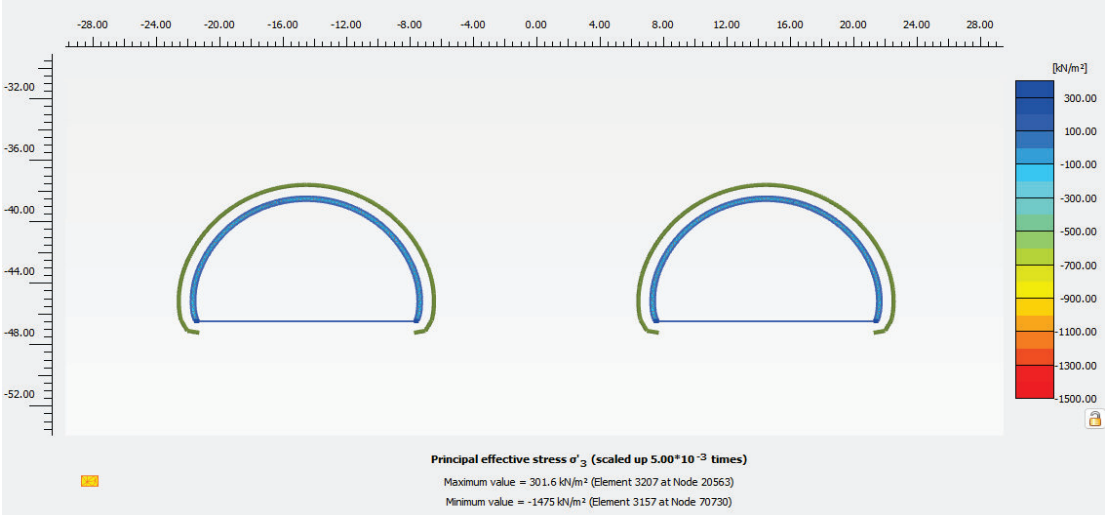


Figure III-44: Minor Principal effective Stress on Support- HSs – Gravel-

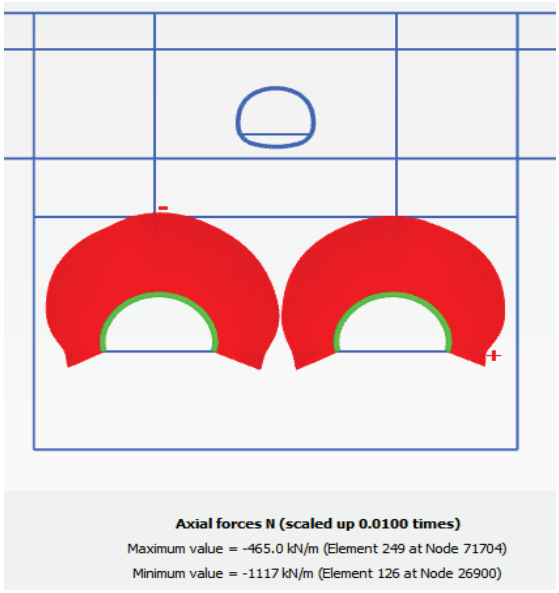
Plane Sole Section in New Tunnels

Table III-21: Verification of Admissible Stress- HSs- Gravel-

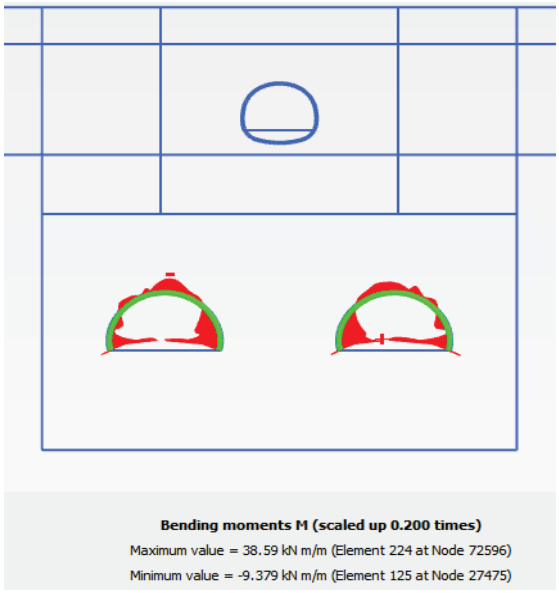
Plane Sole Section in New Tunnels

σ´1 [MPa]	σ´3 [MPa]	σ´1adm [MPa]	σ´3adm [MPa]	σ´1 < σ´1 adm	σ´3 < σ´3 adm
-3.51	0.3	-16	2	CHECK	CHECK

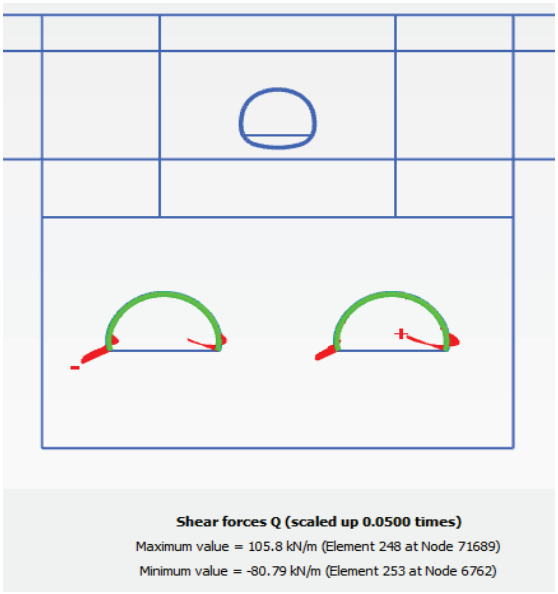
(a.2) Service Stage



Axial forces N (scaled up 0.0100 times)
Maximum value = -465.0 kN/m (Element 249 at Node 71704)
Minimum value = -1117 kN/m (Element 126 at Node 26900)

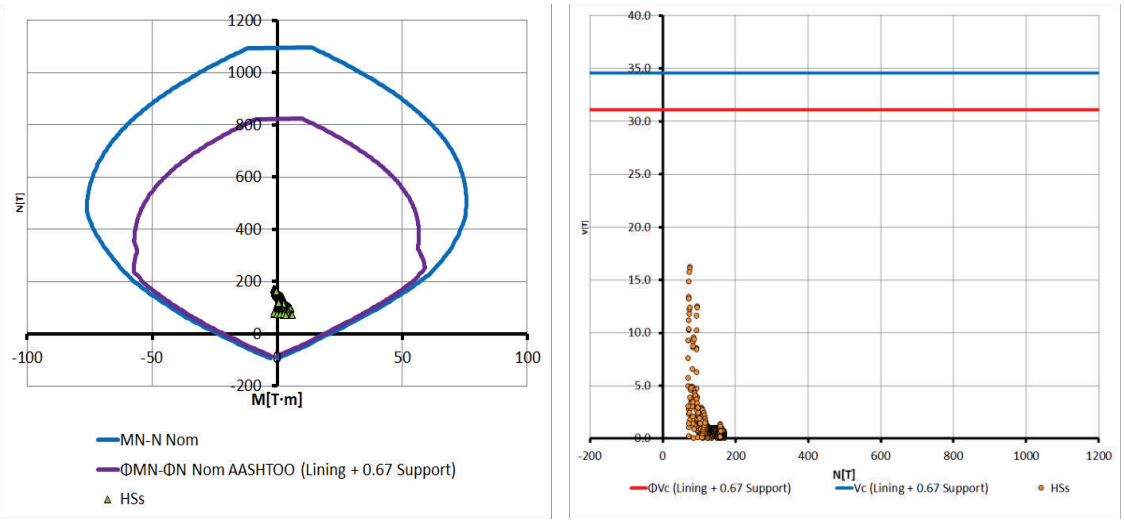


Bending moments M (scaled up 0.200 times)
Maximum value = 38.59 kN m/m (Element 224 at Node 72596)
Minimum value = -9.379 kN m/m (Element 125 at Node 27475)



Shear forces Q (scaled up 0.0500 times)
Maximum value = 105.8 kN/m (Element 248 at Node 71689)
Minimum value = -80.79 kN/m (Element 253 at Node 6762)

Figure III-45: Forces Diagram, Axial, Bending and Shear on Lining- Service Stage- HSs- Gravel- Plane Sole Section in New Tunnels



Graph III-17: : Interaction M-N and N-Q Diagram- Lining of the new road tunnels-

Service Stage- Gravel- Plane Sole Section in New Tunnels

3.1.5 Verification of the Capacity of the Soil

The following shows the plastification of the soil in construction and in service and applies the acceptability criteria explained in section 3.7.4.

(a) Construction Stage

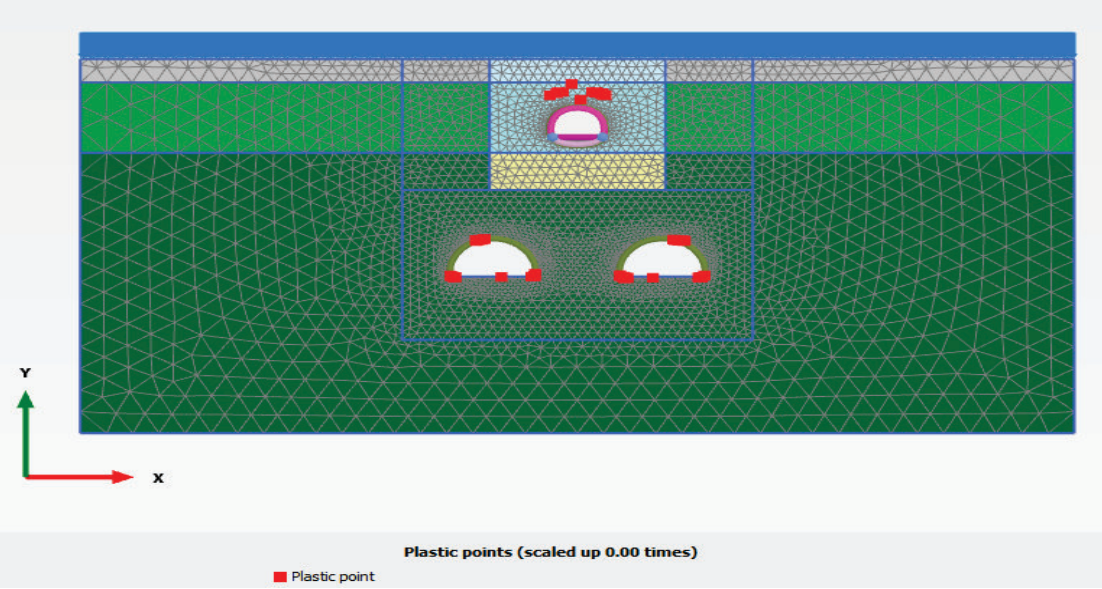


Figure III-46: Plastification Diagram- Construction Stage- HSs- Gravel-

Plane Sole Section in New Tunnels

(b) Service Stage



Figure III-47: Plastification Diagram- Service Stage- HSs- Gravel-Plane Sole Section in New Tunnels

Table III-22: Plastification Verification on Soil- HSs- Gravel-Plane Sole Section in New Tunnels

Stage	R-Plastic [m]	R-Plastic Admissible [m]	Verification
Construction	8	14	CHECK
Service	14	14	CHECK

3.2. Variation of the Constitutive Soil Model with Counter-vault Section in two excavation phases in Mixed and Fine Soil

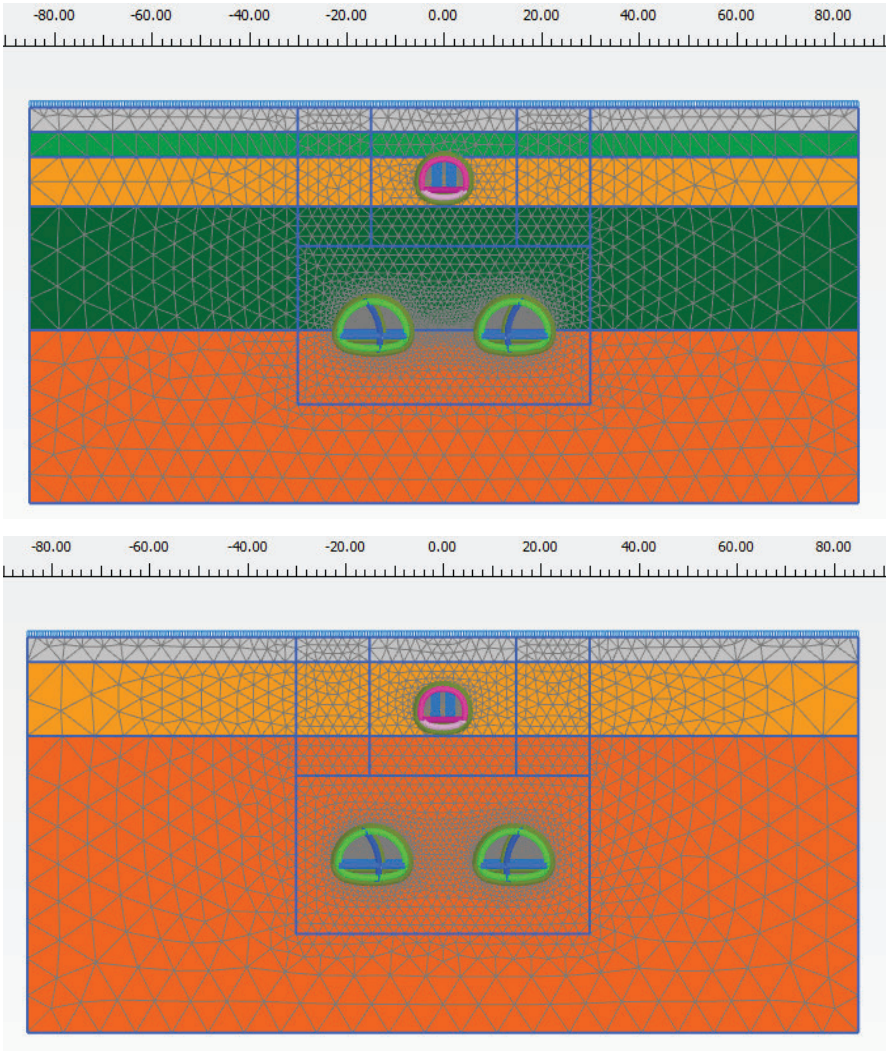


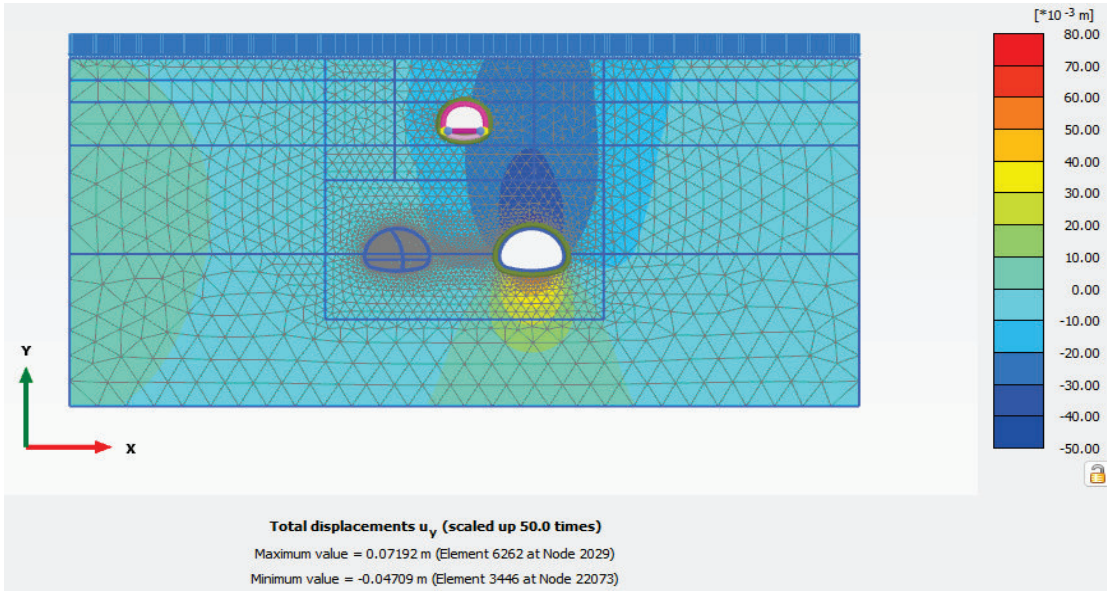
Figure III-48: Soils Models (Mixed-superior and Fine- inferior) with Pre-existing Metro Tunnel and counter-vault section in New Tunnels

3.2.1 Verification of the Deformation in the Metro Tunnel (MT)

Initially, the vertical deformations or settlements are shown for each soil profile, in the most important construction phases and for each soil constitutive model. Then, the settlement profiles located at the inferior level, 18.50 m, and the verification of the acceptance criterion of transverse deformation of the rails of the Metro Tunnel (See Chapter 3.7.1(a)), are presented.

(a) Analysis of the Mixed Profile

(a.1) Construction Stage



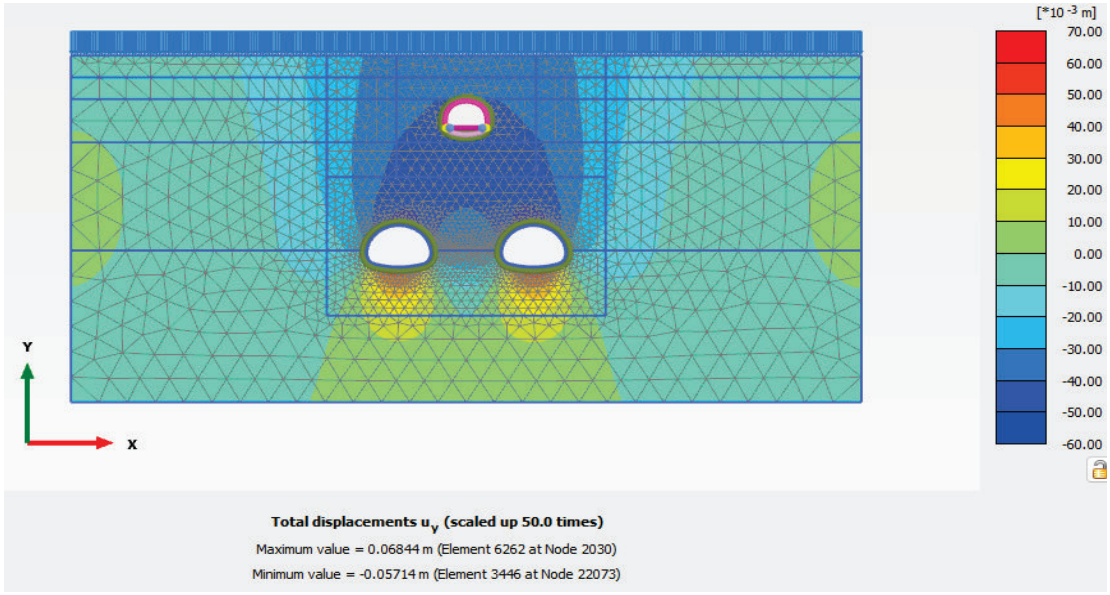


Figure III-49: Vertical Settlement in Construction (WT and ET)- MC- Mixed-Counter-vault Section in New Tunnels

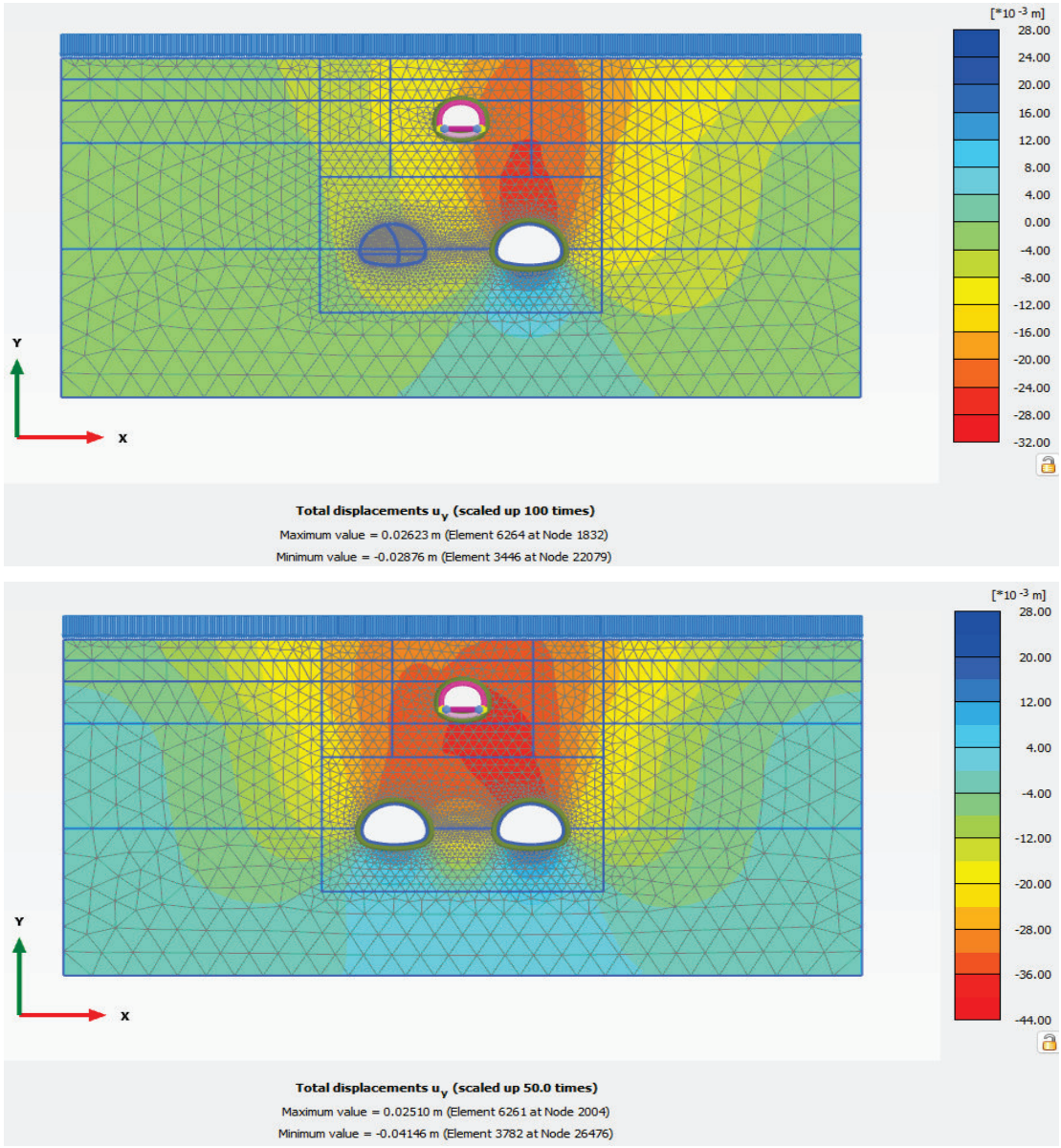


Figure III-50: Vertical Settlement in Construction (WT and ET)- HS- Mixed-Counter-vault Section in New Tunnels

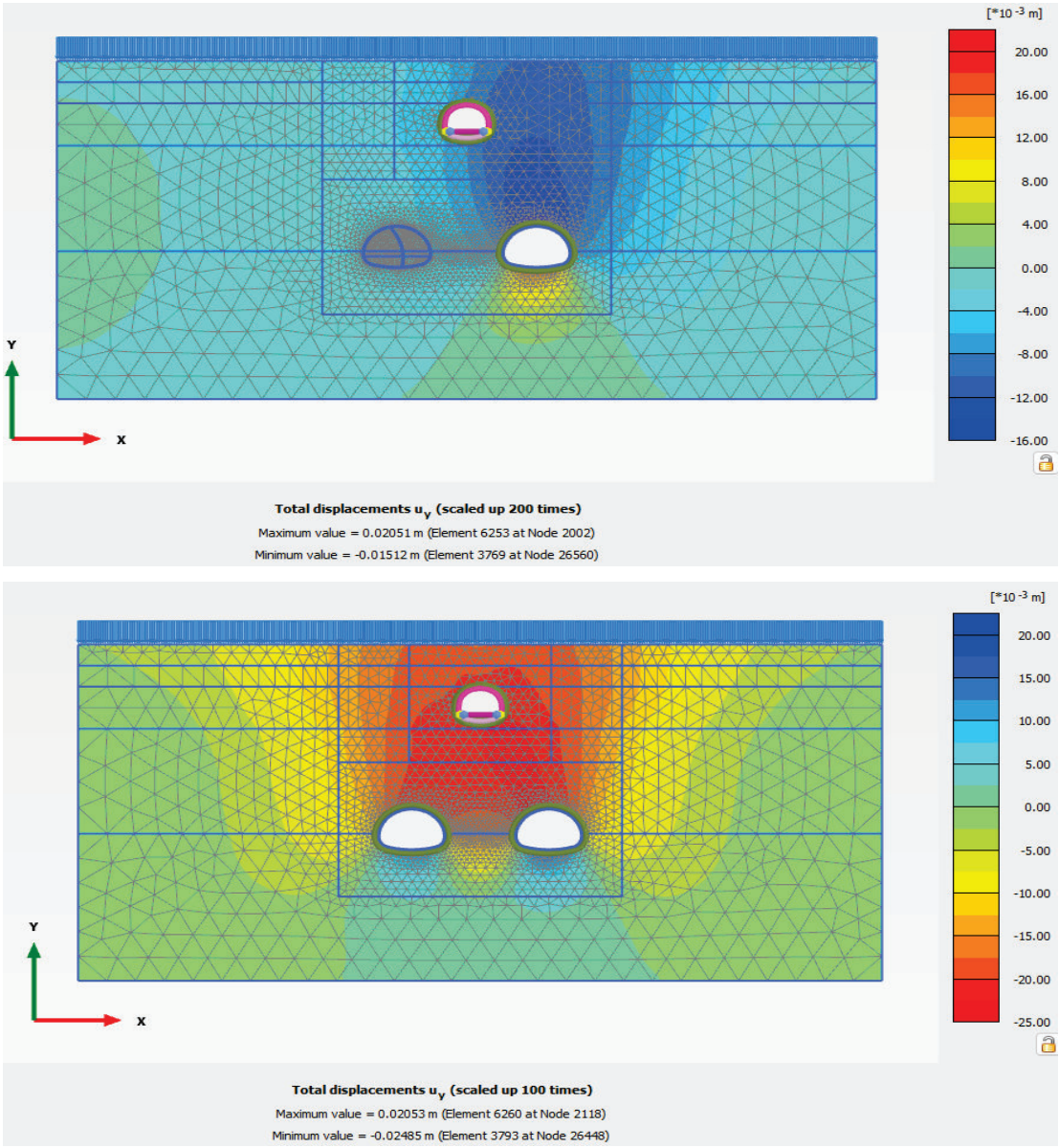
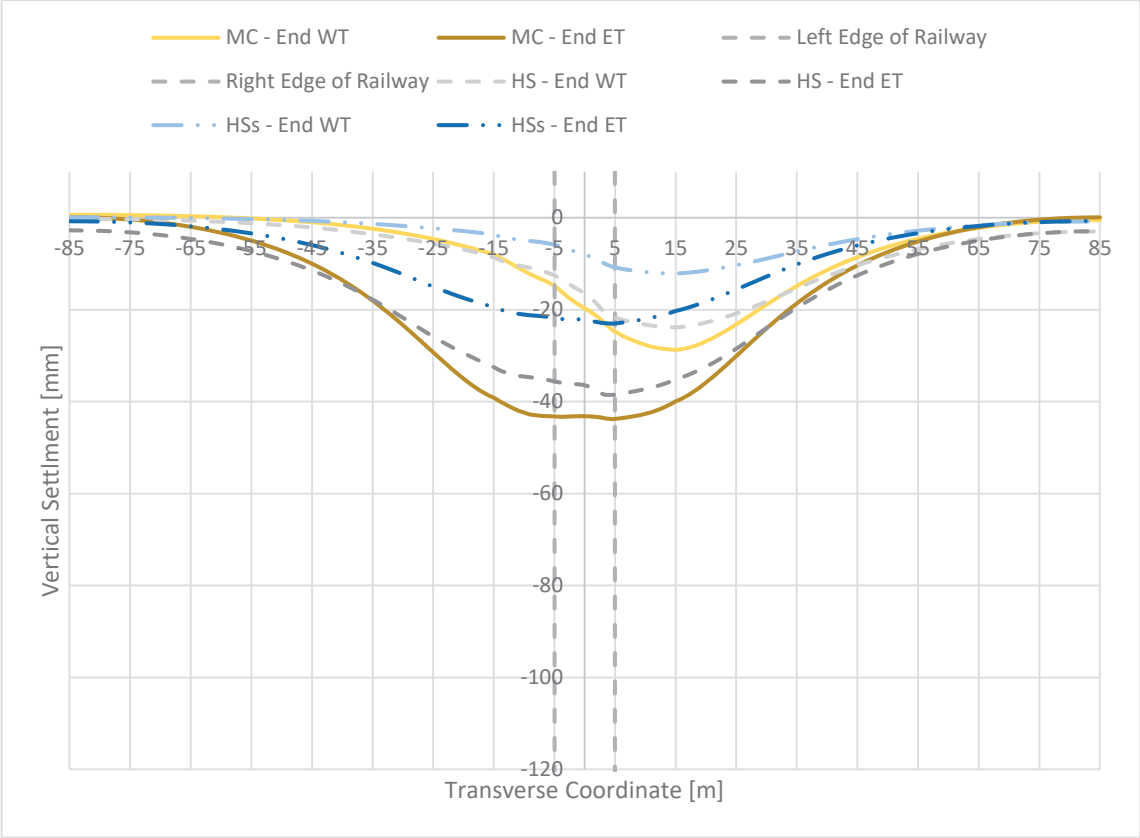


Figure III-51: Vertical Settlement in Construction (WT and ET)-HSs- Mixed-Counter-vault Section in New Tunnels



Graph III-18: Diagram of Transverse Settlement on Metro Tunnel - Construction Stage – Model width Counter-vault Section in New Tunnels- Mixed-Counter-vault Section in New Tunnels

Table III-23: Verification of the Transverse Settlement Limit- MC Model- Construction Stage- Mixed Counter-vault Section in New Tunnels

Phase	Rial 1 Settl (mm)	Rial 2 Settl (mm)	Δ Settl (mm)	Δ Limit (mm)	Verification
Settlement of West Rial					
Excavation WT	-20.33	-21.58	1.25	2	**CHECK**
Excavation ET	-43.19	-43.31	0.12	2	**CHECK**
Settlement of East Rial					
Excavation WT	-19.12	-17.92	1.20	2	**CHECK**
Excavation ET	-43.15	-43.18	0.03	2	**CHECK**

Table III-24: Verification of the Transverse Settlement Limit- HS Model- Construction Stage- Mixed Counter-vault Section in New Tunnels

Phase	Rial 1 Settl (mm)	Rial 2 Settl (mm)	Δ Settl (mm)	Δ Limit (mm)	Verification
Settlement of West Rial					
Excavation WT	-17.18	-19.02	1.84	2	**CHECK**
Excavation ET	-36.79	-37.77	0.98	2	**CHECK**
Settlement of East Rial					
Excavation WT	-15.86	-14.74	1.12	2	**CHECK**
Excavation ET	-36.28	-36.14	0.14	2	**CHECK**

Table III-25: Verification of the Transverse Settlement Limit- HSs Model- Construction Stage- Mixed Counter-vault Section in New Tunnels

Phase	Rial 1 Settl (mm)	Rial 2 Settl (mm)	Δ Settl (mm)	Δ Limit (mm)	Verification
Settlement of West Rial					
Excavation WT	-8.38	-9.28	0.90	2	**CHECK**
Excavation ET	-22.67	-22.75	0.08	2	**CHECK**
Settlement of East Rial					
Excavation WT	-7.69	-7.10	0.59	2	**CHECK**
Excavation ET	-22.12	-22.13	0.01	2	**CHECK**

(a.2) Service Stage

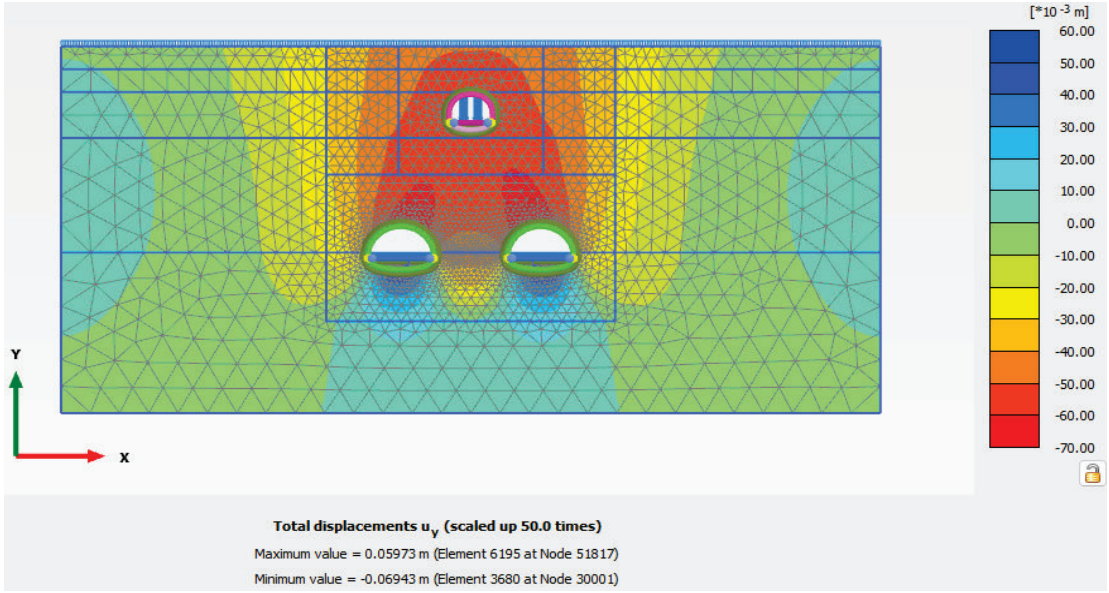


Figure III-52: Vertical Settlement in Service- MC- Mixed-Counter-vault Section in New Tunnels

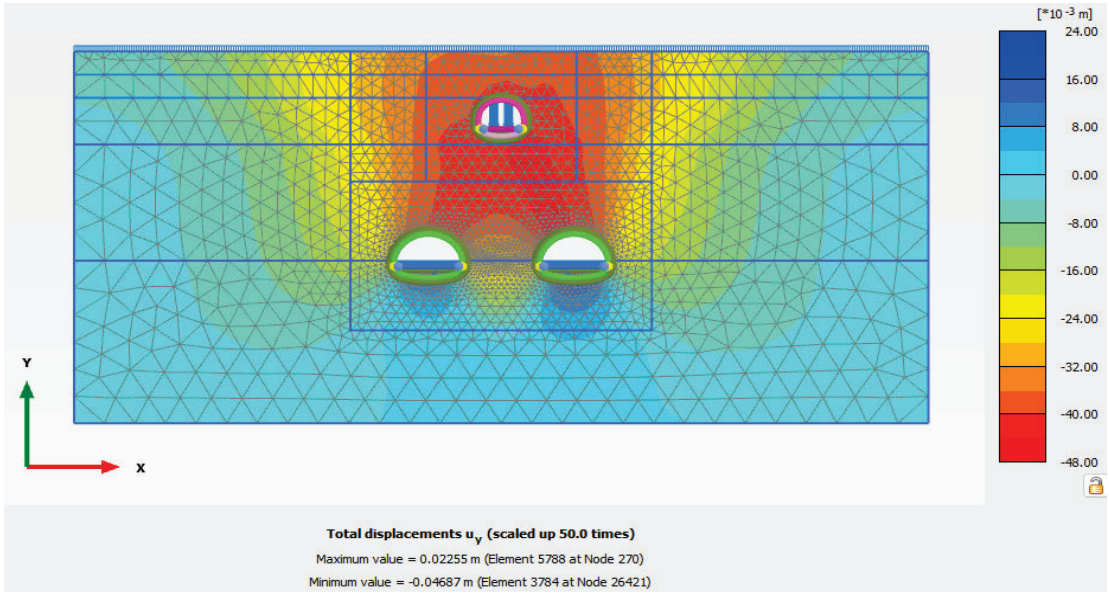


Figure III-53: Vertical Settlement in Service- HS- Mixed-Counter-vault Section in New Tunnels

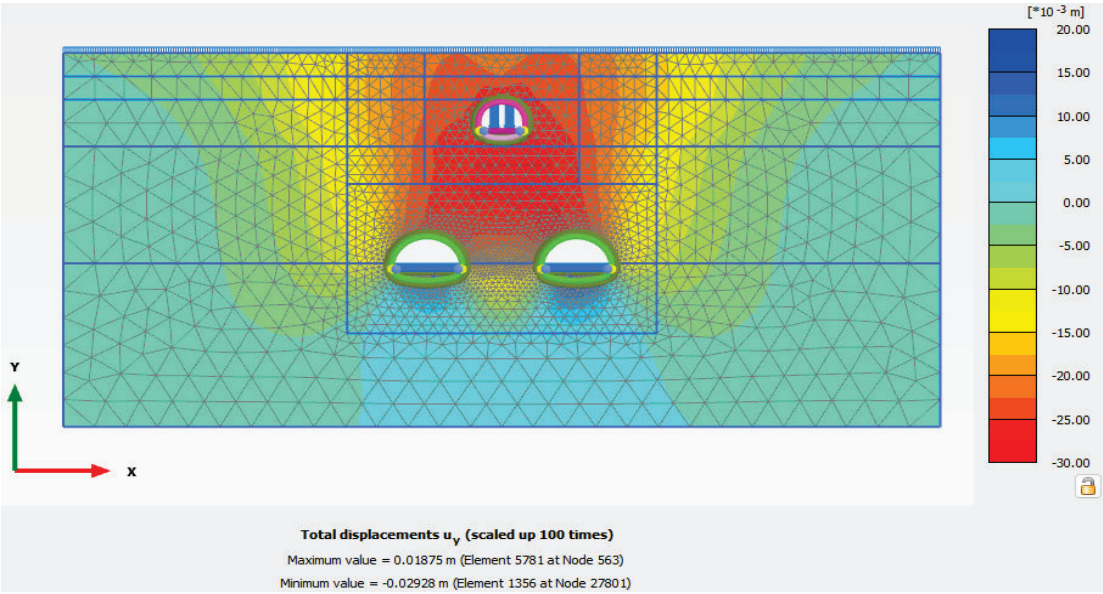
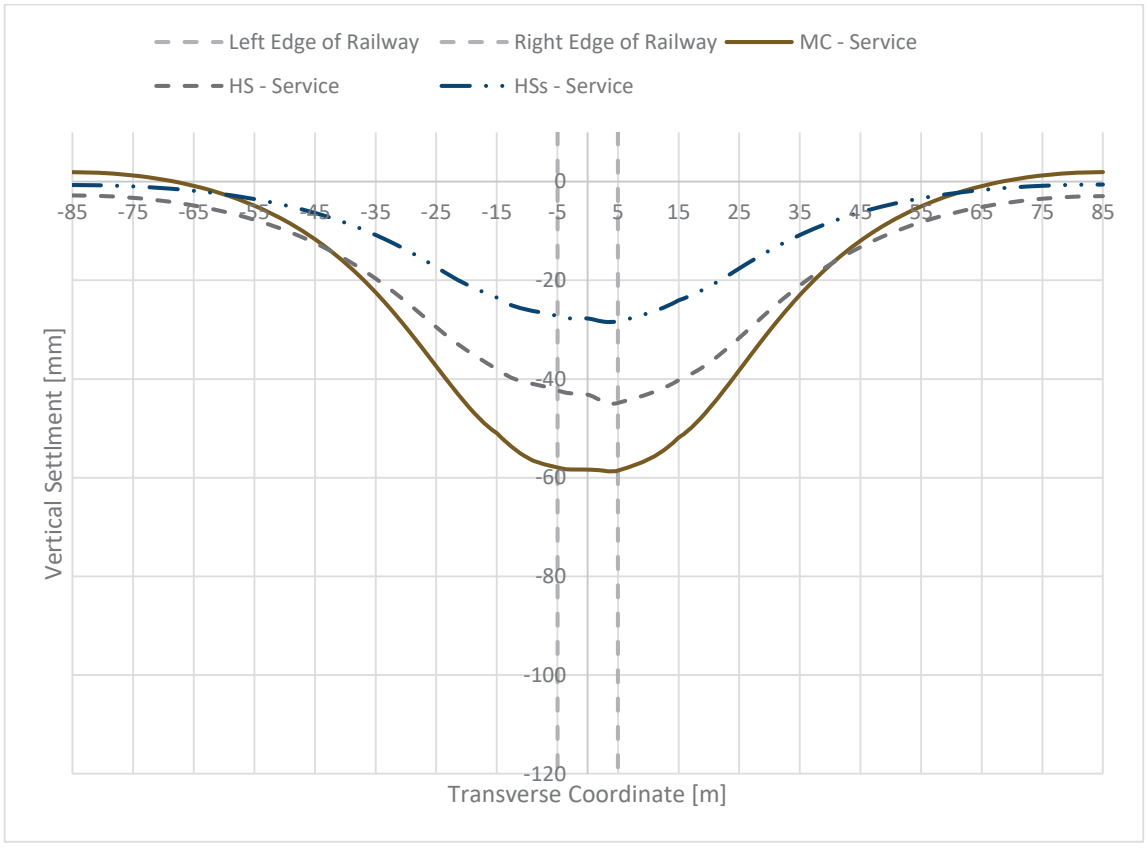


Figure III-54: Vertical Settlement in Service- HSs- Mixed-Counter-vault Section in New Tunnels



Graph III-19: Diagram of Transverse Settlement on Metro Tunnel - Service Stage –

Model with Counter-vault Section in New Tunnels

Table III-26: Verification of the Transverse Settlement Limit- MC Model- Service Stage- Mixed- Counter-vault Section in New Tunnels

Phase	Rial 1 Settl (mm)	Rial 2 Settl (mm)	Δ Settl (mm)	Δ Limit (mm)	Verification
Settlement of West Rial					
Service	-58.38	-58.48	0.09	2	**CHECK**
Settlement of East Rial					
Service	-58.33	-58.32	0.01	2	**CHECK**

Table III-27: Verification of the Transverse Settlement Limit- HS Model- Service Stage- Mixed Counter-vault Section in New Tunnels

Phase	Rial 1 Settl (mm)	Rial 2 Settl (mm)	Δ Settl (mm)	Δ Limit (mm)	Verification
Settlement of West Rial					
Service	-43.48	-44.41	0.93	2	**CHECK**
Settlement of East Rial					
Service	-43.02	-42.94	0.08	2	**CHECK**

Table III-28: Verification of the Transverse Settlement Limit- HSs Model- Service Stage- Mixed Counter-vault Section in New Tunnels

Phase	Rial 1 Settl (mm)	Rial 2 Settl (mm)	Δ Settl (mm)	Δ Limit (mm)	Verification
Settlement of West Rial					
Service	-28.27	-28.26	0.01	2	**CHECK**
Settlement of East Rial					
Service	-27.67	-27.71	0.04	2	**CHECK**

(b) Analysis of the Fine Profile

(b.1) Construction Stage

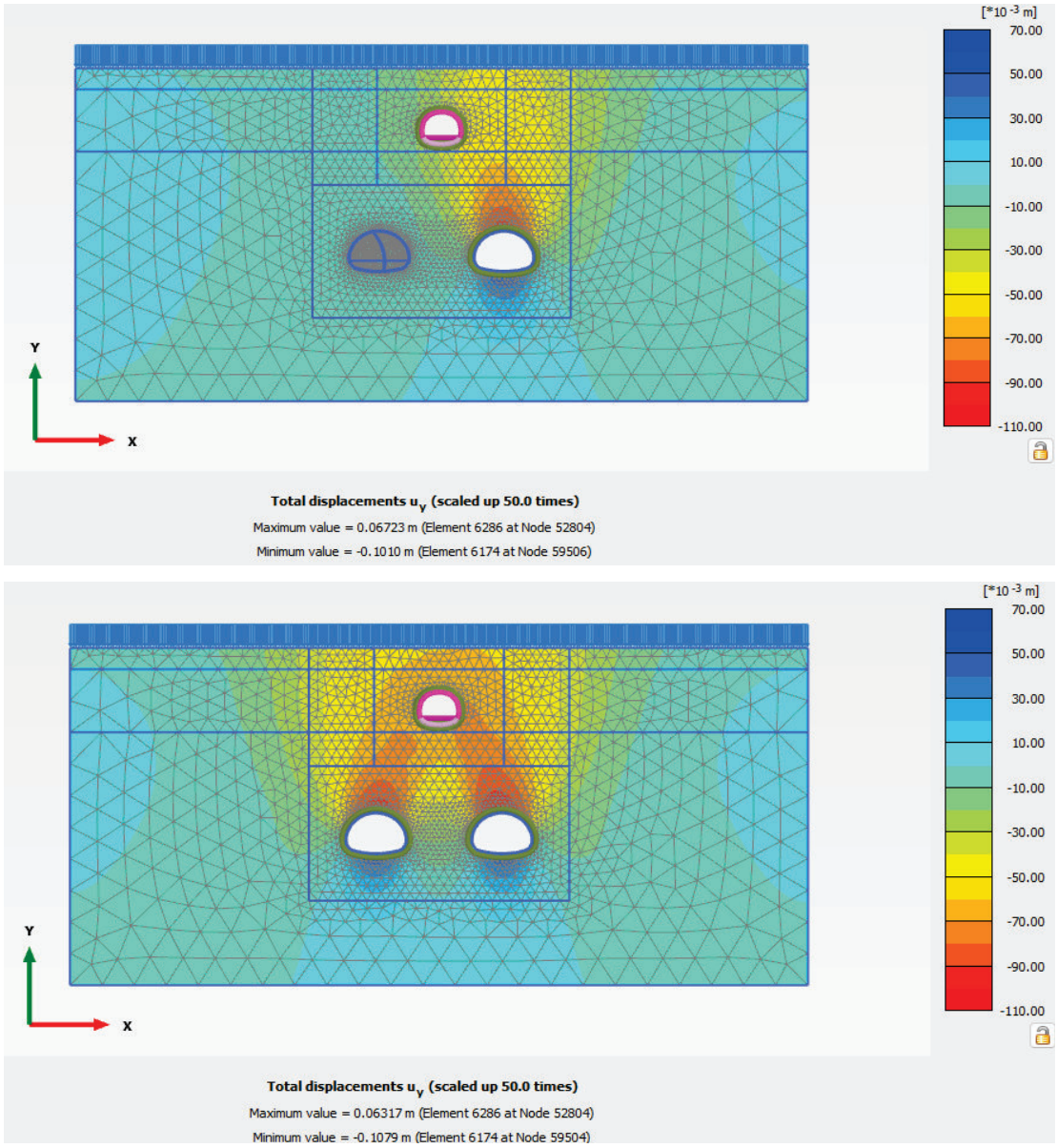
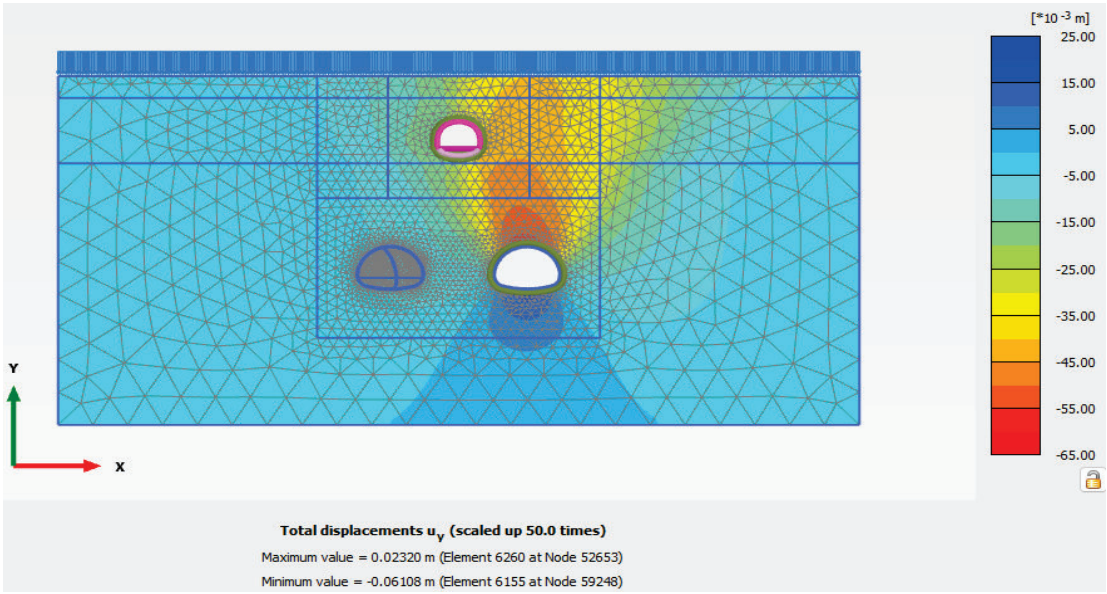


Figure III-55: Vertical Settlement in Construction (WT and ET)- MC- Fine Counter-vault Section in New Tunnels



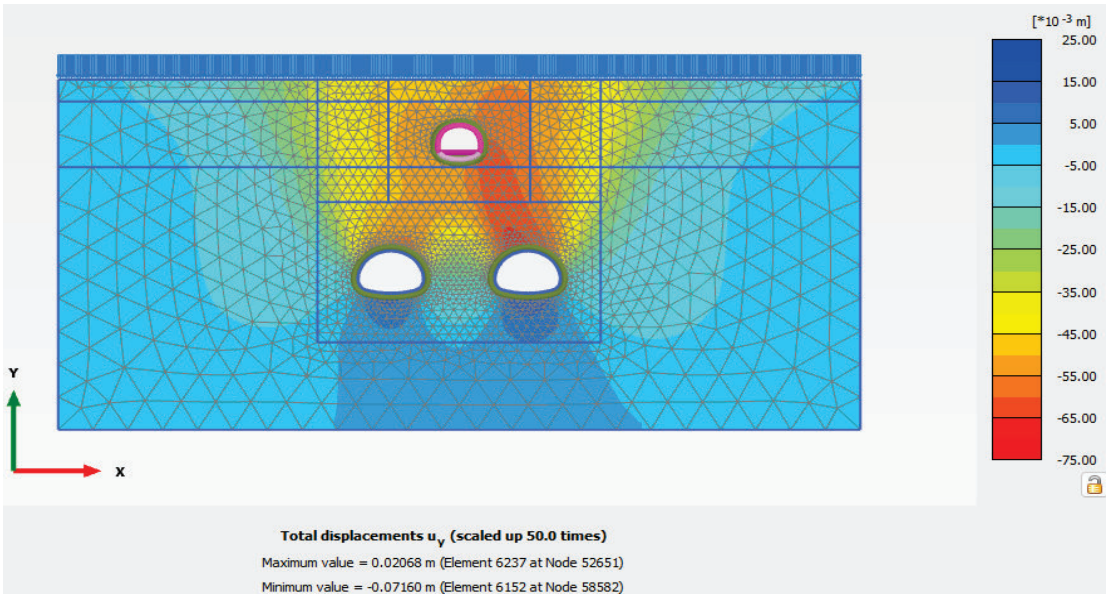


Figure III-56: Vertical Settlement in Construction (WT and ET)- HS- Fine-Counter-vault Section in New Tunnels

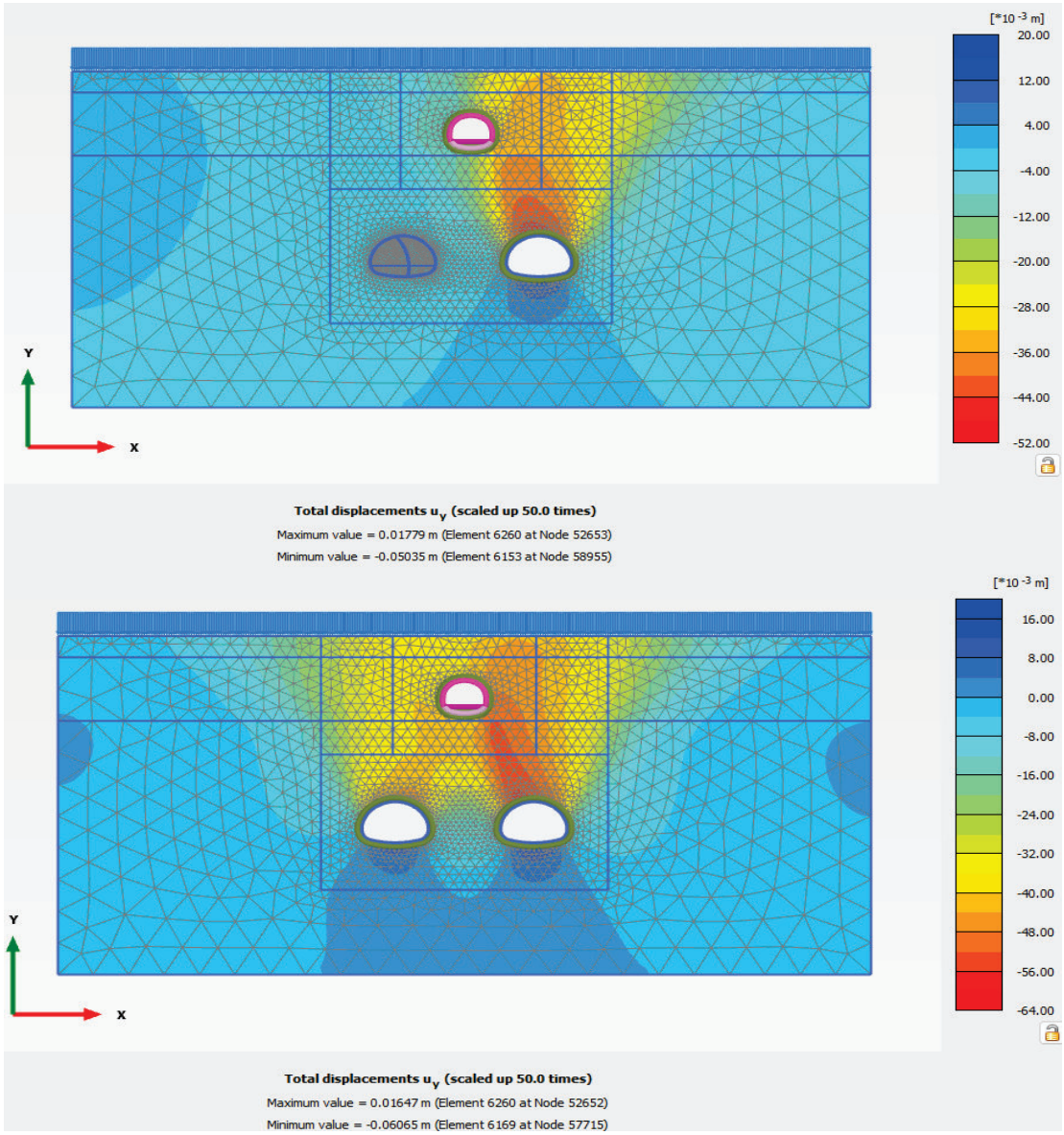
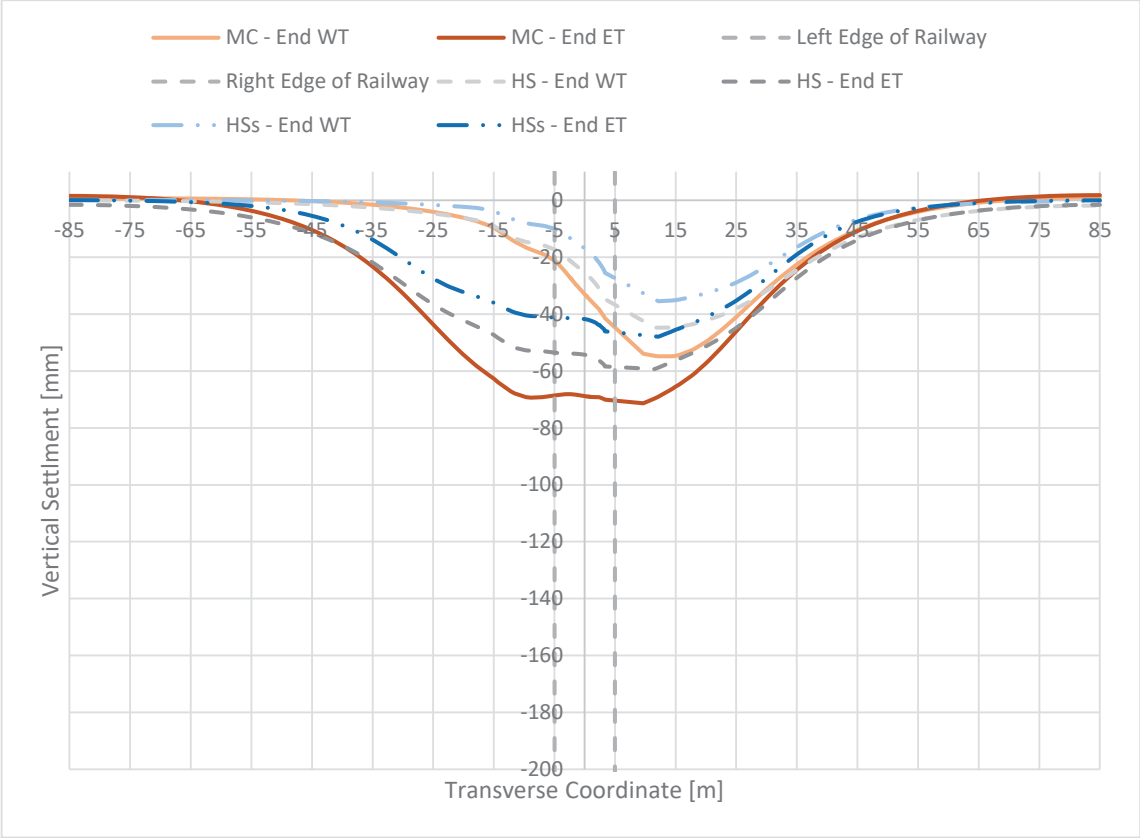


Figure III-57: Vertical Settlement in Construction (WT and ET)- HSs- Fine-Counter-vault Section in New Tunnels



Graph III-20: Diagram of Transverse Settlement on Metro Tunnel - Construction Stage – Model with Plane Sole Section in New Tunnels- Fine- Counter-vault Section in New Tunnels

Table III-29: Verification of the Transverse Settlement Limit- MC Model- Construction Stage- Fine-Counter-vault Section in New Tunnels

Phase	Rial 1 Settl (mm)	Rial 2 Settl (mm)	Δ Settl (mm)	Δ Limit (mm)	Verification
Settlement of West Rial					
Excavation WT	-34.77	-37.94	3.17	2	**NOT CHECK**
Excavation ET	-69.04	-69.19	0.15	2	**CHECK**
Settlement of East Rial					
Excavation WT	-31.32	-27.80	3.53	2	**NOT CHECK**
Excavation ET	-68.57	-68.17	0.40	2	**CHECK**

Table III-30: Verification of the Transverse Settlement Limit- HS Model- Construction Stage- Fine Counter-vault Section in New Tunnels

Phase	Rial 1 Settl (mm)	Rial 2 Settl (mm)	Δ Settl (mm)	Δ Limit (mm)	Verification
Settlement of West Rial					
Excavation WT	-26.93	-30.55	3.62	2	**NOT CHECK**
Excavation ET	-54.72	-56.16	1.43	2	**CHECK**
Settlement of East Rial					
Excavation WT	-24.19	-21.65	2.54	2	**NOT CHECK**
Excavation ET	-54.13	-53.92	0.22	2	**CHECK**

Table III-31: Verification of the Transverse Settlement Limit- HSs Model- Construction Stage- Fine Counter-vault Section in New Tunnels

Phase	Rial 1 Settl (mm)	Rial 2 Settl (mm)	Δ Settl (mm)	Δ Limit (mm)	Verification
Settlement of West Rial					
Excavation WT	-18.16	-21.47	3.31	2	**NOT CHECK**
Excavation ET	-42.11	-43.59	1.48	2	**NOT CHECK**
Settlement of East Rial					
Excavation WT	-15.80	-13.64	2.16	2	**NOT CHECK**
Excavation ET	-41.55	-41.39	0.16	2	**CHECK**

(b.2) Service Stage

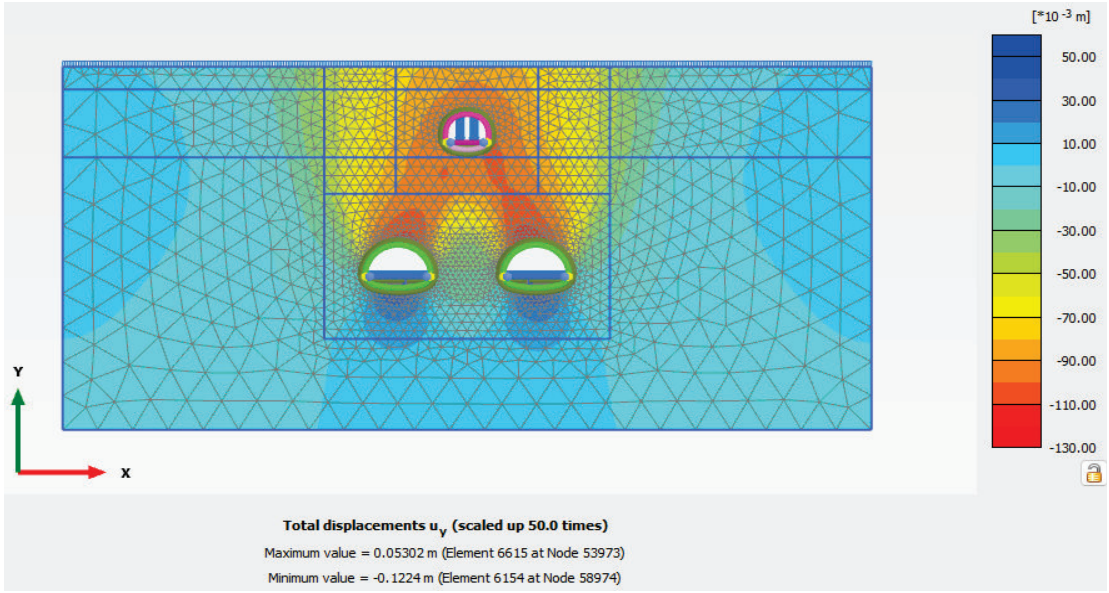


Figure III-58: Vertical Settlement in Service- MC- Fine-Counter-vault Section in New Tunnels

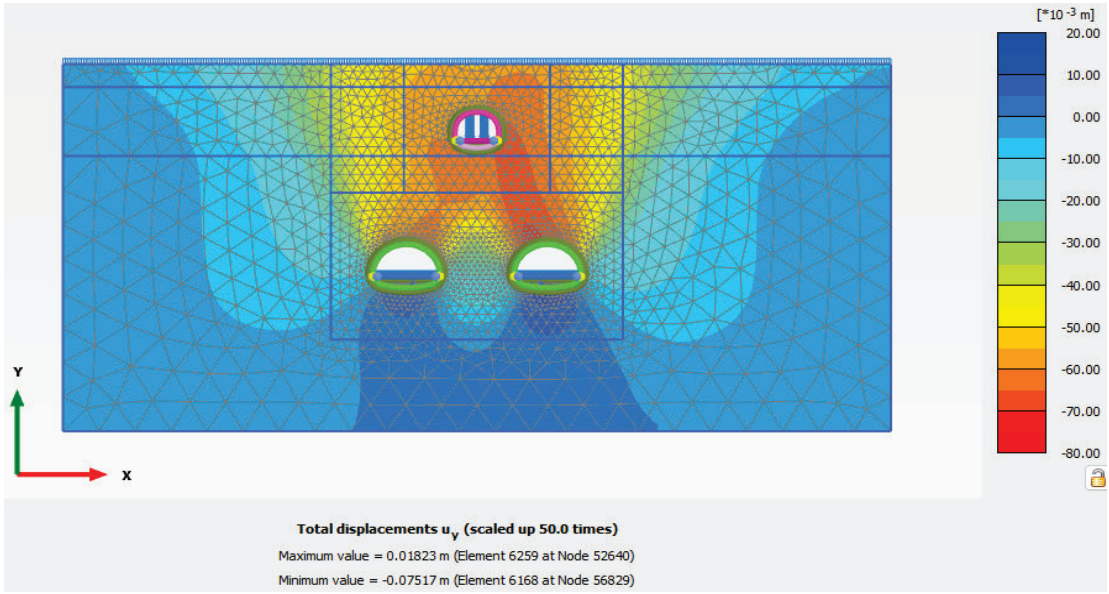


Figure III-59: Vertical Settlement in Service- HS- Fine-Counter-vault Section in New Tunnels

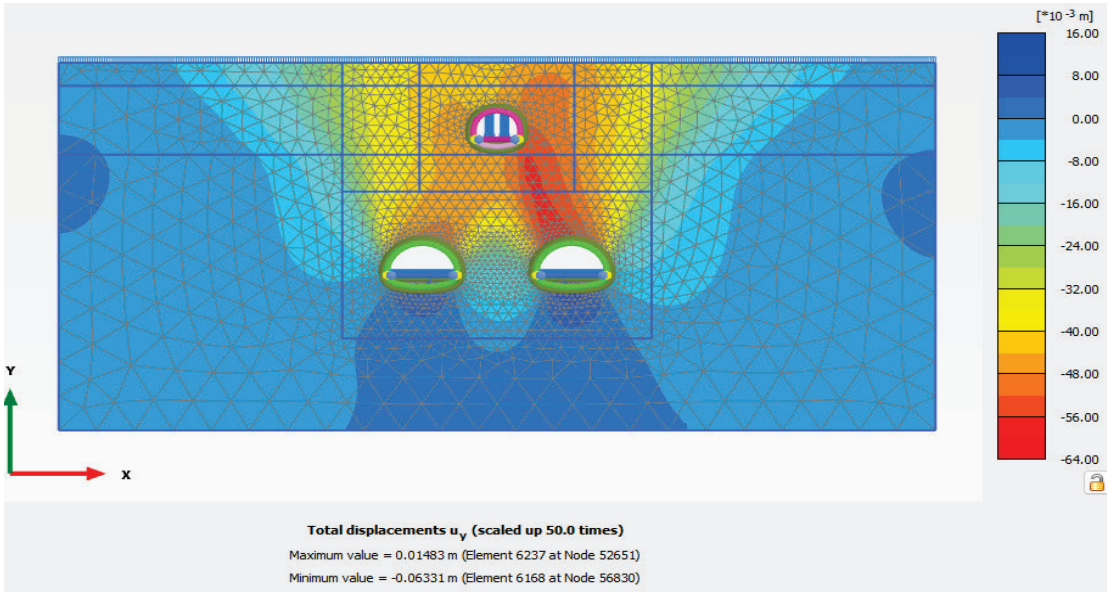
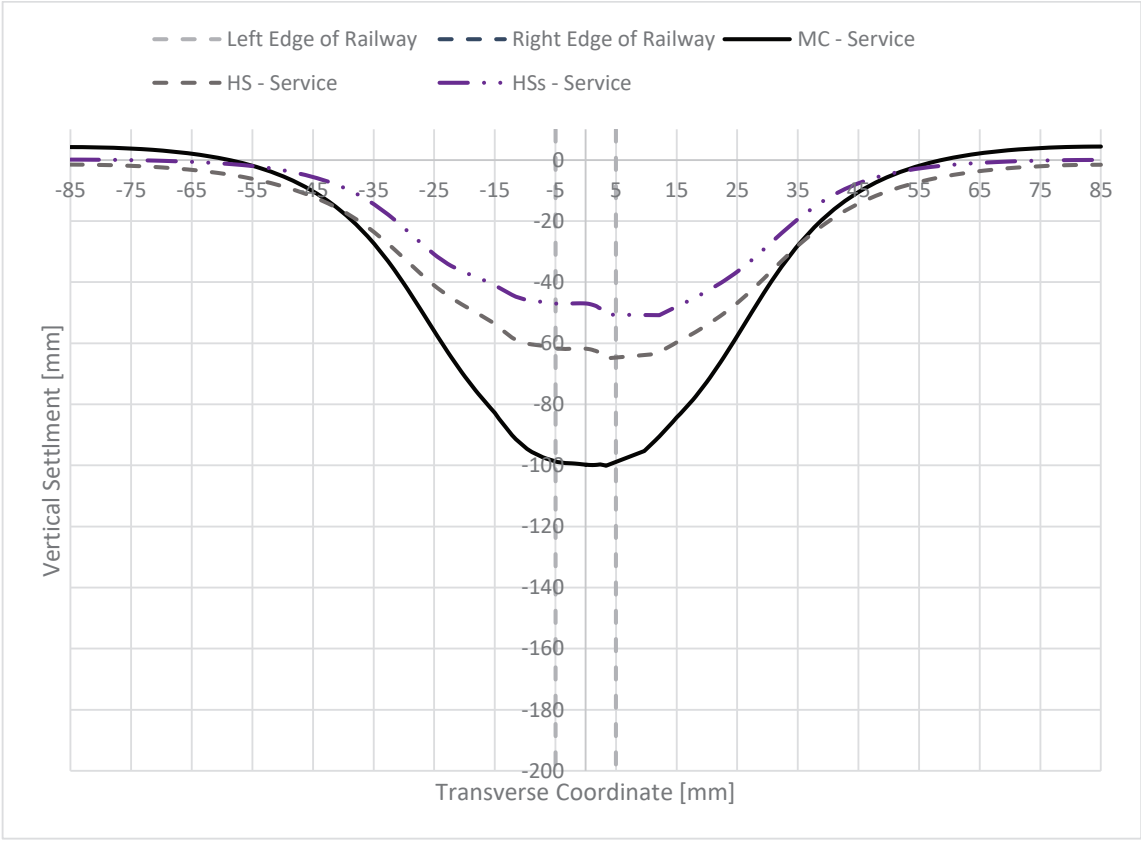


Figure III-60: Vertical Settlement in Service- HSs- Fine- Counter-vault Section in New Tunnels



Graph III-21: Diagram of Transverse Settlement on Metro Tunnel - Service Stage –

Model with Countervault in New Tunnels- Fine

Table III-32: Verification of the Transverse Settlement Limit- MC Model- Service Stage- Fine

Phase	Rial 1 Settl (mm)	Rial 2 Settl (mm)	Δ Settl (mm)	Δ Limit (mm)	Verification
Settlement of West Rial					
Service	-99.83	-99.69	0.14	2	**CHECK**
Settlement of East Rial					
Service	-99.57	-99.30	0.26	2	**CHECK**

Table III-33: Verification of the Transverse Settlement Limit- HS Model- Service Stage- Fine

Phase	Rial 1 Settl (mm)	Rial 2 Settl (mm)	Δ Settl (mm)	Δ Limit (mm)	Verification
Settlement of West Rial					
Service	-62.04	-63.09	1.05	2	**CHECK**
Settlement of East Rial					
Service	-61.77	-61.83	0.05	2	**CHECK**

Table III-34: Verification of the Transverse Settlement Limit- HSs Model- Service Stage- Fine

Phase	Rial 1 Settl (mm)	Rial 2 Settl (mm)	Δ Settl (mm)	Limit (mm)	Verification
Settlement of West Rial					
Service	-47.20	-48.40	1.20	2	**CHECK**
Settlement of East Rial					
Service	-46.91	-46.96	0.05	2	**CHECK**

3.2.2 Verification of the Resistance in the Pre-existing Metro Tunnel considering Counter-vault section in the new tunnels.

At the beginning, the axial force, bending and shear diagrams on the metro-tunnel are presented and then the structural verification is realized through the M-N and N-Q interaction diagrams, as presented in chapter 3.7.1(b).
First the vault and then the counter-vault of the Metro tunnel are verified, with their corresponding concrete thicknesses and reinforcement, as defined in Figure III-14 and Figure III-15.

- Vault of the Metro Tunnel

$e = 0.325\ m$ Concrete thicknesses for the calculation
(Lining thicknesses = 0.20 m + ½ Support thicknesses = 0.125 m)

$A_{s.i} = 3.780\ cm^2/m$ ACMA378 Mesh in Internal face
$A_{s.e} = 2.95\ cm^2/m$ ACMA295 Mesh in External face

- Counter-Vault of the Metro Tunnel

$e = 0.425\ m$ Concrete thicknesses for the calculation
(Lining thicknesses = 0.30 m + ½ Support thicknesses = 0.125 m)

$A_{s.i} = 3.780\ cm^2/m$ ACMA378 Mesh in Internal face
$A_{s.ref} = 6.70\ cm^2/m$ Reinforcement with bars steel 16@30 in Internal face
$A_{s.e} = 2.95\ cm^2/m$ ACMA295 Mesh in External face

(a) Analysis of the Mixed Profile

(a.1) Construction Stage

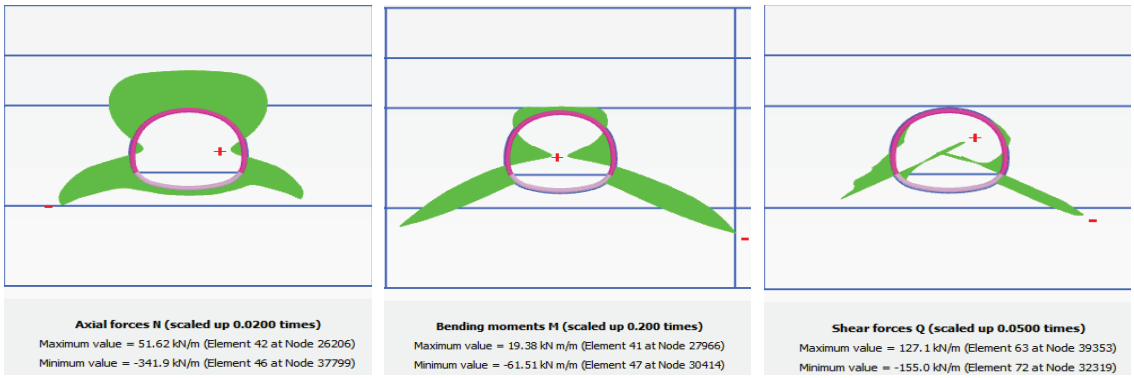


Figure III-61: Forces Diagram, Axial, Bending and Shear- Construction Stage- MC- Mixed

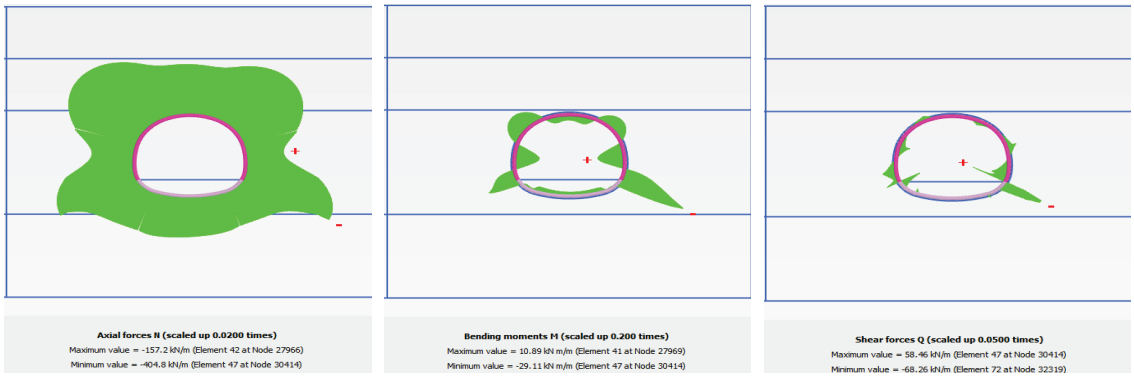


Figure III-62: Forces Diagram, Axial, Bending and Shear- Construction Stage- HS- Mixed

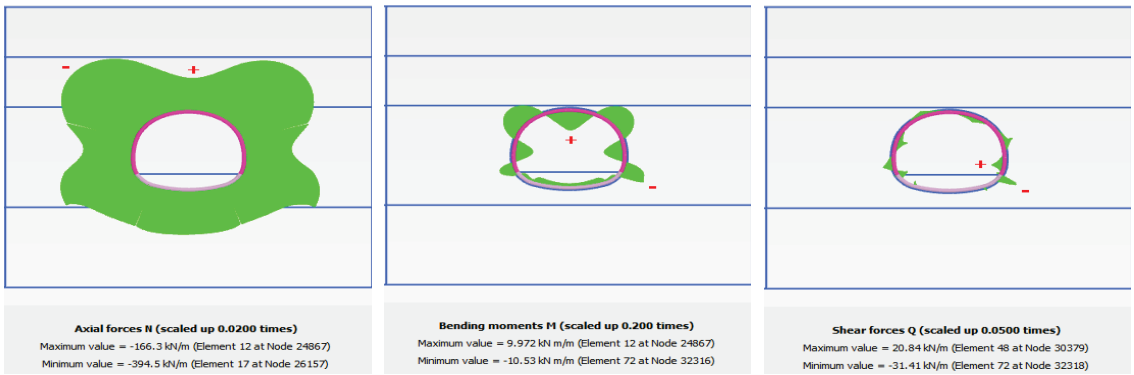
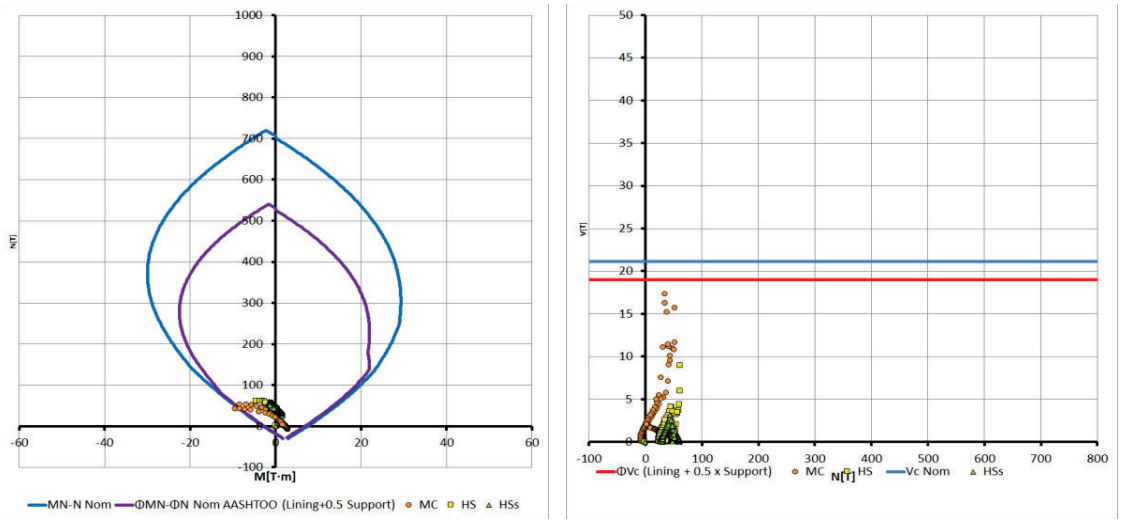
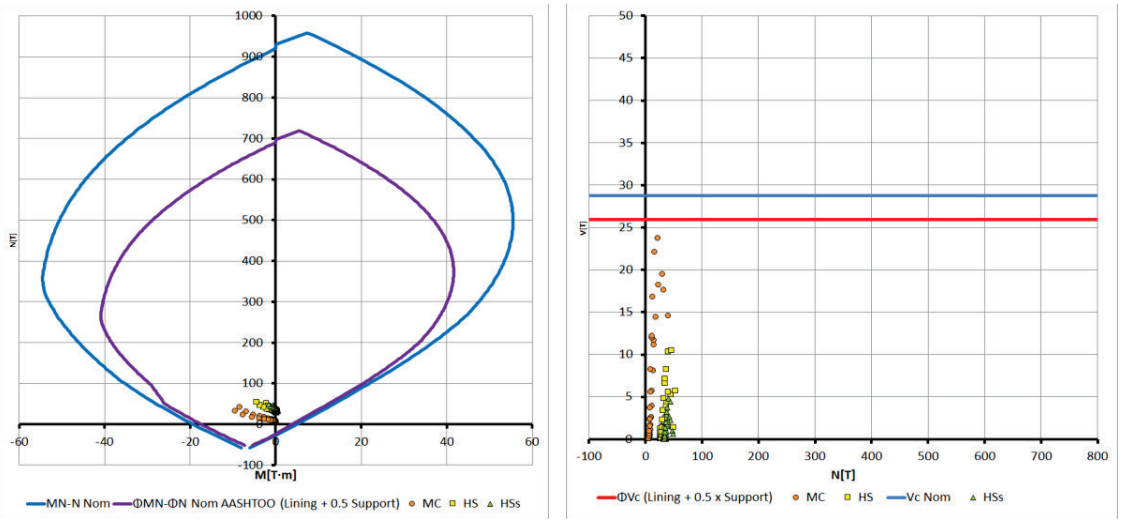


Figure III-63: Forces Diagram, Axial, Bending and Shear- Construction Stage- HSs- Mixed



Graph III-22: Interaction M-N and N-Q Diagram- Vault of Metro Tunnel-

Construction Stage- Mixed



Graph III-23: Interaction M-N and N-Q Diagram- Counter vault of Metro Tunnel-

Construction Stage- Mixed

(a.2) Service Stage

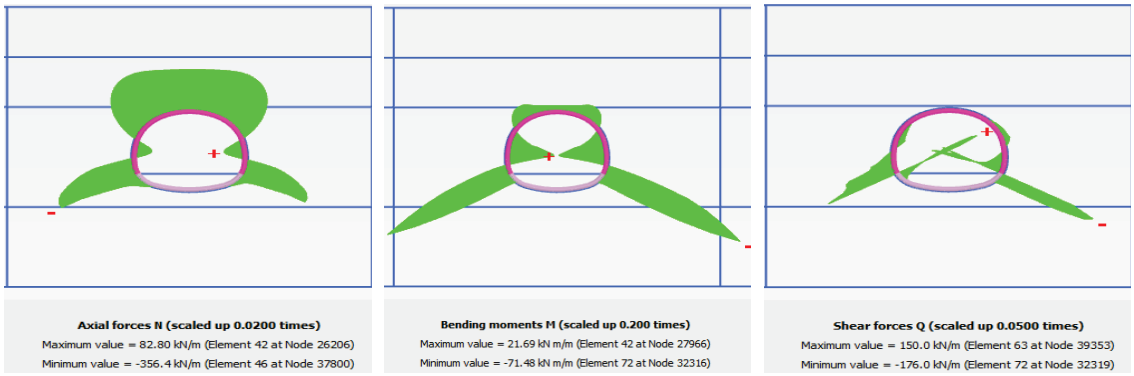


Figure III-64: Forces Diagram, Axial, Bending and Shear- Service Stage- MC- Mixed

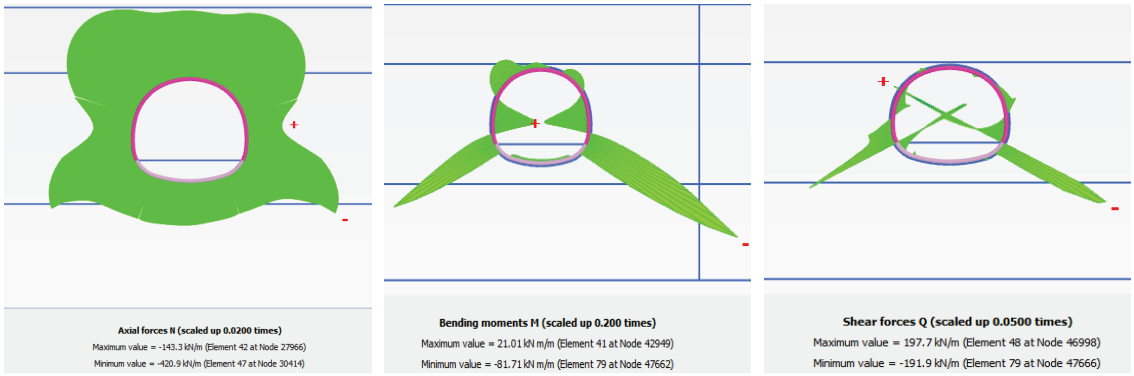


Figure III-65: Forces Diagram, Axial, Bending and Shear- Service Stage- HS- Mixed

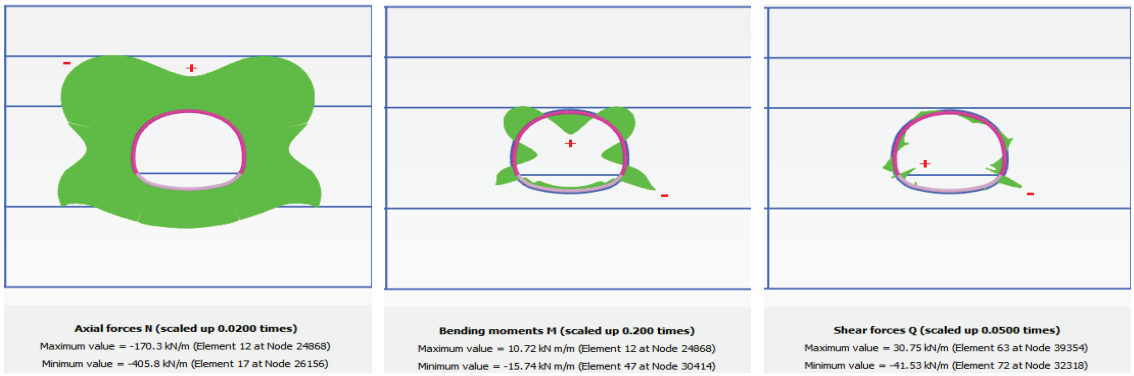
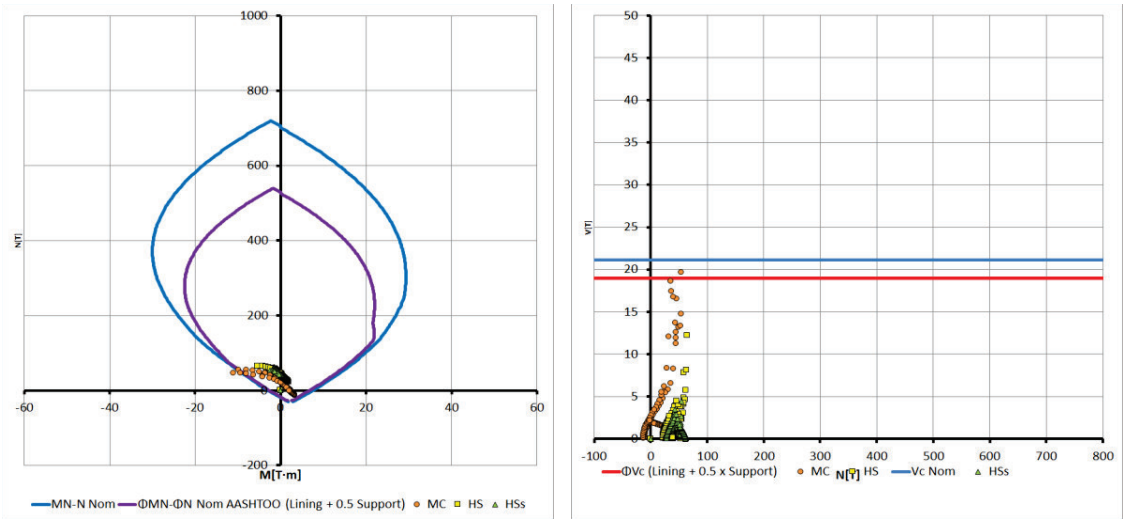
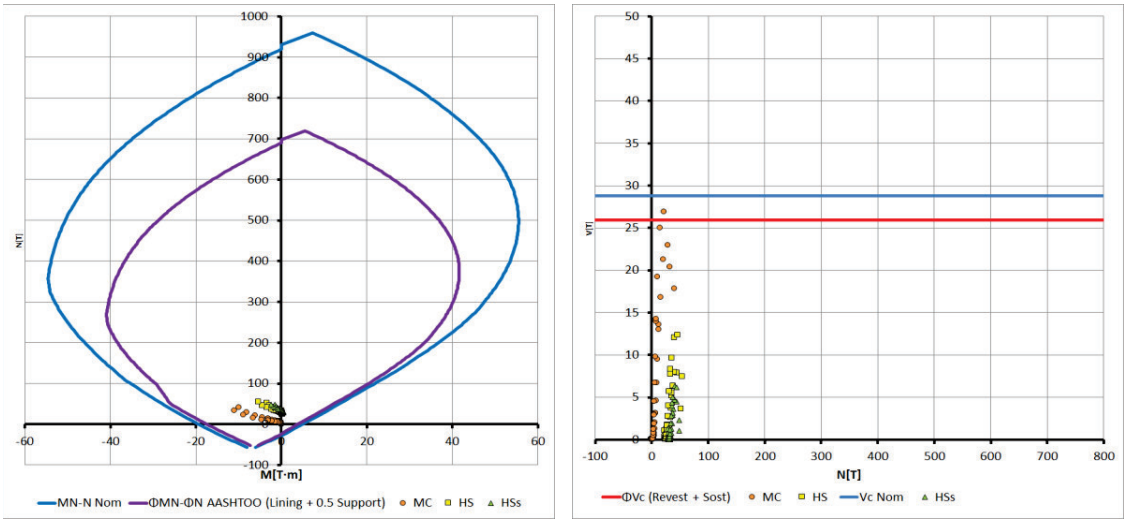


Figure III-66: Forces Diagram, Axial, Bending and Shear- Service Stage- HSs- Mixed



Graph III-24: Interaction M-N and N-Q Diagram- Vault of Metro Tunnel-

Service Stage- Mixed



Graph III-25: : Interaction M-N and N-Q Diagram- Counter vault of Metro Tunnel-

Service Stage- Mixed

(b) Analysis of the Fine Profile

(b.1) Service Stage

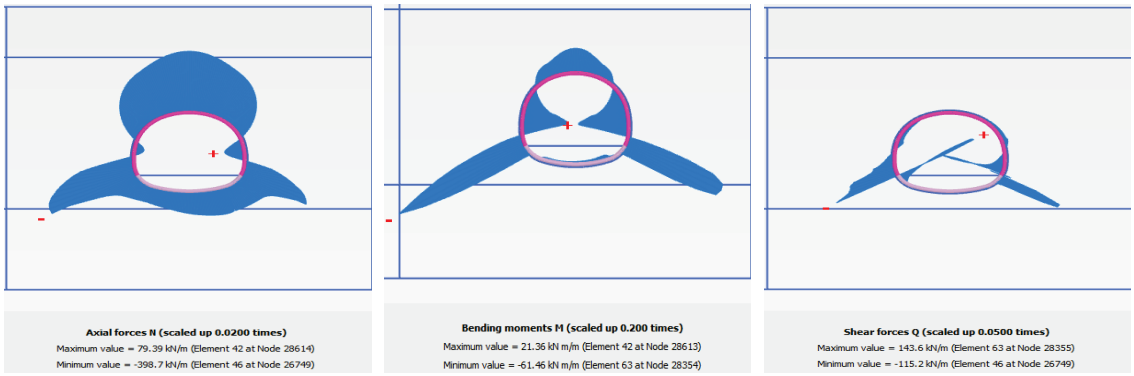


Figure III-67: Forces Diagram, Axial, Bending and Shear- Service Stage- MC- Fine

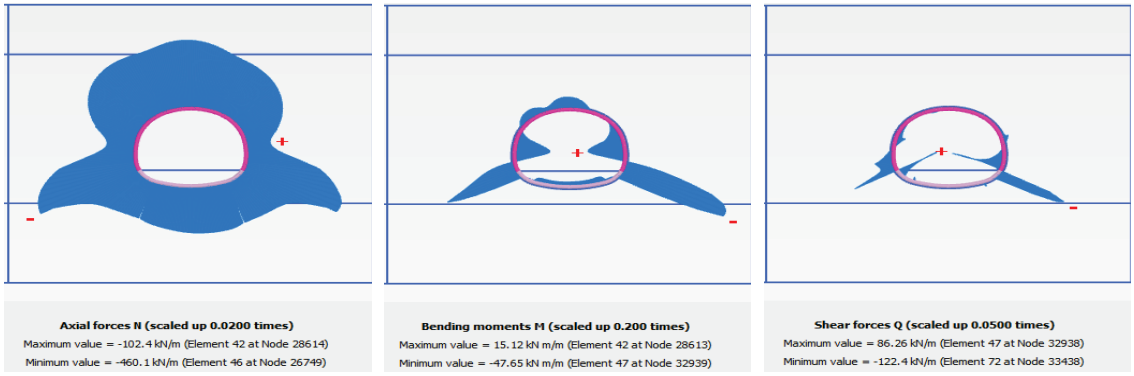


Figure III-68: Forces Diagram, Axial, Bending and Shear- Service Stage- HS- Fine

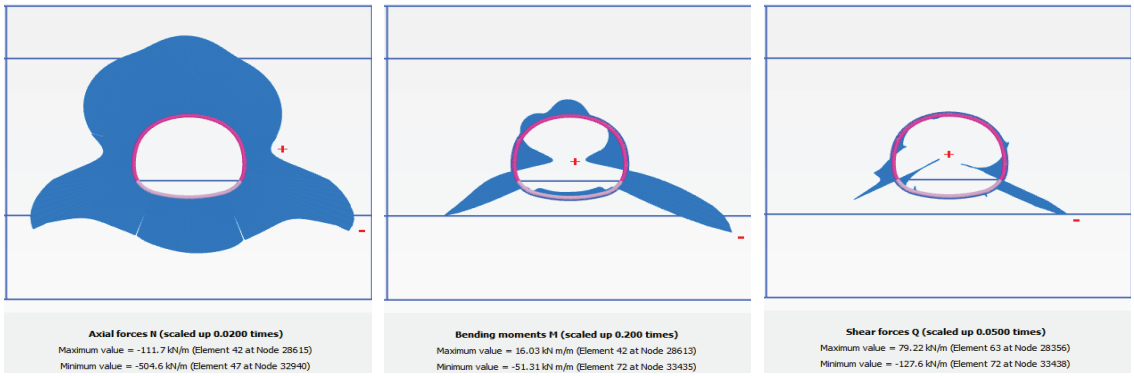
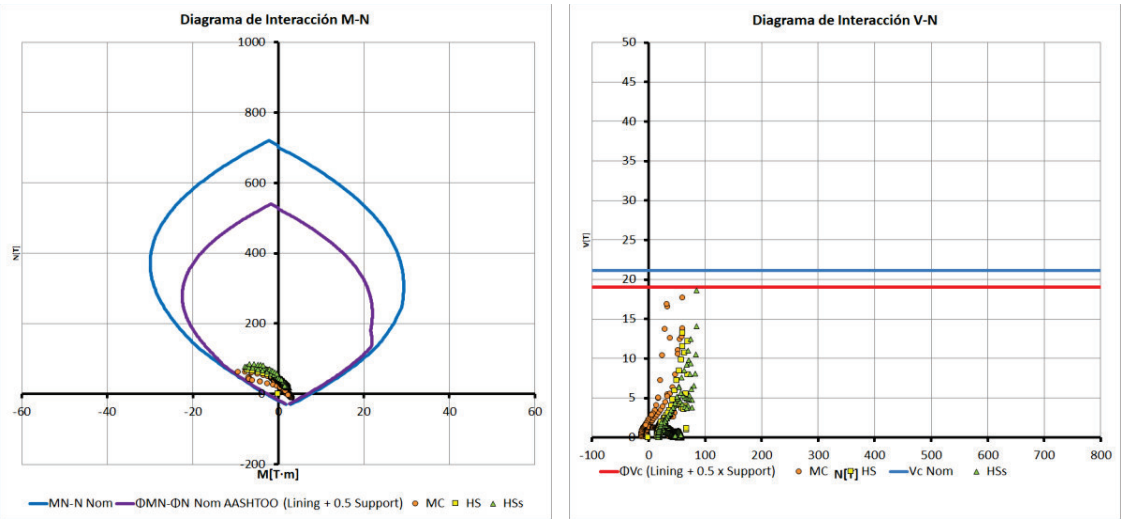
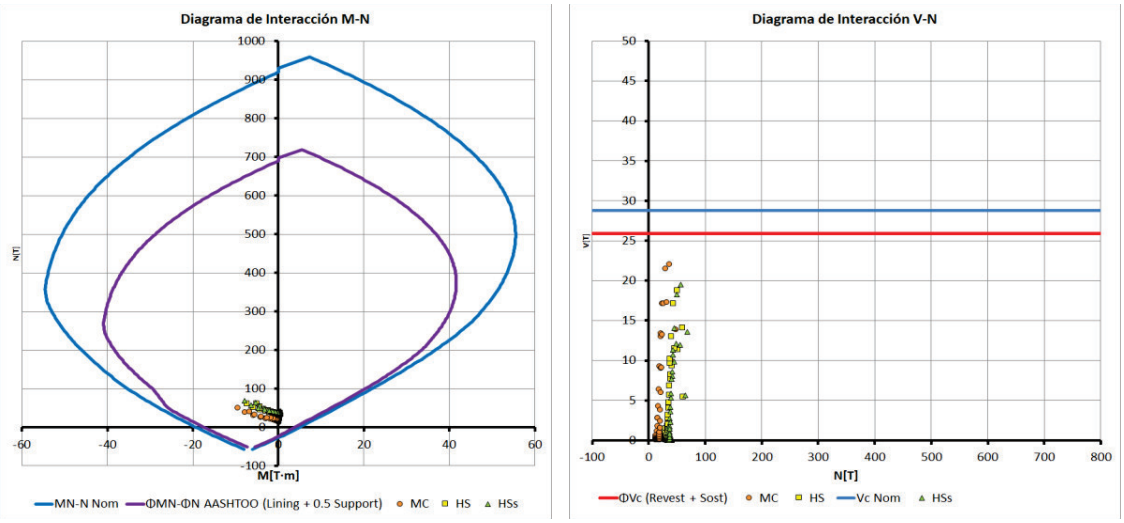


Figure III-69: Forces Diagram, Axial, Bending and Shear- Service Stage- HSs- Fine



Graph III-26: Interaction M-N and N-Q Diagram- Vault of Metro Tunnel-

Service Stage- Fine



Graph III-27: Interaction M-N and N-Q Diagram- Counter vault of Metro Tunnel-

Service Stage- Fine

3.2.3 Verification of the Deformation in the New Road Tunnels

The maximum convergence deformations must be verified with the criterion established in section 3.7.3(a).

(a) Analysis of the Mixed Profile

(a.1) Construction Stage

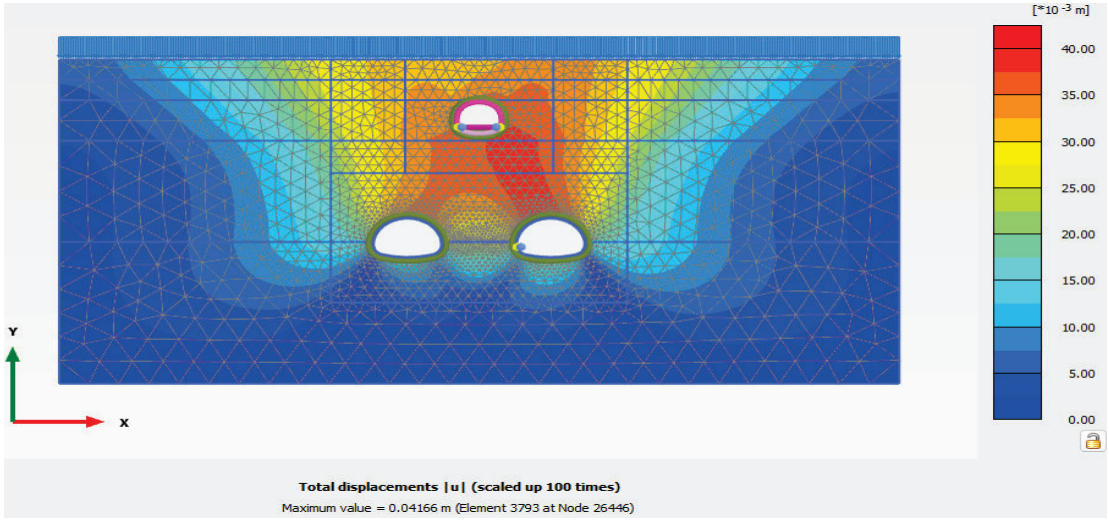


Figure III-70: Maximum Displacement in Construction- HS- Mixed

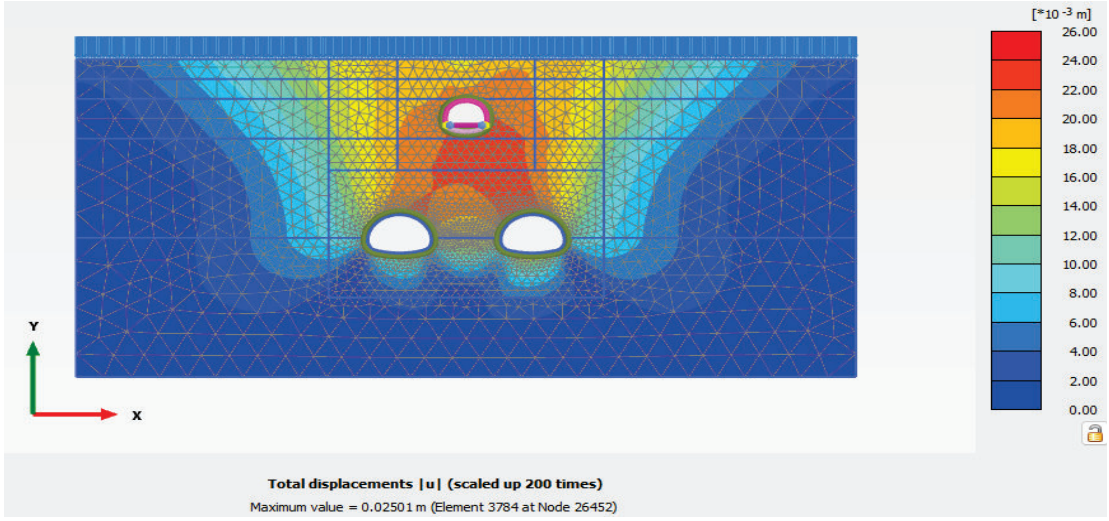


Figure III-71: Maximum Displacement in Construction- HSs- Mixed

i) Service Stage

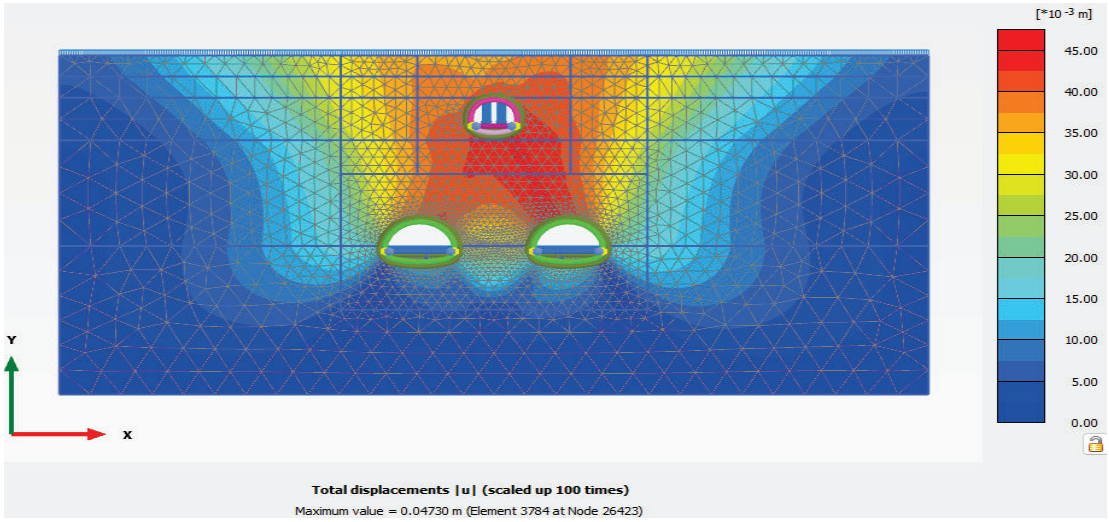


Figure III-72: Maximum Displacement in Service- HS- Mixed

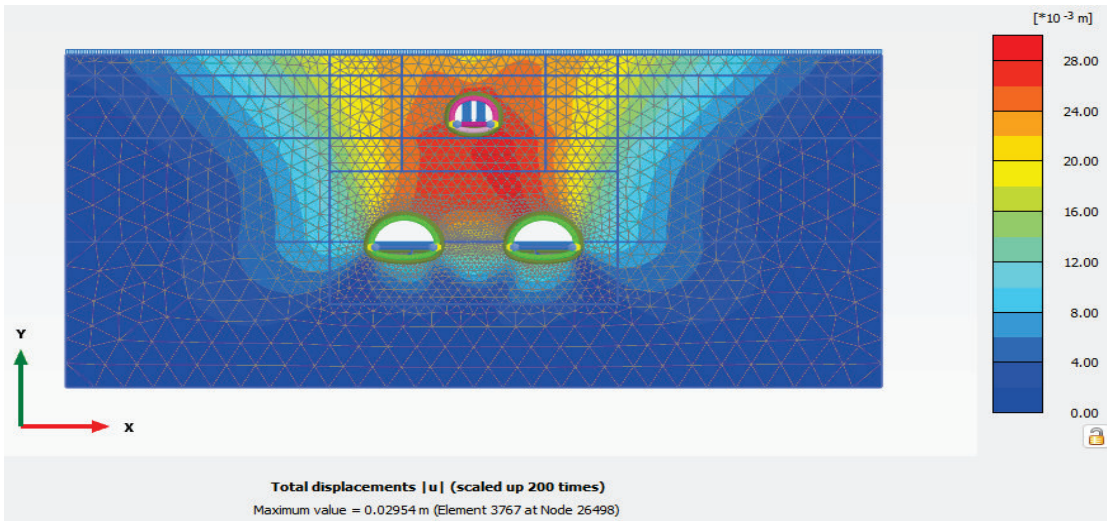


Figure III-73: Maximum Displacement in Service- HSs- Mixed

Table III-35: Summary of Maximum Displacement Checks on New Road Tunnels– Pre-existing Metro Tunnel – Mixed

Maximum Displacement [mm]							
Soil	Construction Stage			Service Stage			Admissible
	MC	HS	HSs	MC	HS	HSs	
Mixed	-	41.66	25.01	-	47.30	29.54	50

3.2.4 Verification of the Resistance in the New Road Tunnels

In the construction stage, the support of the new road tunnels must be verified through the criterion of admissible stresses, as defined in section 3.7.3(b).

In the service stage, the lining of the new road tunnels must be verified through the interaction diagram M-N and N-Q, as defined in section 3.7.3(b)

The lining of the new road tunnels are verified, with their corresponding concrete thicknesses and reinforcement, as defined in Figure III-10 and sections 3.3.2 and 3.3.2(b).

$e = 0.50\ m$ Concrete thicknesses for the calculation
(Lining thicknesses = 0.30 m + 2/3 Support thicknesses = 0.20 m)
$A_s = 3.35\ cm^2/m$ ACMA335 Mesh in Internal and External face
$A_{s1} = 7.60\ cm^2/m$ 2Ø22 Bar of the Reticulate Frame in Internal face
$A_{s1} = 8.04\ cm^2/m$ 1Ø32 Bar of the Reticulate Frame in External face

(a) Analysis of the Mixed Profile

(a.1) Construction Stage

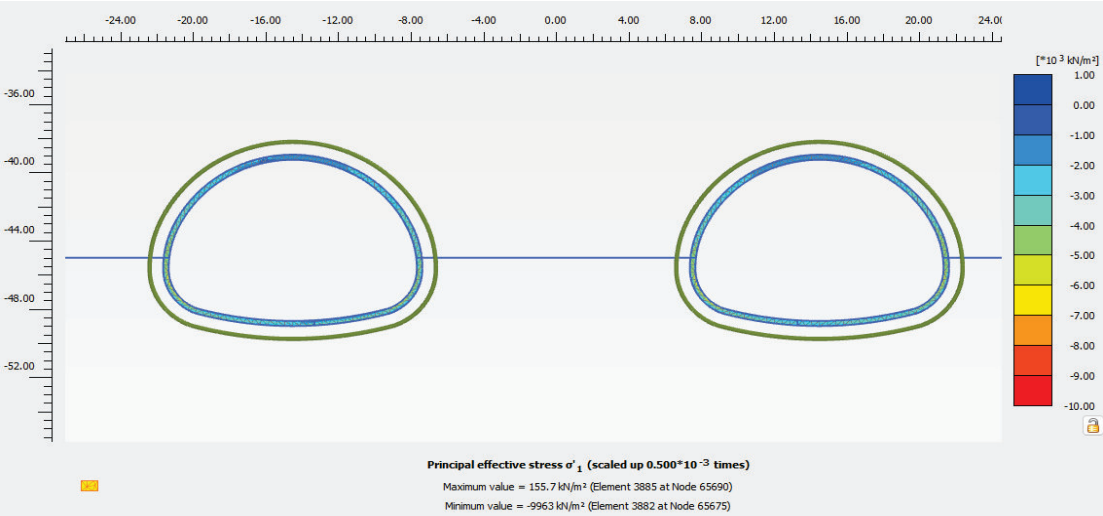


Figure III-74: Major Principal effective Stress on Support- HS - Mixed

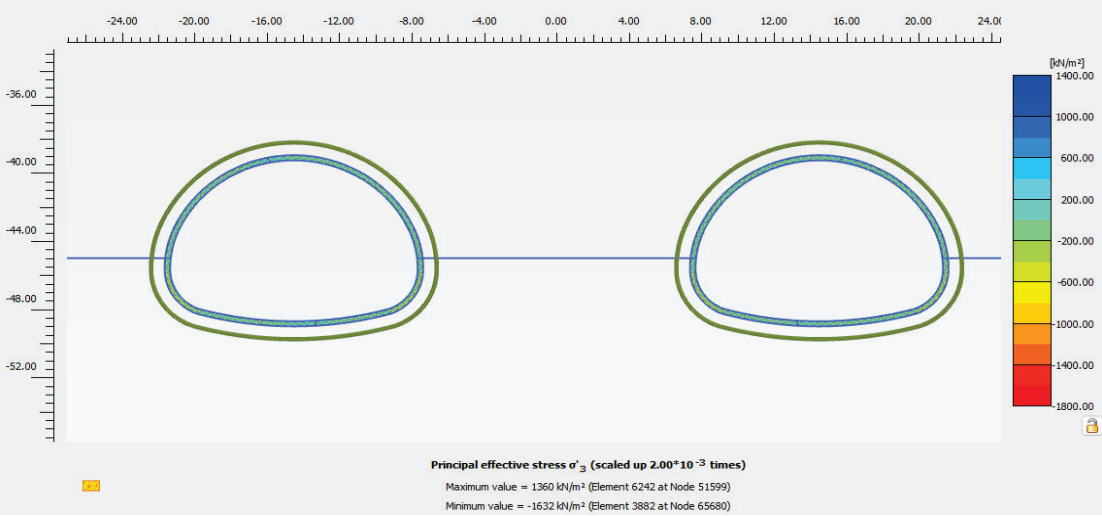


Figure III-75: Minor Principal effective Stress on Support- HS – Mixed

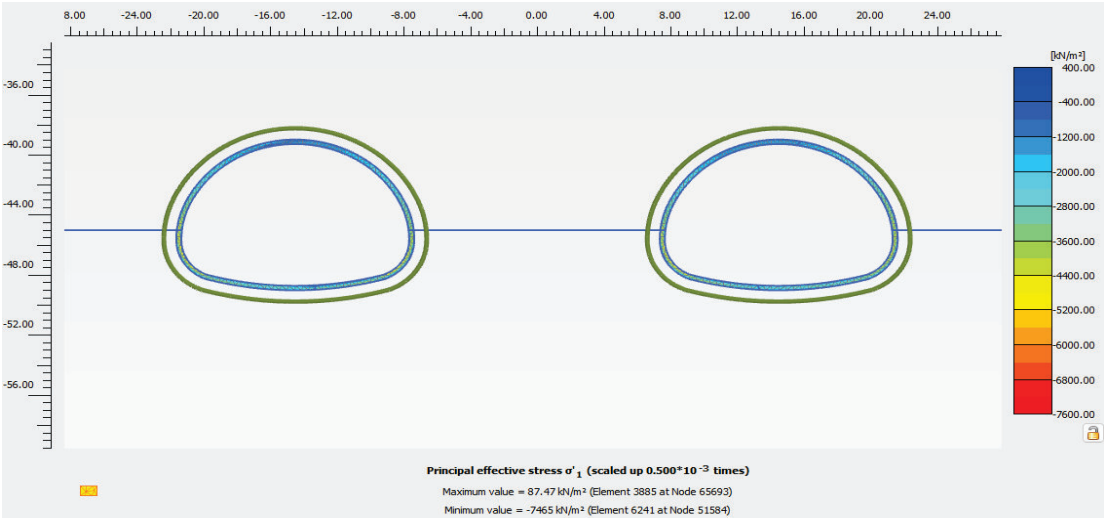


Figure III-76: Major Principal effective Stress on Support- HSs - Mixed

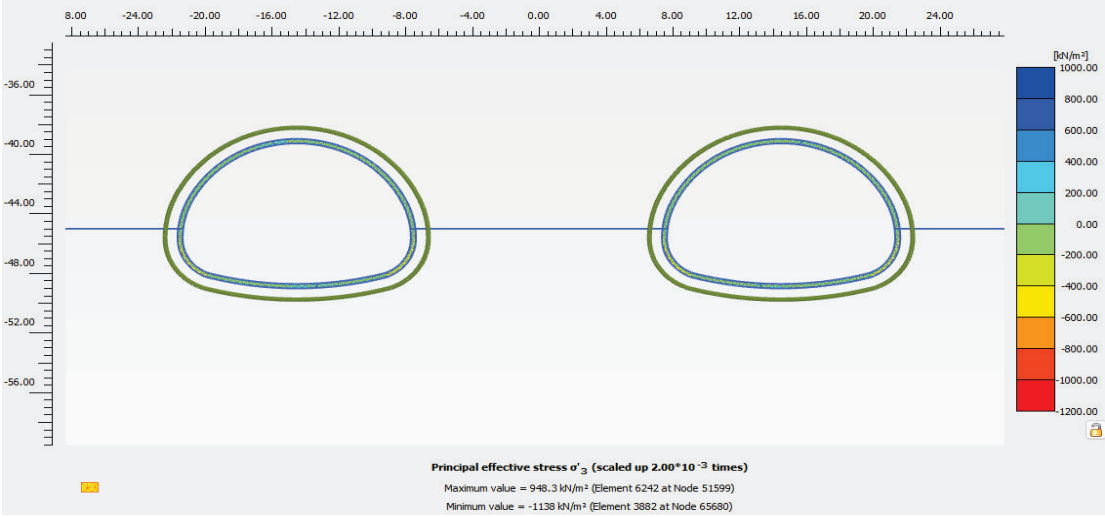


Figure III-77: Minor Principal effective Stress on Support- HSs – Mixed

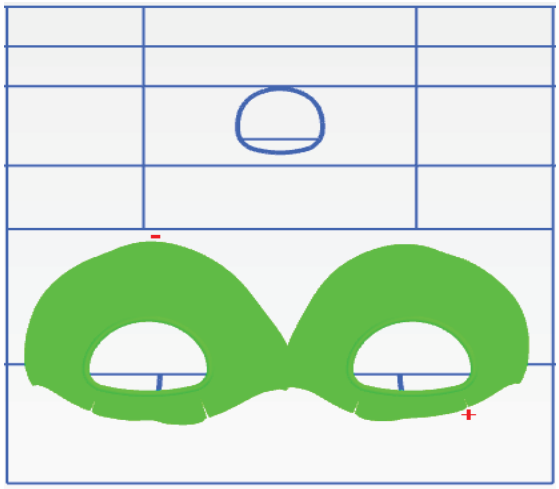
Table III-36: Verification of Admissible Stress- HS- Mixed

´1 [MPa]	σ´3 [MPa]	σ´1adm [MPa]	σ´3adm [MPa]	σ´1 < σ´1 adm	σ´3 < σ´3 adm
-9.96	1.36	-16	2	CHECK	CHECK

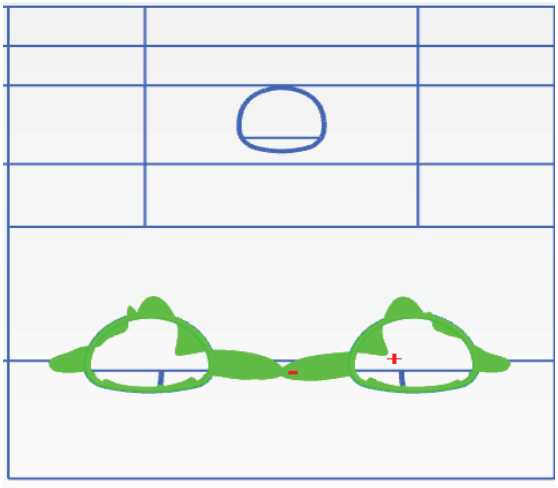
Table III-37: Verification of Admissible Stress- HSs- Mixed

´1 [MPa]	σ´3 [MPa]	σ´1adm [MPa]	σ´3adm [MPa]	σ´1 < σ´1 adm	σ´3 < σ´3 adm
-9.96	1.36	-16	2	CHECK	CHECK

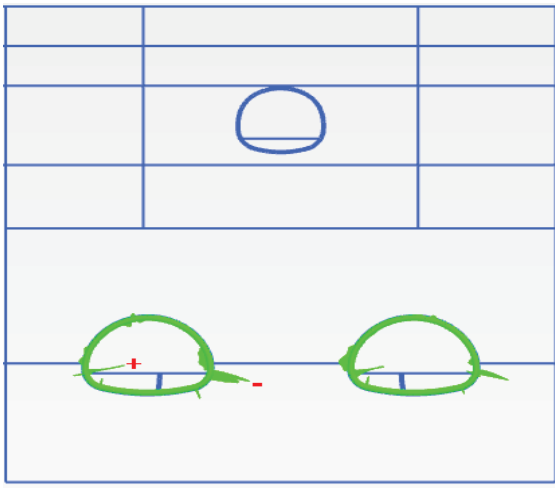
(a.2) Service Stage



Axial forces N (scaled up 0.0100 times)
Maximum value = -249.3 kN/m (Element 376 at Node 2689)
Minimum value = -963.2 kN/m (Element 116 at Node 66100)

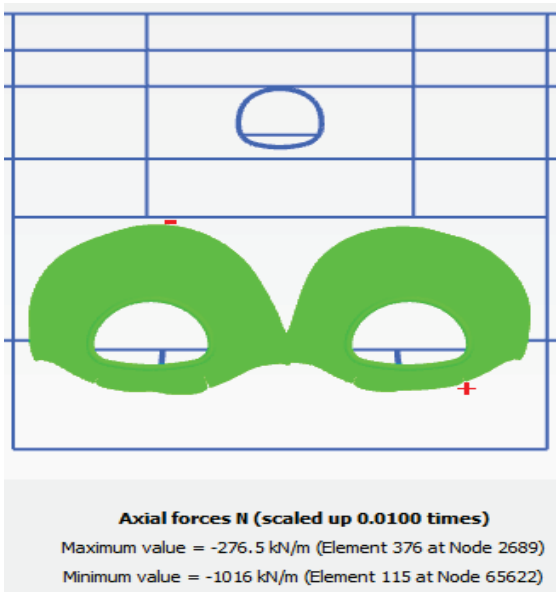


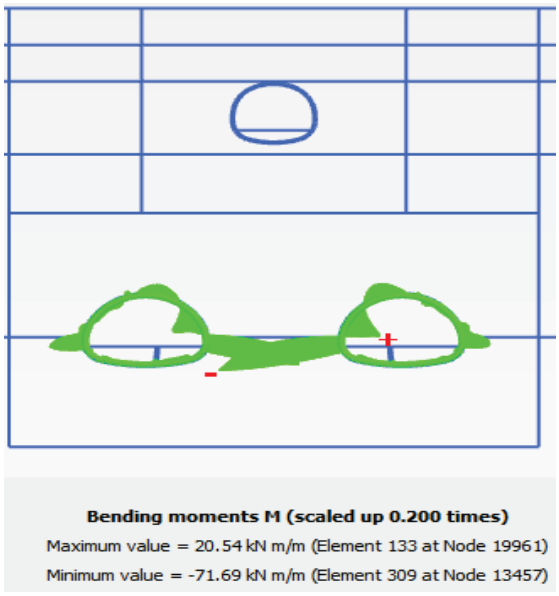
Bending moments M (scaled up 0.200 times)
Maximum value = 16.91 kN m/m (Element 131 at Node 20025)
Minimum value = -40.35 kN m/m (Element 215 at Node 51016)



Shear forces Q (scaled up 0.0500 times)
Maximum value = 86.41 kN/m (Element 227 at Node 53657)
Minimum value = -89.35 kN/m (Element 228 at Node 49632)

Figure III-78: Forces Diagram, Axial, Bending and Shear on Lining- Service Stage- HS- Mixed





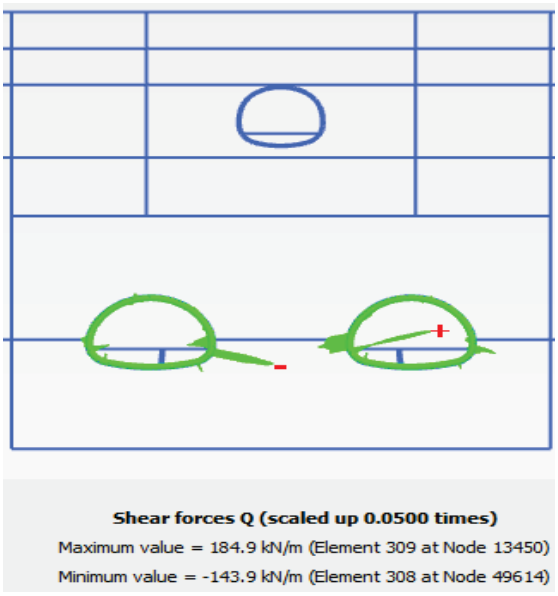
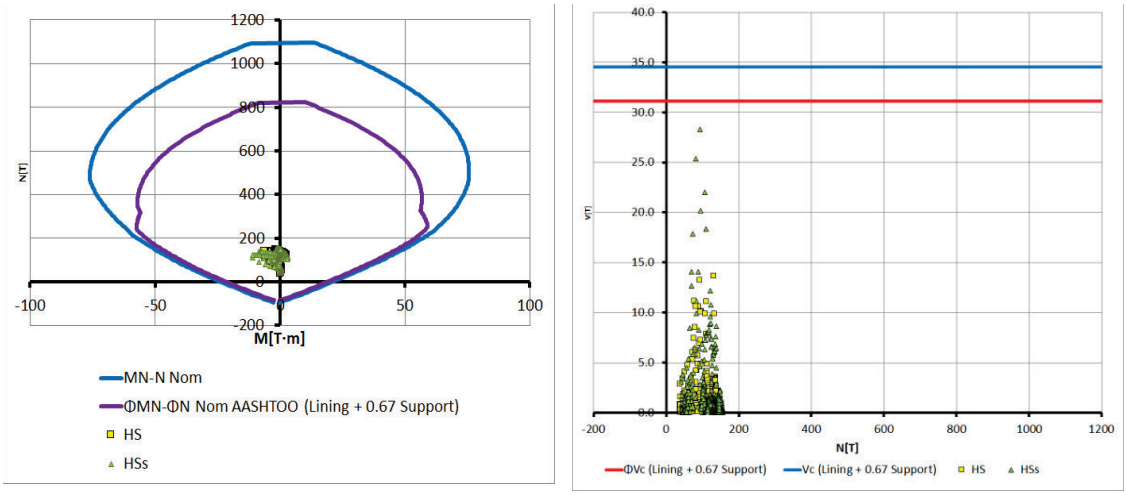


Figure III-79: Forces Diagram, Axial, Bending and Shear on Lining- Service Stage- HSs- Mixed



Graph III-28: : Interaction M-N and N-Q Diagram- Lining of the new road tunnels-

Service Stage- Mixed

3.2.5 Verification of the Capacity of the Soil

The following shows the plastification of the soil in construction and in service and applies the acceptability criteria explained in section 3.7.4.

(a) Construction Stage

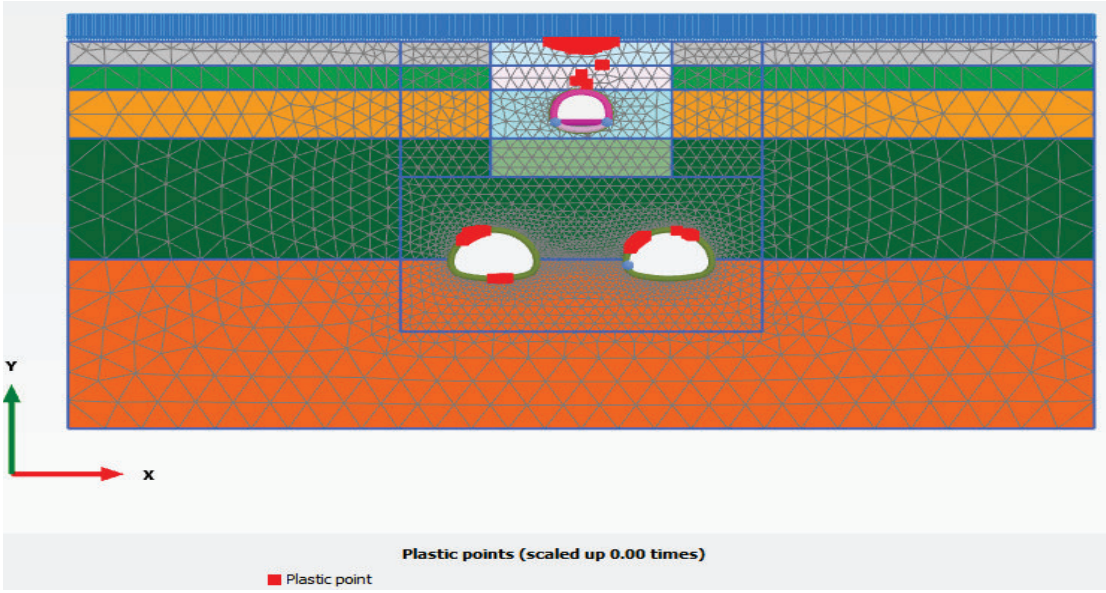


Figure III-80: Plastification Diagram- Construction Stage- HS- Mixed

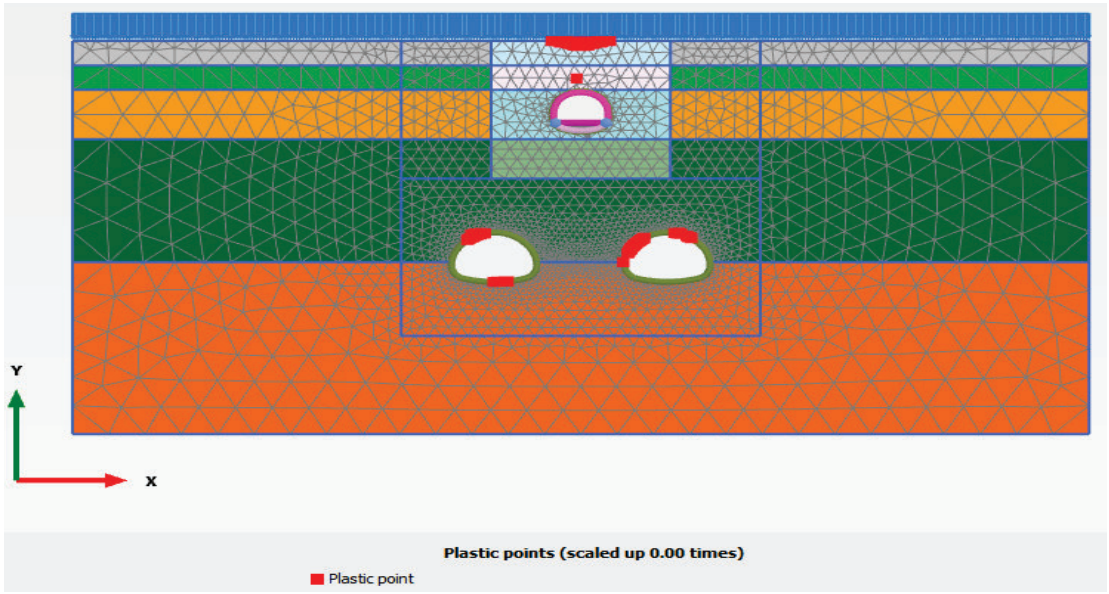


Figure III-81: Plastification Diagram- Construction Stage- HSs- Mixed

(b) Service Stage

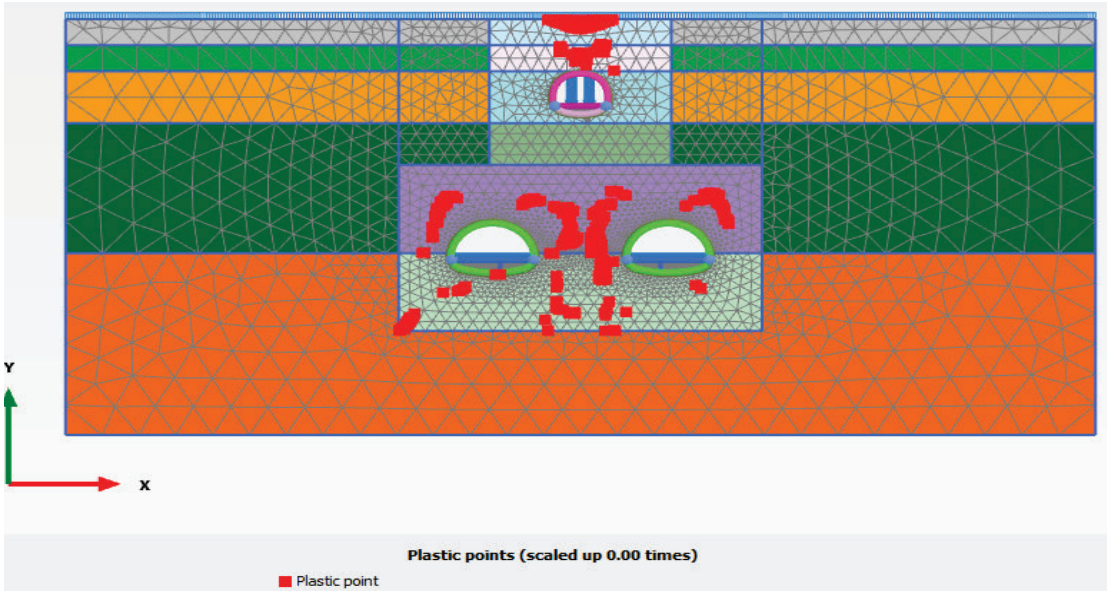


Figure III-82: Plastification Diagram- Service Stage- HS- Mixed

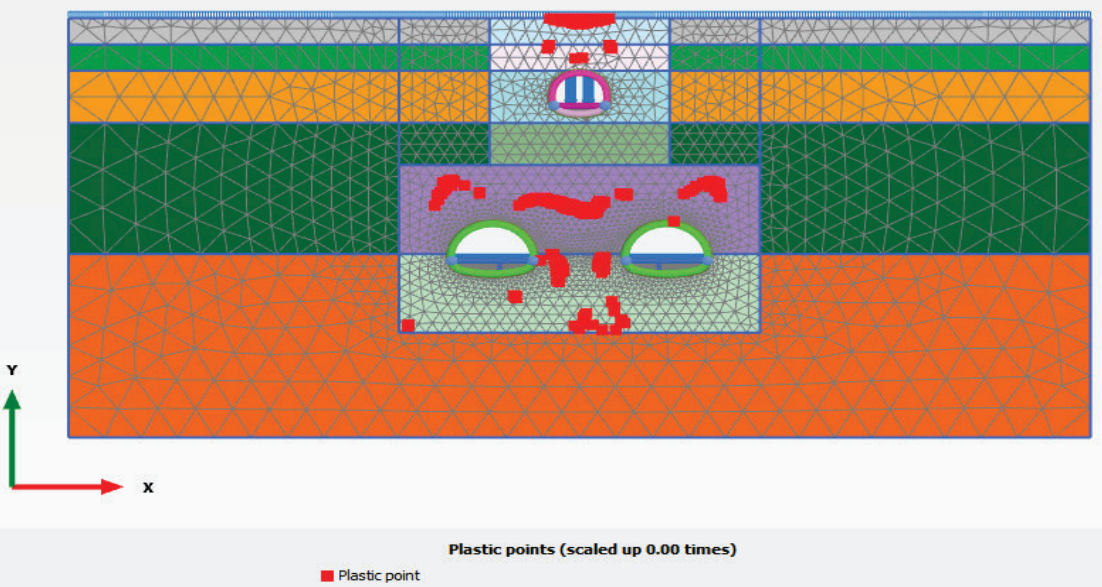


Figure III-83: Plastification Diagram- Service Stage- HSs- Mixed

Table III-38: Plastification Verification on Soil- HS- Mixed

Stage	R-Plastic [m]	R-Plast Adms [m]	Verification
Construction	8	14	CHECK
Service	13	14	CHECK

Table III-39: Plastification Verification on Soil- HSs- Mixed

Stage	R-Plastic [m]	R-Plast Adms [m]	Verification
Construction	8	14	CHECK
Service	12	14	CHECK

3.3. Variation of the Constitutive Soil Model with Counter-vault Section in four excavation phases in Fine Soil

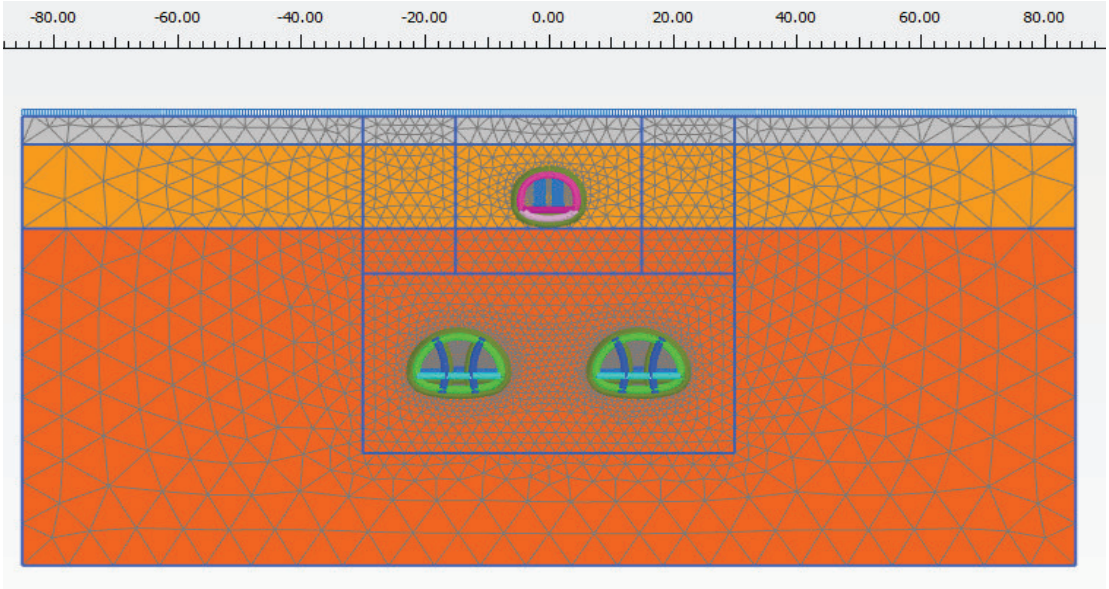


Figure III-84: Fine Soil Model with Pre-existing Metro Tunnel and counter-vault section in New Tunnels with four phases of excavation

3.3.1 Verification of the Deformation in the Metro Tunnel (MT)

Initially, the vertical deformations or settlements are shown for each soil profile, in the most important construction phases and for each soil constitutive model. Then, the settlement profiles located at the inferior level, 18.50 m, and the verification of the acceptance criterion of transverse deformation of the rails of the Metro Tunnel (See Chapter 3.7.1(a)), are presented.

(a) Analysis of the Fine Profile

(a.1) Construction Stage

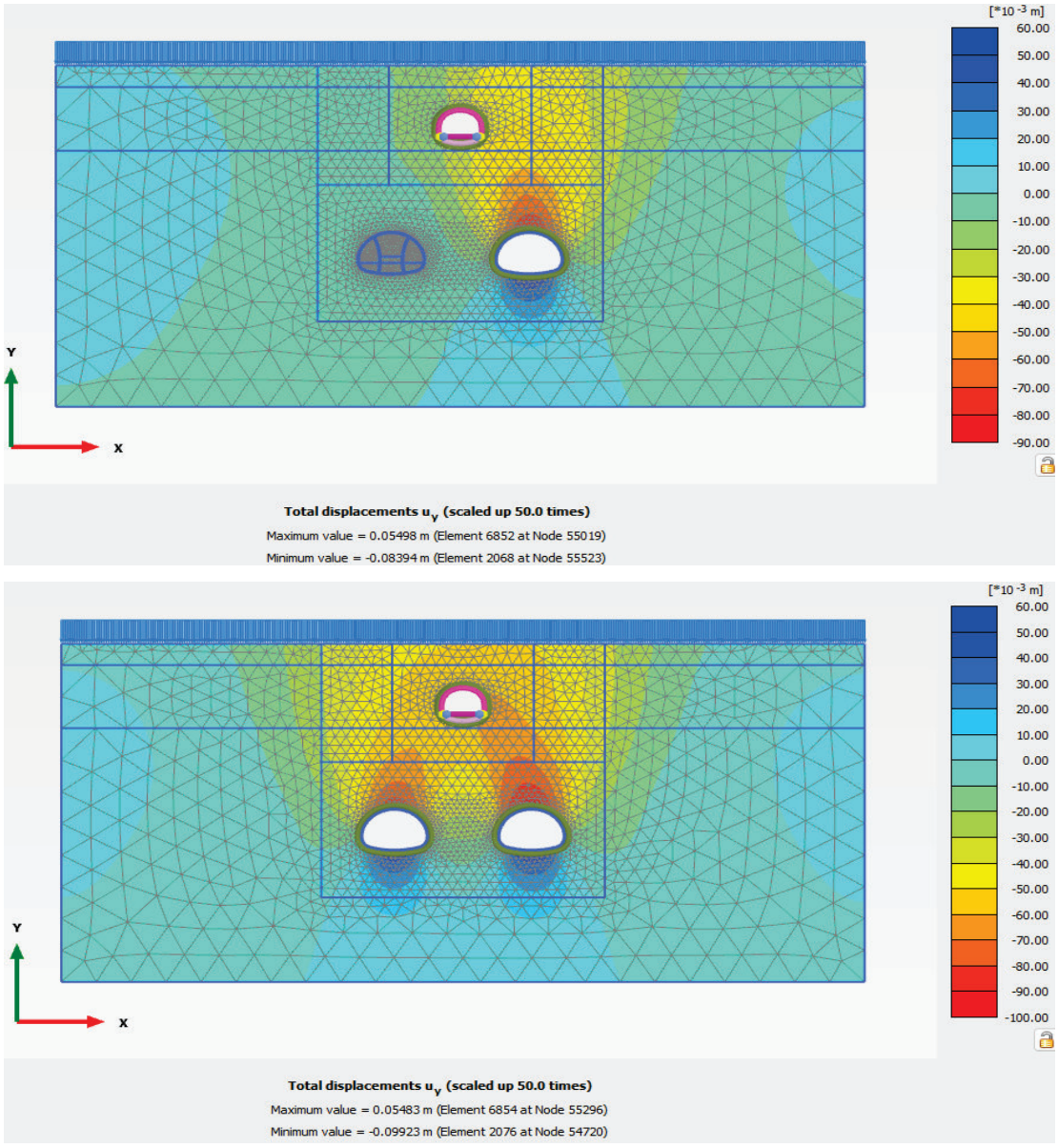


Figure III-85: Vertical Settlement in Construction (WT and ET)- MC- Fine Counter-Vault Section in New Tunnels with four phases of excavation

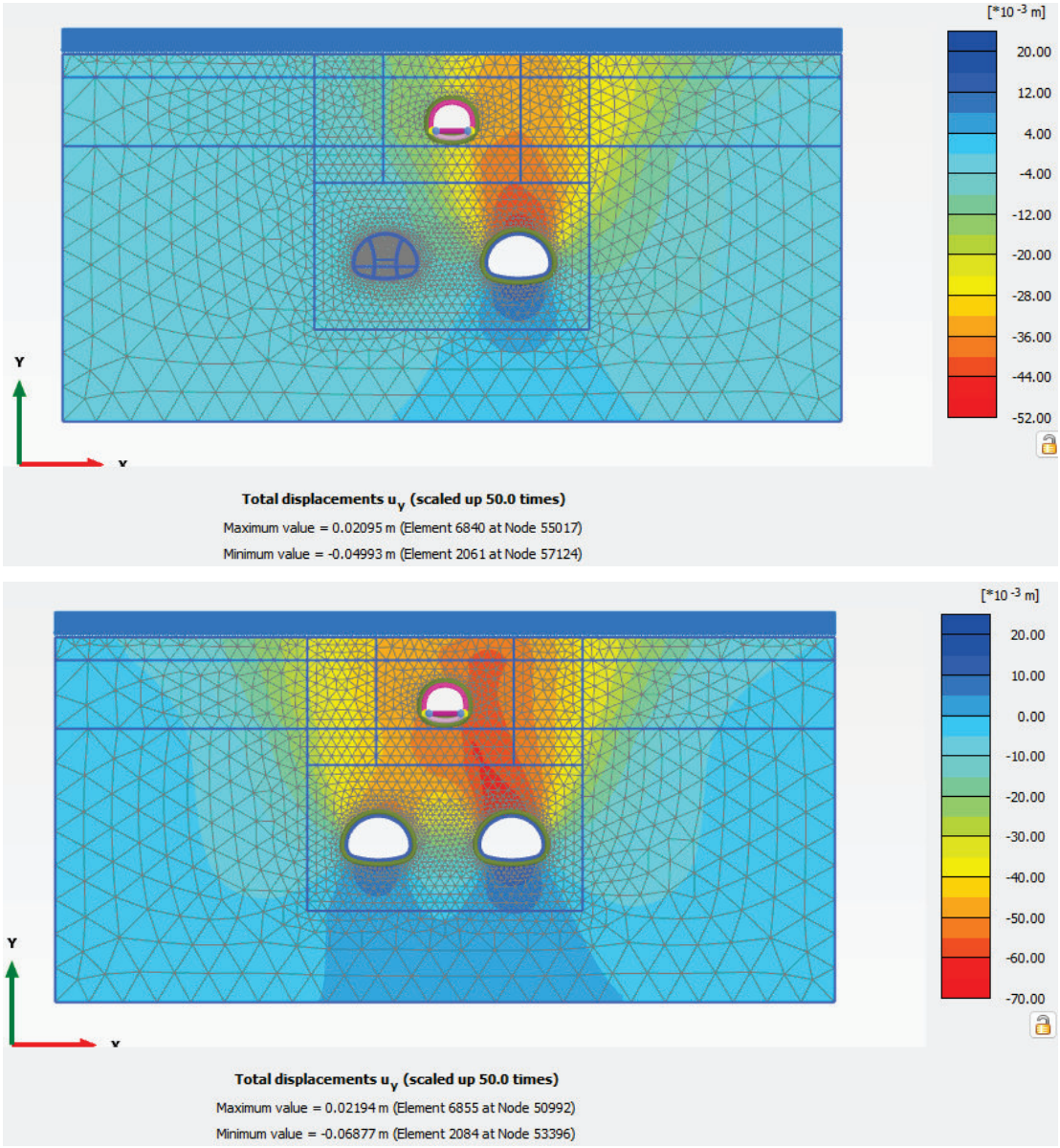


Figure III-86: Vertical Settlement in Construction (WT and ET)- HS- Fine

Counter-Vault Section in New Tunnels with four phases of excavation

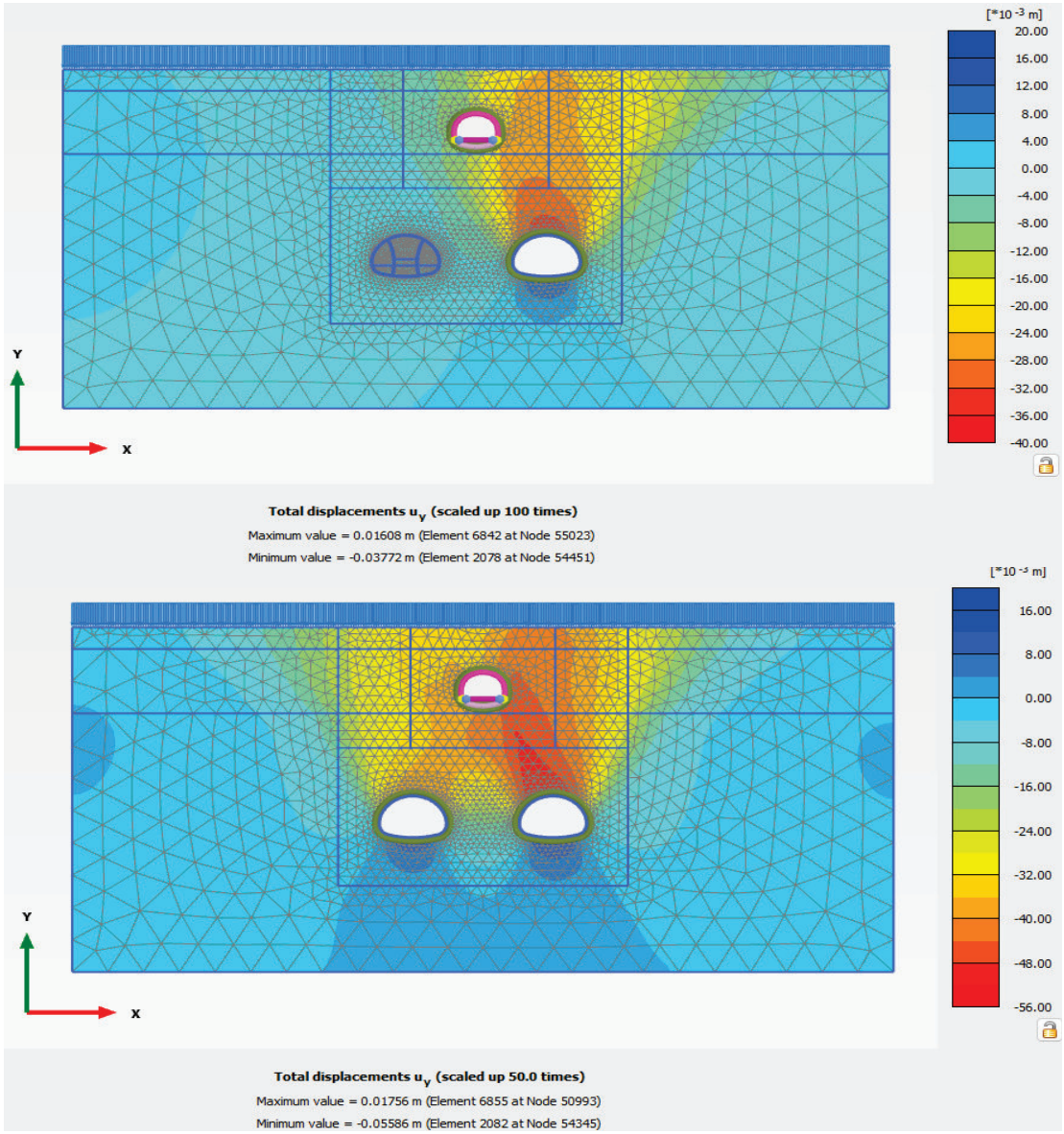
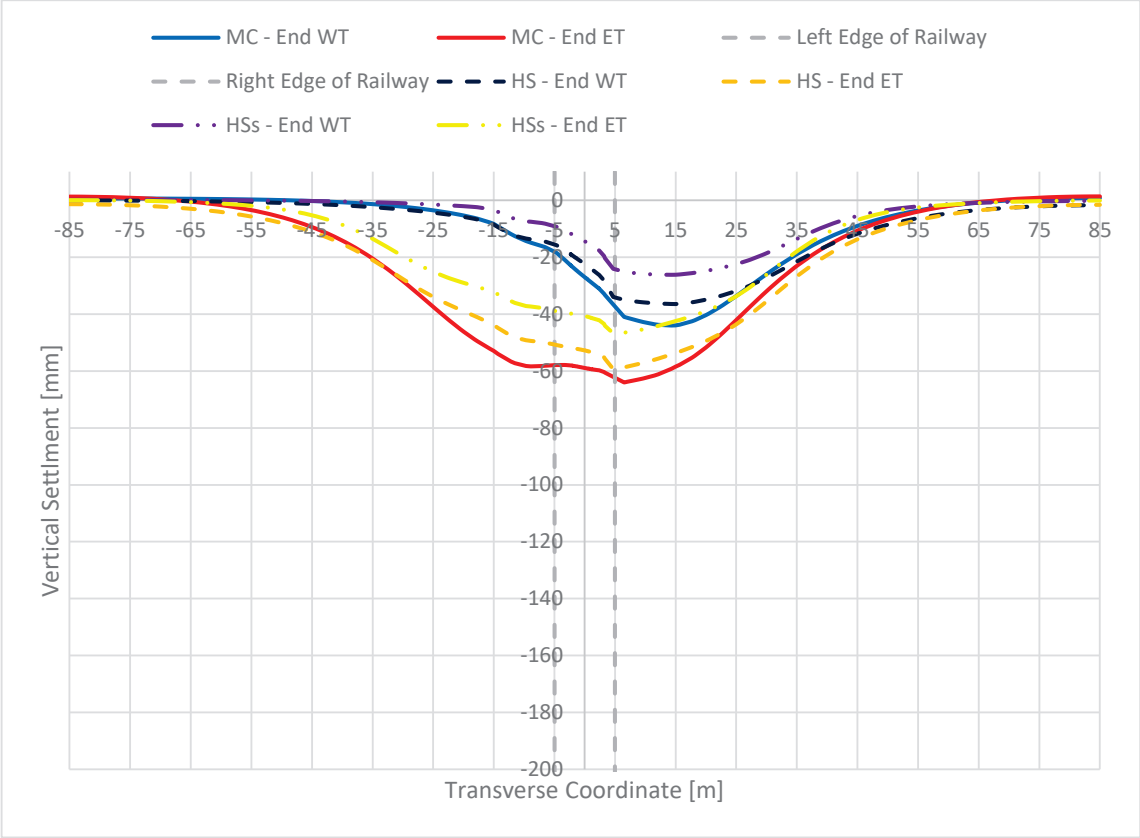


Figure III-87: Vertical Settlement in Construction (WT and ET)- HSs- Fine

Counter-Vault Section in New Tunnels with four phases of excavation



Graph III-29: Diagram of Transverse Settlement on Metro Tunnel - Construction Stage – Model with Counter-Vault Section in New Tunnels and four phases of excavation- Fine

Table III-40: Verification of the Transverse Settlement Limit- MC Model- Construction Stage- Fine Counter-Vault Section in New Tunnels with four phases of excavation

Phase	Rial 1 Settl (mm)	Rial 2 Settl (mm)	Δ Settl (mm)	Δ Limit (mm)	Verification
Settlement of West Rial					
Excavation WT	-28.30	-30.74	2.44	2	**NOT CHECK**
Excavation ET	-59.28	-59.75	0.47	2	**CHECK**
Settlement of East Rial					
Excavation WT	-25.73	-23.11	2.62	2	**NOT CHECK**
Excavation ET	-58.68	-58.14	0.54	2	**CHECK**

Table III-41: Verification of the Transverse Settlement Limit- HS Model- Construction Stage- Fine Counter-Vault Section in New Tunnels with four phases of excavation

Phase	Rial 1 Settl (mm)	Rial 2 Settl (mm)	Δ Settl (mm)	Δ Limit (mm)	Verification
Settlement of West Rial					
Excavation WT	-23.53	-25.93	2.40	2	**NOT CHECK**
Excavation ET	-53.21	-54.09	0.89	2	**CHECK**
Settlement of East Rial					
Excavation WT	-21.30	-19.15	2.15	2	**NOT CHECK**
Excavation ET	-52.47	-51.91	0.57	2	**CHECK**

Table III-42: Verification of the Transverse Settlement Limit- HSs Model- Construction Stage- Fine Counter-Vault Section in New Tunnels with four phases of excavation

Phase	Rial 1 Settl (mm)	Rial 2 Settl (mm)	Δ Settl (mm)	Δ Limit (mm)	Verification
Settlement of West Rial					
Excavation WT	-15.39	-17.39	2.00	2	**CHECK**
Excavation ET	-41.07	-42.01	0.93	2	**CHECK**
Settlement of East Rial					
Excavation WT	-13.54	-11.87	1.68	2	**CHECK**
Excavation ET	-40.29	-39.82	0.47	2	**CHECK**

(a.2) Service Stage

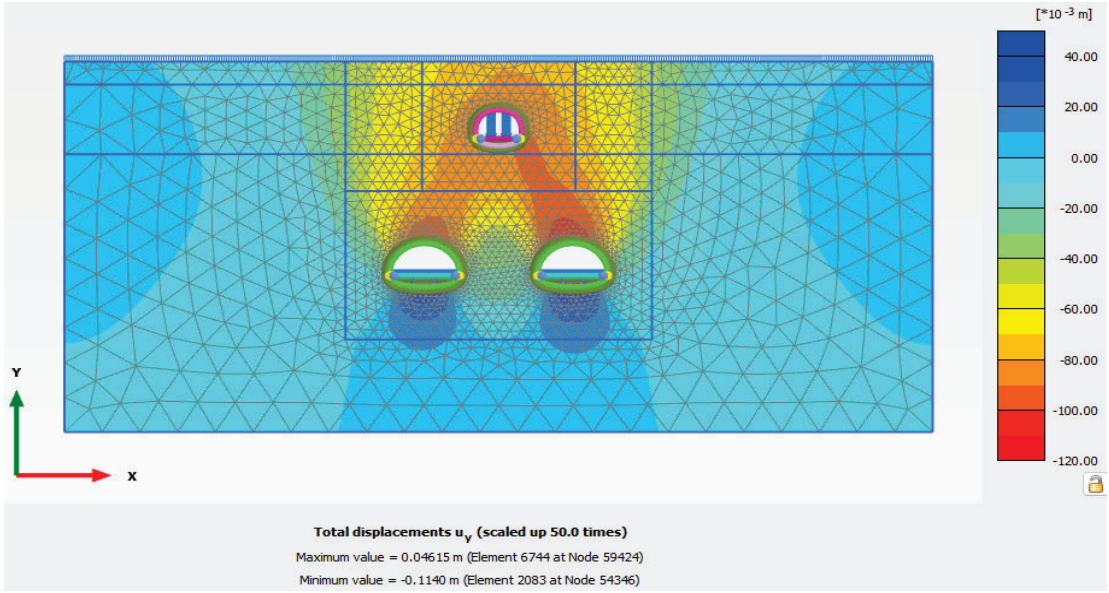


Figure III-88: Vertical Settlement in Service- MC- Fine- Counter-Vault Section in New Tunnels with four phases of excavation

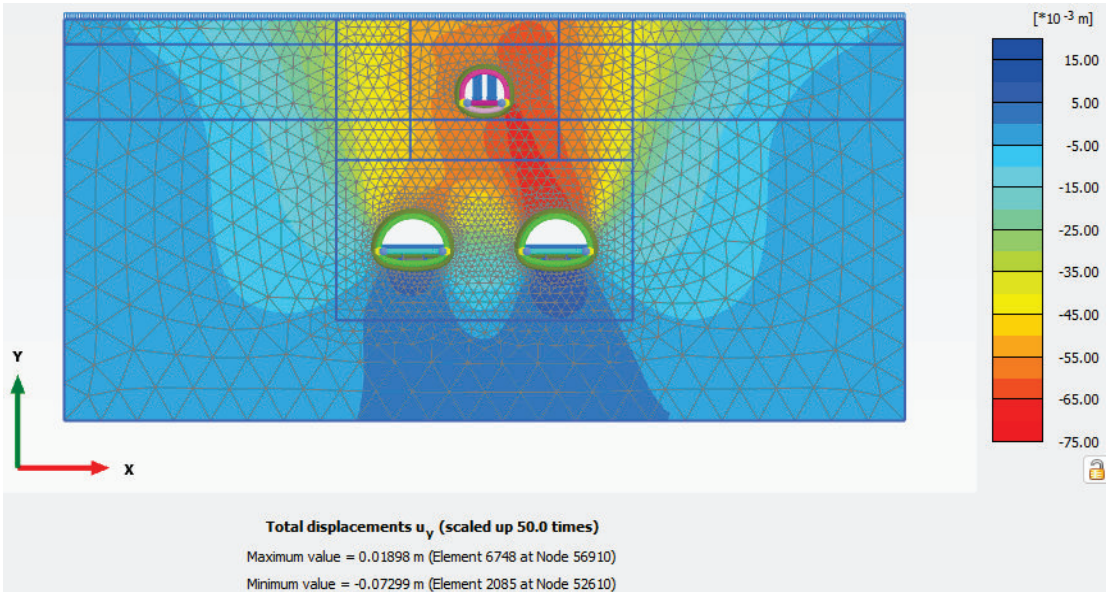


Figure III-89: Vertical Settlement in Service- HS- Fine- Counter-Vault Section in New Tunnels with four phases of excavation

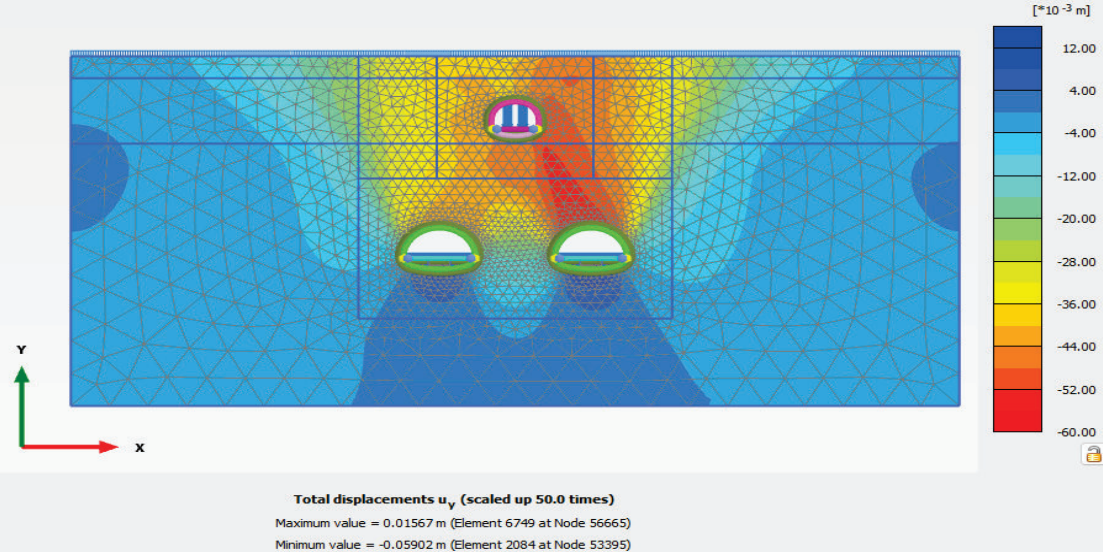
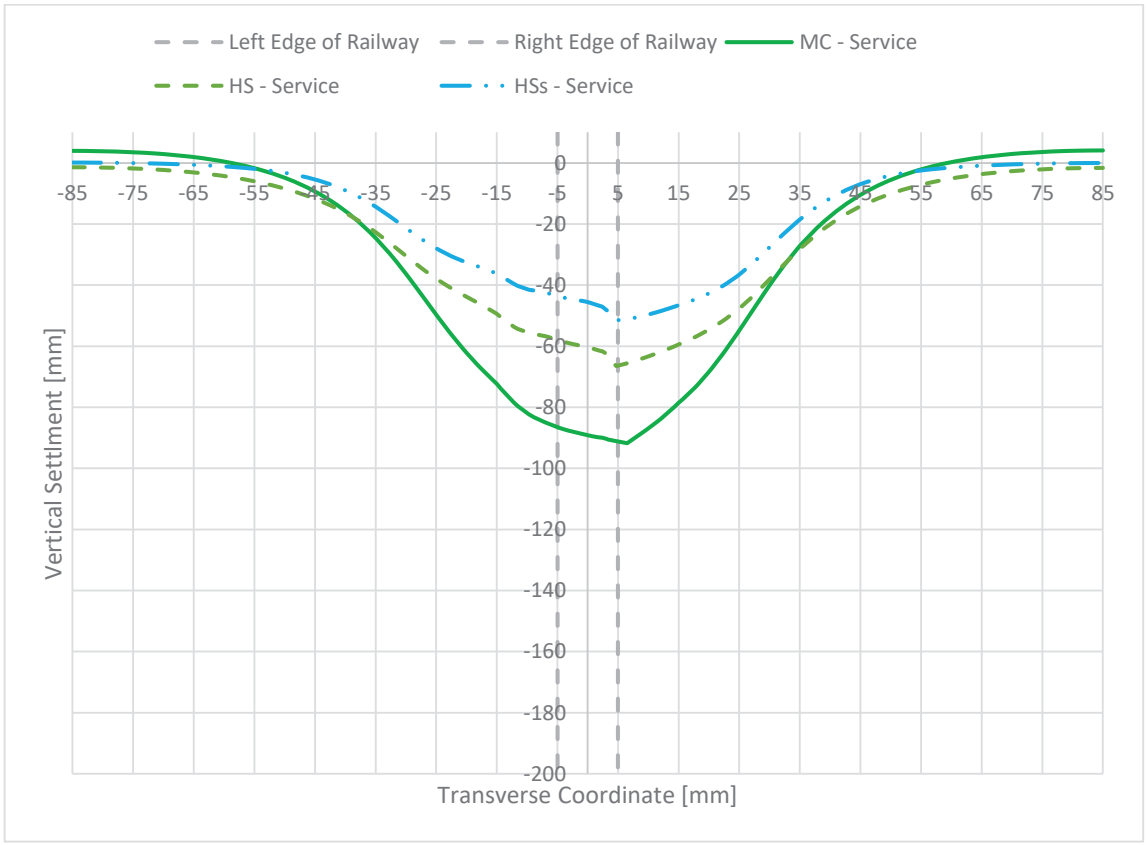


Figure III-90: Vertical Settlement in Service- HSs- Fine- Counter-Vault Section in New Tunnels with four phases of excavation



Graph III-30: Diagram of Transverse Settlement on Metro Tunnel - Service Stage – Model with Counter-Vault Section in New Tunnels with four phases of excavation- Fine

Table III-43: Verification of the Transverse Settlement Limit- MC Model- Service Stage- Fine

Counter-Vault Section in New Tunnels with four phases of excavation

Phase	Rial 1 Settl (mm)	Rial 2 Settl (mm)	Δ Settl (mm)	Δ Limit (mm)	Verification
Settlement of West Rial					
Service	-89.52	-89.97	0.45	2	**CHECK**
Settlement of East Rial					
Service	-88.85	-88.16	0.69	2	**CHECK**

Table III-44: Verification of the Transverse Settlement Limit- HS Model- Service Stage- Fine

Counter-Vault Section in New Tunnels with four phases of excavation

Phase	Rial 1 Settl (mm)	Rial 2 Settl (mm)	Δ Settl (mm)	Δ Limit (mm)	Verification
Settlement of West Rial					
Service	-60.74	-61.56	0.82	2	**CHECK**
Settlement of East Rial					
Service	-60.02	-59.41	0.61	2	**CHECK**

Table III-45: Verification of the Transverse Settlement Limit- HSs Model- Service Stage- Fine

Counter-Vault Section in New Tunnels with four phases of excavation

Phase	Rial 1 Settl (mm)	Rial 2 Settl (mm)	Δ Settl (mm)	Limit (mm)	Verification
Settlement of West Rial					
Service	-46.04	-46.96	0.92	2	**CHECK**
Settlement of East Rial					
Service	-45.27	-44.77	0.49	2	**CHECK**

3.3.2 Verification of the Resistance in the Pre-existing Metro Tunnel considering Counter-vault section in the new tunnels and four phases of excavation.

At the beginning, the axial force, bending and shear diagrams on the metro-tunnel are presented and then the structural verification is realized through the M-N and N-Q interaction diagrams, as presented in chapter 3.7.1(b).
First the vault and then the counter-vault of the Metro tunnel are verified, with their corresponding concrete thicknesses and reinforcement, as defined in Figure III-14 and Figure III-15.

- Vault of the Metro Tunnel

$e = 0.325\ m$ Concrete thicknesses for the calculation
(Lining thicknesses = 0.20 m + ½ Support thicknesses = 0.125 m)

$A_{s.i} = 3.780\ cm^2/m$ ACMA378 Mesh in Internal face
$A_{s.e} = 2.95\ cm^2/m$ ACMA295 Mesh in External face

- Counter-Vault of the Metro Tunnel

$e = 0.425\ m$ Concrete thicknesses for the calculation
(Lining thicknesses = 0.30 m + ½ Support thicknesses = 0.125 m)

$A_{s.i} = 3.780\ cm^2/m$ ACMA378 Mesh in Internal face
$A_{s.ref} = 6.70\ cm^2/m$ Reinforcement with bars steel 16@30 in Internal face
$A_{s.e} = 2.95\ cm^2/m$ ACMA295 Mesh in External face

(a) Analysis of the Fine Profile

(a.1) Construction Stage

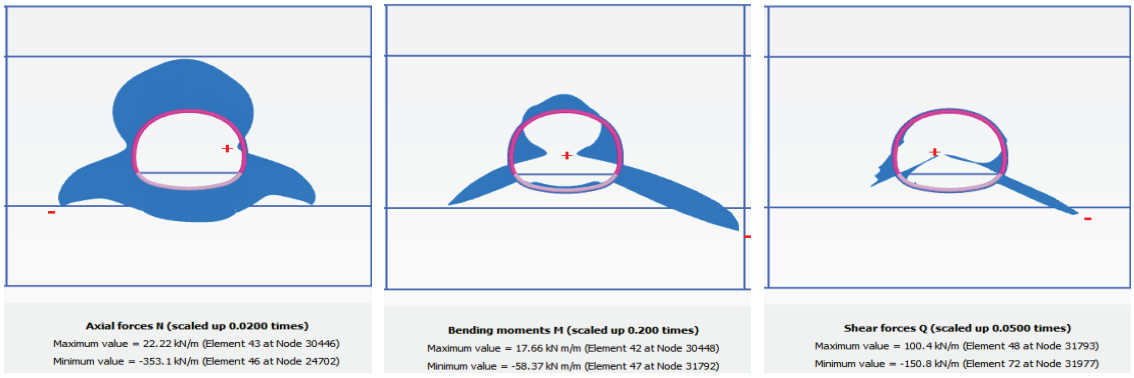


Figure III-91: Forces Diagram, Axial, Bending and Shear- Construction Stage- MC- Fine Counter-Vault Section in New Tunnels with four phases of excavation

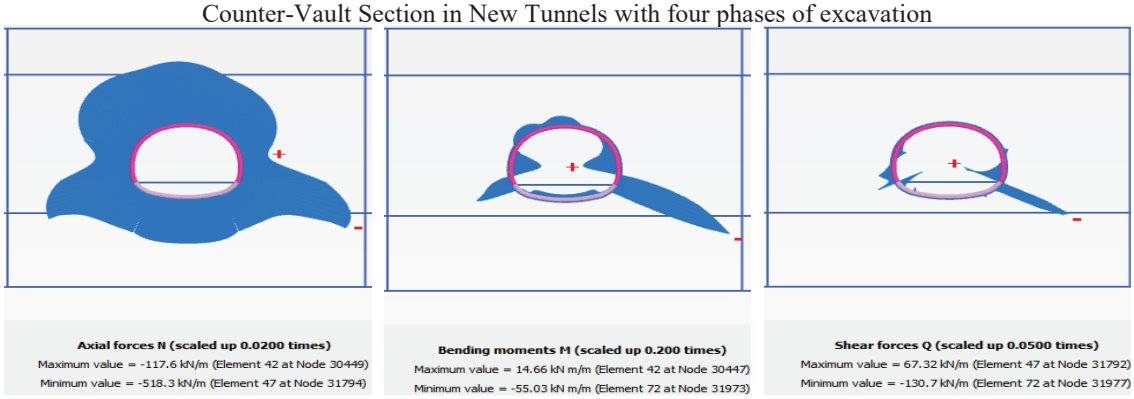


Figure III-92: Forces Diagram, Axial, Bending and Shear- Construction Stage- HS- Fine Counter-Vault Section in New Tunnels with four phases of excavation

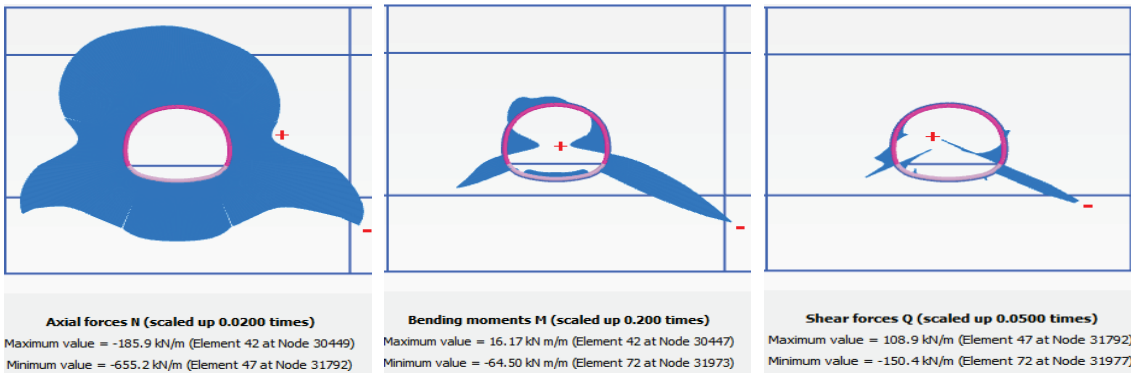
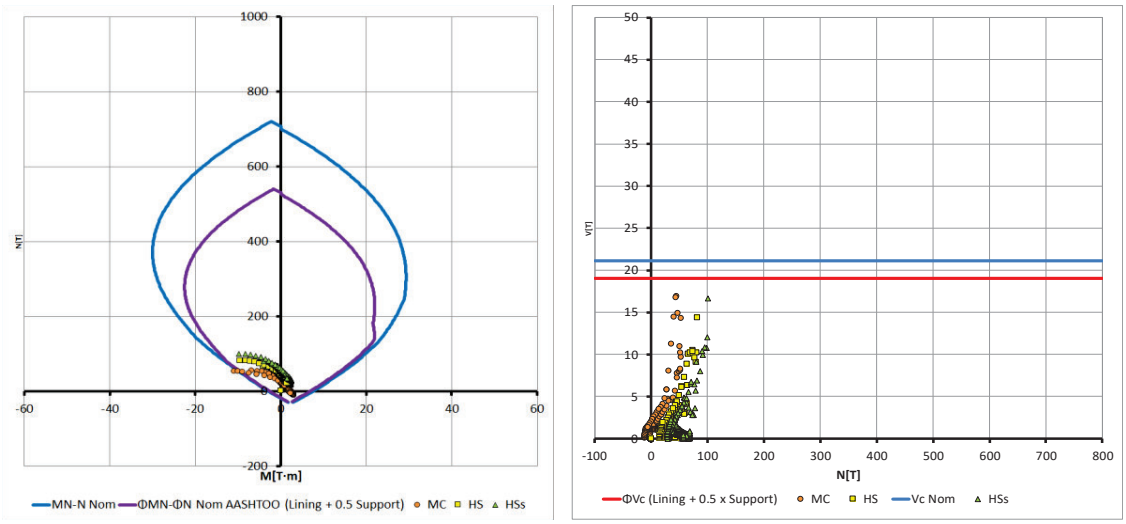
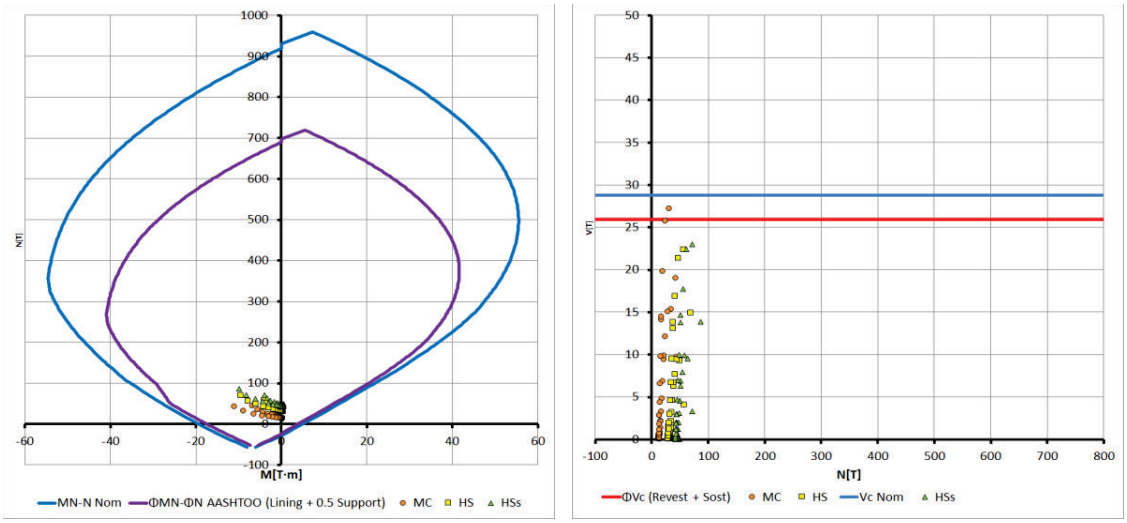


Figure III-93: Forces Diagram, Axial, Bending and Shear - Construction Stage- HSs- Fine Counter-Vault Section in New Tunnels with four phases of excavation



Graph III-31: Interaction M-N and N-Q Diagram- Vault of Metro Tunnel- Construction Stage- Fine- Counter-Vault Section in New Tunnels with four phases of excavation



Graph III-32: Interaction M-N and N-Q Diagram- Counter vault of Metro Tunnel- Construction Stage- Fine- Counter-Vault Section in New Tunnels with four phases of excavation

(a.2) Service Stage

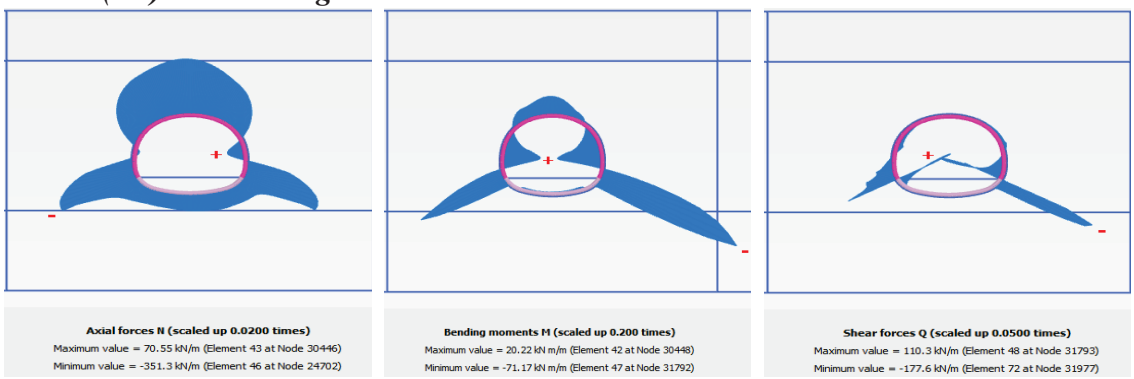


Figure III-94: Forces Diagram, Axial, Bending and Shear- Service Stage- MC- Fine-Counter-Vault Section in New Tunnels with four phases of excavation

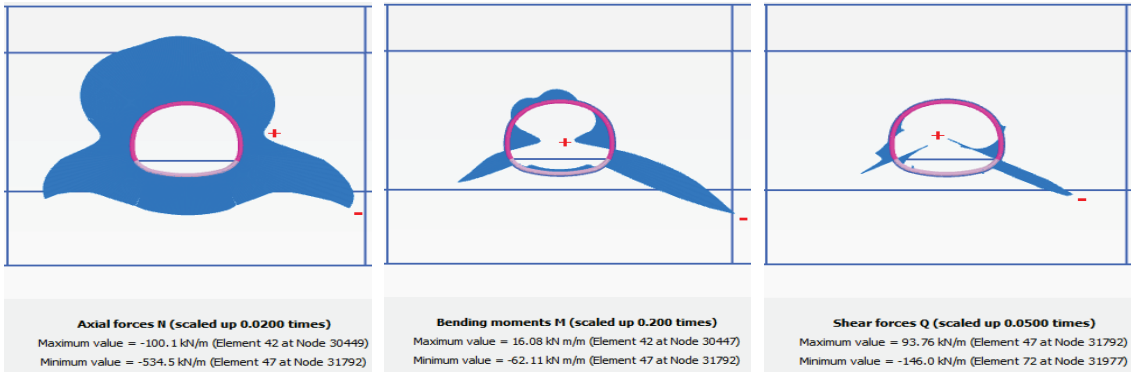


Figure III-95: Forces Diagram, Axial, Bending and Shear- Service Stage- HS- Fine-Counter-Vault Section in New Tunnels with four phases of excavation

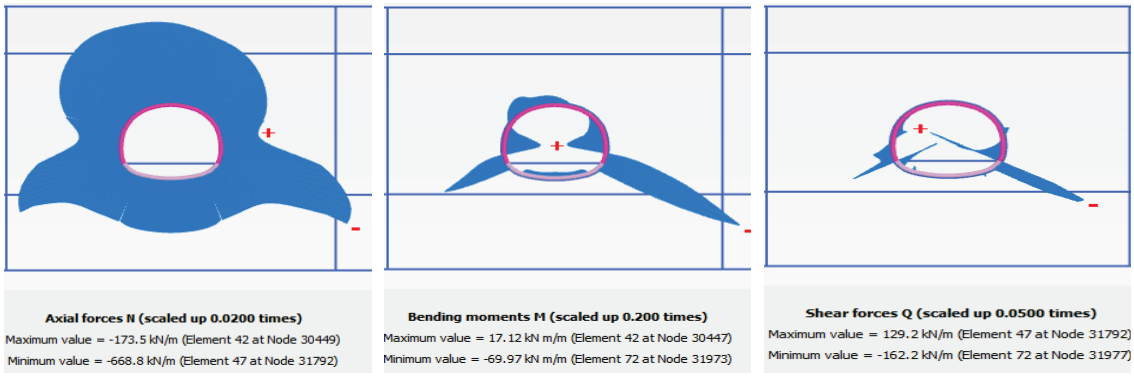
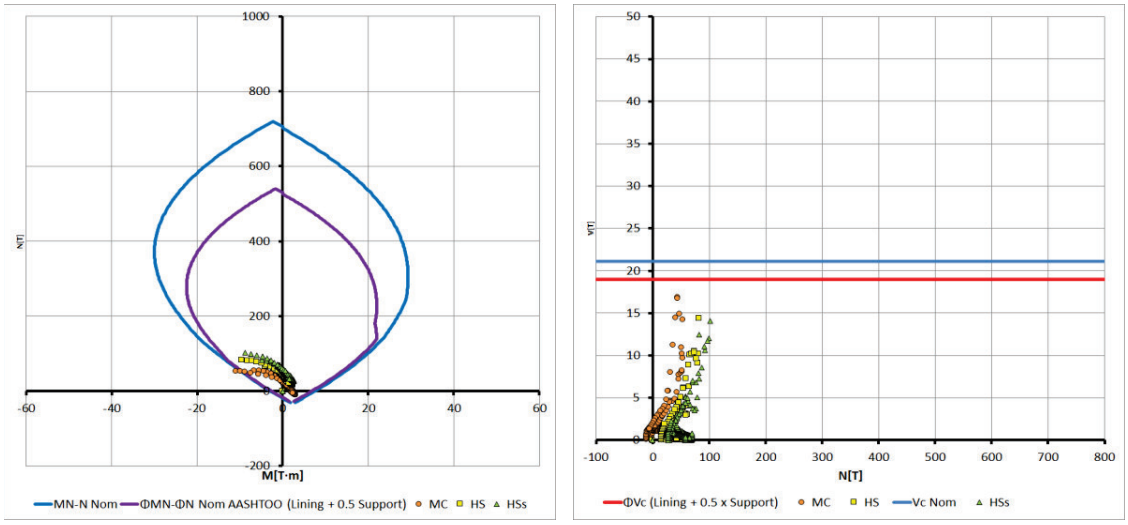
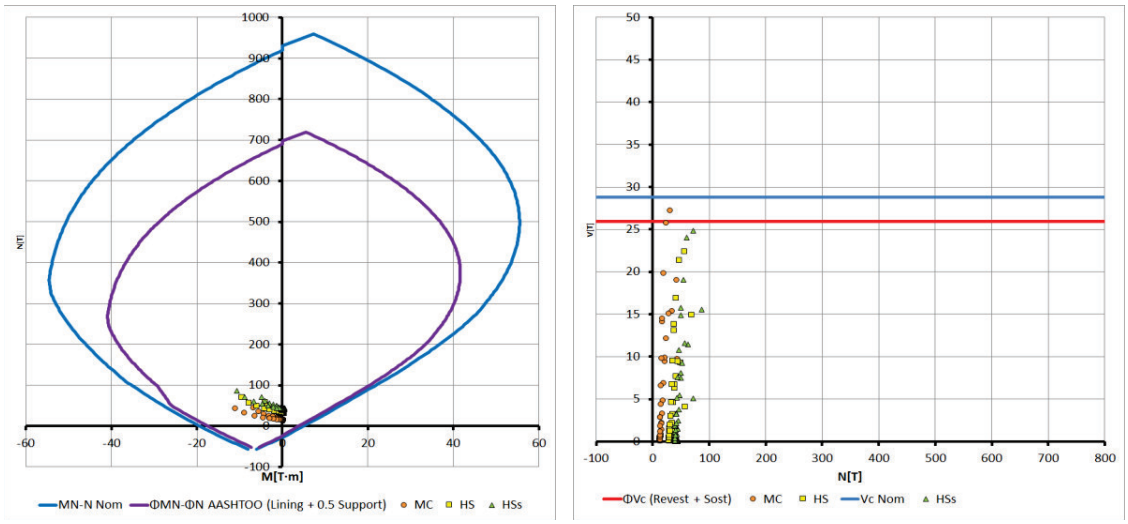


Figure III-96: Forces Diagram, Axial, Bending and Shear- Service Stage- HSs- Fine-Counter-Vault Section in New Tunnels with four phases of excavation



Graph III-33: Interaction M-N and N-Q Diagram- Vault of Metro Tunnel- Service Stage- Fine-Counter-Vault Section in New Tunnels with four phases of excavation



Graph III-34: Interaction M-N and N-Q Diagram- Counter vault of Metro Tunnel- Service Stage- Fine- Counter-Vault Section in New Tunnels with four phases of excavation

3.3.3 Verification of the Deformation in the New Road Tunnels

The maximum convergence deformations must be verified with the criterion established in chapter 3.7.3(a).

(a) Analysis of the Fine Profile

(a.1) Construction Stage

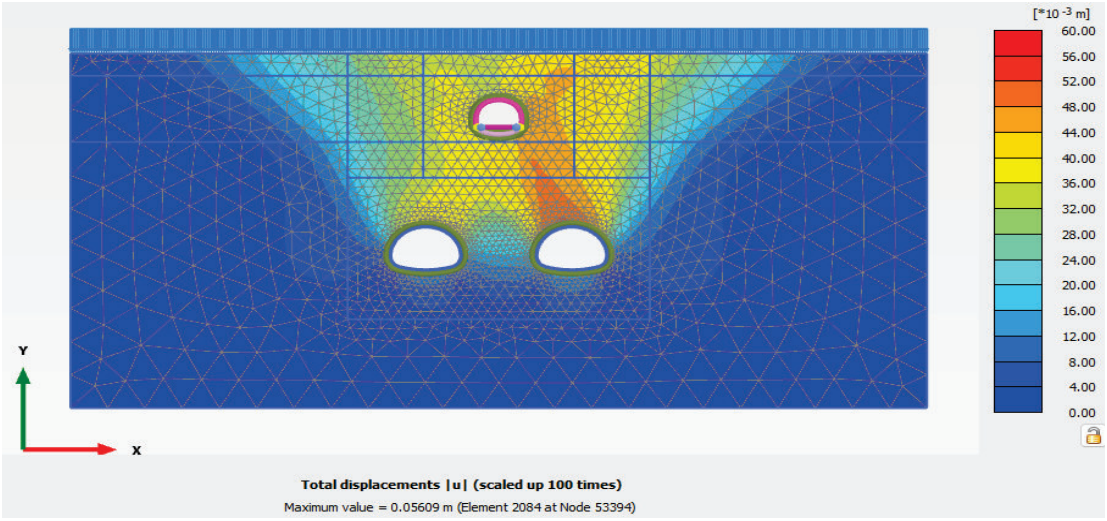


Figure III-97: Maximum Displacement in Construction- HSs- Fine-Counter-Vault Section in New Tunnels with four phases of excavation

(a.2) Service Stage

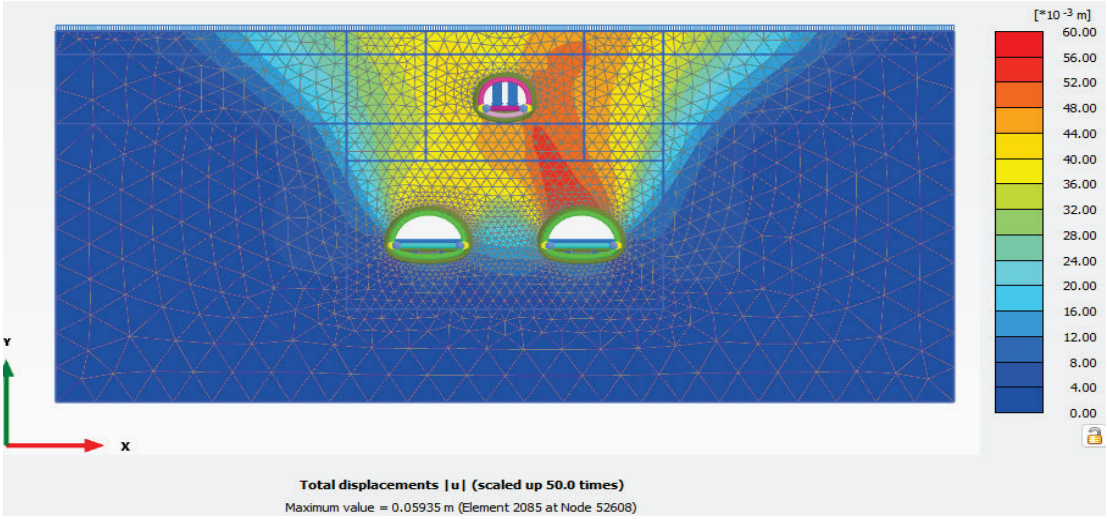


Figure III-98: Maximum Displacement in Service- HSs- Fine- Counter-Vault Section in New Tunnels with four phases of excavation

Table III-46: Summary of Maximum Displacement Checks on New Road Tunnels–Pre-existing Metro Tunnel – Fine- Counter-Vault Section in New Tunnels with four phases of excavation

Maximum Displacement [mm]							
Soil	Construction Stage			Service Stage			Admissible
	MC	HS	HSs	MC	HS	HSs	
Fine	-	-	56.09	-	-	59.35	70

3.3.4 Verification of the Resistance in the New Road Tunnels

In the construction stage, the support of the new road tunnels must be verified through the criterion of admissible stresses, as defined in section 3.7.3(b).

In the service stage, the lining of the new road tunnels must be verified through the interaction diagram M-N and N-Q, as defined in section 3.7.3(b)..

The lining of the new road tunnels are verified, with their corresponding concrete thicknesses and reinforcement, as defined in Figure III-10and sections 3.3.2 and 3.3.2(b).

$e = 0.50\ m$ Concrete thicknesses for the calculation
(Lining thicknesses = 0.30 m + 2/3 Support thicknesses = 0.20 m)
$A_s = 3.35\ cm^2/m$ ACMA335 Mesh in Internal and External face
$A_{s1} = 7.60\ cm^2/m$ 2Ø22 Bar of the Reticulate Frame in Internal face
$A_{s1} = 8.04\ cm^2/m$ 1Ø32 Bar of the Reticulate Frame in External face

(a) Analysis of the Fine Profile

(a.1) Construction Stage

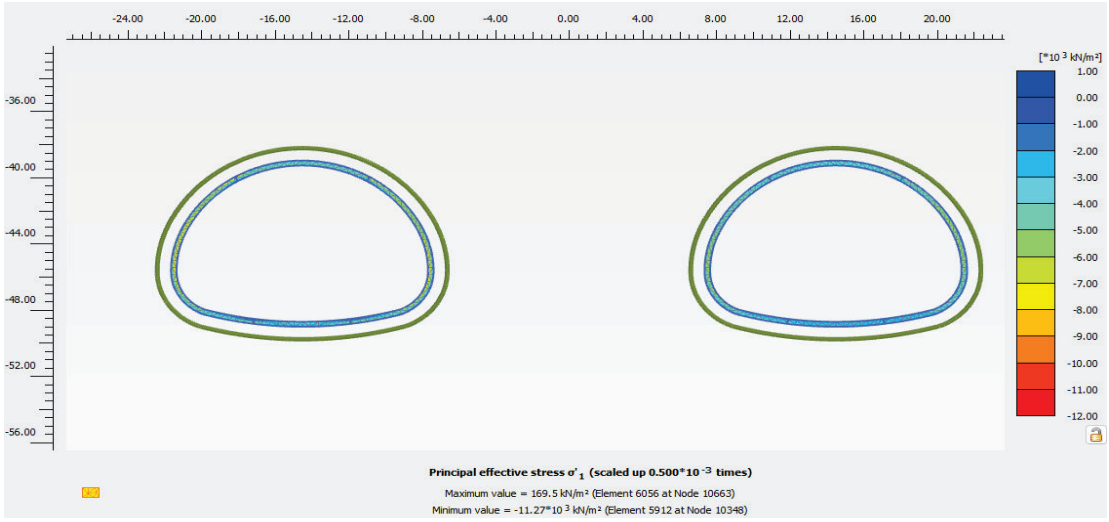


Figure III-99: Major Principal effective Stress on Support- HSs – Fine-Counter-Vault Section in New Tunnels with four phases of excavation

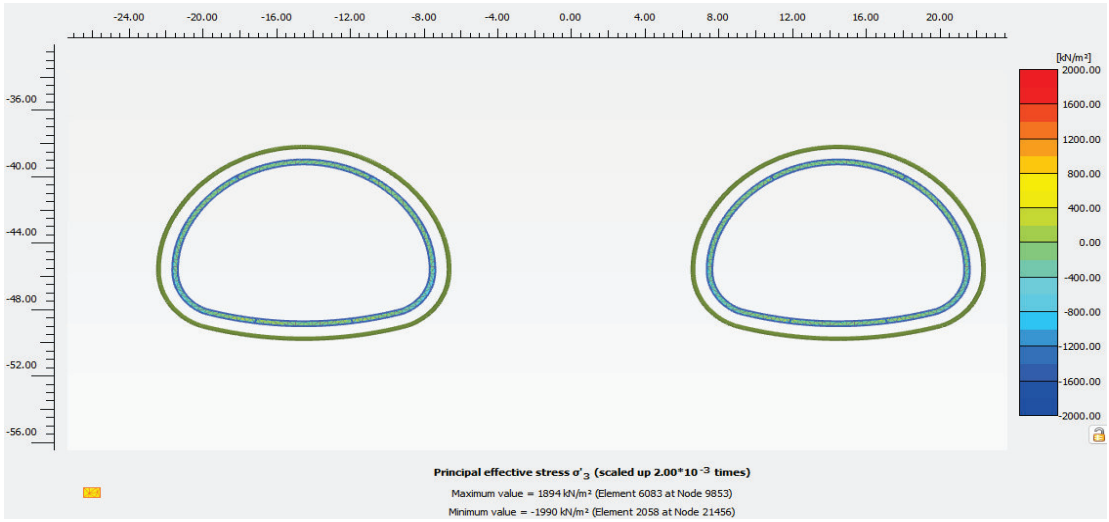


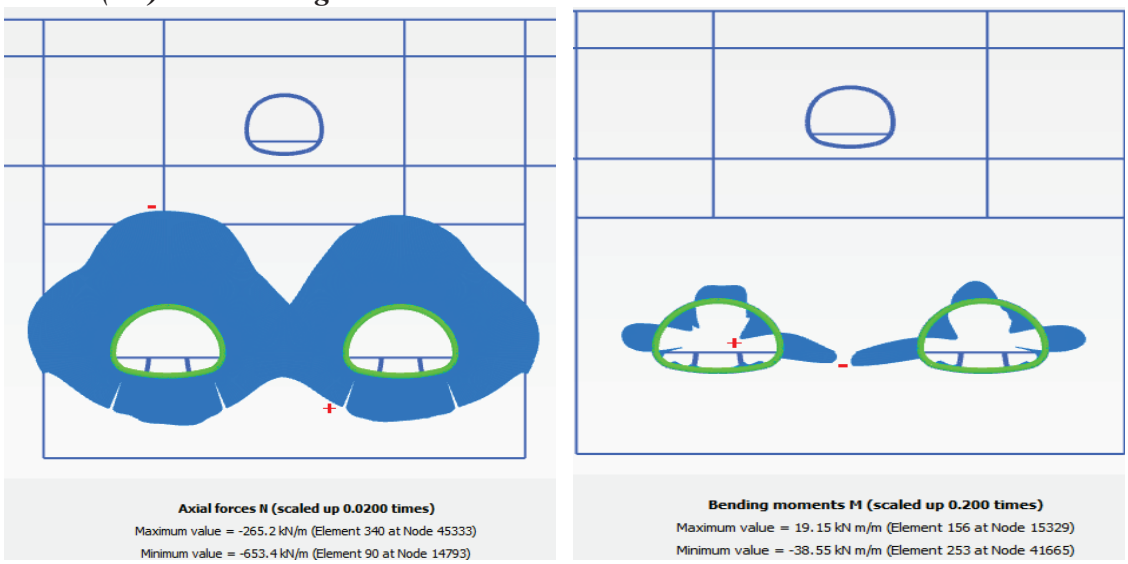
Figure III-100: Minor Principal effective Stress on Support- HSs – Fine-Counter-Vault Section in New Tunnels with four phases of excavation

Table III-47: Verification of Admissible Stress- HSs- Fine-

Counter-Vault Section in New Tunnels with four phases of excavation

σ´1 [MPa]	σ´3 [MPa]	σ´1adm [MPa]	σ´3adm [MPa]	σ´1 < σ´1 adm	σ´3 < σ´3 adm
-11.27	1.89	-16	2	CHECK	CHECK

(a.2) Service Stage



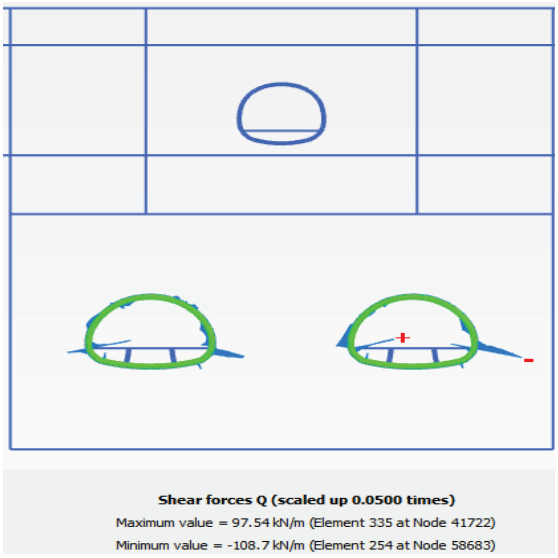
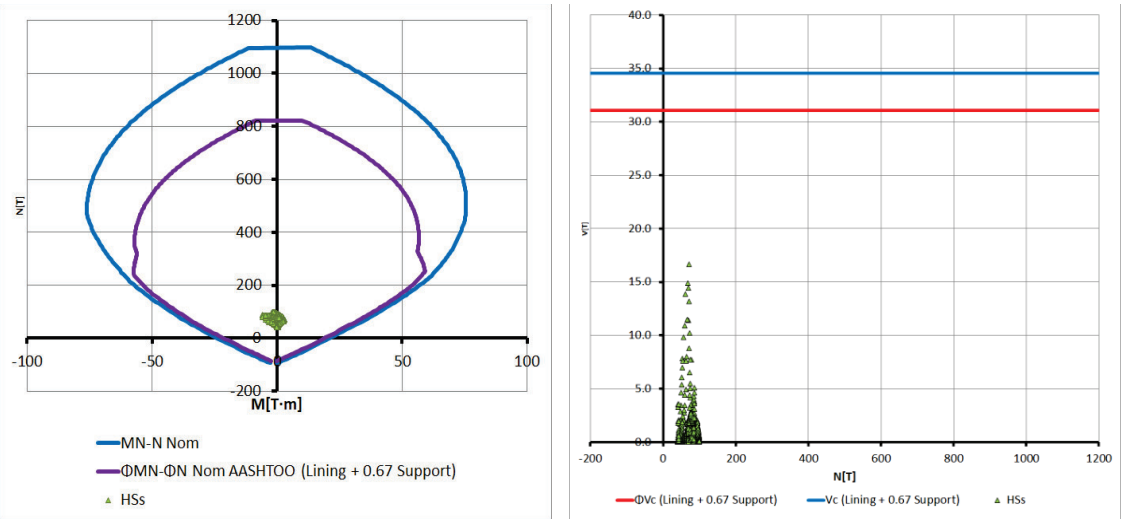


Figure III-101: Forces Diagram, Axial, Bending and Shear on Lining- Service Stage- HSs- Fine- Counter-Vault Section in New Tunnels with four phases of excavation



Graph III-35: : Interaction M-N and N-Q Diagram- Lining of the new road tunnels-

Service Stage- Fine- Counter vault Section in New Tunnels with four phases of excavation

3.3.5 Verification of the Capacity of the Soil

The following shows the plastification of the soil in construction and in service and applies the acceptability criteria explained in section 3.7.4.

(a) Construction Stage

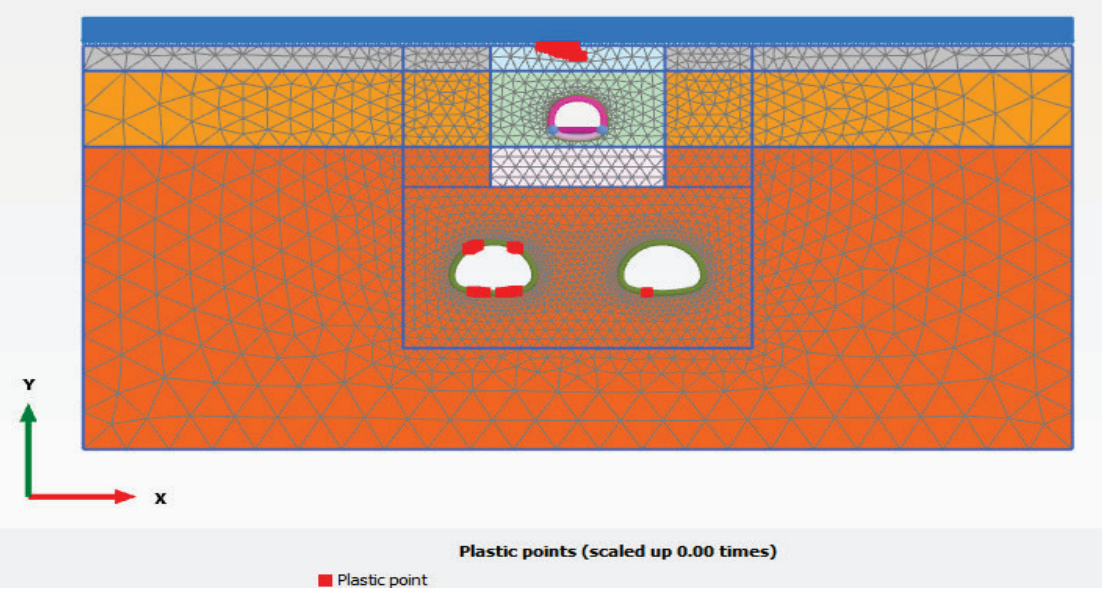


Figure III-102: Plastification Diagram- Construction Stage- HSs- Fine-

Counter-Vault Section in New Tunnels with four phases of excavation

(a.1) Service Stage

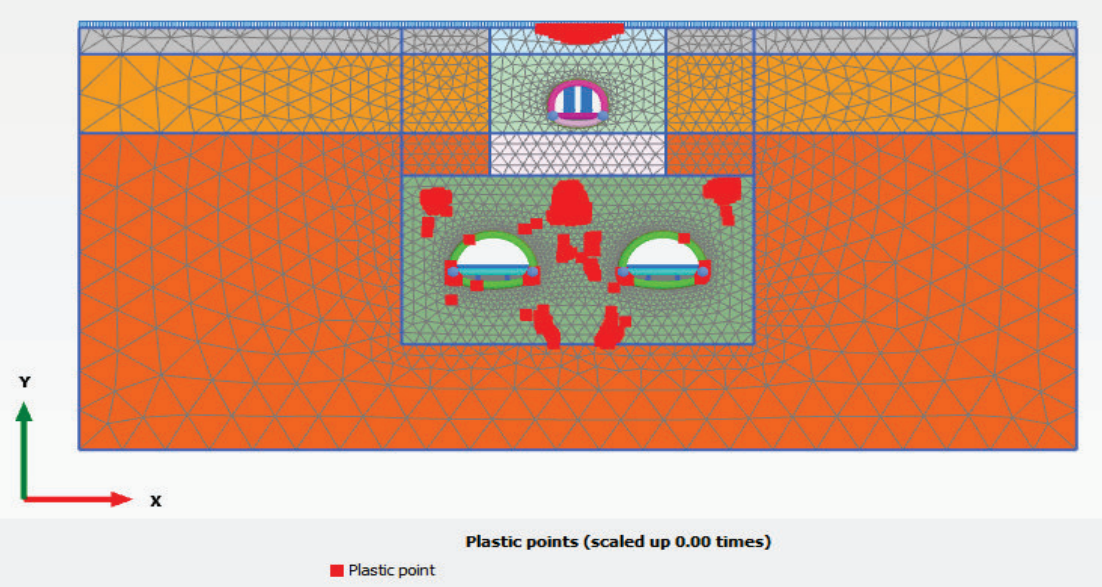


Figure III-103: Plastification Diagram- Service Stage- HSs- Fine-Counter-Vault Section in New Tunnels with four phases of excavation

Table III-48: Plastification Verification on Soil- HSs- Fine-Counter-Vault Section in New Tunnels with four phases of excavation

Stage	R-Plastic [m]	R-Plastic Admissible [m]	Verification
Construction	8	14	CHECK
Service	14	14	CHECK

IV. ANNEX: STRUCTURAL VERIFICATION WITH PRE-EXISTING BUILDING

4.1. Variation of the Constitutive Soil Model with Plane Sole Section in New Tunnels

4.1.1 Verification of the Deformation in the Pre-existing Building (B)

Initially, the vertical and horizontal deformations are shown for each soil profile, in the most important construction phases and for each soil constitutive model. Then, the displacement profiles located at the foundation level, 6.50 m, and the verification of the acceptance criterion of Boscardin & Cording (See Chapter 3.7.2(a)), are presented.

(a) Analysis of the Gravel Profile

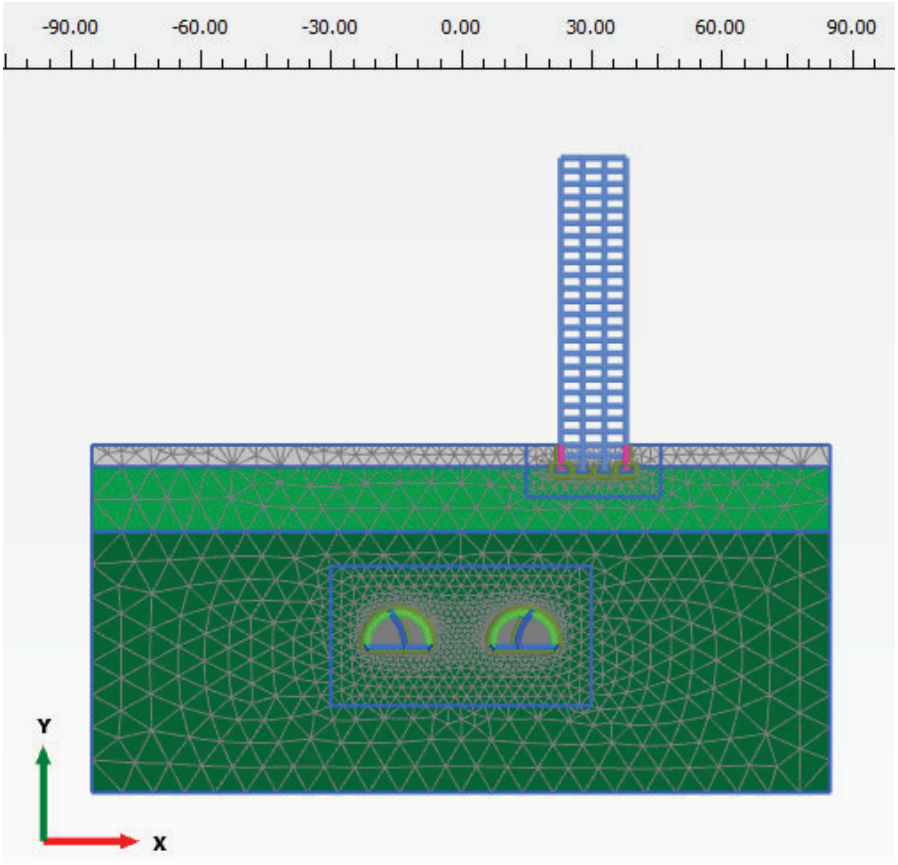


Figure IV-1: Gravel Model with Pre-existing Building and plane sole section in new road tunnels

(a.1) Service Stage

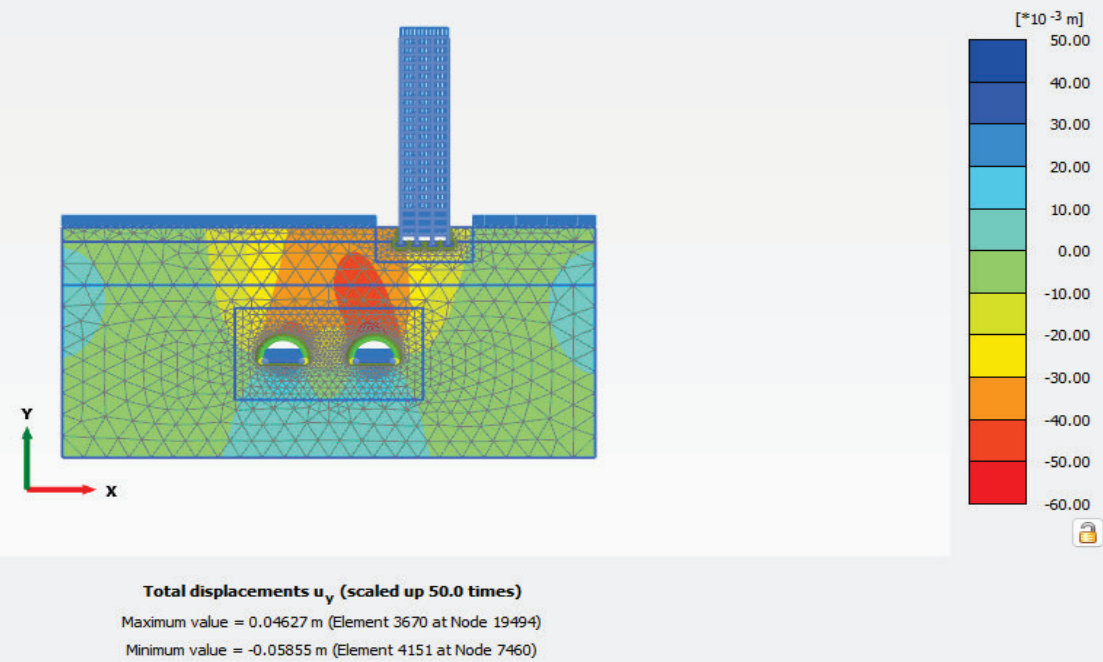


Figure IV-2: Vertical Settlement in Service- MC- Gravel- Plane Sole Section in New Tunnels

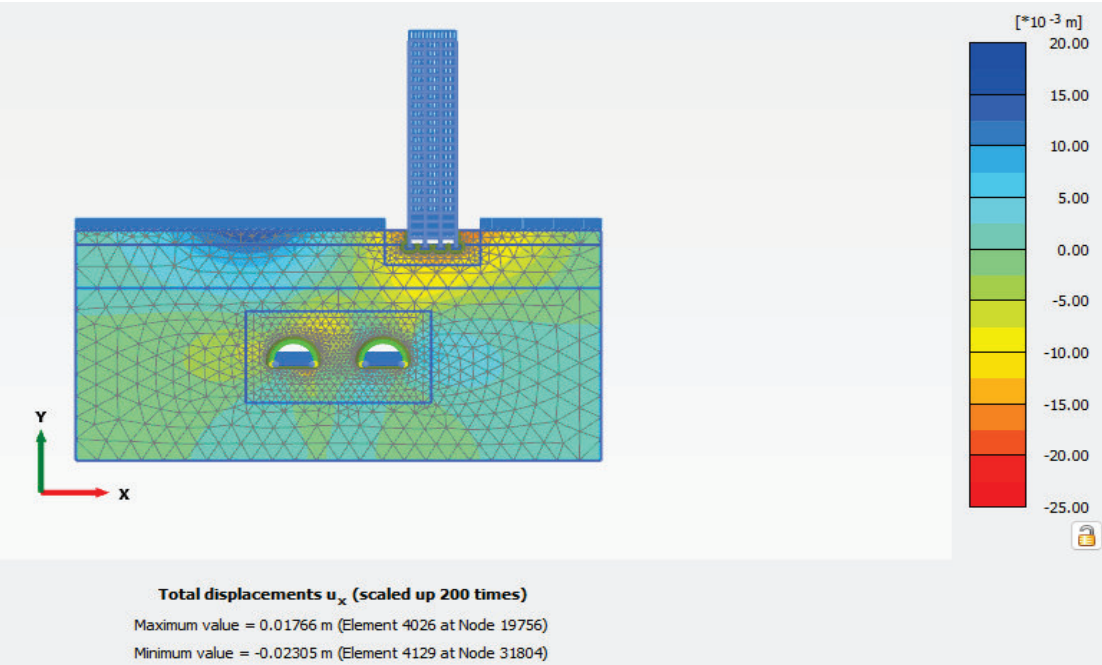


Figure IV-3: Horizontal Displacement in Service- MC- Gravel- Plane Sole Section in New Tunnels

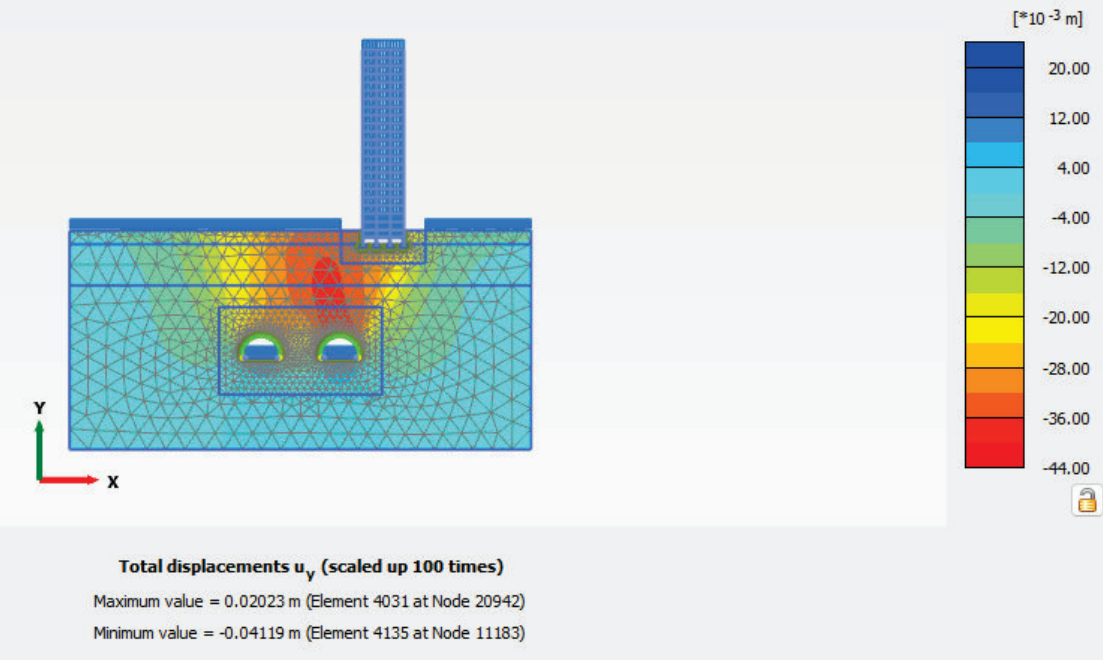


Figure IV-4: Vertical Settlement in Service- HS- Gravel-

Plane Sole Section in New Tunnels

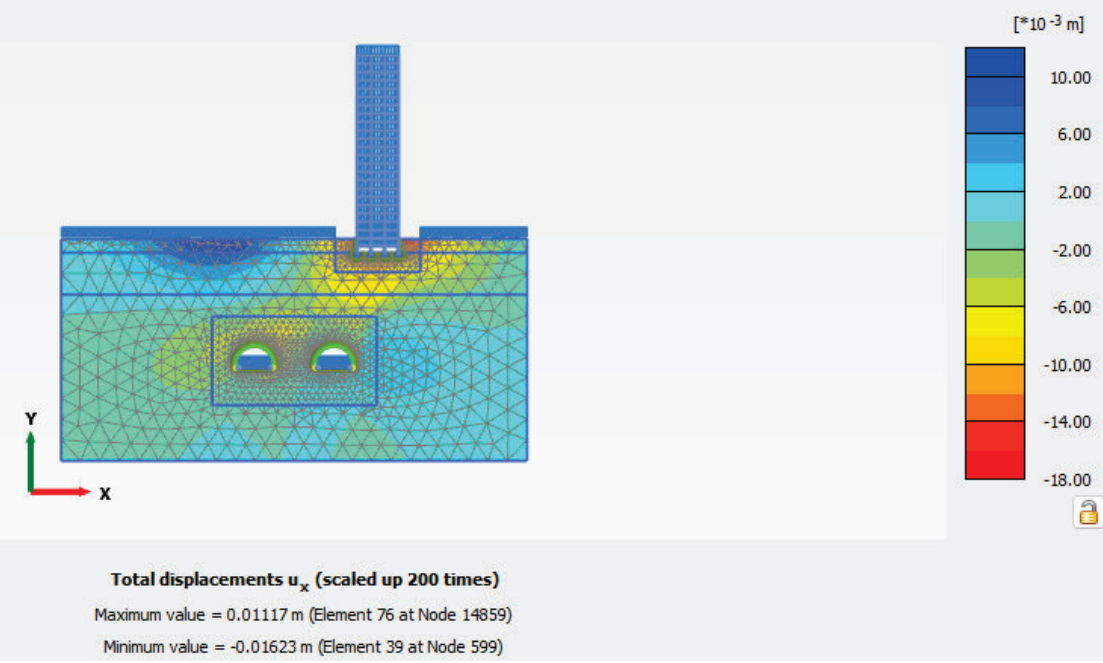


Figure IV-5: Horizontal Displacement in Service- HS- Gravel-

Plane Sole Section in New Tunnels

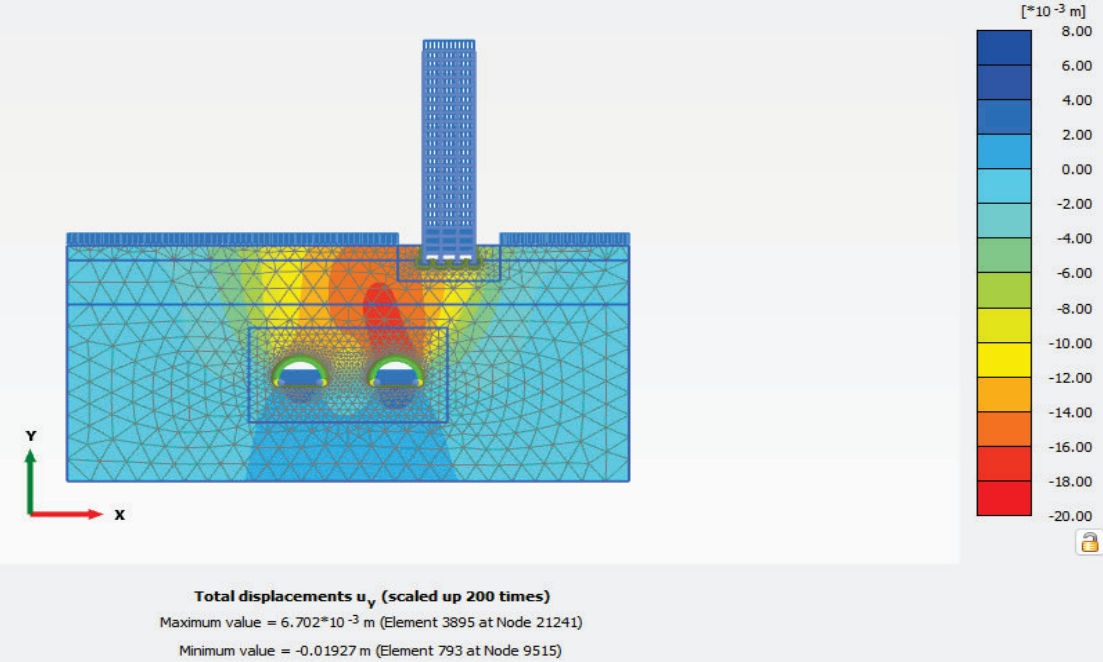


Figure IV-6: Vertical Settlement in Service- HSs- Gravel-

Plane Sole Section in New Tunnels

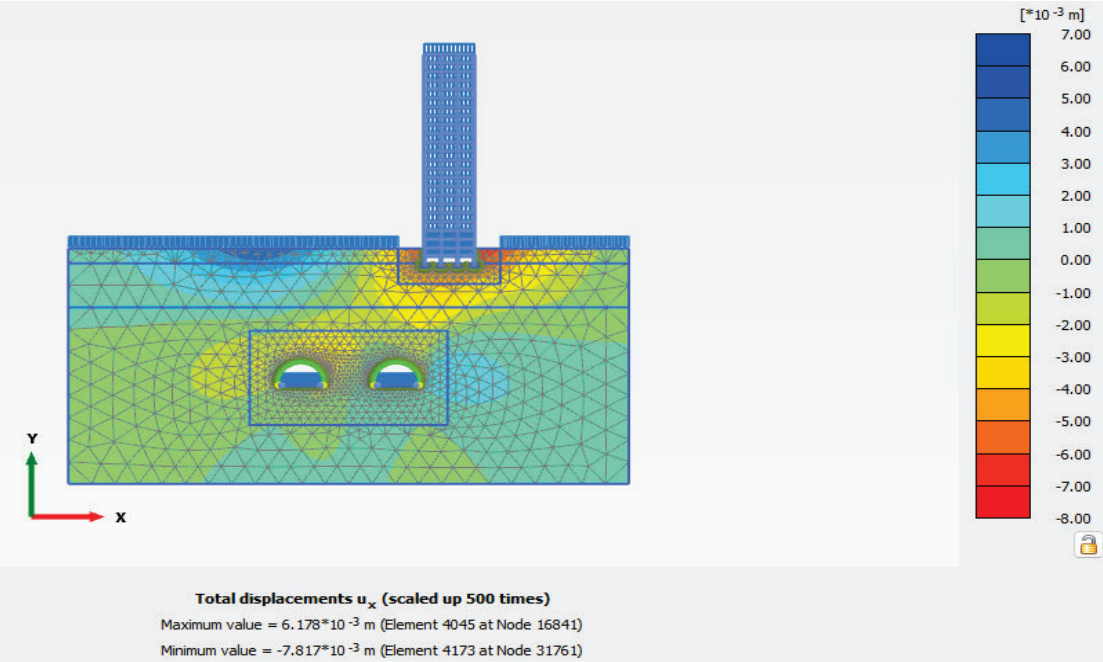
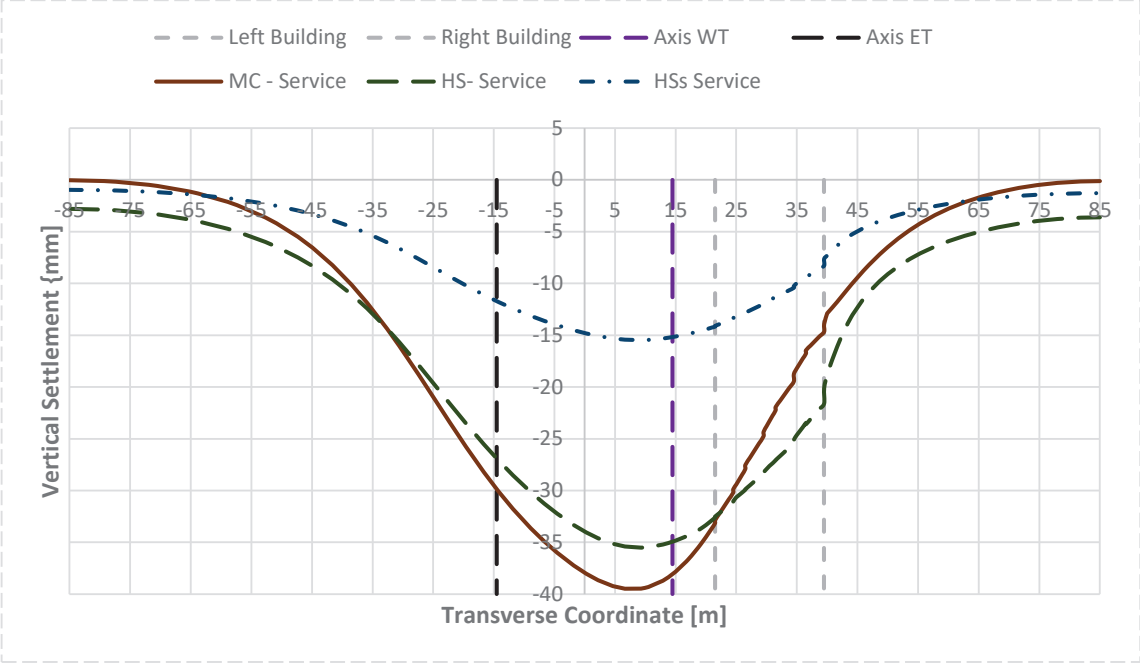
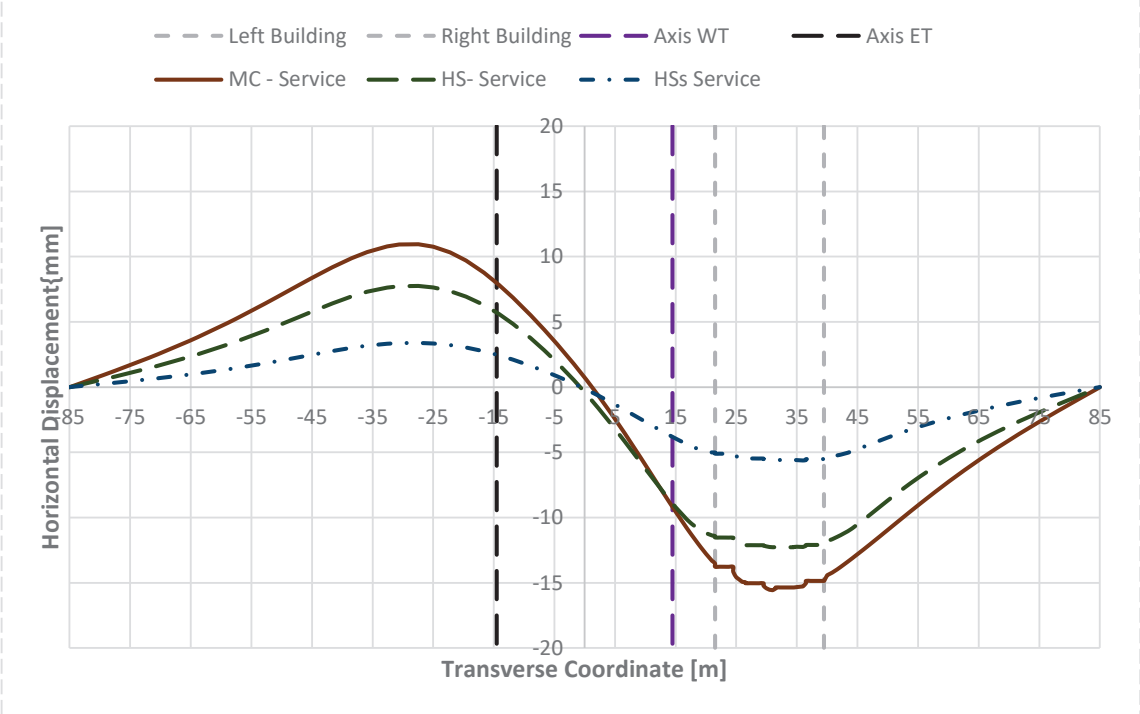


Figure IV-7: Horizontal Displacement in Service- HSs- Gravel-

Plane Sole Section in New Tunnels



Graph IV-1: Diagram of Vertical Settlement on Building Foundation - Service Stage – Model width Plane Sole Section in New Tunnels- Gravel



Graph IV-2: Diagram of Horizontal Displacement on Building Foundation - Service Stage – Model with Plane Sole Section in New Tunnels- Gravel

Table IV-1: Verification of the Deformation in Foundation Building according to Boscardin & Cording- MC Model- Service Stage- Gravel- Plane Sole Section in New Tunnels

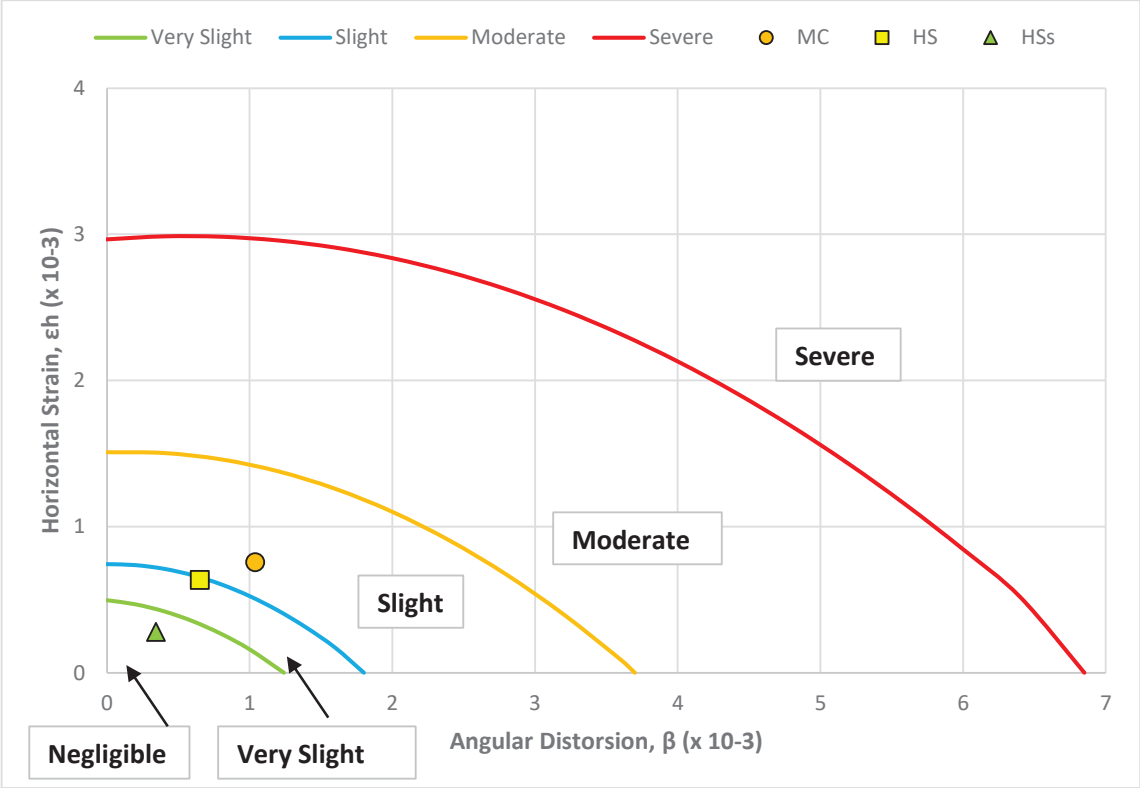
Coord. in model (m)	Settl Left δ_{v1} (mm)		Settl Right δ_{v2} (mm)		Relative Settle $\Delta\delta v$	Horiz Displac δ_H (mm)		Width Found.	Angular Distortion	Lateral Strain
	x	y	x	y	$\delta v1-\delta v2$	x	y	Building	$\beta=\Delta\delta v/L$	$\varepsilon l=\delta_H/L$
Phase	21.5	-6.5	39.5	-6.5	(mm)	21.5	-6.5	L (m)	(x 10-3)	(x 10-3)
Service	-33.01		-14.29		18.71	-13.63		18	1.04	0.76

Table IV-2: Verification of the Deformation in Foundation Building according to Boscardin & Cording- HS Model- Service Stage- Gravel- Plane Sole Section in New Tunnels

Coord. in model (m)	Settl Left δ_{v1} (mm)		Settl Right δ_{v2} (mm)		Relative Settle $\Delta\delta v$	Horiz Displac δ_H (mm)		Width Found.	Angular Distortion	Lateral Strain
	x	y	x	y	$\delta v1-\delta v2$	x	y	Building	$\beta=\Delta\delta v/L$	$\varepsilon l=\delta_H/L$
Phase	21.5	-6.5	39.5	-6.5	(mm)	21.5	-6.5	L (m)	(x 10-3)	(x 10-3)
Service	-32.56		-20.85		11.71	-11.46		18	0.65	0.64

Table IV-3: Verification of the Deformation in Foundation Building according to Boscardin & Cording- HSs Model- Service Stage- Gravel- Plane Sole Section in New Tunnels

Coord. in model (m)	Settl Left δ_{v1} (mm)		Settl Right δ_{v2} (mm)		Relative Settle $\Delta\delta v$	Horiz Displac δ_H (mm)		Width Found.	Angular Distortion	Lateral Strain
	x	y	x	y	$\delta v1-\delta v2$	x	y	Building	$\beta=\Delta\delta v/L$	$\varepsilon l=\delta_H/L$
Phase	21.5	-6.5	39.5	-6.5	(mm)	21.5	-6.5	L (m)	(x 10-3)	(x 10-3)
Service	-14.15		-7.96		6.20	-5.06		18	0.34	0.28



Graph IV-3: Criterion of Boscardin and Cording- Service Stage-

Model with Plane Sole Section in New Tunnels- Gravel

(b) Analysis of the Mixed Profile

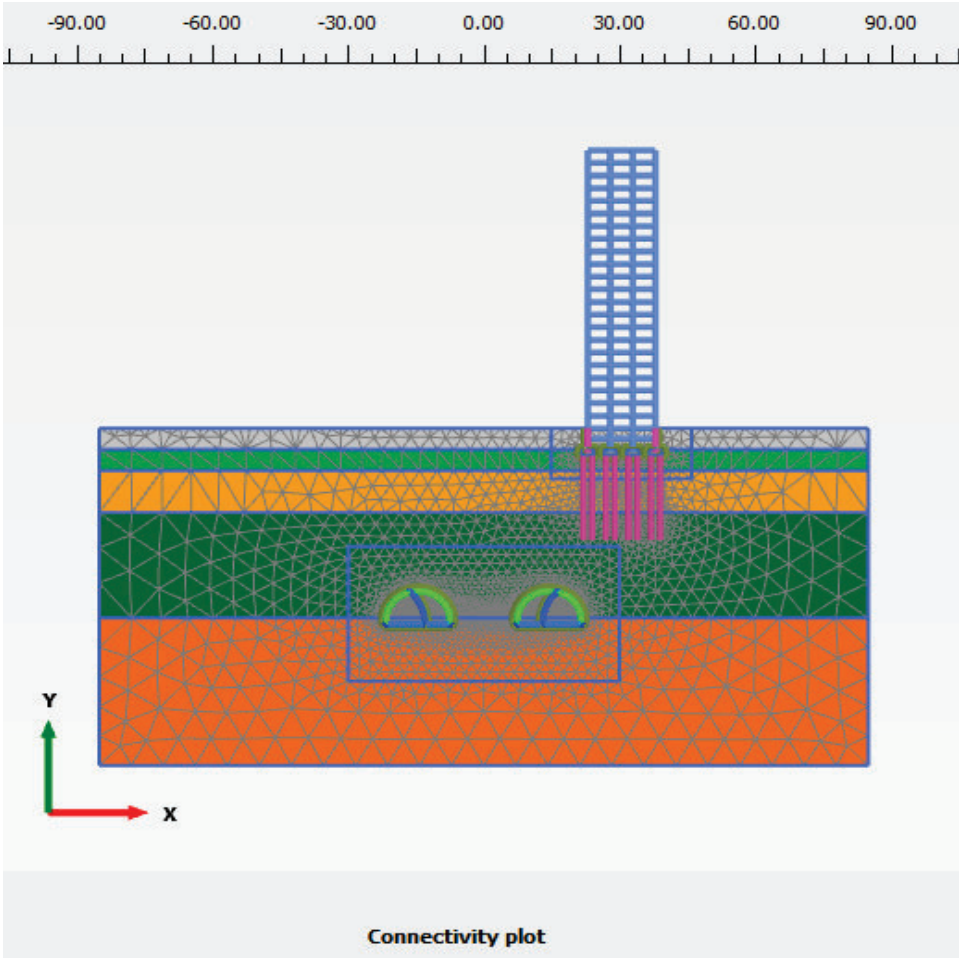


Figure IV-8: Mixed Model with Pre-existing Building and plane sole section in new road tunnels

(b.1) Service Stage

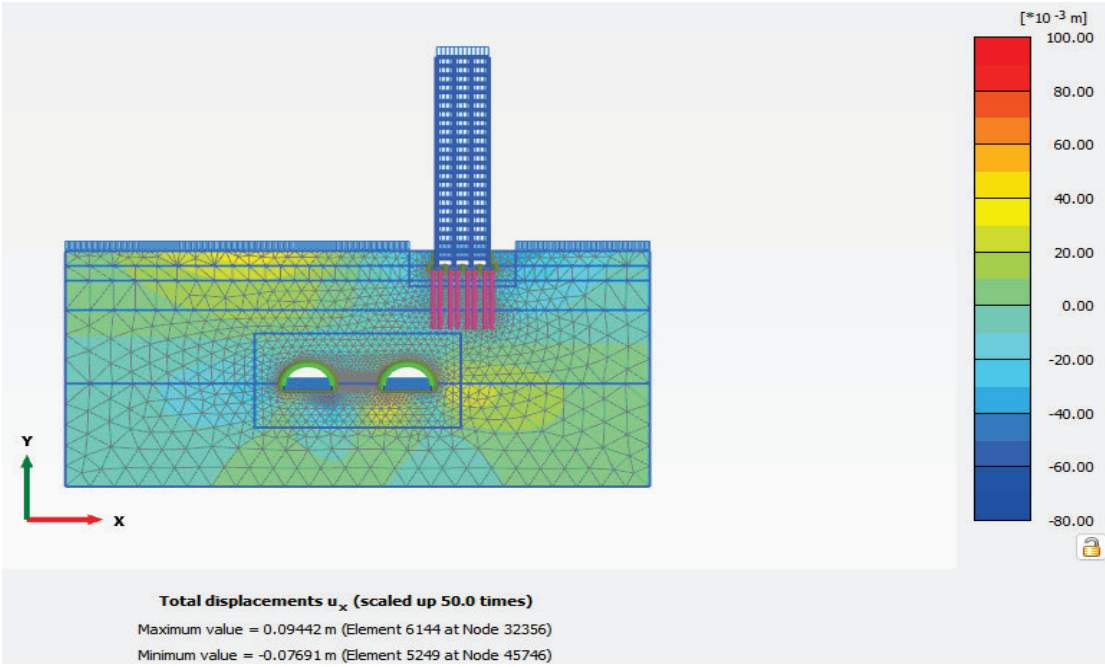


Figure IV-9: Vertical Settlement in Service- MC- Mixed

Plane Sole Section in New Tunnels

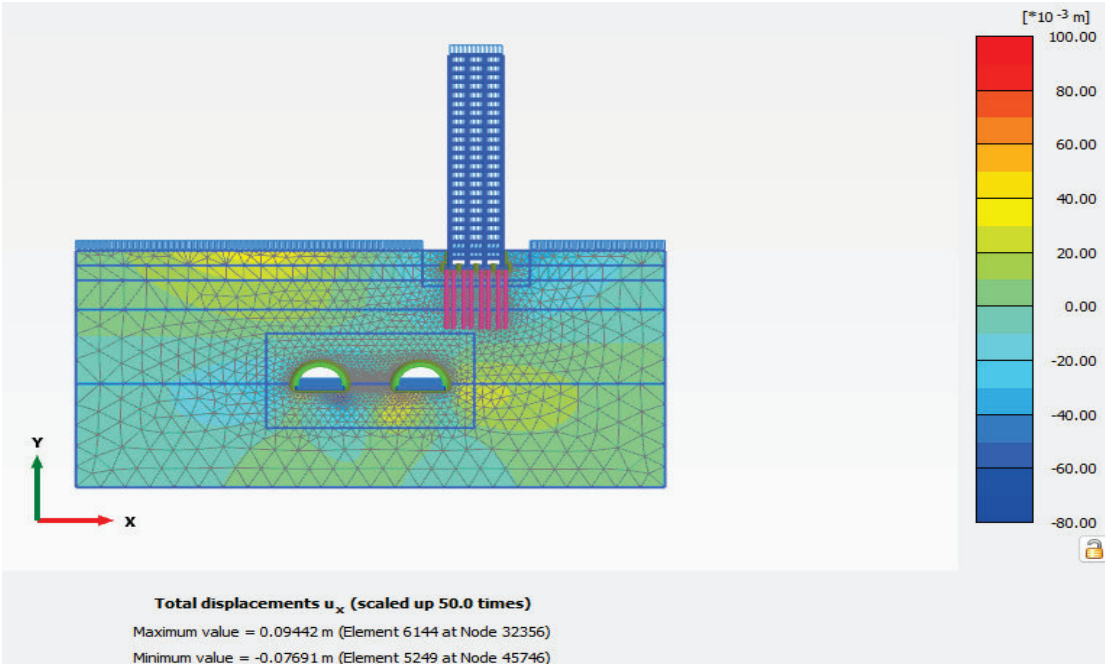


Figure IV-10: Horizontal Displacement in Service (WT and ET)- MC- Mixed

Plane Sole Section in New Tunnels

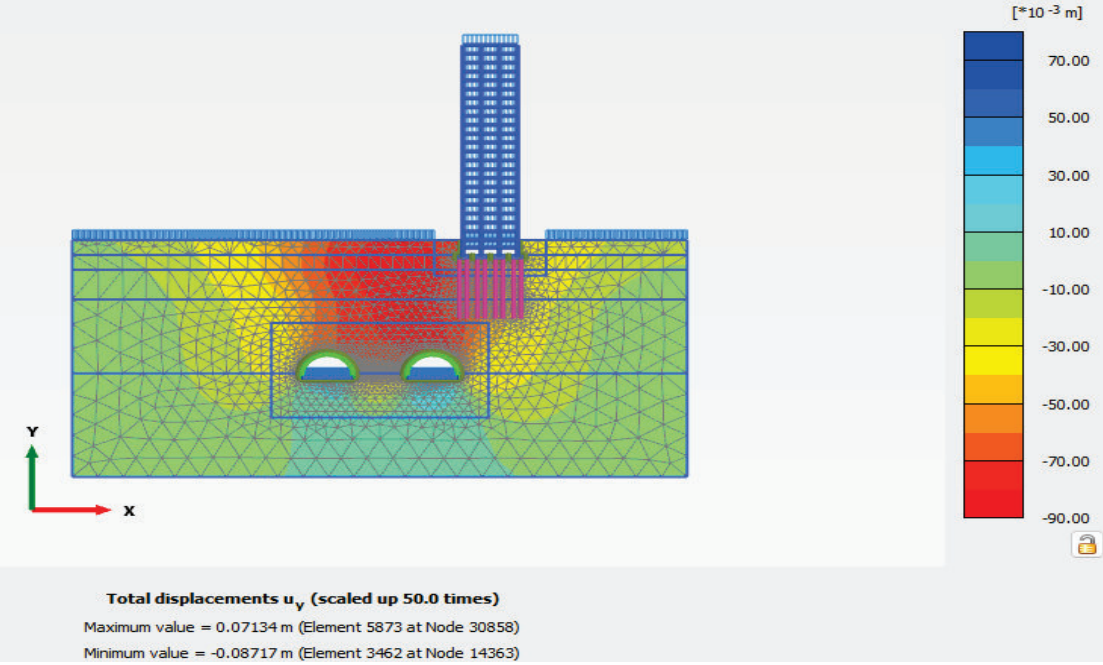


Figure IV-11: Vertical Settlement in Service- HS- Mixed

Plane Sole Section in New Tunnels

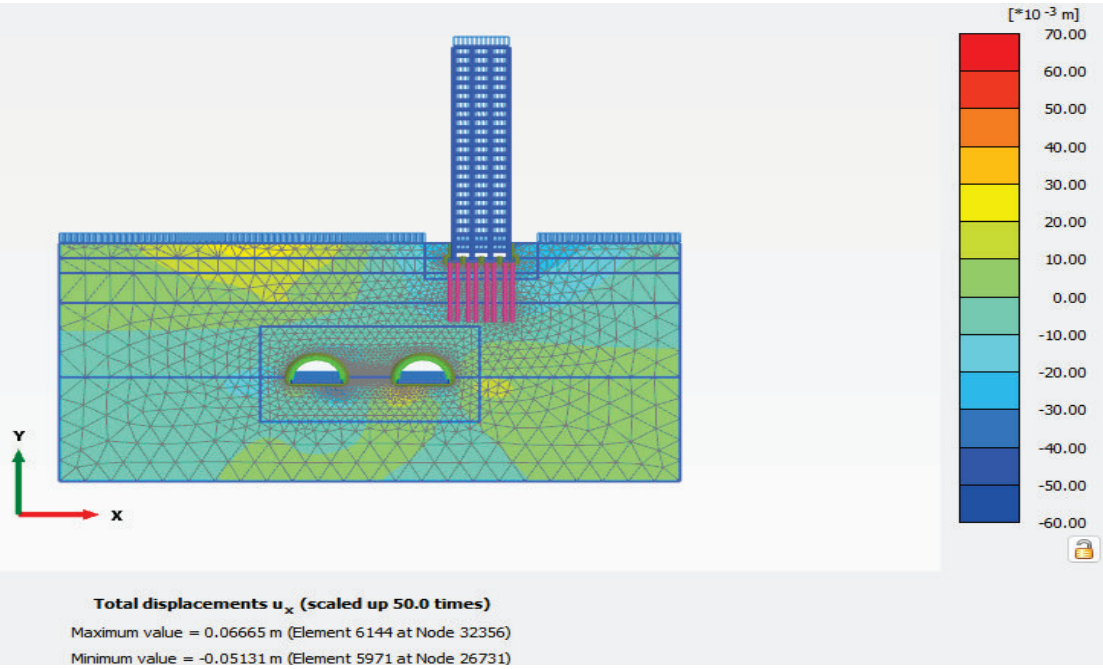


Figure IV-12: Horizontal Displacement in Service (WT and ET)- HS- Mixed

Plane Sole Section in New Tunnels

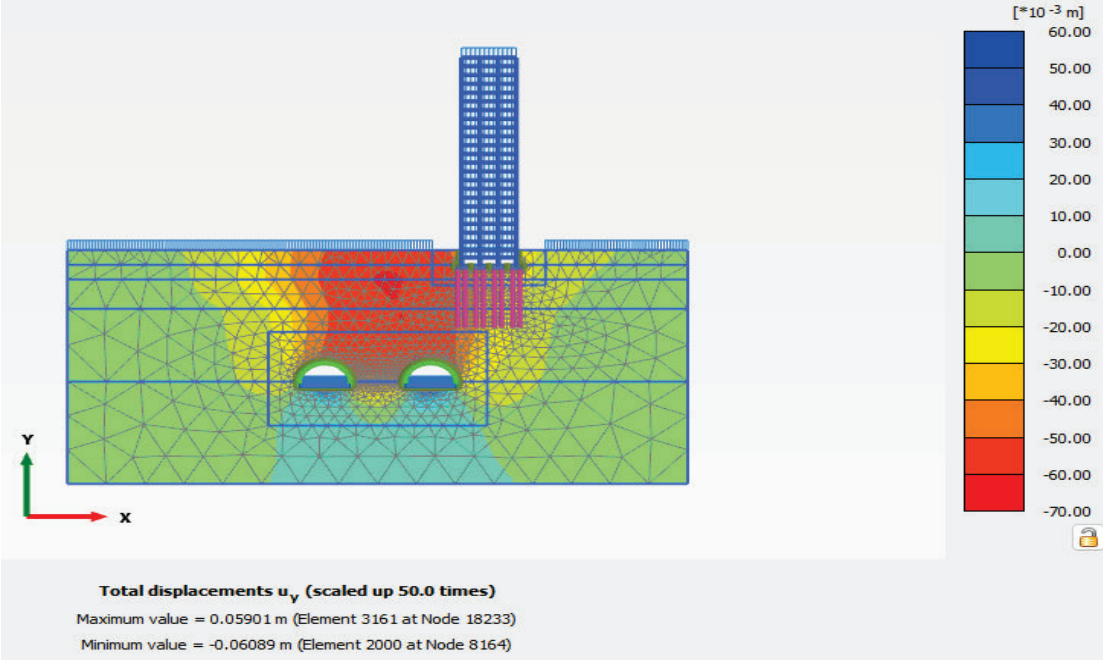


Figure IV-13: Vertical Settlement in Service- HSs- Mixed

Plane Sole Section in New Tunnels

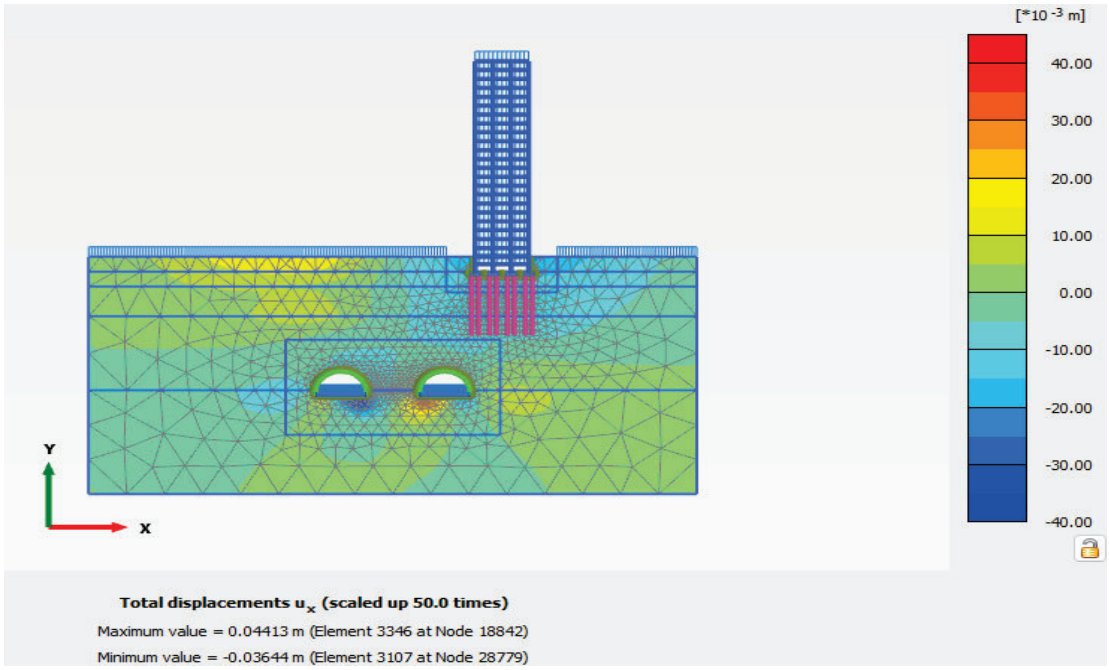
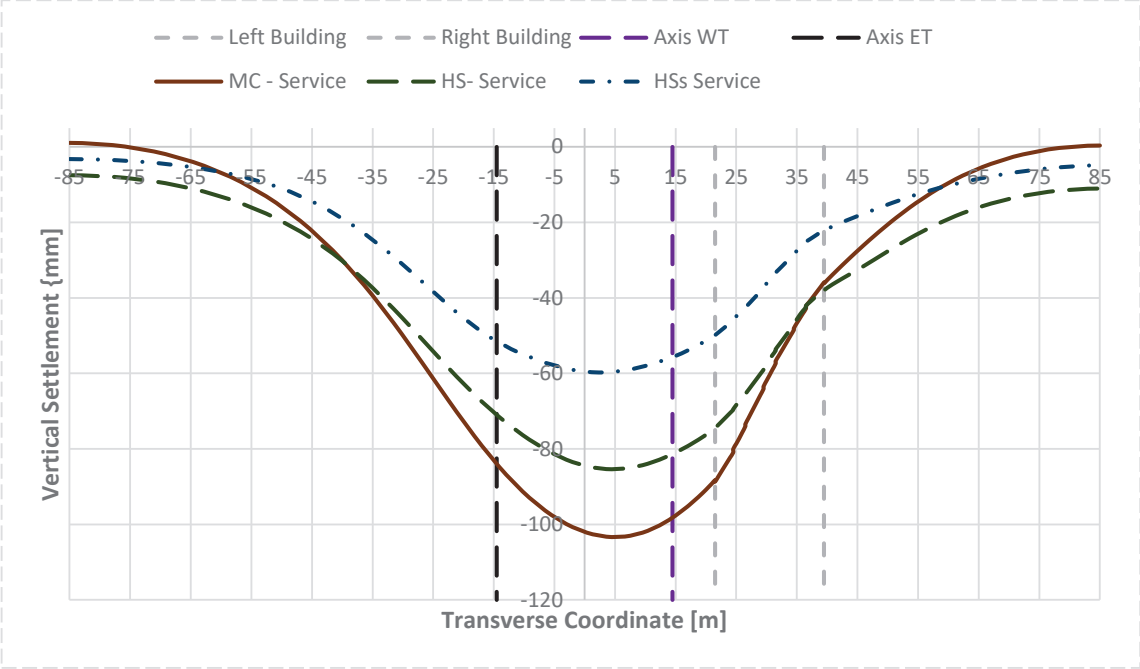
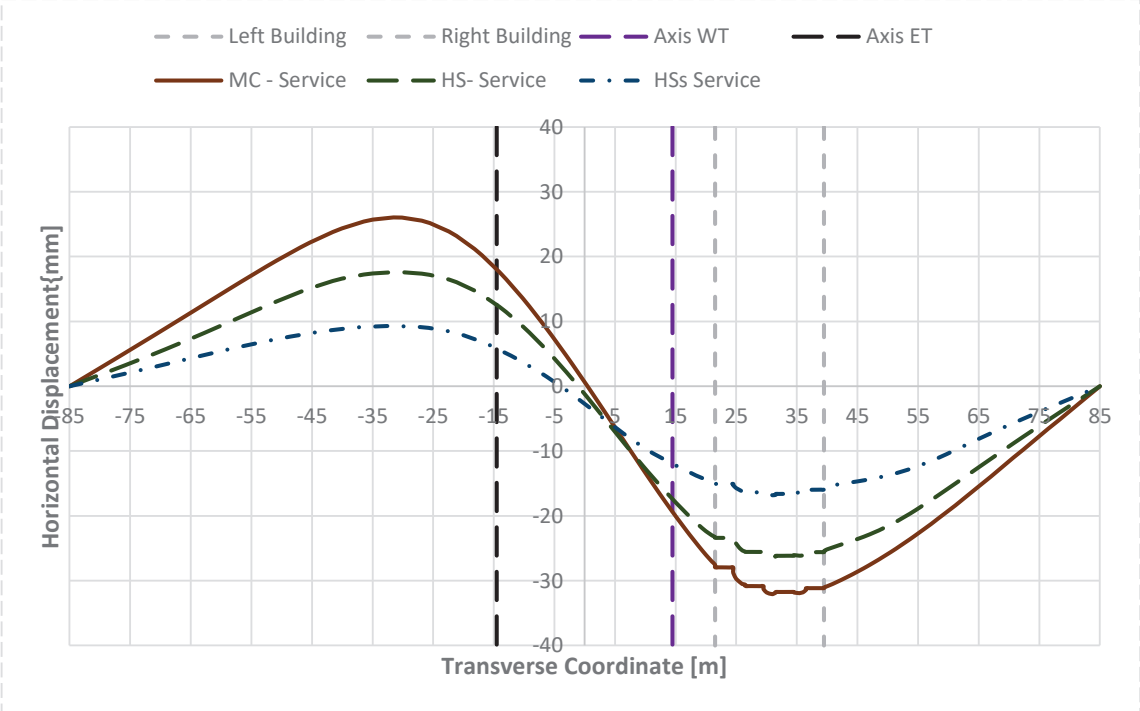


Figure IV-14: Horizontal Displacement in Service (WT and ET)- HSs- Mixed- Plane Sole Section



Graph IV-4: Diagram of Vertical Settlement on Building Foundation - Service Stage – Model with Plane Sole Section in New Tunnels- Mixed



Graph IV-5: Diagram of Horizontal Displacement on Building Foundation - Service Stage – Model with Plane Sole Section in New Tunnels- Mixed

Table IV-4: Verification of the Deformation in Foundation Building according to Boscardin & Cording- MC Model- Service Stage- Mixed- Plane Sole Section in New Tunnels

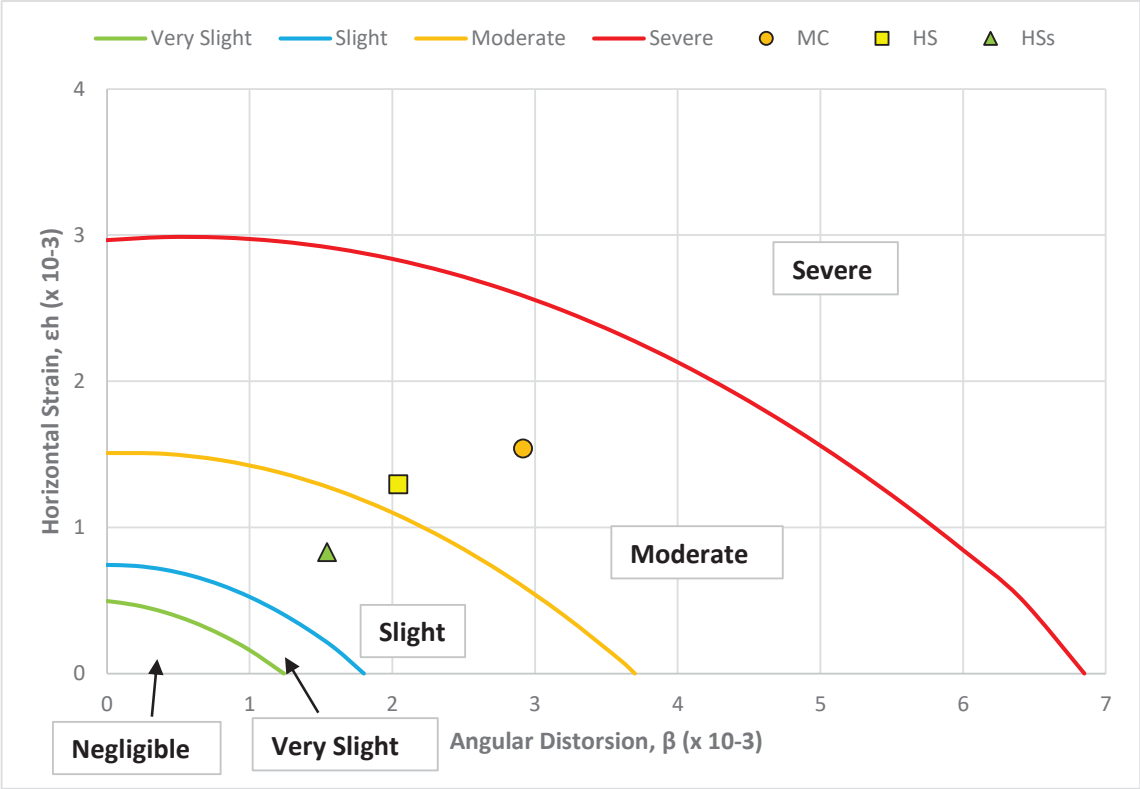
Coord. in model (m)	Settl Left δ_{v1} (mm)		Settl Right δ_{v2} (mm)		Relative Settle $\Delta\delta v$	Horiz Displac δ_H (mm)		Width Found.	Angular Distortion	Lateral Strain
	x	y	x	y	$\delta v1-\delta v2$	x	y	Building	$\beta=\Delta\delta v/L$	$\varepsilon l=\delta_H/L$
Phase	21.5	-6.5	39.5	-6.5	(mm)	21.5	-6.5	L (m)	(x 10-3)	(x 10-3)
Service	-88.49		-36.00		52.49	-27.74		18	2.92	1.54

Table IV-5: Verification of the Deformation in Foundation Building according to Boscardin & Cording- HS Model- Service Stage- Mixed- Plane Sole Section in New Tunnels

Coord. in model (m)	Settl Left δ_{v1} (mm)		Settl Right δ_{v2} (mm)		Relative Settle $\Delta\delta v$	Horiz Displac δ_H (mm)		Width Found.	Angular Distortion	Lateral Strain
	x	y	x	y	$\delta v1-\delta v2$	x	y	Building	$\beta=\Delta\delta v/L$	$\varepsilon l=\delta_H/L$
Phase	21.5	-6.5	39.5	-6.5	(mm)	21.5	-6.5	L (m)	(x 10-3)	(x 10-3)
Service	-74.55		-37.82		36.73	-23.34		18	2.04	1.30

Table IV-6: Verification of the Deformation in Foundation Building according to Boscardin & Cording- HSs Model- Service Stage- Mixed- Plane Sole Section in New Tunnels

Coord. in model (m)	Settl Left δ_{v1} (mm)		Settl Right δ_{v2} (mm)		Relative Settle $\Delta\delta v$	Horiz Displac δ_H (mm)		Width Found.	Angular Distortion	Lateral Strain
	x	y	x	y	$\delta v1-\delta v2$	x	y	Building	$\beta=\Delta\delta v/L$	$\varepsilon l=\delta_H/L$
Phase	21.5	-6.5	39.5	-6.5	(mm)	21.5	-6.5	L (m)	(x 10-3)	(x 10-3)
Service	-49.89		-22.12		27.76	-14.96		18	1.54	0.83



Graph IV-6: Criterion of Boscardin and Cording- Service Stage-

Model with Plane Sole Section in New Tunnels- Mixed

(c) Analysis of the Fine Profile

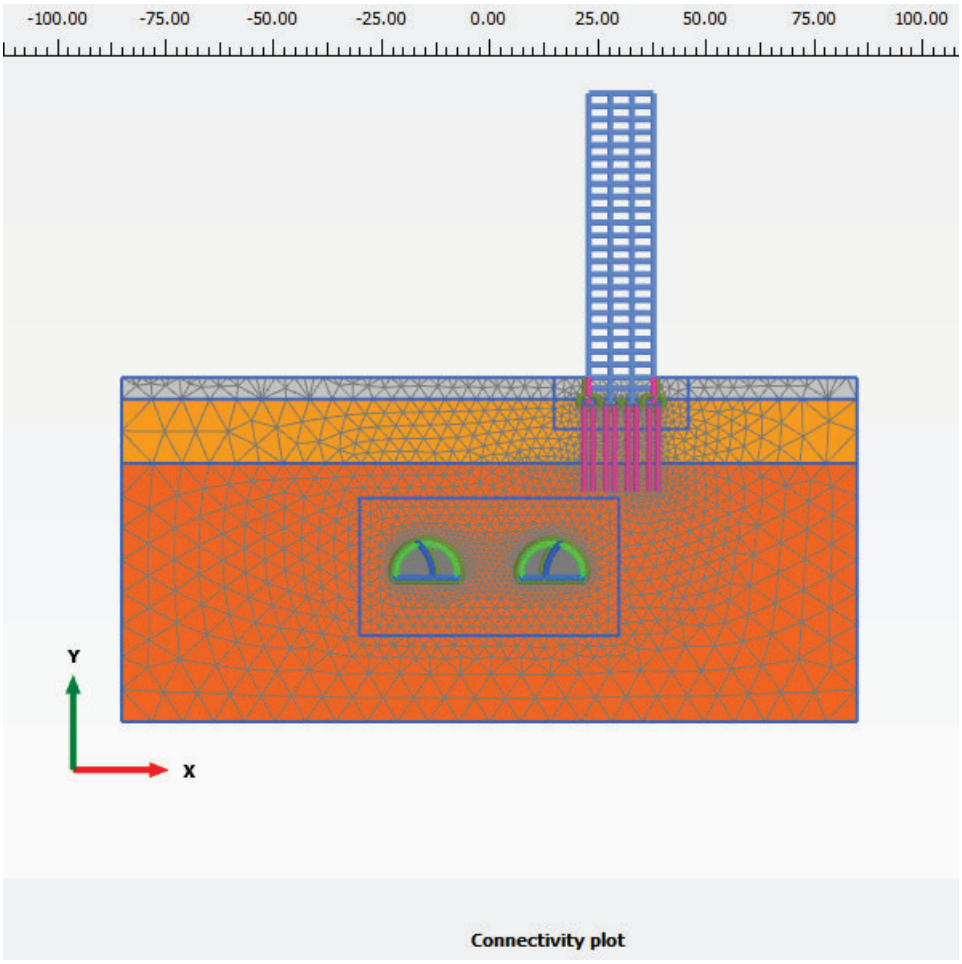


Figure IV-15: Fine Model with Pre-existing Building and plane sole section in new road tunnels

(c.1) Service Stage

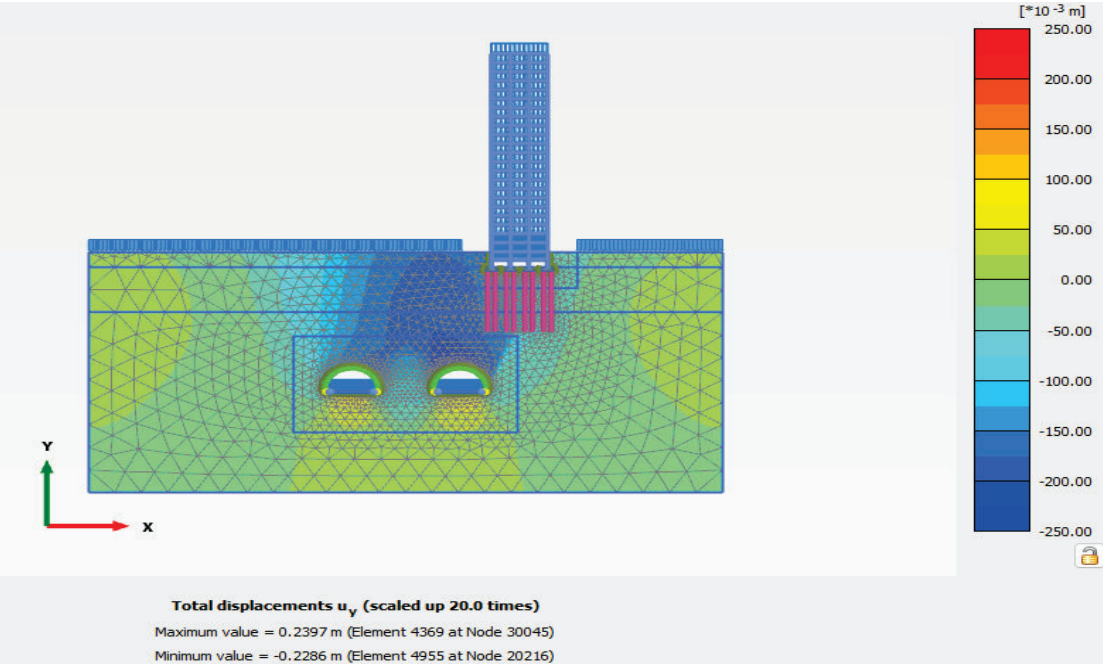


Figure IV-16: Vertical Settlement in Service- MC- Fine

Plane Sole Section in New Tunnels

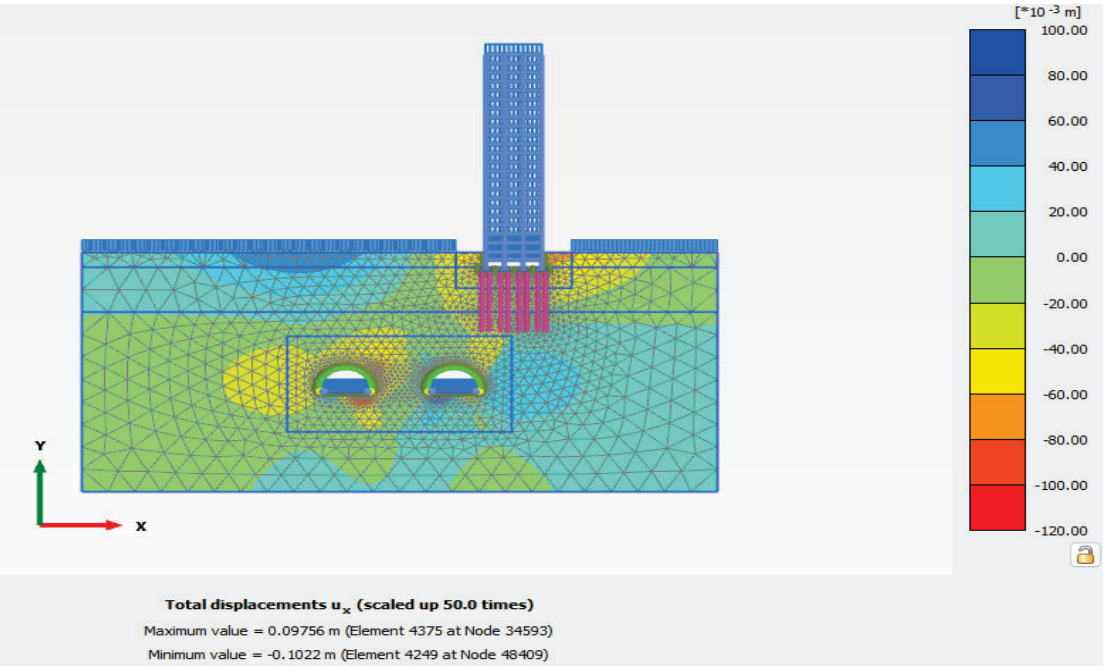


Figure IV-17: Horizontal Displacement in Service (WT and ET)- MC- Fine

Plane Sole Section in New Tunnels

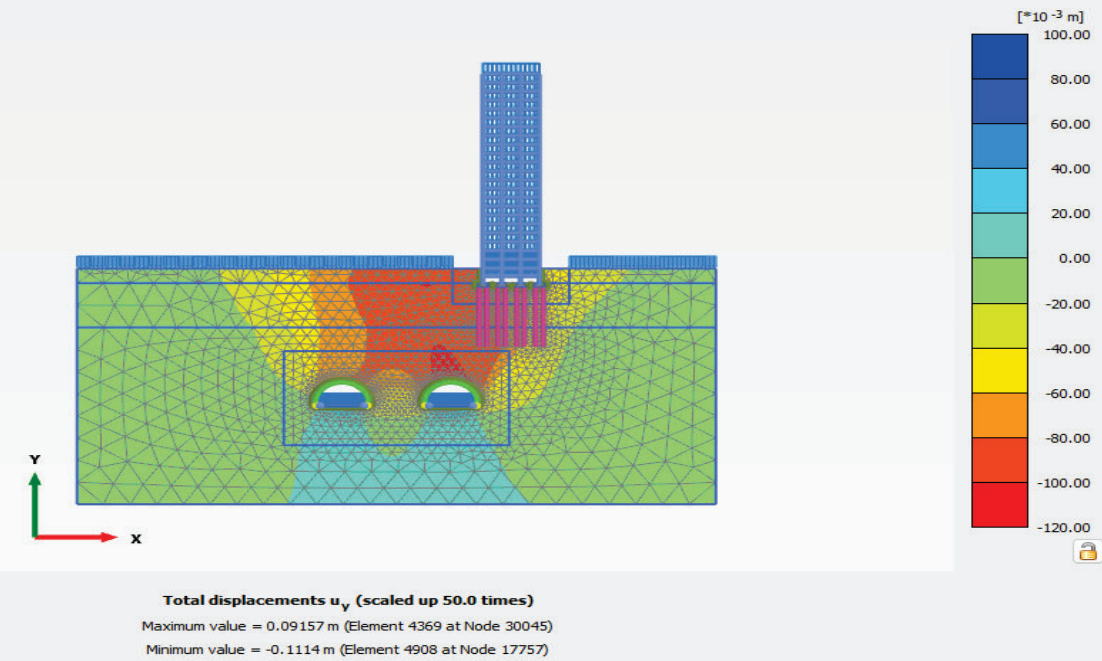


Figure IV-18: Vertical Settlement in Service- HS- Fine

Plane Sole Section in New Tunnels

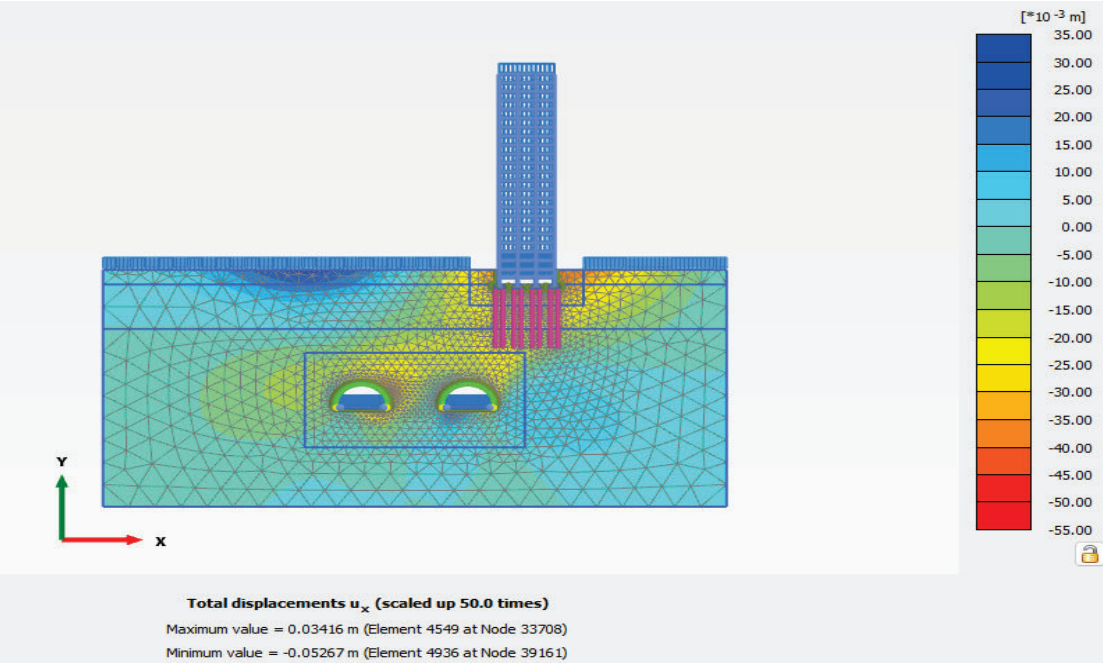


Figure IV-19: Horizontal Displacement in Service (WT and ET)- HS- Fine

Plane Sole Section in New Tunnels

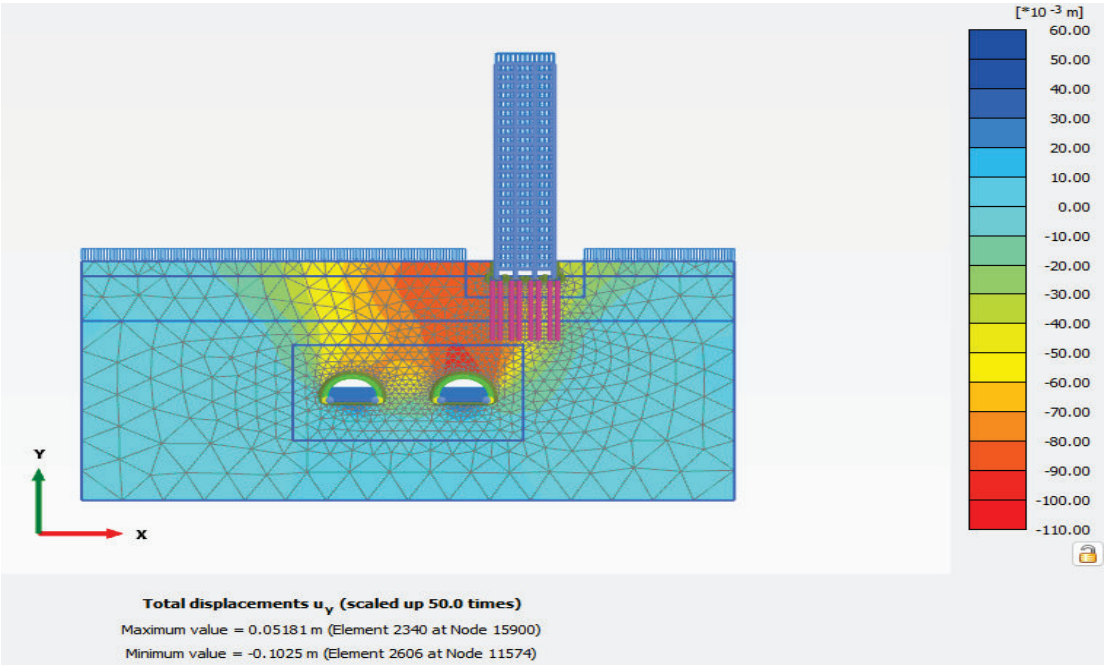


Figure IV-20: Vertical Settlement in Service- HSs- Fine

Plane Sole Section in New Tunnels

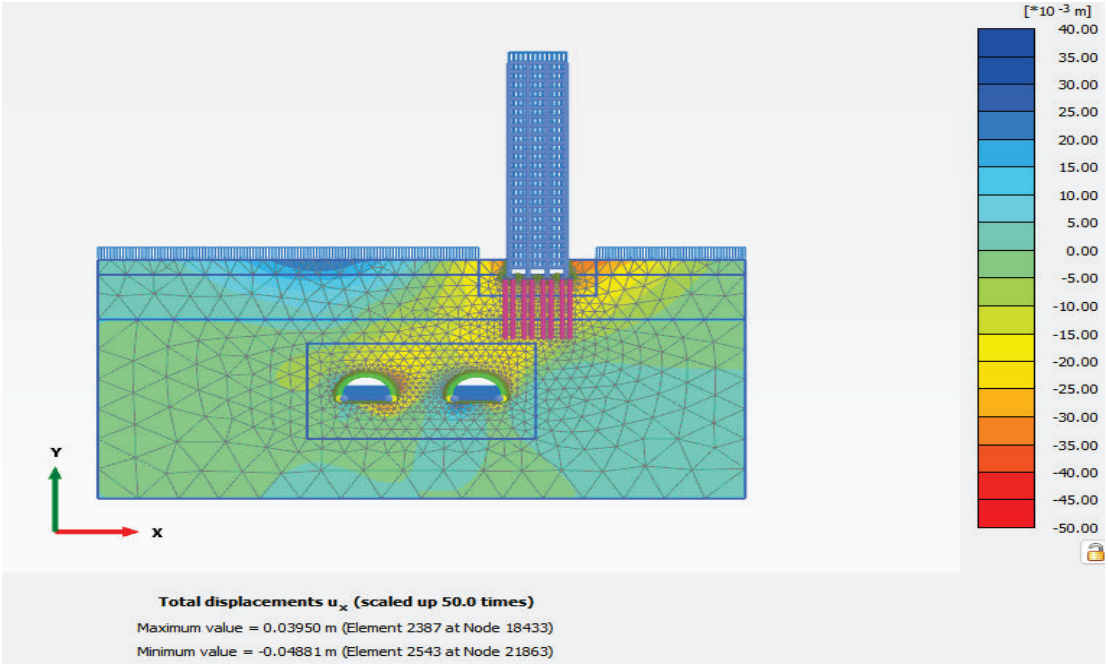
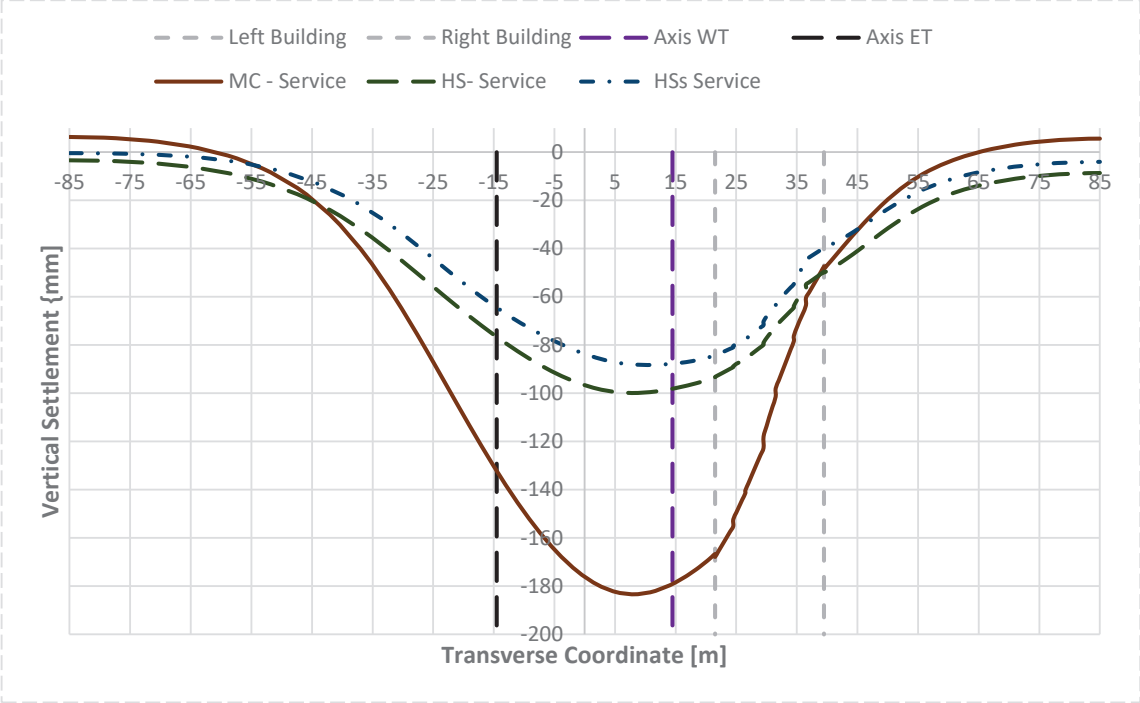
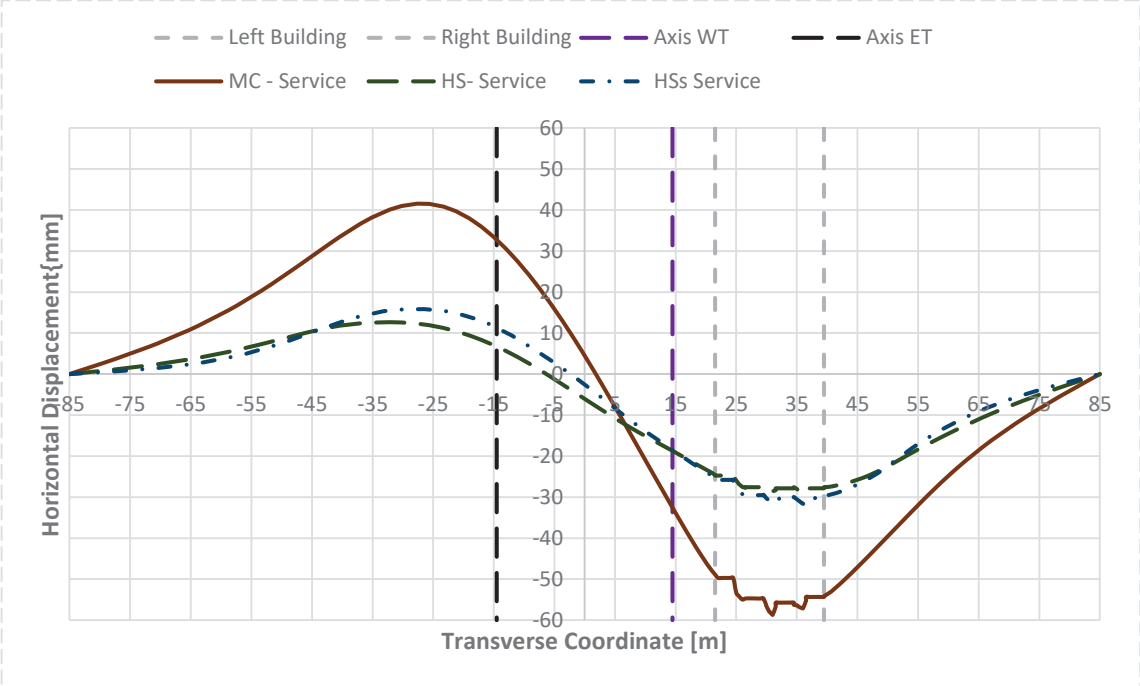


Figure IV-21: Horizontal Displacement in Service (WT and ET)- HSs- Fine

Plane Sole Section in New Tunnels



Graph IV-7: Diagram of Vertical Settlement on Building Foundation - Service Stage – Model with Plane Sole Section in New Tunnels- Fine



Graph IV-8: Diagram of Horizontal Displacement on Building Foundation - Service Stage – Model with Plane Sole Section in New Tunnels- Fine

Table IV-7: Verification of the Deformation in Foundation Building according to Boscardin & Cording- MC Model- Service Stage- Fine- Plane Sole Section in New Tunnels

Coord. in model (m)	Settl Left δ_{v1} (mm)		Settl Right δ_{v2} (mm)		Relative Settle $\Delta\delta v$	Horiz Displac δ_H (mm)		Width Found.	Angular Distortion	Lateral Strain
	x	y	x	y	$\delta v1-\delta v2$	x	y	Building	$\beta = \Delta\delta v/L$	$\varepsilon l = \delta_H/L$
Phase	21.5	-6.5	39.5	-6.5	(mm)	21.5	-6.5	L (m)	(x 10-3)	(x 10-3)
Service	-167.25		-47.88		119.37	-49.31		18	6.63	2.74

Table IV-8: Verification of the Deformation in Foundation Building according to Boscardin & Cording- HS Model- Service Stage- Fine- Plane Sole Section in New Tunnels

Coord. in model (m)	Settl Left δ_{v1} (mm)		Settl Right δ_{v2} (mm)		Relative Settle $\Delta\delta v$	Horiz Displac δ_H (mm)		Width Found.	Angular Distortion	Lateral Strain
	x	y	x	y	$\delta v1-\delta v2$	x	y	Building	$\beta = \Delta\delta v/L$	$\varepsilon l = \delta_H/L$
Phase	21.5	-6.5	39.5	-6.5	(mm)	21.5	-6.5	L (m)	(x 10-3)	(x 10-3)
Service	-93.33		-49.74		43.59	-30.09		18	2.42	1.67

Table IV-9: Verification of the Deformation in Foundation Building according to Boscardin & Cording- HSs Model- Service Stage- Fine- Plane Sole Section in New Tunnels

Coord. in model (m)	Settl Left δ_{v1} (mm)		Settl Right δ_{v2} (mm)		Relative Settle $\Delta\delta v$	Horiz Displac δ_H (mm)		Width Found.	Angular Distortion	Lateral Strain
	x	y	x	y	$\delta v1-\delta v2$	x	y	Building	$\beta = \Delta\delta v/L$	$\varepsilon l = \delta_H/L$
Phase	21.5	-6.5	39.5	-6.5	(mm)	21.5	-6.5	L (m)	(x 10-3)	(x 10-3)
Service	-84.35		-39.72		44.63	-25.56		18	2.48	1.42



Graph IV-9: Criterion of Boscardin and Cording- Service Stage-

Model with Plane Sole Section in New Tunnels- Fine

4.1.2 Verification of the Deformation in the New Road Tunnels

The maximum convergence deformations must be verified with the criterion established in chapter 3.7.3(a).

(a) Analysis of the Gravel Profile

(a.1) Construction Stage

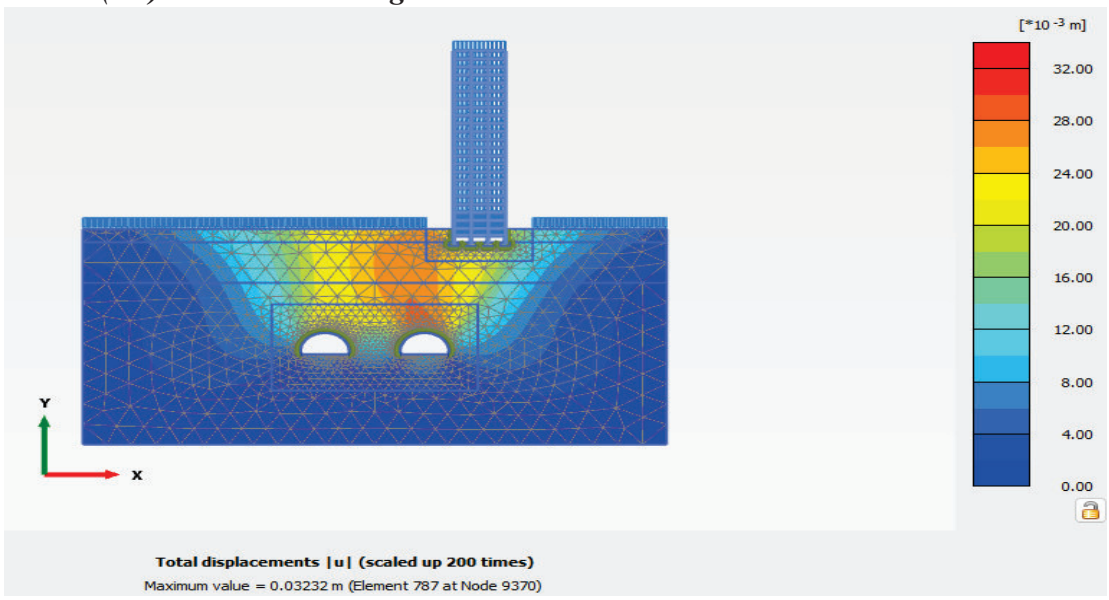


Figure IV-22: Maximum Displacement in Construction- HS- Gravel- Plane Sole Section in New Tunnels

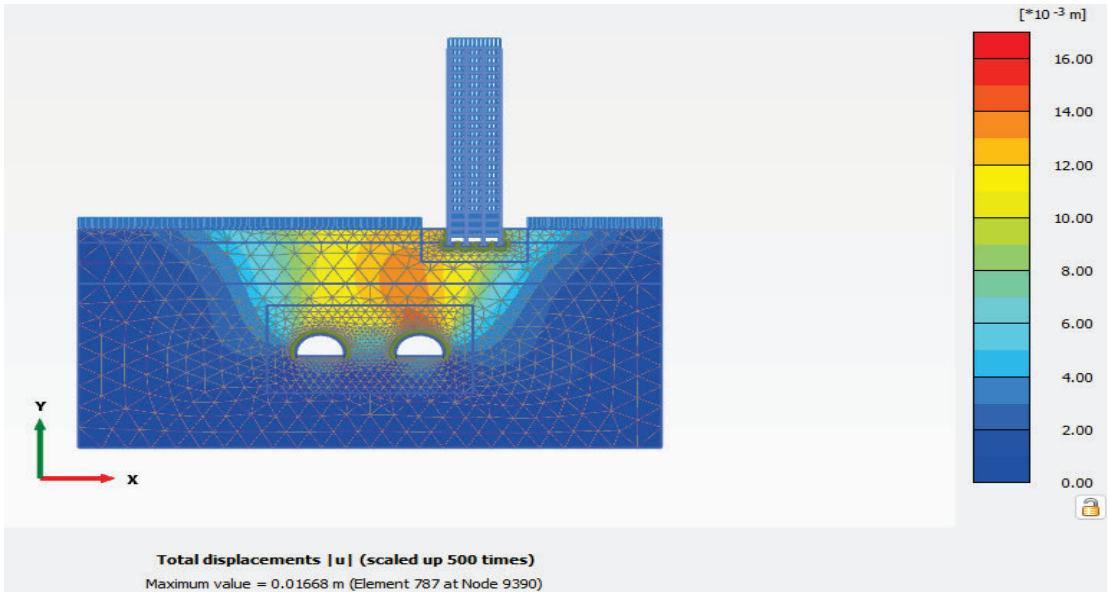


Figure IV-23: Maximum Displacement in Construction- HSs-Gravel- Plane Sole Section in New Tunnels

(a.2) Service Stage

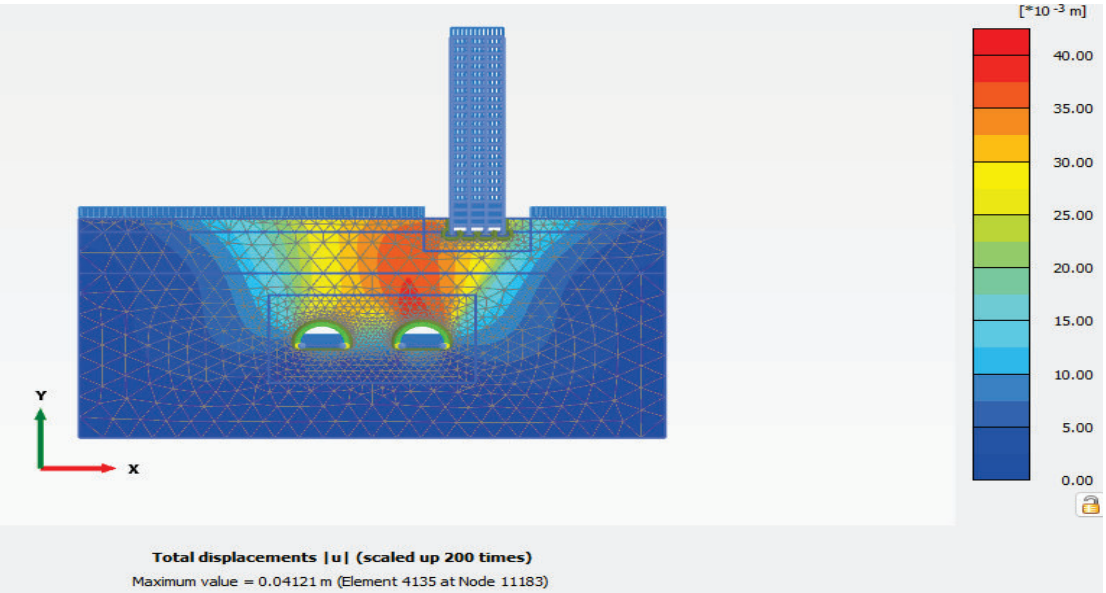


Figure IV-24: Maximum Displacement in Service- HS- Gravel-

Plane Sole Section in New Tunnels

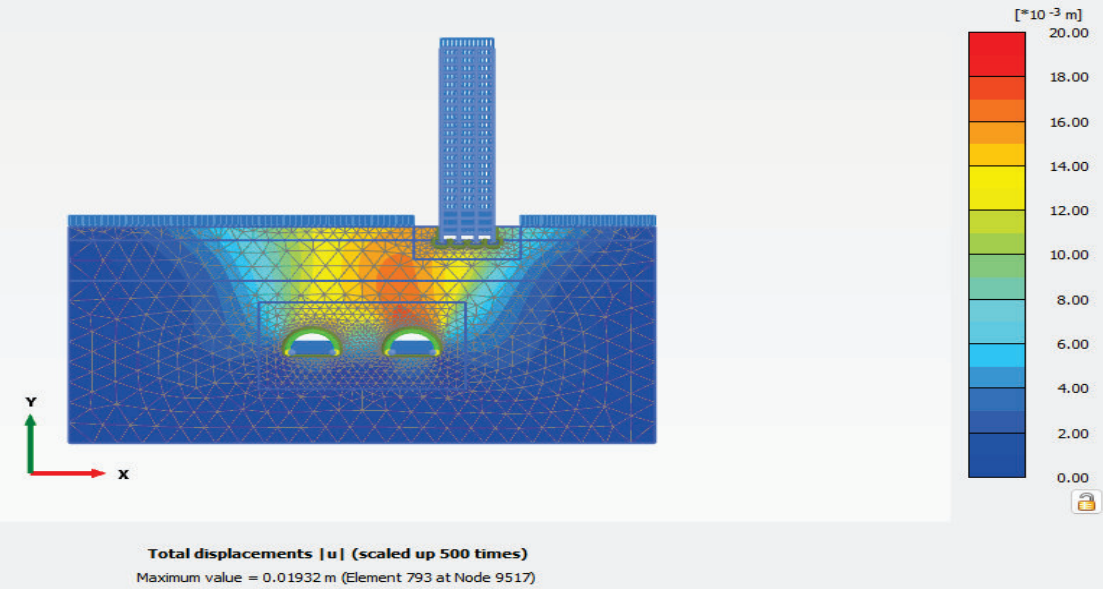


Figure IV-25: Maximum Displacement in Service- HSs- Gravel-

Plane Sole Section in New Tunnels

Table IV-10: Summary of Maximum Displacement Checks on New Road Tunnels–

Pre-existing Building – Gravel- Plane Sole Section in New Tunnels

Maximum Displacement [mm]							
Soil	Construction Stage			Service Stage			Admissible
	MC	HS	HSs	MC	HS	HSs	
Gravel	-	32.32	16.68	-	41.21	19.32	30

4.1.3 Verification of the Resistance in the New Road Tunnels

In the construction stage, the support of the new road tunnels must be verified through the criterion of admissible stresses, as defined in section 3.7.3(b).

In the service stage, the lining of the new road tunnels must be verified through the interaction diagram M-N and N-Q, as defined in section 3.7.3(b)..

The lining of the new road tunnels are verified, with their corresponding concrete thicknesses and reinforcement, as defined in Figure III-10 and sections 3.3.2 and 3.3.2(b).

$e = 0.50\ m$ Concrete thicknesses for the calculation

(Lining thicknesses = 0.30 m + 2/3 Support thicknesses = 0.20 m)

$A_s = 3.35\ cm^2/m$ ACMA335 Mesh in Internal and External face

$A_{s1} = 7.60\ cm^2/m$ 2Ø22 Bar of the Reticulate Frame in Internal face

$A_{s1} = 8.04\ cm^2/m$ 1Ø32 Bar of the Reticulate Frame in External face

(a) Analysis of the Gravel Profile

(a.1) Construction Stage

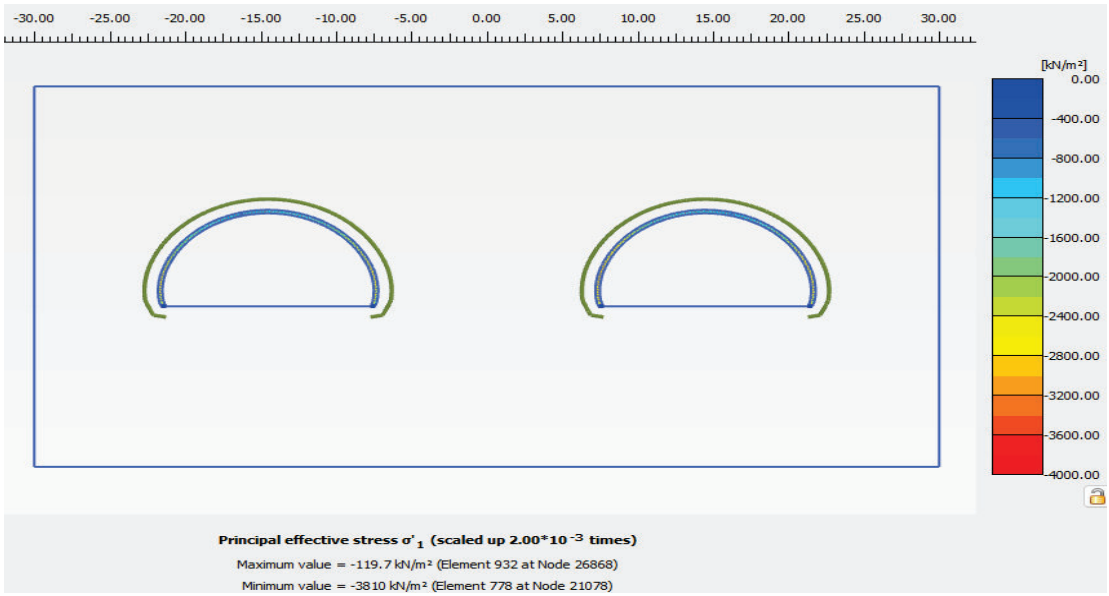


Figure IV-26: Major Principal effective Stress on Support- HSs – Gravel-Plane Sole Section in New Tunnels

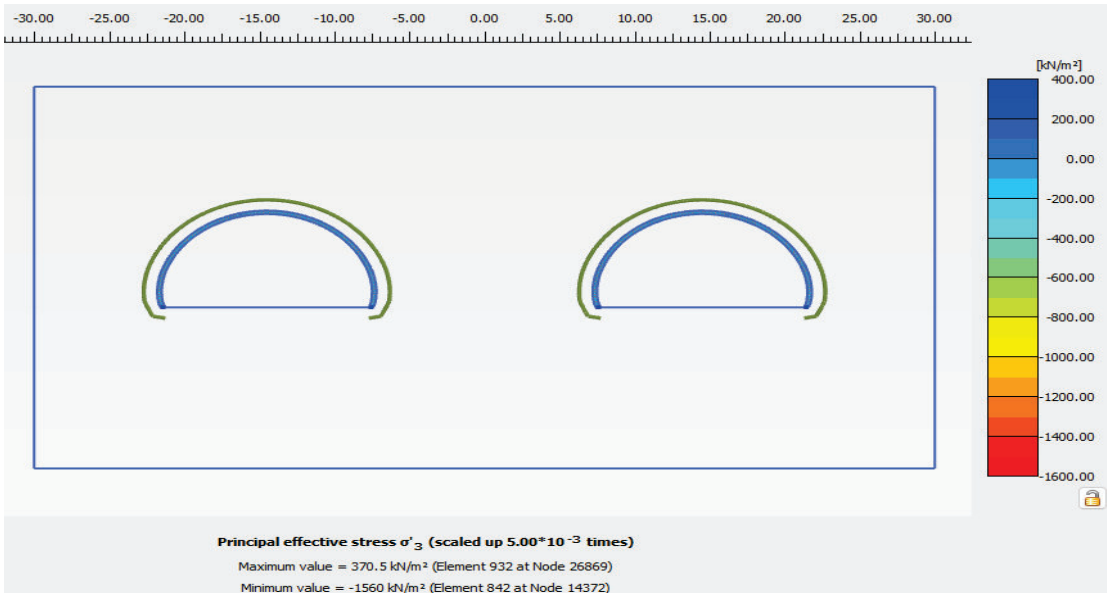


Figure IV-27: Minor Principal effective Stress on Support- HSs – Gravel-Plane Sole Section in New Tunnels

Table IV-11: Verification of Admissible Stress- HSs- Gravel-

Plane Sole Section in New Tunnels

σ´1 [MPa]	σ´3 [MPa]	σ´1adm [MPa]	σ´3adm [MPa]	σ´1 < σ´1 adm	σ´3 < σ´3 adm
-3.81	1.56	-16	2	CHECK	CHECK

(a.2) Service Stage

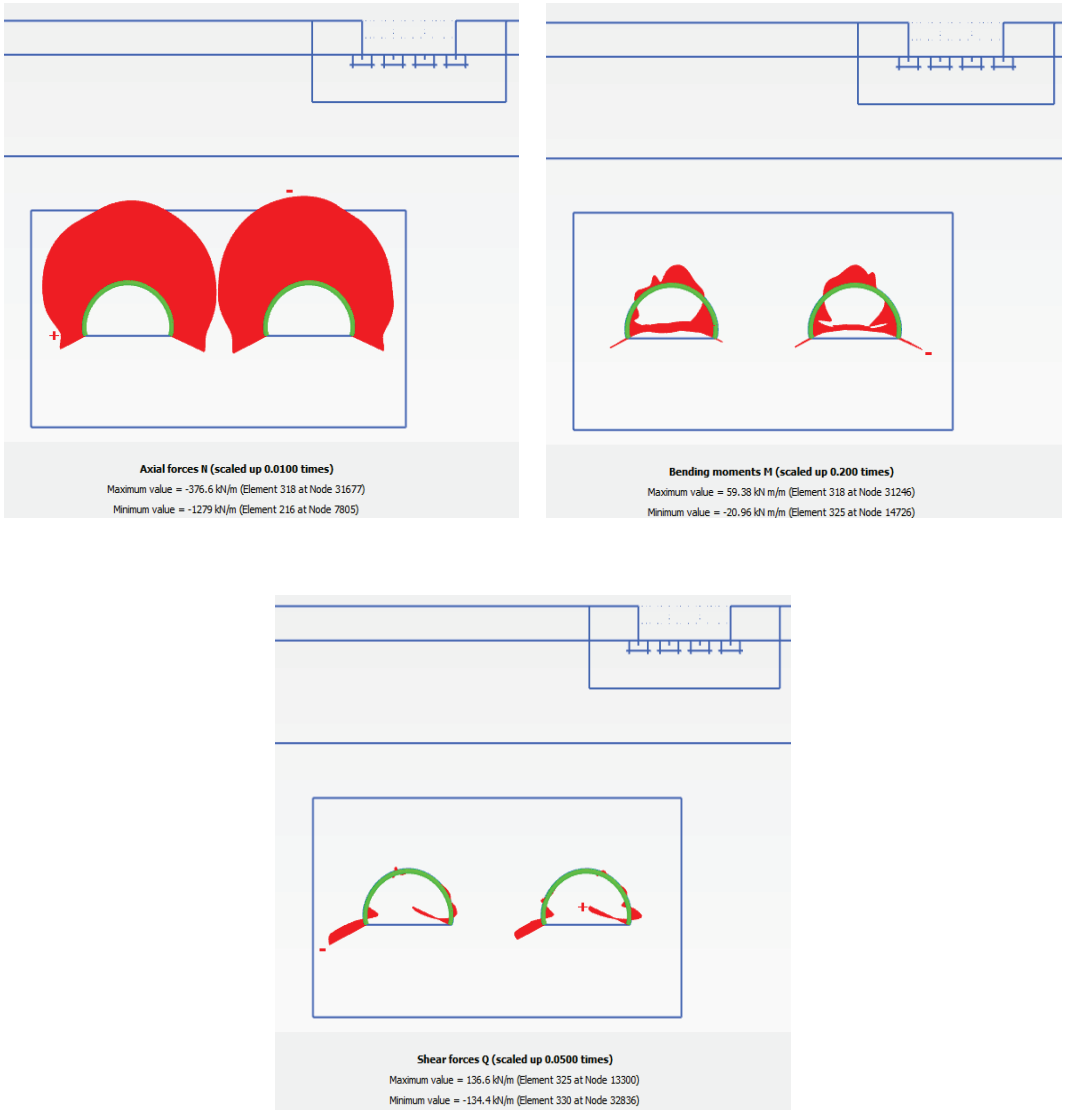
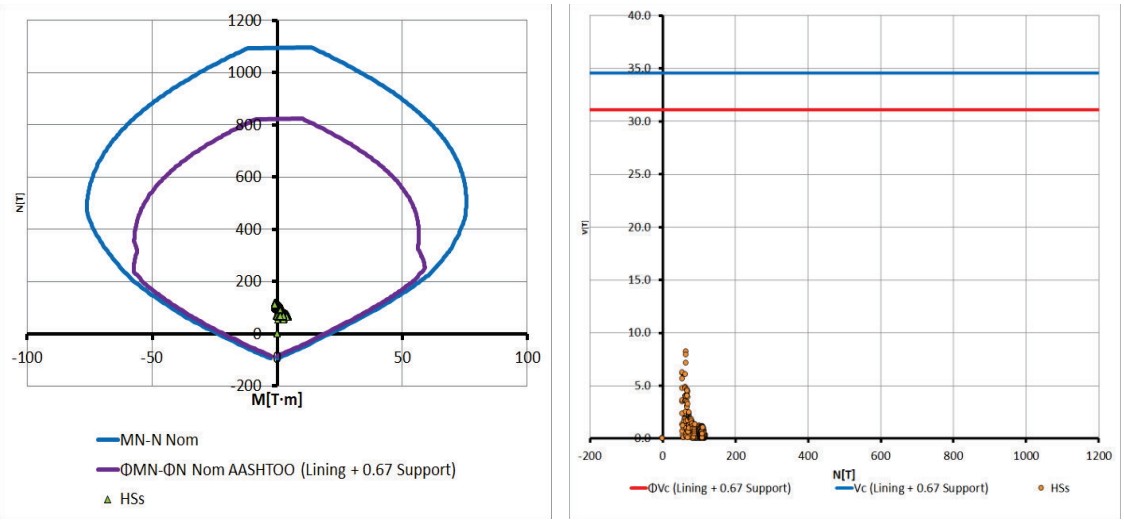


Figure IV-28: Forces Diagram, Axial, Bending and Shear on Lining- Service Stage- HSs- Gravel- Plane Sole Section in New Tunnels



Graph IV-10: : Interaction M-N and N-Q Diagram- Lining of the new road tunnels-

Service Stage- Gravel- Plane Sole Section in New Tunnels

4.1.4 Verification of the Capacity of the Soil

The following shows the plastification of the soil in construction and in service and applies the acceptability criteria explained in section 3.7.4.

(a) Construction Stage

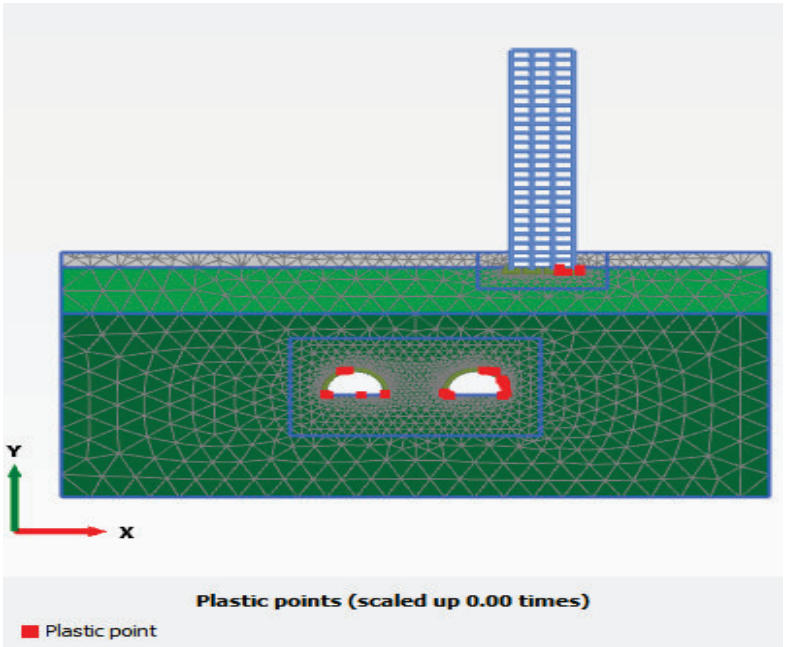


Figure IV-29: Plastification- Construction Stage- HSs- Gravel- Plane Sole Section in New Tunnels

(b) Service Stage

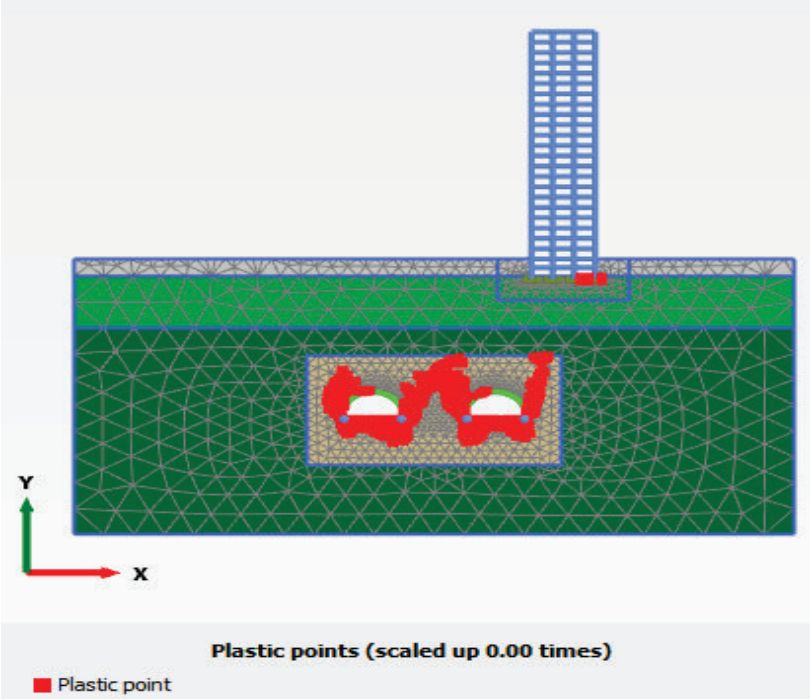


Figure IV-30: Plastification - Service Stage- HSs- Gravel-

Plane Sole Section in New Tunnels

Table IV-12: Plastification Verification on Soil- HSs- Gravel-

Plane Sole Section in New Tunnels

Stage	R-Plastic [m]	R-Plastic Admissible [m]	Verification
Construction	8	14	CHECK
Service	14	14	CHECK

4.2. Variation of the Constitutive Soil Model with Counter-vault Section in two excavation phases in Mixed and Fine Soil

4.2.1 Verification of the Deformation in the Pre-existing Building (B)

(a) Analysis of the Mixed Profile

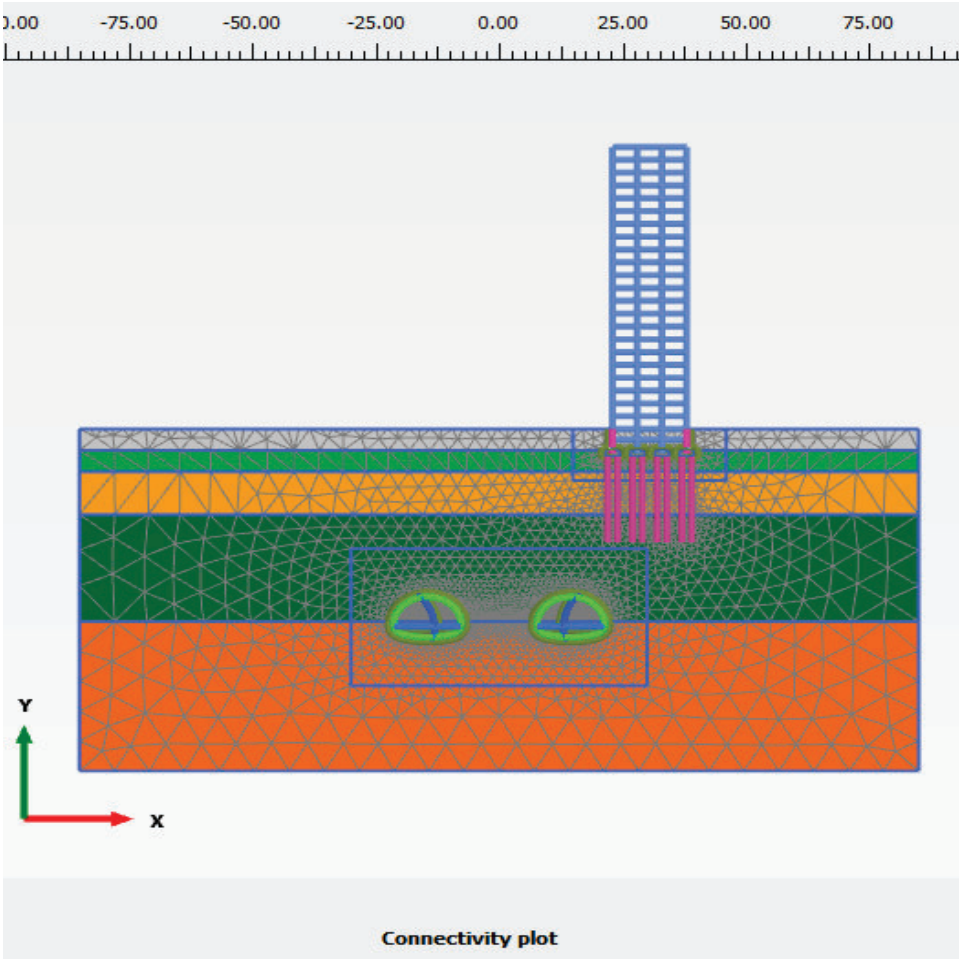


Figure IV-31: Mixed Model with Pre-existing Building and Counter-vault section in new road tunnels

(a.1) Service Stage

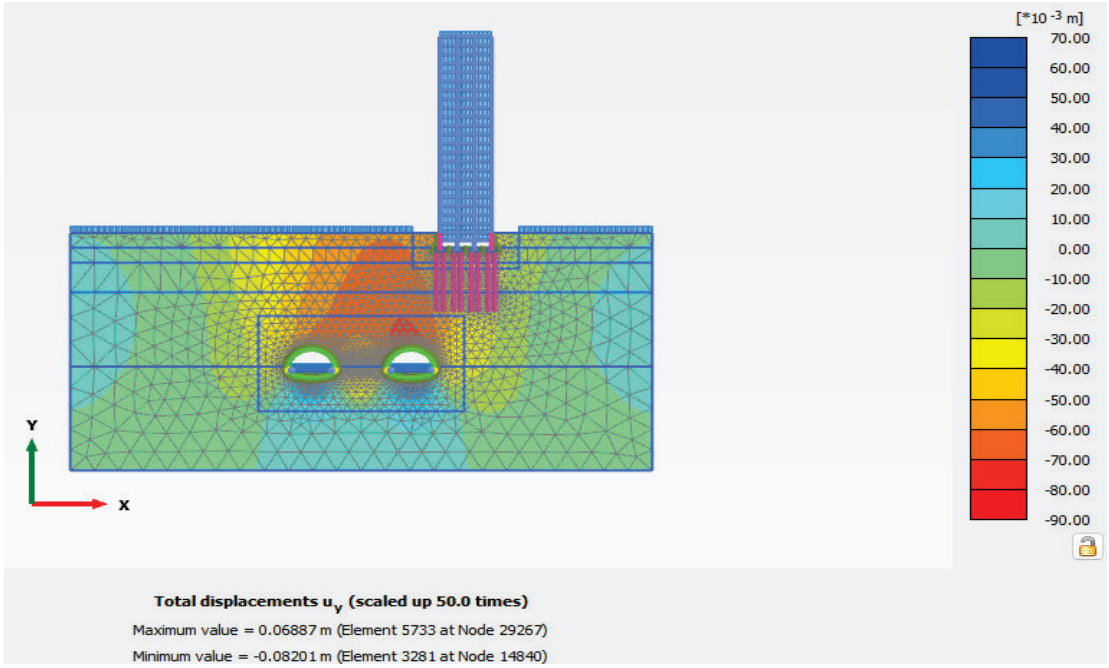


Figure IV-32: Vertical Settlement in Service- MC- Mixed

Counter-vault Section in New Tunnels

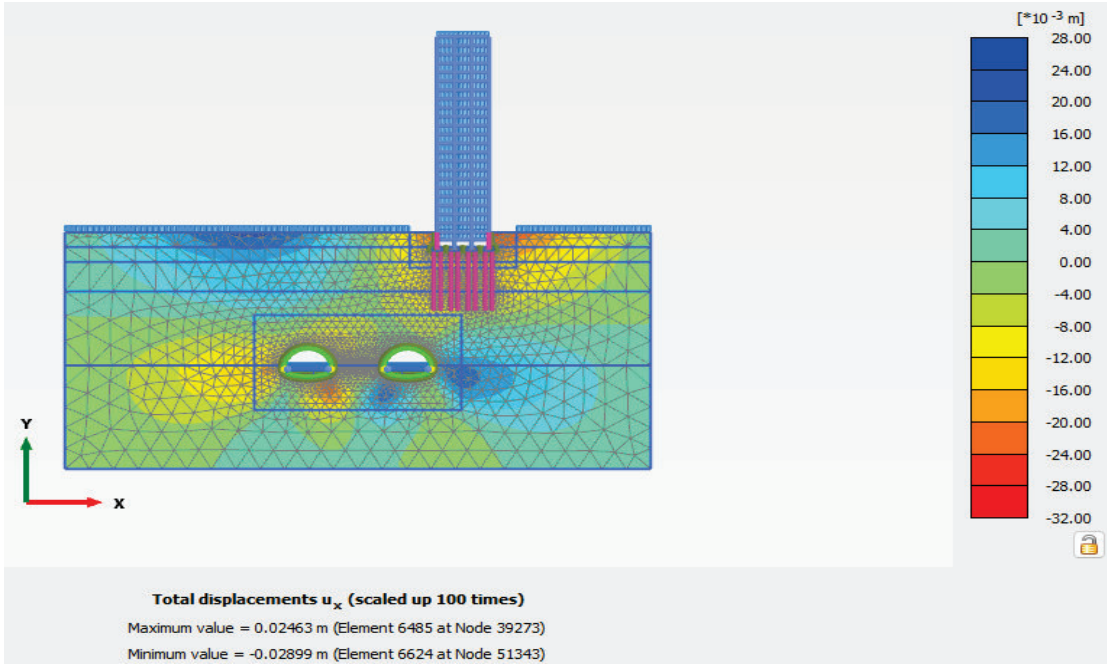


Figure IV-33: Horizontal Displacement in Service (WT and ET)- MC- Mixed

Counter-vault Section in New Tunnels

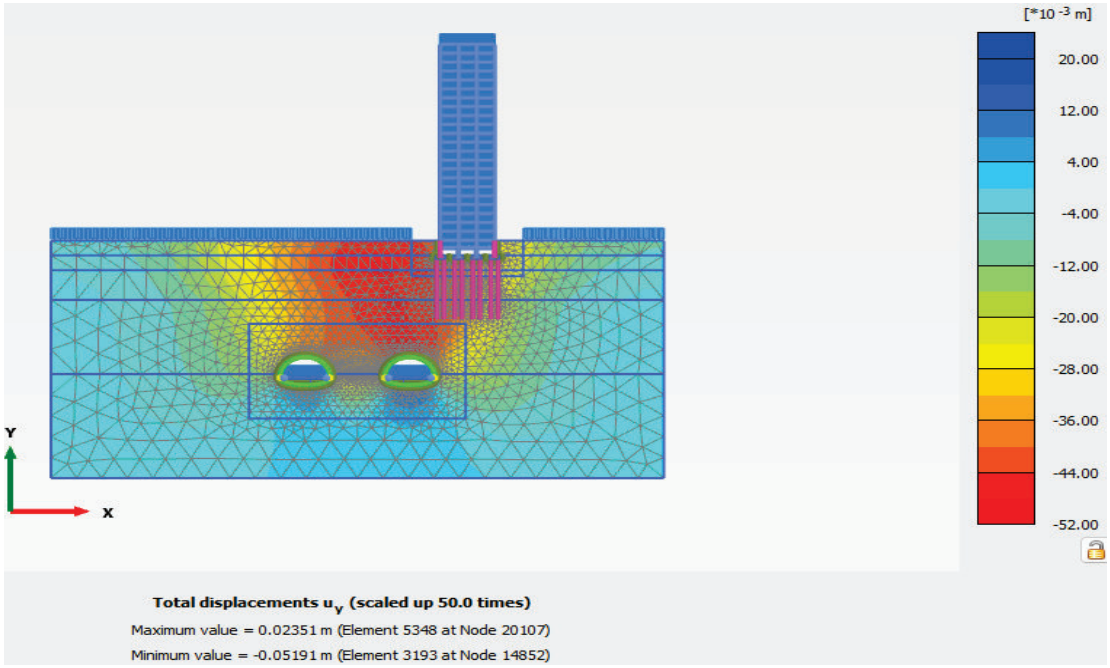


Figure IV-34: Vertical Settlement in Service- HS- Mixed

Counter-vault Section in New Tunnels

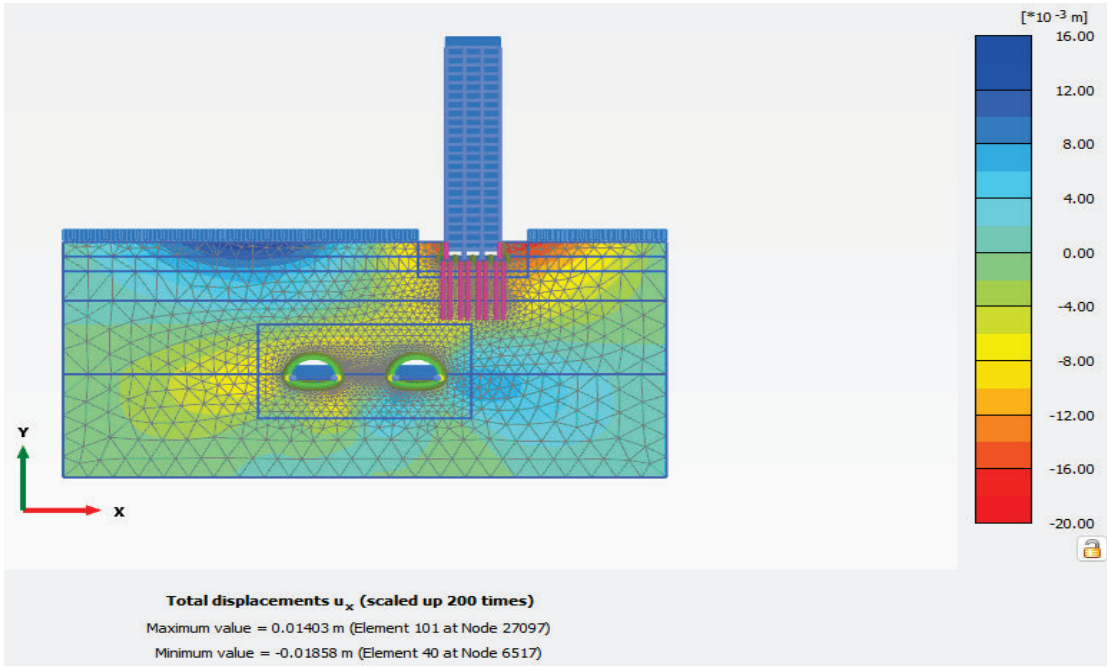


Figure IV-35: Horizontal Displacement in Service (WT and ET)- HS- Mixed

Counter-vault Section in New Tunnels

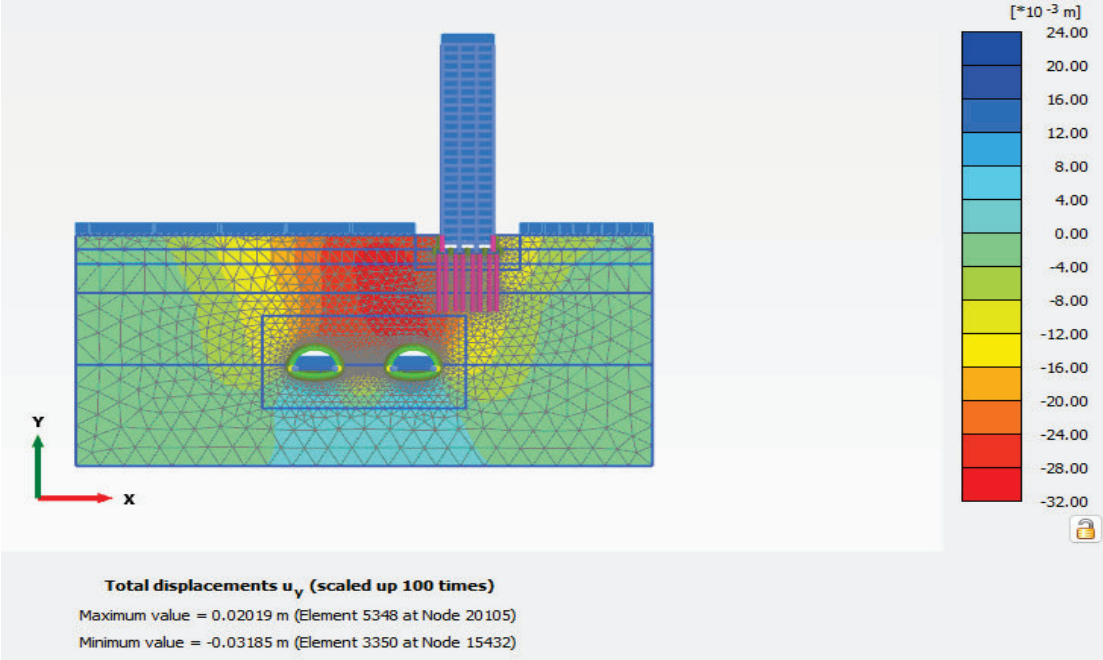


Figure IV-36: Vertical Settlement in Service- HSs- Mixed

Counter-vault Section in New Tunnels

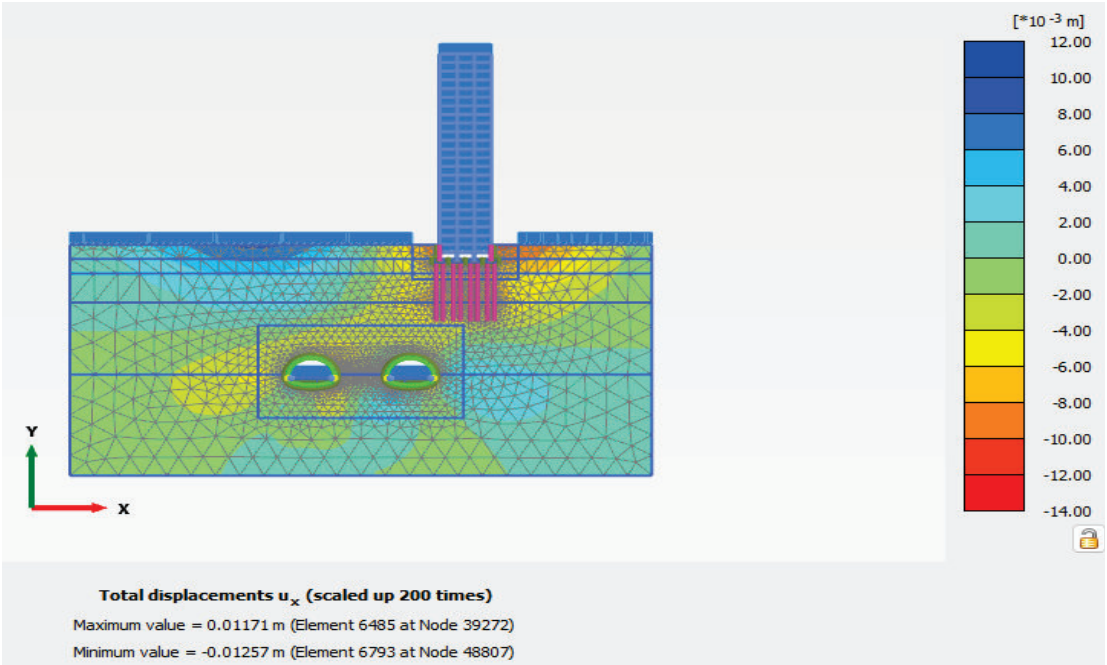
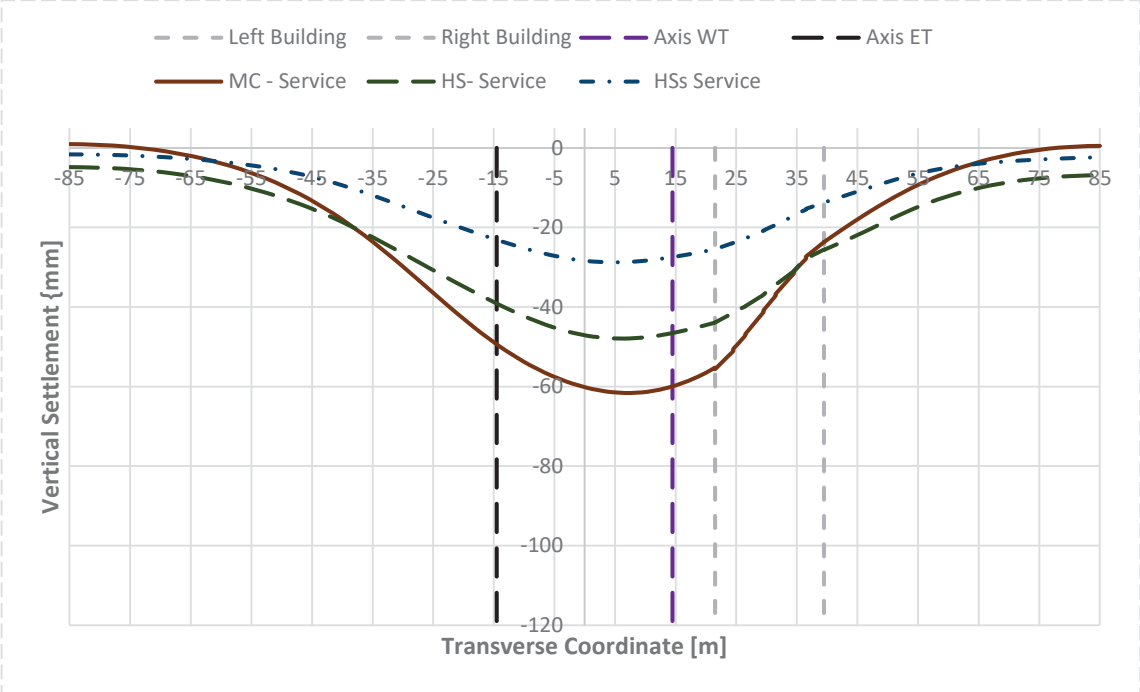
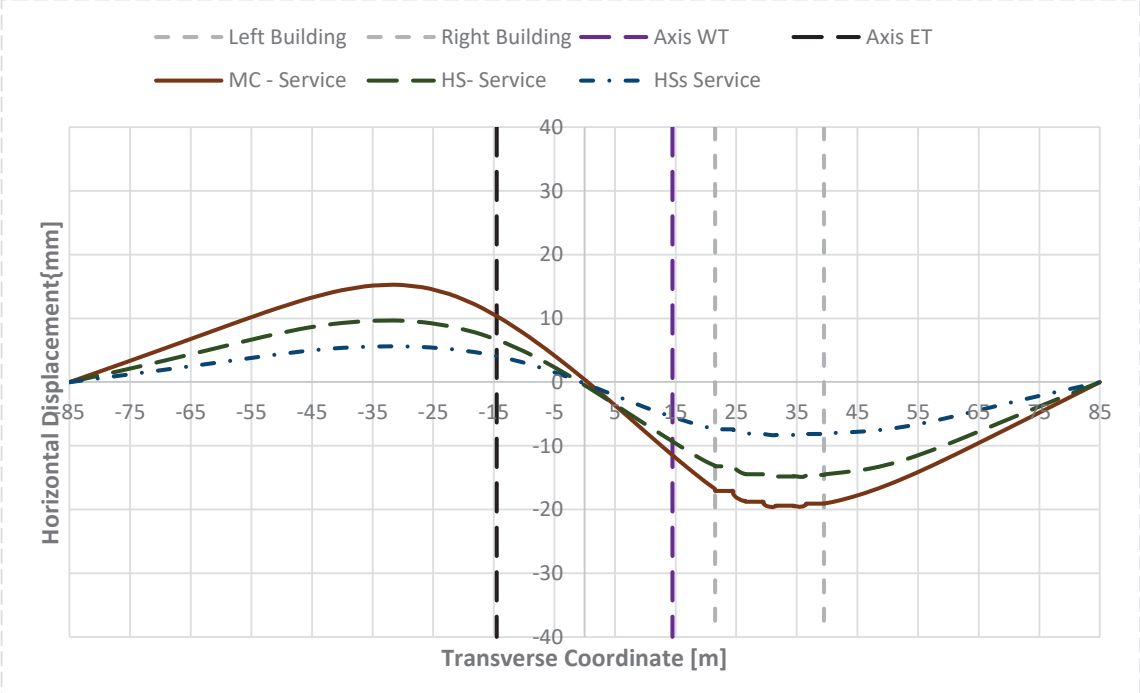


Figure IV-37: Horizontal Displacement in Service (WT and ET)- HSs- Mixed

Counter-vault Section in New Tunnels



Graph IV-11: Diagram of Vertical Settlement on Building Foundation - Service Stage – Model width Counter- vault Section in New Tunnels- Mixed



Graph IV-12: Diagram of Horizontal Displacement on Building Foundation - Service Stage – Model with Counter- vault Section in New Tunnels- Mixed

Table IV-13: Verification of the Deformation in Foundation Building according to Boscardin & Cording- MC Model- Service Stage- Mixed- Counter vault Section in New Tunnels

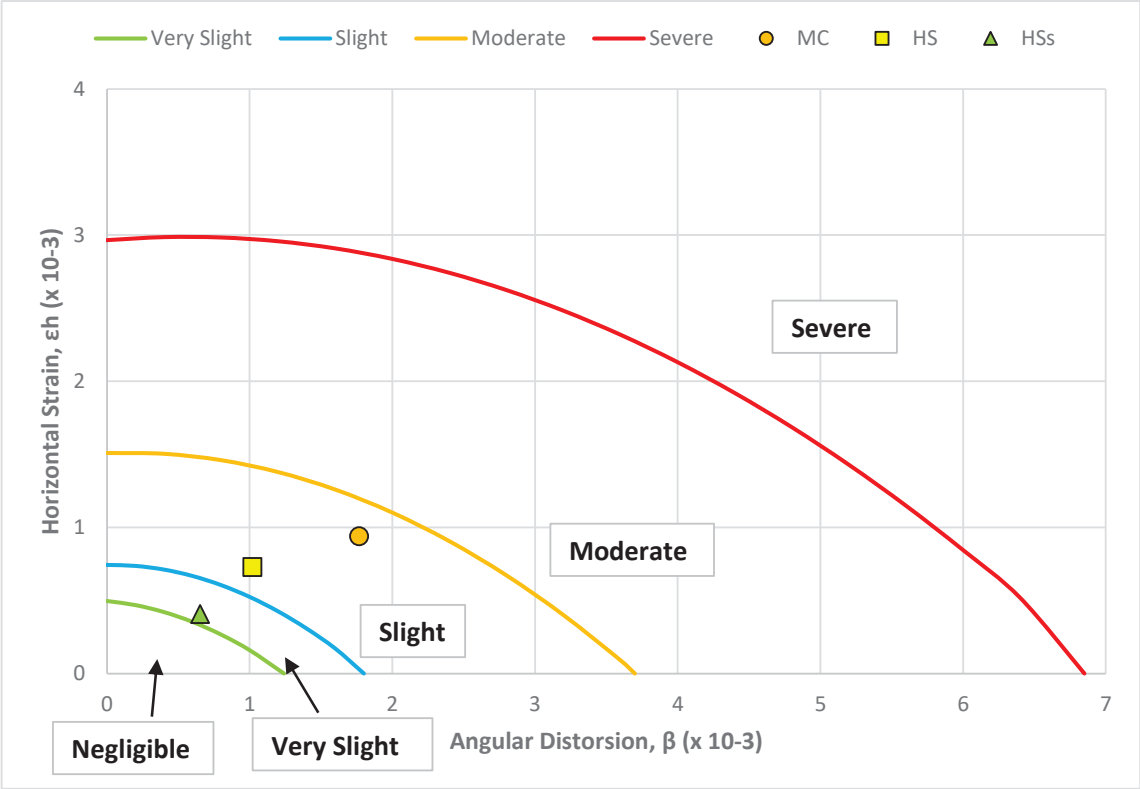
Coord. in model (m) Phase	Settl Left δ_{v1} (mm)		Settl Right δ_{v2} (mm)		Relative Settle $\Delta\delta v$	Horiz Displac δ_H (mm)		Width Found.	Angular Distortion	Lateral Strain
	x	y	x	y	$\delta v1-\delta v2$	x	y	Building	$\beta = \Delta\delta v/L$	$\varepsilon l = \delta_H/L$
	21.5	-6.5	39.5	-6.5	(mm)	21.5	-6.5	L (m)	(x 10-3)	(x 10-3)
Service	-55.42		-23.62		31.80	-16.93		18	1.77	0.94

Table IV-14: Verification of the Deformation in Foundation Building according to Boscardin & Cording- HS Model- Service Stage- Mixed- Counter vault Section in New Tunnels

Coord. in model (m) Phase	Settl Left δ_{v1} (mm)		Settl Right δ_{v2} (mm)		Relative Settle $\Delta\delta v$	Horiz Displac δ_H (mm)		Width Found.	Angular Distortion	Lateral Strain
	x	y	x	y	$\delta v1-\delta v2$	x	y	Building	$\beta = \Delta\delta v/L$	$\varepsilon l = \delta_H/L$
	21.5	-6.5	39.5	-6.5	(mm)	21.5	-6.5	L (m)	(x 10-3)	(x 10-3)
Service	-43.94		-25.61		18.33	-13.15		18	1.02	0.73

Table IV-15: Verification of the Deformation in Foundation Building according to Boscardin & Cording- HSs Model- Service Stage- Mixed- Counter vault Section in New Tunnels

Coord. in model (m) Phase	Settl Left δ_{v1} (mm)		Settl Right δ_{v2} (mm)		Relative Settle $\Delta\delta v$	Horiz Displac δ_H (mm)		Width Found.	Angular Distortion	Lateral Strain
	x	y	x	y	$\delta v1-\delta v2$	x	y	Building	$\beta = \Delta\delta v/L$	$\varepsilon l = \delta_H/L$
	21.5	-6.5	39.5	-6.5	(mm)	21.5	-6.5	L (m)	(x 10-3)	(x 10-3)
Service	-25.47		-13.72		11.74	-7.36		18	0.65	0.41



Graph IV-13: Criterion of Boscardin and Cording- Service Stage-

Model with Counter vault Section in New Tunnels- Mixed

(b) Analysis of the Fine Profile

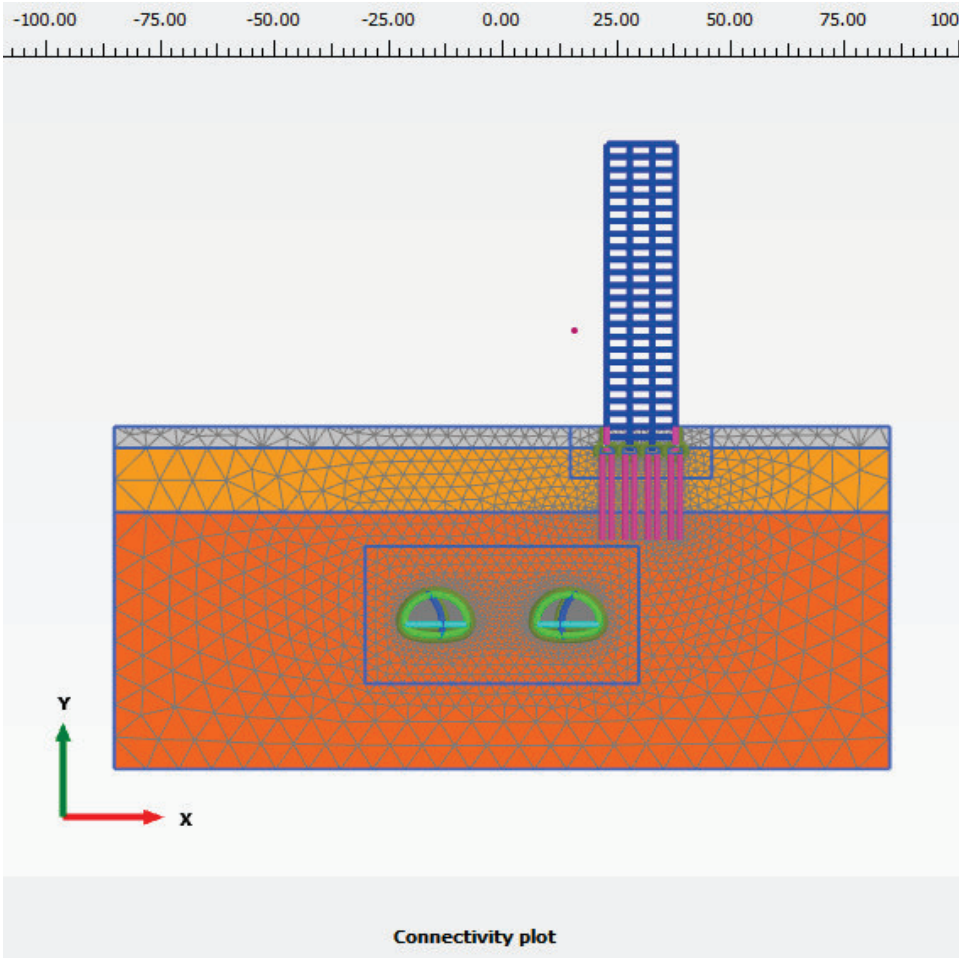


Figure IV-38: Fine Model with Pre-existing Building and counter vault section in new road tunnels

(b.1) Service Stage

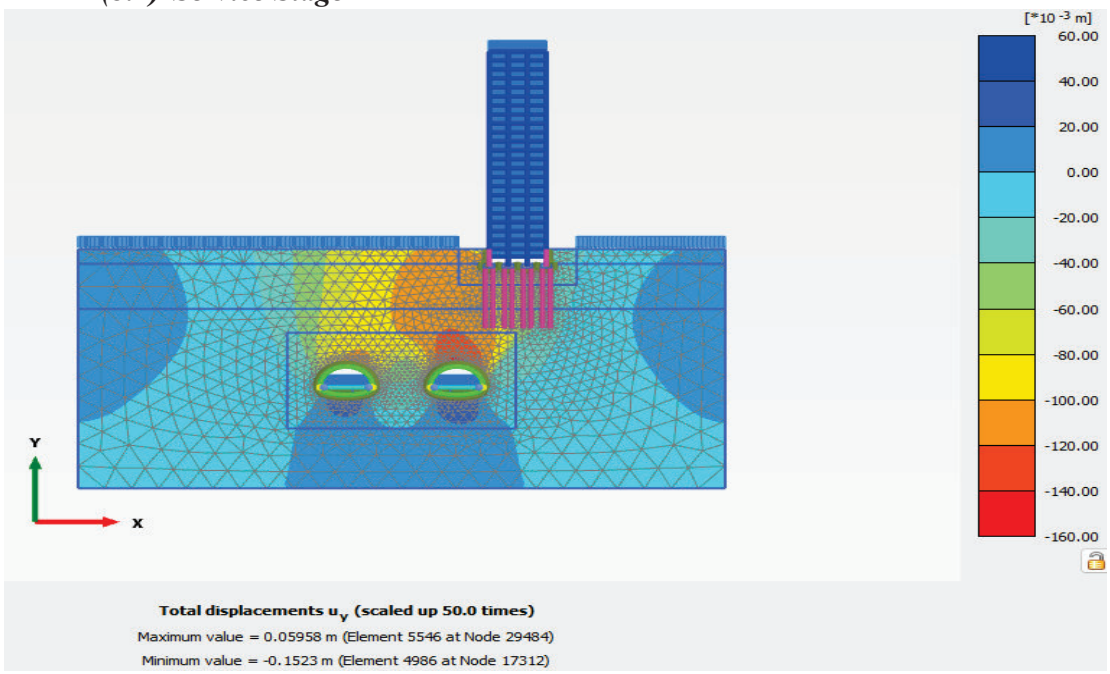


Figure IV-39: Vertical Settlement in Service- MC- Fine

Counter vault Section in New Tunnels

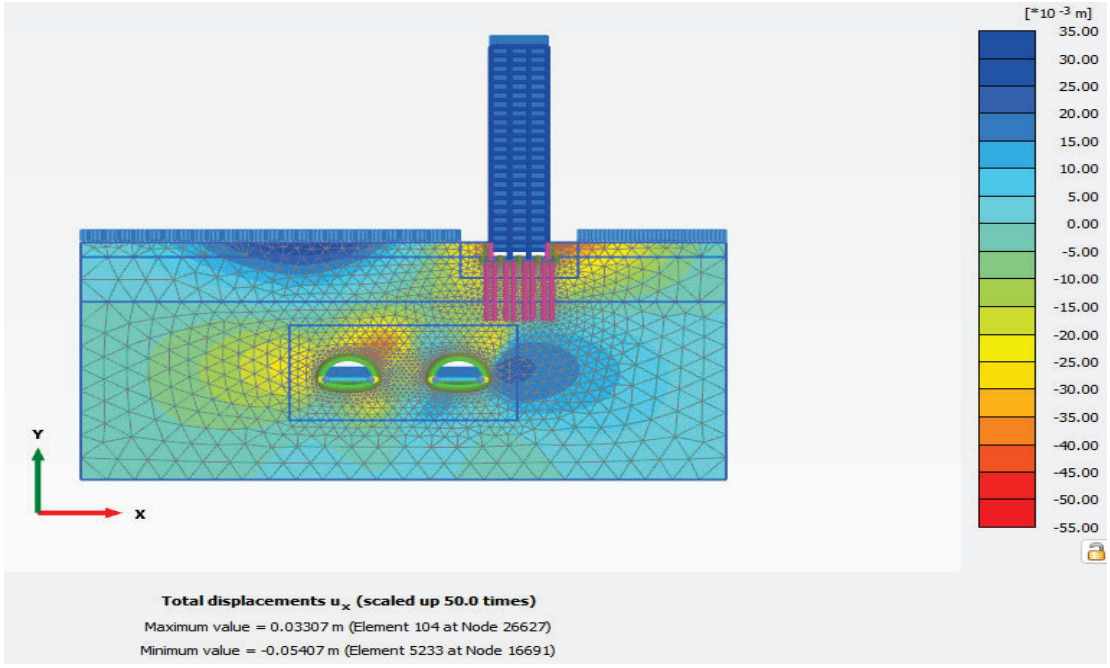


Figure IV-40: Horizontal Displacement in Service (WT and ET)- MC- Fine

Counter vault Section in New Tunnels

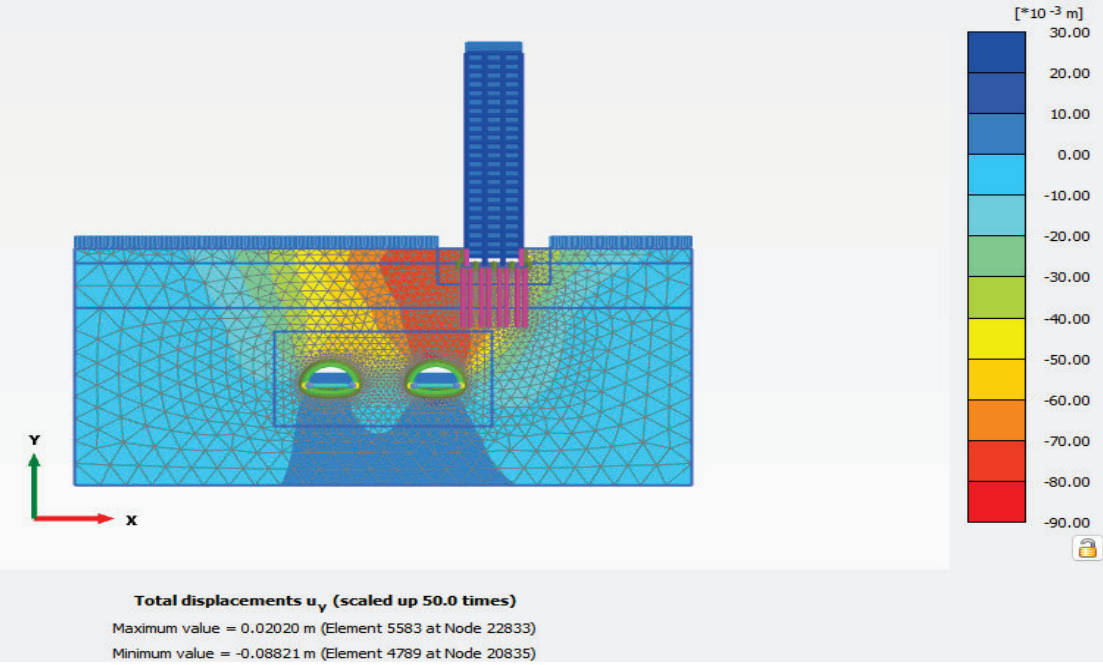


Figure IV-41: Vertical Settlement in Service- HS- Fine

Counter vault Section in New Tunnels

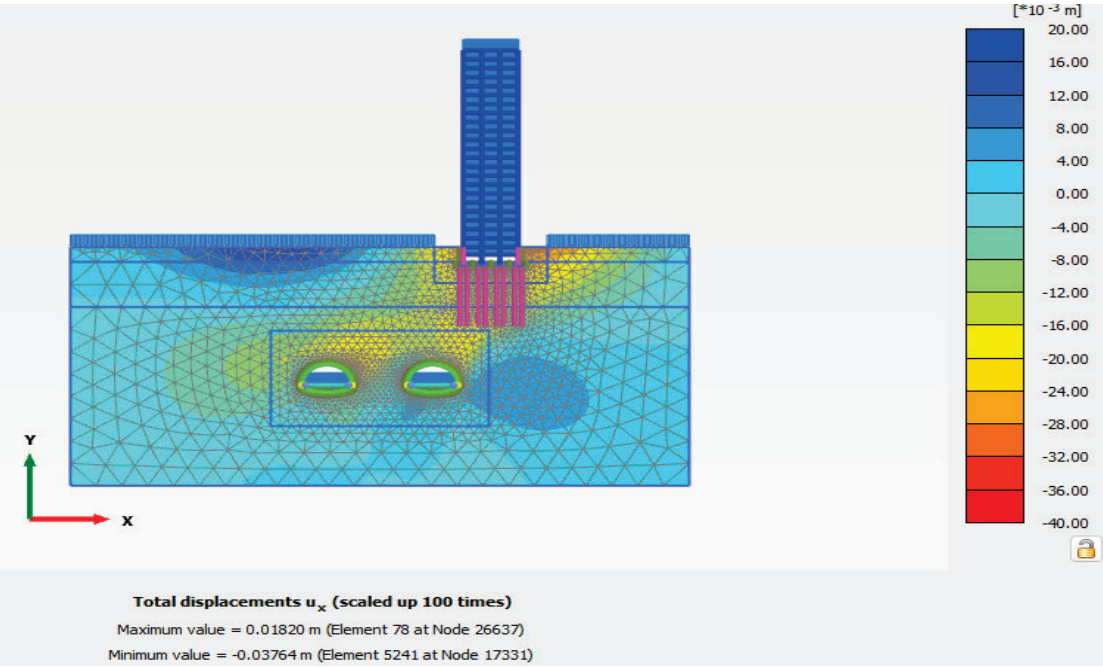


Figure IV-42: Horizontal Displacement in Service (WT and ET)- HS- Fine

Counter vault Section in New Tunnels

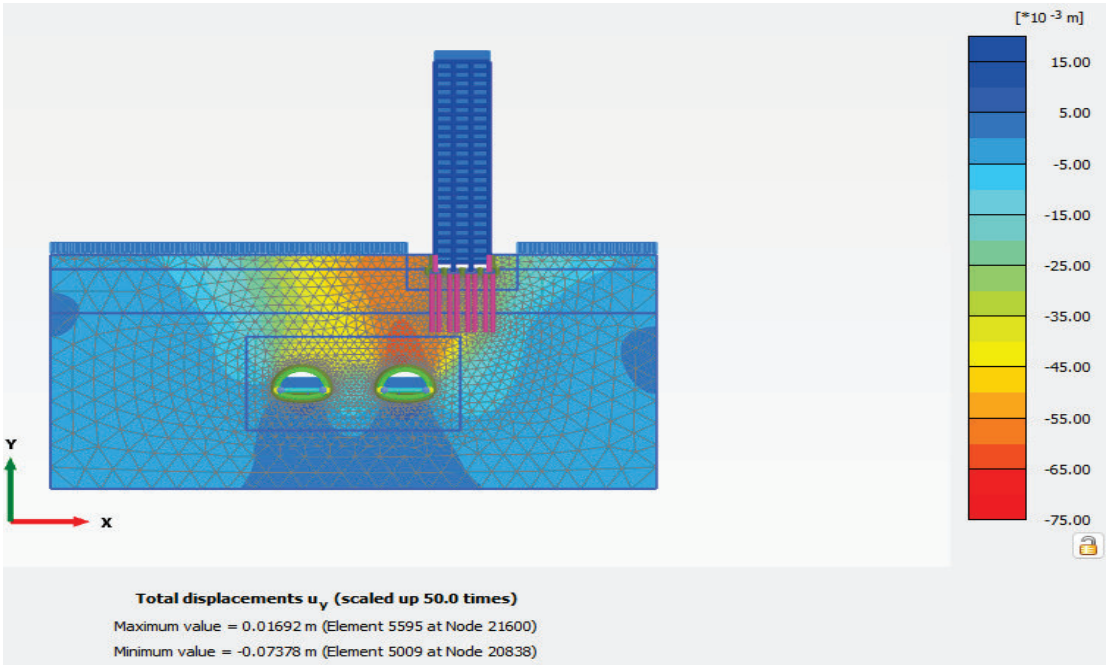


Figure IV-43: Vertical Settlement in Service- HSs- Fine

Counter vault Section in New Tunnels

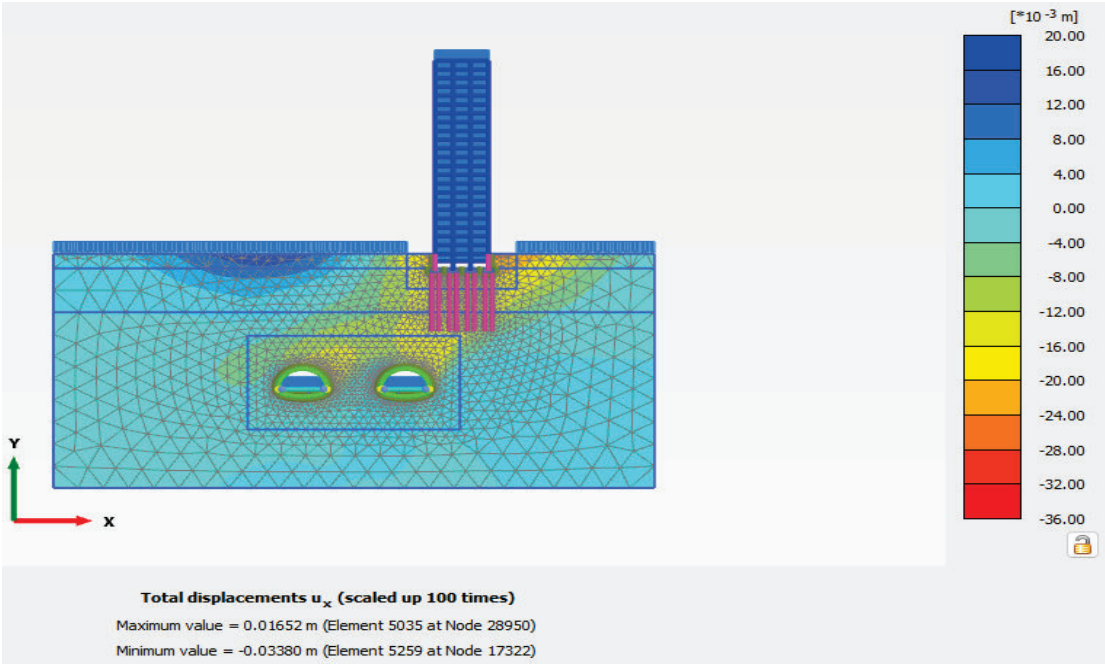
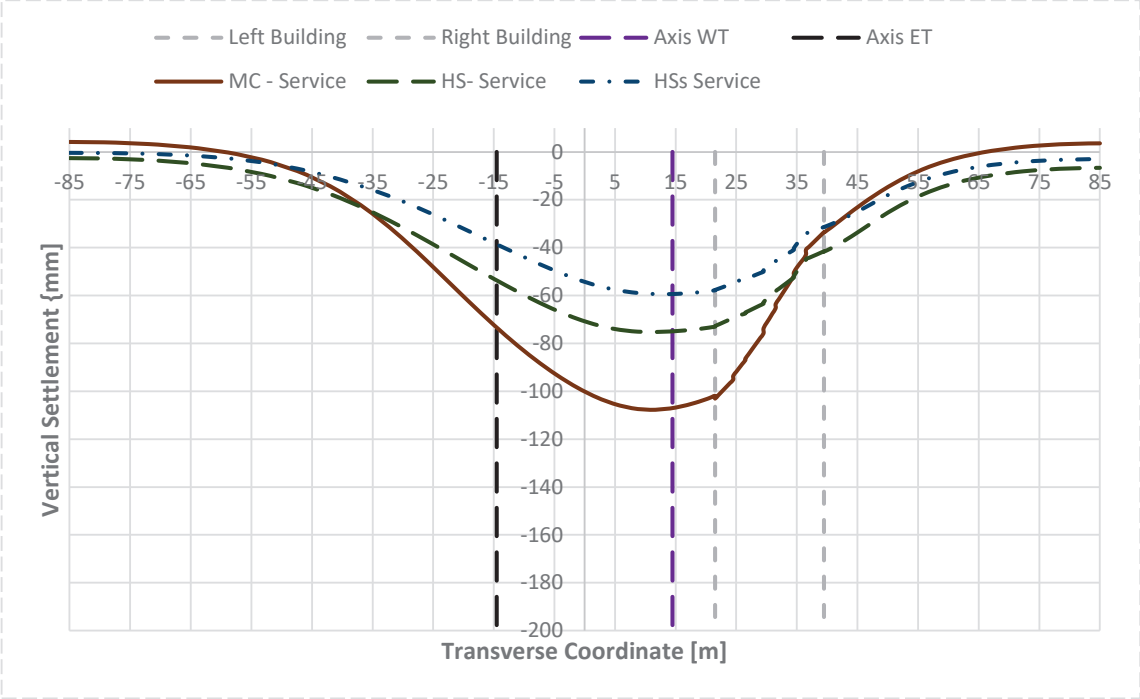
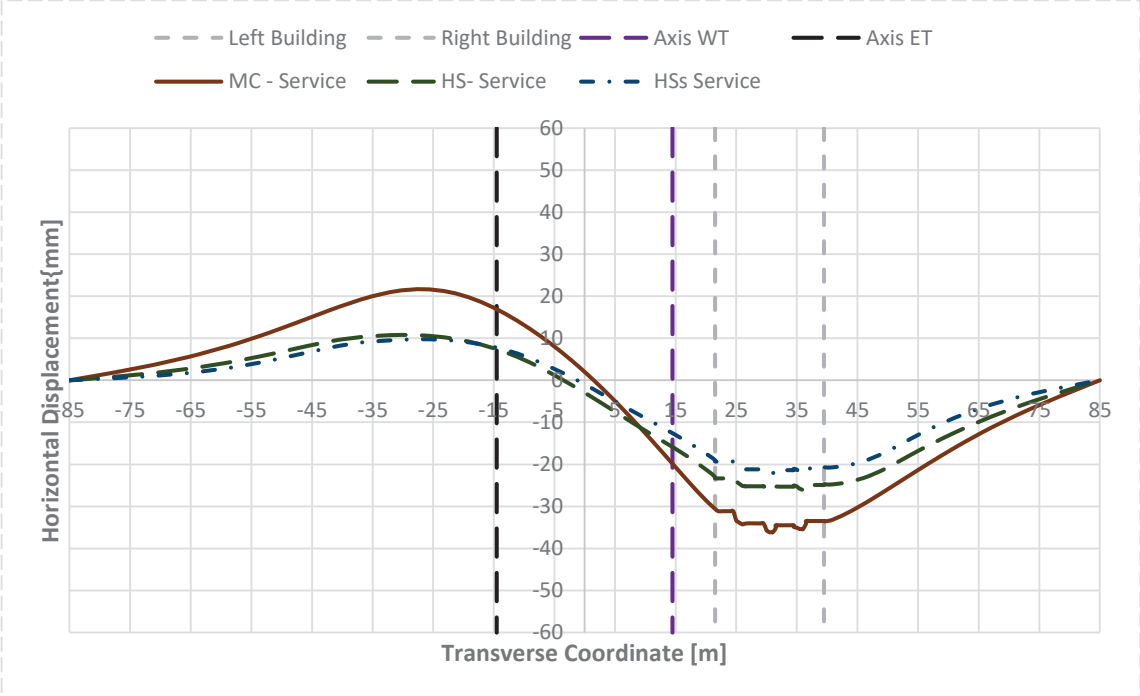


Figure IV-44: Horizontal Displacement in Service (WT and ET)- HSs- Fine

Counter vault Section in New Tunnels



Graph IV-14: Diagram of Vertical Settlement on Building Foundation - Service Stage – Model width Counter- vault Section in New Tunnels- Fine



Graph IV-15: Diagram of Horizontal Displacement on Building Foundation - Service Stage – Model with Counter- vault Section in New Tunnels- Fine

Table IV-16: Verification of the Deformation in Foundation Building according to Boscardin & Cording- MC Model- Service Stage- Fine- Counter vault Section in New Tunnels

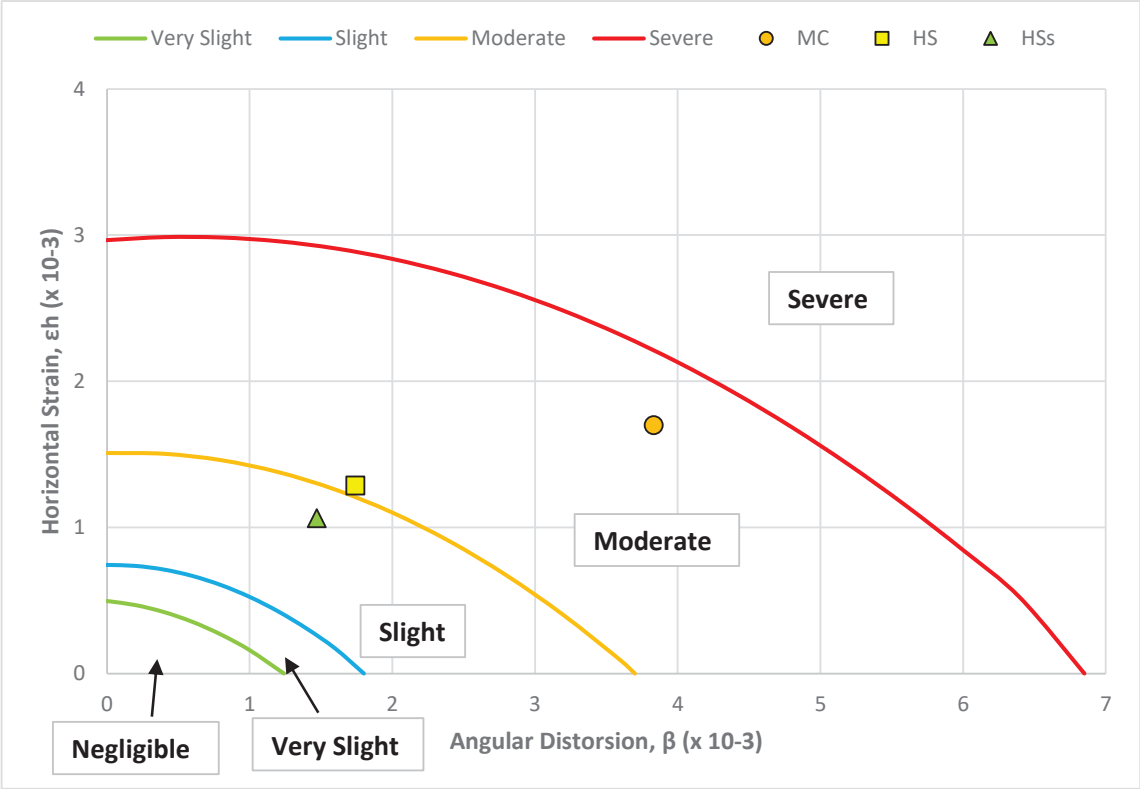
Coord. in model (m) Phase	Settl Left δ_{v1} (mm)		Settl Right δ_{v2} (mm)		Relative Settle $\Delta\delta v$	Horiz Displac δ_H (mm)		Width Found.	Angular Distortion	Lateral Strain
	x	y	x	y	$\delta v1-\delta v2$	x	y	Building	$\beta = \Delta\delta v/L$	$\varepsilon l = \delta_H/L$
	21.5	-6.5	39.5	-6.5	(mm)	21.5	-6.5	L (m)	(x 10-3)	(x 10-3)
Service	-102.54		-33.56		68.98	-30.60		18	3.83	1.70

Table IV-17: Verification of the Deformation in Foundation Building according to Boscardin & Cording- HS Model- Service Stage- Fine- Counter vault Section in New Tunnels

Coord. in model (m) Phase	Settl Left δ_{v1} (mm)		Settl Right δ_{v2} (mm)		Relative Settle $\Delta\delta v$	Horiz Displac δ_H (mm)		Width Found.	Angular Distortion	Lateral Strain
	x	y	x	y	$\delta v1-\delta v2$	x	y	Building	$\beta = \Delta\delta v/L$	$\varepsilon l = \delta_H/L$
	21.5	-6.5	39.5	-6.5	(mm)	21.5	-6.5	L (m)	(x 10-3)	(x 10-3)
Service	-72.91		-41.58		31.33	-23.19		18	1.74	1.29

Table IV-18: Verification of the Deformation in Foundation Building according to Boscardin & Cording- HSs Model- Service Stage- Fine- Counter vault Section in New Tunnels

Coord. in model (m) Phase	Settl Left δ_{v1} (mm)		Settl Right δ_{v2} (mm)		Relative Settle $\Delta\delta v$	Horiz Displac δ_H (mm)		Width Found.	Angular Distortion	Lateral Strain
	x	y	x	y	$\delta v1-\delta v2$	x	y	Building	$\beta = \Delta\delta v/L$	$\varepsilon l = \delta_H/L$
	21.5	-6.5	39.5	-6.5	(mm)	21.5	-6.5	L (m)	(x 10-3)	(x 10-3)
Service	-57.80		-31.35		26.45	-19.14		18	1.47	1.06



Graph IV-16: Criterion of Boscardin and Cording- Service Stage-

Model with Counter- vault Section in New Tunnels- Fine

4.2.2 Verification of the Deformation in the New Road Tunnels

(a) Analysis of the Mixed Profile

(a.1) Construction Stage

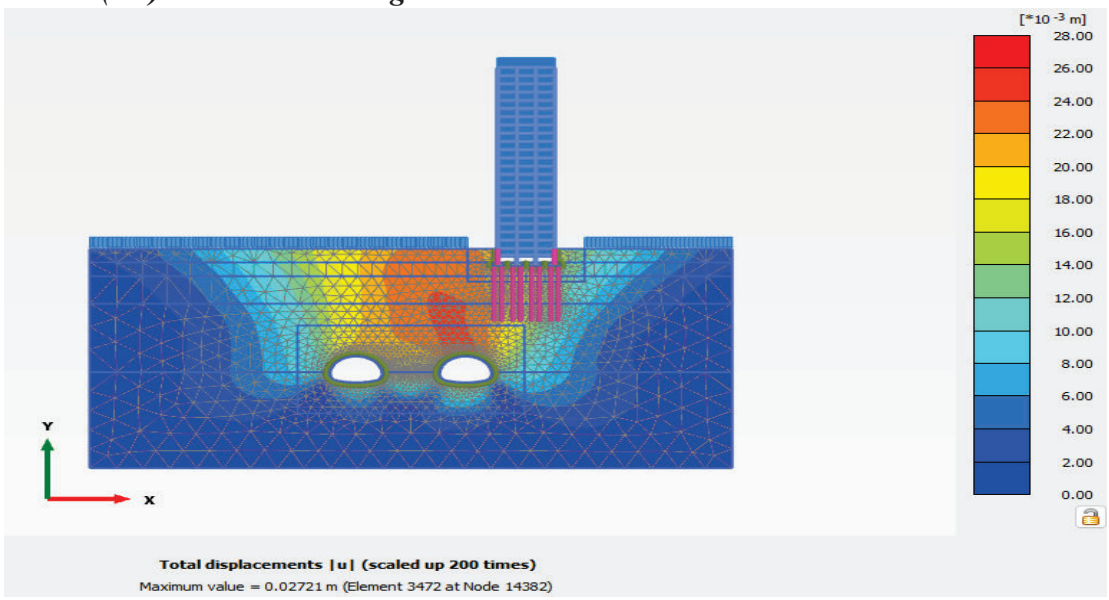


Figure IV-45: Maximum Displacement in Construction-HSs-Mixed-Counter vault Section New Tunnels

(a.2) Service Stage

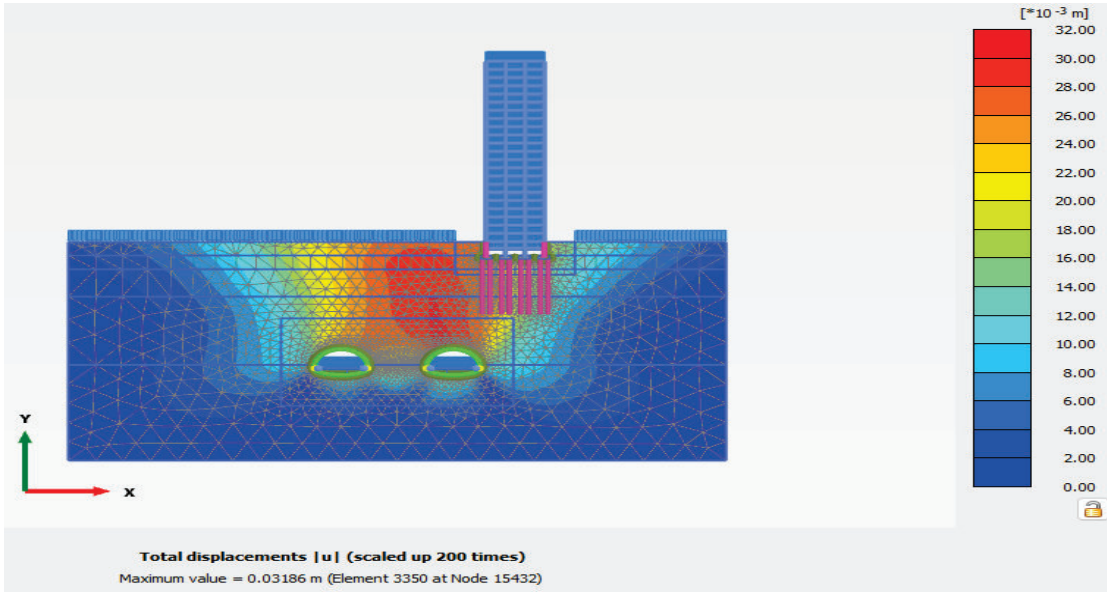


Figure IV-46: Maximum Displacement in Service- HSs- Mixed- Counter-vault Section in New Tunnels

Table IV-19: Summary of Maximum Displacement Checks on New Road Tunnels–

Pre-existing Building – Gravel- Plane Sole Section in New Tunnels

Maximum Displacement [mm]							
Soil	Construction Stage			Service Stage			Admissible
	MC	HS	HSs	MC	HS	HSs	
Mixed	-	-	27.21	-	-	31.86	50

4.2.3 Verification of the Resistance in the New Road Tunnels

In the construction stage, the support of the new road tunnels must be verified through the criterion of admissible stresses, as defined in section 3.7.3(b).

In the service stage, the lining of the new road tunnels must be verified through the interaction diagram M-N and N-Q, as defined in section 3.7.3(b)..

The lining of the new road tunnels are verified, with their corresponding concrete thicknesses and reinforcement, as defined in Figure III-10 and sections 3.3.2 and 3.3.2(b).

$e = 0.50\ m$ Concrete thicknesses for the calculation

(Lining thicknesses = 0.30 m + 2/3 Support thicknesses = 0.20 m)

$A_s = 3.35\ cm^2/m$ ACMA335 Mesh in Internal and External face

$A_{s1} = 7.60\ cm^2/m$ 2Ø22 Bar of the Reticulate Frame in Internal face

$A_{s1} = 8.04\ cm^2/m$ 1Ø32 Bar of the Reticulate Frame in External face

(a) Analysis of the Mixed Profile

(a.1) Construction Stage

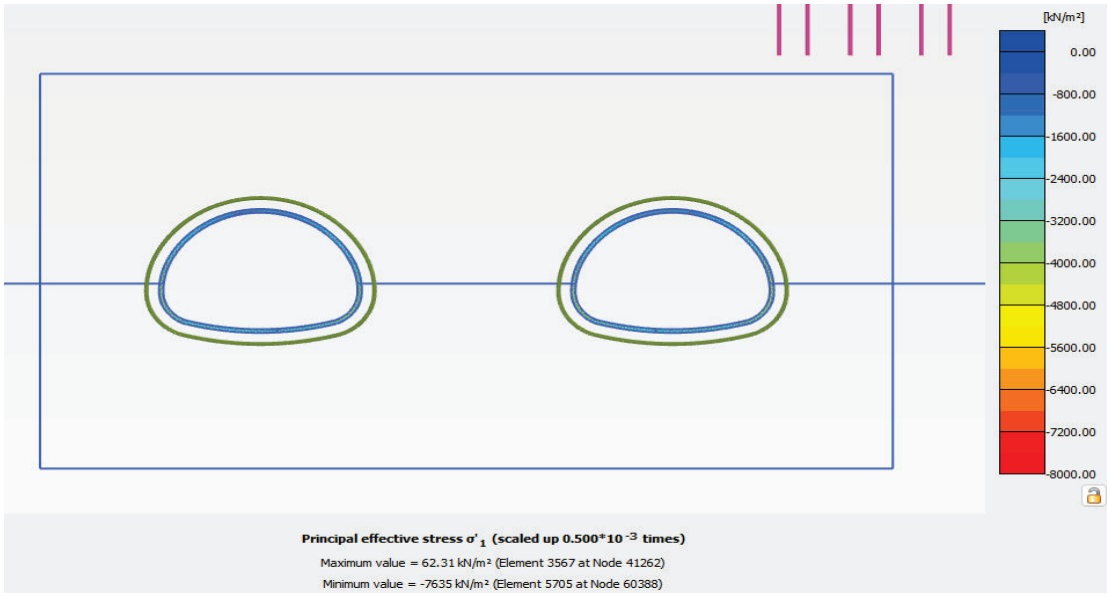


Figure IV-47: Major Principal effective Stress on Support- HSs – Mixed-Counter-vault Section in New Tunnels

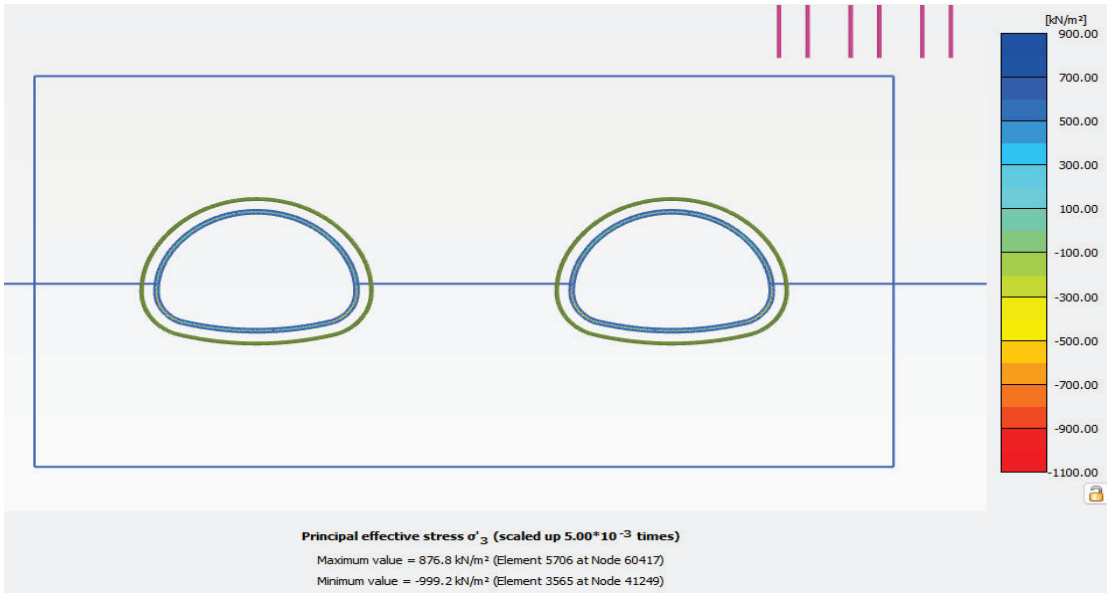


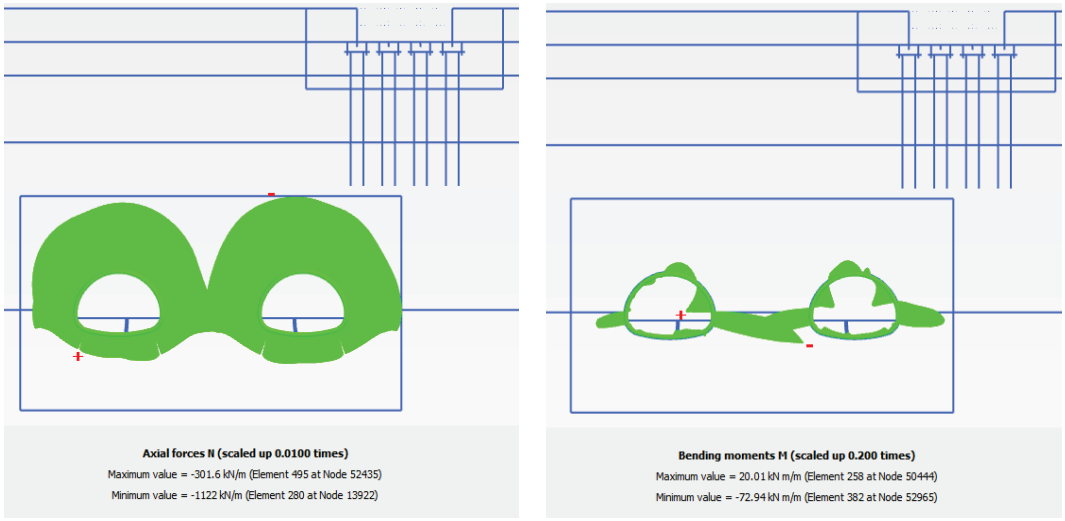
Figure IV-48: Minor Principal effective Stress on Support- HSs – Mixed-Counter-vault Section in New Tunnels

Table IV-20: Verification of Admissible Stress- HSs- Mixed-

Counter vault Section in New Tunnels

σ´1 [MPa]	σ´3 [MPa]	σ´1adm [MPa]	σ´3adm [MPa]	σ´1 < σ´1 adm	σ´3 < σ´3 adm
-7.63	0.87	-16	2	CHECK	CHECK

(a.2) Service Stage



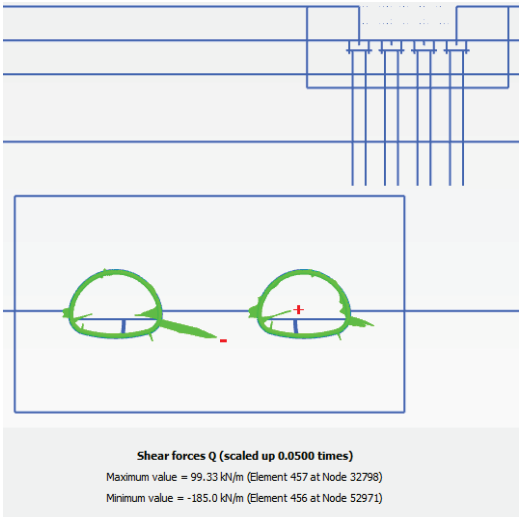
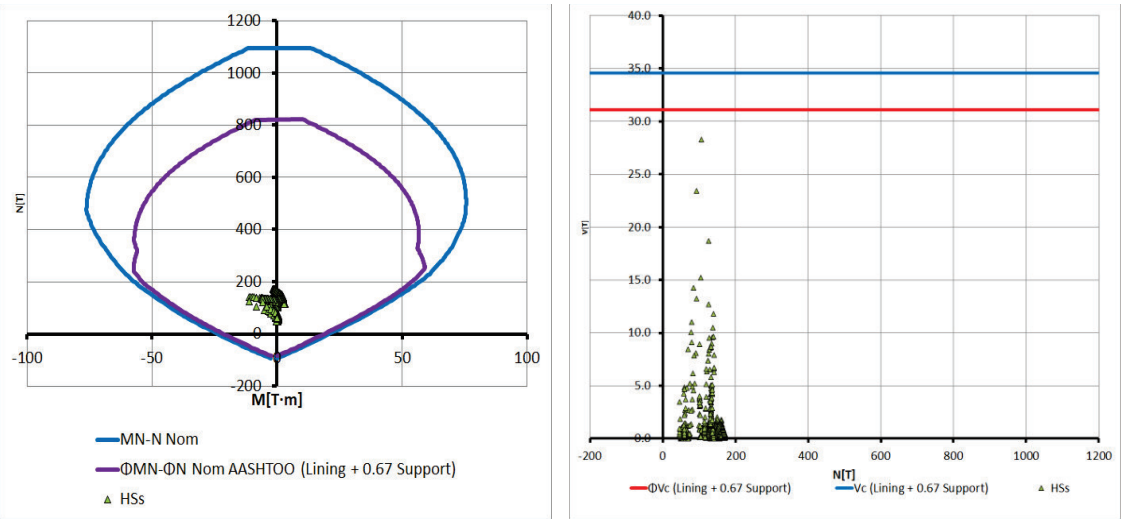


Figure IV-49: Forces Diagram, Axial, Bending and Shear on Lining- Service Stage- HSs- Mixed- Counter vault Section in New Tunnels



Graph IV-17: : Interaction M-N and N-Q Diagram- Lining of the new road tunnels-

Service Stage- Mixed- Counter vault Section in New Tunnels

4.2.4 Verification of the Capacity of the Soil

The following shows the plastification of the soil in construction and in service and applies the acceptability criteria explained in section 3.7.4.

(a) Construction Stage

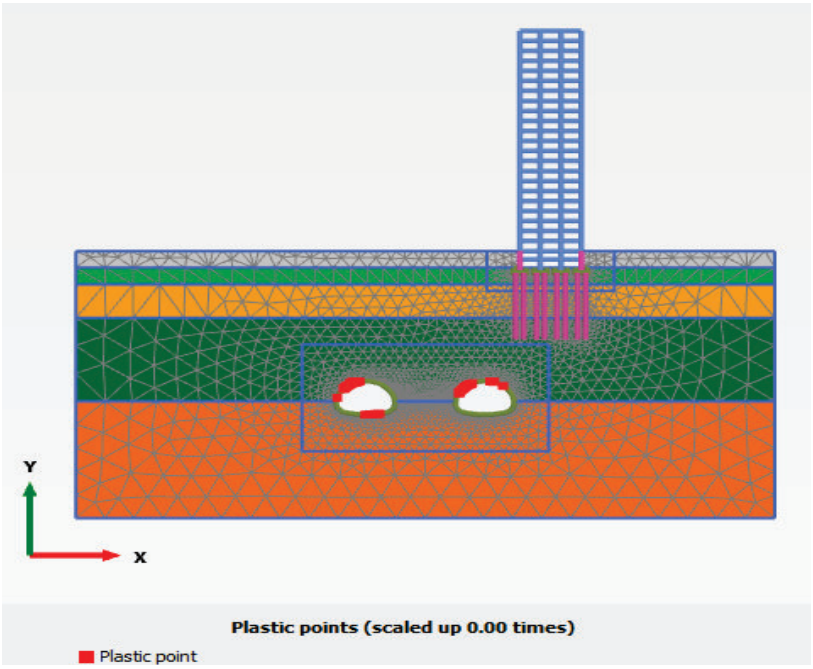


Figure IV-50: Plastification- Construction Stage- HSs- Mixed- Counter vault Section in New Tunnels

(b) Service Stage

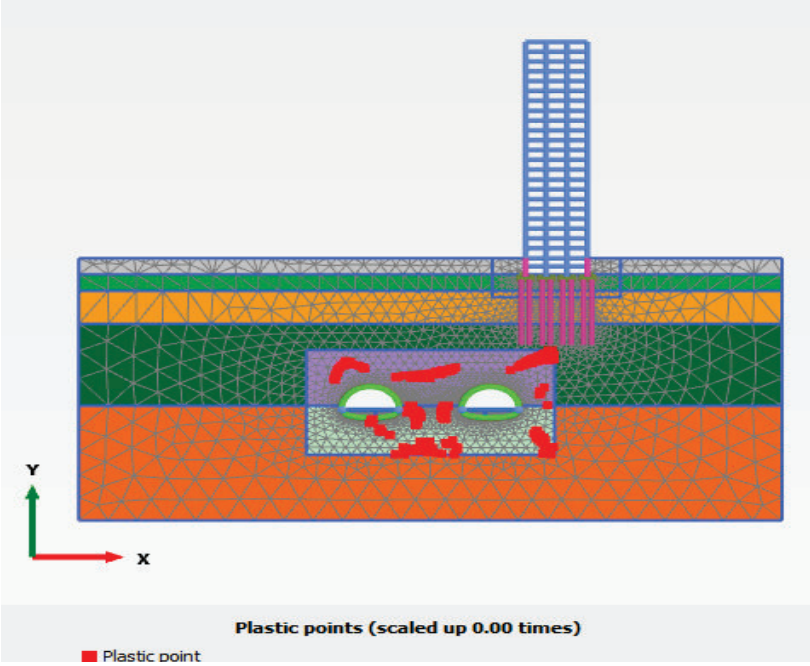


Figure IV-51: Plastification - Service Stage- HSs- Mixed-Counter vault Section in New Tunnels

Table IV-21: Plastification Verification on Soil- HSs- Mixed-Counter vault Section in New Tunnels

Stage	R-Plastic [m]	R-Plastic Admissible [m]	Verification
Construction	8	14	CHECK
Service	12	14	CHECK

4.3. Variation of the Constitutive Soil Model with Counter-vault Section in four excavation phases in Fine Soil

4.3.1 Verification of the Deformation in the Pre-existing Building (B)

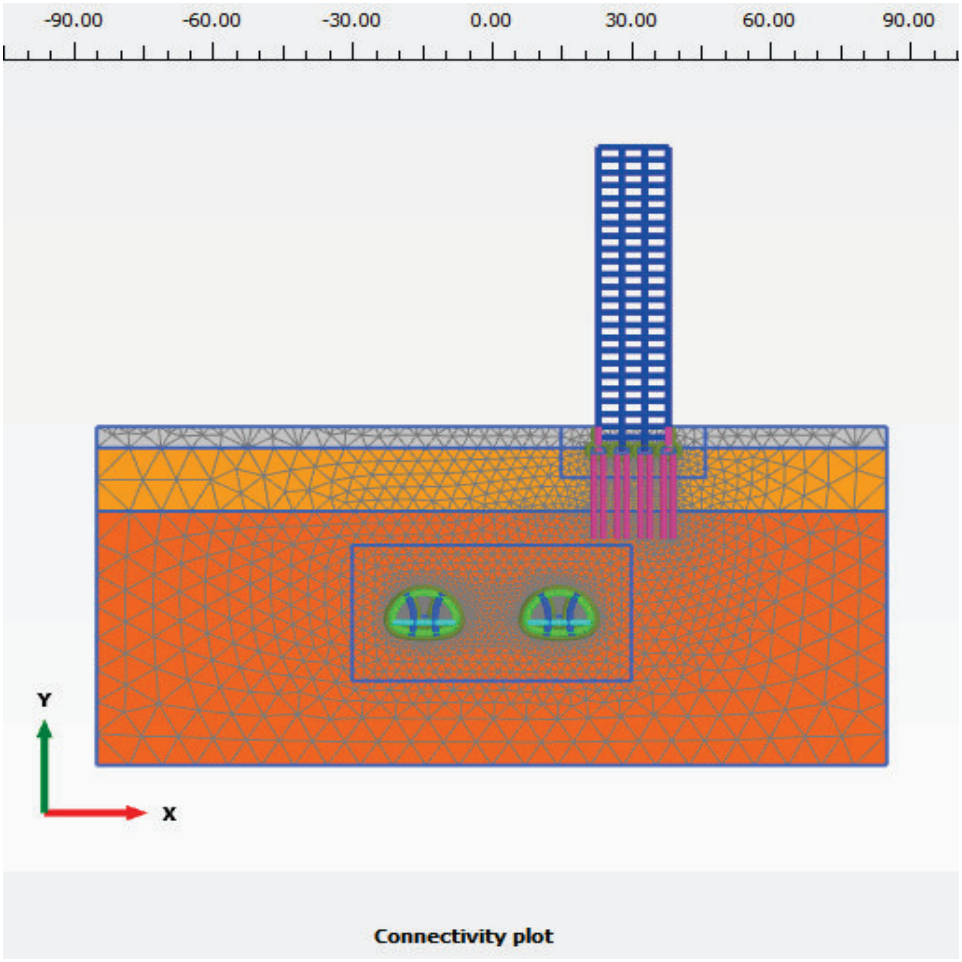


Figure IV-52: Fine Model with Pre-existing Building and counter vault section with four phases of excavation in new road tunnels

(a) Service Stage

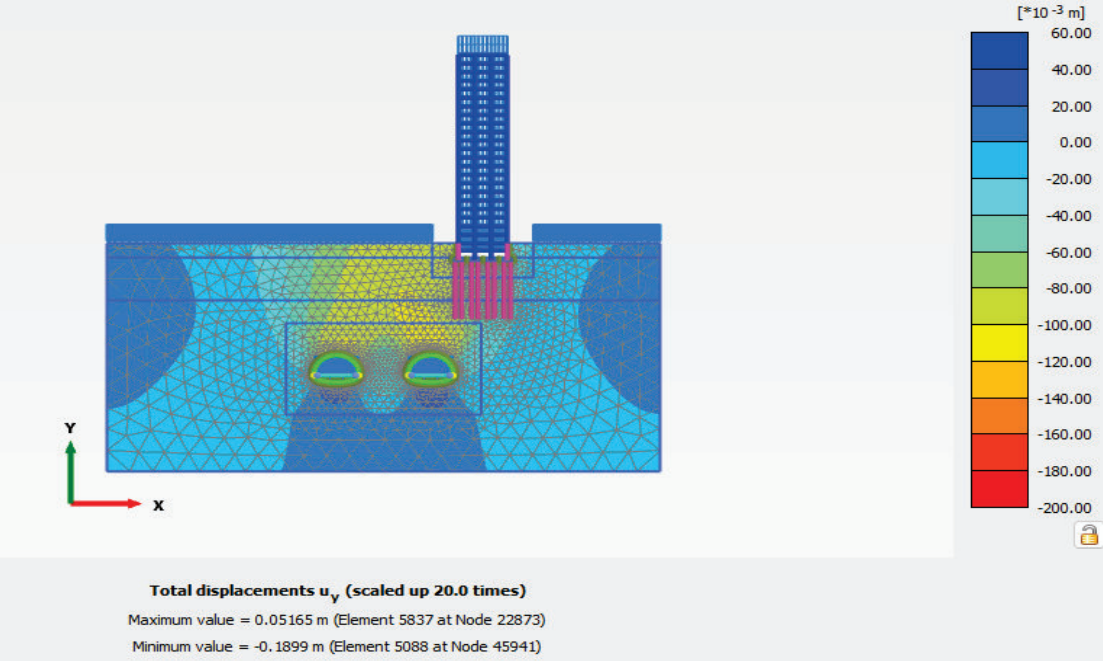


Figure IV-53: Vertical Settlement in Service- MC- Fine

Counter vault Section with four phases in New Tunnels

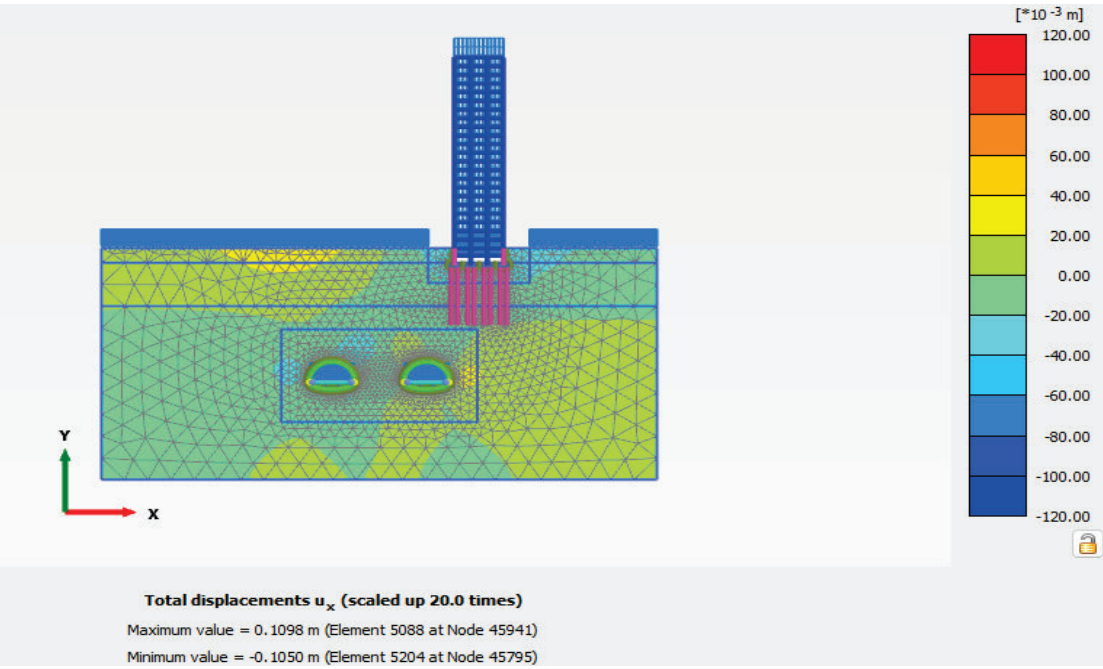


Figure IV-54: Horizontal Displacement in Service- MC- Fine

Counter vault Section with four phases in New Tunnels

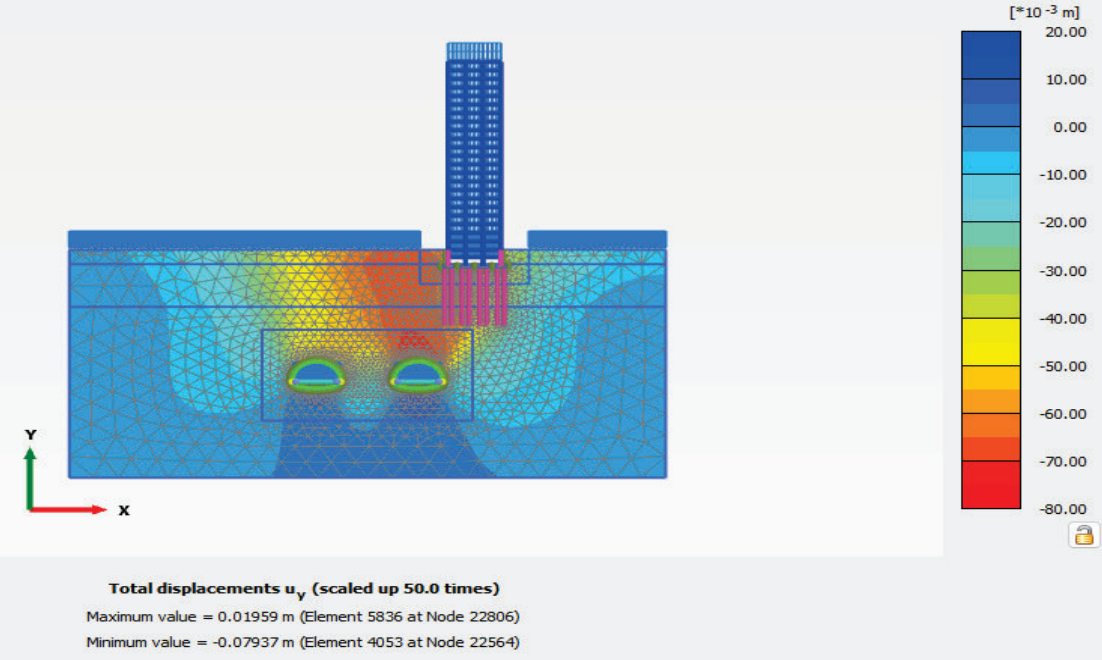


Figure IV-55: Vertical Settlement in Service- HS- Fine

Counter vault Section with four phases in New Tunnels

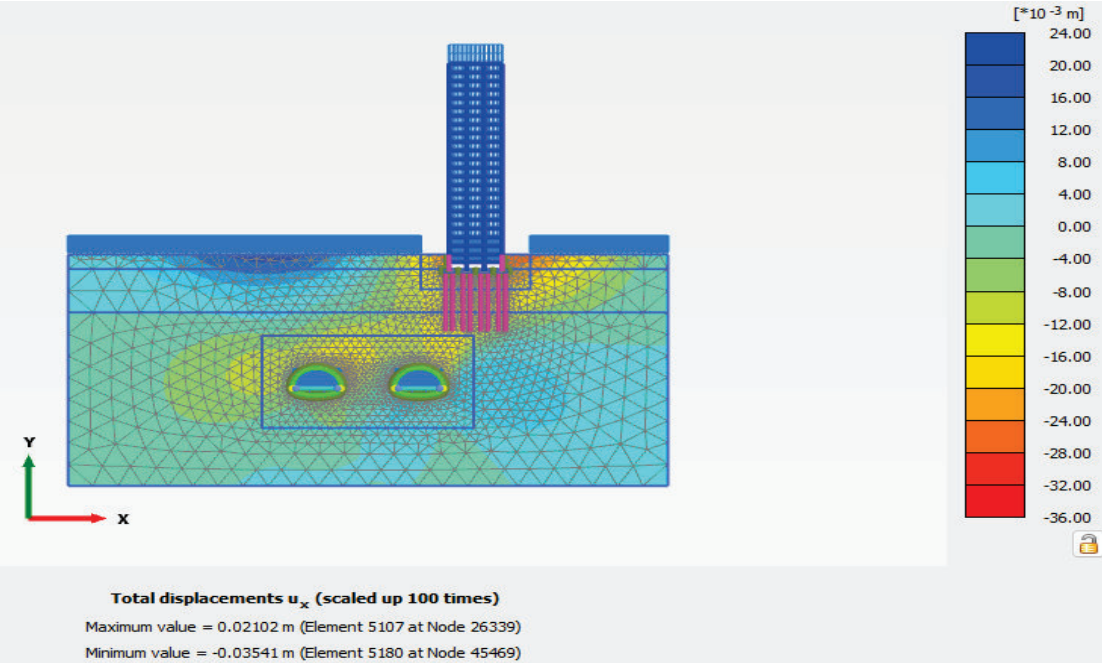


Figure IV-56: Horizontal Displacement in Service- HS- Fine

Counter vault Section with four phases in New Tunnels

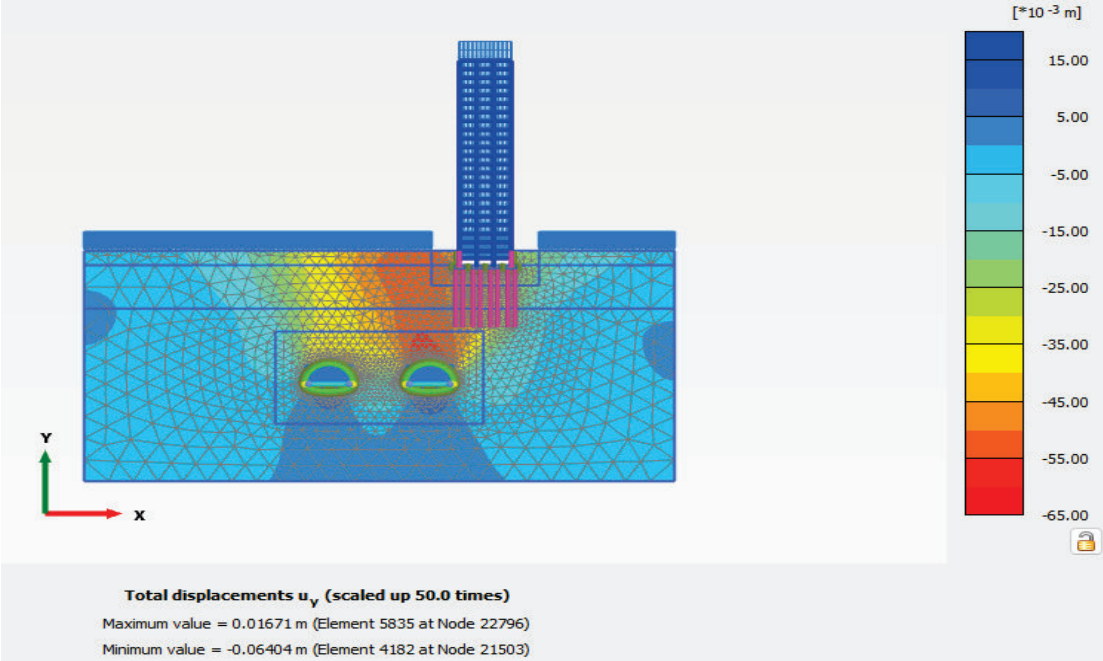


Figure IV-57: Vertical Settlement in Service- HSs- Fine

Counter vault Section with four phases in New Tunnels

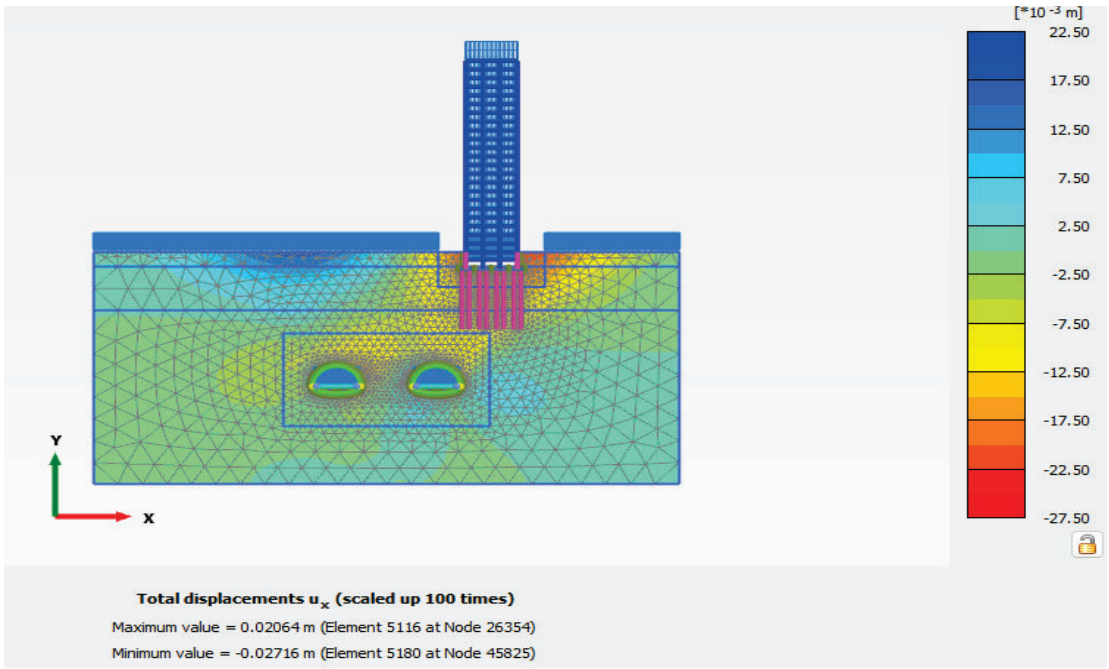
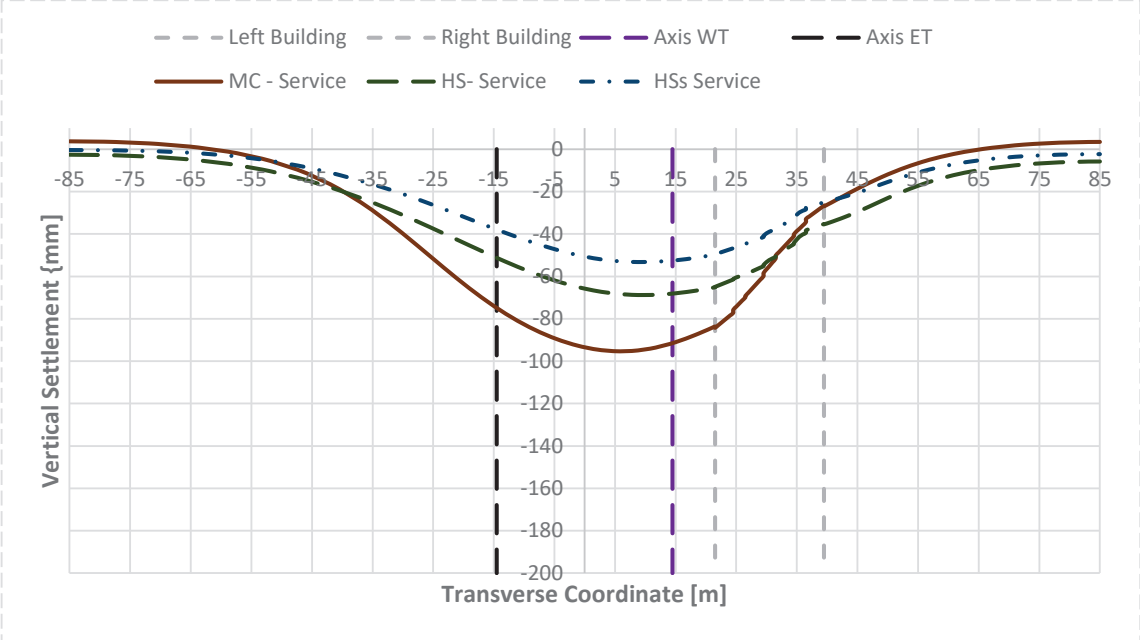
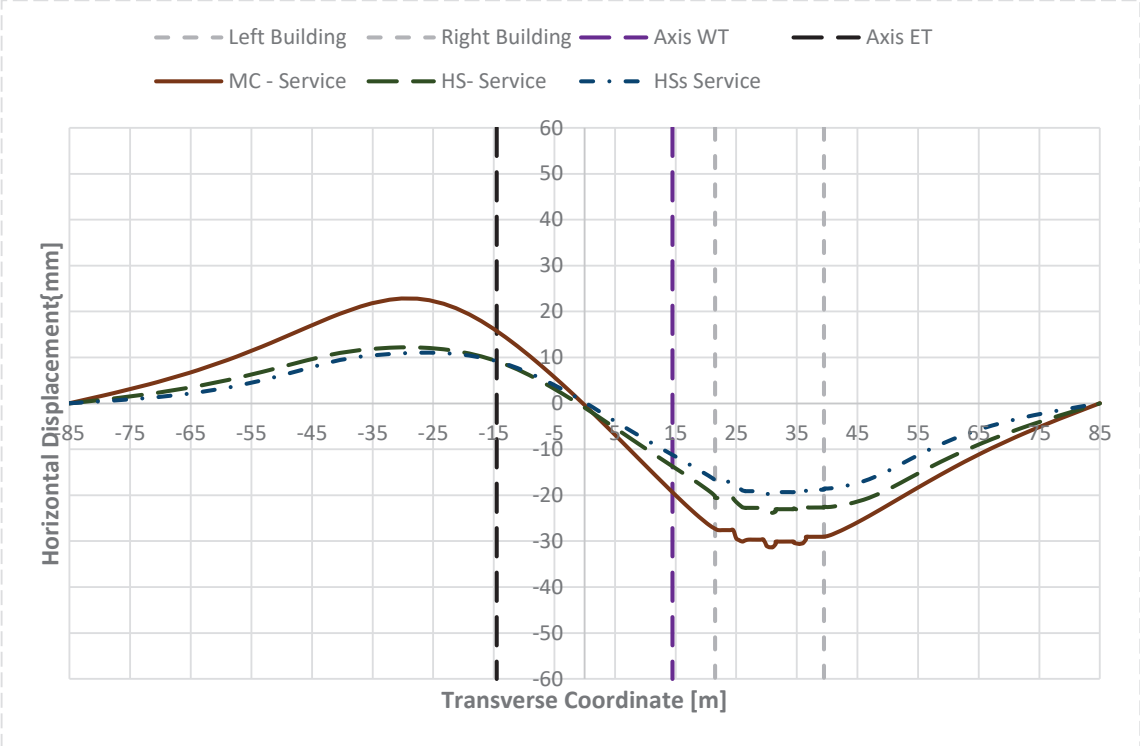


Figure IV-58: Horizontal Displacement in Service- HSs- Fine- Counter vault Section

with four phases in New Tunnels



Graph IV-18: Diagram of Vertical Settlement on Building Foundation - Service Stage – Model width Counter vault Section with four phases in New Tunnels- Fine



Graph IV-19: Diagram of Horizontal Displacement on Building Foundation - Service Stage – Model with Counter Vault Section with four phases in New Tunnels - Fine

Table IV-22: Verification of the Deformation in Foundation Building according to Boscardin & Cording- MC Model- Service Stage- Fine- Counter vault Section with four phases in New Tunnels

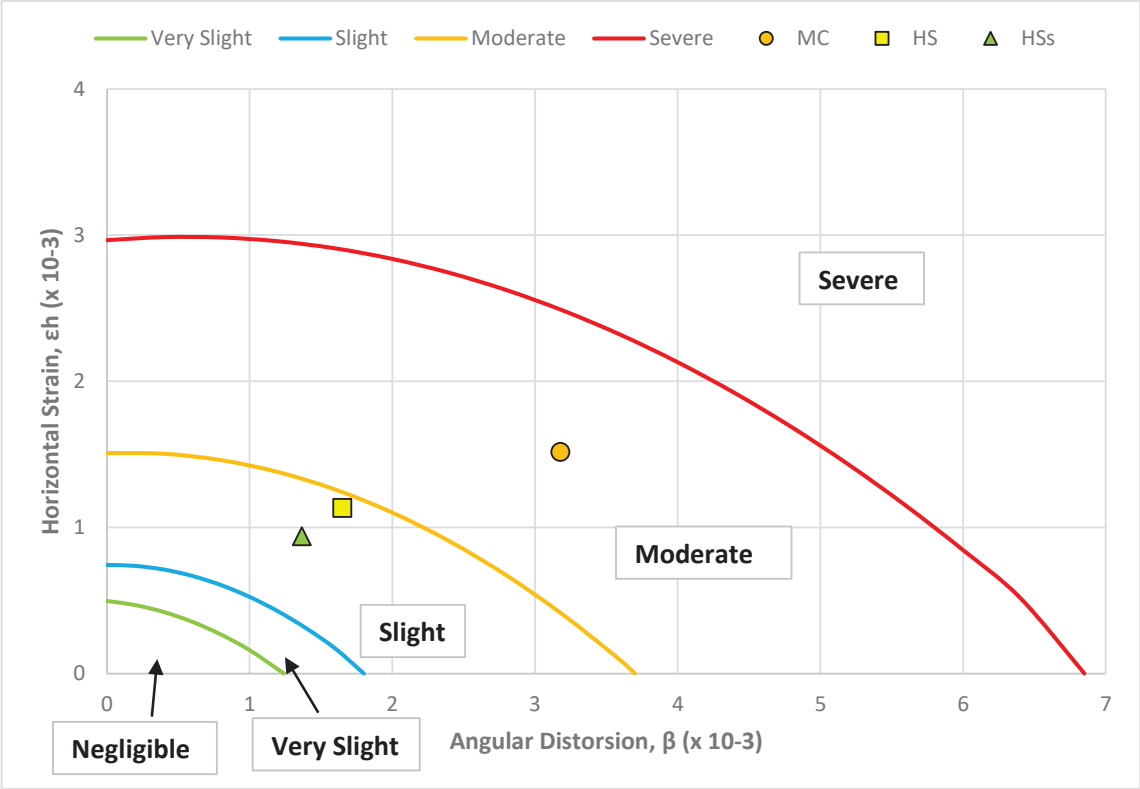
Coord. in model (m)	Settl Left δ_{v1} (mm)		Settl Right δ_{v2} (mm)		Relative Settle $\Delta\delta v$	Horiz Displac δ_H (mm)		Width Found.	Angular Distortion	Lateral Strain
	x	y	x	y	$\delta v1-\delta v2$	x	y	Building	$\beta= \Delta\delta v/L$	$\varepsilon l = \delta_H/L$
Phase	21.5	-6.5	39.5	-6.5	(mm)	21.5	-6.5	L (m)	(x 10-3)	(x 10-3)
Service	-84.00		-26.79		57.21	-27.33		18	3.18	1.52

Table IV-23: Verification of the Deformation in Foundation Building according to Boscardin & Cording- HS Model- Service Stage- Fine- Counter vault Section with four phases in New Tunnels

Coord. in model (m)	Settl Left δ_{v1} (mm)		Settl Right δ_{v2} (mm)		Relative Settle $\Delta\delta v$	Horiz Displac δ_H (mm)		Width Found.	Angular Distortion	Lateral Strain
	x	y	x	y	$\delta v1-\delta v2$	x	y	Building	$\beta= \Delta\delta v/L$	$\varepsilon l = \delta_H/L$
Phase	21.5	-6.5	39.5	-6.5	(mm)	21.5	-6.5	L (m)	(x 10-3)	(x 10-3)
Service	-65.05		-35.38		29.67	-20.42		18	1.65	1.13

Table IV-24: Verification of the Deformation in Foundation Building according to Boscardin & Cording- HSs Model- Service Stage- Fine- Counter vault Section with four phases in New Tunnels

Coord. in model (m)	Settl Left δ_{v1} (mm)		Settl Right δ_{v2} (mm)		Relative Settle $\Delta\delta v$	Horiz Displac δ_H (mm)		Width Found.	Angular Distortion	Lateral Strain
	x	y	x	y	$\delta v1-\delta v2$	x	y	Building	$\beta= \Delta\delta v/L$	$\varepsilon l = \delta_H/L$
Phase	21.5	-6.5	39.5	-6.5	(mm)	21.5	-6.5	L (m)	(x 10-3)	(x 10-3)
Service	-49.67		-25.09		24.57	-16.93		18	1.37	0.94



Graph IV-20: Criterion of Boscardin and Cording- Service Stage-

Model with Counter vault Section with four phases in New Tunnels- Fine

4.4. Variation of the Constitutive Soil Model with Counter-vault Section in four excavation phases in Fine Soil applying Mitigation measure.

4.4.1 Verification of the Deformation in the Pre-existing Building (B)

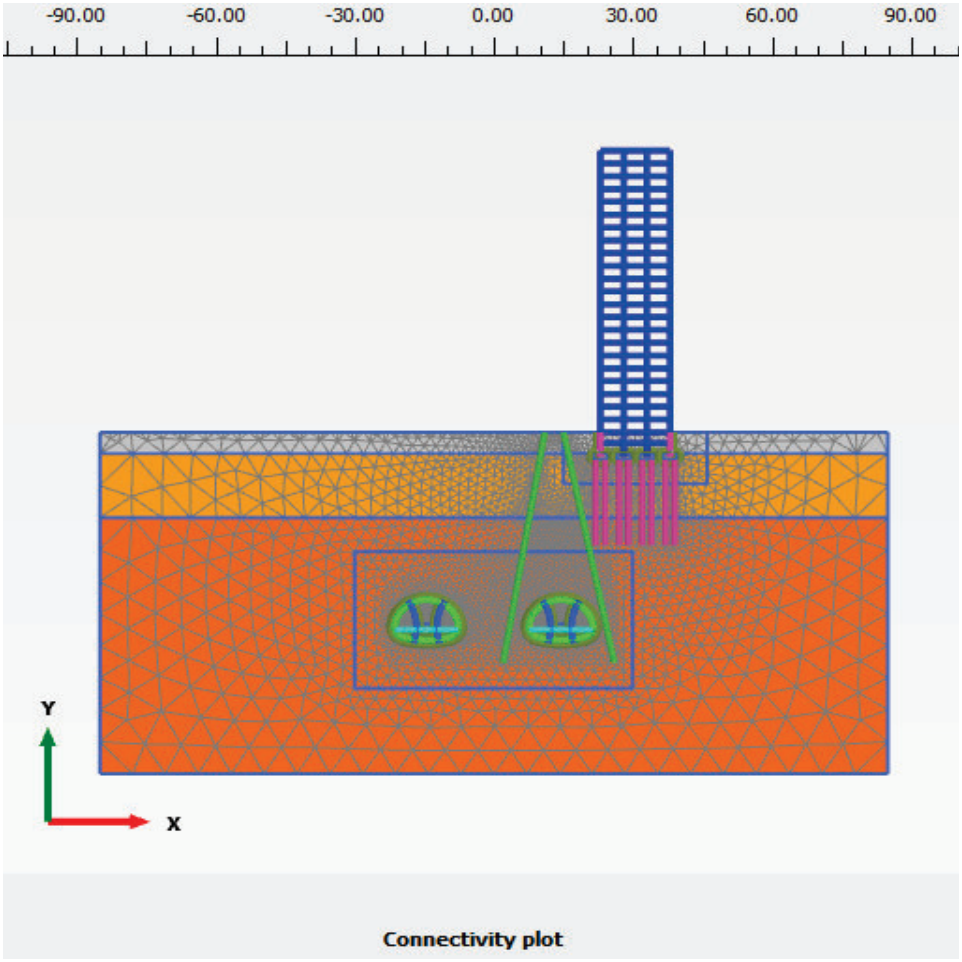


Figure IV-59: Fine Model with Pre-existing Building and counter vault section with four phases of excavation in new road tunnels and Mitigation Measure

(a) Service Stage

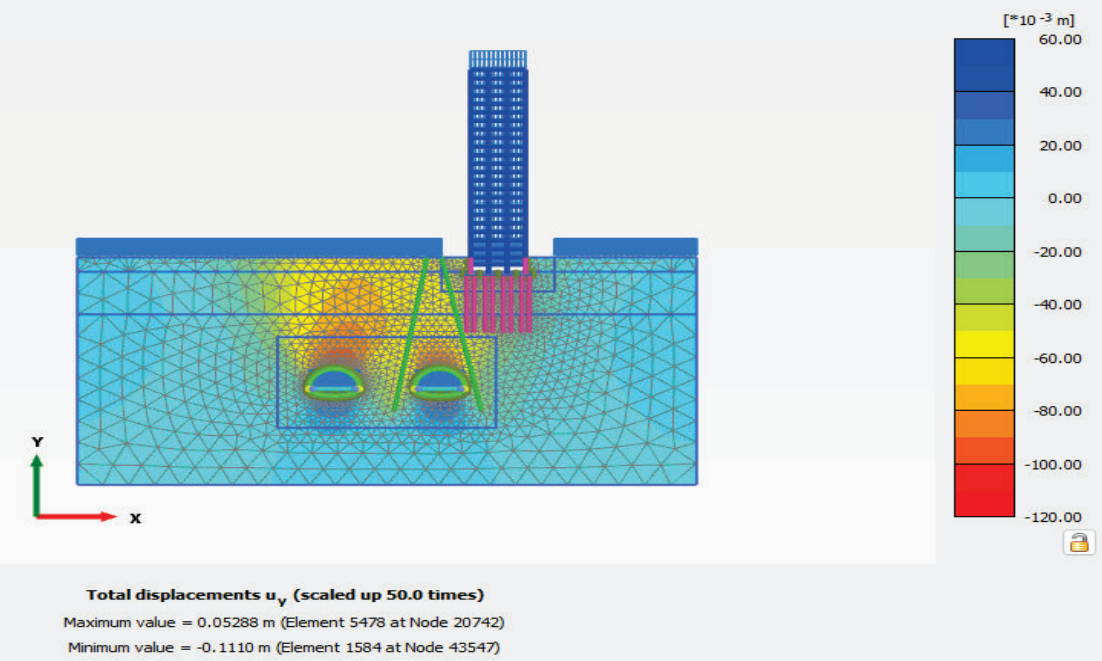


Figure IV-60: Vertical Settlement in Service- MC- Fine

Counter vault Section with four phases in New Tunnels and Mitigation Measure

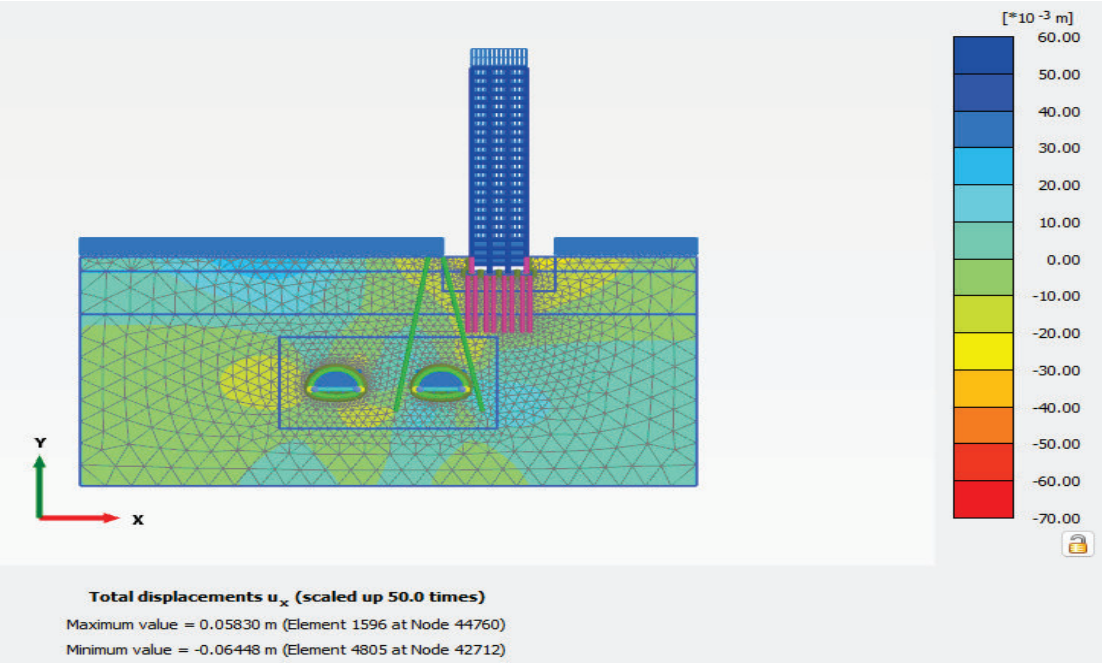


Figure IV-61: Horizontal Displacement in Service- MC- Fine

Counter vault Section with four phases in New Tunnels and Mitigation Measure

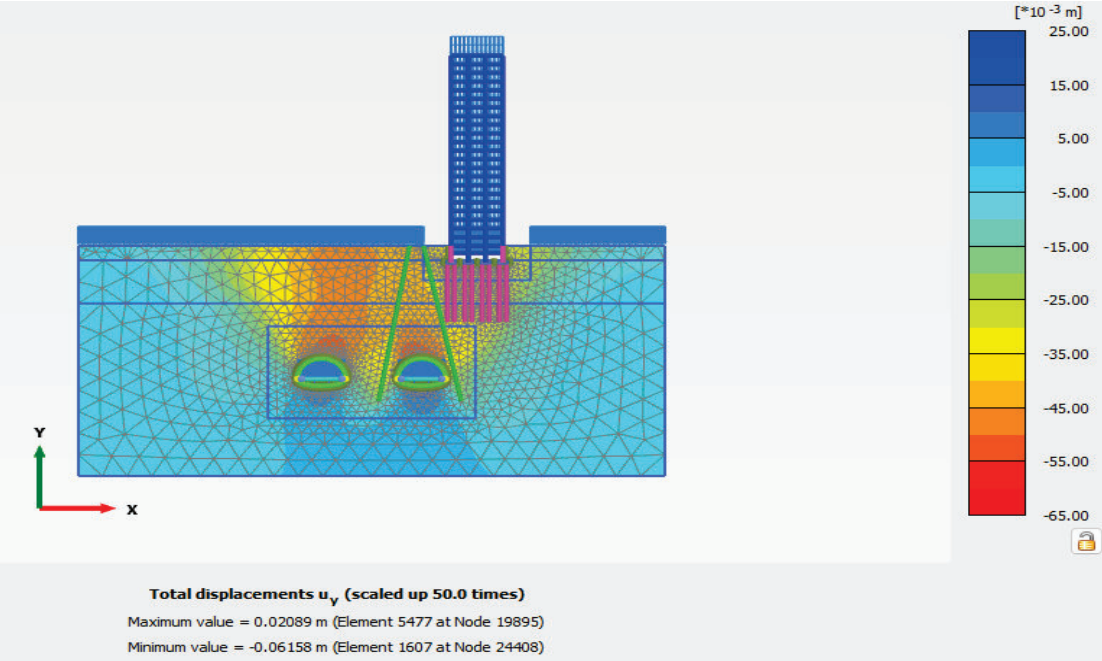


Figure IV-62: Vertical Settlement in Service- HS- Fine

Counter vault Section with four phases in New Tunnels and Mitigation Measure

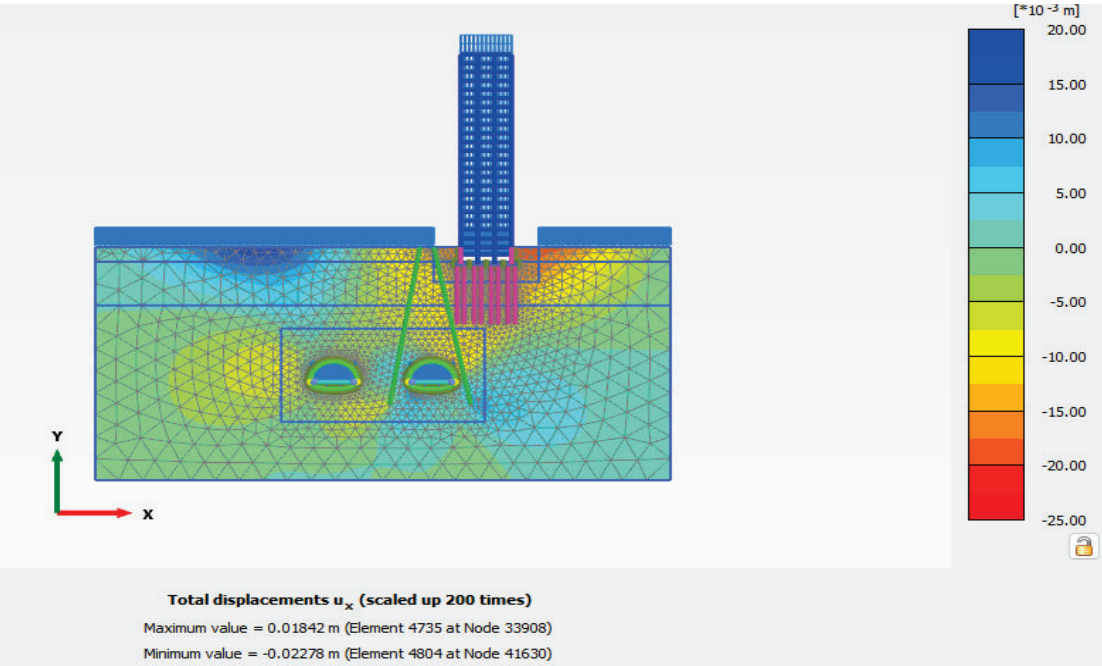


Figure IV-63: Horizontal Displacement in Service- HS- Fine

Counter vault Section with four phases in New Tunnels and Mitigation Measure

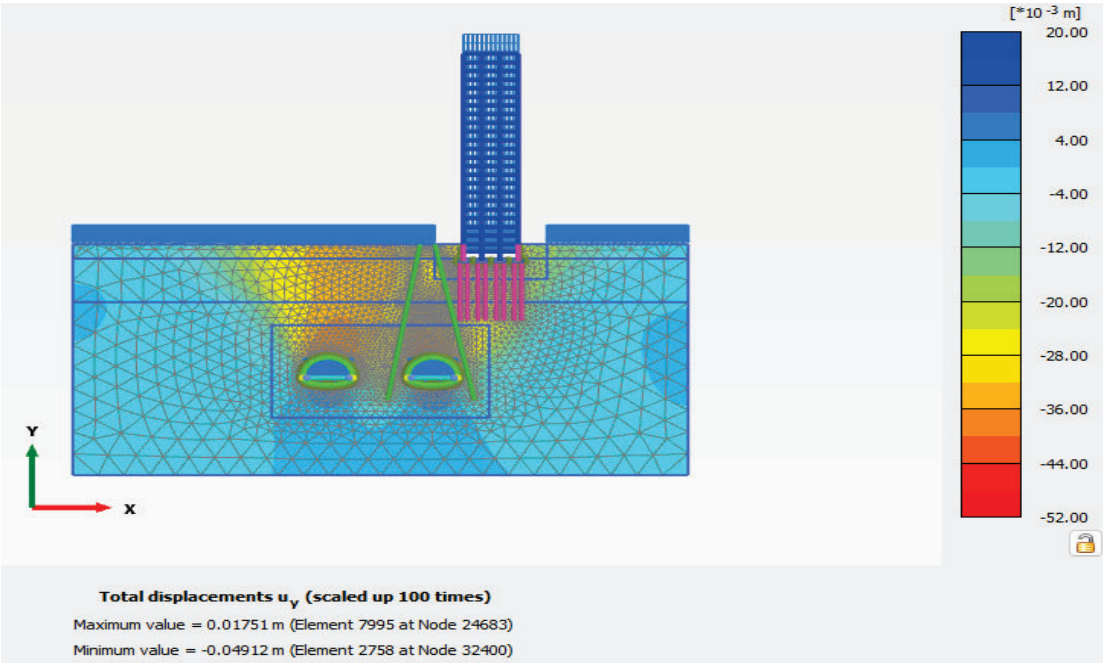


Figure IV-64:Vertical Settlement in Service- HSs- Fine

Counter vault Section with four phases in New Tunnels and Mitigation Measure

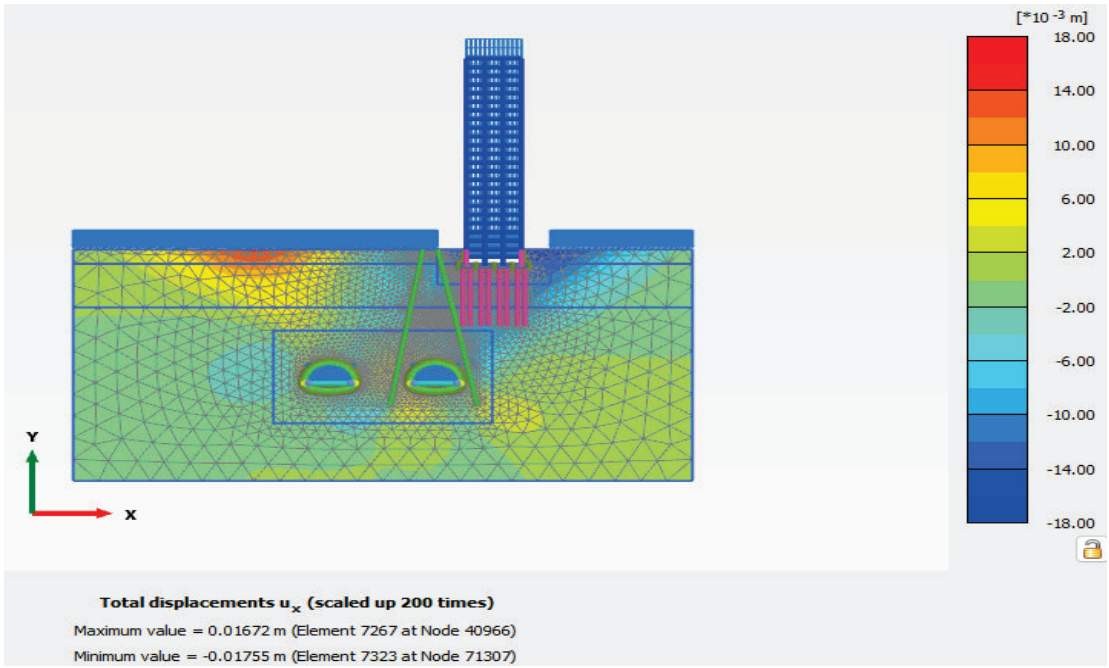
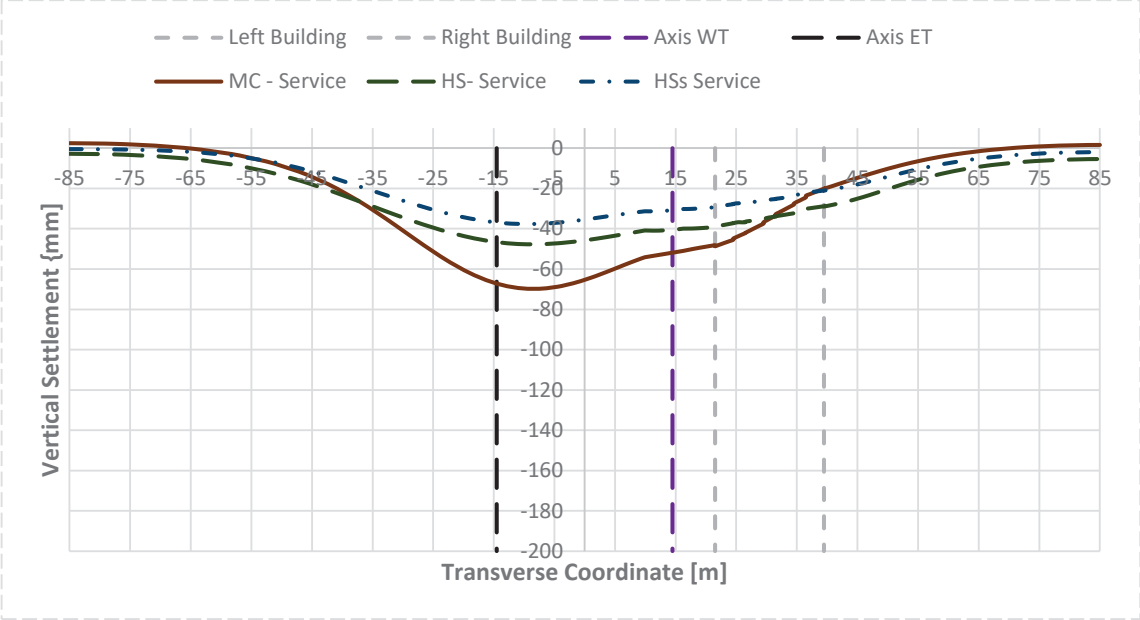
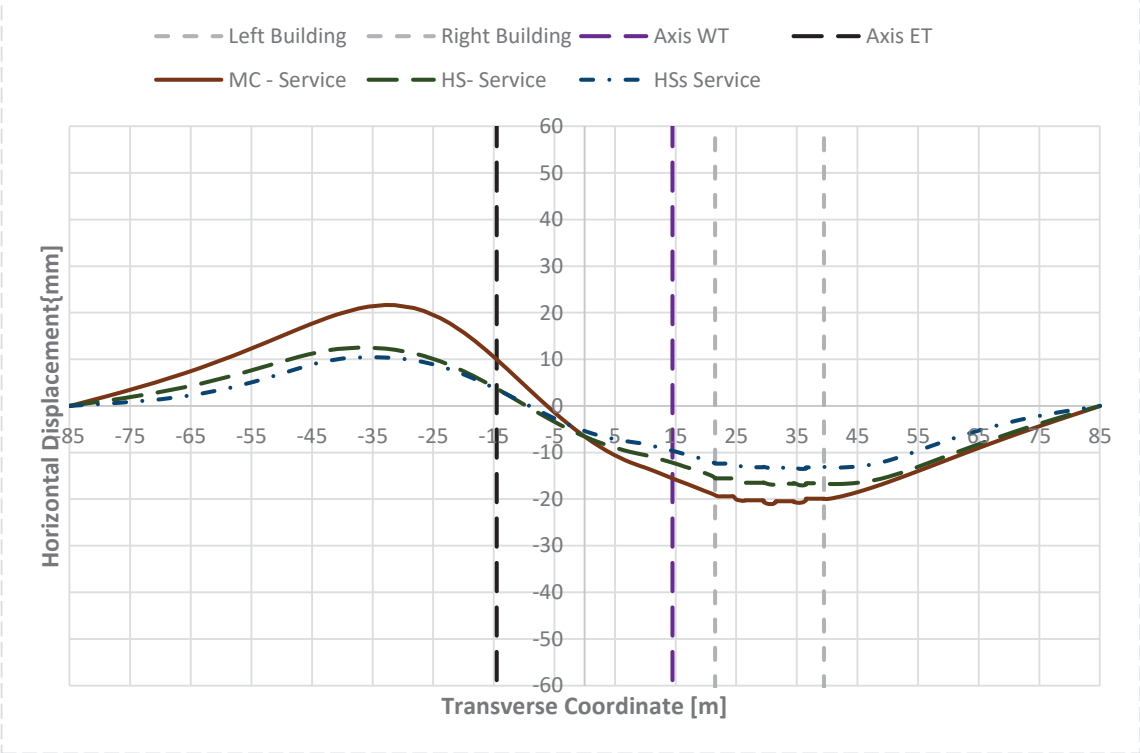


Figure IV-65: Horizontal Displacement in Service- HSs- Fine- Counter vault Section

with four phases in New Tunnels and Mitigation Measure



Graph IV-21: Diagram of Vertical Settlement on Building Foundation - Service Stage – Model with Counter vault Section with four phases in New Tunnels and Mitigation Measure - Fine



Graph IV-22: Diagram of Horizontal Displacement on Building Foundation - Service Stage – Model with Counter Vault Section with four phases in New Tunnels and Mitigation Measure - Fine

Table IV-25: Verification of the Deformation in Foundation Building according to Boscardin & Cording- MC Model- Service Stage- Fine- Counter vault Section with four phases in New Tunnels and Mitigation Measure

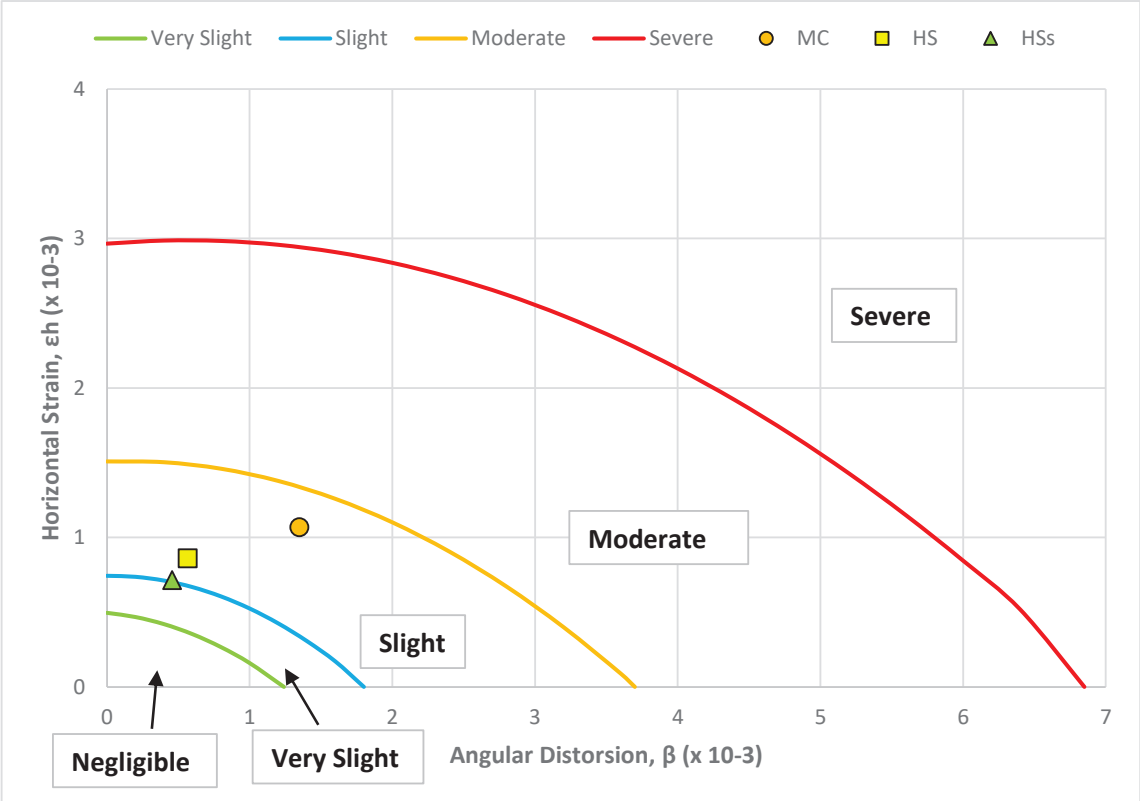
Coord. in model (m)	Settl Left δ_{v1} (mm)		Settl Right δ_{v2} (mm)		Relative Settle $\Delta\delta v$	Horiz Displac δ_H (mm)		Width Found.	Angular Distortion	Lateral Strain
	x	y	x	y	$\delta v1-\delta v2$	x	y	Building	$\beta= \Delta\delta v/L$	$\varepsilon l = \delta_H/L$
Phase	21.5	-6.5	39.5	-6.5	(mm)	21.5	-6.5	L (m)	(x 10-3)	(x 10-3)
Service	-50.95		-26.66		24.28	-19.24		18	1.35	1.07

Table IV-26: Verification of the Deformation in Foundation Building according to Boscardin & Cording- HS Model- Service Stage- Fine- Counter vault Section with four phases in New Tunnels and Mitigation Measure

Coord. in model (m)	Settl Left δ_{v1} (mm)		Settl Right δ_{v2} (mm)		Relative Settle $\Delta\delta v$	Horiz Displac δ_H (mm)		Width Found.	Angular Distortion	Lateral Strain
	x	y	x	y	$\delta v1-\delta v2$	x	y	Building	$\beta= \Delta\delta v/L$	$\varepsilon l = \delta_H/L$
Phase	21.5	-6.5	39.5	-6.5	(mm)	21.5	-6.5	L (m)	(x 10-3)	(x 10-3)
Service	-39.09		-28.93		10.17	-15.51		18	0.56	0.86

Table IV-27: Verification of the Deformation in Foundation Building according to Boscardin & Cording- HSs Model- Service Stage- Fine- Counter vault Section with four phases in New Tunnels and Mitigation Measure

Coord. in model (m)	Settl Left δ_{v1} (mm)		Settl Right δ_{v2} (mm)		Relative Settle $\Delta\delta v$	Horiz Displac δ_H (mm)		Width Found.	Angular Distortion	Lateral Strain
	x	y	x	y	$\delta v1-\delta v2$	x	y	Building	$\beta= \Delta\delta v/L$	$\varepsilon l = \delta_H/L$
Phase	21.5	-6.5	39.5	-6.5	(mm)	21.5	-6.5	L (m)	(x 10-3)	(x 10-3)
Service	-29.25		-21.02		8.23	-12.89		18	0.46	0.72



Graph IV-23: Criterion of Boscardin and Cording- Service Stage-

Model with Counter vault Section with four phases in New Tunnels and Mitigation Measure - Fine

4.4.2 Verification of the Deformation in the New Road Tunnels

(a) Analysis of the Fine Profile

(a.1) Construction Stage

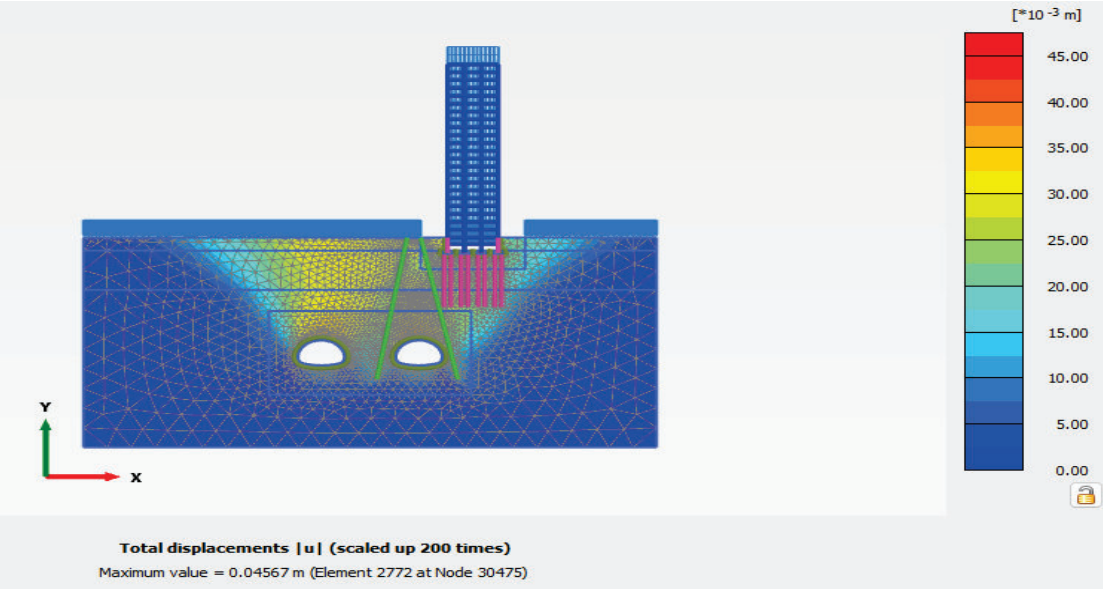


Figure IV-66: Maximum Displacement in Construction-HSs-Fine-Countervault Section

Four Phases-Mitigation measure

(a.2) Service Stage

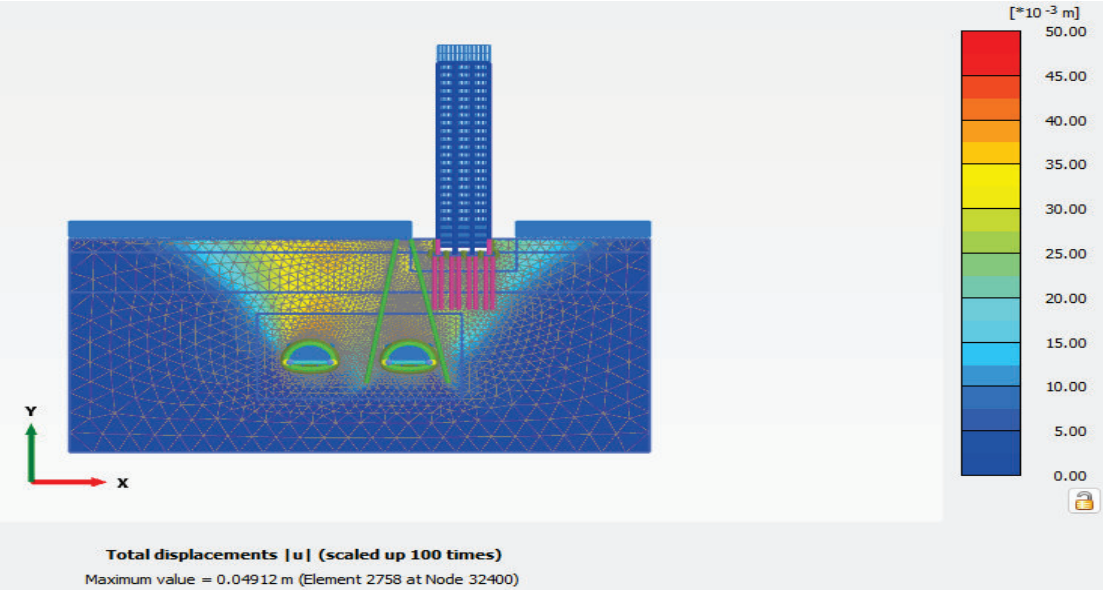


Figure IV-67: Maximum Displacement in Service- HSs- Fine- Counter-vault Section-

Four Phases-Mitigation measure

Table IV-28: Summary of Maximum Displacement Checks on New Road Tunnels– Pre-existing Building – Fine- Countervault Section in New Tunnels with four phases of excavation- Applying Mitigation measure

Maximum Displacement [mm]							
Soil	Construction Stage			Service Stage			Admissible
	MC	HS	HSs	MC	HS	HSs	
Fine	-	-	45.67	-	-	49.12	70

4.4.3 Verification of the Resistance in the New Road Tunnels

In the construction stage, the support of the new road tunnels must be verified through the criterion of admissible stresses, as defined in section 3.7.3(b).

In the service stage, the lining of the new road tunnels must be verified through the interaction diagram M-N and N-Q, as defined in section 3.7.3(b)..

The lining of the new road tunnels are verified, with their corresponding concrete thicknesses and reinforcement, as defined in Figure III-10 and sections 3.3.2 and 3.3.2(b).

$e = 0.50\ m$ Concrete thicknesses for the calculation
(Lining thicknesses = 0.30 m + 2/3 Support thicknesses = 0.20 m)
$A_s = 3.35\ cm^2/m$ ACMA335 Mesh in Internal and External face
$A_{s1} = 7.60\ cm^2/m$ 2Ø22 Bar of the Reticulate Frame in Internal face
$A_{s1} = 8.04\ cm^2/m$ 1Ø32 Bar of the Reticulate Frame in External face

(a) Analysis of the Fine Profile

(a.1) Construction Stage

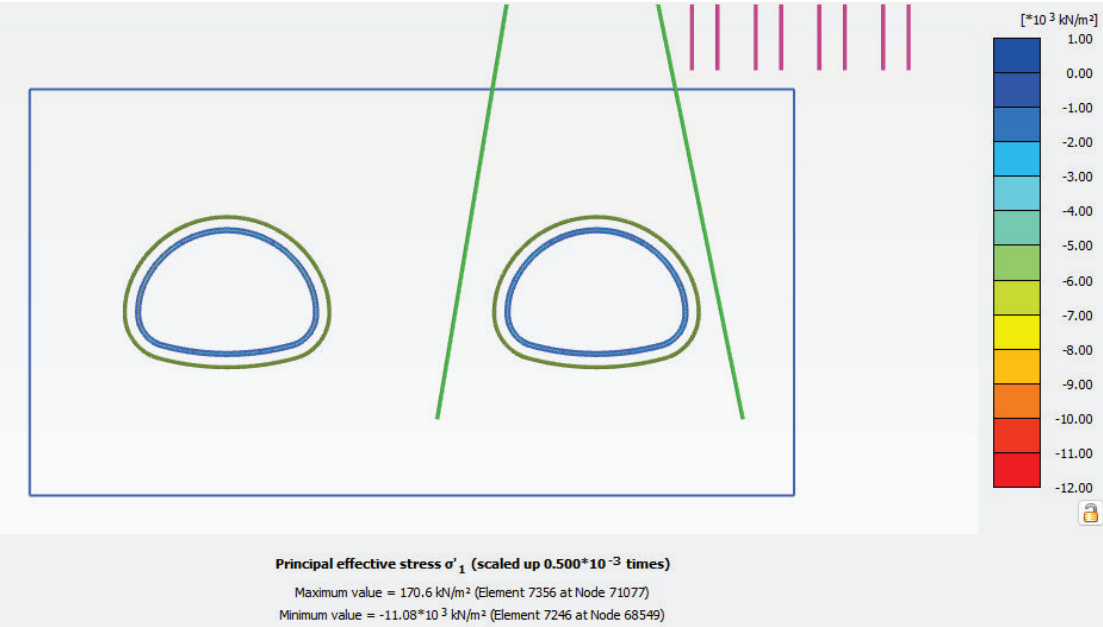


Figure IV-68: Major Principal effective Stress on Support- HSs – Fine-Counter-vault Section in New Tunnels and Mitigation Measure

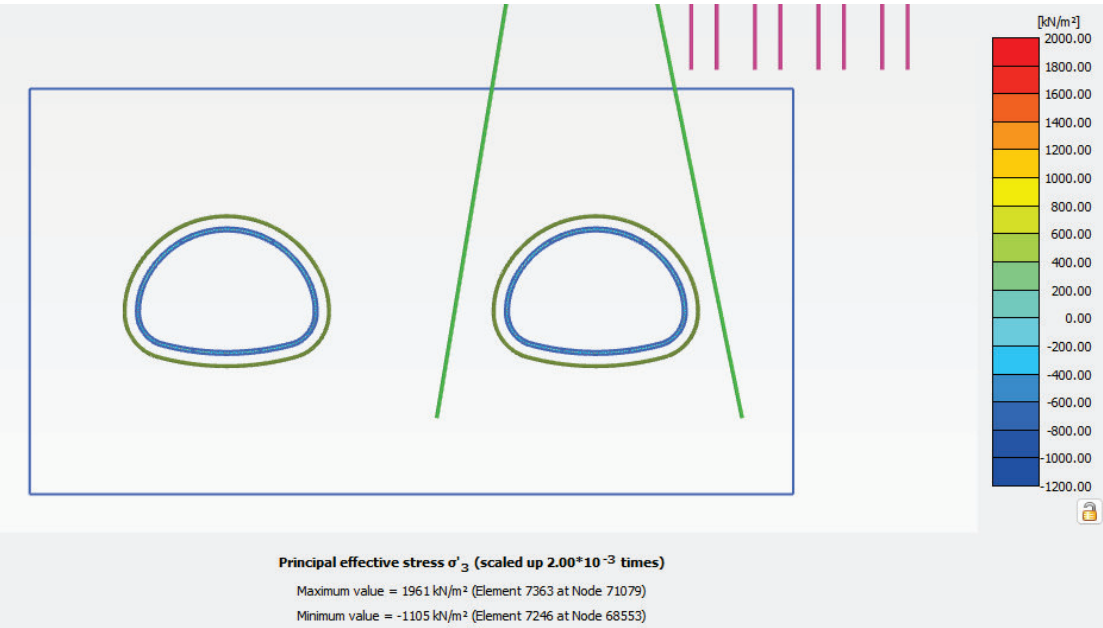


Figure IV-69: Minor Principal effective Stress on Support- HSs – Fine-Counter-vault Section in New Tunnels and Mitigation Measure

Table IV-29: Verification of Admissible Stress- HSs- Fine-

Counter vault Section in New Tunnels and Mitigation Measure

σ´1 [MPa]	σ´3 [MPa]	σ´1adm [MPa]	σ´3adm [MPa]	σ´1 < σ´1 adm	σ´3 < σ´3 adm
-11.08	1.96	-16	2	CHECK	CHECK

(a.2) Service Stage

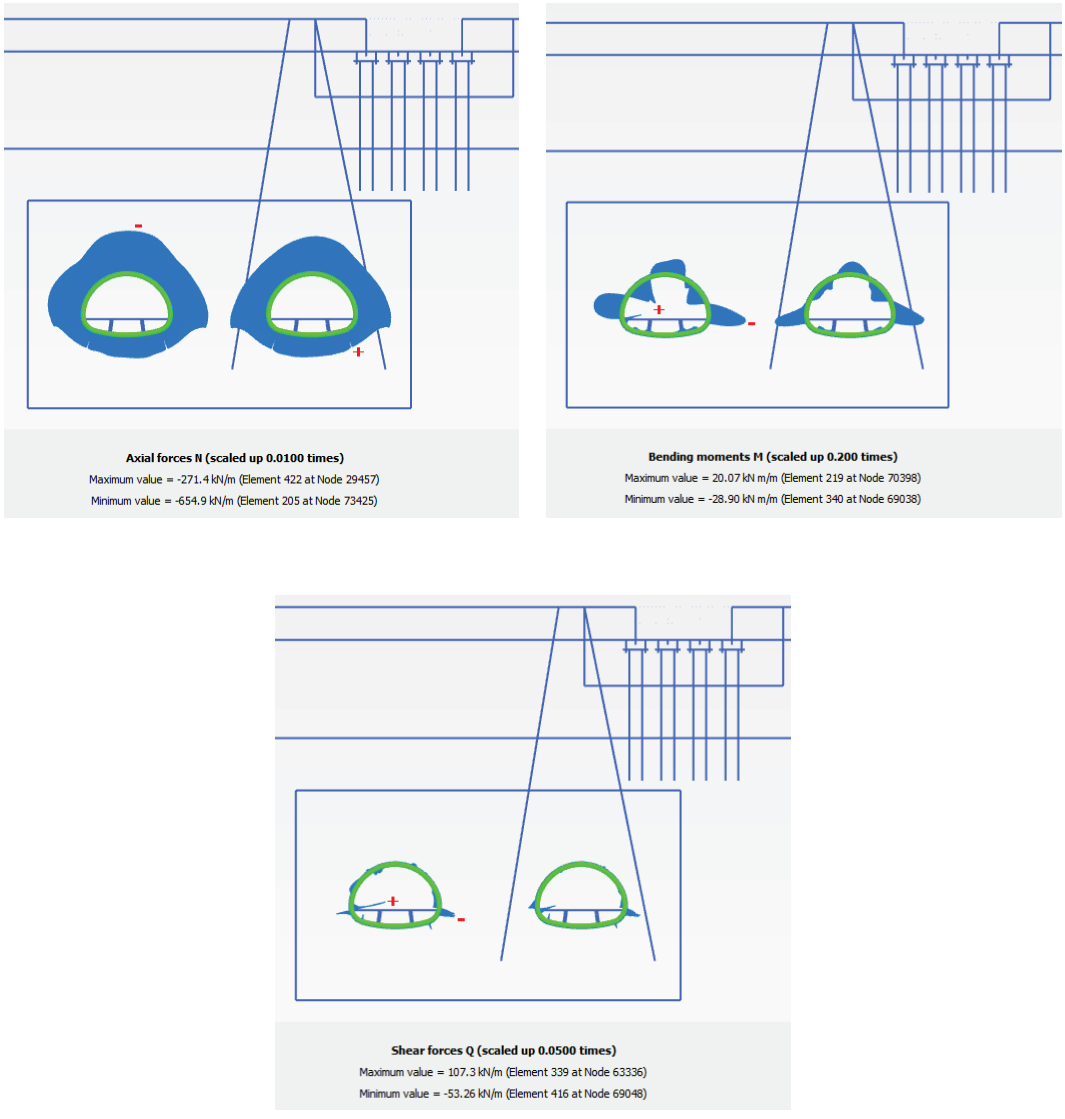
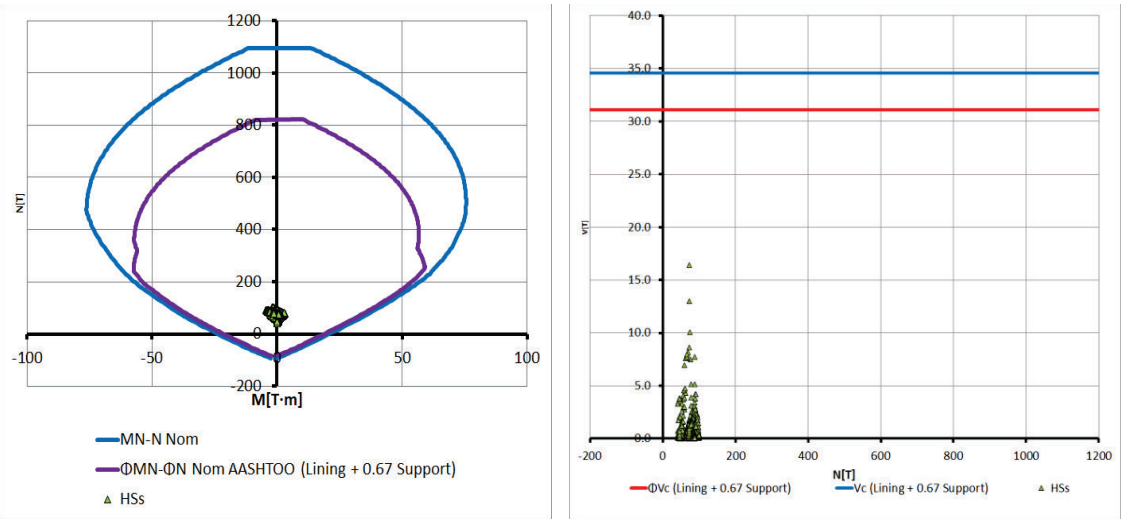


Figure IV-70: Forces Diagram, Axial, Bending and Shear on Lining- Service Stage- HSs- Fine- Counter vault Section in New Tunnels and Mitigation Measure



Graph IV-24: : Interaction M-N and N-Q Diagram- Lining of the new road tunnels- Service Stage- Fine- Counter vault Section in New Tunnels and Mitigation Measure

4.4.4 Verification of the Capacity of the Soil

The following shows the plastification of the soil in construction and in service and applies the acceptability criteria explained in section 3.7.4.

(a) Construction Stage

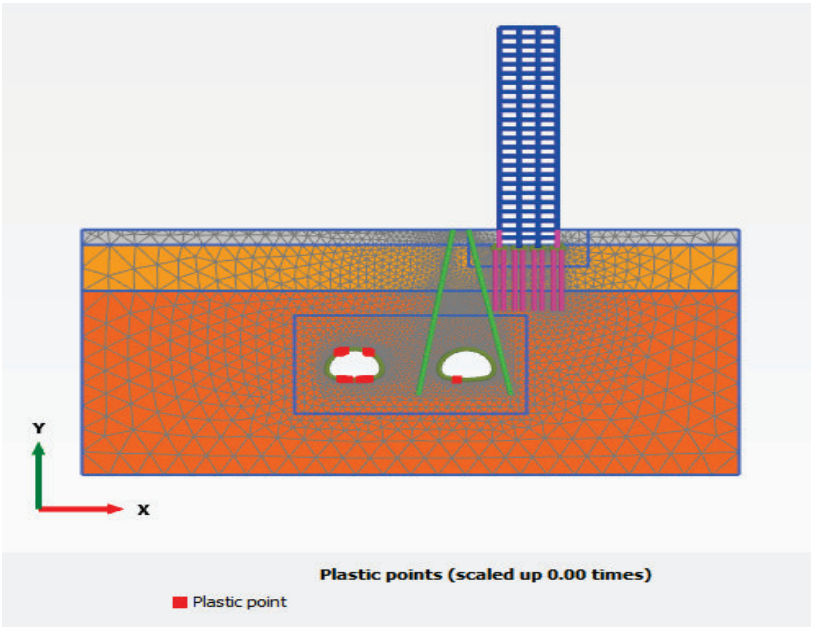


Figure IV-71: Plastification- Construction Stage- HSs- Fine- Counter vault Section in New Tunnels and Mitigation Measure

(b) Service Stage

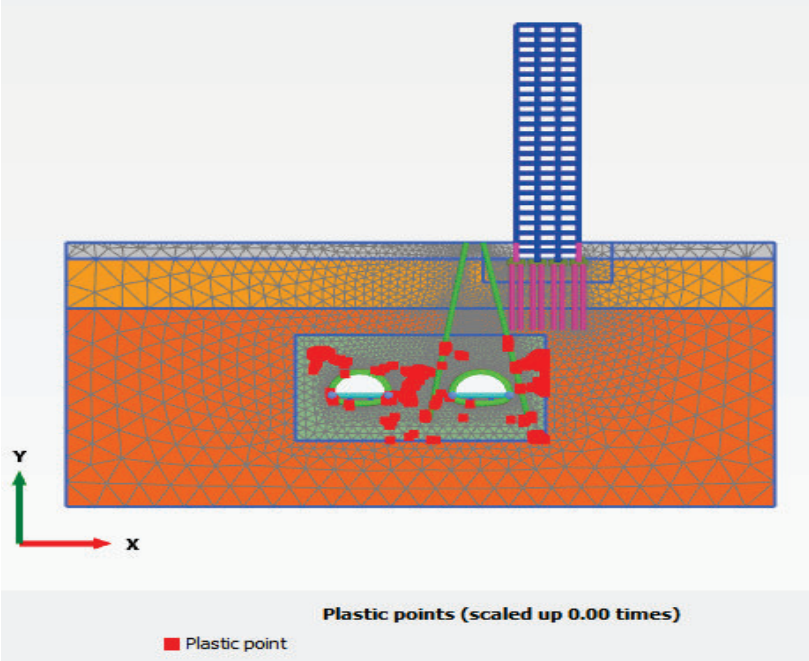


Figure IV-72: Plastification - Service Stage- HSs- Fine-Counter vault Section in New Tunnels and Mitigation Measure

Table IV-30: Plastification Verification on Soil- HSs- Fine-Counter vault Section in New Tunnels and Mitigation Measure

Stage	R-Plastic [m]	R-Plastic Admissible [m]	Verification
Construction	8	14	CHECK
Service	13	14	CHECK

V. PLANS

5.1. Plan N°1: Pre-existing Metro Tunnel- Soil Profiles with Tunnels Excavated in Two phases with Plane Sole Section.

5.2. Plan N°2: Pre-existing Metro Tunnel- Soil Profiles with Tunnels Excavated in Two phases with Counter-vault Section.

5.3. Plan N°3: Pre-existing Metro Tunnel- Soil Profiles with Tunnels Excavated in Four phases with Counter-vault Section.

5.4. Plan N°4: Pre-existing Building- Soil Profiles with Tunnels Excavated in Two phases with Plane Sole Section.

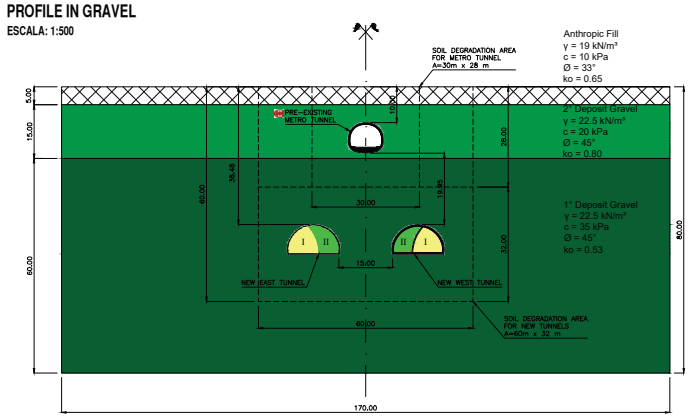
5.5. Plan N°5: Pre-existing Building- Soil Profiles with Tunnels Excavated in Two phases with Counter-vault Section.

5.6. Plan N°6: Pre-existing Building- Soil Profiles with Tunnels Excavated in Four phases with Counter-vault Section.

5.7. Plan N°7: Pre-existing Building- Soil Profiles with Tunnels Excavated in Four phases with Counter-vault Section applying Mitigation measure.

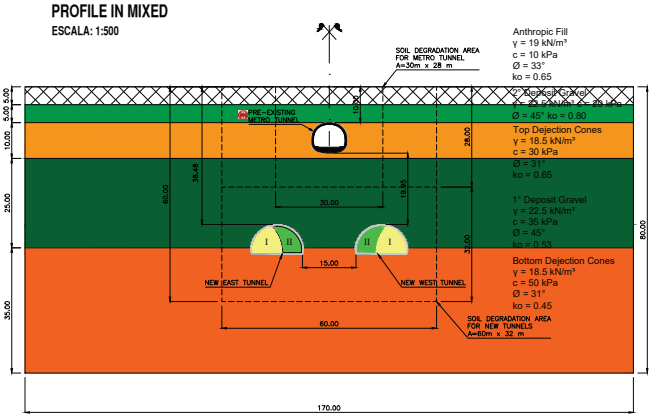
PROFILE IN GRAVEL

ESCALA: 1:500



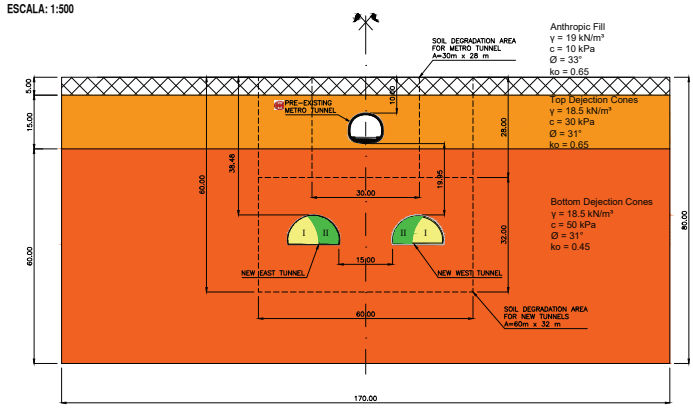
PROFILE IN MIXED

ESCALA: 1:500



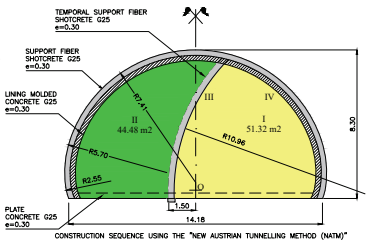
PROFILE IN FINE

ESCALA: 1:500



EAST AND WEST TUNNELS

ESCALA: 1:100



CONSTRUCTION SEQUENCE USING THE "NEW AUSTRIAN TUNNELLING METHOD (NATM)"

Phase I: Excavation and installation of the support of the first phase, with an excavation section of 51.32m2. It will be excavated in advances of 1.00m.

Phase II: The excavation of the section is completed with the excavation of phase II, with an excavation section of 44.48m2. A minimum offset of 20m must be maintained with the advance front. It will also be excavated in 1.00m advances.

Phase III: Maintaining a minimum offset of 20m, with respect to the advance front of Phase II, the demolition of the intermediate wall that forms the temporary support of the tunnel will be executed, in 1.00m steps.

Phase IV: Execution of lining.

GEOLOGICAL REFERENCES:

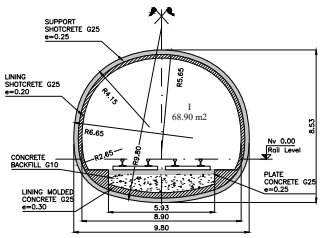
- ANTHROPIC FILL
- 2° DEPOSIT GRAVEL
- 1° DEPOSIT GRAVEL
- TOP DEJECTION CONES
- BOTTOM DEJECTION CONES

NOTES:

UNITS EXPRESSED IN METERS (m)

METRO TUNNEL

ESCALA: 1:100



MATERIALS OF THE PRE-EXISTING METRO TUNNEL:

SHOTCRETE:	G-25 OF σbk=250kg/cm²
MOLDED CONCRETE:	G-25 OF σbk=250kg/cm²
CONCRETE BACKFILL	G-10 OF σbk=100kg/cm²
STEEL FOR ELECTROWELDED MESH:	AT56-50H OF βs=5000kg/cm²
STEEL FOR BARS OF REINFORCEMENT:	A630-420H OF βs=4200kg/cm²

MATERIALS OF THE NEW ROAD TUNNELS:

SHOTCRETE WITH FIBER 3c:	G-25 OF σbk=250kg/cm²
MOLDED CONCRETE:	G-25 OF σbk=250kg/cm²
CONCRETE BACKFILL	G-10 OF σbk=100kg/cm²
STEEL FOR ELECTROWELDED MESH:	AT56-50H OF βs=5000kg/cm²
STEEL FOR RETICULATE FRAMES LG115/32/22	A630-420H OF βs=4200kg/cm²

ESCALA GRAFICA 1:500 (10m 0 10 20m)

ESCALA GRAFICA 1:100 (2m 0 2 4m)

Double Degree Program
Master in Geotechnical Engineering
Master of Sciences in Civil Engineering

TECHNISCHE UNIVERSITÄT MÜNCHEN

Student: Ing. David Enrique Agüero
Advisor: Dr. Ing. Juan Pablo Ibañez
Date: 4 Semester - 2024

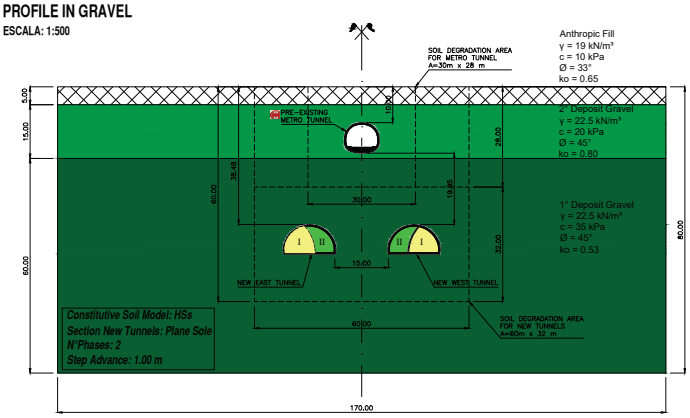
Thesis Title: "Analysis of the Influence of Urban Tunnel Excavation on Pre-existing Structures"

ESCALA	HORIZ.=ESCHOR VERT.=ESCVERT	TWOPHASES_TUNNEL	REV.
		PLA-01	A00

Drawing N°1: Pre-existing Metro Tunnel Soil Profiles with Tunnels Excavated in Two Phases with Plane Sole Section

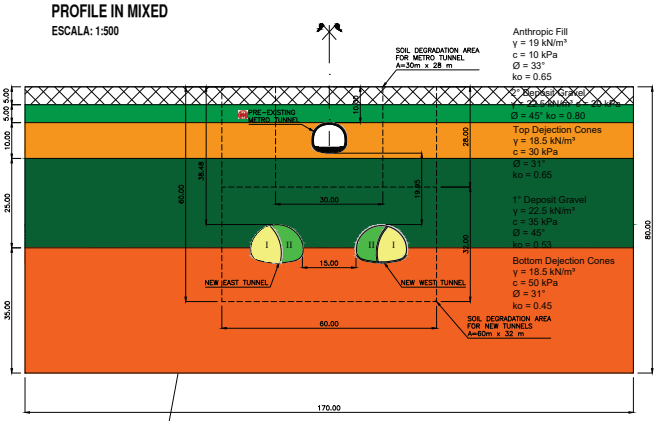
PROFILE IN GRAVEL

ESCALA: 1:500



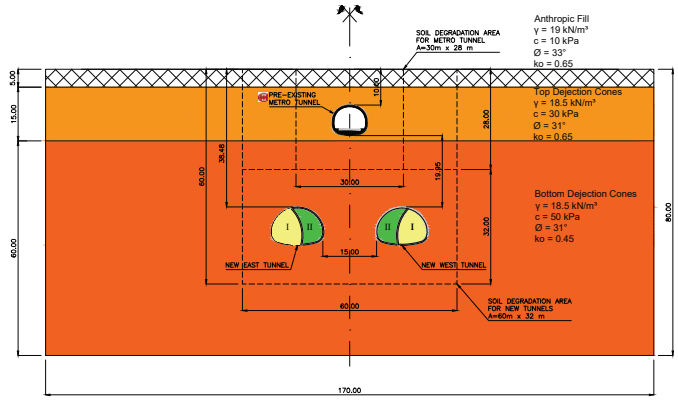
PROFILE IN MIXED

ESCALA: 1:500



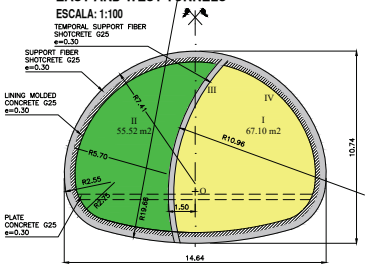
PROFILE IN FINE

ESCALA: 1:500



EAST AND WEST TUNNELS

ESCALA: 1:100



CONSTRUCTION SEQUENCE USING THE "NEW AUSTRIAN TUNNELLING METHOD (NATM)"

Phase I: Excavation and installation of the support of the first phase, with an excavation section of 67.10m2. It will be excavated in advances of 1.00m.

Phase II: The excavation of the section is completed with the excavation of phase II, with an excavation section of 55.52m2. A minimum offset of 20m must be maintained with the advance front. It will also be excavated in 1.00m advances.

Phase III: Maintaining a minimum offset of 20m, with respect to the advance front of Phase II, the demolition of the intermediate wall that forms the temporary support of the tunnel will be executed, in 1.00m steps.

Phase IV: Execution of lining.

REFFERENCIAS GEOLOGICAS:

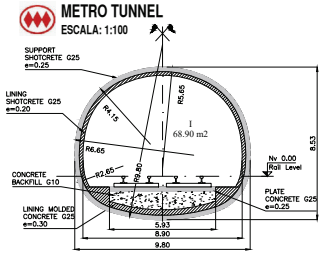
- ANTHROPIC FILL
- 2° DEPOSIT GRAVEL
- 1° DEPOSIT GRAVEL
- TOP DEJECTION CONES
- BOTTOM DEJECTION CONES

NOTES:

UNITS EXPRESSED IN METERS (m)

METRO TUNNEL

ESCALA: 1:100



MATERIALS OF THE PRE-EXISTING METRO TUNNEL:

SHOTCRETE:	G-25 OF σbk=250kg/cm²
MOLDED CONCRETE:	G-25 OF σbk=250kg/cm²
CONCRETE BACKFILL	G-10 OF σbk=100kg/cm²
STEEL FOR ELECTROWELDED MESH:	AT56-50H OF βs=5000kg/cm²
STEEL FOR BARS OF REINFORCEMENT:	A630-420H OF βs=4200kg/cm²

MATERIALS OF THE NEW ROAD TUNNELS:

SHOTCRETE WITH FIBER 3c:	G-25 OF σbk=250kg/cm²
MOLDED CONCRETE:	G-25 OF σbk=250kg/cm²
CONCRETE BACKFILL	G-10 OF σbk=100kg/cm²
STEEL FOR ELECTROWELDED MESH:	AT56-50H OF βs=5000kg/cm²
STEEL FOR RETICULATE FRAMES LG115/32/22	A630-420H OF βs=4200kg/cm²

ESCALA GRAFICA 1:500 (10m 0 10 20m)

ESCALA GRAFICA 1:100 (2m 0 2 4m)

Double Degree Program
Master in Geotechnical Engineering
Master of Sciences in Civil Engineering

TECHNISCHE UNIVERSITÄT MÜNCHEN

Student: Ing. David Enrique Agüero
Advisor: Dr. Ing. Juan Pablo Ibañez
Date: 4 Semester - 2024

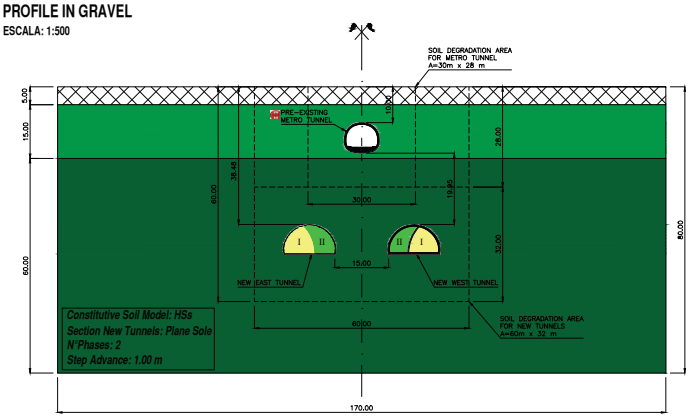
Thesis Title: "Analysis of the Influence of Urban Tunnel Excavation on Pre-existing Structures"

ESCALA	HORIZ.=ESCHOR	TWOPHASES_TUNNEL	REV.
	VERT.=ESCVERT	PLA-01	A00

Drawing N°2: Pre-existing Metro Tunnel
Soil Profiles with Tunnels Excavated
in Two Phases with counter-vault Section

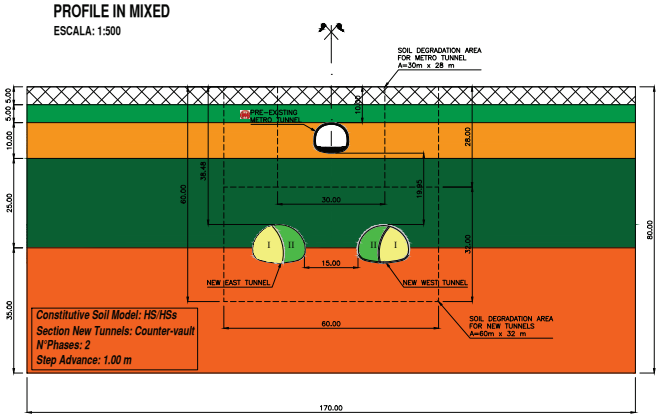
PROFILE IN GRAVEL

ESCALA: 1:500



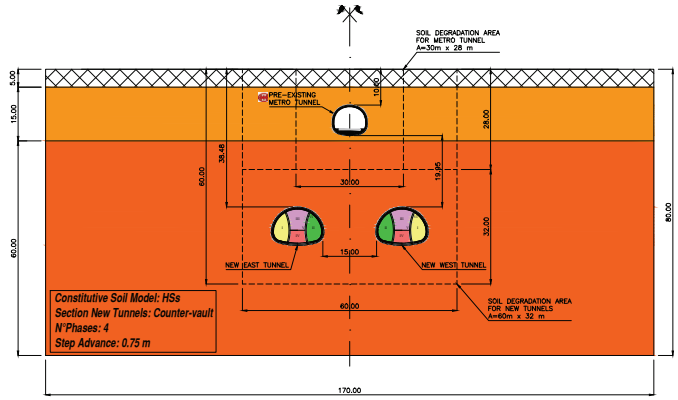
PROFILE IN MIXED

ESCALA: 1:500



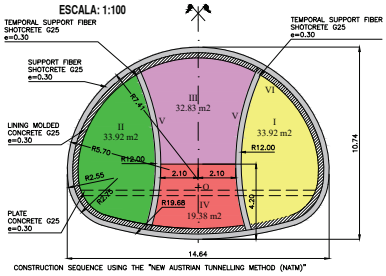
PROFILE IN FINE

ESCALA: 1:500



EAST AND WEST TUNNELS

ESCALA: 1:100



CONSTRUCTION SEQUENCE USING THE "NEW AUSTRIAN TUNNELLING METHOD (NATM)"

Phase I: Excavation and installation of the support of the first phase, with an excavation section of 33.92m2. It will be excavated in advances of 0.75m.

Phase II: Identical to phase I, but a minimum offset of 20 m must be respected with respect to the excavation front of phase I. It will also be excavated in 0.75m advances.

Phase III: Maintaining a minimum offset of 20m, with respect to the advance front of Phase II, Excavation and installation of the support of the third phase, with an excavation section of 32.83m2, in 0.75m advances.

Phase IV: Maintaining a minimum offset of 20m, with respect to the advance front of Phase III, Excavation and installation of the support of the fourth phase, with an excavation section of 19.38m2, in 0.75m advances.

Phase V: Maintaining a minimum offset of 20m, with respect to the advance front of Phase IV, the demolition of the intermediate wall that forms the temporary support of the tunnel will be executed, in 0.75m steps.

Phase VI: Execution of lining.

NOTES:

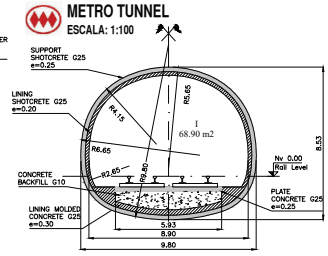
UNITS EXPRESSED IN METERS (m)

REFERENCIAS GEOLOGICAS:

- ANTHROPIC FILL
- 2° DEPOSIT GRAVEL
- 1° DEPOSIT GRAVEL
- TOP DEJECTION CONES
- BOTTOM DEJECTION CONES

METRO TUNNEL

ESCALA: 1:100



MATERIALS OF THE PRE-EXISTING METRO TUNNEL:

SHOTCRETE:	G-25 OF σ_{bk}=250kg/cm²
MOLDED CONCRETE:	G-25 OF σ_{bk}=250kg/cm²
CONCRETE BACKFILL	G-10 OF σ_{bk}=100kg/cm²
STEEL FOR ELECTROWELDED MESH:	AT56-50H OF β_s=5000kg/cm²
STEEL FOR BARS OF REINFORCEMENT:	A630-420H OF β_s=4200kg/cm²

MATERIALS OF THE NEW ROAD TUNNELS:

SHOTCRETE WITH FIBER 3c:	G-25 OF σ_{bk}=250kg/cm²
MOLDED CONCRETE:	G-25 OF σ_{bk}=250kg/cm²
CONCRETE BACKFILL	G-10 OF σ_{bk}=100kg/cm²
STEEL FOR ELECTROWELDED MESH:	AT56-50H OF β_s=5000kg/cm²
STEEL FOR RETICULATE FRAMES LG115/32/22	A630-420H OF β_s=4200kg/cm²

ESCALA GRAFICA 1:500 (10m 0 10 20m)

ESCALA GRAFICA 1:100 (2m 0 2 4m)

Double Degree Program
Master in Geotechnical Engineering
Master of Sciences in Civil Engineering

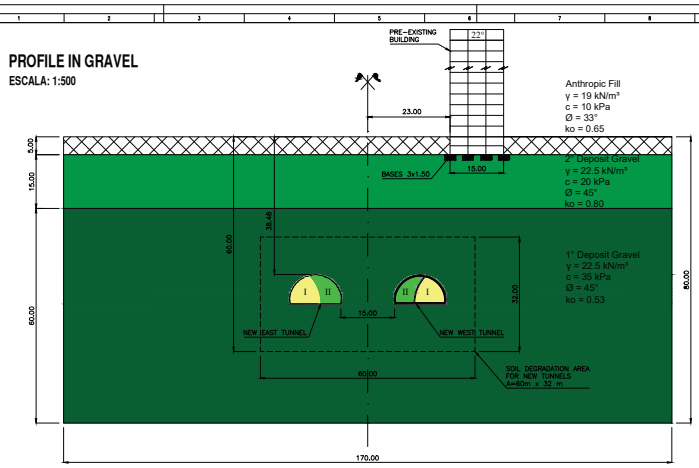
TECHNISCHE UNIVERSITÄT MÜNCHEN

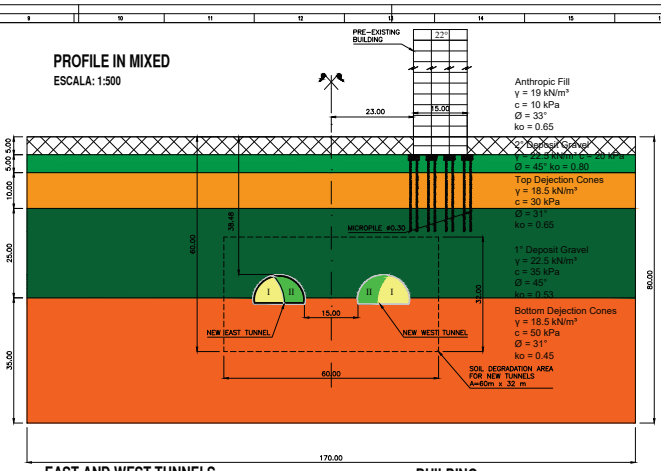
Student: Ing. David Enrique Agüero
Advisor: Dr. Ing. Juan Pablo Ibañez
Date: 4 Semester - 2024

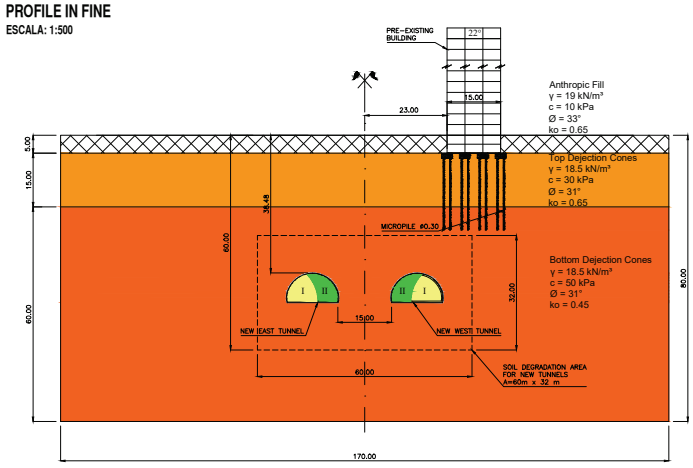
Thesis Title: "Analysis of the Influence of Urban Tunnel Excavation on Pre-existing Structures"

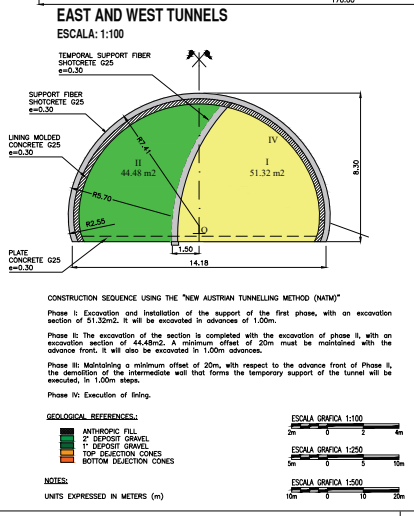
ESCALA	HORIZ.=ESCHOR	TWOPHASES_TUNNEL	REV.
	VERT.=ESCVERT	PLA-01	A00

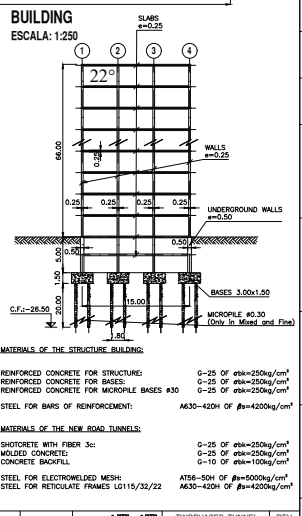
Drawing N°3: Pre-existing Metro Tunnel
Soil Profiles with Tunnels Excavated
in Four Phases with counter-vault Section











Double Degree Program
Master in Geotechnical Engineering
Master of Sciences in Civil Engineering

TECHNISCHE UNIVERSITÄT MÜNCHEN

Student: Ing. David Enrique Agüero
Advisor: Dr. Ing. Juan Pablo Ibañez
Date: 4 Semester - 2024

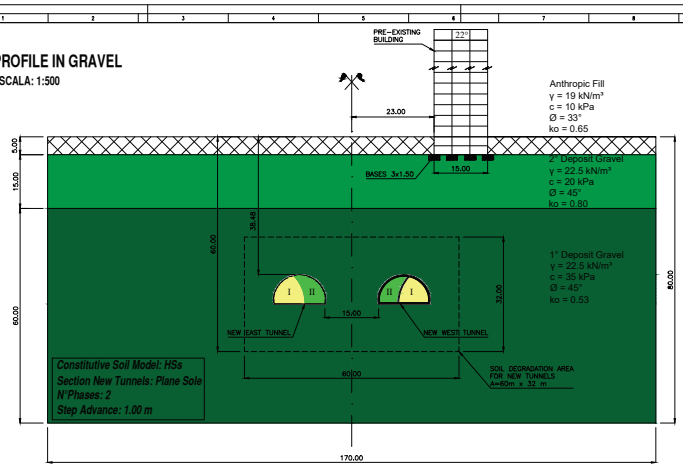
Thesis Title: "Analysis of the Influence of Urban Tunnel Excavation on Pre-existing Structures"

ESCALA	HORIZ.=ESCHOR	TWOPHASES_TUNNEL	REV.
	VERT.=ESCVERT	PLA-01	A00

Drawing N°4: Pre-existing Building
Soil Profiles with Tunnels Excavated
in Two Phases with Plane Sole Section

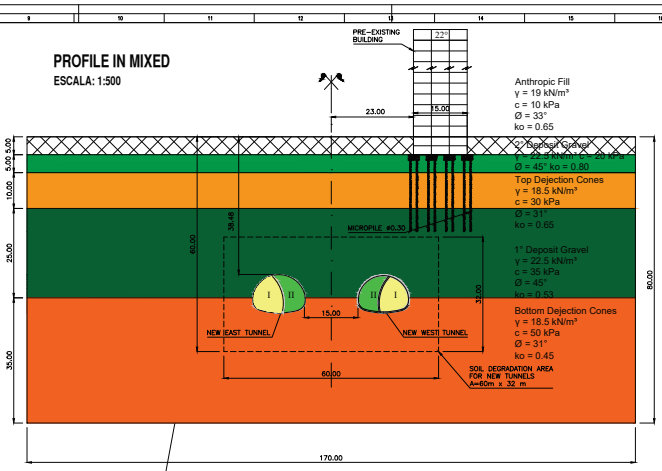
PROFILE IN GRAVEL

ESCALA: 1:500



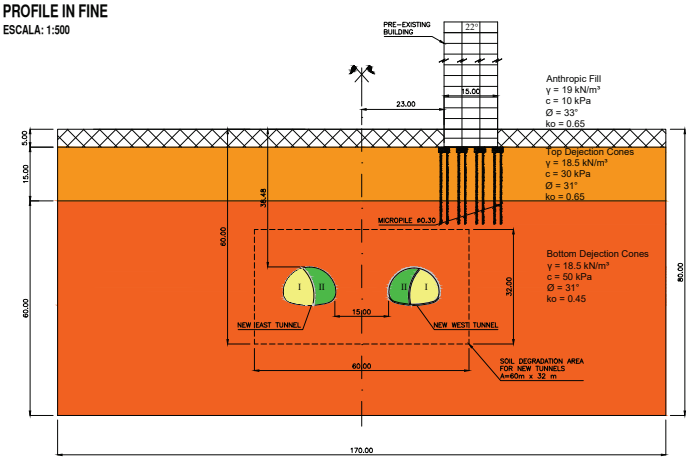
PROFILE IN MIXED

ESCALA: 1:500



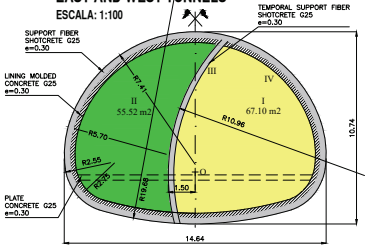
PROFILE IN FINE

ESCALA: 1:500



EAST AND WEST TUNNELS

ESCALA: 1:100



CONSTRUCTION SEQUENCE USING THE "NEW AUSTRIAN TUNNELLING METHOD (NATM)"

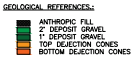
Phase I: Excavation and installation of the support of the first phase, with an excavation section of 51.32m2. It will be excavated in advances of 1.00m.

Phase II: The excavation of the section is completed with the excavation of phase II, with an excavation section of 44.48m2. A minimum offset of 20m must be maintained with the advance front. It will also be excavated in 1.00m advances.

Phase III: Maintaining a minimum offset of 20m, with respect to the advance front of Phase II, the demolition of the intermediate wall that forms the temporary support of the tunnel will be executed, in 1.00m steps.

Phase IV: Execution of lining.

GEOLOGICAL REFFRENCES:-



ESCALA GRAFICA 1:500

ESCALA GRAFICA 1:500

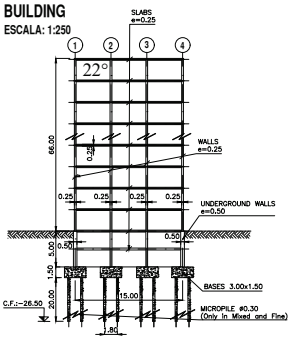
ESCALA GRAFICA 1:500

NOTES:

UNITS EXPRESSED IN METERS (m)

BUILDING

ESCALA: 1:250



MATERIALS OF THE STRUCTURE BUILDING:

REINFORCED CONCRETE FOR STRUCTURE:	G-25 OF σbk=250kg/cm²
REINFORCED CONCRETE FOR BASES:	G-25 OF σbk=250kg/cm²
REINFORCED CONCRETE FOR MICROPILE BASES Ø30	G-25 OF σbk=250kg/cm²
STEEL FOR BARS OF REINFORCEMENT:	A630-420H OF βs=4200kg/cm²

MATERIALS OF THE NEW ROAD TUNNELS:

SHOTCRETE WITH FIBER 3cc:	G-25 OF σbk=250kg/cm²
MOLDED CONCRETE:	G-25 OF σbk=250kg/cm²
CONCRETE BACKFILL	G-10 OF σbk=100kg/cm²
STEEL FOR ELECTROWELDED MESH:	AT56-50H OF βs=5000kg/cm²
STEEL FOR RETICULATE FRAMES LG115/32/22	A630-420H OF βs=4200kg/cm²

Double Degree Program
Master in Geotechnical Engineering
Master of Sciences in Civil Engineering

TECHNISCHE UNIVERSITÄT MÜNCHEN

Student: Ing. David Enrique Agüero
Advisor: Dr. Ing. Juan Pablo Ibañez
Date: 4 Semester - 2024

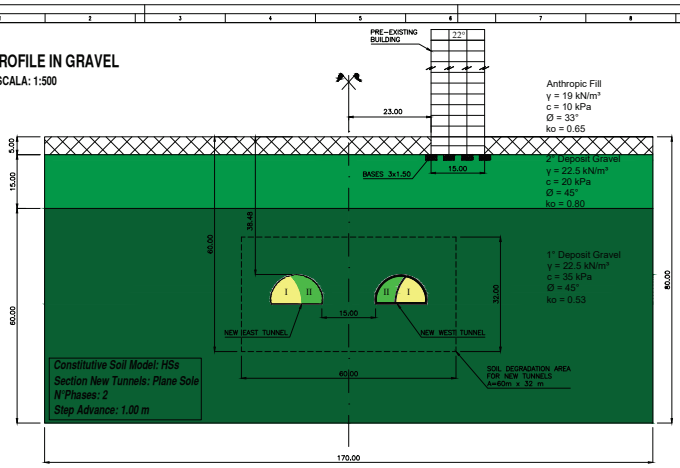
Thesis Title: "Analysis of the Influence of Urban Tunnel Excavation on Pre-existing Structures"

ESCALA	HORIZ.=ESCHOR VERT.=ESCVERT	TWOPHASES_TUNNEL	REV.
		PLA-01	A00

Drawing N°5: Pre-existing Building Soil Profiles with Tunnels Excavated in Two Phases with Counter-vault Section

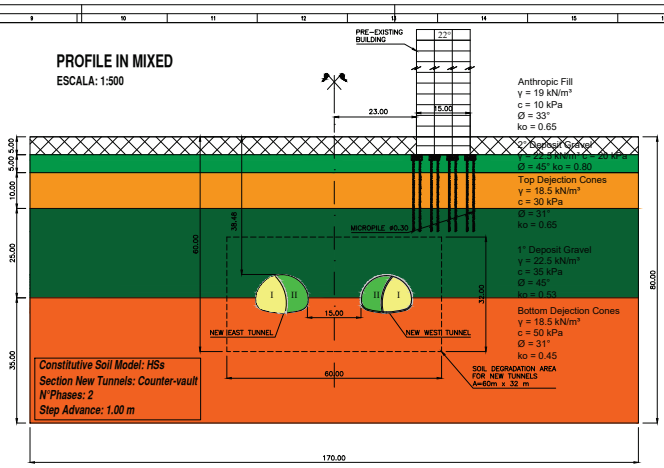
PROFILE IN GRAVEL

ESCALA: 1:500



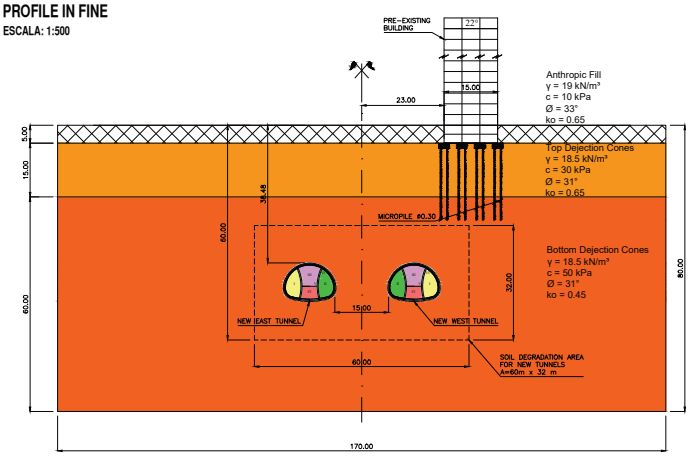
PROFILE IN MIXED

ESCALA: 1:500



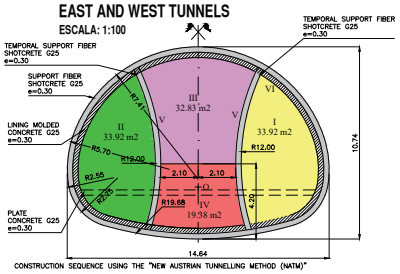
PROFILE IN FINE

ESCALA: 1:500



EAST AND WEST TUNNELS

ESCALA: 1:100



CONSTRUCTION SEQUENCE USING THE "NEW AUSTRIAN TUNNELLING METHOD (NATM)"

Phase I: Excavation and installation of the support of the first phase, with an excavation section of 33.92m2. It will be excavated in advances of 0.75m.

Phase II: Identical to phase I, but a minimum offset of 20 m must be respected with respect to the excavation front of phase I. It will also be excavated in 0.75m advances.

Phase III: Maintaining a minimum offset of 20m, with respect to the advance front of Phase II, Excavation and installation of the support of the third phase, with an excavation section of 32.83m2, in 0.75m advances.

Phase IV: Maintaining a minimum offset of 20m, with respect to the advance front of Phase III, Excavation and installation of the support of the fourth phase, with an excavation section of 19.38m2, in 0.75m advances.

Phase V: Maintaining a minimum offset of 20m, with respect to the advance front of Phase IV, the demolition of the intermediate wall that forms the temporary support of the tunnel will be executed, in 0.75m steps.

Phase VI: Execution of lining.

GEOLOGICAL REFERENCES:

- ANTHROPIC FILL
- 2° DEPOSIT GRAVEL
- 1° DEPOSIT GRAVEL
- TOP DEJECTION CONES
- BOTTOM DEJECTION CONES

NOTES:

UNITS EXPRESSED IN METERS (m)

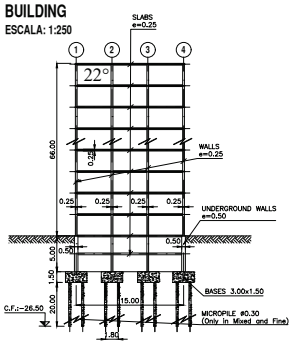
ESCALA GRAFICA 1:100

ESCALA GRAFICA 1:500

ESCALA GRAFICA 1:250

BUILDING

ESCALA: 1:250



MATERIALS OF THE STRUCTURE BUILDING:

REINFORCED CONCRETE FOR STRUCTURE:	G-25 OF σbk=250kg/cm²
REINFORCED CONCRETE FOR BASES:	G-25 OF σbk=250kg/cm²
REINFORCED CONCRETE FOR MICROPILE BASES Ø30	G-25 OF σbk=250kg/cm²
STEEL FOR BARS OF REINFORCEMENT:	A630-420H OF βs=4200kg/cm²

MATERIALS OF THE NEW ROAD TUNNELS:

SHOTCRETE WITH FIBER 3c:	G-25 OF σbk=250kg/cm²
MOLDED CONCRETE:	G-25 OF σbk=250kg/cm²
CONCRETE BACKFILL	G-10 OF σbk=100kg/cm²
STEEL FOR ELECTROWELDED MESH:	AT56-50H OF βs=5000kg/cm²
STEEL FOR RETICULATE FRAMES LG115/32/22	A630-420H OF βs=4200kg/cm²

Double Degree Program
Master in Geotechnical Engineering
Master of Sciences in Civil Engineering

TECHNISCHE UNIVERSITÄT MÜNCHEN

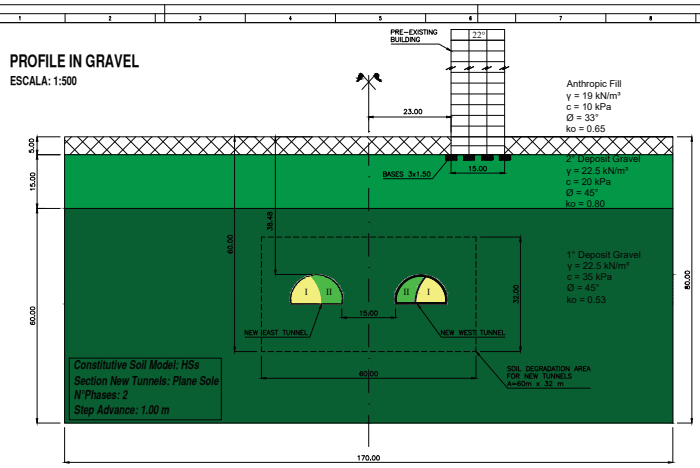
Student: Ing. David Enrique Agüero
Advisor: Dr. Ing. Juan Pablo Ibañez
Date: 4 Semester - 2024

Thesis Title: "Analysis of the Influence of Urban Tunnel Excavation on Pre-existing Structures"

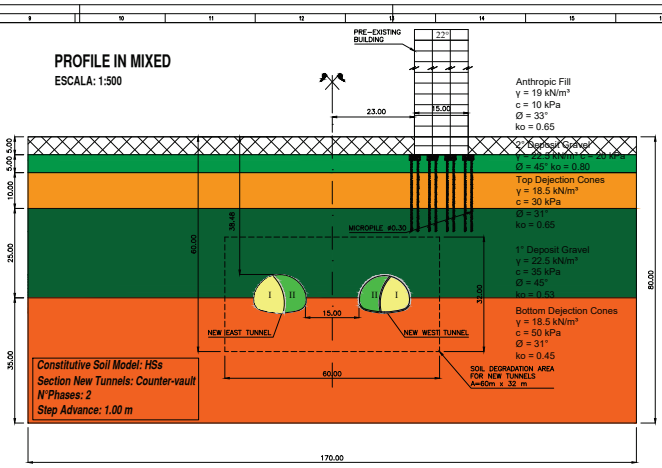
ESCALA	HORIZ.=ESCHOR VERT.=ESCVERT	TWOPHASES_TUNNEL	REV.
		PLA-01	A00

Drawing N°6: Pre-existing Building Soil Profiles with Tunnels Excavated in Four Phases with Counter-vault Section

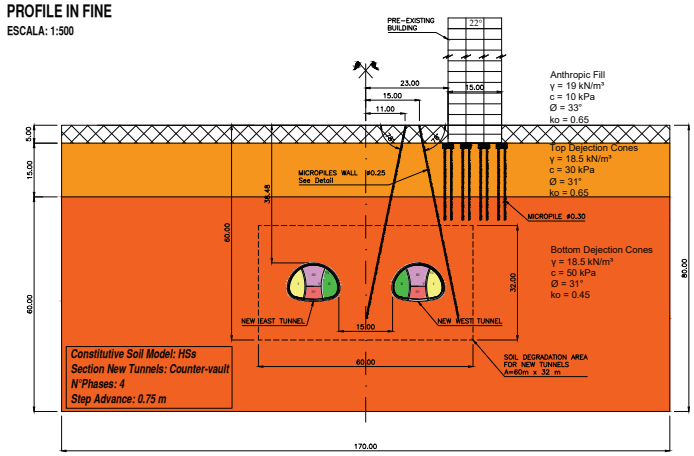
PROFILE IN GRAVEL
ESCALA: 1:500



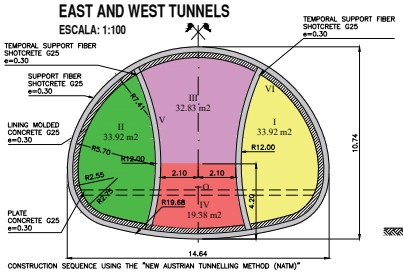
PROFILE IN MIXED
ESCALA: 1:500



PROFILE IN FINE
ESCALA: 1:500



EAST AND WEST TUNNELS
ESCALA: 1:100



CONSTRUCTION SEQUENCE USING THE "NEW AUSTRIAN TUNNELLING METHOD (NATM)"

Phase I: Excavation and installation of the support of the first phase, with an excavation section of 33.92m2. It will be excavated in advances of 0.75m.

Phase II: Identical to phase I, but a minimum offset of 20 m must be respected with respect to the excavation front of phase I. It will also be excavated in 0.75m advances.

Phase III: Maintaining a minimum offset of 20m, with respect to the advance front of Phase II, Excavation and installation of the support of the third phase, with an excavation section of 32.83m2, in 0.75m advances.

Phase IV: Maintaining a minimum offset of 20m, with respect to the advance front of Phase III, Excavation and installation of the support of the fourth phase, with an excavation section of 19.38m2, in 0.75m advances.

Phase V: Maintaining a minimum offset of 20m, with respect to the advance front of Phase IV, the demolition of the intermediate wall that forms the temporary support of the tunnel will be executed, in 0.75m steps.

Phase VI: Execution of lining.

GEOLOGICAL REFERENCES.:

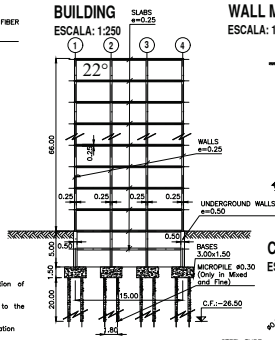
ANTHROPIC FILL
2° DEPOSIT GRAVEL
1° DEPOSIT GRAVEL
TOP DEJECTION CONES
BOTTOM DEJECTION CONES

NOTES:

UNITS EXPRESSED IN METERS (m)

ESCALA GRAFICA 1:500 — 10m 0 10 20m
ESCALA GRAFICA 1:250 — 5m 0 5 10m
ESCALA GRAFICA 1:500 — 10m 0 10 20m
ESCALA GRAFICA 1:250 — 5m 0 5 10m

BUILDING
ESCALA: 1:250



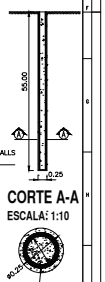
MATERIALS OF THE STRUCTURE BUILDING:

REINFORCED CONCRETE FOR STRUCTURE:	G-25 OF σbk=250kg/cm²
REINFORCED CONCRETE FOR BASES:	G-25 OF σbk=250kg/cm²
REINFORCED CONCRETE FOR MICROPILE BASES #30	G-25 OF σbk=250kg/cm²
REINFORCED CONCRETE FOR MICROPILE WALL #25	G-25 OF σbk=250kg/cm²
STEEL FOR BARS OF REINFORCEMENT:	A630-420H OF fs=4200kg/cm²
STEEL FOR TUBE OF REINFORCEMENT MICROPILE:	S-275 OF ρs=2750kg/cm³

MATERIALS OF THE NEW ROAD TUNNELS:

SHOTCRETE WITH FIBER 3c:	G-25 OF σbk=250kg/cm²
MOLDED CONCRETE:	G-25 OF σbk=250kg/cm²
CONCRETE BACKFILL	G-10 OF σbk=100kg/cm²
STEEL FOR ELECTROWELDED MESH:	A756-50H OF ρs=5000kg/cm²
STEEL FOR RETICULATE FRAMES LG115/32/22	A630-420H OF ρs=4200kg/cm²

WALL MICROPILE
ESCALA: 1:50



CORTE A-A
ESCALA: 1:10

STEEL TUBE e=20mm

Double Degree Program
Master in Geotechnical Engineering
Master of Sciences in Civil Engineering
TECHNISCHE UNIVERSITÄT MÜNCHEN

Student: Ing. David Enrique Agüero
Advisor: Dr. Ing. Juan Pablo Ibañez
Date: 4 Semester - 2024

Thesis Title: "Analysis of the Influence of Urban Tunnel Excavation on Pre-existing Structures"

ESCALA	HORIZ.=ESCHOR	TWOPHASES_TUNNEL	REV.
	VERT.=ESCVERT	PLA-01	A00

Drawing N°7: Pre-existing Building- Soil Profiles with Tunnels Excavated in Four Phases with Counter-vault Section, applying Mitigation Measure.